

SHRP-A-368

# **Binder Characterization and Evaluation**

## **Volume 2: Chemistry**

J.F. Branthaver, J.C. Petersen, R.E. Robertson, J.J. Duvall, S.S. Kim,  
P.M. Harnsberger, T. Mill, E.K. Ensley, F.A. Barbour, J.F. Schabron



**Strategic Highway Research Program**  
National Research Council  
Washington, DC 1993

SHRP-A-368  
Contract A-002A  
ISBN 0-309-05620-9  
Product No.: 1003, 1004, 1009

Program Manager: *Edward T. Harrigan*  
Project Manager: *Jack S. Youtcheff*  
Program Area Secretary: *Juliet Narsiah*  
Production Editor: *Marsha Barrett*

November 1993

key words:  
amphoteric  
asphalt fractionation  
asphalt oxidation  
asphalt rheology  
ion exchange chromatography (IEC)  
molecular structuring  
potentiometric titrations  
pressure aging  
size exclusion chromatography (SEC)  
supercritical fluid chromatography (SFC)  
vapor phase osmometry (VPO)

Strategic Highway Research Program  
National Academy of Sciences  
2101 Constitution Avenue N.W.  
Washington, DC 20418

(202) 334-3774

The publication of this report does not necessarily indicate approval or endorsement of the findings, opinions, conclusions, or recommendations either inferred or specifically expressed herein by the National Academy of Sciences, the United States Government, or the American Association of State Highway and Transportation Officials or its member states.

© 1993 National Academy of Sciences

## Acknowledgments

The research described herein was supported by the Strategic Highway Research Program (SHRP). SHRP is a unit of the National Research Council that was authorized by section 128 of the Surface Transportation and Uniform Relocation Assistance Act of 1987.

At the outset of the A-002A program, J.C. Petersen was Principal Investigator. Co-Principal Investigator was J.F. Branthaver. Project Manager was R.E. Robertson. In 1990, R.E. Robertson succeeded J.C. Petersen as Principal Investigator. D. Geldien served as Project Coordinator and L. Borgman served as Project Statistician. M. Knadler (1988-90) and J. Greaser (1990-93) served as project secretaries.

This report was assembled by J. Greaser. D.C. Colgin assisted with proofreading. Some graphics were prepared by T. Munari and G. Wong. Assistance in the preparation of previous reports was rendered by M. Hauff and M. Knadler. Members of the Technical Staff of the Exploratory and New Products Division, Office of Physical Sciences of Western Research Institute performed most of the work that is the subject of the report. Some analytical work was performed by the Analytical Services Division, Office of Physical Sciences of Western Research Institute.

Chapter 1 was written by J.F. Branthaver, who supervised most of the research reported therein. Ion exchange chromatography separations were performed by M.W. Catalfomo, D.C. Colgin, S.S. Kim, and S.C. Preece. The supercritical fluid chromatography separations were carried out by F.A. Barbour. Rheological studies were performed by H. Plancher, F.A. Reid, and M.V. Aldrich.

Chapter 2 was written by J.J. Duvall, who supervised the work reported therein. Size exclusion chromatography separations were performed by M.W. Catalfomo, D.C. Colgin, A.A. Gwin, S.S. Kim, G. Miyake, S.C. Preece, and J. Wolf. Rheological studies were performed by H. Plancher and F.A. Reid.

Chapter 3 was written by J.F. Branthaver. The laboratory work was performed by M.W. Catalfomo, D.C. Colgin, and A.A. Gwin. The extensive rheological work was performed by F.A. Reid.

Chapter 3 was written by J.F. Branthaver. The laboratory work was performed by M.W. Catalfomo, D.C. Colgin, and A.A. Gwin. The extensive rheological work was performed by F.A. Reid.

Chapter 4 was written by J.F. Branthaver. The work described in the chapter was supervised by R.E. Robertson, J.F. Schabron, and J.F. Branthaver. A.A. Gwin performed the titrations.

Chapter 5 was written by J.F. Branthaver and S.S. Kim. Laboratory work was performed by D.C. Colgin, A.A. Gwin, and S.S. Kim. The extensive rheological studies were carried out by F.A. Reid.

Chapter 6 was written by J.F. Branthaver. The extensive rheological studies were supervised by H. Plancher and performed by H. Plancher and F.A. Reid.

Chapter 7 was written by T. Mill of SRI International, who supervised the work performed therein. Laboratory studies were carried out by B. Loo, M. Rossi, and D. Tse.

Chapter 8 was written by P.M. Harnsberger. The oxidation studies were supervised by E.K. Ensley and P.M. Harnsberger. Reduced specific viscosity studies and size exclusion chromatography studies were supervised by J.J. Duvall. J.F. Branthaver supervised the titration studies. Oxidations were performed by M.V. Aldrich, M. Meyer, S. Rickard, S. Smith, J. Tauer, and J. Wolf. A.A. Gwin and G. Miyake performed other laboratory work. The extensive rheological work was performed by H. Plancher and F.A. Reid.

Chapter 9 was written by J.F. Branthaver. Asphaltene studies were supervised by P.M. Harnsberger. Heithaus determinations and reduced specific viscosity studies were supervised by J.J. Duvall. Nuclear magnetic resonance data were obtained by D. Netzel. Molecular weights were determined by G.W. Gardner. Infrared spectra were obtained by M.V. Aldrich, A.A. Gwin, G. Miyake, and J. Wolf. Heithaus titrations were performed by M.V. Aldrich, A.A. Gwin, B. Lowry, and J. Wolf. Asphaltenes were prepared by M.W. Catalfomo, D.C. Colgin, A.A. Gwin, S.C. Preece, and M. Scott. Rheological measurements were performed by H. Plancher and F.A. Reid.

Preparation of all entries for Database B was performed by J. Tauer, M.V. Aldrich, and A.A. Gwin.



# Contents

Acknowledgments	iii
List of Figures	vii
List of Tables	xvii
Abstract	xxxiii
Executive Summary	xxxv
Introduction	xxxix
Chapter 1 Separation of Asphalts by Chemical Functionality	1
Chapter 2 Size Exclusion Chromatography Separations of Asphalts	39
Chapter 3 Rheological Studies of Mixtures of Model Compounds with Asphalts	77
Chapter 4 Potentiometric Titration Studies	87
Chapter 5 Polarity of Asphalt	101
Chapter 6 Molecular Structuring Studies	149
Chapter 7 Oxidation Pathways for Asphalt	157
Chapter 8 Aging Studies of Asphalt	189
Chapter 9 Characterization of Asphalts by Classical Methods	287
References	313

Appendix A	Supplementary Figures and Tables . . . . .	321
Appendix B	List of Tables Available in Database . . . . .	457
Appendix C	Lot Numbers for Resins Used in Ion Exchange Chromatography Separations . . . . .	461
Appendix D	Separation of a Quinolone-Enriched Fraction from SHRP Asphalts . . . .	467

## List of Figures

1.1	Flow Sheet for Separation of Asphalts into Five Fractions by IEC	17
1.2	Viscosity vs. Molecular Weight for IEC Neutrals	18
1.3	Plot of Tan Delta (Constant Torque) Values of Seven Core Asphalts vs. Number-Average Molecular Weights of Their IEC Strong Acid Fractions	19
1.4	Flow Sheet for Isolation of Amphoterics by IEC	20
1.5	SFC Chromatograms of IEC Neutral, SEC Fraction-II, and Maltene Fractions of AAA-1	21
1.6	SFC Chromatograms of IEC Neutral, SEC Fraction-II, and Maltene Fractions of AAB-1	21
1.7	SFC Chromatograms of IEC Neutral, SEC Fraction-II, and Maltene Fractions of AAC-1	22
1.8	SFC Chromatograms of IEC Neutral, SEC Fraction-II, and Maltene Fractions of AAD-1	22
1.9	SFC Chromatograms of IEC Neutral, SEC Fraction-II, and Maltene Fractions of AAF-1	23
1.10	SFC Chromatograms of IEC Neutral, SEC Fraction-II, and Maltene Fractions of AAG-1	23
1.11	SFC Chromatograms of IEC Neutral, SEC Fraction-II, and Maltene Fractions of AAK-1	24

1.12	SFC Chromatograms of IEC Neutral, SEC Fraction-II, and Maltene Fractions of AAM-1 .....	24
2.1	Size Exclusion Chromatograms of Core Asphalts .....	53
2.2	Relationship Between Tan Delta (25°C and torque at 400 g·cm) and SEC Fraction-II for Streamlined Preparative Size Exclusion Chromatography (SPSEC) and Preparative Size Exclusion Chromatography (PSEC) .....	55
2.3	SEC Fraction-II vs. Phase Angle .....	56
2.4	PSEC Separation of Asphalt AAB-1 and of its Recombined Fractions 1 and 2 .....	57
2.5	PSEC Separation of Asphalt AAD-1 and its IEC Neutrals, Weak Acids, and Weak Bases .....	58
2.6	Fast SEC Refractive Index Chromatograms for Unaged Core Asphalts, Toluene Carrier, $10^4$ Å and $10^3$ Å Columns in Series .....	59
2.7	Fast SEC of AAK-1, Aged by Thin-Film Accelerated Aging Test (TFAAT) (0, 24, 48, and 72 hours), Scanned at 300 nm .....	60
2.8	Fast SEC of AAK-1 Aged by TFAAT (0, 24, 48, and 72 hrs), Scanned at 575 nm .....	61
2.9	Relationship Between Percent SEC Fraction-II Equivalent by High Performance Liquid Chromatography and Tan Delta (25°C and torque at 400 g·cm) for the Differential Refractive Index Detector at 100 minutes into Run .....	62
2.10	SFC Chromatograms of SEC Fractions of IEC Neutral Fractions of AAA-1 .....	63
2.11	Fast SEC Refractive Index Chromatograms for Maltenes from Unaged Core Asphalts, toluene carrier, $10^4$ Å and $10^3$ Å columns in series .....	341
2.12	Fast SEC Refractive Index Chromatograms for Asphaltenes from Unaged Core Asphalts, toluene carrier, $10^4$ Å and $10^3$ Å columns in series .....	342
2.13	Fast SEC of AAK-1 Aged by Thin-Film Accelerated Aging Test (0, 24, 48, and 72 hours), Scanned at 340 nm .....	343

2.14	Fast SEC of AAK-1 Aged by TFAAT (0, 24, 48, and 72 hours), Scanned at 380 nm	344
2.15	Fast SEC of AAK-1 Aged by TFAAT (0, 24, 48, and 72 hours), Scanned at 410 nm	345
2.16	Fast SEC of AAK-1 Aged by TFAAT (0, 24, 48, and 72 hours), Scanned at 420 nm	346
2.17	Fast SEC of AAK-1 Aged by TFAAT (0, 24, 48, and 72 hours), Scanned at 500 nm	347
2.18	Fast SEC of AAK-1 Aged by TFAAT (0, 24, 48, and 72 hours), by Fluorescence Detector	348
2.19	Fast SEC of AAK-1 Aged by TFAAT (0, 24, 48, and 72 hours), by Differential Refractive Index Detector	349
2.20	Fast SEC of Blends of Asphaltenes/Maltenes of AAA-1, Scanned at 300 nm	350
2.21	Fast SEC of Blends of Asphaltenes/Maltenes of AAA-1, Scanned at 340 nm	351
2.22	Fast SEC of Blends of Asphaltenes/Maltenes of AAA-1, Scanned at 380 nm	352
2.23	Fast SEC of Blends of Asphaltenes/Maltenes of AAA-1, Scanned at 420 nm	353
2.24	Fast SEC of Blends of Asphaltenes/Maltenes of AAA-1, Scanned at 500 nm	354
2.25	Fast SEC of Blends of Asphaltenes/Maltenes of AAA-1, Scanned at 575 nm	355
2.26	Fast SEC of Blends of Asphaltenes/Maltenes of AAA-1, by Fluorescence Detector	356
2.27	Fast SEC of Blends of Asphaltenes/Maltenes of AAA-1, by Differential Refractive Index Detector	357
2.28	Relationship Between SEC Fraction-II and Tan Delta (25°C and torque at 400 g·cm) for the Refractive Index Detector at 9 Minutes into Run	358

2.29	Relationship Between SEC Fraction-II and Tan Delta (25°C and torque at 400 g·cm) for the Refractive Index Detector at 9.5 Minutes into Run . . . . .	359
2.30	Relationship Between SEC Fraction-II and Tan Delta (25°C and torque at 400 g·cm) for the Refractive Index Detector at 10.5 Minutes into Run . . . . .	360
2.31	Relationship Between SEC Fraction-II and Tan Delta (25°C and torque at 400 g·cm) for the Refractive Index Detector at 11 Minutes into Run . . . . .	361
2.32	Relationship Between SEC Fraction-II and Tan Delta (25°C and torque at 400 g·cm) at 305 nm and 10 Minutes into Run . . . . .	362
2.33	Relationship Between SEC Fraction-II and Tan Delta (25°C and torque at 400 g·cm) at 340 nm and 10 Minutes into Run . . . . .	363
2.34	Relationship Between SEC Fraction-II and Tan Delta (25°C and torque at 400 g·cm) at 380 nm and 10 Minutes into Run . . . . .	364
2.35	Relationship Between SEC Fraction-II and Tan Delta (25°C and torque at 400 g·cm) at 410 nm and 10 Minutes into Run . . . . .	365
2.36	Relationship Between SEC Fraction-II and Tan Delta (25°C and torque at 400 g·cm) at 420 nm and 10 Minutes into Run . . . . .	366
2.37	Relationship Between SEC Fraction-II and Tan Delta (25°C and torque at 400 g·cm) at 460 nm and 10 Minutes into Run . . . . .	367
2.38	Relationship Between SEC Fraction-II and Tan Delta (25°C and torque at 400 g·cm) at 500 nm and 10 Minutes into Run . . . . .	368
2.39	Relationship Between SEC Fraction-II and Tan Delta (25°C and torque at 400 g·cm) at 575 nm and 10 Minutes into Run . . . . .	369
2.40	Relationship Between Total Response of the Fluorescence Detector at 10 Minutes Run and Tan Delta (25°C and torque at 400 g·cm) . . . . .	370
2.41	SFC Chromatograms of Aliphatic and Aromatic Components of AAA-1 SEC Fraction 4 . . . . .	371
2.42	SFC Chromatograms of Aliphatic and Aromatic Components of AAA-1 SEC Fraction 5 . . . . .	372
3.1	Structures of Model Compounds Mixed with Asphalts . . . . .	82

4.1	Potentiometric Titration Curves (Bases) of Tank and Thin-Film Oven Pressure Oxidation Vessel (TFO-POV) Aged Core Asphalts . . . . .	94
5.1	Viscosities of Neutrals Measured and Predicted by Molecular Weight and Amount of IR Functional Group . . . . .	120
5.2	Viscosity vs. Molecular Weight for Core Asphalts . . . . .	121
5.3	Viscosity vs. Amount of Polar Components for AAM-1 . . . . .	122
5.4	Viscosity vs. Amount of Polar Components for Four Core Asphalts . . . . .	123
5.5	Effect of Amphoterics on Viscosity for AAD-1 . . . . .	124
5.6	Viscosity at 25°C vs. Polarity for Four Core Asphalts . . . . .	125
5.7	Viscosity Prediction by Viscosity-Polarity Relationship for AAD-1 . . . . .	126
5.8	Viscosity vs. Polarity for SEC Cross-Blending Mixtures Containing SEC Fraction-II of AAD-1 . . . . .	127
5.9	Viscosity vs. Polarity for SEC Cross Blending Mixtures Containing SEC Fraction-II of AAG-1 . . . . .	128
5.10	Viscosity vs. Polarity for SEC Cross Blending Mixtures Containing SEC Fraction-II of AAK-1 . . . . .	129
5.11	Viscosity vs. Polarity for SEC Cross Blending Mixtures Containing SEC Fraction-II of AAM-1 . . . . .	130
5.12	Viscosities of SEC Cross Blending Mixtures Measured and Predicted . . . . .	131
5.13	Dielectric Constant vs. Polarity . . . . .	132
5.14	Glass Transition Temperature vs. Viscosity of Core Asphalt at 25°C . . . . .	133
5.15	Glass Transition Temperature vs. Viscosity of IEC Neutrals at 25°C . . . . .	134
5.16	Glass Transition Temperature vs. Viscosity of Maltenes at 25°C . . . . .	135
5.17	Glass Transition Temperature vs. Viscosity of SEC Fraction-II at 25°C . . . . .	136
5.18	Glass Transition Temperature vs. Retention Time for Peak Maxima in Fast SEC . . . . .	137

5.19	Activation Energy for Viscous Flow vs. Glass Transition Temperature . . . . .	138
5.20	Viscosity at 45°C vs. Polarity . . . . .	139
5.21	Viscosity at 60°C vs. Polarity . . . . .	140
5.22	Activation Energy for Viscous Flow vs. Polarity . . . . .	141
5.23	Activation Energy for Viscous Flow vs. Ratio of Weakly Polar Fraction to Strongly Polar Fraction Determined from IEC Separation . . . . .	142
7.1	Oxidizable Structures in Representative Asphalt Molecules . . . . .	175
7.2	Relative CL Intensities in Air . . . . .	176
7.3	Effect of Oxygen Concentration on CL . . . . .	177
7.4	Correlation of Sulfoxide with Sulfur in Core Asphalts . . . . .	178
7.5	ESCA Sulfur Spectrum for ROOH Oxidized AAA-1 . . . . .	179
7.6	Formation of Sulfoxide Band at 1030 cm <sup>-1</sup> in Core Asphalts Using t-BuOOH in Toluene at 25°C . . . . .	180
7.7	Cooxidation of AAA-1 with Dimethyl Sulfide at 110°C, 48 Hours . . . . .	181
7.8	Possible Pathways for Sulfoxide Formation . . . . .	182
8.1	Pressure Oxidation Vessel (POV) Oxidation of Core Asphalt AAD-1 With and Without TFO . . . . .	220
8.2	Pressure Oxidation Vessel (POV) Oxidation of Core Asphalt AAD-1 . . . . .	221
8.3	Pressure Oxidation Vessel (POV) Oxidation of Core Asphalt AAD-1 after TFO . . . . .	222
8.4	Mass Change versus Log Viscosity Increase During TFO Aging . . . . .	223
8.5	Relationship Between Viscosity Change and Carbonyl (Ketone) Formation on POV Oxidation of Asphalt AAD-1 With and Without Prior TFO Oxidation . . . . .	224
8.6	Kinetic Plots of the POV Aging of SHRP Core Asphalts at 60°C, 2.07 MPa Oxygen . . . . .	225



8.7	Kinetic Aging Plot of SHRP Asphalts Using the PAV Method at 2.07 MPa, 60°C .....	226
8.8	Sensitivity of SHRP Core Asphalts to Carbonyl (Ketone) Produced During PAV-Aging at 2.7 MPa, 60°C .....	227
8.9	Sensitivity of SHRP Core Asphalts to Carbonyl (Ketone) Produced During PAV-Aging at 2.7 MPa, 60°C .....	228
8.10	Oxidation Products Formed in Selected SHRP Asphalts as a Function of Time During PAV Aging at 60°C .....	229
8.11	Comparison of the Low Temperature Aging Kinetics of Asphalts AAD-1 and AAG-1 Using the POV, PAV, and TFAAT Methods .....	230
8.12	Aging Kinetics of SHRP Core Asphalts Using the TFAAT Method at 85°C ...	231
8.13	Aging Kinetics of SHRP Core Asphalts Using the TFAAT Method at 113°C .....	232
8.14	Aging Kinetics of SHRP Core Asphalts Using the TFAAT Method at 130°C .....	233
8.15	PAV Aging of Selected SHRP Prior TFO-Aged Asphalts at Different Temperatures .....	234
8.16	Aging Indices after TFO of SHRP Asphalts Aged by the PAV Method at Different Temperatures .....	235
8.17	144 Hour Aging Indices at Three Temperatures of SHRP Core Asphalts .....	236
8.18	Comparison of 80°C PAV 144 Hour Aging Indices Including and Excluding TFO Aging .....	237
8.19	TFAAT Oxidation of Asphalt AAG-1 at 113°C .....	238
8.20	Relationship Between the Carbonyls Formed and Dynamic Viscosity Increase Using the TFAAT Method at 85, 113, and 130°C for Core Asphalts AAF-1, AAG-1, AAK-1, and AAM-1 .....	239
8.21	Relationship Between the Carbonyls Formed and Dynamic Viscosity Increase Using the TFAAT Method at 85, 113, and 130°C for Core Asphalts AAA-1, AAB-1, AAC-1, and AAD-1 .....	240

8.22	Reduced Specific Viscosity Measurements at 45°C for Asphalts AAD-1 and AAG-1 Both Before and After TFAAT Aging at 113°C 72 Hours . . . . .	241
8.23	Effects of Temperature on the Aging Characteristics of Asphalts AAD-1 and AAG-1 . . . . .	242
8.24	Reduced Specific Viscosities at Two Temperatures for TFAAT Aged AAA-1 . . . . .	243
8.25	Reduced Specific Viscosities at Two Temperatures for TFAAT Aged AAB-1 . . . . .	244
8.26	Reduced Specific Viscosities at Two Temperatures for TFAAT Aged AAC-1 . . . . .	245
8.27	Reduced Specific Viscosities at Two Temperatures for TFAAT Aged AAD-1 . . . . .	246
8.28	Reduced Specific Viscosities at Two Temperatures for TFAAT Aged AAF-1 . . . . .	247
8.29	Reduced Specific Viscosities at Two Temperatures for TFAAT Aged AAG-1 . . . . .	248
8.30	Reduced Specific Viscosities at Two Temperatures for TFAAT Aged AAK-1 . . . . .	249
9.1	Functional Groups in Neat and Aged Asphalts Measured by IR-FGA . . . . .	296
9.2	Reduced Specific Viscosities at Two Temperatures for Unaged AAA-1 . . . . .	297
9.3	Reduced Specific Viscosities at Two Temperatures for Unaged AAB-1 . . . . .	298
9.4	Reduced Specific Viscosities at Two Temperatures for Unaged AAC-1 . . . . .	299
9.5	Reduced Specific Viscosities at Two Temperatures for Unaged AAD-1 . . . . .	300
9.6	Reduced Specific Viscosities at Two Temperatures for Unaged AAF-1 . . . . .	301

9.7	Reduced Specific Viscosities at Two Temperatures for Unaged AAG-1 .....	302
9.8	Reduced Specific Viscosities at Two Temperatures for Unaged AAK-1 .....	303
9.9	Reduced Specific Viscosities at Two Temperatures for Unaged AAM-1 .....	304

## List of Tables

1.1	Separation of Seven Asphalts into Five Fractions by IEC	25
1.2	Ratios of IEC Fractions for Eight Core Asphalts	25
1.3	Infrared Functional Group Analysis of IEC Fractions of Asphalt AAA-1	26
1.4	Elemental Analyses and Molecular Weights of IEC Neutral Fractions of Eight Core Asphalts	27
1.5	Elemental Analyses and Molecular Weights of IEC Strong Acid Fractions of Seven Core Asphalts	28
1.6	Viscosities (Pa·s) of Core Asphalts, Their IEC Neutral Fractions, and Mixtures of IEC Fractions at 25°C, 1.0 rad/s	29
1.7	Molecular Weights by Vapor Phase Osmometry in Toluene at 60°C for Strong Acid Fractions of Seven Core Asphalts Compared with Tan Delta <sub>ct</sub> Values for Whole Asphalts at 25°C	30
1.8	Mass Fractions of Amphoteric, Base, Acid, and Neutral Fractions Isolated from Four Core Asphalts by IEC	31
1.9	Infrared Functional Group Analysis for IEC Amphoteric, Base, and Neutral Plus Acid Fractions of Four Core Asphalts	32
1.10	Molecular Weights of IEC Amphoteric and Base Fractions	33
1.11	Carbon, Hydrogen, and Nitrogen Contents of Amphoteric Fractions	34
1.12	NMR Analysis of IEC Amphoteric Fractions of Four Core Asphalts	35

1.13	Viscosities (Pa·s) of Mixtures of Four Core Asphalts with Their IEC Amphoteric, Base, Acid, or Neutral Fractions at 60°C and 1.0 rad/s . . . . .	35
1.14	Viscosities (Pa·s) of Mixtures of Neutral Plus Acid and Base Fractions of Four Asphalts at Three Temperatures Compared with Viscosities of Parent Asphalts at 1 rad/s . . . . .	36
1.15	Mass Fractions of Amphoterics, Bases, and Neutrals Plus Acids Isolated from Four Asphalts Aged TFO-PAV (60°C, 144 hours) by IEC . . . . .	37
1.16	Peak Height Maxima and Width at One-Half Maximum Height in SFC Chromatograms of IEC Neutral Fractions of Eight Asphalts, and Number-Average Molecular Weights of IEC Neutral Fractions . . . . .	37
1.17	Peak Height Maxima and Width at One-Half Maximum Height in SFC Chromatograms of Iso-Octane Maltenes of Eight Asphalts . . . . .	38
1.18	Separation of Seven Asphalts by IEC . . . . .	323
1.19	Separation of Asphalt AAC-1 by IEC . . . . .	325
1.20	Quantitative IR Analyses of IEC Fractions of AAB-1 . . . . .	325
1.21	Quantitative IR Analyses of IEC Fractions of AAD-1 . . . . .	326
1.22	Quantitative IR Analyses of IEC Fractions of AAF-1 . . . . .	327
1.23	Quantitative IR Analyses of IEC Fractions of AAG-1 . . . . .	328
1.24	Quantitative IR Analyses of IEC Fractions of AAK-1 . . . . .	329
1.25	Quantitative IR Analyses of IEC Fractions of AAM-1 . . . . .	330
1.26	Elemental Analyses of IEC Strong Base Fractions of Seven Core Asphalts . . . . .	331
1.27	Elemental Analyses of IEC Weak Acid Fractions of Seven Core Asphalts . . . . .	331
1.28	Elemental Analyses of IEC Weak Base Fractions of Seven Core Asphalts . . . . .	332
1.29	Metal and Porphyrin Contents of IEC Fractions of Asphalt AAD-1 . . . . .	333

1.30	Rheological Data for Six Core Asphalt IEC Neutral Fractions at 25°C (50 mm Parallel Plates) . . . . .	334
1.31	Rheological Data for IEC Neutral Fractions of Asphalts AAC-1 and AAF-1 at 25°C and 45°C (50 mm Parallel Plates) . . . . .	335
1.32	Rheological Data for IEC Neutral Fractions at 0°C (10% Strain, 25 mm Parallel Plates) . . . . .	336
1.33	Viscosities (Pa·s) of Mixtures of Core Asphalts (95 wt %) with Their Own IEC Neutral Fractions (5 wt %) Compared with Original Asphalt Viscosities at 25°C and 60°C, 1.0 rad/s . . . . .	337
1.34	Viscosities (Pa·s) of Mixtures of Asphalt AAD-1 with Its IEC Fractions at 25°C, 45°C, 60°C, 1.0 rad/s . . . . .	337
1.35	Viscosities (Pa·s) of Neutral Plus Acid Fractions of Four Asphalts at 25°C and 45°C, 1.0 rad/s . . . . .	338
1.36	$G^*/\sin \delta$ (dyne/cm <sup>2</sup> ) Values of Mixtures of Four Core Asphalts with Their IEC Amphoteric, Base, Acid, or Neutral Fractions at 60°C, 1.0 rad/s . . . . .	338
1.37	Yields of Moderate Base Fractions and Moderate Base-Free Fractions by IEC Separation of Five Core Asphalts . . . . .	339
1.38	Molecular Weights of IEC Amphoteric and Base Fractions of TFO-POV Aged (60°C, 144 hours) Asphalts . . . . .	340
2.1	Preparative SEC Separation of Core Asphalts . . . . .	64
2.2	Number-Average Molecular Weights ( $M_n$ ) of Preparative SEC Fractions of Asphalts . . . . .	65
2.3	Viscosities (Pa·s) of Core Asphalts and SEC Fraction-II of Core Asphalts at 25°C, 1.0 rad/s . . . . .	67
2.4	Elemental Analyses of SEC Fractions of Asphalts AAB-1, AAG-1, and AAM-1 . . . . .	68
2.5	Tan Delta <sub>α</sub> Values of Core Asphalts at 25°C and Mass Fractions of SEC Fraction-II in Core Asphalts . . . . .	69

2.6	Tan Delta <sub>ct</sub> Values for Expanded Set of Asphalts at 25°C and Mass Fractions of SEC Fraction-II Components of Expanded Set of Asphalts . . . . .	70
2.7	Comparison of PSEC and SPSEC Fraction-I Data for Core Asphalts . . . . .	71
2.8	Comparison of PSEC and SPSEC Fraction-I Data for Noncore Asphalts . . . . .	72
2.9	Comparison of PSEC and SPSEC Fraction-I Data for Aged Asphalts . . . . .	73
2.10	Peak Height Maxima and Width at One-Half Maximum Height in SFC Chromatograms of SEC Fraction-II of Eight Asphalts . . . . .	74
2.11	Number Average Molecular Weights of PSEC Fractions and SFC Carbon Number Distributions of the IEC Neutral Fraction of Asphalt AAA-1 . . . . .	75
2.12	Carbon Number Distribution for AAG-1 PSEC Fractions . . . . .	76
2.13	Quantitative IR Analyses of SEC Fractions of AAD-1 . . . . .	373
2.14	Quantitative IR Analyses of SEC Fractions of AAG-1 . . . . .	374
2.15	Carbon Number Distribution for AAG-1 Saturate/Aromatic Fractions . . . . .	375
2.16	Carbon Number Distributions of Saturate Fractions Compared with Aromatic Fractions by SFC Asphalt AAA-1 . . . . .	375
3.1	Properties of Model Compounds Used in Asphalt-Model Compound Mixtures . . . . .	84
3.2	Viscosities (Pa·s) at Two Temperatures for Mixtures of Model Compounds (1 mass %) with Asphalt AAA-1 . . . . .	85
3.3	Rheological Data of Mixtures of Model Compounds (1 mass %) with AAA-1 at 25°C . . . . .	376
3.4	Rheological Data of Mixtures of Model Compounds (1 mass %) with AAA-1 at 60°C . . . . .	377
3.5	Rheological Data of Mixtures of Model Compounds (1 mass %) with AAB-1 at 25°C . . . . .	378
3.6	Rheological Data of Mixtures of Model Compounds (1 mass %) with AAB-1 at 60°C . . . . .	379

3.7	Rheological Data of Mixtures of Model Compounds (1 mass %) with AAC-1 at 25°C .....	380
3.8	Rheological Data of Mixtures of Model Compounds (1 mass %) with AAC-1 at 60°C .....	381
3.9	Rheological Data of Mixtures of Model Compounds (1 mass %) with AAD-1 at 25°C .....	382
3.10	Rheological Data of Mixtures of Model Compounds (1 mass %) with AAD-1 at 60°C .....	383
3.11	Rheological Data of Mixtures of Model Compounds (1 mass %) with AAF-1 at 25°C .....	384
3.12	Rheological Data of Mixtures of Model Compounds (1 mass %) with AAF-1 at 60°C .....	385
3.13	Rheological Data of Mixtures of Model Compounds (1 mass %) with AAG-1 at 25°C .....	386
3.14	Rheological Data of Mixtures of Model Compounds (1 mass %) with AAG-1 at 60°C .....	387
3.15	Rheological Data of Mixtures of Model Compounds (1 mass %) with AAK-1 at 25°C .....	388
3.16	Rheological Data of Mixtures of Model Compounds (1 mass %) with AAK-1 at 60°C .....	389
3.17	Rheological Data of Mixtures of Model Compounds (1 mass %) with AAM-1 at 25°C .....	390
3.18	Rheological Data of Mixtures of Model Compounds (1 mass %) with AAM-1 at 60°C .....	391
3.19	Rheological Data for Mixtures of Model Compounds (2 mass %) with AAA-1 at 25°C and 60°C .....	392
3.20	Rheological Data for Mixtures of Model Compounds (2 mass %) with AAB-1 at 25°C and 60°C .....	393
3.21	Rheological Data for Mixtures of Model Compounds (2 mass %) with AAC-1 at 25°C and 60°C .....	394



3.22	Rheological Data for Mixtures of Model Compounds (2 mass %) with AAD-1 at 25°C and 60°C .....	395
3.23	Rheological Data for Mixtures of Model Compounds (2 mass %) with AAF-1 at 25°C and 60°C .....	396
3.24	Rheological Data for Mixtures of Model Compounds (2 mass %) with AAG-1 at 25°C and 60°C .....	397
3.25	Rheological Data for Mixtures of Model Compounds (2 mass %) with AAK-1 at 25°C and 60°C .....	398
3.26	Rheological Data for Mixtures of Model Compounds (2 mass %) with AAM-1 at 25°C and 60°C .....	399
3.27	Rheological Data for Mixtures of Model Compounds with AAA-1 at 25°C and 60°C .....	400
3.28	Rheological Data for Mixtures of Model Compounds with AAB-1 at 25°C and 60°C .....	401
3.29	Rheological Data for Mixtures of Model Compounds with AAC-1 at 25°C and 60°C .....	402
3.30	Rheological Data for Mixtures of Model Compounds with AAD-1 at 25°C and 60°C .....	403
3.31	Rheological Data for Mixtures of Model Compounds with AAF-1 at 25°C and 60°C .....	404
3.32	Rheological Data for Mixtures of Model Compounds with AAG-1 at 25°C and 60°C .....	405
3.33	Rheological Data for Mixtures of Model Compounds with AAK-1 at 25°C and 60°C .....	406
3.34	Rheological Data for Mixtures of Model Compounds with AAM-1 at 25°C and 60°C .....	407
4.1	Nonaqueous Titrations of Bases in Core Asphalts (Mettler) .....	96
4.2	Nitrogen Concentrations and Base Concentrations of Core Asphalts .....	97
4.3	Nonaqueous Titrations of Bases in Core Asphalts (Metrohm) .....	97

4.4	Nonaqueous Titrations of Bases (Mettler) in TFO-POV Aged Core Asphalts .....	98
4.5	Nonaqueous Potentiometric Titrations of Iso-Octane Maltenes of Core Asphalts .....	99
4.6	Potentiometric Titrations for Bases in IEC Fractions of Four Asphalts .....	100
4.7	Potentiometric Titrations of Bases in Expanded Set of Asphalts .....	408
4.8	Potentiometric Titrations of Acids in Core Asphalts .....	408
4.9	Potentiometric Titrations of Acids in Aged Core Asphalts .....	409
4.10	Potentiometric Titrations of Acids in Iso-Octane Maltenes of Core Asphalts .....	409
4.11	Potentiometric Titrations of IEC Strong Acid Fractions of Core Asphalts .....	410
4.12	Potentiometric Titrations of IEC Amphoteric and Total Acid Fractions of Core Asphalts .....	411
4.13	Potentiometric Titrations of Core Asphalts Performed at Various Times after Dissolution of Sample .....	412
5.1	PSEC Separation of IEC Amphoteric Fraction of AAD-1 and AAG-1 .....	143
5.2	IEC Separation of SEC Fraction-I of AAD-1 and AAG-1 .....	143
5.3	Yields of Extracts of IEC Cation and Anion Resins by Toluene, Ethanol, and Water Mixture .....	144
5.4	Separation of SEC Fraction-II of AAD-1 and AAG-1 .....	144
5.5	IEC Separation of SEC Fractions-I and -II of AAD-1 and AAG-1 .....	145
5.6	Molecular Weight of Amphoterics of SEC-I and SEC-1 of Amphoterics of AAD-1 and AAG-1 .....	145
5.7	Polarity Factors of Nine IEC Fractions .....	146
5.8	Calculated Polarities of Four Core Asphalts .....	146

5.9	Regression Equations of Viscosity-Polarity Relationship for Four Core Asphalts . . . . .	147
5.10	Polarities of Various Fractions of Four Core Asphalts . . . . .	147
5.11	Activation Energy of Viscous Flow and Glass Transition Temperatures for Eight Core Asphalts . . . . .	148
5.12	Tan Delta Values at Three Temperatures of Mixtures of SEC Fractions of Asphalts AAD-1 and AAK-1 . . . . .	413
5.13	Tan Delta Values at Three Temperatures of Mixtures of SEC Fractions of Asphalts AAD-1 and AAM-1 . . . . .	414
5.14	Tan Delta Values at Three Temperatures of Mixtures of SEC Fractions of Asphalts AAG-1 and AAK-1 . . . . .	415
5.15	Tan Delta Values at Three Temperatures of Mixtures of SEC Fractions of Asphalts AAG-1 and AAM-1 . . . . .	416
5.16	Viscosities at Three Temperatures of Mixtures of SEC Fractions of Asphalts AAD-1 and AAK-1 . . . . .	417
5.17	Viscosities at Three Temperatures of Mixtures of SEC Fractions of Asphalts AAD-1 and AAM-1 . . . . .	418
5.18	Viscosities at Three Temperatures of Mixtures of SEC Fractions of Asphalts AAG-1 and AAK-1 . . . . .	419
5.19	Viscosities at Three Temperatures of Mixtures of SEC Fractions of Asphalts AAG-1 and AAM-1 . . . . .	420
5.20	Comparison of Viscosities (60°C) of Sets of Mixtures of SEC Fractions of Asphalts AAD-1 and AAK-1 . . . . .	421
5.21	Comparison of Viscosities (60°C) of Sets of Mixtures of SEC Fractions of Asphalts AAD-1 and AAM-1 . . . . .	422
5.22	Comparison of Viscosities (60°C) of Sets of Mixtures of SEC Fractions of Asphalts AAG-1 and AAK-1 . . . . .	423
5.23	Comparison of Viscosities (60°C) of Sets of Mixtures of SEC Fractions of Asphalts AAG-1 and AAM-1 . . . . .	424

5.24	Relative Viscosities at 25°C of Mixtures of SEC .....	425
5.25	Polarity Factors of Mixtures of SEC Fractions .....	425
6.1	Viscoelastic Properties of Asphalt AAK-1 after Extended Cure Time at 25°C .....	155
6.2	Viscoelastic Properties of Asphalt AAM-1 after Extended Cure Time at 25°C .....	156
6.3	Viscoelastic Properties of Asphalt AAB-1 after Extended Cure Time at 25°C .....	156
6.4	Viscoelastic Properties of Asphalt AAM-1 after Extended Cure Time at 45°C .....	426
6.5	Viscoelastic Properties of Asphalt AAM-1 after Extended Cure Time at 60°C .....	426
6.6	Viscoelastic Properties of Asphalt AAG-1 after Extended Cure Time at 60°C .....	427
6.7	Rheological Properties of Aged AAK-1 at 25°C (110°C loading temperature) .....	427
6.8	Rheological Properties of Aged AAK-1 at 25°C (150°C loading temperature) .....	428
6.9	Viscoelastic Properties of Aged Asphalt AAM-1 After Extended Cure Time at 25°C .....	428
6.10	Viscoelastic Properties of TFO-POV Aged Asphalt AAM-1 After Extended Cure Time at 45°C .....	429
6.11	Viscoelastic Properties of TFO-POV Aged Asphalt AAM-1 after Extended Cure Time at 60°C .....	429
6.12	Viscoelastic Properties of Asphalt AAM-1 n-Heptane Maltenes After Extended Cure Time at 0°C .....	430
6.13	Viscoelastic Properties of Asphalt AAM-1 Neutral Fraction After Extended Cure Time at 0°C .....	430

6.14	Viscoelastic Properties of Aged Core Asphalts After Cure Times of 2 Hours and 1080 Hours (45 Days) at 25°C .....	431
7.1	Concentrations of Phenols in Core Asphalts by Several Methods and Comparison with Asphaltene Content .....	183
7.2	Concentrations of Phenols in Modified Asphalts .....	183
7.3	Comparison of Sulfur Contents of Core Asphalts and Sulfoxide Contents in Core Asphalts Oxidized by a Chemical and Two Thermal Methods .....	184
7.4	Analysis of Sulfur XANES and ESCA Spectra of Asphalt Samples .....	185
7.5	Thermal Changes in Sulfoxide and Carbonyl in Preoxidized Asphalts in Argon at 165°C .....	186
7.6	Oxidation of AAD-1 and AADT .....	186
7.7	Oxidation of AAG-1 and AAGT .....	187
7.8	Oxidation of AAK-1 and AAKT .....	187
7.9	Long Term Oxidation of Asphalts .....	188
7.10	Oxidation of AAM-1 and AAMT .....	188
8.1	Change in Dynamic Shear Viscosity With Time During Aging of Asphalt AAD-1 and TFO-Oxidized AAD-1 in Oxygen Pressure Vessel at 60°C, 300 psi .....	250
8.2	Changes in Dynamic Shear Viscosity with Time During Aging of Annealed, 400-Hour Pressure Oxidized Asphalt AAD-1 with and without TFO Aging Prior to Initial Pressure Oxidation .....	251
8.3	Effect of Thermal Treatment to Disrupt Molecular Structuring on the Rheological Properties at 60°C of Low-Temperature, Pressure-Oxidized (300 psi) Asphalt AAD-1 .....	252
8.4	Chemical Functionality Formed On Oxidative Aging of AAD-1 .....	252
8.5	Changes in Rheological and Chemical Properties with POV Aging of Asphalt AAD-1 at Different Temperatures .....	253

8.6	Relationship of Weight Loss to Log Viscosity Increase During TFO Test . . . . .	254
8.7	Changes in Rheological and Chemical Properties of SHRP Core Asphalts During POV Aging at 60°C, 300 psi . . . . .	255
8.8	Changes in Rheological and Chemical Properties During Thin-Film Oven Aging Followed by 60°C PAV (300 psi) Oxidation of SHRP Core Asphalts . . . . .	257
8.9	Correction of Viscosities for Prior TFO-Aged Asphalts Subsequently Aged by POV and PAV Methods for TFO Aging . . . . .	259
8.10	Changes in Rheological and Chemical Properties of Selected SHRP Asphalts During TFAAT Aging at 65°C . . . . .	260
8.11	Changes in Rheological and Chemical Properties of SHRP Core Asphalts During TFAAT Aging at 85°C . . . . .	261
8.12	Changes in Rheological and Chemical Properties of SHRP Core Asphalts During TFAAT Aging at 113°C . . . . .	263
8.13	Changes in Rheological and Chemical Properties of SHRP Core Asphalts During TFAAT Aging at 130°C . . . . .	265
8.14	Changes in Rheological and Chemical Properties During TFO Aging Followed by 70°C PAV (300 psi) Oxidation of SHRP Asphalts . . . . .	267
8.15	Changes in Rheological and Chemical Properties During TFO Aging Followed by 80°C PAV (300 psi) Oxidation of SHRP Asphalts . . . . .	268
8.16	Oxidation Products Formed in Asphalt AAG-1 as a Function of Time During TFAAT Aging at 113°C . . . . .	269
8.17	Comparison of POV and PAV Aging of Selected SHRP Asphalts, 300 psi, 60°C, 144 Hours . . . . .	269
8.18	Comparison of Results from TFO Oxidation and TFO Followed by 60°C POV-Argon (300 psi) Oxidation of SHRP Asphalts . . . . .	270
8.19	Results of Vanadyl Acetonylacetonate Catalyzed Oxidation of SHRP Asphalts Using the RTFO Method . . . . .	271
8.20	IR Spectroscopic Analysis Results of Vanadyl Acetonylacetonate Catalyzed Oxidation of SHRP Asphalts . . . . .	272

8.21	Results of IR Analysis of Extracted Asphalts from Asphalt-Aggregate PAV Aging, 144 Hours, 60°C . . . . .	273
8.22	Results from Thermal Annealing Experiments on Extracted Asphalts from Asphalt-Aggregate PAV Aging . . . . .	274
8.23	Preparative Size Exclusion Fraction-I Data for Aged Core Asphalts (mass %) . . . . .	275
8.24	Carbonyl Absorbance and Sulfoxide Concentrations of Aged Asphalts . . . . .	276
8.25	Preparative SEC of Aged Core Asphalts (mass %) . . . . .	276
8.26	Comparison of PSEC and SPSEC Fraction-I Data for Aged Asphalts . . . . .	277
8.27	Mass Fractions of SEC Fraction-I of Aged Asphalts . . . . .	278
8.28	Molecular Weights in Toluene and Pyridine of SEC Fractions of Aged Asphalts . . . . .	279
8.29	Potentiometric Titration of Bases in Core Asphalts TFO-PAV Aged at 100°C . . . . .	280
8.30	Potentiometric Titration of Bases in TFO and TFO-PAV Aged Asphalts . . . . .	281
8.31	Asphaltene and Maltene Yields from TFAAT-Aged Core Asphalts . . . . .	282
8.32	Heithaus P (state of peptization) for Unaged and TFAAT Aged Core Asphalts . . . . .	282
8.33	Heithaus $p_a$ (peptizability of asphaltenes) for Unaged and TFAAT Aged Core Asphalts . . . . .	283
8.34	Heithaus $p_o$ (peptizing power of maltenes) for Unaged and TFAAT Aged Core Asphalts . . . . .	283
8.35	Reduced Specific Viscosity of Selected SHRP Asphalts Before and After Aging at 45°C as a Function of Percent Natural Abundance of Asphaltenes . . . . .	284
8.36	Kinetic Data for Comparison of 113°C TFAAT Test and 60°C PAV (Corrected for TFO) . . . . .	285
8.37	Viscosities and Aging Indices of Core Asphalts after TFO . . . . .	432

8.38	Changes in Rheological and Chemical Properties During TFO + 60°C PAV (300 psi) Oxidation of SHRP Asphalts . . . . .	433
8.39	Changes in Rheological and Chemical Properties During TFO + 70°C PAV (300 psi) Oxidation of SHRP Asphalts . . . . .	435
8.40	Changes in Rheological and Chemical Properties During TFO + 80°C PAV (300 psi) Oxidation of SHRP Asphalts . . . . .	436
8.41	Viscosities and Yields of SEC Fraction-II Materials of Core Asphalts and TFAAT (130°C; 4 Hrs; 12 Hrs) Aged Asphalts . . . . .	437
8.42	Molecular Weights of SEC Fraction I of Both Unaged Asphalts and of TFAAT (130°C; 12 Hrs) Aged Asphalts, and Sulfur Concentrations of Parent Asphalts . . . . .	438
8.43	Sulfoxide and Carbonyl Concentrations of SEC Fractions of TFO-PAV (60°C; 144 hours) Aged Asphalts . . . . .	439
8.44	Mass Fractions of Core Asphalt SEC Fraction-II, Aged Asphalt SEC Fraction-II, and Molecular Weights of Core Asphalt SEC Fraction-I and Aged Asphalt SEC Fraction-I . . . . .	440
8.45	Viscosities and Yields of SEC Fraction-II of Core Asphalts and Aged Asphalts . . . . .	441
8.46	Reduced Specific Viscosity Measurements of TFAAT Aged AAA-1 Maltenes and Asphaltenes . . . . .	442
8.47	Reduced Specific Viscosity Measurements of TFAAT Aged AAB-1 Maltenes and Asphaltenes . . . . .	442
8.48	Reduced Specific Viscosity Measurements of TFAAT Aged AAC-1 Maltenes and Asphaltenes . . . . .	443
8.49	Reduced Specific Viscosity Measurements of TFAAT Aged AAD-1 Maltenes and Asphaltenes . . . . .	443
8.50	Reduced Specific Viscosity Measurements of TFAAT Aged AAF-1 Maltenes and Asphaltenes . . . . .	444
8.51	Reduced Specific Viscosity Measurements of TFAAT Aged AAG-1 Maltenes and Asphaltenes . . . . .	444



8.52	Reduced Specific Viscosity Measurements of TFAAT Aged AAK-1 Maltenes and Asphaltenes .....	445
8.53	Reduced Specific Viscosity Measurements of TFAAT Aged AAK-1 Maltenes and Asphaltenes .....	445
9.1	Carbon and Hydrogen Analyses of Core Asphalts Performed by Two Analytical Laboratories .....	305
9.2	Determination of Nitrogen, Oxygen, and Sulfur in Eight Core Asphalts .....	306
9.3	Determination of Vanadium and Nickel in Eight Core Asphalts .....	306
9.4	Number-Average Molecular Weights ( $M_n$ ) of Core Asphalts by Vapor Phase Osmometry at 60°C .....	307
9.5	IR Functional Group Analysis of Neat SHRP Core Asphalts .....	307
9.6	Asphaltene Yields and Asphaltene Compatibility Indices of Core Asphalts .....	308
9.7	Elemental Analyses and Molecular Weights of Core Asphalt Asphaltenes .....	309
9.8	Heithaus Parameter Values for Seven Asphalts .....	310
9.9	Viscosities of Core Asphalts Determined at 60°C .....	311
9.10	Viscosities of Core Asphalts at 25°C .....	312
9.11	Elemental Analyses and Molecular Weights of Expanded Set of Asphalts .....	446
9.12	Infrared Functional Group Analysis of Expanded Set of Asphalts .....	447
9.13	Asphaltene Yields of Expanded Set Asphalts Determined by Different Operators .....	448
9.14	Comparison of Asphaltene Yields and Asphaltene Compatibility Indices of Selected Core Asphalts and Lower Viscosity Grades of Core Asphalts .....	449
9.15	Heithaus Parameters of Members of the Expanded Set of Asphalts .....	450

9.16	Core Asphalt Viscosities by Brabender Rheotron and Rheometric Mechanical Spectrometer at 45°C .....	450
9.17	Viscosities of Expanded Set of Asphalts at 60°C After Argon Annealing (50% strain, 25 mm parallel plates) .....	451
9.18	Viscosities of Heptane Maltenes of Core Asphalts at Three Temperatures .....	452
9.19	Reduced Specific Viscosity Measurements of Mixtures of AAA-1 Maltenes and Asphaltenes .....	452
9.20	Reduced Specific Viscosity Measurements of Mixtures of AAB-1 Maltenes and Asphaltenes .....	453
9.21	Reduced Specific Viscosity Measurements of Mixtures of AAC-1 Maltenes and Asphaltenes .....	453
9.22	Reduced Specific Viscosity Measurements of Mixtures of AAD-1 Maltenes and Asphaltenes .....	454
9.23	Reduced Specific Viscosity Measurements of Mixtures of AAF-1 Maltenes and Asphaltenes .....	454
9.24	Reduced Specific Viscosity Measurements of Mixtures of AAG-1 Maltenes and Asphaltenes .....	455
9.25	Reduced Specific Viscosity Measurements of Mixtures of AAK-1 Maltenes and Asphaltenes .....	456
9.26	Reduced Specific Viscosity Measurements of Mixtures of AAM-1 Maltenes and Asphaltenes .....	456

## **Abstract**

Experimental results from the chemical composition studies in the SHRP Binder Characterization and Evaluation Program are described. Asphalts were separated into components by means of preparative ion exchange chromatography, preparative size exclusion chromatography, and other methods. As a result of these separations, asphalt rheological properties were rationalized by chemical parameters such as molecular weight, molecular size distributions, and polarity factors. Analytical methods such as streamlined preparative size exclusion chromatography, supercritical fluid chromatography, and potentiometric titration were adapted for asphalt analysis.

Results of a study of the mechanism of asphalt oxidation indicate that oxidative aging at service temperatures proceeds by some pathway other than a classical radical-chain. Extensive kinetic experiments at moderate temperatures and high partial pressures of oxygen show that the physical state of an asphalt affects the aging process, and that aging tests conducted at temperatures much greater than service temperatures are likely to yield results that do not correspond to actual field aging.

# **Binder Characterization and Evaluation**

## **Related Reports**

### **Volume 1     Project Summary (SHRP-A-367)**

- Chapter 1     Introduction and Discussion of Asphalt Model
- Chapter 2     Prediction of Performance
- Chapter 3     Chemical Composition--Physical Property Relationships

### **Volume 3     Physical Characterization (SHRP-A-369)**

- Chapter 1     Linear Viscoelastic Model
- Chapter 2     Rheological Measurements
- Chapter 3     Low-Temperature Physical Hardening
- Chapter 4     Fracture and Fatigue
- Chapter 5     Oxidative Aging Studies
- Chapter 6     Miscellaneous Tests

### **Volume 4     Test Methods (SHRP-A-370)**

- Chapter 1     Dynamic Shear Rheometer
- Chapter 2     Bending Beam Rheometer
- Chapter 3     Direct Tension
- Chapter 4     Pressure Aging Vessel
- Chapter 5     Rotational Viscometer
- Chapter 6     Analyses of Asphalt by Standard Analytical Techniques
- Chapter 7     Separation of Asphalts by Ion Exchange Chromatography
- Chapter 8     Analysis of Nonpolar Fractions of Asphalts by Supercritical Fluid Chromatography

## Executive Summary

The SHRP Binder Characterization and Evaluation Program had as a principal objective the study of relationships between asphalt chemical composition and performance-related physical properties. Volume 2 of this report summarizes results of the chemical composition studies performed at Western Research Institute and SRI International. Studies of physical properties performed at The Pennsylvania State University and Texas Transportation Institute are reported in Volume 3. Major conclusions drawn from the study are described in Volume 1. Details of selected experimental procedures are presented in Volume 4.

The chemical composition studies focused on eight asphalts that were designated "core" asphalts. The core asphalts vary widely in chemical and physical properties. All have been used in building roads, and their performance characteristics vary considerably, hence their selection for these studies. Information obtained by studying these asphalts was verified on a larger group of asphalts designated the expanded set of asphalts. The conclusions are derived from investigation of a variety of binders and were not based on the intensive study of a few "pet" asphalts.

At the beginning of the SHRP Binder Characterization and Evaluation Program, experimentation was guided by a model of asphalt structure in which polar, aromatic molecules that tend to form associations are dispersed in a bulk solvent moiety consisting of relatively nonpolar, aliphatic molecules. According to this model, asphalt physical properties can best be described by the effectiveness with which the polar, associating materials are dispersed by the solvent, rather than being described by global chemical parameters such as elemental composition. Accordingly, attempts were made to separate asphalts into solvent and dispersed moieties. The model requires that the dispersed moiety of an asphalt be of larger overall apparent molecular size than the solvent moiety and that the two moieties differ chemically. Separation of asphalt solutions was accomplished by size exclusion chromatography and by ion exchange chromatography. Materials were isolated by both methods, which correspond to the dispersed and solvent moieties. It was demonstrated that the polar, aromatic, polyfunctional amphoteric fraction of asphalts isolated by ion exchange chromatography is the principal viscosity-building component of asphalts. Neutral materials isolated by ion exchange chromatography have properties consistent with asphalt solvent moieties. These separation studies show that asphalt rheological properties are determined by contributions from the solvent moiety and contributions from the dispersed materials, designated as polarity factors. Numerical values

can be assigned to these contributing factors and used for prediction of rheological properties.

Several novel techniques were developed for the analysis of asphalts. A fast size exclusion chromatography method featuring a gravimetric finish was used to characterize tank and aged asphalts. The results can be used to predict asphalt rheological properties. Supercritical fluid chromatography was used in the "fingerprinting" of asphalt solvent moieties. This technique revealed striking differences among solvent moieties of various asphalts. Nonaqueous potentiometric titration for bases and acids was adapted for use with asphalts. Different kinds of basic species can be quantified using this technique. It was verified that oxidative aging of asphalts results in increased amounts of polar acidic and weakly basic species and some destruction of native moderately strong bases, compared with tank asphalts.

A significant effort in the SHRP Binder Characterization and Evaluation Program was directed toward the study of asphalt age hardening, both reversible and irreversible. Isothermal reversible age hardening was shown to be a significant phenomenon in asphalts, particularly those already oxidatively aged. Understanding of the mechanisms of asphalt oxidation was greatly enhanced by work done at SRI International. Oxidation of carbon atoms in asphalts is probably by a nonchain process involving radical intermediates. Asphalts contain varying amounts of natural oxidation inhibitors, probably phenols. The oxidation of aliphatic (sulfide) sulfur compounds to sulfoxides, but not thiophenic sulfur compounds, was verified. Asphalts contain substances that react with oxygen to form intermediates, which then oxidize aliphatic sulfur compounds to sulfoxides. The sulfur compounds do not react directly with oxygen to form sulfoxides at service temperatures. The presence of large amounts of aliphatic sulfur compounds in asphalts serves to inhibit oxidation of carbon compounds.

Aging studies were performed on many asphalts using standard methods such as the thin-film oven test and the thin-film accelerated-aging test. Extensive studies of low-temperature asphalt aging under elevated oxygen pressure were also performed. The results of these experiments provide the basis for selection of a realistic aging test. It was found that the aging characteristics of asphalts are a function of their physical state and therefore aging is temperature dependent. Some asphalts do not exhibit greatly different aging behavior over a fairly wide temperature range, while others exhibit significant differences. The choice of aging temperature was shown to be important in the design of an aging test. The more test temperatures deviate from service temperatures, the less predictive such a test is likely to be.

Aging experiments were also conducted on loose mixtures of asphalts and closely graded aggregate particles at temperatures in the pavement service temperature range. The results showed an effect of aggregate on asphalt aging, but the effect was not large. These results may not hold true for all asphalt-aggregate combinations, since only a small number of combinations were tested.

In conclusion, the understanding of the contribution of each chemically distinct material in asphalt to the observed physical properties was greatly advanced in this SHRP project.

Further, much of the historical mystery surrounding the effects of oxidation on asphalt performance properties was dispelled. Finally, several new applications of rapid chemical separation and analytical methods were refined to a point that each can be considered readily applicable by highway laboratories.

## Introduction

The studies of asphalt chemistry performed during the SHRP Binder Characterization and Evaluation Program (A-002A) are the subject of Volume 2 of this report. The work was performed at Western Research Institute (WRI) and at SRI International.

The chemical composition of a substance determines its physical properties. For simple molecules, physical properties can be estimated from a knowledge of molecular structures. For complex mixtures such as asphalts, which comprise many thousands of different molecular species, quantification of individual molecular entities is not practicable; even if it were, interactions between the many different kinds of molecules would have to be known in order to calculate physical properties of mixtures such as asphalts. Unfortunately, the simplification of predicting asphalt physical properties from averages of a few single global chemical variables of whole asphalts does not produce sufficiently accurate results.

A number of techniques and tests historically have been used to determine asphalt composition. Some examples are ultimate analysis, carbon-and-hydrogen-type determination using nuclear magnetic resonance (NMR) methods, measurements of polar functionalities by infrared functional group analysis (IR-FGA), chemical affinity (Rostler analysis), liquid chromatographic separation of maltenes after asphaltene precipitation (Corbett analysis), response to test compounds (phenol interaction test), molecular weight determinations; and molecular size range by size exclusion chromatography (SEC). Much important information about the composition of asphalts has been obtained by these classical techniques.

In Volume 1, chapter 1 it was explained how the colloidal model of asphalt structure evolved to rationalize differences in asphalt performance-related properties. In that model, the asphaltene content of an asphalt was an important indicator. Asphalts with large asphaltene concentrations, designated "gel" types, tended to behave differently from asphalts with few asphaltenes, designated as "sol" types. However, it was also observed that many asphalts are of an intermediate nature. Although it was established that asphaltenes are the principal viscosity-enhancing components of asphalts (and disproportionately influence other properties as well), it was observed that equiviscous (at a given temperature) asphalts could have varying asphaltene concentrations. Similarly, asphalts with identical asphaltene concentrations could have different rheological properties. Failure modes of asphalts (when mixed with aggregates) such as low-temperature cracking propensities, stripping behaviors,



tendencies to rut, and susceptibilities toward oxidative aging could not be predicted except in general ways.

A better model of asphalt structure, which better relates asphalt chemical properties to performance-related physical properties, was required than was offered by the colloidal theory. Therefore, at the outset of the Binder Characterization and Evaluation Program, the principal objectives were testing the fundamental validity of the model, and then either replacing or refining it. To do this, it was essential to improve classical methods of asphalt analysis and adapt novel methods to the study of asphalts in order to better understand asphalt chemistry.

Two of the most fundamental chemical properties of any organic substance are molecular weight and chemical functionality. Many physical properties, particularly rheological properties, are in theory functions of molecular weight and (for complex mixtures) molecular weight distribution. Chemical functionality determines extent of intermolecular associations; it therefore influences effective molecular weights, as distinct from true molecular weights, of organic materials. Hence, chemical functionality governs those physical properties that depend on effective molecular weight. Chemical functionality also influences aging and stripping behaviors. These relationships were explained in Volume 1, chapter 1. Briefly, molecules composed of carbon and hydrogen tend to associate with one another less strongly than molecules composed of carbon, hydrogen, and heteroatoms such as nitrogen and oxygen. The latter kinds of molecules are considered to be polar; they form relatively strong associations of molecules, depending on such factors as temperature, shear, and solvation. These associations have the effect of increasing effective molecular weights of polar molecules.

Therefore methods for separation of asphalts into distinct chemical fractions and into fractions of differing molecular sizes were emphasized from the beginning of the Binder Characterization and Evaluation Program. The separation of asphaltenes by solvent precipitation was not considered sufficient, based on considerations explained in Volume 1, chapter 1, to accomplish these goals. The technique of ion exchange chromatography (IEC) had been shown to provide good separations of petroleum fractions into neutral, acidic, and basic components, but had only been used in one asphalt study. The advantages of the technique were that neutral materials free of polar heteroatoms could be obtained, and that acidic and basic species could be separated. These results cannot be achieved by asphaltene precipitation.

SEC has long been used for analysis of molecular weight distributions in asphalts. However, there has not been a great deal of study of the different fractions generated by SEC. If there is any validity at all to the classical theory of asphalt structure, it should be possible to separate associating from nonassociating components of asphalts by SEC. Moreover, it should be possible, because of quantitative recoveries usually observed in SEC separations, to separate aged asphalts into fractions of different molecular size and study them. Because SEC studies relate to all objectives of the program, a great deal of effort was expended on the improvement of existing methods.

Hardening of asphalts with age is a phenomenon that was intensively studied during the Binder Characterization and Evaluation Program. Hardening has physical and chemical components, and both were studied. A comprehensive study of the reaction of oxygen with asphalts was begun, which included the investigation of the mechanism of asphalt oxidation conducted at SRI International. In order to develop a realistic aging test for asphalts, much fundamental knowledge is required. Any aging test that simulates service lifetimes, requires the use of elevated temperatures, elevated pressures, or a catalyst to accelerate the reaction of oxygen with asphalt. The effect of the accelerated reaction on asphalt properties in test procedures must resemble the effect of years of service on the same properties. The work done in this program provided baseline data for the development of a practical aging test for binders. Arriving at an aging protocol was a principal objective of the program.

The objectives outlined above for the Binder Characterization and Evaluation Program guided the course of research for the duration of the program.

This report consists of nine chapters. Chapters 1 and 2 report results of various separation methods on asphalts and differences in properties among various asphalt components. Chapter 3 describes rheological investigations of mixtures of asphalts with selected model compounds. The model compounds chosen were those chemically similar in some respects to fractions isolated in the separations described in chapters 1 and 2. Chapter 4 describes the development of potentiometric titration as a rapid method for studying acidic and basic components of asphalts. Chapter 5 describes methods for predicting asphalt rheological properties based on chemical parameters. These methods were applied to mixtures of components of different asphalts. A study of isothermal reversible age hardening (nonoxidative) is reported in chapter 6. The progress made in understanding the mechanism of asphalt oxidation is discussed in chapter 7. Chapter 8 includes studies of asphalt aging kinetics performed in a variety of ways. These studies emphasize the importance of asphalt physical structure in asphalt oxidative aging. Chapter 9 reports studies of SHRP asphalts using conventional methods. The global chemical variables reported are used to compare the asphalts with results of previous studies.

# 1

## Separation of Asphalts by Chemical Functionality

### Introduction

Most asphalts are the distillation residua of crude oils, although some are products of solvent precipitation processes. As a result of either process, the most polar, most aromatic, and highest molecular weight components in crude oils become concentrated in asphalts. The composition of asphalts is therefore diverse and may include such different kinds of compounds as nonpolar saturated hydrocarbons of relatively high molecular weight and relatively small, polar, aromatic molecules. Many of the polar components may be polyfunctional. The presence of such materials complicates separations of asphalts into compound classes.

Many earlier asphalt fractionation studies used liquid chromatography on stationary phases such as alumina or silica gel. Before performing separations on these materials, the most polar components of asphalts were removed. The pretreatment step was found to be necessary because the highly polar components have poor solubility characteristics and tend to adsorb irreversibly on silica gel and alumina. The usual method for removal of polar materials was asphaltene precipitation using hydrocarbon solvents such as n-pentane or n-heptane. This is unfortunate, because in many respects the constituents of asphaltenes (which may include high molecular weight nonpolar molecules in addition to polar species) are the most interesting components of asphalts. It is therefore desirable to be able to fractionate solutions of whole asphalts without pretreatment and without too much irreversible adsorption on the solid materials used in separations. Asphaltene precipitation separates molecules according to solubility and not chemical functionality. In the Binder Characterization and Evaluation Program, emphasis was placed on ion exchange chromatography (IEC), which had been used to separate petroleum and petroleum-derived materials into defined chemical fractions and which offers acceptable recoveries. This technique had seen little application to asphalts. A column chromatographic procedure in which the adsorbent has been chemically modified to allow high recoveries was also employed. The novel technique of supercritical fluid chromatography (SFC) is also described, although in a strict sense it does not separate asphalts entirely by chemical functionality.

## **Ion Exchange Chromatography (IEC) Separations**

Ion exchange chromatography (IEC) has long been used to separate shale oil, tar sand bitumen, petroleum and petroleum-derived materials into defined chemical fractions (Boduszynski, Chadha, and Pochopien 1977; Green et al. 1984; Kircher 1991; McKay et al. 1975; Selucky et al. 1981). When used to separate organic substrates such as those described above, IEC works as a form of affinity chromatography and does not function in an actual ion exchange mode (as in water softeners). In order to separate asphalts into defined chemical fractions using IEC, samples of asphalts are dissolved in selected solvents, and the solutions are pumped into columns filled with activated anion or cation resins. Asphalt components containing acidic functional groups become adsorbed on anion resins, from which they can be desorbed. Asphalt components having basic functional groups are adsorbed on cation resins. Components containing neither acidic nor basic functional groups will not be adsorbed by either anion or cation columns. Components having both acidic and basic substituents (amphoterics) will be adsorbed by both anion or cation resins; when columns of both resins are arranged in series, amphoteric will be adsorbed by whichever resin is contacted first.

The separation of asphalts by IEC was first reported by Boduszynski, Chadha, and Pochopien (1977), who separated Romashkino bitumen into neutral, acidic, and basic fractions with total recoveries of more than 90%. A refined IEC method for separation of petroleum and petroleum fractions was developed by Green et al. (1984) after a systematic study of experimental variables. This procedure generates well-defined neutral, acidic, and basic fractions and was used for many of the separations reported herein.

A disadvantage of the IEC procedure applied to petroleum residua is that some material is irreversibly adsorbed on resin columns, so total recoveries never are 100%. These irreversibly adsorbed materials almost certainly are components that are highly polar and aromatic, and therefore strongly influence asphalt physical properties. Another disadvantage of the IEC procedure is the great time and expense required to activate resins and perform separations. The technique is extremely sensitive to many experimental variables, such as temperature, flow rate, column dimensions, and column packing. Rapid flow rates do not allow for breakup of asphalt microstructural units (Selucky et al. 1981). The strength of the solvent used to dissolve asphalt samples and as eluant significantly affects results of IEC separations. When cyclohexane is used as a solvent, almost all polar materials in asphalts are adsorbed on the resins. If asphalts are dissolved in a more polar solvent, such as the mixture of benzene, tetrahydrofuran, and ethanol used in some of the IEC separations performed in this study, weakly acidic and weakly basic components of asphalts are not adsorbed on the columns. Above all, proper resin activation is vitally important. Attempts to shortcut the elaborate activation procedure result in excessive irreversible adsorption of polar materials, particularly from asphalts dissolved in cyclohexane. Needless to say, highly trained personnel are required for IEC separations.

At the outset of the SHRP Binder Characterization and Evaluation (A-002A) Program, eight asphalts were selected for special study and were designated as core asphalts. These asphalts are coded as AAA-1, AAB-1, AAC-1, AAD-1, AAF-1, AAG-1, AAK-1, and AAM-1. All other asphalts studied in the program are referred to as the expanded set of

asphalts. Some chemical and physical properties of the core asphalts and the expanded set of asphalts are reported in chapter 9.

Initial separations of the eight core asphalts followed the procedure published by Green et al. (1984) as closely as possible so that results would have some basis of comparison with data obtained in their investigation. Since Green et al. (1984) published their method, they have recommended using resins of larger mesh size, and their suggestion was followed in this study. Green et al. employed longer and thinner columns than were used in the SHRP Binder Characterization and Evaluation study, but when a Wilmington crude oil distillate fraction was separated by the method used in this program, results were obtained close to those published by Green et al. (1984) for the same material (Volume IV, Chapter 7).

In the procedure described above, a solution of an asphalt can be separated into as many as five distinct fractions. Asphalts to be separated were dissolved in a mixed solvent consisting of benzene, tetrahydrofuran, and ethanol; this solution was then pumped through two columns, one filled with activated anion resin and the other filled with activated cation resin. The columns were arranged so that the asphalt solution contacted the anion resin first. Desorption of the materials collected on the anion resin and solvent removal yielded strong acids. Desorption of materials collected on the cation resin and solvent removal yielded strong bases. Solvent removal from the eluates yielded a mixture of neutrals, weak acids, and weak bases. In some runs, the procedure was interrupted at this point. In other runs, the cation resin column was not used, so eluates in these runs consisted of a mixture of strong and weak bases, weak acids, and neutrals.

In the complete IEC separation of an asphalt into five fractions, the eluates from the initial separation, consisting of neutrals, weak acids, and weak bases, were redissolved in cyclohexane and this solution was pumped through another pair of columns filled with activated resins. Again, the solution contacted the anion resin column first. Desorption of the anion resin followed by solvent removal yielded weak acids. Desorption of the cation resin followed by solvent removal yielded weak bases. Both weakly polar fractions retained solvent tenaciously and were difficult to dry completely. Materials eluted through both columns, after solvent removal, constituted the neutral fraction.

A flow sheet illustrating the above procedure is presented in figure 1.1. Detailed descriptions of the methods used in this study are presented in Volume IV, chapter 7 of this report.

The IEC separation procedure described above does not isolate amphoteric components of asphalts into a single fraction. As mentioned earlier, these materials are polar components containing both acidic and basic functional groups. In the IEC separation procedure described above, amphoteric components become distributed among the strong acid, strong base, and weak acid fractions. Collection of amphoteric components into one fraction requires another separation strategy, which will be described later.

One core asphalt, AAC-1, is waxy and would not completely dissolve in the mixed solvent of benzene, tetrahydrofuran, and alcohol. This asphalt is soluble in cyclohexane. In order to fractionate AAC-1 by IEC, a solution of the asphalt in cyclohexane was pumped through

two columns, one filled with anion resin and the other with cation resin. The columns were arranged so that the solution contacted the anion resin first. Three fractions, consisting of neutrals, total acids, and total bases, were collected in this separation. When the anion resin column was used alone, a mixture of neutrals plus total bases was collected in the eluates. The other core asphalts also were separated into the same fractions using these procedures.

Average yields of four polar fractions (strong acid, weak acid, strong base, weak base) and the neutral fraction, and total recoveries for replicate IEC separations of seven core asphalts are listed in table 1.1. Data for each of the individual separations are provided in supplementary table 1.18<sup>1</sup>. A separation of core asphalt AAC-1 into total acid, total base, and neutral fractions was performed due to incomplete solubility of this asphalt in the mixed solvent. These results are reported in supplementary table 1.19. The data in supplementary tables 1.18 and 1.19 include confidence intervals for the separations. For each of the five IEC fractions of seven of the asphalts, values of confidence intervals vary. These values are relatively large for the weak acid and weak base fractions, and relatively small for the other fractions. The larger values of the confidence intervals associated with the weak acid and weak base fractions can be attributed to difficulties in removing solvent from these materials and the nature of the IEC separation, in which the five fractions generated do not undergo identical vicissitudes. For example, neutral materials pass through four resin columns, but are adsorbed on none. Strong acids are adsorbed on the first column they encounter, after which they are desorbed. Weak bases pass through three columns and are adsorbed on the fourth.

Confidence interval values for a given IEC fraction are similar among the asphalts, indicating that the separation technique is applied consistently and is not asphalt-dependent. There do not appear to be large operator effects. The IEC separations of the core asphalts have not been replicated in other laboratories. Fractionation patterns vary among the asphalts and serve to uniquely characterize (fingerprint) each asphalt. Some ratios of mass percentages of various IEC fractions are listed in table 1.2. A discussion of the significance of these ratios is presented in chapter 5.

To verify that the five IEC fractions collected from each of the seven core asphalts are distinct and have properties that are in accordance with predictions based on the microstructural model (see Volume I, chapter 1), each IEC fraction from each core asphalt was analyzed using conventional analytical methods. Elemental analyses and infrared functional group analyses (IR-FGA) were performed, and number-average molecular weight ( $M_n$ ) data were obtained in toluene at 60°C (140°F) by vapor phase osmometry (VPO). These conventional analytical methods as applied to asphalts are discussed in chapter 9.

Representative IR-FGA data for IEC fractions of asphalt AAA-1 are listed in table 1.3. The IR-FGA data for IEC fractions of the other core asphalts are listed in supplementary tables 1.20 through 1.25. The data in the tables show that, with the exception of AAG-1, carboxylic acids and phenols are concentrated in the strong acid fractions, as are the amphoteric 2-quinolones. Pyrroles occur in all four polar fractions but are concentrated in

---

<sup>1</sup>All supplementary tables in this report can be found in appendix A.

the weak acid fractions. Sulfoxides and ketones, which result from oxidation, are concentrated in the weak base fractions. The neutral fractions are virtually free of the functional groups whose concentrations are measured by IR-FGA. In asphalt AAG-1, phenols are concentrated in the weak acid fraction, and the 2-quinolones are equally divided between the strong acid and strong base fractions. The neutral fraction of this asphalt contains measurable amounts of pyrroles and phenols. Unusual acid-base properties of this asphalt were noted in another SHRP study (Labib and Zanzucchi 1991). Overall, the IR-FGA results show that the IEC separation produces fractions that contain the expected functional groups.

Elemental analyses and  $M_n$  determinations for the IEC neutral fractions of eight core asphalts and strong acid fractions of seven core asphalts are listed in tables 1.4 and 1.5. As expected, the IEC neutral fractions are much more aliphatic (they contain more hydrogen) than the IEC strong acid fractions. Nitrogen was detected in only two of the neutral fractions, but ranges from 0.9-1.8% in the strong acid fractions. The strong acid fractions also are much more enriched in oxygen. Interestingly, sulfur concentrations of the IEC neutral fractions are either equivalent to or only slightly less than sulfur concentrations of the IEC strong acid fractions. The  $M_n$  values of the neutral materials are lower than  $M_n$  values of their parent asphalts (chapter 9, table 9.4), whereas  $M_n$  values of the IEC strong acid fractions are much higher. The  $M_n$  value of the neutral fraction of AAM-1 is significantly higher than the  $M_n$  values of the other seven whole asphalts. The high  $M_n$  of the nonpolar neutral fraction of this asphalt cannot be due to the polar interactions presumed to be characteristic of the acidic and basic fractions. The  $M_n$  value of the strong acid fraction of this asphalt is comparable to  $M_n$  values of the strong acid fractions of asphalts AAA-1 and AAK-1. In these polar IEC fractions, associations (the formation of which were discussed in Volume I, chapter 1) are believed to be responsible for high  $M_n$  values. A discussion of the problems involved in  $M_n$  determinations of asphalts and asphalt fractions by vapor phase osmometry (VPO) is included in chapter 9. The  $M_n$  values of the neutral fractions determined by VPO probably are reasonably accurate. The  $M_n$  values are confirmed by the supercritical fluid chromatography (SFC) profiles discussed below. The  $M_n$  values for polar fractions of asphalts obtained by VPO are probably higher than their average "true" molecular weights. Note that the  $M_n$  value of the IEC strong acid fraction of asphalt AAG-1 is relatively low.

Elemental analyses of strong base, weak acid, and weak base fractions of seven of the core asphalts have been determined and are reported in supplementary tables 1.26 through 1.28. In general, the IEC strong base fractions are less aromatic than corresponding IEC strong acid fractions. Nitrogen concentrations of IEC strong base fractions are equal to or higher than nitrogen concentrations of corresponding IEC strong acid fractions. Weak acid fractions are less aromatic than corresponding strong base fractions, and weak bases are the least aromatic of all the polar fractions. All four polar fractions have substantial amounts of heteroatoms (nitrogen, oxygen, and sulfur).

Asphalt AAD-1 is rich in the metals vanadium and nickel. These metals are known to exist in asphalts as organic chelates, some of which are metalloporphyrins. Porphyrins are readily identified in asphalts because of distinctive bands in their ultraviolet-visible spectra. Each of the five IEC fractions of asphalt AAD-1 was analyzed for vanadium, nickel, and

porphyrin content to determine how these metals become distributed during IEC separation. These results are listed in supplementary table 1.29. The nonpolar neutral fraction contains small amounts of metals, mostly nickel. All four polar fractions contain substantial amounts of both metals. The weak base fraction contains a particularly high concentration of nickel and most of the identifiable porphyrins. Vanadium occurs in high concentrations in both acid fractions and the weak base fraction. The weak acid fraction contains particularly large amounts of vanadium compared with nickel. The metal chelates in the acid fraction may not be porphyrins. The nickel complexes in asphalt AAD-1 appear to be more basic, on the average, than the vanadyl complexes. In the weak base fractions, most of the metals are accounted for as porphyrin complexes. Metalloporphyrin chelates, unless they possess carboxylic acid side-chains, would be expected to be weakly basic in character. Thus, IEC separation of AAD-1 results in a predictable concentration of this class of readily detectable compounds according to their chemical nature.

Vanadium closure for the sum of the fractions is not particularly good (73%). It is likely that the highly polar materials that irreversibly adsorb on the anion resin are higher in vanadium than nickel. The nickel closure is about 81% of the total nickel in the asphalt.

The IEC neutral fractions of each of the asphalts are viscous liquids at ambient temperatures. Upon standing at room temperature for several months in the dark and under an inert gas atmosphere, all of the IEC neutral fractions except that of AAA-1 were observed to deposit what appeared to be wax crystals. The asphalts were analyzed for wax content by Dr. F. Fleitas of INTEVEP, and values of up to 5% were observed. Asphalt AAA-1 was determined to be low in wax content. Similar behavior might occur in whole asphalts and not be observed due to asphalt opacity. Wax precipitation could significantly affect the low-temperature properties of asphalts. All other IEC fractions are dark friable solids or tacky semisolids.

Rheological data for the neutral fractions of the core asphalts at 25°C (77°F) and three different rates of shear are reported in supplementary tables 1.30 and 1.31. Rheological data for the neutral fractions of AAC-1 and AAF-1 were also obtained at 45°C (113°F). The viscosities of the neutral fractions can be compared with viscosities of the parent asphalts at 25°C (77°F) and 1.0 radians per second (rad/s) rate of shear (chapter 9, table 9.10). It is evident that at 25°C (77°F), the whole asphalt viscosities are two to three orders of magnitude greater than neutral fraction viscosities of the same asphalt. Neutral fractions constitute 50-60% of these asphalts but are not the viscosity-enhancing components of asphalts; obviously the polar fractions, in whole or in part, are the viscosity-enhancing components of asphalts. Thus, IEC neutral fractions fulfill very well the properties of a bulk solvent predicted by the model of asphalt structure described in Volume I, chapter 1. They are the least aromatic components of asphalts, contain small amounts of nitrogen and oxygen, and are of lower  $M_n$  than the parent asphalts. With respect to rheological properties, samples of neutral fractions of a given asphalt from different IEC runs are not greatly different at 25°C (77°F), with the exception of AAM-1.

The  $\tan \delta$  values listed in supplementary tables 1.30 and 1.31 represent ratios of viscous ( $G''$ ) to elastic ( $G'$ ) moduli of viscoelastic liquids.  $\tan \delta$  values vary with temperature and rate of shear, as do viscosities. For whole asphalts,  $\tan \delta$  decreases with increased rate of



shear. Remarkably,  $\tan \delta$  values of the IEC neutral fractions increase with increasing shear rates at 25°C (77°F). In order to verify this phenomenon, rheological studies were performed on three of the IEC neutral fractions at 0°C (32°F). Viscosities and  $\tan \delta$  values of the three neutral fractions at this temperature are reported in supplementary table 1.32. Lowering the temperature by 25°C (77°F) increases the viscosity of these three IEC neutral fractions by more than two orders of magnitude. At 0°C (32°F),  $\tan \delta$  values are low, but they still increase with increasing rate of shear. At present, the authors cannot offer an explanation for this phenomenon. The viscosity determinations at 0°C (32°F) of two different preparations of IEC neutral fractions of AAK-1 were not reproducible within the 10% instrumental variation of the mechanical spectrometer, and there was some variance between two different viscosity measurements of the same sample of the IEC neutral fraction of AAD-1. It is not known whether these variances are due to difficulties in measuring viscosities on the mechanical spectrometer at low temperatures or to some phenomenon related to the low-temperature hardening of asphalts.

Rheological theory predicts that liquid viscosities should be a function of molecular weight. Inspection of supplementary table 1.30 shows that the viscosity of the IEC neutral fraction of asphalt AAM-1 at 25°C (77°F) is much greater than the viscosities of any of the other IEC neutral fractions at the same temperature. The molecular weight of the AAM-1 IEC neutral fraction also is much greater than the molecular weights of the other IEC neutral fractions (table 1.4). These molecular weights were determined at 60°C (140°F) by VPO in toluene. Similarly, the IEC neutral fraction of AAD-1 is the least viscous of the eight IEC neutral fractions at 25°C (77°F), and its molecular weight is lowest. For the IEC neutral fractions of the eight core asphalts, with the exception of AAG-1, there is a fairly good correlation of viscosity and molecular weight (figure 1.2). The IEC neutral fraction of AAG-1 is the only neutral material that contains significant amounts of oxygen and nitrogen-containing compounds (possibly carbazoles, indoles, and ethers), and the presence of such compounds might be responsible for the greater viscosity of AAG-1 neutrals. Due to the non-polar nature of the components of the IEC neutral fractions, the VPO method should provide fairly accurate  $M_n$  values (Green, Diehl, and Shay 1991).

Rheological properties of various mixtures of IEC fractions of core asphalts were studied at 25°C (77°F). The mixture of neutrals, weak acids, and weak bases can be obtained by separating asphalts using only the first step of the IEC separation procedure described earlier, dissolving each asphalt (except AAC-1) in a mixed solvent and pumping it through only one pair of anion and cation resin columns. The mixture of neutrals plus total bases can be obtained by dissolving each asphalt in cyclohexane and pumping the solution through one column filled with anion resin. The combination of neutrals, total bases, and weak acids is obtained by dissolving each asphalt (except AAC-1) in mixed solvent and pumping the solution through one column filled with anion resin. Each of these separations removes one or two polar fractions from the rest of the components of an asphalt.

Table 1.6 lists viscosities of several of these mixtures compared with viscosities of the parent asphalts and their IEC neutral fractions determined at 25°C (77°F). More detailed descriptions of the rheological properties of these materials are found in SHRP Database B (appendix B). The data in table 1.6 show that as polar materials become mixed with the neutral materials, in natural abundance levels, viscosities increase. The data in table 1.6

imply that the strong acid fraction, the most abundant polar fraction and also the most polar and aromatic, contains most of the viscosity-enhancing components of seven of the core asphalts. When all of the other four IEC fractions are mixed together, viscosities of the mixtures at 25°C (77°F) are an order of magnitude less than corresponding viscosities of the parent asphalts. However, there are relatively more neutral materials (of low viscosity compared with parent asphalts) in these IEC fraction mixtures.

Mixtures were also prepared in which each of the core asphalts was combined with 5% by weight of its own neutral fraction. The mixtures are characterized by viscosities that are roughly 60-70% those of parent asphalts measured under identical conditions. These data are listed in supplementary table 1.33. Asphalt AAD-1 was combined with 5% by weight of its strong base fraction. A solvent treatment was required to effect mixing. The viscosity of the mixture was compared with that of a sample of AAD-1 subjected to an equivalent solvent treatment. At three temperatures of measurement, the viscosity of the mixture was about 25% greater than that of the solvent treated asphalt. Combining AAD-1 with 2% by weight of its strong acid fraction yielded a mixture having a viscosity about the same as the mixture containing 5% strong bases. Based on these data, which are listed in supplementary table 1.34, the strong acid fraction contains more viscosity-enhancing materials than the strong base fraction, and the effect of adding the neutral fraction to asphalts results in mixtures having lower viscosities than the parent asphalts. Later in this chapter, rheological studies of mixtures of asphalts with IEC fractions obtained by a different separation method are reported. Fractions generated by the other IEC separation are referred to as acid and base fractions and should not be confused with the strong acid and strong base fractions discussed above. Neutral fractions generated by both methods are identical.

The  $M_n$  values of the strong acid fractions determined by VPO in toluene are much higher than those of the neutral fractions, and  $M_n$  values of the strong acids vary significantly among seven of the core asphalts. Large  $M_n$  values should, according to the microstructural model, reflect stronger, more extensive associations. Stronger, extensive associations (particularly those that may be of three-dimensional extent) should be reflected in rheological properties, particularly in the size of the elastic modulus (and therefore  $\tan \delta$  values) of an asphalt measured at ambient temperatures. Table 1.7 lists  $\tan \delta_{ct}$  values of seven of the core asphalts at 25°C (77°F) and  $M_n$  values of their strong acid fractions. (A discussion of the difference between conventional  $\tan \delta$  and  $\tan \delta_{ct}$  values is reserved until chapter 2.) These data are plotted in figure 1.3. With the exception of AAA-1,  $\tan \delta_{ct}$  values correlate inversely with  $M_n$  of the IEC strong acid fractions. The reason for the anomaly in the case of AAA-1 may be the relatively large amount of neutral materials in this asphalt compared with the other core asphalts. It may be speculated that asphalts having polar fractions with large values of  $M_n$  would be more resistant to rutting when used in mixes, compared with asphalts having polar fractions with low values of  $M_n$ .

The above results show that asphalts can be separated into well-defined chemical fractions using an IEC technique developed to characterize crude oils and materials derived from crude oils. For seven core asphalts, a neutral fraction and four polar fractions are obtained. The microstructural model emphasizes the influence of associations of polyfunctional chemical species in determining asphalt properties, and considerations of acidity and

basicity are not of themselves paramount. A polyfunctional molecule may contain more than one acidic group, more than one basic group, or multiple acidic and basic groups (amphoteric). It is desirable to be able to separate polyfunctional molecules per se rather than acidic or basic species. A hypothesis was advanced that the dominant associating species in asphalts are amphoteric molecules, and a program was designed to test this hypothesis. The hypothesis is inherently credible for aged asphalts in particular, due to the formation of weakly basic ketone and sulfoxide functionalities (chapters 7 and 8).

Amphoteric molecules can be classified into four categories based on interactions with ion exchange resins. They may be strong acid-strong base type, strong acid-weak base type, weak acid-strong base type, or weak acid-weak base type. Obviously other more complex combinations of amphoteric molecules can be envisioned, but they can be reduced to one of the above four with respect to interactions with ion exchange resins. In the separation scheme described earlier, amphoteric molecules will be distributed among the strong acid, strong base, and weak base fractions. If it is desired to collect all amphoteric molecules in one fraction, each of the aforementioned materials must be further separated, a tedious undertaking, or a new scheme must be devised. One new scheme is illustrated in figure 1.4. In this scheme, four fractions are collected: a neutral fraction (presumably identical to the fraction collected in the conventional separation), an amphoteric fraction, an acid fraction, and a base fraction. The latter two fractions will contain polyacid and polybasic materials, respectively. The salient features of this scheme are that asphalt solutions are pumped through a cation resin column as a first step, and four fractions are obtained instead of five. Experimental details of this modified IEC procedure are described in Volume IV, chapter 7.

Table 1.8 lists weight fractions of neutral, amphoteric, base, and acid fractions of four of the core asphalts. Yields of neutral fractions are virtually identical with yields of neutrals obtained by the conventional IEC separation in which asphalt solutions are separated into five fractions and contact anion resins first. For all of the four asphalts, the amphoteric fraction is the dominant polar fraction. Yields of amphoteric molecules are similar to those reported by Selucky et al. (1981) for Athabasca bitumens. The amphoteric fractions are observed to be black friable solids that swell when contacted with small amounts of solvents. All base fractions of each of the four asphalts are tacky semisolids. Mixtures of neutrals and acids are viscous liquids (although the acid fractions are tacky semisolids by themselves), and their viscosities were measured at 25°C (77°F) and 45°C (113°F). These data are listed in supplementary table 1.35. Viscosities of the neutral plus acid fractions are orders of magnitude lower than viscosities of the parent asphalts measured at the same temperatures.

Infrared analyses (IR-FGA) of amphoteric molecules, bases, and combinations of acids and neutrals were performed. The results are listed in table 1.9. It is noteworthy that 2-quinolones (which are amphoteric compounds) are found in abundance only in the amphoteric fractions, as would be expected. Ketones and sulfoxides are concentrated in base fractions. These functionalities presumably are generated during workup. The  $M_n$  values of the amphoteric and base fractions were determined ( $M_n$  measurements were not performed on neutral and acid fractions) in toluene and pyridine. These data are listed in table 1.10. The  $M_n$  values of the base fractions range from approximately 800 daltons to 1,350 daltons, and are the same in toluene as in pyridine, indicating that by themselves the bases do not engage in strong associations. The  $M_n$  values of the amphoteric fractions range from 3,700

daltons (AAK-1) to 1,500 daltons (AAG-1) in toluene, and from 2,700 daltons (AAK-1) to 1,200 daltons (AAG-1) in pyridine. Differences in  $M_n$  in toluene compared with pyridine (a better solvent for polar materials than toluene) indicate that amphoteric materials engage in associative interactions. Elemental analyses of the amphoteric fractions (table 1.11) show that these materials are aromatic and also have high nitrogen concentrations. The above observations are confirmed by nuclear magnetic resonance (NMR) data (table 1.12), which show that about 50% of the carbon atoms in the amphoteric fractions are aromatic. Aromatic hydrogen concentrations are not very large, which implies that some aromatic molecules having more than two rings may be present.

All of the above observations confirm the hypothesis that the amphoteric component of asphalt consists of the most polar and most aromatic molecules, which are of highest  $M_n$  value (resulting from tendencies to associate). If the microstructural model is correct, amphoteric fractions will be found to be the principal viscosity-enhancing component of asphalts, the component contributing most to elastic moduli of asphalts, and the component most responsible for asphalt strength.

In order to test this hypothesis directly, mixtures of each asphalt with each of the four IEC fractions (neutral, amphoteric, acid, and base) were prepared. The compositions of these mixtures were calculated based on the observation that a specific natural abundance of each IEC fraction characterizes each asphalt. For example, asphalt AAD-1 consists of about 54% neutrals, 25% amphoterics, 9% bases, and 8% acids. Asphalt AAG-1 consists of 52% neutrals, 18% amphoterics, 12% bases, and 14% acids. It was decided initially to add amphoterics to asphalts such that the resulting mixtures would contain double the natural abundance levels of amphoterics. However, the resulting materials were observed to be coal-like, and viscosities were barely measurable at 60°C (140°F). Solvent removal from the prepared mixtures proved to be very tedious. The amphoteric fractions impart great surface activities to the mixtures, and under vacuum, meringues form that flow from distillation flasks into the rotary evaporators used in the solvent removal process.

Accordingly, it was decided to formulate mixtures for each of the four asphalts such that amphoterics constituted a 50% excess of their natural abundance for each of the asphalts. For example, a 10.0 g sample of AAD-1 contains ~ 2.5 g amphoterics, a 25% natural abundance; 50% excess would be 37.5%. So to make 10.0 g of a mixture having 37.5% amphoterics, enough amphoteric material (1.67 g in this case) 8.33 g was added to AAD-1 to yield 10.0 g of a mixture containing 3.75 g amphoterics. For AAG-1, the natural abundance level for amphoterics is 18%, much less than for AAD-1. A mixture of AAG-1 containing a 50% excess of this natural abundance would contain 27% amphoterics. Similar considerations apply to AAK-1 and AAM-1. Natural abundances of amphoterics in these asphalts are similar to those in AAD-1 and AAG-1, respectively.

Mixtures were also prepared by adding neutral, acid, and base fractions to the asphalts. In every case, the same amount of each fraction was added as for the amphoteric fraction. For example, in the AAD-1 mixtures, 1.67 g amphoterics was added to 8.33 g AAD-1. In the mixtures of AAD-1 with its neutral fraction, 1.67 g neutrals were added to 8.33 g AAD-1. Similarly, 1.67 g bases were added to 8.33 g AAD-1, and 1.67 g acids were added to 8.3 g AAD-1. The neutral, acid, and base fractions were not added in amounts commensurate

with their own natural abundances but in amounts corresponding to the natural abundance of the amphoteric fraction, so that effects of each fraction on rheological properties could be compared on an equivalent mass basis within an asphalt.

Viscosities of all these mixtures at 60°C (140°F) are listed in table 1.13. It is obvious that, as a fraction, the amphetics are the components of the asphalts governing high viscosities, as predicted by the microstructural model. Bases added to each of the four asphalts cause moderate viscosity increases in the resulting mixtures, and addition of acids to asphalts causes only small viscosity increases in the resulting mixtures. These results indicate that there are few polyfunctional acidic and basic compounds present, assuming these types of compounds would have effects on rheological properties similar to those of amphetics. Mixtures of asphalts with neutrals are characterized by viscosities that are much lower than parent asphalt viscosities measured under the same conditions. These results do not mean that no viscosity-enhancing species exist in acid, base, or neutral materials, or that no viscosity-reducing species exist in the amphoteric fractions. The results apply to the fractions as a whole.

Rheological measurements of materials on a mechanical spectrometer produce values for dynamic viscosities ( $\eta^*$ ), complex modulus ( $G^*$ ), elastic modulus ( $G'$ ), viscous modulus ( $G''$ ), and  $\tan \delta$  ( $G''/G'$ ). For many rheological studies, the quantity  $G^*/\sin \delta$  (complex modulus divided by the sine of the phase angle  $\delta$ ) is of greater interest than  $\eta^*$ . Accordingly, this quantity has been calculated for the mixtures of four asphalts with their amphoteric, base, acid, and neutral fractions (supplementary table 1.36). The  $G^*/\sin \delta$  values are numerically approximately 10 times the corresponding values of dynamic viscosity. This is because rheological measurements were performed at 60°C (140°F) and 1.0 rad/s. Under these conditions for asphalts,  $G^*$  values (reported in dyne/cm<sup>2</sup>) are 10 times  $\eta^*$  values (reported in Pa·s) and phase angles are not greatly different from 90°, hence the sine of the phase angle is nearly unity. Most measurements of dynamic viscosity reported in this volume were performed under conditions such that  $G^*/\sin \delta$  is numerically 10 times that of the corresponding dynamic viscosities, and so  $G^*/\sin \delta$  values are not calculated elsewhere.

In the mixtures discussed above, which are combinations of IEC fractions with whole asphalts, the ratios of neutrals to polars are different from the relative abundance of neutrals and polars in neat asphalts. Acids, bases, and amphetics are considered to be the polar fractions.

To verify the effect of the absence of amphetics on asphalt properties, mixtures consisting only of neutral, base, and acid fractions were prepared. In these amphoteric-free mixtures, the relative amounts of neutrals and total polars were the same as in the parent asphalts. However, amphetics were replaced by bases, and so the amphoteric-free mixtures contain much more than their natural abundances of bases. In table 1.14, viscosities at three temperatures and  $\tan \delta$  values at 25°C (77°F) of four such mixtures are compared with the same measurements on the parent asphalts. Viscosities of the mixtures are much lower than those of the parent asphalts at all three temperatures. The  $\tan \delta$  values of the mixtures are high, particularly the mixture made up of IEC fractions of AAG-1. High  $\tan \delta$  values are the result of low values of the elastic ( $G'$ ) modulus. The rheological data reported for all of

the above mixtures (with and without amphoteric) in tables 1.13 and 1.14 demonstrate that the amphoteric materials as defined by IEC are largely responsible for viscosity-enhancing phenomena in asphalts and are the main contributors to asphalt elastic moduli at 25°C (77°F). Therefore, amphoteric (as defined by IEC separation) have the chemical properties that the microstructural model predicts for asphalt dispersed moieties, as discussed earlier. Similarly, IEC neutral fractions are relatively nonviscous, aliphatic, and nonpolar and have properties that the microstructural model would attribute to asphalt solvent moieties. The other IEC fractions cannot be so readily characterized and may be distributed among the dispersed and solvent moieties as a function of temperature and other variables.

Other IEC separations were performed in which samples of asphalts were dissolved in a mixed solvent consisting of benzene, tetrahydrofuran, and ethanol, and the solutions then were pumped into columns of activated cation resin. Molecules having moderate to strong basic functional groups, including some amphoteric (strong base-strong acid, strong base-weak acid), are adsorbed on the cation resin, and any molecules not containing moderate to strong basic functional groups are eluted. This procedure generates two fractions, which (to avoid confusion with fractions generated in other IEC procedures) will be arbitrarily designated as a moderate base fraction, and a moderate base-free fraction. Yields of these materials for four of the core asphalts are reported in supplementary table 1.37. This table also lists  $M_n$  values for the moderate base fraction (a tacky semisolid) and viscosities of the moderate base-free fraction at 25°C (77°F). Viscosities of the moderate base-free materials are low compared with those of the parent asphalts. Again, the highly polar fraction, in this case the moderate base fraction, is found to be the viscosity-enhancing component of the asphalt. The moderate base fractions also have high  $M_n$  values. Yields of these fractions and some analytical data can be found in SHRP Database B (appendix B).

The IEC separations of asphalts described above are the result of the first attempt to use the technique for the fractionation of several asphalts. All operational variables in the IEC procedure were not rigorously evaluated in the Binder Characterization and Evaluation Program, due to time and budgetary constraints. In particular, not enough runs were made to evaluate the effect of different batches of resin received from the manufacturer on the separation. In appendix C, manufacturer's batch numbers of resins are listed. These resins were used in the separations whose results are reported in tables 1.8, 1.15, and supplementary tables 1.18 and 1.19. The data in appendix C do not indicate any clear trends. Occasionally, batches of anion resins that could not be properly activated were received during the course of the Binder Characterization and Evaluation Program. These batches of resins failed to develop a characteristic pink color after the activation procedure. When used in separations, these resins did not effectively adsorb polar materials.

Asphalts have been separated by IEC by three different procedures. In all three procedures, strongly polar, aromatic materials having high  $M_n$  values (compared with other components), which also are the viscosity-enhancing components of asphalts, were isolated. These strongly polar, aromatic materials are designated as strong acids in one procedure, amphoteric in the second, and moderate bases in the third. It is speculated that all three fractions contain mostly the same components, which can be characterized as having an aromatic nucleus with at least one strongly acidic and one basic functional group. It would thus be predicted that, if in a subsequent IEC separation procedure amphoteric were further

fractionated into materials containing strongly polar and weakly polar functional groups, the former would be found to be far more viscosity-enhancing than the latter. Some studies on separations of amphoteric fractions by other methods are reported in chapter 5.

The microstructural model predicts that, as asphalts oxidatively age, chemical reactions will take place, resulting in the formation of relatively more amphoteric materials at the expense of less polar materials. It is not known whether the amphoteric materials formed during oxidative aging closely resemble those already present in asphalts. Samples of asphalts AAD-1, AAG-1, AAK-1, and AAM-1 were subjected to an aging procedure that will be discussed in detail in chapter 8. Briefly, each asphalt sample was given a preliminary thin-film oven (TFO) treatment, a procedure that simulates hot-mix conditions. The TFO-aged samples were transferred to a pressure vessel. The pressure vessel then was filled with air to a pressure of  $2.07 \times 10^6$  Pa (300 psi) and placed in an oven. The oven temperature was maintained at 60°C (140°F) for 144 hours. The whole procedure, known as the TFO-PAV procedure, was adopted because it is believed to simulate several years of pavement service. The temperature (60°C/140°F) of reaction is near the maximum pavement temperature for most temperate climates. The high pressure accelerates the reaction of asphalt with oxygen.

Separation of TFO-PAV aged asphalts into neutral plus acid, base, and amphoteric fractions proved to be feasible. More materials were irreversibly adsorbed on the cation and anion resins than when unaged asphalts were separated. Neutrals were not separated from acids for reasons of economy. Yields of IEC fractions of asphalts aged by TFO-PAV (60°C/140°F, 144 hours) are reported in table 1.15. Yields of IEC amphoteric fractions in the oxidatively aged asphalts are extremely variable, but it appears that there are more of them than in unaged asphalts, particularly in the cases of AAG-1 and AAM-1. Unfortunately, losses to irreversible adsorption on the ion exchange resins were large for TFO-PAV aged AAD-1 and AAK-1. It is likely that the irreversibly adsorbed materials resemble amphoteric materials in polarity and aromaticity more than the other IEC fractions. Concentrations of bases in oxidatively aged samples are higher than in unaged samples; this is confirmed by potentiometric titration studies described in chapter 4.

The  $M_n$  values for amphoteric and base fractions of the aged asphalts were determined in toluene and pyridine by VPO at 60°C (140°F). For the amphoteric fractions in toluene,  $M_n$  values of both aged and unaged asphalts are much the same, within experimental error. The same is true for  $M_n$  values determined in pyridine. For both aged and unaged materials,  $M_n$  values determined in toluene are much greater than  $M_n$  values determined in pyridine. These data are reported in table 1.10 and in supplementary table 1.38. The  $M_n$  values in toluene of the base fractions of the aged asphalts are somewhat less than those of the base fractions of the unaged asphalts. For the base fractions of aged and unaged asphalts,  $M_n$  values in toluene and pyridine are nearly the same. It appears that one result of oxidative aging is that amphoteric and basic species are generated, but the species generated do not differ from those already present in molecular size. It can be speculated that oxidative aging does not result in formation of molecules greatly different from those already present, at least for those materials not irreversibly adsorbed on resins.

The IEC technique has been pressed to its practical limits in the separation of oxidatively aged asphalts. Nevertheless, the data obtained provide support for the predictions of the

microstructural model with regard to oxidative aging of asphalts. A more detailed discussion of oxidative aging is included in chapters 7 and 8, where it is shown that two principal products of oxidative aging of asphalts appear to be ketones and sulfoxides. These compounds would be expected to become part of IEC base or amphoteric fractions.

## **Concentration of Quinolones by Liquid Chromatography**

One constituent of petroleum residua that is known to be amphoteric is the class of compounds known as 2-quinolones. These compounds have been identified in asphalts by spectrometric methods (Petersen et al. 1971). It is believed that 2-quinolones interact strongly by hydrogen bonding with each other, with carboxylic acids, and probably with other polar compounds.

A separation scheme for concentration of these interesting compounds therefore was developed. Quinolone concentrates make up 2-5% of the four asphalts studied. The nitrogen, oxygen, and sulfur concentrations of the 2-quinolone concentrates are much higher than in the parent asphalts. The sulfur functionality associated with 2-quinolones also is readily oxidizable to sulfoxide, as shown by infrared spectra. The  $M_n$  values of the 2-quinolone concentrates at 60°C (140°F), measured by VPO in toluene, are about twice those of the parent asphalts. Thus, a chemical fraction containing specific identifiable compounds that are definitely amphoteric exists in asphalts and has some chemical properties that resemble IEC amphoteric and strong acid fractions. The analytical data for the quinolone concentrates are in SHRP Database B (appendix B) and are discussed in a separate publication (Preece, Branthaver, and Kim 1992), which is appended to this report as appendix D.

## **Supercritical Fluid Chromatography (SFC) Studies**

Asphalts contain significant amounts of compounds that are appreciably volatile at atmosphere pressure and mix-plant temperatures, as well as large amounts of compounds that are distillable under conditions of high heat and low pressure. Most of these compounds are relatively nonpolar and aliphatic. They are not readily separated by column chromatographic methods, and are in the main not analyzable by gas chromatography (GC). Most of the distillable compounds in asphalts have carbon numbers greater than 40, which are not volatile enough for GC analysis. The novel technique of supercritical fluid chromatography (SFC) has been developed to analyze hydrocarbons in the higher carbon number range (C-40 through C-80). A supercritical fluid has the solubility power of a liquid but the mobility of a gas. The technique involves injecting a sample dissolved in a solvent into a conventional GC column using supercritical carbon dioxide as the mobile phase. Experimental details are presented in Volume IV (chapter 8) of this report. Samples must be largely free of polars, which will not be chromatographed and will become irreversibly adsorbed on the columns. IEC neutral fractions, which are largely free of polar material, are a good candidate for SFC separation.



Replicate SFC chromatograms of the IEC neutral fractions of the eight core asphalts are shown in figures 1.5 through 1.12. These data are reduced to report form in table 1.16. The IEC neutral fractions consist mostly of hydrocarbons in the C-25 to C-80 range. All contain some large hydrocarbons greater than C-80. It is difficult to quantify such large hydrocarbons in the C-80 to C-110 (limit of detectability) range because accurate response factors are not known, but such materials are not likely, based on trends in the traces in figures 1.5 through 1.12, to be present in large quantities, except in the IEC neutral fraction of AAM-1 (figure 1.12). It is unfortunate that these larger hydrocarbons cannot be accurately quantified, because they may disproportionately influence rheological properties. Carbon numbers corresponding to maximum peak heights differ greatly among the IEC fractions, as do peak widths at one-half peak height. The latter parameter is a measure of molecular weight distribution of the material. The IEC neutral fractions of AAA-1, AAD-1, and AAK-1 are of relatively low carbon number, and their SFC chromatograms are similar. The IEC neutral fractions of AAB-1 and AAG-1 also are similar and are of somewhat higher overall carbon number. The SFC chromatogram of the IEC neutral fraction of AAM-1 is very distinct and indicates that this material consists of relatively high molecular weight aromatic species. Possible reasons for this will be discussed in chapter 2.

In chapter 9, the preparation of maltenes by solvent precipitation with n-heptane followed by iso-octane is described. The iso-octane maltenes of each of the core asphalts were separated by SFC. Chromatograms are shown in figures 1.5 through 1.12. Data based on these chromatograms are listed in table 1.17. The SFC chromatograms of iso-octane maltenes resemble those of corresponding IEC neutral fractions. When equivalent amounts of materials are chromatographed, the peak heights of the maltene spectra are not as high as peak heights of the neutral fraction SFC spectra. There are more polar materials in the maltenes, which are not separated by SFC. Nevertheless, based on the SFC spectra, both materials might be treated as surrogates for asphalt solvent moieties in studies directed at verifying the microstructural model, although the IEC neutrals are definitely preferable. Figures 1.5 through 1.12 also illustrate traces of size exclusion chromatography (SEC) fractions of the core asphalts, which will be discussed in chapter 2.

## Summary

The chromatographic methods discussed herein effectively separate asphalts into defined chemical fractions (IEC) in sufficient amounts to permit further study, or can be used to obtain characteristic fractionation patterns of nonpolar asphalt fractions (SFC). Information can be obtained through these methods that cannot be obtained from any simple measurement on bulk asphalts. The results of these separations show that asphalts are composed of polar aromatic materials dispersed in a somewhat less aromatic solvent that contains relatively few polar groups. The nature of the two kinds of materials differ among asphalts. Based on the separations described above, a significant component of asphalts (15-20 mass %) consists of aromatic molecules having moderately strong acidic and basic functional groups, and these amphoteric materials engage in associations that greatly influence asphalt properties. The largest component of asphalts (50-60%) consists of relatively nonpolar molecules, which are orders of magnitude less viscous than parent asphalts. Other polar components of varying amounts, some acidic and others basic, are

found in asphalts. When asphalts are aged, more highly polar materials are formed at the expense of less polar materials. Further discussion of the relationship between the composition of these materials and physical properties is found in chapter 5.

The results of the IEC separations support the model of asphalt structure advanced in Volume I, chapter 1. The results suggest that asphalt physical properties and performance can be predicted in part by knowledge of aromaticity and  $M_n$  data of IEC neutral materials and of polarities of other IEC fractions. In particular, low-temperature properties may be greatly influenced by the nature of the nonpolar IEC neutral materials.

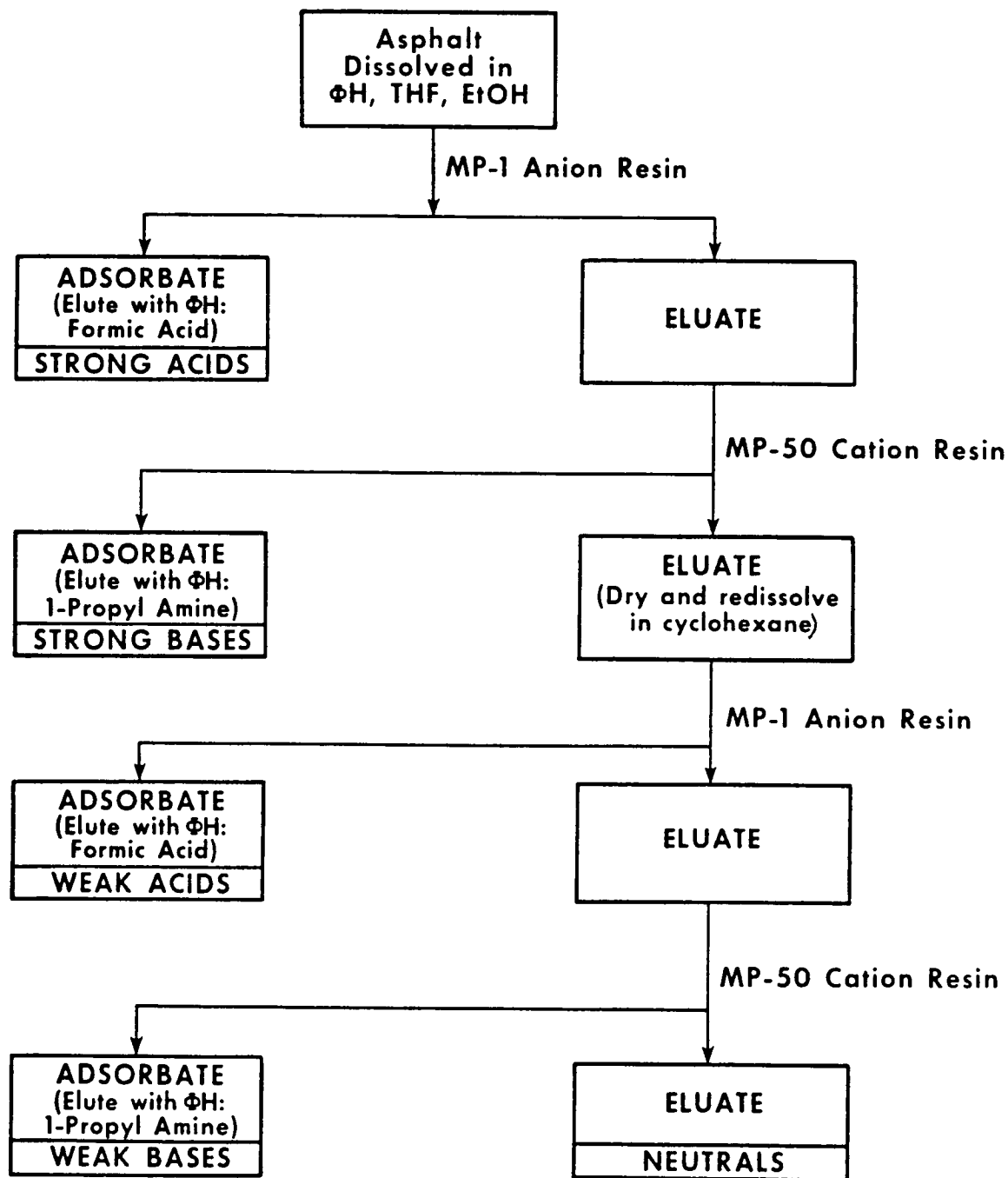


Figure 1.1. Flow Sheet for Separation of Asphalts into Five Fractions by Ion Exchange Chromatography (IEC)

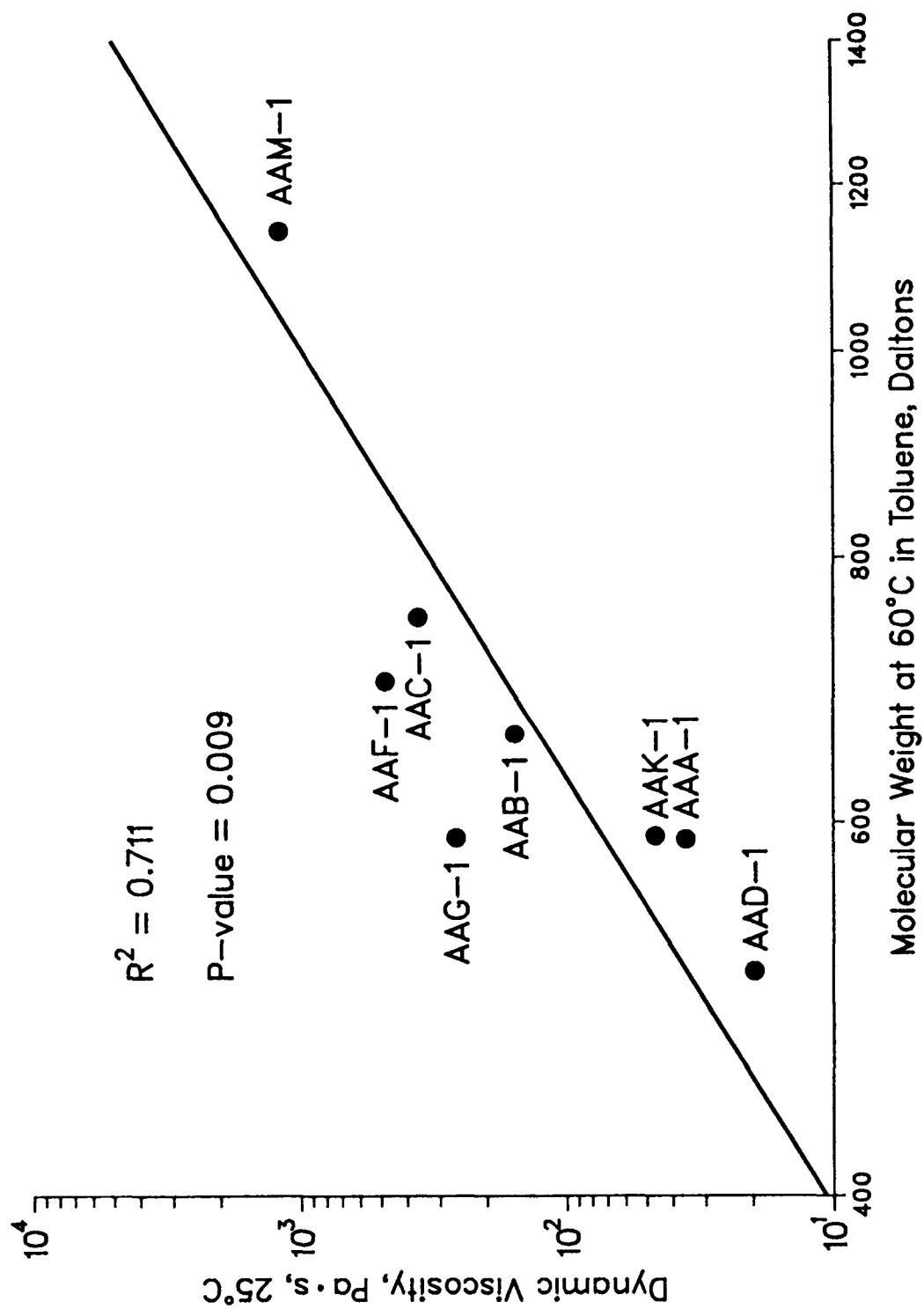


Figure 1.2 Viscosity vs. Molecular Weight for IEC Neutrals

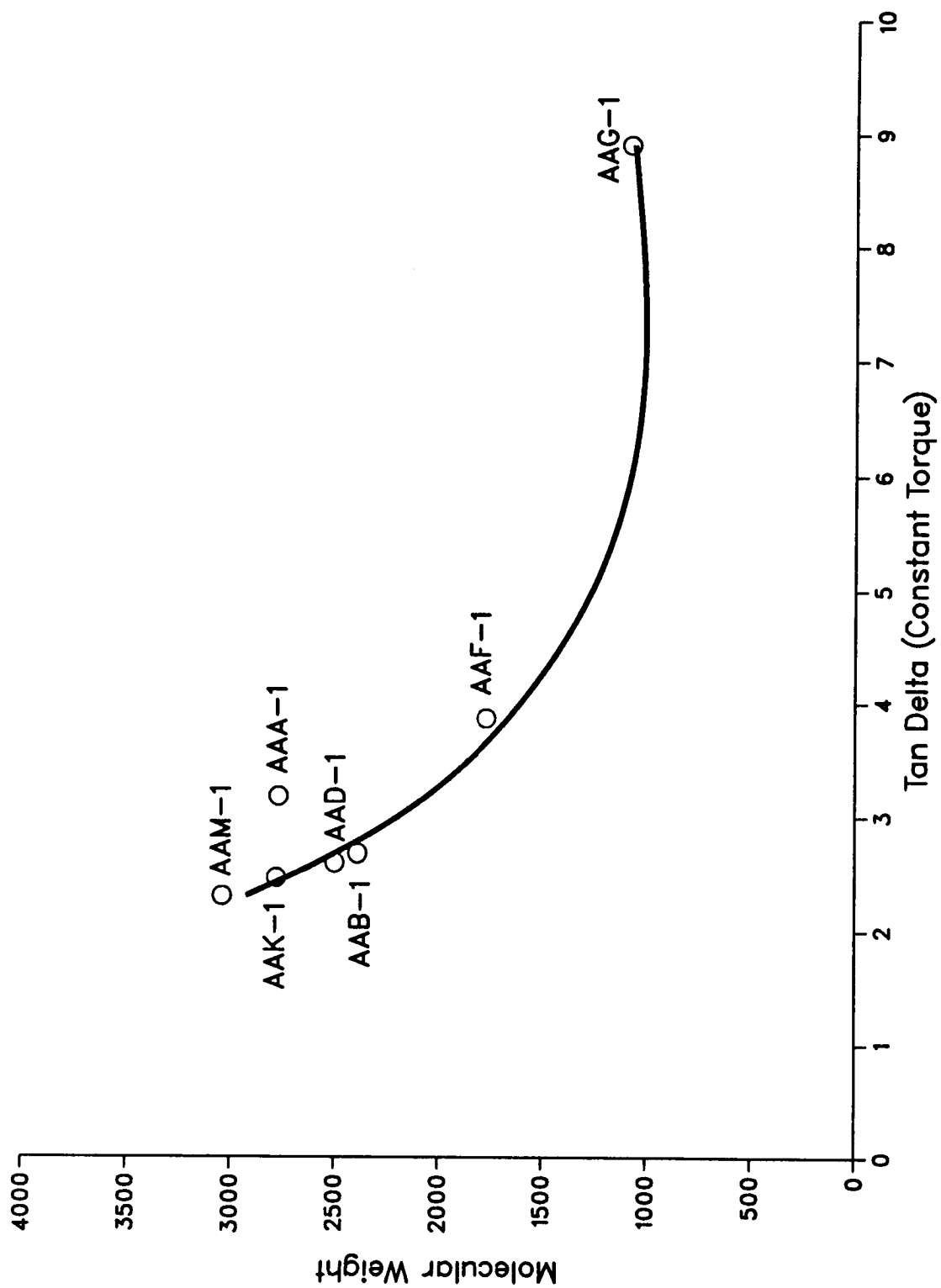


Figure 1.3 Plot of  $\tan \delta_{ct}$  Values of Seven Core Asphalts vs. Number-Average Molecular Weights of Their IEC Strong Acid Fractions

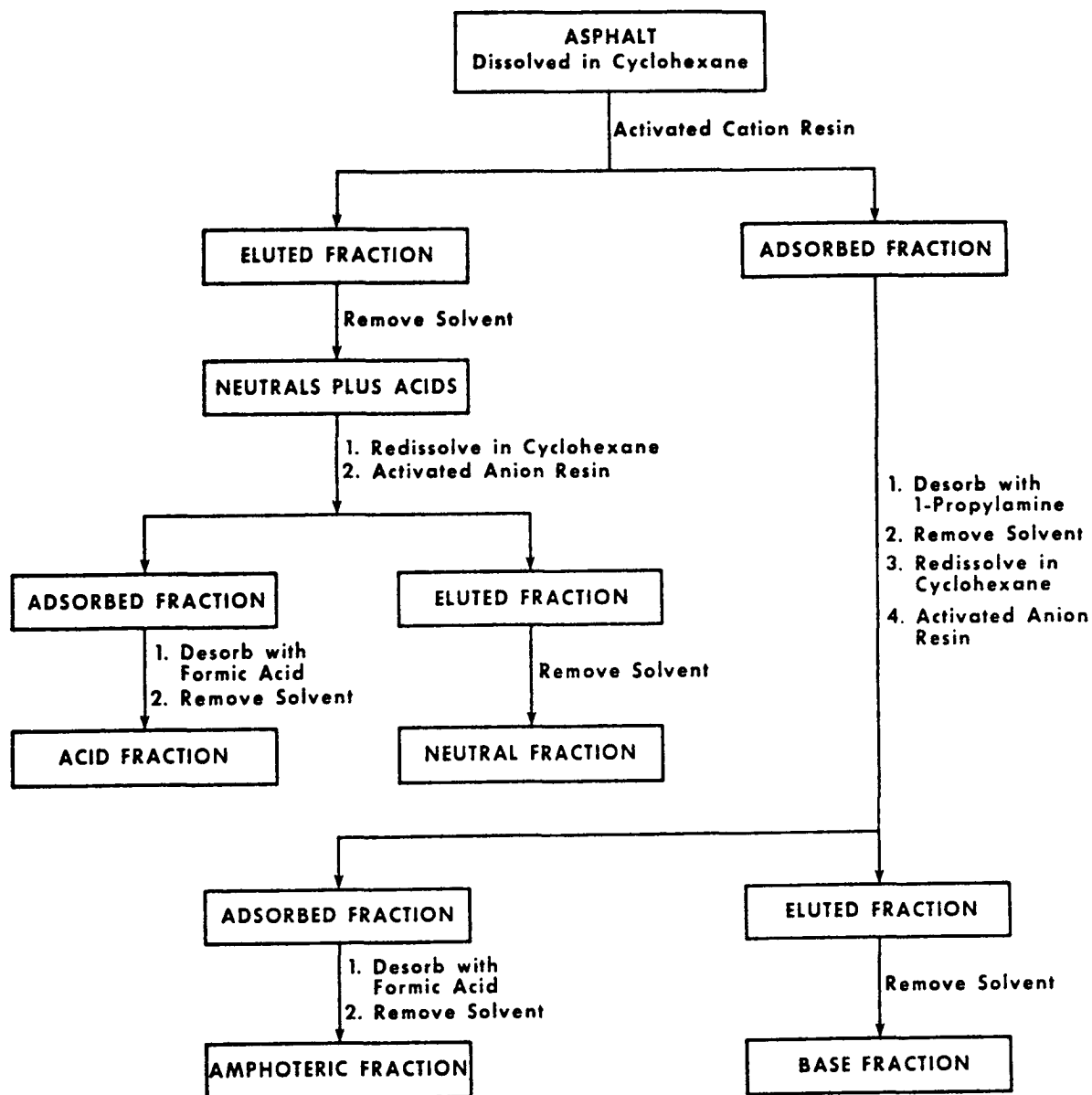
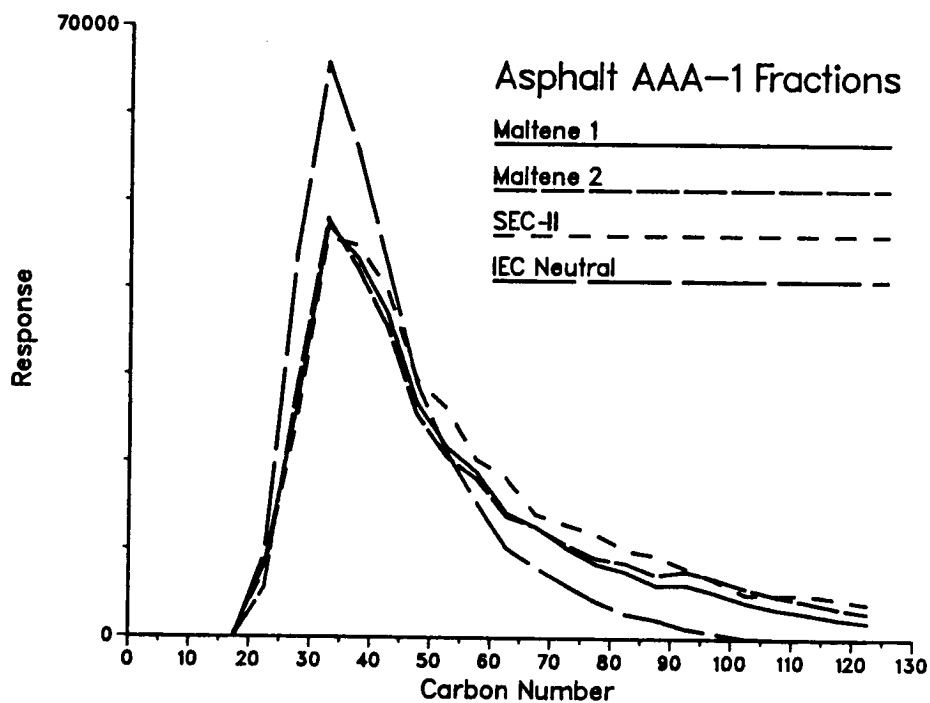
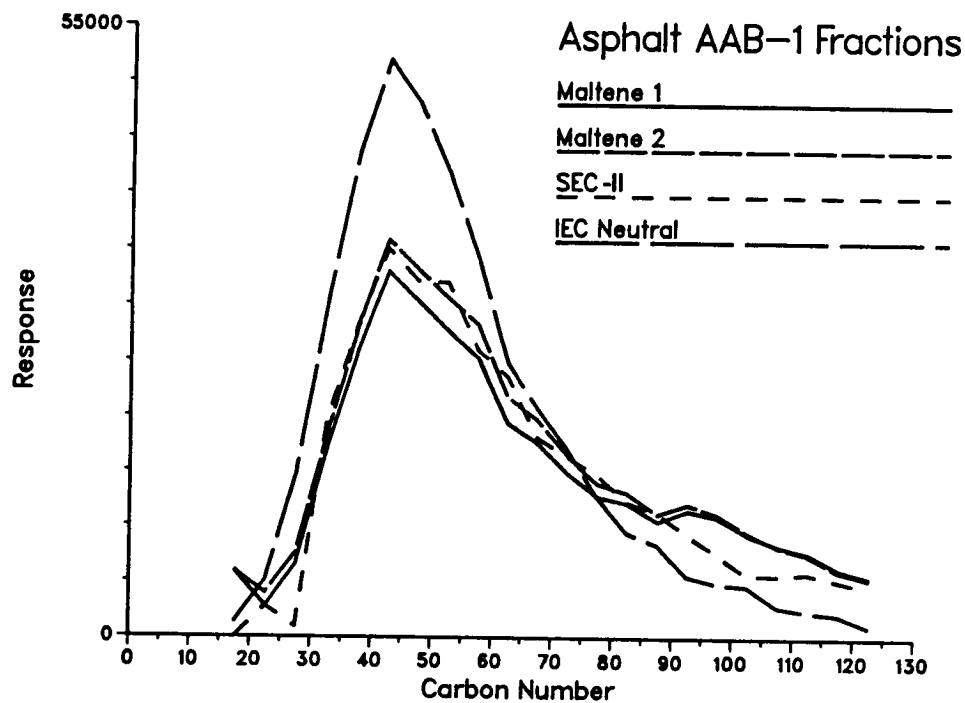


Figure 1.4 Flow Sheet for Isolation of Amphoteric by IEC



**Figure 1.5** Supercritical Fluid Chromatography (SFC) Chromatograms of IEC Neutral, Size Exclusion Chromatography (SEC) Fraction-II, and Maltene Fractions of AAA-1



**Figure 1.6** SFC Chromatograms of IEC Neutral, SEC Fraction-II, and Maltene Fractions of AAB-1

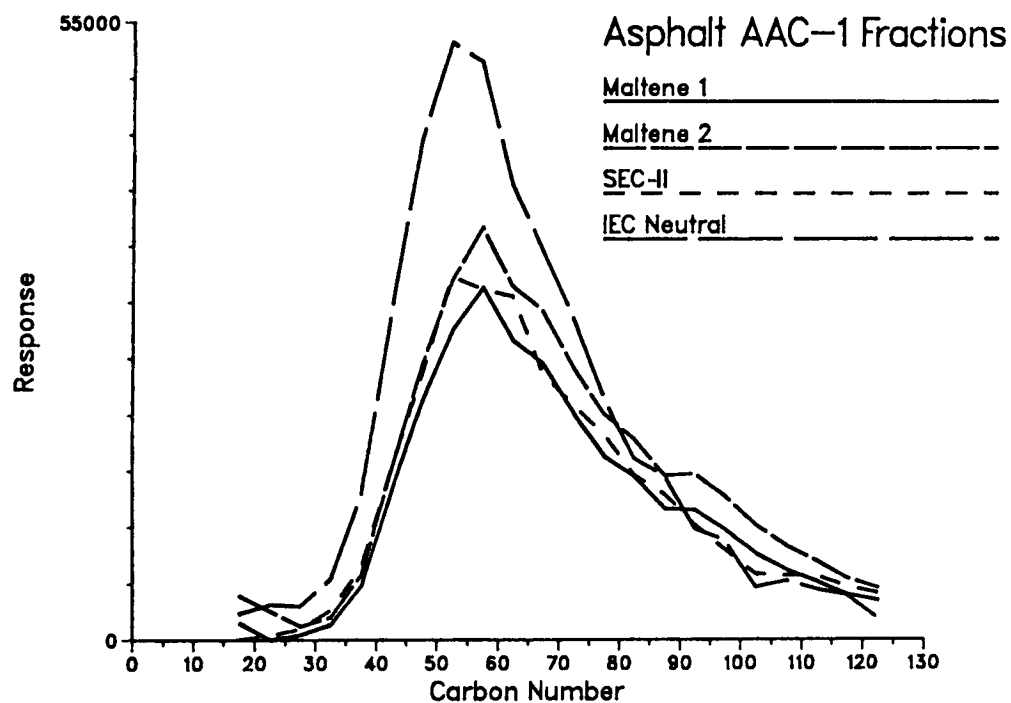


**Figure 1.7** SFC Chromatograms of IEC Neutral, SEC Fraction-II, and Maltene Fractions of AAC-1

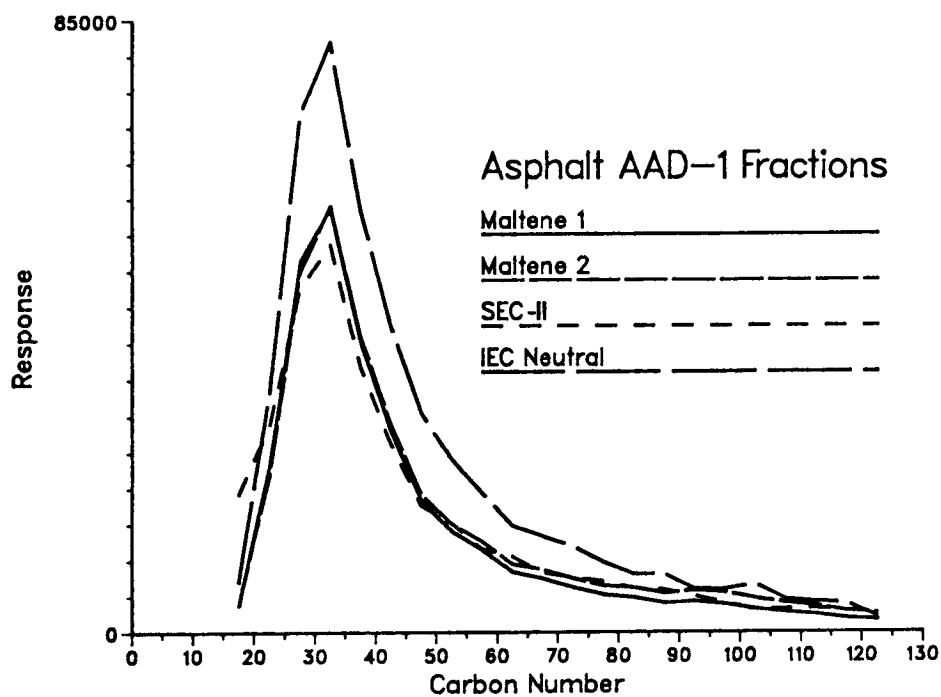


**Figure 1.8** SFC Chromatograms of IEC Neutral, SEC Fraction-II, and Maltene Fractions of AAD-1



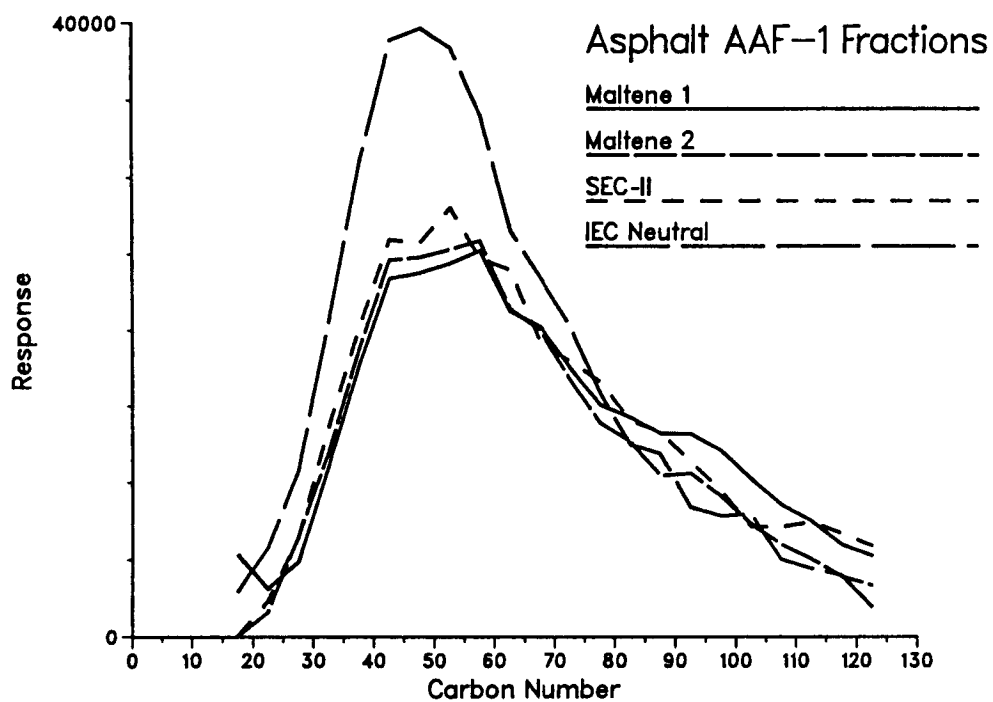


**Figure 1.9** SFC Chromatograms of IEC Neutral, SEC Fraction-II, and Maltene Fractions of AAF-1

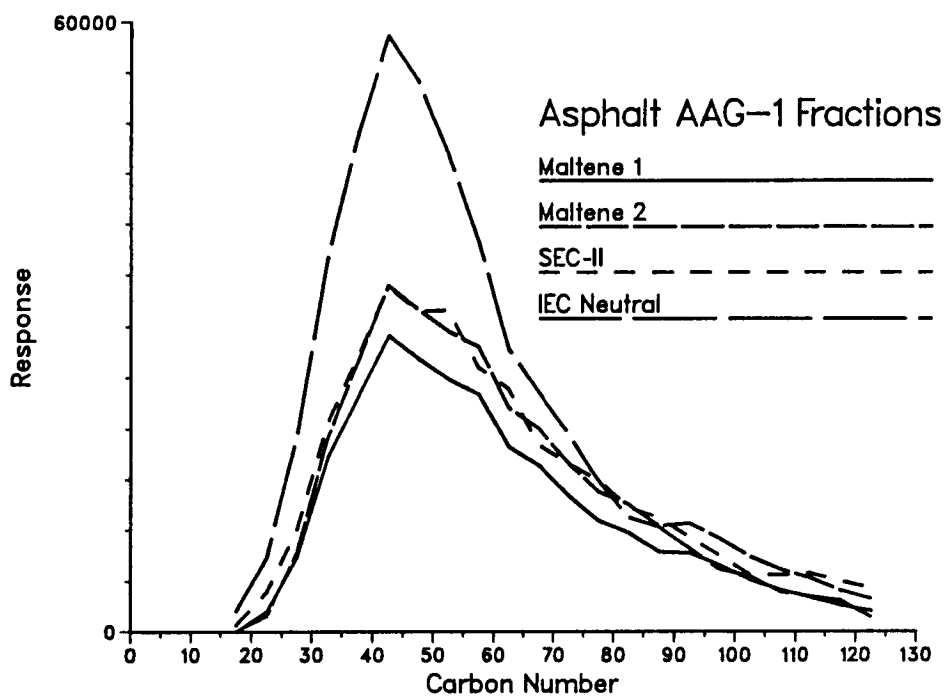


**Figure 1.10** SFC Chromatograms of IEC Neutral, SEC Fraction-II, and Maltene Fractions of AAG-1

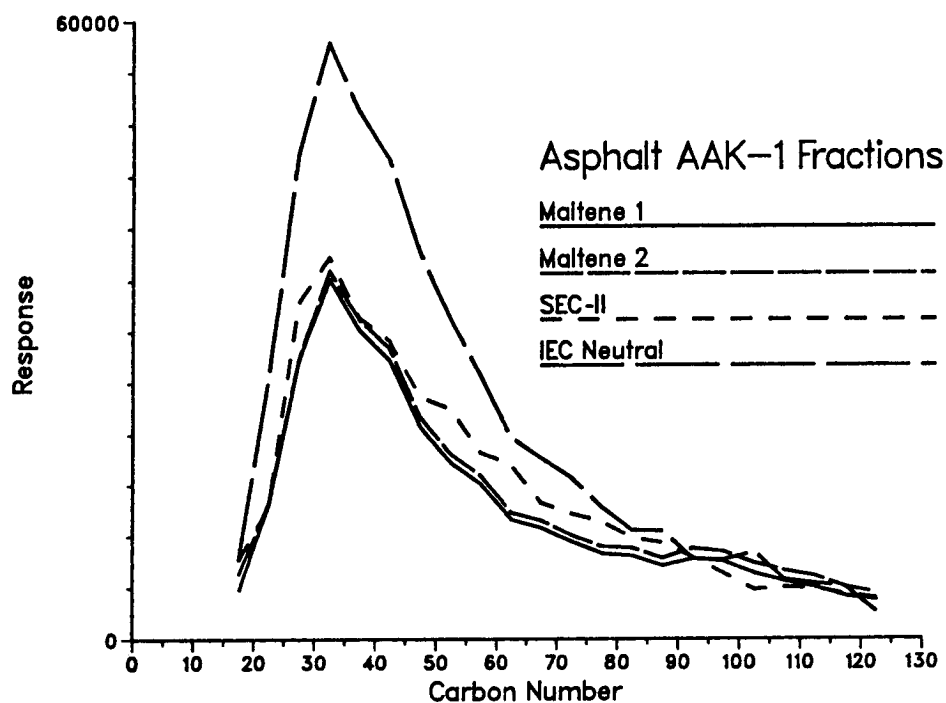


Figure 1.11 SFC Chromatograms of IEC Neutral, SEC Fraction-II, and Maltene Fractions of AAK-1

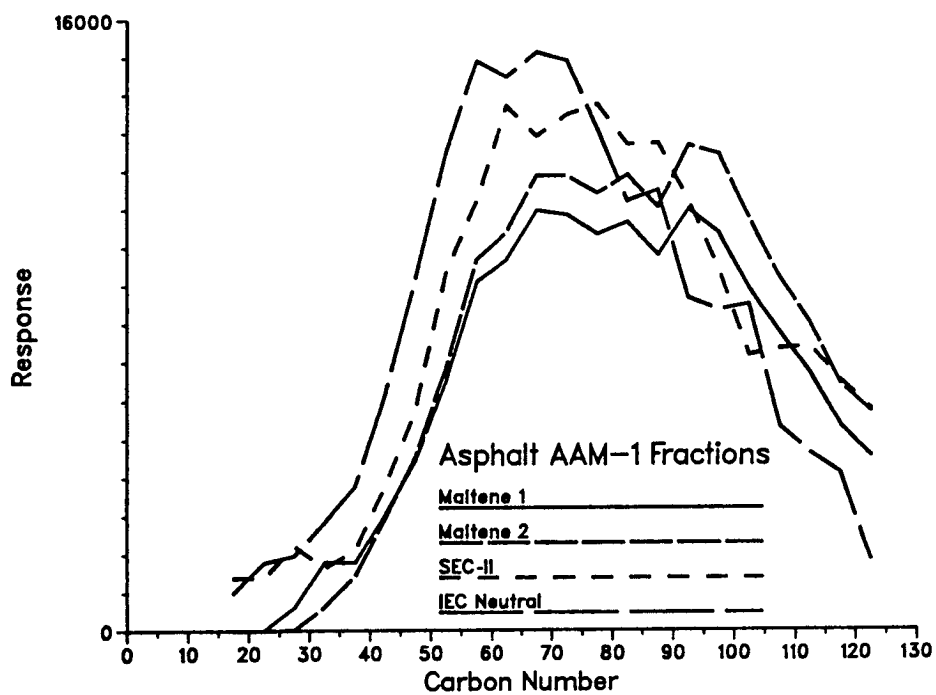


Figure 1.12 SFC Chromatograms of IEC Neutral, SEC Fraction-II, and Maltene Fractions of AAM-1

**Table 1.1 Separation of Seven Asphalts into Five Fractions by Ion Exchange Chromatography (IEC)**

Asphalt	IEC Fraction (mass %) <sup>1</sup>					Total Recovery (mass %)
	Strong Acid	Strong Base	Weak Acid	Weak Base	Neutral	
AAA-1	18.0	6.2	8.6	5.0	59.6	97.2
AAB-1	15.3	9.1	8.6	6.7	56.9	96.5
AAD-1	25.1	7.7	7.8	5.6	51.6	97.8
AAF-1	16.9	6.2	9.9	7.6	56.8	97.7
AAG-1	18.1	12.1	11.4	9.0	50.4	99.8
AAK-1	20.6	8.3	8.2	7.7	52.2	96.4
AAM-1	13.7	10.4	10.0	9.1	53.4	96.7

<sup>1</sup> Statistical treatment of these data is found in the Appendix, Supplementary Table 1.18.

**Table 1.2 Ratios of IEC Fractions for Eight Core Asphalts**

Asphalt	Ratio <sup>1, 2, 3</sup>		
	Neutral Fraction	Weakly Polar Fractions	Total Acids
	Polar Fractions	Strongly Polar Fractions	Total Bases
AAA-1	1.58	0.56	2.37
AAB-1	1.43	0.63	1.51
AAC-1	1.63	-	1.71
AAD-1	1.11	0.41	2.48
AAF-1	1.39	0.76	1.94
AAG-1	1.00	0.68	1.40
AAK-1	1.17	0.55	1.81
AAM-1	1.23	0.79	1.22

<sup>1</sup> These ratios are calculated using averages in Table 1.1.

<sup>2</sup> The polar fractions are calculated as the sum of the total acids and total bases.

<sup>3</sup> The weakly polar fractions are the sum of the weak acids and weak bases, and the strongly polar fractions are the sum of the strong acids and strong bases.

**Table 1.3 Infrared (IR) Function Group Analysis of IEC Fractions of Asphalt AAA-1**

Fraction	Run	Functional Group (Moles/L) <sup>1</sup>					
		Sulfoxides	Ketones	Carboxylic Acid	2-Quinolone	Pyrrolic N-H	Phenolic O-H
Strong Acid	1	0.06	<0.01	0.08	0.04	0.2	0.3
	2	0.10	<0.01	0.07	0.04	0.3	0.2
Strong Base	1	0.08	0.04	<0.01	0.01	0.2	0.1
	2	0.10	0.04	<0.01	<0.01	0.2	<0.1
Weak Acid	1	0.09	0.11	0.01	0.01	0.6	0.1
	2	0.13	0.07	0.02	0.02	0.6	0.1
Weak Base	1	0.19	0.25	<0.01	<0.01	0.2	<0.1
	2	0.19	0.24	<0.01	<0.01	0.2	<0.1
Neutral	1	<0.01	<0.01	<0.01	<0.01	<0.1	<0.1
	2	<0.01	<0.01	<0.01	<0.01	<0.1	<0.1

<sup>1</sup> Based on prior experience with asphalts, standard deviations are (Moles/L): sulfoxides, 0.027; ketones, 0.006; carboxylic acids, 0.005; 2-quinolones, 0.002. The analyses for N-H and O-H are qualitative.

**Table 1.4 Elemental Analyses and Molecular Weights of IEC Neutral Fractions of Eight Core Asphalts**

Parent Asphalt	Element (mass %) <sup>1</sup>					Total (mass %)	H/C	M <sub>n</sub> <sup>2</sup>
	C	H	N	O	S			
AAA-1	83.6	10.7	0.0	0.5,0.4	4.5,4.6	99.3	1.52	590
AAB-1	84.5	11.1	0.0	0.4	4.1	100.1	1.57	660
AAC-1	86.2,86.0	11.6	0.1,0.2	0.4	1.8	100.1	1.61	750
AAD-1	82.3	11.0	0.0	0.4	6.2	99.9	1.59	510
AAF-1	85.0	10.7	0.0	0.8	3.4	99.9	1.50	700
AAG-1	86.5	10.7	0.2	0.5	1.3	99.2	1.47	590
AAK-1	82.9	10.4	0.0	0.6,0.6	5.9	99.8	1.49	590
AAM-1	86.4	11.7	0.0	0.7	0.9	99.7	1.61	1,140

<sup>1</sup> Standard deviations for the elemental analyses are estimated to be (mass %): carbon, 0.36; hydrogen, 0.20; nitrogen, 0.09; oxygen, 0.41; sulfur, 0.36.

<sup>2</sup> Determined at 60 °C by vapor phase osmometry in toluene. Error bars are ± 5% for the measurements below 1,000 Daltons, and ± 10% for measurements greater than 1,000 Daltons.

**Table 1.5 Elemental Analyses and Molecular Weights of IEC Strong Acid Fractions of Seven Core Asphalts**

Parent Asphalt	Run	Element (mass %) <sup>1</sup>					Total (mass %)	H/C	M <sub>n</sub> <sup>2</sup>
		C	H	N	O	S			
AAA-1	1	81.0	7.8	0.9	2.4	6.9	99.0	1.15	2,770
	2	80.2	7.4	0.9	2.4	7.0	97.9	1.10	2,810
AAB-1	1	83.2	7.2	1.2	2.6	4.9	99.1	1.03	2,390
	2	83.0	7.4	1.4	-	-	99.3	1.06	-
AAD-1	1	79.5	8.0	1.7	2.6	7.3	99.1	1.20	2,500
AAF-1	1	82.7	7.3	1.0	2.9	4.7	98.6	1.05	1,770
AAG-1	1	83.7	8.4	1.8	3.5, 3.6	1.2	98.7	1.20	1,080
AAK-1	1	80.2	7.9	1.6	2.6	6.2	98.5	1.17	2,780
AAM-1	1	85.8	8.0	1.2	2.0	1.5	98.5	1.11	3,040

<sup>1</sup> Standard deviations for the elemental analyses are estimated to be (mass %): carbon, 0.36; hydrogen, 0.20; nitrogen, 0.09; oxygen, 0.41; sulfur, 0.36.

<sup>2</sup> Determined at 60 °C by vapor phase osmometry in toluene. Error bars are estimated to be ± 10% for these determinations.

**Table 1.6 Viscosities (Pa · s) of Core Asphalts, Their IEC Neutral Fractions, and Mixtures of IEC Fractions at 25 °C and 1.0 rad/s**

Asphalt	Run Number	Viscosity <sup>1</sup> of Whole Asphalt	Viscosity of Neutral Fraction	Viscosity of Neutral + Weak Bases + Strong Bases	Viscosity of Neutral + Weak Acids + Weak Bases	Viscosity of Neutral + Weak Acids + Weak Bases + Strong Bases
AAA-1	1	30,070	36	111	246	468
	2	-	-	-	214	-
AAB-1	1	85,020	155	-	446	1,302
AAC-1	1	74,710	360	916	-	-
AAD-1	1	39,440	20	62	73	216
	2	-	-	-	65	-
AAF-1	1	287,900	480	-	4,296	14,030
AAG-1	1	230,300	261	-	2,951	17,670
AAK-1	1	157,900	46	-	355	1,045
	2	-	-	-	368	-
AAM-1	1	230,000	1,191	2,714	3,826	15,210

<sup>1</sup> Five viscosity measurements at 25 °C and 1.0 rad/s on the Rheometrics Mechanical Spectrometer were obtained for AAK-1. A standard deviation of 2,000 Pa · s and a coefficient of variance of 2.5% were calculated for this set of measurements. For four similar viscosity determinations of AAM-1, a standard deviation of 7,500 Pa · s and a coefficient of variance of 4.7% were calculated. In these experiments and for the whole asphalts in the above table, asphalts were annealed at 150 °C for 1 hour, and then were cooled. Measurements were completed before two more hours elapsed. As a general rule, viscosity determinations on the Rheometrics Mechanical Spectrometer are believed to be accurate to ± 10%.

**Table 1.7 Molecular Weights by Vapor Phase Osmometry in Toluene at 60 °C for Strong Acid Fractions of Seven Core Asphalts Compared with Tan  $\delta_{ct}$  Values for Whole Asphalts at 25 °C**

Parent Asphalt	Run No.	Molecular Weight (Daltons) <sup>1</sup>	Tan $\delta_{ct}$ <sup>2</sup>
AAA-1	1	2,770	3.18
	2	2,810	-
AAB-1	1	2,390	2.68
AAD-1	1	2,500	2.60
AAF-1	1	1,770	3.87
AAG-1	1	1,080	8.91
AAK-1	1	2,780	2.47
AAM-1	1	3,040	2.31

<sup>1</sup> ASTM Method D2503 is estimated to have an error of  $\pm 10\%$  at this molecular weight range.

<sup>2</sup> Ratio of Viscous ( $G''$ ) to Elastic ( $G'$ ) Modulus. A standard deviation of 0.020 for tan  $\delta$  was calculated from data for AAK-1 and AAM-1.



**Table 1.8 Mass Fractions of Amphoteric, Base, Acid, and Neutral Fractions Isolated from Four Core Asphalts by IEC**

Asphalt	Operator Initials and Run Number	IEC Fraction (mass %)					Total Recovery (% of Charge)	
		Amphoterics plus Bases	Amphoterics	Bases	Neutrals plus Acids	Acids		Neutrals
AAD-1	MC1		25.9	9.3	59.8			95.0
	SK1		25.5	9.5	60.4			95.4
	MC2		25.0	8.6	62.2			96.7
	SK2		25.8	7.7		8.6	54.0	96.0
	DG1		22.3	12.1		7.3	53.1	94.9
	Avg. + Std. Dev.		24.9±1.3	9.4±1.5	60.8±1.0	8.0	53.6	95.6±0.7
AAG-1	MC3		18.6	13.3	66.4			98.3
	SK3		18.4	10.7	68.8			98.0
	DG2		18.8	12.9		13.4	51.9	96.9
	DG3		18.2	13.1		15.3	52.8	99.5
	Avg. + Std. Dev.		18.5±0.2	12.5±1.0	67.6	14.4	52.4	98.2±0.9
	AAK-1	MC4		24.1	9.6	61.7		
SK4			24.6	10.9	61.5			97.1
SK5			24.2	8.7		8.1	53.8	94.8
DG4			23.5	12.9	59.0			95.4
DG5			17.9	7.3		7.6	55.2	90.5
Avg. ± Std. Dev.			22.9±2.5	9.88±1.9	60.7±1.2	7.9	54.6	94.6±2.2
AAM-1	MC5		18.9	15.6	63.9			98.5
	SK6		18.1	12.9	66.1			97.1
	SK7		18.9	13.4		10.0	54.0	96.3
	DG6	34.5				8.5	56.5	99.4
	Avg. + Std. Dev.		18.6±0.4	14.0±1.2	65.0	9.3	55.3	97.8±1.2

**Table 1.9 Infrared Functional Group Analysis for IEC Amphoteric, Base, and Neutral Plus Acid Fractions of Four Core Asphalts<sup>1</sup>**

Asphalt	IEC Fraction	Functional Group Concentration, Moles/L					
		Sulfoxides	Ketones	Carboxylic Acids	2-Quinolones	Pyrrolic N-H	Phenolic O-H
AAD-1	Neutrals Plus Acids	0.05	<0.01	0.01	<0.01	0.2	<0.1
	Bases	0.15	0.17	<0.01	<0.01	0.2	<0.1
	Amphoterics	0.09	<0.01	0.02	0.07	0.4	0.1
AAG-1	Neutrals Plus Acids	0.05	<0.01	0.05	<0.01	0.3	0.1
	Bases	0.08	0.13	<0.01	<0.01	0.2	<0.1
	Amphoterics	0.08	<0.01	0.03	0.07	0.6	0.1
AAK-1	Neutrals Plus Acids	0.08	<0.01	0.02	<0.01	0.1	<0.1
	Bases	0.15	0.10	<0.01	<0.01	0.2	<0.1
	Amphoterics	0.10	<0.01	0.06	0.04	0.3	<0.1
AAM-1	Neutrals Plus Acids	<0.01	<0.01	<0.01	<0.01	0.2	<0.1
	Bases	0.08	0.10	<0.01	<0.01	0.2	<0.1
	Amphoterics	0.06	<0.01	0.02	0.02	0.3	<0.1

<sup>1</sup> Based on prior experience with asphalts, standard deviations (Moles/L) are: sulfoxides, 0.027; ketones, 0.006; carboxylic acids, 0.005; 2-quinolones, 0.002. Analyses of N-H and O-H are qualitative.

**Table 1.10 Molecular Weights of IEC Amphoteric and Base Fractions**

Asphalt	Run No.	Fraction	Molecular Weight (Daltons) <sup>1</sup>	
			Toluene	Pyridine
AAD-1	1	Amphoteric	2,960	2,260
		Base	1,100	1,100
	2	Amphoteric	2,930	2,180
		Base	1,060	1,200
AAG-1	1	Amphoteric	1,540	1,170
		Base	880; 880 <sup>2</sup>	-
	2	Amphoteric	1,620	1,240
		Base	815	835
AAK-1	1	Amphoteric	3,690	2,730
		Base	1,260; 1,240 <sup>2</sup>	1,340
	2	Amphoteric	3,540	2,160
		Base	1,300	1,350
AAM-1	1	Amphoteric	3,560	insol.
		Base	1,740	insol.
	2	Amphoteric	3,410	insol.
		Base	1,670	insol.

<sup>1</sup> These analyses were performed by vapor phase osmometry at 60 °C, and the results are number-average molecular weights. Error bars are estimated to be  $\pm 5\%$  for values below 1,000 Daltons, and  $\pm 10\%$  at the higher values.

<sup>2</sup> Replicate determinations

**Table 1.11 Carbon, Hydrogen, and Nitrogen Contents of Amphoteric Fractions**

Parent Asphalt	Run No.	Element (mass %) <sup>1</sup>			H/C ratio
		C	H	N	
AAD-1	1	80.3	8.6	1.9	1.28
	<u>2</u>	<u>81.1</u>	<u>8.6</u>	<u>1.9</u>	<u>1.26</u>
	Avg.	80.6	8.6	1.9	1.27
AAG-1	1	84.7	8.4	2.5	1.18
	2	84.8	8.6	2.5	1.21
	3	<u>84.8</u>	<u>8.6</u>	<u>2.4</u>	<u>1.21</u>
	Avg. + St. Dev.	84.8 ± 0.1	8.5 ± 0.1	2.5 ± 0.1	1.20 ± 0.01
AAK-1	1	81.5	8.3	1.7	1.21
	2	78.5	8.2	1.6	1.24
	3	81.2	8.2	1.9	1.20
	4	80.9	8.2	2.0	1.19
	5	<u>80.6</u>	<u>8.1</u>	<u>2.0</u>	<u>1.20</u>
	Avg. + Std. Dev.	80.5 ± 1.1	8.2 ± 0.1	1.8 ± 0.2	1.21 ± 0.02
AAM-1	1	88.0	8.5	1.2	1.15
	2	<u>86.4</u>	<u>8.6</u>	<u>1.1</u>	<u>1.19</u>
	Avg.	87.2	8.6	1.2	1.17

<sup>1</sup> Analyses for C, H, and N are by a standard method and their standard deviations are (mass %): carbon, 0.36; hydrogen, 0.20; nitrogen, 0.09.

**Table 1.12 Nuclear Magnetic Resonance (NMR) Analysis of IEC Amphoteric Fractions of Four Core Asphalts**

Asphalt	Run No.	% Aromatic Carbon		% Aromatic Hydrogen	
		Tank Asphalt <sup>1</sup>	Amphoteric Fraction <sup>2</sup>	Tank Asphalt <sup>1</sup>	Amphoteric Fraction <sup>2</sup>
AAD-1	1	23.7	41.1	6.8	7.1
	2		45.0		8.1
AAG-1	1	28.3	49.3	7.3	11.8
	2		51.8		12.9
AAK-1	1	31.9	44.8	6.8	8.3
	2		43.6		6.2
AAM-1	1	24.7	47.1	6.5	9.4
	2		46.1		9.2

<sup>1</sup> Data obtained from Montana State University

<sup>2</sup> Errors are estimated to be  $\pm 10\%$

**Table 1.13 Viscosities (Pa · s) of Mixtures of Four Core Asphalts with Their IEC Amphoteric, Base, Acid, or Neutral Fractions at 60°C and 1.0 rad/s**

Asphalt	Run Number	Viscosity <sup>1</sup> of Asphalt	Viscosity of Asphalt + Amphoterics	Viscosity of Asphalt + Bases	Viscosity of Asphalt + Acids	Viscosity of Asphalt + Neutrals
AAD-1	1	131	2,462	327	174	37
	2	-	2,815	301	212	43
AAG-1	1	240	1,740	346	285	132
	2	-	1,139	402	437	129
AAK-1	1	413	6,836	656	517	110
	2	-	6,755	1,004	550	124
AAM-1	1	258	4,032	399	292	140
	2	-	3,901	470	342	135

<sup>1</sup> Viscosities measured on the Rheometrics Mechanical Spectrometer are estimated to have an error bar of  $\pm 10\%$ .

**Table 1.14 Viscosities (Pa · s) of Mixtures of Neutral Plus Acid and Base Fractions of Four Asphalts at Three Temperatures Compared with Viscosities of Parent Asphalts at 1 rad/s**

Asphalt	Run No.	Viscosity of Asphalt <sup>1</sup>			Tan $\delta$ , <sup>2</sup> Asphalt (25 °C)	Viscosity of Mixture			Tan $\delta$ , Mixture (25 °C)
		25 °C	45 °C	60 °C		25 °C	45 °C	60 °C	
AAD-1	1	40,570	1,083	130.8	2.60	1,264	54.3	10.1	17.09
	2	-	-	-	-	1,950	72.6	14.4	10.83
AAG-1	1	354,000	3,202	239.9	8.91	41,260	559.3	57.6	97.85
	2	-	-	-	-	34,360	569.7	62.4	129.1
AAK-1	1	81,050	4,203	412.7	2.47	7,272	220.9	35.4	14.01
	2	-	-	-	-	2,850	121.7	20.8	14.04
AAM-1	1	161,550	2,769	258.0	2.31	18,450	318.7	51.4	12.48
	2	-	-	-	-	15,770	243.0	43.8	13.84

<sup>1</sup> Standard deviations of 1,700 Pa · s for AAK-1, and 5,200 Pa · s for AAM-1 were determined for measurements at 25 °C.

<sup>2</sup> A standard deviation of 0.020 at 25 °C was determined from data for AAK-1 and AAM-1.

**Table 1.15 Mass Fractions of Amphoterics, Bases, and Neutrals Plus Acids Isolated from Four Asphalts Aged by Thin-Film Oven Pressure Air Vessel (TFO-PAV) (60°C, 144 hours), by IEC**

Asphalt	Run No.	IEC Fraction (mass %)			Total Recovery, % of Charge
		Amphoterics	Bases	Neutrals Plus Acids	
AAD-1	1	30.7	14.2	48.9	93.8
	2	23.5	16.4	47.7	87.6
AAG-1	1	24.7	16.7	55.5	96.9
AAK-1	1	26.4	16.6	50.4	93.4
	2	23.9	16.8	50.8	90.2
AAM-1	1	27.4	14.5	55.9	97.8
	2	21.1	17.4	55.9	94.5

**Table 1.16 Peak Height Maxima and Width at One-Half Maximum Height in SFC Chromatograms of IEC Neutral Fractions of Eight Asphalts, and Number-Average Molecular Weights of IEC Neutral Fractions**

Parent Asphalt of IEC Neutral Fraction	Peak Maximum, Carbon Number	Width of Carbon Numbers at One-Half Height of Peak Maximum	Molecular Weight ( $M_n$ ) <sup>1</sup> of IEC Neutral Fraction (Daltons)
AAA-1	33	20.5	590
AAB-1	43	30.7	660
AAC-1	52	32.0	750
AAD-1	33	19.2	510
AAF-1	48	41.0	700
AAG-1	43	30.7	590
AAK-1	33	30.7	590
AAM-1	65	60.2	1,140

<sup>1</sup> ASTM Method D 2503 is estimated to have an error bar of  $\pm 10\%$  in the molecular weight range over 1,000 Daltons and  $\pm 5\%$  below 1,000 Daltons

**Table 1.17 Peak Height Maxima and Width at One-half Maximum Height in SFC Chromatograms of Iso-octane Maltenes of Eight Asphalts**

Parent Asphalt of SEC Low MW Fraction	Run No.	Peak Maximum Carbon Number	Range of Carbon Numbers at One-Half Height of Peak Maximum
AAA-1	1	33	27-52
	2	33	27-52
AAB-1	1	43	33-71
	2	43	33-71
AAC-1	1	58	44-80
	2	58	45-83
AAD-1	1	33	24-43
	2	33	24-43
AAF-1	1	58	33-88
	2	58	33-88
AAG-1	1	43	31-70
	2	43	33-73
AAK-1	1	33	24-53
	2	33	24-53
AAM-1	1	92	50- >110
	2	92	50- >110



## 2

# Size Exclusion Chromatography Separations of Asphalts

### Introduction

The microstructural model proposed for asphalt (Volume I, Chapter 1) suggests that polar and aromatic molecules in asphalt interact through relatively weak attractive forces (compared with intramolecular covalent bonding) to form molecular associations. One consequence of the formation of molecular associations is that the associations have effective molecular weights considerably larger than the true molecular weights of their component individual molecules. The molecular associations also have hydrodynamic volumes much larger than most unassociated molecules found in asphalt; therefore, a separation of associated from non-associated species should be possible by techniques that separate mixtures into fractions of different molecular size. The most common such method is size exclusion chromatography (SEC), also known as gel permeation chromatography (GPC). Separations of solutions of asphalts into fractions of varying molecular sizes by means of SEC and correlation of SEC fractionation behavior with asphalt properties have been reported by a number of workers (Altgelt and Hirsch 1970; Bynum and Traxler 1970; Haley 1975; Reerink and Lijzenga 1975; Huynh et al. 1978; Brule, Raymond, and Such 1986; Beazley, Hawsey, and Plummer 1987; Donaldson et al. 1988; Jennings et al. 1988; Bishara, McReynolds, and Lewis 1991). The existence of many reports of earlier asphalt separations by SEC was one reason for the emphasis on SEC separations in the Strategic Highway Research Program.

According to the microstructural model the intermolecular forces that hold asphalt molecular associations together are hydrogen bonds and other interactions between polar molecules. Because these forces are much weaker than intramolecular covalent bonds, the technique used to separate asphalt associating from nonassociating components must disturb the associations as little as possible. During an SEC separation of a solution of an asphalt at ambient temperatures, the solvent used would be the most likely agent for breaking up the associations and must be chosen with care. Therefore, the solubility parameter of the solvent used in an SEC experiment should resemble that of the asphalt's natural solvent moiety as closely as possible. In addition, the solvent must be relatively low-boiling and nonpolar because it is necessary to obtain associated materials free of solvent for subsequent studies. The solvent chosen was toluene, which has a solubility parameter of 8.9, believed to approximate the average solubility parameter of asphalt solvent moieties. Analytical SEC separations of small amounts of asphalts commonly use tetrahydrofuran, a

much more polar solvent than toluene. However, the objectives of these separations are not the preservation of natural asphalt molecular associations to the greatest possible extent. It would be ideal to separate asphalts into fractions by SEC without use of any solvent. The high viscosities of asphalts preclude such separation.

All SEC separations operate on the principle that the column packing material behaves somewhat like a molecular sieve. In the separations described below, column packings are particles of cross-linked copolymers of styrene and divinyl benzene that swell when in contact with organic liquids of appropriate polarity. The swelled column packings, or gels, are porous, and the sizes of the pores vary over a wide range. As a solution of an asphalt passes through a column of swelled gel particles, molecules (or associations of molecules) that are small enough may enter into some of the pores of the gel, and reside there for a time, and thus are slowed in their passage through the column. The smaller the molecule, the more pores it can enter into and the longer it takes to pass through the column. Molecules (or associations of molecules) that are too large to enter any of the pores of the gel pass through the column between the gel particles without experiencing any residence time within the gel pores. Obviously, the pore size distribution of the gel used in an SEC separation must be chosen based on an estimate of the molecular size distribution of the mixture to be separated.

In practice, all of the molecules (or associations of molecules) that are excluded from the pores pass through the column in one initially collected "slug" and all others are spread out according to size, with the smallest molecules emerging from the column last. If asphalt associations are extremely weak and largely broken up by dissolution in toluene, SEC separation will separate molecules according to molecular sizes only, and isolation of associations by SEC will fail. If a gel with the correct pore size distribution is chosen for the separation, associations not broken up by dissolution will be separated from nonassociated molecules by SEC. The fractionation pattern of the materials separated by SEC is a function of the pore size distribution and average pore size of the gel used in the separation.

## **SEC Separations in the Binder Characterization and Evaluation Program**

It was proposed from the beginning of the Binder Characterization and Evaluation Project (A-002A) that two kinds of SEC separations of asphalts be attempted. The first is a preparative procedure used to obtain fractions of sufficient size that they could be analyzed by methods requiring large amounts of sample. This procedure became known in this project as preparative SEC, or PSEC. Because it was desired to obtain fractions containing as much of the larger molecular associations as possible, the pore size of the gel was critical to the success of the project. Tests of column packings of several pore sizes showed that Bio-Rad Bio-Beads S-X1, with a molecular weight exclusion limit of 14,000 daltons (a pore size of about 170 Å), was best suited for PSEC separations. A method to differentiate between molecular associations and the rest of the asphalt while separations were in progress was also necessary. The method that was used is based on the principle that some polar molecules found in asphalt are highly aromatic hence their solutions should fluoresce under the influence of ultraviolet (UV) radiation. However, if some of these

polar, aromatic molecules become part of molecular associations, fluorescence is largely quenched. The fluorescence of organic dyes in solution and in the solid state is discussed by Langhals, Demming, and Potrawa (1991), who claimed there is no general theory to explain fluorescence quenching effects. They stated that when molecules containing chromophoric groups associate, electronic energy is lost to thermal vibrations. Therefore, as an SEC separation of an asphalt solution progresses, a zone that is weakly fluorescent should be eluted initially, followed by more strongly fluorescent materials, assuming the validity of the microstructural model. If the model is invalid, or if molecular associations are largely broken up during SEC separation, the above pattern of fluorescence as a function of elution volume would be unlikely to be observed.

The second approach arose from the need for an analytical technique that could be completed in a short time and yield results that could be compared with data obtained by other workers. This procedure uses high performance liquid chromatography (HPLC) equipment and became known as fast SEC or analytical SEC. A pair of small columns are used that contain gels with pore sizes of 10,000 Å and 1,000 Å respectively. Detectors used included differential refractive index (DRID), fluorescence, and UV/visible diode array (DAD).

Later in the project, a third procedure was developed that uses small preparative columns. This procedure separates samples of asphalts larger than are analyzed in the fast SEC technique, but not nearly as large as the samples processed in the preparative method. Detection is gravimetric. This procedure known as streamlined preparative size exclusion chromatography (SPSEC) is discussed below.

## **Preparative Size Exclusion Chromatography**

The detailed experimental procedure for this method is given in Volume IV, Chapter 9. In brief, a water-jacketed column 5 cm inner diameter (ID) by 102.4 cm long was packed with Bio-Rad Bio-Beads S-X1 swelled in toluene. Column temperatures usually were 40°C (104°F). The column was calibrated using various high molecular weight molecules of known structure. For asphalt separations, 16 g asphalt in 150 mL toluene was charged into the bottom of the column at a flow rate of 3.5 mL/min. At this rate, each separation takes several hours to complete. Either two or nine fractions were collected, depending on the objectives of the particular separations. In either case SEC Fraction-I (the first eluting fraction) was always the same, with the cutpoint between SEC Fraction-I and subsequent fractions determined by the point at which the eluate reached a uniform brightness of fluorescence in response to 350 nm light. This point is very sharp for most unaged asphalts. For aged asphalts and some unaged asphalts there is a transition zone in which fluorescence gradually increases with elution volume of solute. The cutpoint for these asphalts is therefore somewhat operator-dependent. When nine total fractions were collected, all fractions after the first consisted of 200 mL volumes of eluate each. When only two fractions were collected, the fluorescent material, SEC Fraction-II, consisted of 1600 mL of eluate. Solvent removal was accomplished using a rotary evaporator under vacuum. After solvent removal, the samples were weighed and then stored under an inert gas atmosphere.

Recoveries of material are virtually quantitative. Any losses are due to loss of volatiles in workup and not to irreversible adsorption on the gel. In this respect, PSEC has an advantage over ion exchange chromatography (IEC) in asphalt separation. As much as 6% or more of some asphalts become irreversibly adsorbed to the resins used in IEC (chapter 1). The excellent material recoveries are another reason for the emphasis on SEC separation in the Binder Characterization and Evaluation Program.

Mass percentages of each of nine SEC fractions of the core asphalts are listed in table 2.1. Two identical columns packed with Bio-Beads S-X1 gel were used, and four different operators performed the separations. Averages of several runs for each asphalt are reported in table 2.1, and results are satisfactorily reproducible. For the larger SEC fractions, deviations of over 5.0 mass % of averages of several runs seldom were observed. For fractions containing little material, somewhat more variance was noted. The mass percentage data in table 2.1 are plotted vs. elution bed volumes corresponding to each of the SEC fractions in figure 2.1. In the plots in figure 2.1, the first point nearest the origin on the x-axis represents initial breakthrough of colored eluates, has zero weight, and corresponds to about 21% of the total column bed volume. The second point from the origin (based on distance along the x-axis) corresponds to the column bed volume at which SEC Fraction-I has been completely collected. Elution bed volume for these nonfluorescent materials is about 35-40% of the total column bed volume. Subsequent points plotted along the x-axis are at an additional 10.38% total column bed volume, after which each of the later fractions has been completely collected. The y-axis values of each point correspond to the masses of each of the fractions. The points in the plots are connected for purposes of illustration in figure 2.1. It should be emphasized that the plots have been designed to emphasize relative amounts of SEC Fraction-I materials, as the second data point corresponds to more volume of eluate than subsequent data points. The graphs also do not plot cumulative masses of material collected and so further emphasize bimodal mass distributions of SEC Fraction-I and the fractions collected subsequently (collectively designated SEC Fraction-II). In the following discussions, these plots are also referred to as SEC chromatograms.

Seven of the plots in figure 2.1 exhibit bimodal distributions of mass fractions. Inspection of these bimodal distributions allows a rough measure of the relative amounts of asphalt dispersed and solvent moieties. The dispersed components can be considered to be the materials eluted up to the second data point of each of the chromatograms. These plots show that each asphalt has a distinctive molecular size distribution, as defined by SEC.

Number-average molecular weight ( $M_n$ ) data (determined in toluene by vapor phase osmometry at 60°C/140°F) and mass fraction data for the first six fractions (of the nine fraction separations) eluted in the SEC separations of the eight core asphalts are listed in table 2.2. There was not enough material in the last three fractions for determination of  $M_n$  values. The molecular weight values for each fraction were multiplied by the mass fractions, and these products were summed for each of the asphalts to obtain approximate weight-average molecular weight ( $M_w$ ) values (Gratzfeld-Husgen 1989). For materials composed of large molecules, this latter value is a good indicator of mechanical strength. It may be possible to relate these indirectly obtained  $M_w$  values to important asphalt physical

properties. Because of the nature of asphalts, direct measurement of  $M_w$  by standard methods is virtually impossible.

Noted in table 2.2 the relatively large (compared with the molecular weights of the succeeding fractions)  $M_n$  values of the initial SEC fractions (SEC Fraction-I), which vary considerably among the eight asphalts. The values of  $M_n$  progressively decrease, as expected, for each succeeding SEC fraction of each of the asphalts. A discussion of the problems involved in  $M_n$  determinations of petroleum fractions by VPO is presented in chapter 9.

It is therefore believed that the asphalt dispersed phases have been effectively separated from the asphalt solvent phases by PSEC in the case of the seven asphalts characterized by bimodal plots in figure 2.1. The SEC chromatogram of asphalt AAM-1, however, is not bimodal. There are reasons to believe that this asphalt contains substantial amounts of molecules of relatively high true molecular weight (Jennings et al. at press). Of all of the asphalts tested, AAM-1 contains the most SEC Fraction-I materials. However, AAM-1 is peculiar in that its asphaltene content is low (chapter 9, table 9.6), which shows that asphaltene and SEC Fraction-I materials are not identical. Asphaltenes are operationally defined by solvent precipitation, as discussed in Volume I, chapter 1. In discussions of models of asphalt structure, asphaltenes are sometimes considered to be representative of dispersed moieties. For AAM-1, this is obviously not the case. For the other seven asphalts, yields of SEC Fraction-I (table 2.1) are similar to or slightly higher than yields of heptane plus iso-octane asphaltenes (chapter 9, table 9.6). Presumably most, but not all, components of asphaltenes will be included in the SEC Fraction-I of a particular asphalt. However, as AAM-1 illustrates, there can be much material of high apparent  $M_n$  in asphalts that does not precipitate when an asphalt is mixed with alkanes such as n-heptane.

The microstructural model of asphalt requires that the most polar, associating components (presumably SEC Fraction-I) of asphalts will have high apparent molecular weights and will be the principal viscosity-enhancing components of asphalts. The remainder of an asphalt, SEC Fraction-II or collective SEC Fractions 2-9, should correspond roughly to the asphalt solvent moiety. In all cases the SEC Fraction-II materials were observed to be stiff liquids at ambient temperature, so their viscosities could be measured. SEC Fraction-I materials, on the other hand, are black friable solids. The viscosities of the SEC Fraction-II materials are reported in table 2.3, as are the viscosities of the parent asphalts. Under the conditions of measurement, the viscosities of SEC Fraction-II materials, which constitute the bulk of each asphalt, are considerably lower than the viscosities of the whole asphalts. In particular, the viscosities of the SEC Fraction-II materials of AAA-1, AAB-1, AAD-1, and AAK-1 are very much lower than those of the parent asphalts. The viscosities of the SEC Fraction-II materials of asphalts AAF-1, AAG-1, and AAM-1 are not nearly so much lower than parent asphalt viscosities. In asphalts, AAF-1 and AAG-1, the highly associated SEC Fraction-I materials are not such a large proportion of the asphalts (table 2.1). Clearly, the result of removing the high apparent molecular weight components from asphalts is that the residual materials have much lower viscosities than the respective parent asphalts, particularly for AAA-1, AAB-1, AAD-1, and AAK-1.

Nine SEC fractions of three of the core asphalts were generated and the first six analyzed for elemental composition (table 2.4). The latter three fractions were too small to perform complete analyses. The SEC fractions of other asphalts were not analyzed for elements due to the expense involved. The data in table 2.4 show that SEC Fraction-I materials are relatively aromatic, based on atomic H/C ratios. However, some of the later eluted SEC fractions of AAG-1 and AAM-1 are even more aromatic and represent significant amounts of material. A similar trend is observed for heteroatom content (N, O, S). The SEC Fraction-I materials of the three asphalts contain more heteroatoms than the fractions eluted immediately afterward in SEC separations. Heteroatom content trends upward in the latest eluted materials. While SEC Fraction-I materials contain more heteroatoms and are more aromatic than SEC Fraction-II materials as a whole, there are components of SEC Fraction-II that are highly aromatic and contain large amounts of heteroatoms. The reason why these materials are not part of the associations represented by SEC Fraction-I is not clear.

The SEC fractions from the nine fraction separations of two of the core asphalts were also subjected to infrared functional group analysis (IR-FGA). Results are listed in supplementary tables 2.13 and 2.14. In general, ketones and sulfoxides, which are products of oxidation during handling, are observed to be concentrated in low molecular weight fractions. Phenols and 2-quinolones are observed to be concentrated in the highest molecular weight fractions. Carboxylic acids are observed to be concentrated in intermediate molecular weight fractions, whereas carboxylic acid salts are detected only in SEC Fraction-I of asphalt AAG-1. This asphalt had been treated with lime, which formed salts, and carboxylic acid salts are classic soaps. Carboxylic acid salts (soaps) are known to associate strongly, and their presence in the SEC fraction of the highest apparent molecular weight fraction of AAG-1 (whereas the presumably structurally similar carboxylic acids of other asphalts are concentrated in the later SEC eluates) strongly supports the model of asphalt structure based on molecular association.

An objective of SHRP is to relate fundamental physical properties of asphalts with compositional data. Asphalt viscosities have not been easily correlated with bulk composition data because viscosity is a made-to-order property. For example, all asphalts of AC-20 grade should have a viscosity of  $200 \text{ Pa}\cdot\text{s} \pm 20\%$  at  $60^\circ\text{C}$  ( $140^\circ\text{F}$ ). However, other rheological properties of asphalts of the same grade can vary markedly. The ratio of the viscous modulus ( $G''$ ) to the elastic modulus ( $G'$ ), defined as  $\tan \delta$ , is a fundamental physical property and is indicative of the rheological nature of asphalts.  $\tan \delta$  values of asphalts vary with temperature and usually are compared at equivalent shear rates. An exception to this latter convention is discussed below.

Careful measurements of  $\tan \delta_{ct}$  values were made for each core asphalt at  $25^\circ\text{C}$  ( $77^\circ\text{F}$ ), and these values are reported in table 2.5 along with their respective mass fractions of SEC Fraction-II materials. These  $\tan \delta_{ct}$  values were measured under similar ( $400 \text{ g}\cdot\text{cm}$ ) torque values for all of the asphalts, hence the use of the subscript *ct* indicating constant torque. This was done because of the wide range of stiffness of the asphalts at  $25^\circ\text{C}$  ( $77^\circ\text{F}$ ). Shear rates in each of the measurements, therefore, were varied somewhat. There is a good relationship between  $\tan \delta_{ct}$  values of the asphalts at  $25^\circ\text{C}$  ( $77^\circ\text{F}$ ) and the mass percentages of their SEC Fraction-II components. This type of correlation is predicted by the microstructural model. For example, a large proportion of SEC Fraction-II in an asphalt is

characteristic of an asphalt that is relatively deficient in molecules that engage in associative behavior and are responsible for elastic properties. The  $\tan \delta_{ct}$  values of such asphalts at ambient temperatures would be expected to be fairly large. In contrast, an asphalt containing a relatively large proportion of SEC Fraction-I will have substantial quantities of associating materials and small  $\tan \delta_{ct}$  values.

The  $\tan \delta_{ct}$  values at 25°C (77°F) of several of the expanded set of asphalts were also determined. These asphalts were separated into two fractions by PSEC. Table 2.6 lists the mass fractions of SEC Fraction-II materials and the  $\tan \delta_{ct}$  values for these asphalts. The data in tables 2.5 and 2.6 are illustrated in figure 2.2. It is evident that for all the asphalts studied, there is a good relationship between  $\tan \delta_{ct}$  at 25°C (77°F) for an asphalt and the mass % of SEC Fraction-II of that asphalt. Figure 2.3 illustrates the relationship between mass fractions of SEC Fraction-II materials of the asphalts and phase angle values, calculated from the  $\tan \delta_{ct}$  values. The relationship is linear and a value of  $R^2 = 81.9$  was calculated, which represents a reasonably satisfactory correlation. It is speculated that when the mass % of the SEC Fraction-II component exceeds 85%, the elastic modulus ( $G'$ ) tends to be small at ambient temperatures compared with the viscous modulus ( $G''$ ). This may mean that mixtures of such an asphalt with most aggregates may be prone to exhibit more rutting behavior than equivalent mixes using other asphalts.

Correlations of mass percentages of SEC fractions with complex moduli ( $G^*$ ) divided by  $\sin \delta$  were observed to be weak. This is because most rheological studies performed at Western Research Institute (WRI) were directed toward measuring dynamic viscosity values of asphalts and asphalt fractions at low rates of shear, usually 1.0 rad/s. At this shear rate, the complex modulus is numerically 10 times that of the viscosity, and phase angles are in the 70-90° range, so  $\sin \delta$  values are near unity. Since asphalt viscosities at 25°C (77°F) do not correlate well with amounts of SEC fractions, neither will  $G^*/\sin \delta$  values.

Note that some of the expanded set of asphalts are generically related to the core group of asphalts. Asphalt AAE is air-blown AAA-1 and, as expected, the mass fraction of SEC Fraction-II of AAE is less than that of AAA-1 and the  $\tan \delta_{ct}$  value at 25°C (77°F) of AAE is significantly lower. Asphalt AAG-1 is derived from the same crude source as ABD, but AAG-1 has been lime treated. These two asphalts have similar  $\tan \delta_{ct}$ s at 25°C (77°F) and similar SEC fractionation behavior. Asphalt AAC-2 is a lower viscosity grade of AAC-1 and, as expected, has a larger SEC Fraction-II component and a greater  $\tan \delta_{ct}$  at 25°C (77°F).

A unique experiment was performed for asphalt AAB-1. SEC Fractions-1 and -2 (of nine) were recombined, redissolved in toluene, and rechromatographed. The result is illustrated in figure 2.4 and is compared with the result from a regular SEC separation of tank asphalt AAB-1. The amount of material in the initial fraction from the separation of combined Fractions 1 and 2 is slightly larger than that obtained in the original separation of AAB-1, and only a small amount of material elutes at a higher percent of bed volume in the second separation than in the initial one. This result indicates that the associating species in this asphalt are stable and are only slightly broken up by dilution.

In another singular experiment, the material remaining when the strong acids and strong bases were removed by IEC from a sample of asphalt AAD-1 (chapter 1) was separated by SEC. The results are shown in figure 2.5 along with the results of an SEC separation of tank asphalt AAD-1. Almost no material of large apparent molecular size was observed in the SEC chromatogram of the strong acid, strong base-free material. Similarly, when the SEC fractions 2 through 6 of asphalt AAD-1 were combined and separated into five fractions (neutral, weak and strong acids, weak and strong bases) by IEC, much lower yields of strong acid and strong base fractions were obtained than for the whole asphalt. This results suggests that the nonfluorescent, associating material obtained by SEC and the strongly polar material obtained by IEC from asphalt AAD-1 correspond fairly closely, as suggested by the microstructural model.

The possibility that the molecular associations could be weakened by higher temperatures was tested by performing the SEC separation of asphalt AAK-1 at 60°C (140°F) instead of the usual 40°C (104°F). The mass percentages of fractions obtained in this experiment are in the right direction, that is, the higher temperature gave a somewhat lower yield of SEC Fraction-I materials and slightly higher yields of lower molecular weight materials. The changes are small, however (only slightly greater than experimental error). In the temperature range of these experiments, asphalt molecular associations appear to be stable.

## Fast or Analytical SEC

The PSEC procedure discussed above requires about 12 hours for a complete separation and several more hours to complete solvent removal from the fractions generated. An analytical SEC procedure also was devised that can be performed in much less time. This procedure separates molecules according to their relative sizes, as does PSEC, but on a smaller scale using HPLC equipment with all of its associated hardware and software. The time required is measured in minutes rather than hours.

The experimental procedure is described in detail in Volume IV (chapter 9) and is based on published methods (Brule, Raymond, and Such 1986; Donaldson et al. 1988; Jennings et al. 1988). Briefly, a 1.25 mg sample is injected into a system consisting of two columns connected in series. The columns are 7.8 mm ID by 300 mm long and are packed with a gel made of a copolymer of styrene and divinylbenzene, like the PSEC columns, but with different pore sizes. The first column contains a gel with a very large average pore size (10,000 Å), and the second column contains a 1,000 Å gel. These pore sizes are much larger than the average pore size of the gel used in the PSEC separations. The pore sizes were selected to spread out the high apparent molecular weight material found in asphalts. Toluene is used as the carrier, as in PSEC. The HPLC is equipped with a UV/visible diode array detector (DAD) and is augmented with a differential refractive index detector (DRID) and a fluorescence detector (FD). Each detector is equipped with an integrating device that is programmed to give 30-second data slice areas. The system was calibrated using polystyrene standards with molecular weights of 2,300, 4,016, 6,287, and 30,013 daltons. Larger molecules or molecular associations are eluted at shorter times than small molecules, as for preparative SEC.



The DRID detects differences in refractive index between the carrier, toluene in this case, and the sample stream. The greater the difference, the greater the response. While the DRID is a fairly good universal detector, it should be realized that the compound types that make up asphalts can vary considerably in their refractive indices. The DAD detects differences in light intensity between a sample beam and a reference beam caused by absorbance of light by the sample. Materials that absorb UV/visible light in the 290-395 nm range include those with conjugated double bonds, such as aromatic compounds. Materials that do not absorb UV/visible in the 290-395 nm range include aliphatic hydrocarbons, alcohols, and ethers. Also, it is well known that the more condensed rings that comprise the aromatic part of a molecule (e.g., pyrene as opposed to toluene), the longer the wavelength of the absorption maximum of the molecule. In addition, if a polar molecule such as phenol becomes hydrogen bonded to another molecule, the wavelength of absorbance increases. Hydrogen bonds are among those believed to be important in the intermolecular bonding that forms the dispersed phase of asphalts. The FD works on a different principle. In the FD, light of a particular wavelength is focused on the sample stream; the aromatic portions of the sample absorb some of the incident radiation and then emit radiation at a longer wavelength. Again, the FD and the DAD respond to the aromatic portion of an asphalt.

The SEC chromatograms, obtained by utilizing the DRID, of the unaged core asphalts are shown in figure 2.6. That this system detects differences between asphalts is readily apparent. The negative peaks on the trailing edge of DRID chromatograms seem to be inherent in the system and occur even when only the solvent is injected. SEC chromatograms for the maltenes and asphaltenes (obtained by n-heptane precipitation) from the unaged core asphalts are shown in supplementary figures 2.11 and 2.12. The peaks for the maltenes are similar in shape to those of the asphalts (figure 2.6) except that the inflections observed in asphalt chromatograms at shorter elution times are diminished or absent in the maltene chromatograms. This is because more associated species with the higher molecular weights are concentrated in the asphaltenes. The peaks in the asphaltene chromatograms (supplementary figure 2.12) are different in shape from peaks in chromatograms of the corresponding asphalts and tend to spread out, suggesting that some asphaltene molecular associations are broken up in the analytical system, in which solutions of asphalts are much more dilute and gel pore sizes larger than in PSEC. It is assumed that asphaltenes consist mostly of molecules that tend to form molecular associations.

Chromatograms, obtained by using the DAD, for core asphalt AAK-1 aged by the thin film accelerated aging test (TFAAT) for 0, 24, 48, or 72 hours are shown for a scan at 300 nm in figure 2.7 and for a scan at 575 nm in figure 2.8 (the use of TFAAT in the oxidative aging of asphalts is discussed in chapter 8). For scans at other wavelengths and by the DRID and FD methods for the same samples, see supplementary figures 2.13 through 2.19. The figures demonstrate that as aging time increases, large apparent molecular size (LAMS) material increases, and this increase occurs at the expense of smaller molecular weight (SMW) material. It is also apparent that as aging time increases, the molecular associations appear to become more extensive; the first peak (shoulder) increases in size and the initial breakthrough of sample elution also occurs at an earlier time. It is interesting to note that the DAD chromatograms at 300 nm, a wavelength at which essentially all aromatic molecules are detected (a "general" type detector), shows the second peak as the largest.

The DAD chromatograms taken at 575 nm, a longer wavelength at which larger aromatic ring systems and hydrogen bonded systems are detected, show the first peak as the largest. This is expected, as large aromatic ring systems tend to become part of extensive associations. Some of the larger molecules and/or associations were produced at the expense of smaller molecules during TFAAT aging. These results can be rationalized as follows: Reaction of asphalt components with oxygen produces materials that tend to be more polar than their precursors and can therefore associate with other polar molecules through hydrogen bonding and other polar interactions. Also, naphthenic materials might be dehydrogenated as a result of reaction with oxygen to produce aromatic ring systems that can interact through  $\pi - \pi$  bonding.

Similar chromatograms are obtained using the DAD for asphalt AAA-1, its maltene fraction, and mixtures prepared by adding varying amounts of AAA-1 asphaltenes to AAA-1 maltenes (supplementary figures 2.20 through 2.25). In each of these figures, the maltene chromatograms are symmetrical. Buildup of the smaller peak corresponding to LAMS material parallels asphaltene concentration of the mixtures. Relatively more LAMS material is detected in all the chromatograms (including those of the maltenes) as wavelength increases from 300 nm to 575 nm. This is attributed to shorter wavelengths being more sensitive to the SMW material and longer wavelengths being more sensitive to the LAMS material. In chromatograms of these materials using FD (supplementary figure 2.26) LAMS materials are not detected, so all the chromatograms are identical. In chromatograms of the mixtures using the DRID (supplementary figure 2.27), LAMS materials are detected at approximately the same levels as in the chromatograms using the DAD at 300 nm (supplementary figure 2.20). The amount of LAMS material detected in these samples is a function of the detector used.

It is interesting to note that chromatograms produced using the FD detector, supplementary figure 2.18 for aged samples and supplementary figure 2.26 for asphaltene-maltene blends, are unchanged with increased amounts of LAMS, regardless of asphaltene concentration. This result corroborates the observation that as molecules form large intermolecular associations, which are believed to be the principal component of asphaltenes, fluorescence is quenched.

A set of 23 unaged and 5 thin film oven (TFO) aged samples were analyzed using fast SEC. (The use of TFO in asphalt aging is discussed in chapter 8). The unaged samples included the core asphalts and 15 of the extended set of asphalts including AAC-2, AAD-2, AAG-2, AAK-2, and AAM-2, which are lower viscosity grade samples from the same source as the corresponding core asphalts. Also included were samples that were derived from the same crude sources as the core asphalts but were not merely different viscosity grades. For example, AAE is air-blown AAA-1; ABD is from the same source as AAG-1, but the latter has been lime treated. The aged samples included AAB-1, AAC-1, AAG-1, AAK-1, and AAM-1. These samples were run to establish a possible relationship between  $\tan \delta_{ct}$  of asphalts and amounts of smaller molecular size material determined by fast SEC. Such a relationship for PSEC separations was discussed earlier.

Analysis of the chromatograms of these samples showed that the inflection point between the first peak (shoulder) and the subsequent peak occurred at about 10 minutes into the run

and was essentially the same for all asphalts tested. Average times were  $10.05 \pm 0.17$  minutes for the DAD and  $10.22 \pm 0.18$  minutes for the DRID (the DRID followed the DAD in the sample stream). This inflection point is believed to correspond to the onset of fluorescence observed in the PSEC separations. In order to test this theory, total areas under the chromatographic curves obtained were normalized. Then, because the data had been collected as 30-second area slices, it was a simple matter to sum those slices, beginning at 10 minutes into the run, to the end of the run. This integrand which is thought to correspond to the SEC Fraction-II of the preparative run was divided by the total area under the curve to give the HPLC percent equivalent of SEC Fraction-II. These percent equivalents were then plotted vs.  $\tan \delta_{ct}$  in figure 2.9 for the DRID. Similar plots were constructed for areas under each curve for 9.0, 9.5, 10.5, and 11.0 minutes into each run. These plots are illustrated in supplementary figures 2.28 through 2.31. In addition, because the DAD records data for up to eight wavelengths, plots were made for 10 minutes into each run for the following wavelengths: 305, 340, 380, 410, 420, 460, 500, and 575 nm. These results are shown in supplementary figures 2.32 through 2.39. Also, a plot of  $\tan \delta_{ct}$  at 25°C (77°F) for each asphalt vs. actual area from the FD is shown in supplementary figure 2.40.

All plots show the same general form as the plot from the PSEC data (figure 2.2). Of all the DRID plots, the one corresponding to the 10-minute breakpoint (figure 2.9) most closely resembles the curve in figure 2.2 for the PSEC separations. For the DAD, the plots for the data at the lower wavelengths show "tighter formations" than those for the longer wavelengths. This is to be expected because the lower wavelengths are characterized by a more general response. For the DRID plots at different times, the shorter times show the tighter formations which may indicate that the separation of associating and non-associating components is not as complete as in PSEC separations. The plot for the FD shows the most scatter and is the least satisfactory.

## **Streamlined Preparative Size Exclusion Chromatography (SPSEC)**

The streamlined preparative SEC (SPSEC) procedure was developed to provide gravimetric finish data in a shorter time than possible using the PSEC method. The PSEC procedure requires about 12 hours run time and another 8 to 12 hours solvent removal time. The fast SEC procedure is completed in a very short time, but none of the detectors is able to account for the whole sample, due to the diverse nature of asphalts. The SPSEC procedure developed requires about 3 hours run time, and solvent removal can be performed either in another 1 to 2 hours using a rotary evaporator or overnight using a static inert gas flow evaporator. If it is only required to determine quickly the mass % of an asphalt contained in SEC Fraction-I and SEC Fraction-II, the simplest way to obtain these data is to subtract the mass % of SEC Fraction-I from 100%. Therefore, it is not necessary to weigh or even collect SEC Fraction-II. However, SEC Fraction-II is usually weighed as a check on each individual run. SEC Fraction-I material is easier to manipulate because it is a friable solid and is therefore less likely to suffer loss of material during the solvent evaporation process. Solvent removal from SEC Fraction-I material also is easier because Fraction-II materials are tacky semisolids.

The procedure is fully described in Volume IV (chapter 9). Briefly, a 0.15 g sample dissolved in enough toluene to make 3 mL solution is pumped into the bottom of a 0.9 cm ID by 52.0 cm column packed with Bio-Rad Bio-Beads S-X1 gel. Toluene is used as the eluant at about 0.27 mL/min. After about 10 mL colorless eluate is collected, sample begins to emerge. Colored eluate (6.0 mL) is collected, the receiver is changed, and 25 mL more is collected. The 6.0 mL fraction contains the nonfluorescent material plus some transitional material and (when divested of solvent) is weighed as SEC Fraction-I. The 25 mL fraction contains some transitional material and the fluorescent material and (when divested of solvent) is weighed as SEC Fraction-II. As explained in Volume IV (chapter 9), a standard asphalt must be run occasionally to determine whether the volume collected for SEC Fraction-I needs to be adjusted. Six columns are customarily used, which allows one sample to be run in triplicate in the morning and another sample to be run in triplicate in the afternoon. Three determinations are enough to give statistically significant data.

Samples of all of the unaged core asphalts and 27 of the unaged extended group of asphalts were separated using the SPSEC procedure. In addition, samples of all of the core asphalts aged at 100°C (212°F) and four asphalts aged at 113°C (235°F) at the Pennsylvania Transportation Institute (PTI) were separated. A sample of one member of the extended set of asphalts, AAN, aged two different ways at 100°C (212°F) at PTI was separated. The results for the unaged core asphalts are listed in table 2.7 along with results from the PSEC for comparison purposes. Results for the noncore asphalts and the asphalts aged at PTI are listed in tables 2.8 and 2.9, respectively.

The results in the tables show that, in general, the SPSEC procedure gives the same results, within  $\pm 10\%$ , as the PSEC procedure. It is evident that the results from SPSEC have, in general, larger standard deviations than the results from PSEC. These results are quite acceptable considering the time saved. Continuing development of the SPSEC procedure should give better and more reproducible results.

The data for  $\tan \delta_{ct}$  at 25°C (77°F) of asphalts vs. percent SEC Fraction-II relationship for PSEC and SPSEC are combined in figure 2.2. The two curves are essentially the same, so the relationship holds for either procedure. The SPSEC procedure can therefore be used effectively to give worthwhile results in a much shorter time than the PSEC procedure.

## **Supercritical Fluid Chromatographic (SFC) Analysis of SEC Fraction-II Materials and Ion Exchange Chromatography (IEC) Neutral Fractions**

SFC is a relatively new analytical technique that is being applied to analysis of asphalt fractions. The principles of the SFC method were described in chapter 1. The method can be applied to relatively nonpolar fractions such as neutral fractions generated by IEC, maltenes, and SEC Fraction-II materials. Results of SFC analyses of core asphalt maltenes and IEC neutral fractions were discussed in chapter 1. These fractions appear to consist mainly of aromatic and aliphatic hydrocarbons ranging from carbon-number 20 (C-20) to above C-100. The maltene fractions are more polar than the IEC neutral fractions. Profiles of carbon-number distributions of maltenes and IEC neutral fractions obtained by SFC resemble each other but differ among the various asphalts. These profiles are illustrated in

chapter 1, figures 1.5 through 1.12, which also contain SFC profiles for SEC Fraction-II materials of the core asphalts. Data on which the profiles are based are listed in table 2.10. These data list peak height maxima and peak widths at one-half peak height as a function of carbon numbers. It is evident from figures 1.5 through 1.12, that the SEC Fraction-II materials resemble iso-octane maltenes more than IEC neutral fractions for a given asphalt.

To investigate further the possibilities that SFC offers to asphalt analysis, other asphalt fractions were examined. In addition to SFC analysis of the core asphalt IEC neutral fractions, SFC analysis was performed on seven of the eight SEC fractions obtained from the PSEC separation of the IEC neutral fractions from asphalts AAA-1 and AAG-1. In this particular study, the three techniques of IEC, SEC, and SFC were combined. Core asphalt neutral fractions obtained by IEC are nonpolar but are made up of hydrocarbons having a wide molecular weight, or carbon-number, distribution. Therefore, these IEC neutral fractions are amenable to SEC separation. In the SEC separation of IEC neutral fractions of AAA-1 and AAG-1, cutpoints were chosen to correspond exactly to those determined for PSEC separations of the parent asphalts into nine fractions. Mass fraction data and  $M_n$  values for individual SEC fractions derived from IEC neutral fractions of AAA-1 and AAG-1 are listed in tables 2.11 and 2.12. From these data it is clear that SEC effectively separates the neutral materials into fractions of widely varying  $M_n$  values. Significantly, there is a substantial amount of material of high  $M_n$  in the neutral materials. Because of their nonpolar nature; these high  $M_n$  values can hardly be caused by association phenomena. The SFC profiles of the SEC fractions confirm this. No SFC data could be obtained for the highest molecular weight SEC fractions listed in tables 2.11 and 2.12 because the molecules that constitute these materials are too large to be analyzed by SFC. The data in table 2.11 for the AAA-1 IEC neutral fraction separation and SFC analysis are plotted in figure 2.10. The lowering of the SFC carbon number peak maximum with increasing SEC fraction number is apparent.

To further complicate matters, SEC Fractions 4 and 5 of the AAA-1 IEC neutral fraction and SEC Fractions 3, 4, and 5 of the AAG-1 IEC neutral fraction were chromatographed on silica gel to generate saturate and aromatic subfractions. These subfractions were analyzed by SFC, and the data are listed in supplementary tables 2.15 and 2.16. For the separation of the AAA-1 fractions, the data in supplementary table 2.16 are plotted in supplementary figures 2.41 and 2.42. It is apparent that the aromatic fractions are of much greater carbon number (and  $M_n$ ) than saturate fractions in the same SEC fraction. This is because SEC separates according to molecular size. For a given carbon number, a saturated hydrocarbon will have a much larger molecular volume than a corresponding aromatic hydrocarbon. These results further illustrate the sensitivity of the SEC procedure to molecular size differences.

Inspection of supplementary figures 2.41 and 2.42 shows that the sums of the saturate and aromatic materials essentially reconstitute those of the original SEC fractions. It is important to note that the chromatograms of the saturate materials are more symmetrical, and have narrower molecular size distributions, and their peaks occur at a lower carbon number than those for the corresponding aromatic fractions.

## Summary

A preparative SEC method has been developed that separates substantial amounts (16.0 g) of asphalts into fractions of varying molecular size. The fractions are sufficiently large that they can be subsequently studied by methods requiring substantial amounts of material. The materials in the first eluted SEC fraction (Fraction-I) have been related to the molecular associations predicted by the microstructural model. The correspondence is verified by the relative lack of fluorescence of these materials to light of 350 nm wavelength and by their high number average molecular weight as determined by vapor phase osmometry. The SEC Fraction-I materials are friable solids and comprise 10-30% of the asphalts studied. The mass % values of the later, more fluorescent SEC eluates (all materials not contained in SEC Fraction-I and referred to as SEC Fraction-II) have been related to  $\tan \delta_{ct}$  (the ratio of viscous modulus to elastic modulus) values at 25°C (77°F) for many asphalts. The SEC Fraction-II materials constitute the bulk of all asphalts studied. These materials are much less viscous than parent asphalts at the same temperature of measurement.

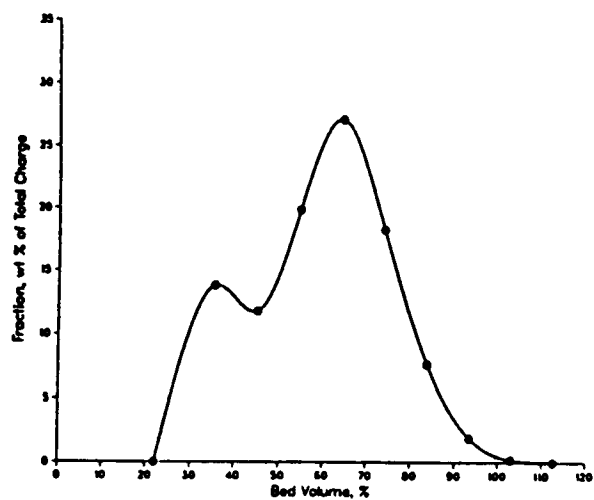
A small-scale SEC procedure that uses gravimetric detection has also been developed that provides data that demonstrate the SEC Fraction-II/ $\tan \delta_{ct}$  relationship. The same relationship was verified by an analytical SEC method adapting HPLC procedures.

The IEC separations showed that asphalts can be separated into distinct chemical fractions. The SEC separations, which are much more rapid and convenient, have shown that asphalts can be separated into fractions of widely different molecular sizes, and that these fractions differ chemically. Both of these results are required for the microstructural model to be valid.

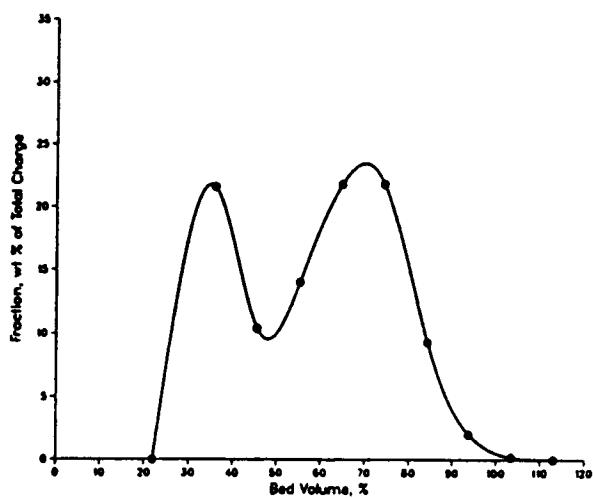
The SEC separation of asphalts into more than two fractions can be used as the basis for crude estimates of weight-average molecular weights.

Work with SFC, a technique developed for the study of asphalts during this program, has shown that information can be obtained about an important portion of asphalt, the solvent or dispersing moiety, that cannot be gained any other way. These materials, approximated by the neutral fractions obtained from IEC of asphalts (or less so by asphalt SEC Fraction-II materials or iso-octane maltene fractions), comprise the bulk of an asphalt and are difficult to characterize but have a great influence on asphalt properties. Results from this work show, for example, that the solvent moiety of asphalt AAM-1 differs greatly from those of other asphalts. Further work using this technique may provide useful information about solvent components that may allow prediction of rheological behavior of asphalts.

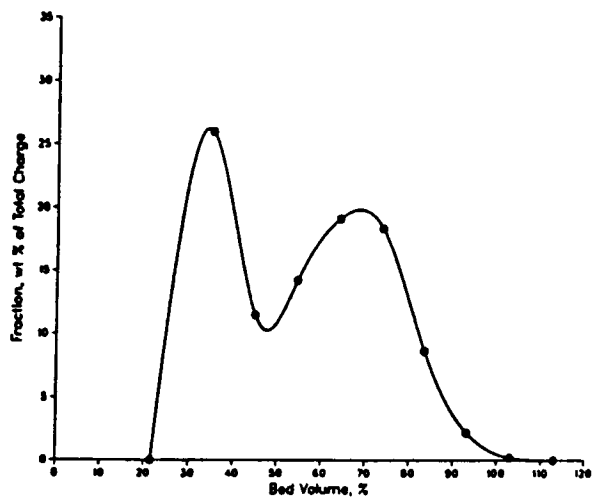
SEC CHROMATOGRAM OF AAF-1



SEC Chromatogram of AAA-1



SEC Chromatogram of AAK-1



SEC Chromatogram of AAM-1

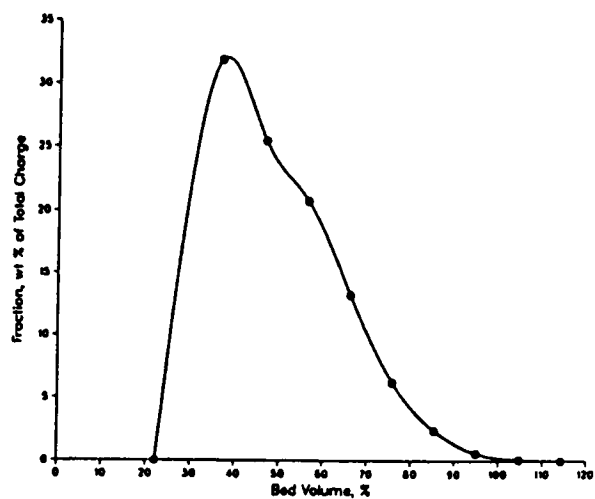
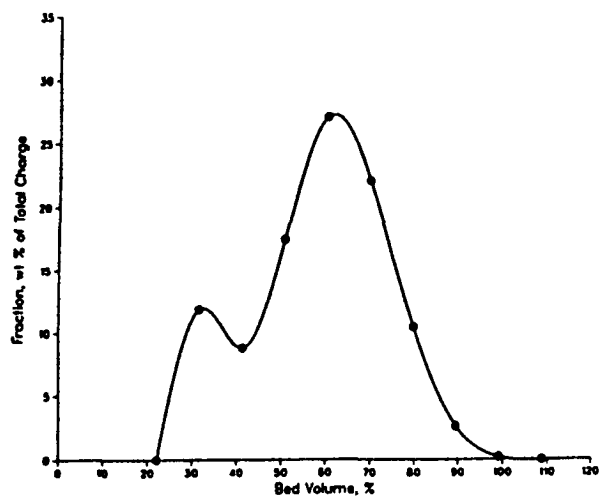
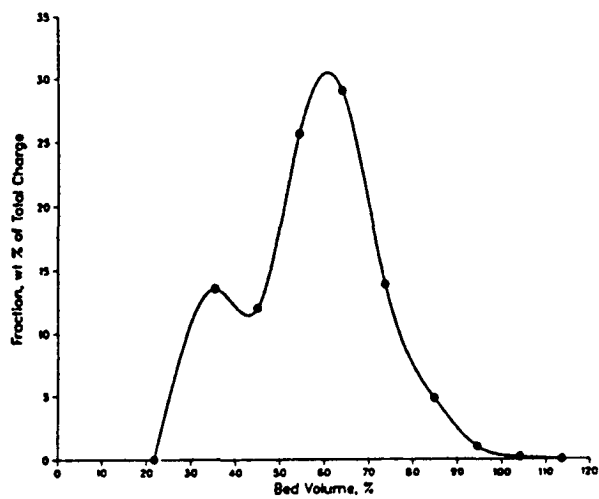


Figure 2.1 SEC Chromatograms of Core Asphalts

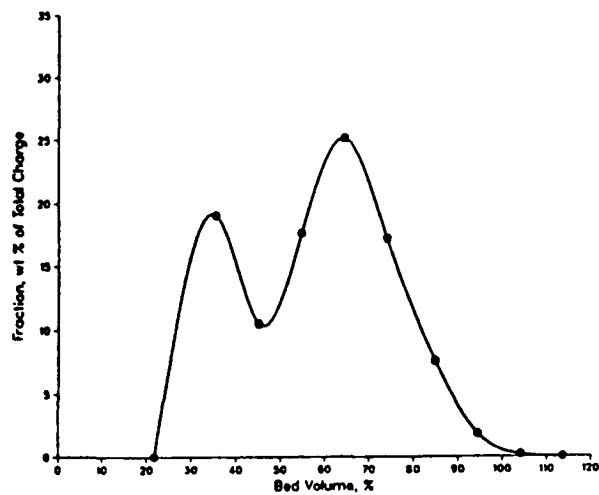
SEC Chromatogram of AAG-1



SEC Chromatogram of AAC-1



SEC Chromatogram of AAB-1



SEC Chromatogram of AAD-1

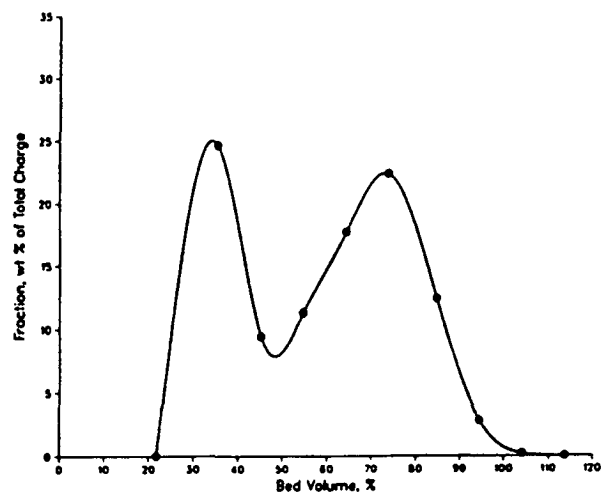
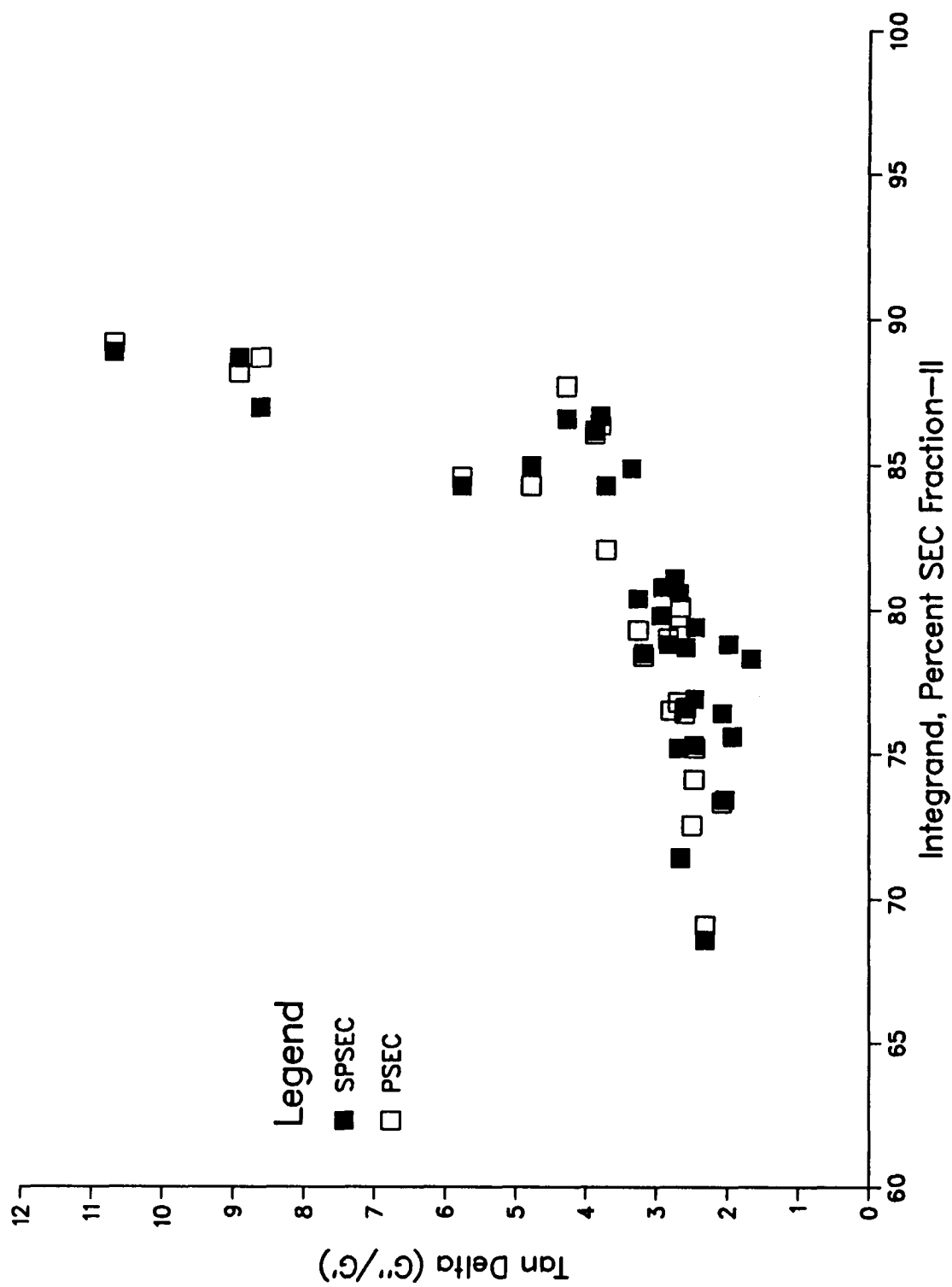


Figure 2.1 (continued)





**Figure 2.2** Relationship Between  $\tan \delta$  (25°C and torque at 400 g·cm) and SEC Fraction-II for Streamlined Preparative Size Exclusion Chromatography (SPSEC) and Preparative Size Exclusion Chromatography (PSEC)

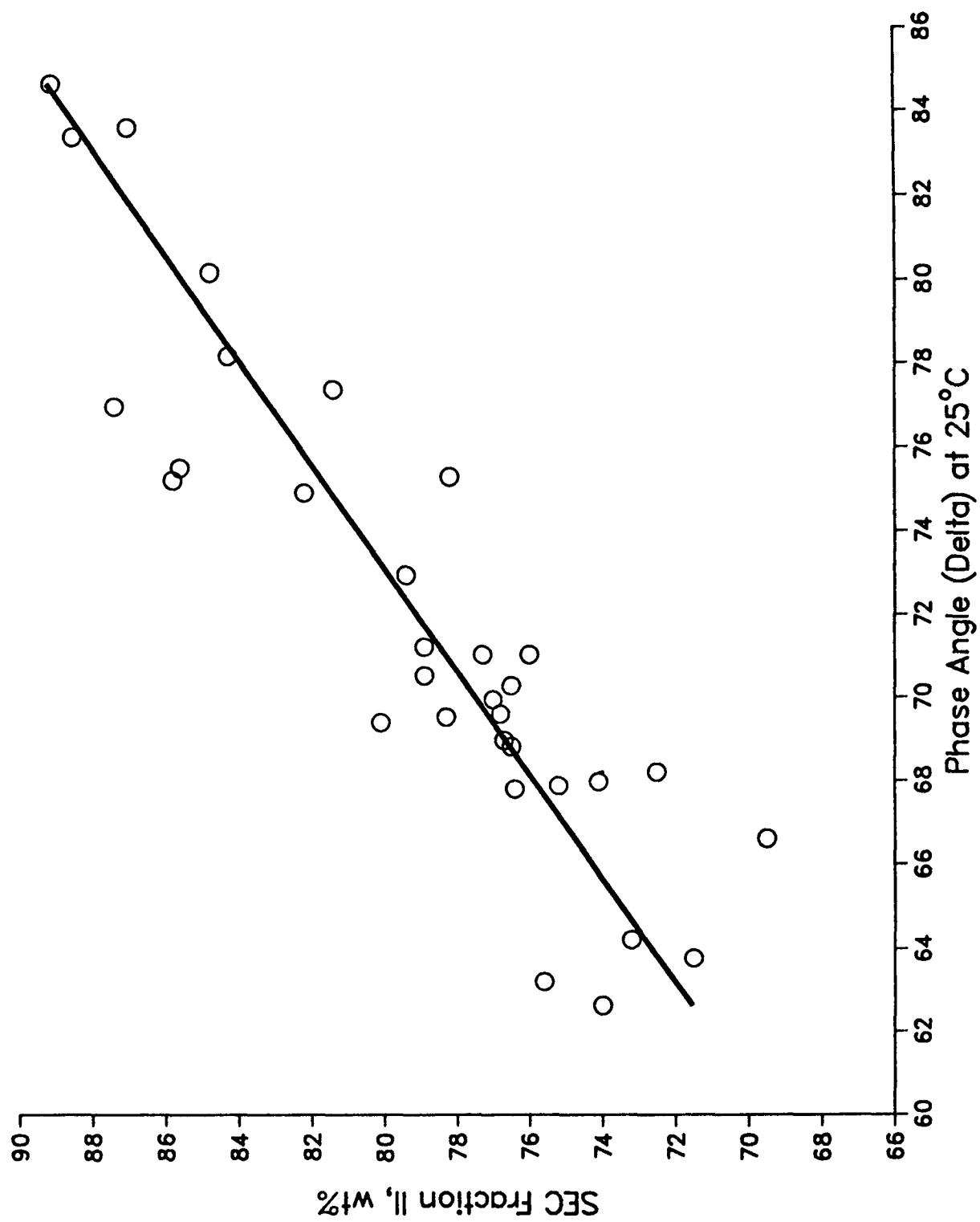


Figure 2.3 SEC Fraction-II vs. Phase Angle

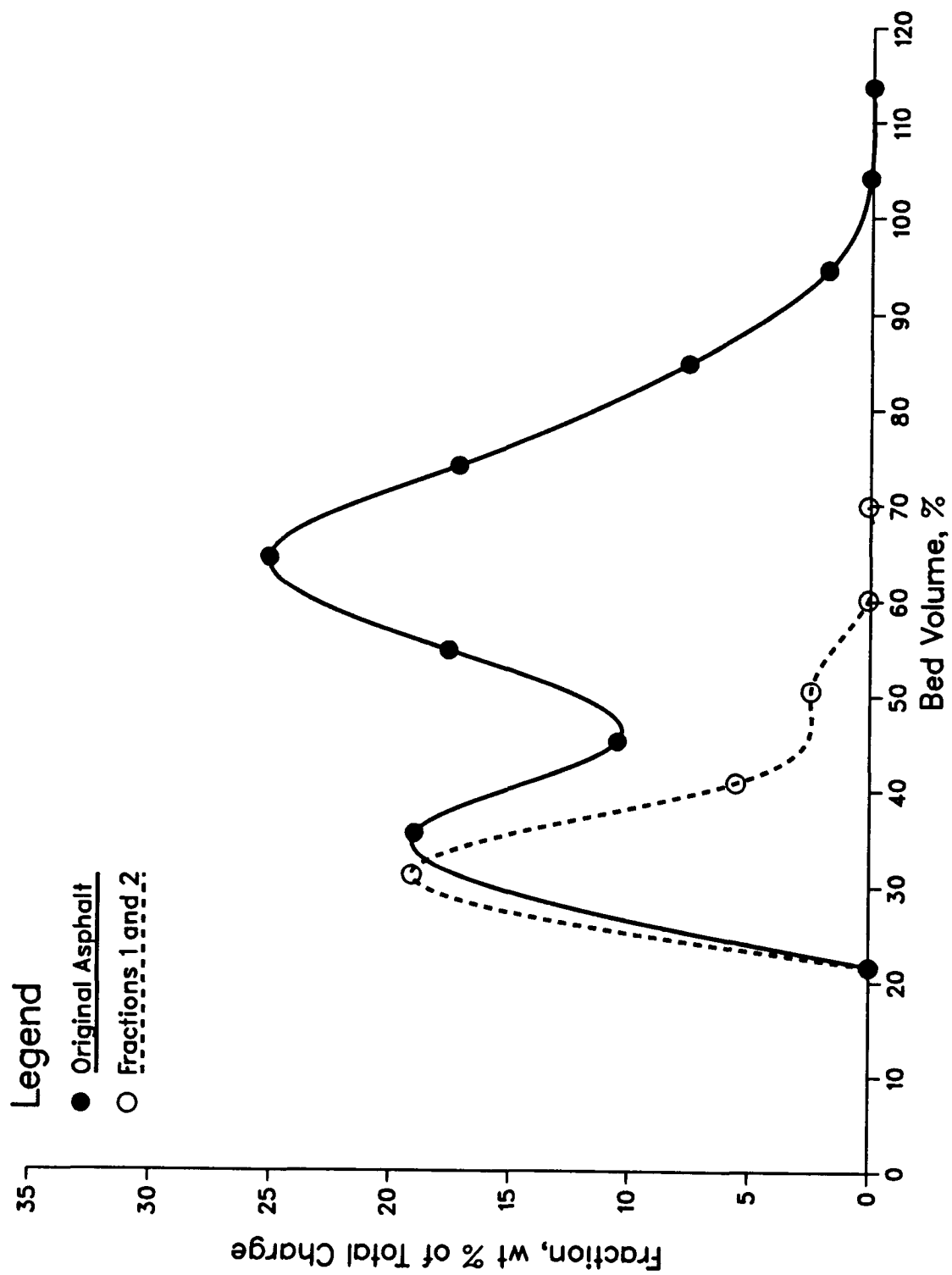
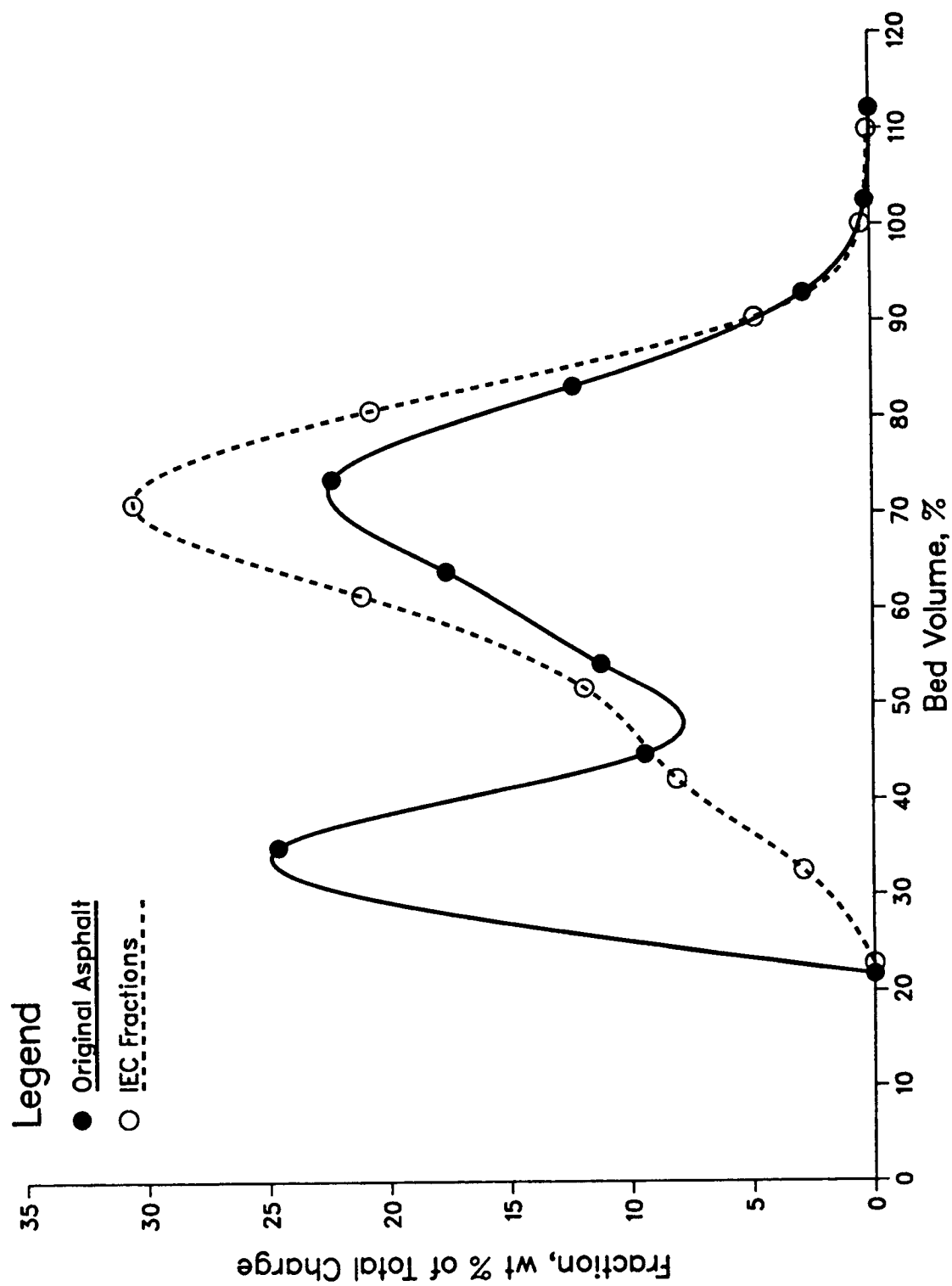
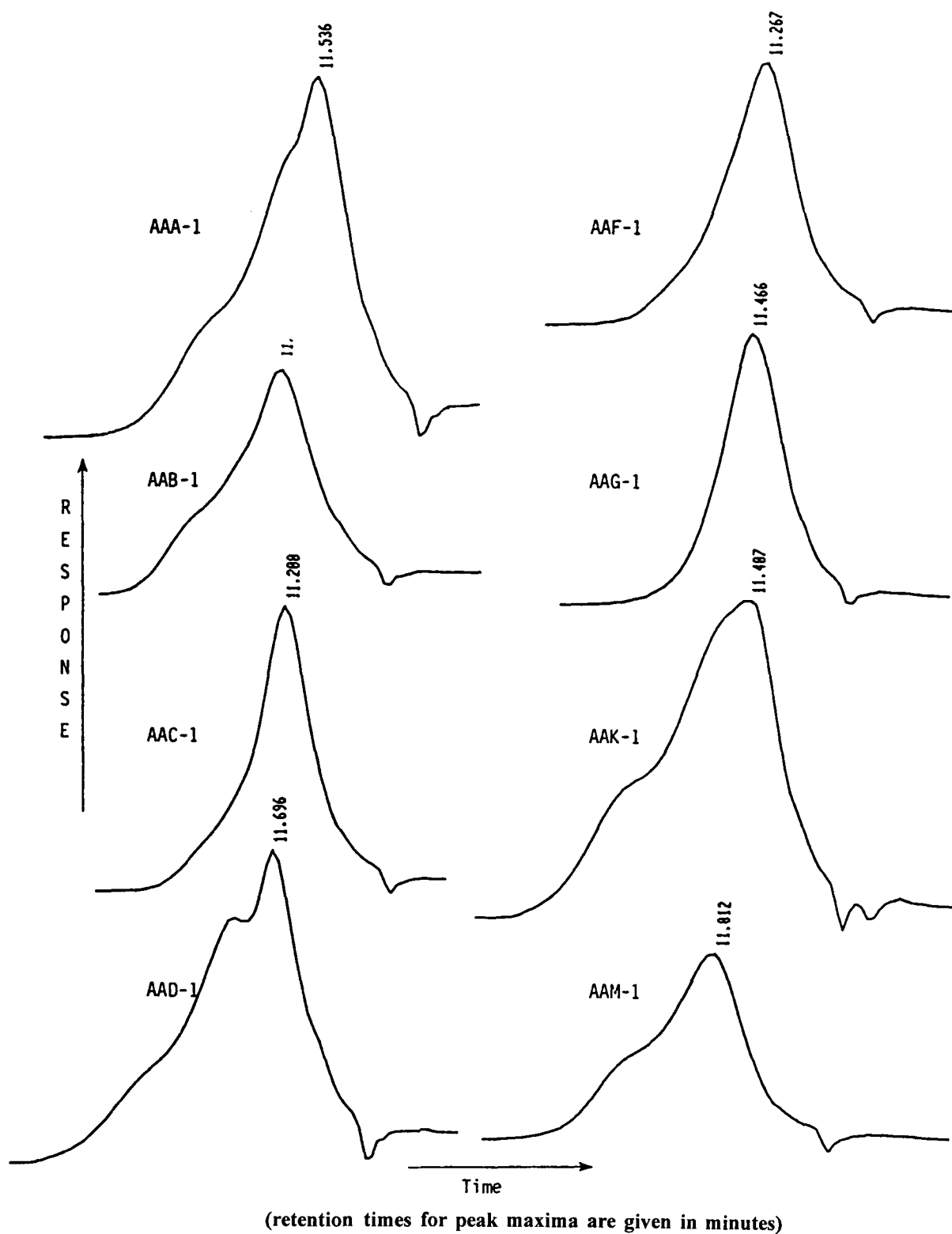


Figure 2.4 PSEC Separation of Asphalt AAB-1 and its Recombined Fractions 1 and 2



**Figure 2.5** PSEC Separation of Asphalt AAD-1 and its IEC Neutrals, Weak Acids, and Weak Bases



**Figure 2.6** Fast SEC Refractive Index Chromatograms for Unaged Core Asphalts (toluene carrier,  $10^4$  Å and  $10^3$  Å columns in series)

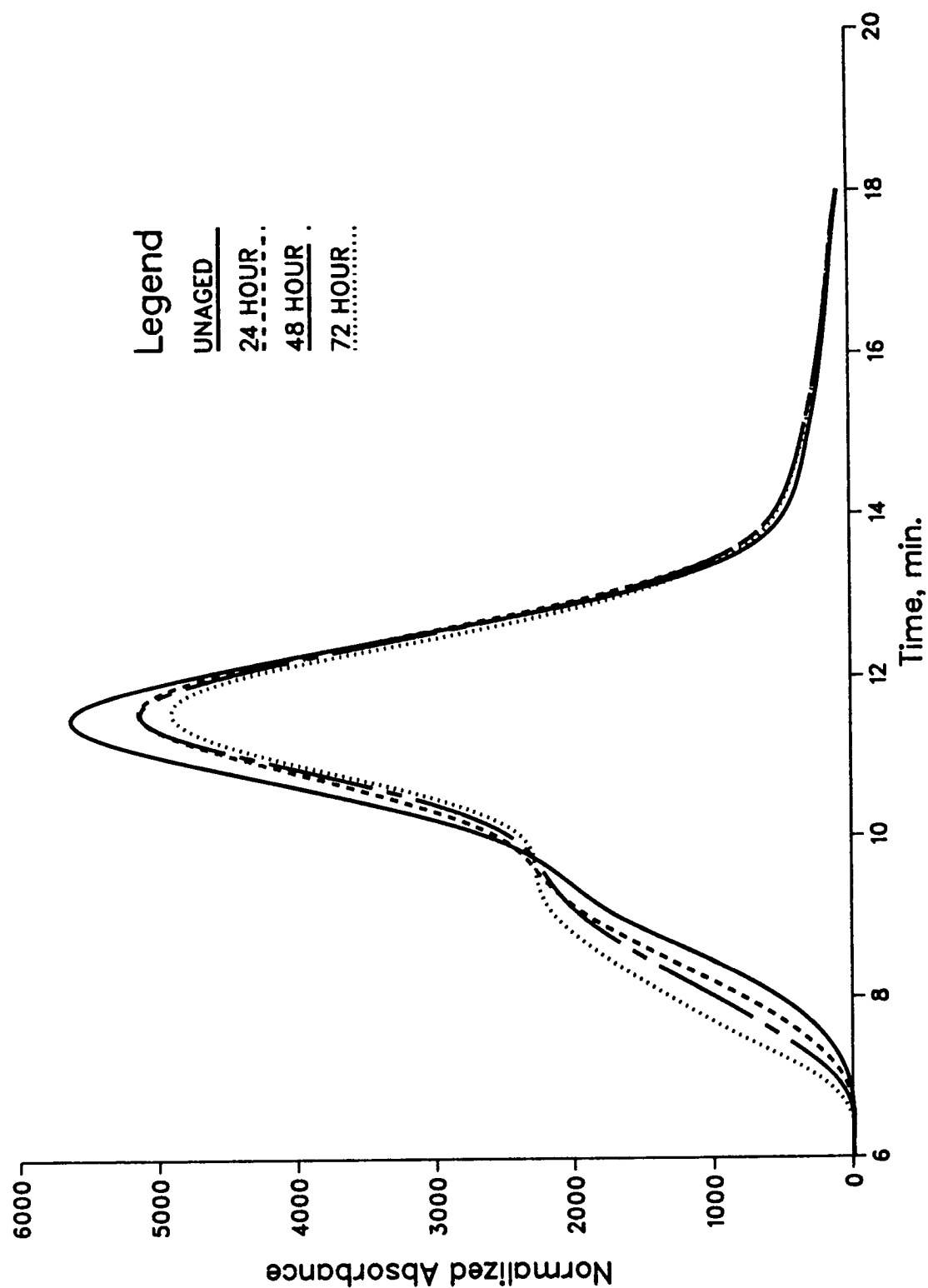


**Figure 2.7** Fast SEC of AAK-1 by Thin-Film Accelerated Aging Test (TFAAT) Aged (0, 24, 48, and 72 hours), Scanned at 300 nm

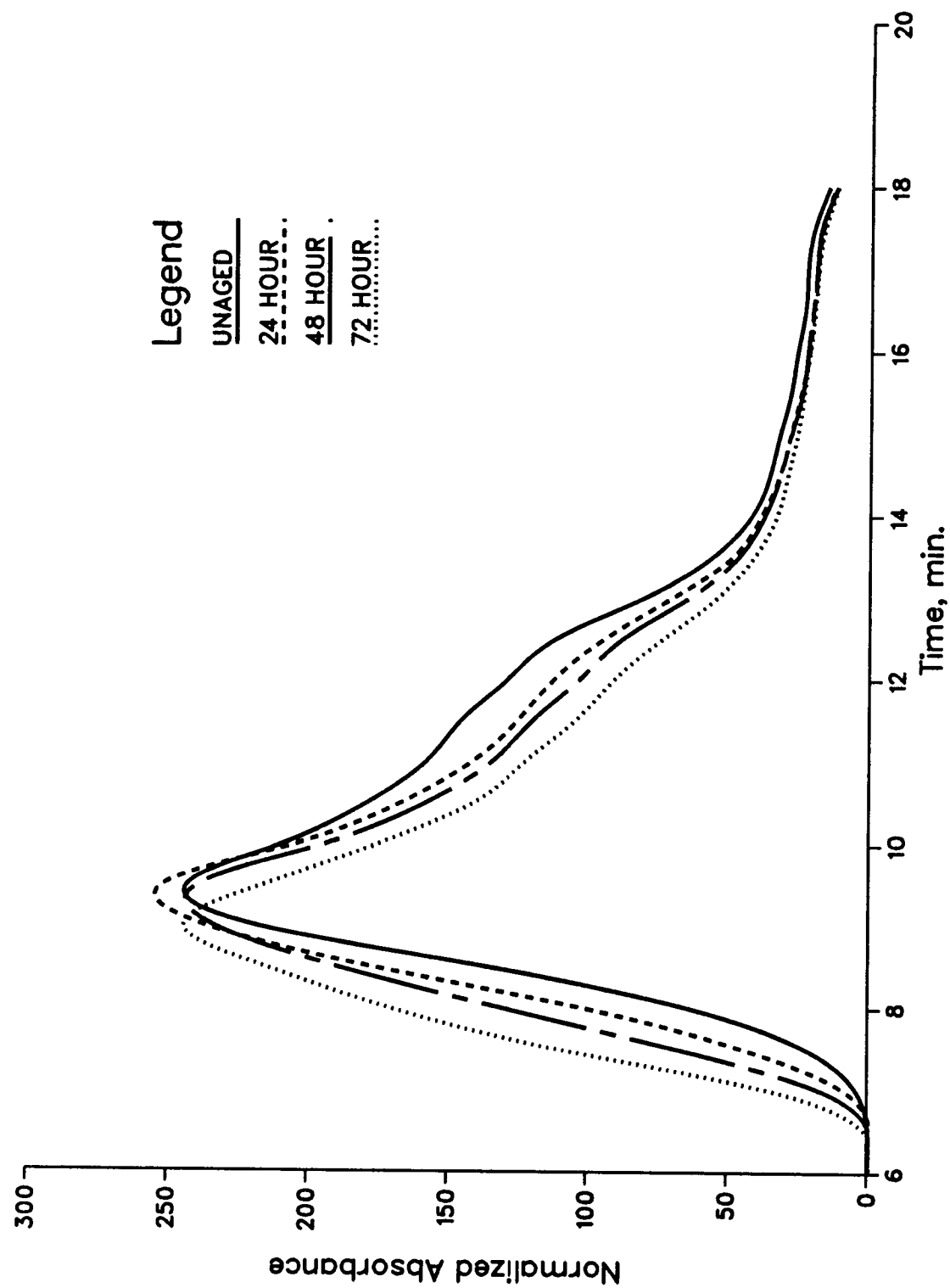


Figure 2.8 Fast SEC of AAK-1 Aged by TFAAT (0, 24, 48, and 72 hours), Scanned at 575 nm

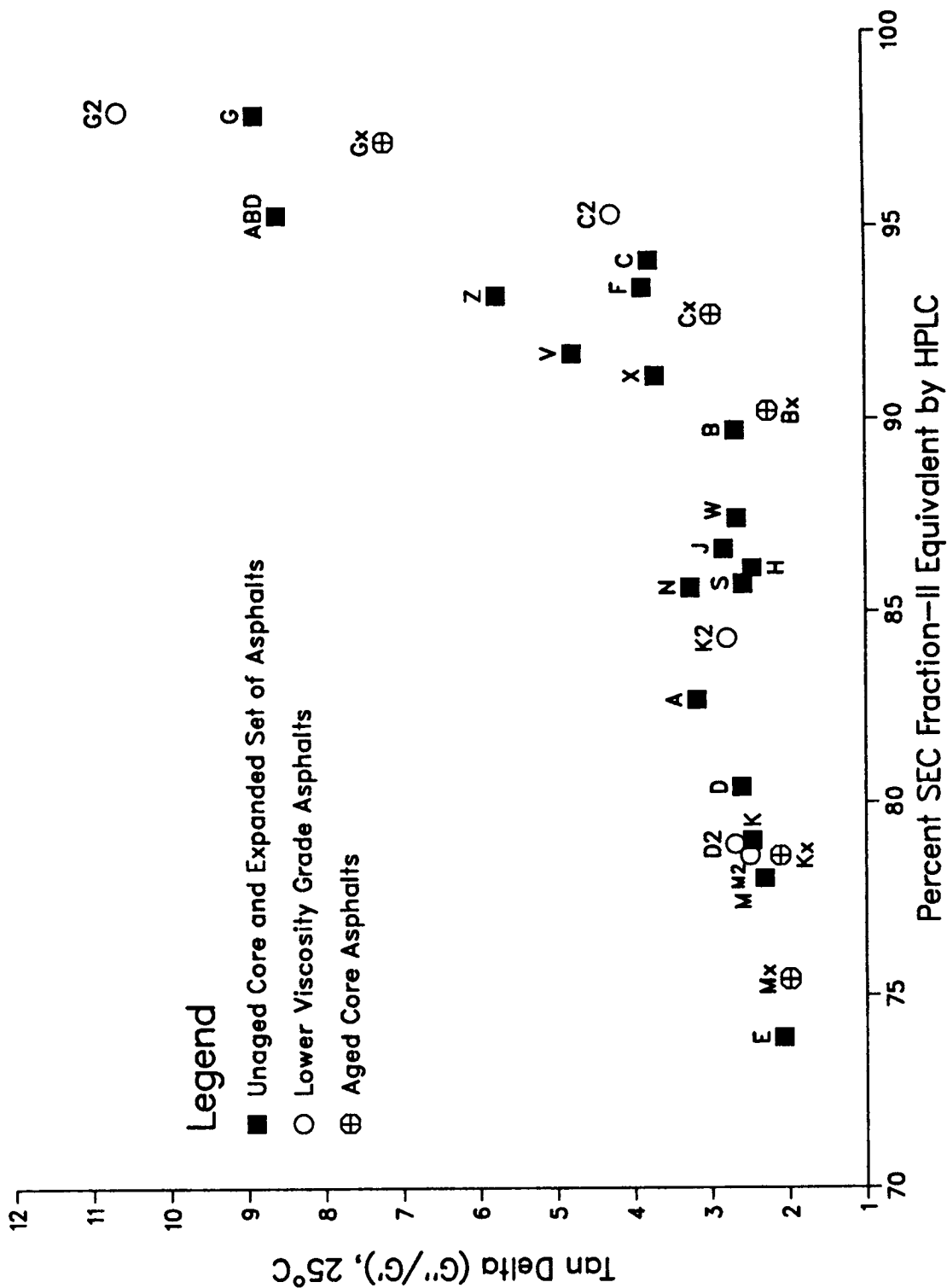
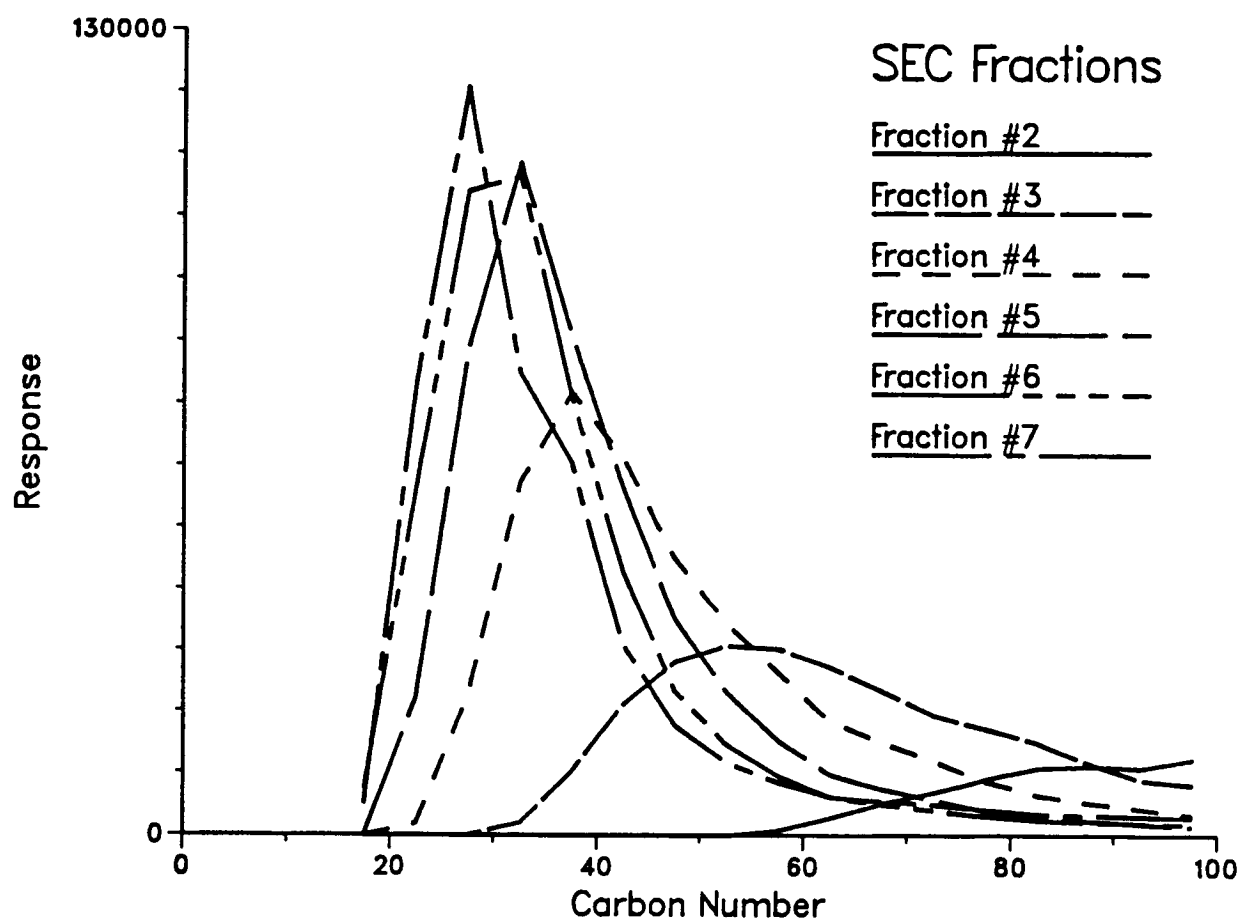


Figure 2.9 Relationship Between Percent SEC Fraction-II Equivalent by High Performance Liquid Chromatography and  $\tan \delta$  (25°C and torque at 400 g · cm) for the Differential Refractive Index Detector at 10 Minutes into Run





**Figure 2.10** SFC Chromatograms of Size Exclusion Chromatography Fractions of IEC Neutral Fractions of AAA-1

Table 2.1 Preparative SEC Separation of Core Asphalts

Fraction Number	Mass Percent of Whole Asphalt for Fraction with Standard Deviations								Std. Dev. <sup>1</sup>
	AAA-1	AAB-1	AAC-1	AAD-1	AAF-1	AAG-1	AAK-1	AAM-1	
1	21.6 ± 0.5	20.9 ± 0.7	13.6 ± 0.1	23.4 ± 0.2	13.9 ± 0.2	11.9 ± 0.4	25.8 ± 0.3	30.8 ± 0.5	-
2	10.4	10.7 ± 0.2	12.0	9.4	11.8	8.8	11.5	25.4	0.2
3	14.0	18.0 ± 0.6	25.6	11.2	19.9	17.4	14.3	20.7	0.6
4	21.3	25.0 ± 0.3	29.1	17.6	27.0	27.0	19.2	13.2	0.4
5	21.1	16.7 ± 0.8	13.8	22.3	18.2	22.0	18.3	6.2	0.5
6	9.3	7.2 ± 0.6	4.7	12.3	7.6	10.4	8.7	2.4	0.6
7	2.0	1.8 ± 0.2	1.1	2.8	1.9	2.6	2.2	0.6	0.2
8	0.1	0.1 ± 0.02	0.1	0.2	0.1	0.2	0.2	0.1	0.01
9	0.02	0.04	0.02	0.02	0.03	0.06	0.06	0.03	-
Total	99.8	100.4	100.0	99.2	100.4	100.4	100.2	99.4	-

<sup>1</sup> Standard deviations in this column estimated by multiplying the average range for a fraction over all asphalts by 0.886.

**Table 2.2 Number-Average Molecular Weights ( $M_n$ ) of Preparative SEC Fractions of Asphalts**

Asphalt	SEC Fraction Number	Mass Fraction	$M_n$ (Daltons) <sup>1</sup>	$M_n \times$ Mass Fraction
AAA-1	1	0.216	11,000	2,376
	2	0.104	2,200	229
	3	0.140	1,200	168
	4	0.213	730	155
	5	0.211	540	114
	6	0.093	390	36
				<u>36</u>
				$\Sigma = 3,078$
AAB-1	1	0.203	9,200	1,868
	2	0.104	1,800	187
	3	0.173	1,000	173
	4	0.255	710	181
	5	0.173	550	95
	6	0.077	430	33
				<u>33</u>
				$\Sigma = 2,537$
AAC-1	1	0.135	7,380	996
	2	0.121	1,610	195
	3	0.256	1,000	256
	4	0.291	780	227
	5	0.138	610	84
	6	0.047	490	23
				<u>23</u>
				$\Sigma = 1,781$
AAD-1	1	0.247	7,000	1,729
	2	0.093	2,200	205
	3	0.112	1,200	134
	4	0.177	700	124
	5	0.223	470	105
	6	0.123	360	44
				<u>44</u>
				$\Sigma = 2,341$
AAF-1	1	0.139	8,690	1,208
	2	0.119	1,970	234
	3	0.199	1,110	221
	4	0.270	770	208
	5	0.182	610	111
	6	0.077	450	35
				<u>35</u>
				$\Sigma = 2,017$

Table 2.2 continued

AAG-1	1	0.118	7,900	932
	2	0.088	1,700	150
	3	0.174	990	172
	4	0.271	710	192
	5	0.220	550	121
	6	0.104	420	44
				$\Sigma = 1,611$
AAK-1	1	0.260	10,000	2,600
	2	0.115	1,700	196
	3	0.143	1,000	143
	4	0.192	650	125
	5	0.183	410	75
	6	0.087	340	30
				$\Sigma = 3,169$
AAM-1	1	0.318	4,600	1,463
	2	0.255	1,700	434
	3	0.207	1,100	228
	4	0.132	810	107
	5	0.062	600	37
	6	0.025	480	12
				$\Sigma = 2,281$

<sup>1</sup> ASTM Method D 2503 is estimated to have an error bar of  $\pm 10\%$  in the molecular range of over 1,000 Daltons, and  $\pm 5\%$  below 1,000 Daltons

**Table 2.3 Viscosities (Pa · s) of Core Asphalts and SEC Fraction-II of Core Asphalts at 25 °C and 1.0 rad/s**

Asphalt	Viscosity <sup>1</sup> of Asphalt	Mass % SEC Fraction-II in Asphalt <sup>2</sup>	Viscosity of SEC Fraction-II
AAA-1	27,540	78.2	506
AAB-1	112,500	78.3	1,367
AAC-1	94,540	85.8	8,602
AAD-1	40,570	76.7	336
AAF-1	307,800	85.6	53,350
AAG-1	354,000	87.1	62,380
AAK-1	107,700	74.1	1,124
AAM-1	112,300	69.5	26,350

<sup>1</sup> Viscosities measured on the mechanical spectrometer are estimated to have an error bar of  $\pm 10\%$ .

<sup>2</sup> Averages of two determinations

Table 2.4 Elemental Analyses of SEC Fractions of Asphalts AAB-1, AAG-1, and AAM-1

Asphalt	SEC Fraction	Element <sup>1</sup> , mass %					H/C	Total N,O,S, mass %
		C	H	N	O	S		
AAB-1	1	84.1	7.9	1.2	0.9	5.3	1.12	7.4
	2	84.4	11.1	0.6	0.6	4.2	1.57	5.4
	3	84.0	12.2	0.3	0.6	3.3	1.73	4.2
	4	82.4	11.8	0.3	0.5	3.6	1.71	4.4
	5	83.9	10.6	0.4	0.5	5.0	1.51	5.9
	6	84.6	8.2	0.7	0.6	6.4	1.15	7.7
AAG-1	1	82.7	9.0	1.7	3.3	0.9	1.30	5.9
	2	86.0	11.2	1.2	1.0	1.2	1.55	3.4
	3	85.8	12.0	0.9	0.7	1.1	1.67	2.7
	4	86.3	11.8	0.8	0.6	1.1	1.63	2.5
	5	86.9	10.7	0.4	0.6	1.2	1.47	2.2
	6	88.4	8.9	1.2	0.7	1.1	1.20	3.0
AAM-1	1	86.9	10.8	0.6	0.5	1.0	1.48	2.1
	2	84.6	12.1	0.4	0.6	0.8	1.70	1.8
	3	84.8	11.9	0.4	0.6	0.9	1.67	1.9
	4	87.0	11.1	0.5	0.7	1.1	1.52	2.3
	5	87.5	9.1	0.8	0.9	1.1	1.24	2.8
	6	89.1	7.5	0.8	1.0	1.8	1.00	3.6

<sup>1</sup> Analyses for the elements were by standard methods. Standard deviations are (mass %): carbon, 0.36; hydrogen, 0.20; nitrogen, 0.09; oxygen, 0.41; sulfur, 0.36.

**Table 2.5 Tan  $\delta_{ct}$  Values of Core Asphalts at 25 °C and Mass Fractions of SEC Fraction-II in Core Asphalts**

Asphalt	SEC Fraction-II, mass % <sup>1</sup>	Phase Angle, $\delta$ degree	Tan $\delta_{ct}$ ( $G''/G'$ ) <sup>2</sup> of Asphalt
AAA-1	78.2	72.54	3.18
AAB-1	78.3	69.54	2.68
AAC-1	85.8	75.22	3.79
AAD-1	76.7	68.96	2.60
AAF-1	85.6	75.51	3.87
AAG-1	87.1	83.60	8.91
AAK-1	74.1	67.96	2.47
AAM-1	69.5	66.59	2.31

<sup>1</sup> Averages of two determinations

<sup>2</sup> A standard deviation of 0.020 for tan  $\delta_{ct}$  was calculated from data for AAK-1 and AAM-1.

**Table 2.6 Tan  $\delta_{ct}$  Values for Expanded Set of Asphalts at 25 °C and Mass Fractions of SEC Fraction-II Components of Expanded Set of Asphalts**

Asphalt	SEC Fraction-II, mass % <sup>1</sup>	Phase Angle, $\delta$ degree	Tan $\delta_{ct}$ ( $G''/G'$ ) <sup>2</sup> of Asphalt
AAC-2	87.4	76.82	4.27
AAD-2	76.8	69.61	2.69
AAE	73.2	64.22	2.07
AAG-2	89.2	84.65	10.68
AAH	75.2	67.88	2.46
AAJ	78.9	70.54	2.83
AAK-2	76.5	70.28	2.79
AAL	77.3	71.04	2.91
AAM-2	72.5	68.20	2.50
AAN	79.4	72.95	3.26
AAO	77.0	69.95	2.74
AAP	75.6	63.20	1.98
AAQ	81.4	73.38	3.35
AAR	76.4	67.80	2.45
AAS-1	76.5	68.81	2.58
AAT	76.0	71.04	2.91
AAU	78.9	71.22	2.94
AAV	84.3	78.18	4.78
AAW	80.1	69.40	2.66
AAX	82.2	74.91	3.71
AAZ	74.0	62.61	1.93
AAZ	84.8	80.17	5.77
ABC	71.5	63.77	2.03
ABD	88.6	83.38	8.61

<sup>1</sup> Averages of two determinations

<sup>2</sup> A standard deviation of 0.20 for tan  $\delta_{ct}$  was calculated from data for AAK-1 and AAM-1.



**Table 2.7 Comparison of PSEC and Streamlined Preparative Size Exclusion Chromatography (SPSEC) Fraction-I Data for Core Asphalts**

Asphalt	PSEC, mass %	SPSEC, mass %
AAA-1	21.6 ± 0.5	21.5 ± 0.7
AAB-1	20.9 ± 0.7	19.6 ± 0.6
AAC-1	13.6 ± 0.1	13.4 ± 0.7
AAD-1	23.4 ± 0.2	23.4 ± 0.8
AAF-1	13.9 ± 0.2	14.4 ± 1.2
AAG-1	11.9 ± 0.4	10.8 ± 0.8
AAK-1	25.8 ± 0.3	24.8 ± 1.5
AAM-1	30.8 ± 0.5	32.3 ± 1.7

**Table 2.8 Comparison of SPSEC and PSEC Fraction-I Data for the Noncore Asphalts**

Asphalt	PSEC, mass %	SPSEC, mass %
AAE	26.7 ± 0.2	24.6 ± 1.3
AAH	24.8 ± 0.2	22.1 ± 1.0
AAJ	21.0 ± 0.2	22.8 ± 0.6
AAL	22.7 ± 0.4	20.4 ± 0.6
AAN	20.7 ± 0.2	20.4 ± 0.9
AAO	23.0 <sup>1</sup>	19.1 ± 0.3
AAP	24.4	21.2 ± 0.4
AAQ	18.6 <sup>1</sup>	14.5 ± 0.5
AAR	23.6 ± 1.8	21.7 ± 1.0
AAS-1	23.4 ± 0.1	21.3 ± 0.6
AAT	24.0 <sup>1</sup>	19.2 ± 0.8
AAU	21.1 ± 1.3	20.2 ± 0.3
AAV	15.7 ± 0.1	15.0 ± 0.6
AAW	19.9 ± 0.1	21.8 ± 0.4
AAX	17.9 ± 0.1	15.7 ± 1.0
AAZ	26.0 <sup>1</sup>	24.4 ± 1.8
AAZ	15.4 ± 0.1	15.7 ± 0.6
AAC-2	12.3 ± 0.4	13.6 ± 0.2
AAD-2	23.2 <sup>1</sup>	24.8 ± 0.4
AAG-2	10.8 <sup>1</sup>	11.1 ± 0.5
AAK-2	23.5 <sup>1</sup>	22.6 ± 0.7
AAM-2	27.5 <sup>1</sup>	29.7 ± 0.4
ABA	ND <sup>2</sup>	21.7 ± 0.1
ABC	28.5 <sup>1</sup>	26.6 ± 0.5
ABD	11.3 ± 0.1	13.0 ± 0.4
ABG	ND	20.6 ± 0.3
ABH	ND	13.4 ± 0.2

<sup>1</sup> Average based on 2 runs. Average standard calculated by multiplying the average of the range of determinations by 0.886 to be ± 0.8.

<sup>2</sup> ND = Not determined

**Table 2.9 Comparison of PSEC and SPSEC Fraction-I Data for Aged<sup>1</sup> Asphalts**

Asphalt	Aging Protocol <sup>2</sup>	PSEC <sup>3</sup> , mass %	SPSEC, mass %
AAA-1	A	ND <sup>4</sup>	27.8 ± 0.5
AAB-1	A	ND	26.2 ± 0.7
AAC-1	A	ND	18.1 ± 0.2
AAD-1	B	33.8	31.0 ± 0.4
AAD-1	A	ND	27.8 ± 0.8
AAD-1	C	36.2	34.6 ± 0.4
AAF-1	A	ND	20.6 ± 0.4
AAG-1	B	18.0	17.7 ± 0.8
AAG-1	A	ND	15.2 ± 1.0
AAG-1	C	19.2	19.6 ± 0.4
AAK-1	B	34.7	33.0 ± 0.6
AAK-1	A	ND	29.9 ± 0.3
AAK-1	C	39.9	37.0 ± 0.3
AAM-1	B	49.3	42.3 ± 1.6
AAM-1	A	ND	38.2 ± 1.4
AAM-1	C	47.1	47.3 ± 0.6
AAE	A	32.5	ND
AAE	D	~28.5	ND
AAN	A	24.6	24.5 ± 0.8
AAN	D	22.6	21.5 ± 1.0
AAS-1	D	26.4	ND

<sup>1</sup> Aged at The Pennsylvania State University

<sup>2</sup> Aging protocols:

A = Thin-film oven test followed by pressure air vessel aging at 100 °C (212 °F) for 20 hr with a 3.2 mm (1/8") film thickness

B = Thin-film oven test followed by pressure air vessel aging at 100 °C (212 °F) for 24 hr with a 1.6 mm (1/16") film thickness

C = Thin-film oven test followed by pressure air vessel aging at 113 °C (235 °F) for 24 hr with a 1.6 mm (1/16") film thickness

D = Thin-film oven test (ASTM D 1754)

<sup>3</sup> These PSEC results are for one run only. A study of the results from PSEC runs of unaged asphalts gives a standard deviation of 0.8

<sup>4</sup> ND = Not determined

**Table 2.10 Peak Height Maxima and Width at One-Half Maximum Height in SFC Chromatograms of SEC Fraction-II of Eight Asphalts**

Parent Asphalt SEC Fraction-II	Peak Maximum, Carbon Number	Range of Carbon Numbers at One-half Height of Peak Maximum
AAA-1	33	28-56
AAB-1	43	33-70
AAC-1	58	43-83
AAD-1	33	23-42
AAF-1	53	34-78
AAF-1	43	32-72
AAG-1	43	32-72
AAK-1	33	23-57
AAM-1	78	50->110

**Table 2.11 Number Average Molecular Weights of PSEC Fractions and SFC Carbon Number Distributions of the IEC Neutral Fraction of Asphalt AAA-1**

SEC Fraction	IEC Neutral Fraction (Mass %)	M <sub>n</sub> <sup>1</sup> (Daltons)	Carbon Number			
			Initial	Mid	Final	Calculated from MW
1	3.0	-	-	-	-	-
2	9.5	2,200	57	100	>100	169
3	20.5	1,200	27	62	>100	92
4	32.6	730	17	43	>100	56
5	26.4	540	17	37	95	41
6	7.0	390	15	34	90	27
7	0.7	290	15	33	90	22
8	0.1	-	-	-	-	-

<sup>1</sup> ASTM Method D 2503 is estimated to have an error bar of ± 10% in the molecular weight range of over 1,000 Daltons, and ± 5% below 1,000 Daltons.

**Table 2.12 Carbon Number Distribution for AAG-1 PSEC Fractions**

Fraction	Mass % of Fraction	M <sub>n</sub> <sup>1</sup> (Daltons)	Carbon Number			
			Initial	Mid	Final	Calculated from MW
1	0.7	7,900	-	-	-	-
2	4.8	1,700	55	91	>100	130
3	18.7	990	37	62	>100	76
4	36.2	710	22	52	>100	55
5	28.1	550	17	44	92	42
6	10.4	420	15	38	90	32
7	1.2	-	15	36	90	-

<sup>1</sup> ASTM Method D 2503 is estimated to have an error of ± 10% in the molecular weight range of over 1,000 Daltons, and ± 5% below 1,000 Daltons.

### 3

## Rheological Studies of Mixtures of Model Compounds with Asphalts

### Introduction

In order to supplement rheological studies of asphalts mixed with chemically defined fractions derived from asphalts, mixtures of asphalts with model compounds were prepared. Even the chemically defined asphalt fractions are complex mixtures of various compounds that can be characterized only approximately at best. Adding compounds of known structure in definite amounts to asphalts permits some quantification of effects of chemical composition on asphalt properties.

### Mixtures of Model Compounds with Asphalts

The criteria used for choosing model compounds were molecular size, polarity, similarity of carbon skeleton, resemblance to compounds known to be present in crude oils, and availability. With one exception, compounds of carbon number lower than 12 (C-12) were not chosen in order to minimize small molecule effects on the rheology of model compound-asphalt mixtures. All but two model compounds selected for mixing with asphalts are n-alkanes or n-alkane derivatives. It is known that n-alkanes are one of the most abundant types of compounds found in crude oils that have not been biodegraded. Most even carbon number n-alkanes and many of their simpler derivatives are readily obtainable.

Two n-alkanes and three of their more polar derivatives were mixed with each of the core asphalts at the 1% and 2% (mass) level. The two alkanes were dodecane (C-12) and hexadecane, otherwise known as cetane (C-16). The derivatives chosen were the terminal alcohols (hydroxy group on carbon number 1), monocarboxylic acids, and dicarboxylic acids. Within each of the series, there is a polarity gradient from the parent alkane through the alcohol and the monocarboxylic acid to the more polar dicarboxylic acids. The dicarboxylic acids are capable of engaging in extensive associations and would be expected to become parts of asphalt molecular associations. The parent alkanes should augment solvent moieties and are not present in amounts sufficient to induce flocculation. The influence of molecular size on rheological properties can be estimated by comparing mixtures of analogous compounds of the two series. Of the four compound types discussed

above, the two n-alkanes and the monocarboxylic acids are found in many crude oils and may be present in asphalts. Minor amounts of dicarboxylic acids have been detected in crude oils. Alcohols are not significant components of petroleum.

Four other model compounds were chosen that do not resemble known petroleum constituents. Aliphatic amines are common asphalt antistripping agents, so 1,12-aminododecane was selected. The corresponding C-16 compound was unavailable from known vendors. The benzene derivative 5-phenylvaleric acid (C-11) was selected in order to include an aromatic compound possessing a polar functional group in the series of test compounds. The difunctional compound 12-aminododecanoic acid was selected as an example of an amphoteric material. The large, bulky molecule tetrastearoylpentaerythritol was selected to allow comparison of the mixtures of asphalts with model compounds of carbon number 16 or lower with mixtures of asphalts with a much larger compound having an entirely different carbon skeleton. The C-11 compound (phenylvaleric acid) and C-12 compounds are not of greatly different size, ranging from molecular weight 170 (dodecane) to 230 (dodecanedioic acid). The C-16 compounds range from molecular weight 226 (hexadecane) to 286 (thapsic acid). Structures of the model compounds are illustrated in figure 3.1. Some properties of the model compounds are listed in table 3.1.

As a first step in mixing model compounds with asphalts, a 10-15 g sample of asphalt is weighed into a tared 100 mL round-bottom flask by heating the asphalt until it is easily scooped out of its container. Aliquots of model compound are added to the flask so that the model compound comprises 1.0% or 2.0% of the total mixture. When model compound-asphalt mixtures are made up, a control sample of asphalt is always treated in an identical way except that no model compounds are added to it. Each flask is then attached to a rotary evaporator and the flask immersed in an 80°C (176°F) waterbath and heated with rotation for 2 hours. The flasks are then immersed into an oil bath for 10 minutes at 125°C (257°F) while being rotated, and the vacuum line is turned on. When the sample begins to exhibit bubble formation, the vacuum is shut off. The flasks are blanketed with argon and submitted for rheological analyses at 25°C (77°F) and 60°C (140°F).

Prior to rheological analysis, the samples were annealed for 30 minutes at 110°C (230°F) and measurements were performed within 48 hours (C-12 compounds), or they were annealed at 150°C (302°F) for 60 minutes and measurements were performed within 2 hours (C-16 compounds).

The microstructural model predicts that addition of a small amount of a nonpolar, miscible compound of low viscosity, such as dodecane, to an asphalt will result in a mixture less viscous than the neat asphalt; the reduction in mixture viscosity depends on the amount of diluent added. Dodecane cannot engage in associative interactions other than Van der Waals interactions because it contains no polar functional groups. Therefore, according to the model, dodecane will become part of an asphalt solvent moiety (whose properties it more closely resembles than components of asphalt polar associations) and will serve to increase the amount of and reduce the polarity of the solvent moiety. More polar model compounds will either distribute themselves between the two moieties or become part of polar associations, depending on the polarity of the model compound. Mixtures of model compounds of differing polarities with a given asphalt should have different rheological



properties. A given model compound should cause similar, but not identical, changes in the rheological properties of different asphalts when mixed with them. Other properties of asphalts, such as glass transition temperatures ( $T_g$ ), also should be affected by addition of model compounds.

Table 3.2 lists viscosities of mixtures of asphalt AAA-1 (99.0 mass %) with several model compounds (1.0 mass %) at 25°C (77°F) and 60°C (140°F), along with viscosities of samples of AAA-1 with no model compound added but otherwise subjected to the same workup treatment as the model compound mixtures. At both temperatures of measurement, the viscosity of the mixture containing dodecane is considerably less than that of the control. The long-chain alcohol 1-dodecanol behaves much like dodecane, as does the monobasic lauric acid, which presumably is dimeric in solution. The difunctional compound 1,12-diaminododecane also has a viscosity-reducing effect when mixed with AAA-1, as does the benzene derivative 5-phenylvaleric acid.

Mixtures of AAA-1 with 1.0 mass % of either of the difunctional compounds dodecanedioic acid or 12-aminododecanoic acid are more viscous than mixtures containing dodecane, and at 25°C (77°F) are more viscous than the controls. It is not known why the control samples are more viscous than other samples of neat asphalts. Possibly the light vacuum and heating to which they are subjected during processing removes small amounts of light ends.

Supplementary tables 3.3-3.18 list more detailed rheological data for mixtures of the eight core asphalts with C-11 and C-12 model compounds at the 1.0 mass % level. Rheological data for mixtures containing 1.0% of the bulky molecule tetrastearoylpentaerythritol (MW = 1,202), the structure of which is illustrated in figure 3.1, also are included in these supplementary tables. Data were obtained at 25°C (77°F) and 60°C (140°F). For a given asphalt, mixtures containing dodecane, 1-dodecanol, or lauric acid are lowest in viscosity, and mixtures containing dodecanedioic acid or 12-aminododecanoic acid are highest. Mixtures containing 1,12-diaminododecane, 5-phenylvaleric acid, or tetrastearoylpentaerythritol are intermediate. The  $\tan \delta$  values of the mixtures containing dodecane, 1-dodecanol, or lauric acid, at the same temperature of measurement, are consistently higher than  $\tan \delta$  values of mixtures containing dodecanedioic or 12-aminododecanoic acid. Addition of the latter two model compounds appears to enhance the magnitude of the elastic modulus of mixtures compared with mixtures of asphalts with the other compounds. The  $\tan \delta$  values in these tables are reported for different rates of shear and are not to be confused with  $\tan \delta_{\alpha}$  values discussed in chapter 2. Insofar as they are accurately measured, the  $\tan \delta$  values of the model compound mixtures decrease with increasing shear rate. The degree to which a given model compound causes reduced or enhanced viscosity when mixed with asphalts varies among the asphalts. Interestingly, mixtures of the bulky molecule tetrastearoylpentaerythritol with asphalts usually are lower in viscosity than the controls, although not as low in viscosity as the dodecane, lauric acid, or 1-dodecanol mixtures. Tetrastearoylpentaerythritol, which is much larger than any of the other model compounds, contains no unhindered polar functional groups.

Supplementary tables 3.19-3.26 list rheological data for mixtures of the above model compounds with the core asphalts at the 2.0 mass % level. Data were obtained at 25°C

(77°F) and 60°C (140°F). Compared with the 1.0% mixtures of dodecane, 1-dodecanol, and lauric acid, viscosities of the 2.0% mixtures of these compounds are further reduced. At the 2% level, 1,12-diaminododecane and phenylvaleric acid also have viscosity-reducing effects. Dodecanedioic acid or 12-aminododecanoic acid mixtures at the 2.0% level have relatively high viscosities, particularly when compared with the dodecane mixtures. Replicates of the data in supplementary tables 3.3-3.26 can be found in SHRP Database B (appendix B).





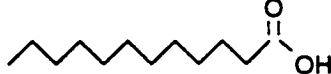




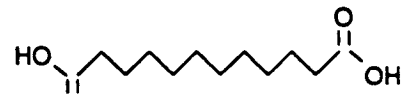
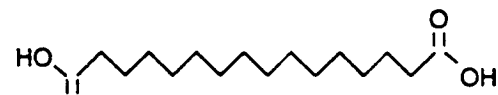
Mixtures of the core asphalts at both 1.0% and 2.0% levels were prepared with four C-16 compounds: hexadecane, 1-hexadecanol, palmitic acid, (hexadecanoic acid), and thapsic acid (hexadecanedioic acid). Structures of these compounds are illustrated in figure 3.1, and properties are listed in table 3.1. Rheological data were measured by a different annealing method than was used for the C-12 compounds. During the course of the Binder Characterization and Evaluation Program it was eventually decided that the annealing method described below should be used in all viscosity determinations. The mixtures were heated to 150°C (302°F) under an inert gas for 1 hour. After 30 minutes cooling, rheological measurements were obtained within 2 hours. These data are listed in supplementary tables 3.27 through 3.34.

The viscosities of mixtures of C-16 compounds are somewhat higher than viscosities of C-12 analogues at the 1% level. Thus, dodecane mixtures are less viscous than corresponding hexadecane mixtures. The same is true for mixtures of lauric vs. palmitic acid, 1-dodecanol mixtures vs. those of 1-hexadecanol, and mixtures of dodecanedioic vs. thapsic acid (hexadecanedioic acid). This is expected due to the larger size of the C-16 compounds. Greater viscosity reductions (or, in some cases with thapsic acid, viscosity increases) are observed in mixtures of the C-16 compounds at the 2.0% level. Where viscosity decreases in mixtures are observed, temperature coefficients of viscosity also are lowered, and vice versa.

Reproducibilities in supplementary tables 3.25 through 3.34 are poor. The procedure involved in manufacture of the mixtures is simple and is likely not operator-dependent. Small differences in amounts of model compounds weighed into flasks were observed, but these differences cannot account for the variances in viscosity. One explanation is that model compounds affect asphalt isothermal reversible molecular structuring differently. The mixtures were stored for different times even though they all were annealed the same way for a given set of compounds. Until these variables are investigated, the data cannot be statistically evaluated. Nevertheless, within a given data set, the trends are the same. Thapsic acid mixtures with asphalts have higher viscosities than mixtures containing hexadecane, palmitic acid, or 1-hexadecanol. The scatter in the data is unfortunate because some of the measured rheological properties of some of the model compound mixtures (particularly the hydrocarbons dodecane and hexadecane) may be useful in predicting aging tendencies of asphalts, as discussed in chapter 8.

## Summary

The above results conform to predictions based on the microstructural model. With one exception, the model compounds are small compared with most constituents of asphalts. Adding miscible model compounds of relatively small size, unless they are polar and capable of associative behavior to form extended structures, will result in mixtures of reduced viscosity. Molecules that contain no functional groups, such as dodecane and hexadecane, behave in this manner when added to asphalts. Rheological properties of the mixture containing these compounds are the real bases for comparison in this study. Monofunctional polar molecules also do not engage in associative interactions other than dimer formation, so they also act to lower viscosity when mixed with asphalts. Four of the polar difunctional compounds mixed with asphalts exhibit viscosity-enhancing effects compared with mixtures containing hydrocarbons. The diamine mixtures tested did not exhibit increased viscosities compared with other polar difunctional compounds, in keeping with observations of mixtures of IEC base fractions discussed in chapter 1. Anomalously, the large molecule tetrastearoylpentaerythritol also acts to reduce viscosity when mixed with asphalts. This implies that the associations in which the viscosity-enhancing model compounds are involved are larger than 1,200 daltons. The dicarboxylic acids and amino acids are known to associate strongly in concentrated solutions. The result of these associations is manifest in rheological behavior.

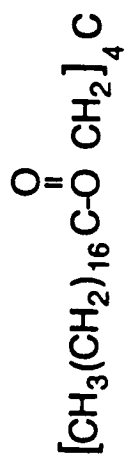
Name	Formula	Structure
Dodecane	$\text{CH}_3(\text{CH}_2)_{10}\text{CH}_3$	
Hexadecane	$\text{CH}_3(\text{CH}_2)_{14}\text{CH}_3$	
1-Dodecanol	$\text{CH}_3(\text{CH}_2)_{10}\text{CH}_2\text{OH}$	
1-Hexadecanol	$\text{CH}_3(\text{CH}_2)_{14}\text{CH}_2\text{OH}$	
Dodecanoic Acid (Lauric Acid)	$\text{CH}_3(\text{CH}_2)_{10}\text{CO}_2\text{H}$	
Hexadecanoic Acid (Palmitic Acid)	$\text{CH}_3(\text{CH}_2)_{14}\text{CO}_2\text{H}$	
5-Phenylpentanoic Acid (Phenylvaleric Acid)	$\text{C}_6\text{H}_5(\text{CH}_2)_4\text{CO}_2\text{H}$	
1,12 Diaminododecane	$\text{H}_2\text{N}(\text{CH}_2)_{12}\text{NH}_2$	
12-Aminododecanoic Acid	$\text{H}_2\text{N}(\text{CH}_2)_{11}\text{CO}_2\text{H}$	
Dodecanedioic Acid	$\text{HO}_2\text{C}(\text{CH}_2)_{10}\text{CO}_2\text{H}$	
Hexadecanedioic Acid (Thapsic Acid)	$\text{HO}_2\text{C}(\text{CH}_2)_{14}\text{CO}_2\text{H}$	

**Figure 3.1 Structures of Model Compounds Mixed with Asphalts**

\_\_\_\_\_  
Name

\_\_\_\_\_  
Formula

Tetraстеаройпентаэритритол



\_\_\_\_\_  
Structure

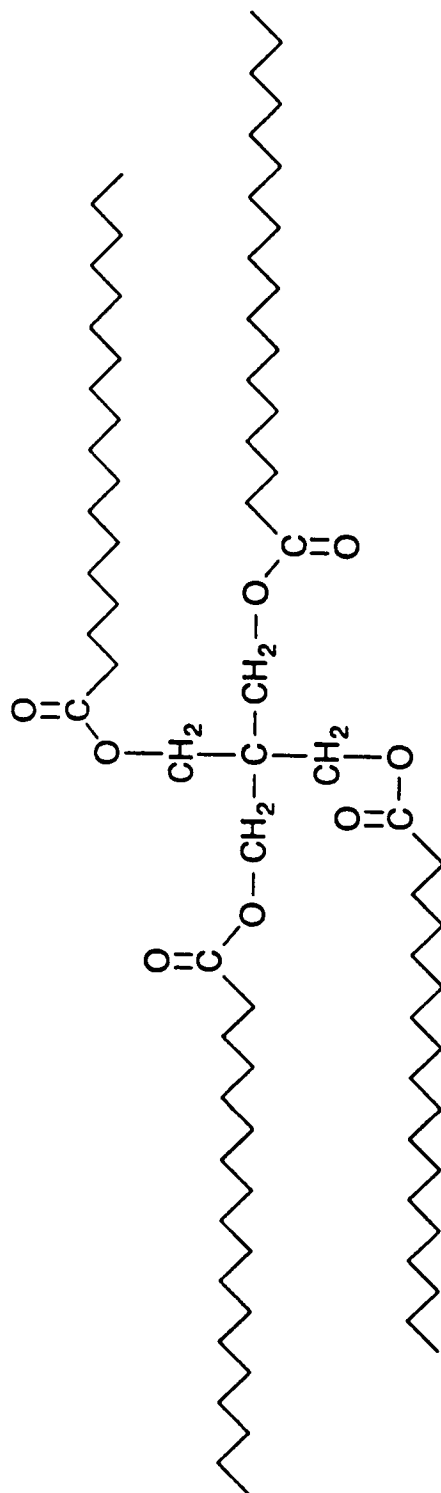


Figure 3.1 continued

**Table 3.1 Properties<sup>1</sup> of Model Compounds Used in Asphalt-Model Compound Mixtures**

Model Compound	Molecular Weight, Daltons	Boiling Point, °C	Melting Point, °C
Dodecane	170.3	216.2	-12
Hexadecane	226.4	283-286	17-19
1-Dodecanol	186.3	260-262	24-27
1-Hexadecanol	242.4	179-181 (10 mm)	54-56
Dodecanoic Acid (Lauric Acid)	200.3	225 (100 mm)	44-46
Hexadecanoic Acid (Palmitic Acid)	256.4	-	61-64
5-Phenylpentanoic Acid (Phenylvaleric Acid)	178.2	177-178 (13 mm)	58-60
1,12 Diaminododecane	200.4	-	69-71
12-Aminododecanoic Acid	215.3		185-187
Dodecanedioic Acid	230.3	245 (10 mm)	128-130
Hexadecanedioic Acid (Thapsic Acid)	286.4	-	124-126
Tetrastearoylpentaerythritol	1,202.0	-	71

<sup>1</sup> Values published in Aldrich Catalog Handbook of Fine Chemicals, 1992-1993, Aldrich Chemical Company, Milwaukee, Wisconsin

**Table 3.2 Viscosities (Pa · s) at Two Temperatures for Mixtures of Model Compounds (1 mass %) with Asphalt AAA-1**

Model Compound	Temperature, °C	Viscosities (Pa · s) <sup>3</sup>	
		Run 1	Run 2
None	25 <sup>1</sup>	30,690	27,540
Dodecane	25	18,530	16,690
Lauric Acid	25	21,050	26,400
1-Dodecanol	25	14,870	15,020
12-Aminolauric Acid	25	35,400	32,550
Dodecanedioic Acid	25	33,330	34,900
1,12 Diaminododecane	25	25,920	24,000
5-phenylvaleric Acid	25	20,780	15,780
None	60 <sup>2</sup>	128	124
Dodecane	60	85	75
Lauric Acid	60	88	83
1-Dodecanol	60	71	72
12-Aminoldecanoic Acid	60	121	119
Dodecanedioic Acid	60	126	149
1,12 Diaminododecane	60	102	95

<sup>1</sup> 1.0 rad/s, 25 mm PP, 3% Strain

<sup>2</sup> 1.0 rad/s, 25 mm PP, 50% Strain

<sup>3</sup> Viscosity determinations on the Rheometrics Mechanical Spectrometer are estimated to have error bars of ± 10%

## 4

# Potentiometric Titration Studies

### Introduction

Ion exchange chromatography (IEC) and liquid chromatography (LC) are valuable techniques for separating asphalts into defined chemical fractions and separating polar from nonpolar materials. However, separation of asphalts into fractions by these methods is time-consuming and expensive. It is highly desirable to be able to identify and quantify functional groups of interest in asphalts in less time (i.e., several minutes) than it takes to perform IEC and LC separations (days). For purposes of functional group quantification it is not necessary to separate asphalts into discrete chemical fractions.

Infrared functional group analysis (IR-FGA) measures a number of important functional groups in asphalt, particularly those produced on oxidation. However, the IR-FGA technique does not adequately quantify some basic functional groups, such as pyridinic nitrogens, which are known to occur in asphalts and which would be expected to engage in relatively strong associative interactions. One method that might be used for quantification of bases (and also acids) in asphalt is nonaqueous potentiometric titration. In potentiometric titrations, changes in potentials of electrodes immersed in solutions of titrated materials are measured as titrating reagents are added. The changes in electrode potential should be unique for a given chemical functionality and proportional to its abundance.

### Nonaqueous Potentiometric Titrations of Bases

Nonaqueous potentiometric titration methods for acids and bases in whole crudes and distillate fractions have been published by Buell (1967a; 1967b), McKay, Weber, and Latham (1976), Dutta and Holland (1983; 1984), Ali and Ali (1988), and Green et al. (1989). The method of Dutta and Holland (1984) was found to be most suitable for determining bases in asphalts. In this procedure, chlorobenzene is the solvent, acetic anhydride scavenges water, and perchloric acid is the titrant. Electrodes are immersed in beakers containing stirred samples of asphalt dissolved in chlorobenzene-acetic anhydride. Electrode potentials in millivolts (mV) are measured as perchloric acid (0.1 N) is added to the solution. Inflections in the curves obtained by plotting electrode potential (mV) vs. titrant (mL) are observed at 300-400 mV and 600-700 mV. These inflections correspond to



strong and weak bases, respectively. Initially, titrations were performed on a venerable Mettler DK-10/DK-11 titrator with a calomel electrode. Unfortunately, this instrument suffered irreversible breakdown during the course of the study. Subsequently, a Metrohm 670 Titroprocessor with a silver chloride electrode was used. Standards employed were 8-hydroxy quinoline, caffeine, and di-n-decyl sulfoxide. Adaptation of the method used to titrate whole crudes and distillate fractions to asphalts did not prove to be routine. Asphalts contain surfactants that interfere with titrations by tenaciously adhering to glass electrodes (Giraudeau et al. 1991). Some asphalts contain finely divided inorganic contaminants that must be removed by filtration. These and other problems were finally resolved, and a procedure described in Volume IV, chapter 11 was adopted.

Asphalts are petroleum residua, so basic components found in asphalts will be those that naturally occur in petroleum. Pyridinic-type compounds (pyridines, quinolines, phenanthridines, acridines) are the only moderately strong bases found in petroleum in significant amounts. Weakly basic compounds include quinolones, amides, sulfoxides, and ketones (the latter two are products of oxidation).

Results of nonaqueous potentiometric titration of the eight core asphalts for bases using the Mettler apparatus are listed in table 4.1, and titration curves are illustrated in figure 4.1. The first endpoint, corresponding to the inflection in the titration curves that occurs at approximately 200-450 mV, is the point at which all moderately strong bases have been neutralized. Three of the asphalts, AAA-1, AAK-1, and AAM-1, are relatively deficient in moderately strong bases. Asphalts AAD-1 and AAG-1 have the largest concentrations of moderately strong bases. Weak bases were quantified from the inflection in the titration curve ranging from 690-800 mV. With the exception of asphalt AAG-1, the core asphalts contain more weak than moderately strong bases. Asphalt AAG-1 is characterized by a third inflection having an average endpoint of 560 mV. It is not known what compound types give rise to this inflection. Total titratable bases do not correlate very well with nitrogen concentrations of the asphalts (table 4.2). The average ratio of mmol nitrogen (total nitrogen in asphalt) to meq base per unit weight of asphalt ranges from 1.7 to 2.4. This suggests that basic nitrogen content cannot be accurately predicted from percent total nitrogen. Nonbasic nitrogen-containing molecules, such as pyrroles, indoles, carbazoles, and porphyrins, also occur in petroleum and become concentrated in residua but would not be detected by nonaqueous potentiometric titration using the method adopted in this study. Hence, a quantitative method to measure all basic materials, including basic nitrogen (not total nitrogen), is useful because of the variation of the relative amounts of total base to total nitrogen among various asphalts. Basic nitrogen compounds are more likely to be involved in molecular associations of various kinds than nonbasic nitrogen compounds.

Titration of solutions of core asphalts using the Metrohm apparatus and a silver chloride electrode were also performed. These data are listed in table 4.3. The results are reasonably close to those obtained using the Mettler apparatus, except that good values for weak bases of AAF-1 and AAK-1 could not be obtained using the Metrohm apparatus. The amount of bases in AAG-1 found by the Metrohm was significantly greater than that found by the Mettler titrimeter. At the current stage of the investigation, these discrepancies are unexplained.

When asphalts undergo oxidative aging, the principal products of oxygen incorporation are ketones and sulfoxides, which are weakly basic molecules. Buildup of polar species such as these affects asphalt rheological properties (Petersen 1984). Table 4.4 lists nonaqueous potentiometric titration data for the eight core asphalts subjected to laboratory aging by means of an initial thin-film oven (TFO) treatment followed by pressure vessel oxidation with oxygen for 1,000 hours at 60°C (140°F) and 300 psi ( $2.07 \times 10^6$  Pa). This procedure is known as the TFO-POV method and is discussed at length in chapter 8. The result of aging of asphalts is a marked increase in weak bases and an increase in total titratable bases. The increase in total titratable bases appears to parallel sulfur contents (chapter 9, table 9.2) of neat asphalts. This is because of the formation of sulfoxides during the aging process, which are weak bases. Except for asphalt AAG-1, aging also results in some reduction in the concentration of moderately strong bases, possibly due to their conversion to weak bases. For example, pyridine-type compounds might be converted to N-oxides. Titration curves of each of the aged core asphalts are also illustrated in figure 4.1.

Table 4.5 lists nonaqueous titration data for iso-octane maltenes of the core asphalts. The properties of these materials are discussed in chapter 9. The concentrations of total titratable bases in the iso-octane maltenes are not much lower than in the parent asphalts. The results also show that these maltenes, which are both heptane soluble and iso-octane soluble, are similar to the whole asphalts in base types and amounts. Surprisingly large amounts of moderately strong bases are present in the maltenes, which are assumed to be composed mostly of nonpolar materials. If, according to the microstructural model that describes asphalts, maltenes are considered to constitute most of or are representative of asphalt-dispersing moieties, then basic components would not be greatly concentrated in asphalt-dispersed moieties. Based on this premise, some of the basic functional groups may be parts of molecules that are nonpolar as a whole and do not engage in strong associations. Large molecules that are almost entirely hydrocarbon with one sterically hindered basic functional group might fit this description.

IEC unlike solvent precipitation, separates asphalts into definable chemical fractions. A description of this method and its application to asphalts is provided in chapter 1. Four of the whole core asphalts were separated into basic, amphoteric, and neutral plus acidic fractions by IEC. Nonaqueous potentiometric titrations of these fractions were performed, and results are listed in table 4.6. The IEC neutral plus acid fractions comprise more than 60% of the masses of each asphalt, but the only basic materials present are small amounts of weak bases, as would be expected. The IEC base fractions, accounting for 10-15% of each asphalt, have large concentrations of total titratable bases, particularly moderately strong bases. The amphoteric fractions of the asphalts, believed to contain most of the polyfunctional materials that engage in extended associative interactions and therefore greatly influence asphalt rheological properties, contain large amounts of titratable bases, predominantly weak bases. The associative interactions of asphalt-dispersed materials, of which amphoteric are an important component, must be fairly weak because asphalt rheological properties are shear-susceptible and are markedly affected by small temperature changes.

Some members of the expanded set of asphalts were analyzed for base concentrations by the potentiometric titration method. Among the asphalts investigated are different viscosity

grades of two of the core asphalts, AAG-2 and AAK-2. For AAG-2, only two endpoints were used to calculate two base fractions, whereas for AAG-1, three endpoints corresponding to three inflections in the titration curve were used (supplementary table 4.7). Total base concentrations for the two asphalts are virtually the same. Asphalts ABD and AAG-1 are AR-4000 grades from the same source. The difference between the two is that AAG-1 has undergone lime treatment. Total base concentration in AAG-1 is slightly higher than in ABD. For the related asphalts ABD, AAG-1, and AAG-2, strong base concentrations and total base concentrations are higher than in any other asphalts studied.

The total base concentration of AAK-2 (AC-10 grade) is not greatly different from that of AAK-1 (AC-30 grade). However, AAK-2 contains twice the strong base concentration of AAK-1 and about half the concentration of weak bases. The reasons for these differences are not apparent, but it can be speculated that production of the higher viscosity grade material results in conversion of moderately strong bases into weak bases, or that some moderately strong bases are removed during manufacture of higher viscosity grades. Alternatively, a basic material may have been added to the lower viscosity grade asphalt.

The asphalts AAH and AAJ contain amounts of titratable weak and moderately strong bases similar to AAK-2. Asphalt AAV more closely resembles AAC-1 in its weak base-moderately strong base distribution.

## **Nonaqueous Potentiometric Titrations of Acids**

Development of a method for nonaqueous potentiometric titration of asphalts for acidic species also has been a subject of investigation. After a literature search, it was decided to adopt a method published by Dutta and Holland (1983) for potentiometric titrations of coal fractions. In this method, the solvent is chlorobenzene and the titrant is the base tetra-n-butyl ammonium hydroxide in 2-propanol. The Metrohm apparatus (silver chloride electrode) was used in this study. Standard model compounds such as acetic acid, lauric acid, adipic acid, picolinic acid, and 2-ethyl phenol were titrated to determine operational parameters. Results from titration of asphalts and asphalt fractions so far are qualitative. Both carboxylic acids and phenols are detected in strong acid fractions obtained from core asphalts by IEC. However, no inflections were observed in titration curves of the whole asphalts AAB-1, AAC-1, AAF-1, AAG-1, and AAM-1, although infrared analysis (chapter 9) proves the presence of both carboxylic acids and phenols in these asphalts. Small inflections were observed when asphalts AAA-1, AAD-1, and AAK-1 were titrated with tetra-n-butyl ammonium hydroxide. Accordingly, it was decided to employ a mixture of chlorobenzene and pyridine, a moderately strong organic base, as solvent. Pyridine disrupts asphaltene associations, which might persist in pure chlorobenzene and would almost surely involve acidic species. Inflection points in the titration curves of AAB-1, AAC-1, AAF-1, AAG-1, and AAM-1 were observed when pyridine was used as cosolvent with chlorobenzene. A disadvantage of using pyridine is that all carboxylic acids, regardless of their relative strengths, will titrate at approximately the same potential since it is actually pyridinium ion that is titrated.

The observation that pyridine disrupts asphalt associations that are apparently not disturbed by chlorobenzene supports the microstructural model. Clearly, this observation is consistent with the observation that vapor phase osmometry (VPO) molecular weights determined in pyridine are significantly lower than molecular weights determined in toluene for polar fractions. Both observations are important in establishing the existence and importance of a multimolecular, or intermolecular, structure in petroleum asphalt.

Supplementary table 4.8 lists nonaqueous potentiometric titration data for acids in the eight core asphalts using the pyridine-chlorobenzene system. Inspection of the titration curves shows that strengths of acidic species in asphalts form more of a continuum than for bases, which can be classified as moderately strong or weak. Acids can be classified as strong, moderate, or weak, corresponding to carboxylic acids, phenols, quinolones, and possibly some pyrroles. By potentiometric titration, there are far more weak and moderately strong acids than strong acids. This also was noted in the infrared (IR-FGA) spectra of these asphalts (chapter 9, table 9.5). The continuum of acid strengths is such that only arbitrary division into strong acids and moderate to weak acids is possible for the acids. When the potentiometric titrations for acids in the core asphalts were replicated, total acids replicated within 10-20%, but the division between strong and moderate to weak acids could not be replicated with any accuracy, so values for these classes of acids are not reported for the second run in supplementary table 4.8. More work clearly is needed in this area. There appear to be more titratable acids than bases in the core asphalts. Asphalts AAG-1 and AAD-1 contain the largest amounts of total titratable acids. Asphalts AAA-1, AAC-1, and AAM-1 contain the smallest amounts of total titratable acids.

Assuming that most acid molecules contain no more than one or two functional groups, more acids are found by titration than by IR-FGA if it is assumed that most pyrroles are not titratable. Both methods verify the existence of large total acid concentrations in asphalt AAG-1, but potentiometric titration data indicate that AAF-1 contains a significant amount of acidic species, whereas IR-FGA finds few acids. Similar discrepancies are noted for other asphalts. It may be that polyfunctionality is more widespread than previously realized (titration data are reported in equivalents, IR-FGA data in moles), or that titration overcounts (or IR-FGA undercounts) acidic species. Supplementary table 4.9 lists potentiometric titration data for total acids in aged core asphalts. These aged core asphalts are the same samples that were titrated to determine base concentration. The asphalts were TFO-PAV aged at 60°C (140°F) and 300 psi ( $2.07 \times 10^6$  Pa) for 1,000 hours. The aged asphalts contain more titratable acids than the parent unaged asphalts. For AAK-1, total titratable acids in the aged asphalts are twice the amount of total titratable acids in the unaged asphalt. The TFO-PAV aged AAG-1 contains only 20% more acids than unaged AAG-1. The percentage increases in total titratable acids resulting from aging of the other acids range from 36-46%.

The iso-octane maltenes of the core asphalts also were titrated to quantify acidic species. These data are listed in supplementary table 4.10. The maltene fractions of the asphalts contain somewhat fewer acidic species (except for AAG-1) than the parent asphalts, but the amount of titratable acids in these supposedly nonpolar materials is substantial. Earlier, it was observed that maltenes contain almost as much titratable bases as the parent asphalts.

In chapter 1, two different methods of separation of asphalts into chemically defined fractions by IEC were described. In one method, a polar fraction designated strong acids was generated from seven of the core asphalts. Potentiometric titrations of acids in these fractions were performed, and the results are listed in supplementary table 4.11. This table lists data for titrations performed at varying times after samples were dissolved in the chlorobenzene-pyridine solvent. The reason for doing this will be discussed later. The data in supplementary table 4.11 show that total titratable acids are highly concentrated in the IEC strong acid fractions, as would be expected.

In another IEC separation of asphalts, amphoteric, total acid, total base, and neutral fractions were generated (chapter 1). Potentiometric titrations of acids in these fractions were performed. Virtually none were found in the neutral and base fractions. Data for the amphoteric and total acid fractions of four core asphalts are listed in supplementary table 4.12. The total acid fractions measured contain somewhat more titratable acids than corresponding amphoteric fractions, but values are high for both fractions.

The poor reproducibilities observed in the potentiometric titrations of acids led to an examination of several variables in the experimental procedure that could influence results. One variable was discovered to be the time elapsed between dissolution of a sample into chlorobenzene-pyridine and titration of the solution. Solutions of four core asphalts were prepared, and aliquots were titrated after standing for 4 hours, 72 hours, and 168 hours (1 week). Results of these experiments are listed in supplementary table 4.13. These results can be compared with data in supplementary table 4.8 in which solutions were titrated within 15 minutes after dissolution of samples in the solvent. Total titratable acids in the solutions that had been stored for several days are significantly less (even allowing for scattering the data) than were found in the samples of the same asphalts titrated minutes after they were dissolved. The same phenomenon was observed in the IEC strong acid fractions of AAG-1 and AAM-1 (supplementary table 4.11) and in the amphoteric fraction of AAD-1 (supplementary table 4.12). It is speculated that some self-assembly of polar materials over time into associations is occurring in the chlorobenzene-pyridine solutions of asphalts and IEC fractions. The phenomenon can be rationalized by the microstructural model, but other explanations may be advanced. It is known that incorporation of polar species into associations may result in changes in acidity (Skold and Tunius 1992).

## Summary

A method used for nonaqueous potentiometric titration of bases in petroleum has been shown to be applicable to asphalts. It has been found that total titratable bases in neat asphalts consist of moderately strong and weak bases, the relative amounts of which correlate poorly with total nitrogen. Somewhat surprisingly, base concentrations of iso-octane maltenes, prepared by removal of the most polar, aromatic moieties of asphalts, were only slightly lower than parent asphalts. Titration data show that the IEC procedure cleanly separates asphalts into definable chemical fractions. Almost all bases in asphalts are found in base and amphoteric fractions as defined by IEC, and not in neutral and acidic fractions.

Aging of asphalts results in buildup of sulfoxides and ketones, which are weak bases. Nonaqueous potentiometric titration confirms this buildup of weak bases, but also shows that moderately strong base concentrations decrease upon aging. Whether pyridinic and quinolonic compounds are converted to weaker bases or are even further degraded is not known. A method for potentiometric titration of asphalts for acidic species was also studied. This method is not as well developed as the base titration method.

Reproducibilities in the acid titration method are not entirely satisfactory, and breakdown of total titratable acids into fractions of different acid strengths has not been adequately accomplished. Potentiometric titrations of oxidatively aged asphalts show that aging causes a significant buildup of acidic species. Titrations of solutions of asphalts in chlorobenzene-pyridine are affected by the length of time elapsing between titration and preparation of solutions. This indicates that acidic components of asphalts undergo self-assembly in solution.

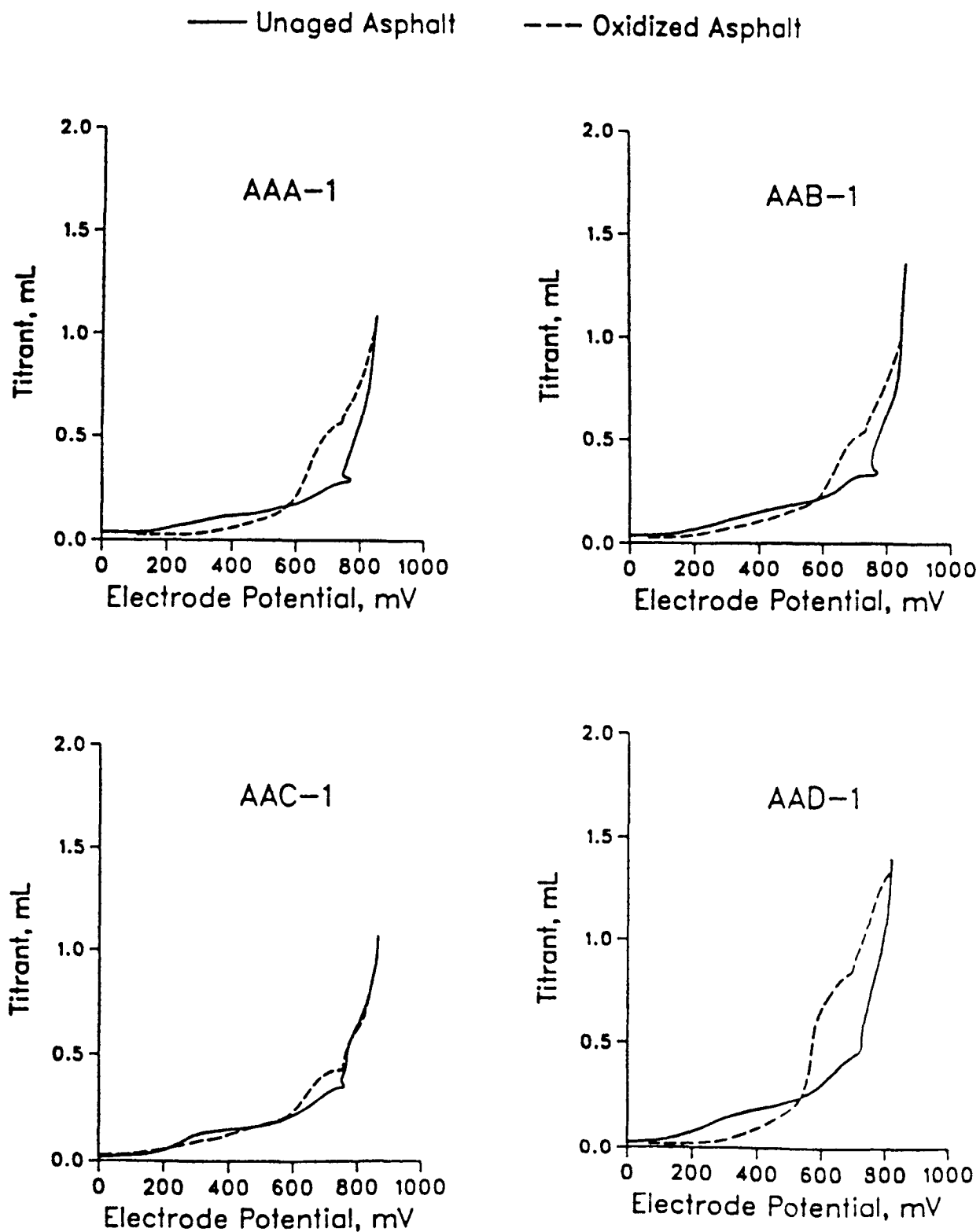


**Figure 4.1 Potentiometric Titration Curves (Bases) of Tank and Thin Film Oven Pressure Oxidation Vessel (TFO-POV) Aged Core Asphalts**

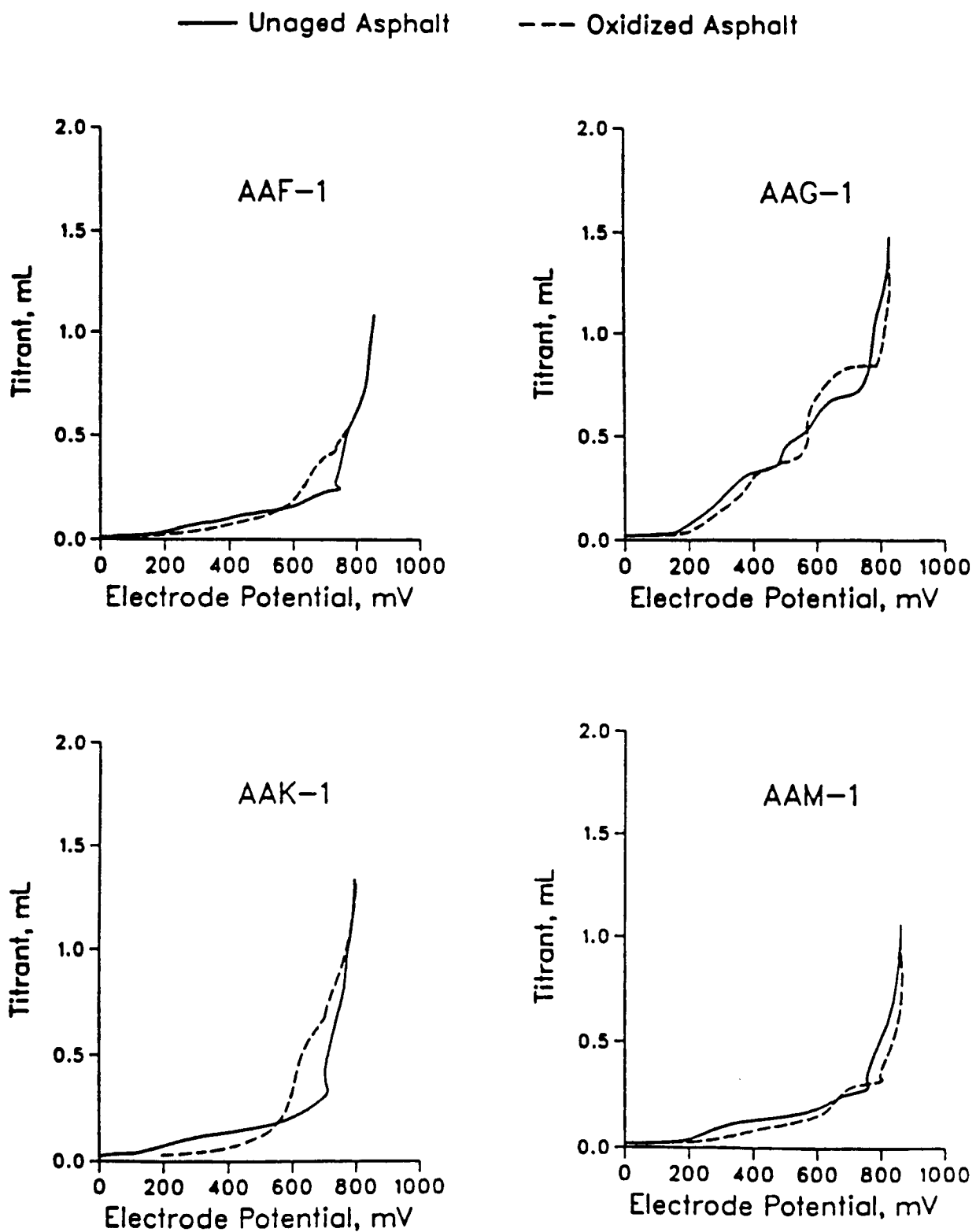


Figure 4.1 Continued



**Table 4.1 Nonaqueous Titration of Bases in Core Asphalts (Mettler)**

Asphalt	Run No.	End Point #1		End Point #2 <sup>1</sup>		End Point #3		Total <sup>1</sup> Titratable Base, meq/g
		mv	meq/g	mv	meq/g	mv	meq/g	
AAA-1	1	440	0.06	740	0.12			0.18
	2	440	0.06	740	0.12			0.18
AAB-1	1	440	0.09	740	0.13			0.22
	2	440	0.09	740	0.13			0.22
AAC-1	1	450	0.09	740	0.12			0.22
	2	450	0.09	740	0.12			0.22
AAD-1	1	420	0.11	700	0.17			0.28
	2	440	0.11	710	0.17			0.28
AAF-1	1	480	0.07	740	0.10			0.17
	2	500	0.07	730	0.10			0.17
AAG-1	1	440	0.20	520	0.10	690	0.12	0.42
	2	480	0.20	600	0.12	720	0.13	0.45
AAK-1	1	440	0.06	800	0.17			0.23
	2	420	0.06	800	0.17			0.23
AAM-1	1	460	0.06	720	0.10			0.16
	2	460	0.06	750	0.10			0.16

<sup>1</sup> Standard deviations were calculated by multiplying the averages of the ranges in columns 6 and 9 by 0.866. These values are: 0.002 for end point #2, 0.003 for total titratable bases.

**Table 4.2 Nitrogen Concentrations and Base Concentrations of Core Asphalts**

Asphalt Code Number	Nitrogen, mass %	mmol/g	<u>mmol Nitrogen</u> meq base
AAA-1	0.49	0.35	1.9
AAB-1	0.53	0.38	1.7
AAC-1	0.67	0.48	2.2
AAD-1	0.77	0.55	2.0
AAF-1	0.55	0.39	2.3
AAG-1	1.10	0.78	1.8
AAK-1	0.71	0.51	2.2
AAM-1	0.55	0.39	2.4

**Table 4.3 Nonaqueous Titration of Bases in Core Asphalts (Metrohm)**

Asphalt	Endpoint #1, moderately strong bases (meq/g)	Endpoint #2, weak bases (meq/g)	Total Titratable Bases, meq/g
AAA-1	0.06	0.13	0.19
AAB-1	0.11	0.10	0.21
AAC-1	0.11	0.08	0.19
AAD-1	0.12	0.16	0.28
AAF-1 <sup>1</sup>	0.07	-	-
AAG-1	0.23	0.29	0.52
AAK-1 <sup>1</sup>	0.09	-	-
AAM-1	0.08	0.07	0.15

<sup>1</sup> Reproducible numbers for the weak bases of these two asphalts were not obtained.

**Table 4.4    Nonaqueous Titrations of Bases (Mettler) in Core Asphalts Aged by Thin-Film Oven Pressure Oxidation Vessel (TFO-POV)**

Asphalt	End Point #1		End Point #2		End Point #3		Total Titratable Bases, meq/g
	mv	meq/g	mv	meq/g	mv	meq/g	
AAA-1	440	0.03	740	0.34			0.37
AAB-1	440	0.06	740	0.30			0.36
AAC-1	450	0.08	740	0.20			0.28
AAD-1	430	0.06	700	0.50			0.56
AAF-1	490	0.05	740	0.21			0.26
AAG-1	440	0.20	560	0.05	690	0.23	0.48
AAK-1	430	0.03	710	0.41			0.44
AAM-1	460	0.04	760	0.15			0.19

**Table 4.5 Nonaqueous Potentiometric Titration of Iso-octane Maltenes of Core Asphalts**

Asphalt	Run No.	End Point #1 <sup>1</sup>		End Point #2 <sup>1</sup>		End Point #3		Total <sup>1</sup> Titratable Base, meq/g
		mv	meq/g	mv	meq/g	mv	meq/g	
AAA-1	1	440	0.03	720	0.14 <sup>1</sup>			0.17
	2	440	0.04	730	0.12			0.16
AAB-1	1	470	0.06	730	0.14			0.20
	2	470	0.06	730	0.13			0.19
AAC-1	1	470	0.08	710	0.13			0.21
	2	490	0.07	790	0.14			0.21
AAD-1	1	460	0.08	710	0.18			0.26
	2	460	0.08	740	0.19			0.27
AAF-1	1	460	0.05	710	0.12			0.17
	2	460	0.05	710	0.12			0.17
AAG-1	1	480	0.18	560	0.07	740	0.16	0.41
	2	460	0.18	560	0.08	710	0.14	0.40
AAK-1	1	430	0.04	730	0.14			0.18
	2	430	0.02	740	0.15			0.17
AAM-1	1	460	0.05	710	0.10			0.15
	2	460	0.05	710	0.11			0.16

<sup>1</sup> Standard deviations were calculated by multiplying the averages of the ranges in columns 4, 6, and 9 by 0.886. These values are: 0.004 for end point #1, 0.009 for end point #2, and 0.007 for total titratable bases.

Table 4.6 Potentiometric Titrations for Bases in IEC Fractions of Four Asphalts

Asphalt	IEC Fraction	End Point #1		End Point #2		Total Base, meq/g	Closure	
		mv	meq/g	mv	meq/g		calc.	obs.
AAD-1	Base Amphoteric Neutral Plus Acid	460	0.38	700	0.42	0.80	0.075	
		450	0.17	700	0.35	0.52	0.134	
		-	-	740	0.04	0.04	0.024	
							0.23	0.28
AAG-1	Base Amphoteric Neutral Plus Acid	480	0.86	700	0.34	1.20	0.144	
		420	0.25	620	0.39	0.64	0.118	
		-	-	720	0.06	0.06	0.041	
							0.30	0.43
AAK-1	Base Amphoteric Neutral Plus Acid	470	0.32	720	0.34	0.66	0.065	
		430	0.13	700	0.34	0.47	0.114	
		-	-	-	-	-	-	
							0.18	0.23
AAM-1	Base Amphoteric Neutral Plus Acid	480	0.26	740	0.29	0.55	0.08	
		460	0.16	690	0.19	0.35	0.06	
		-	-	-	-	-	0.14	
								0.16

## 5

# Polarity of Asphalt

### Introduction

The viscosities of chemically similar organic systems should be functions of molecular weights. For example, a polymer mixture composed of components of relatively low carbon number will be less viscous than a mixture of the same polymer composed of components of higher carbon number. Viscosities of the neutral fractions obtained from the eight core asphalts by ion exchange chromatography (IEC) correlate fairly well with the number-average molecular weights ( $M_n$ ) of these materials, as shown in chapter 1, table 1.4 and figure 1.2. Some of the IEC neutral fractions contain marginal amounts of polar functional groups (supplementary tables 1.22 and 1.23). The  $M_n$  values of the IEC neutral fractions can be corrected for the small amounts of polar materials, and new values of the viscosities calculated, as shown in regression equation (5.1):

$$\text{Log } \eta^* = -12.4 + 5.09 \text{ Log } M_n + 3.26 C_{fg} \quad (5.1)$$

where  $\eta^*$  is the viscosity of the IEC neutral fraction (Pa·s) at 25°C (77°F),  $M_n$  is the number-average molecular weight in daltons of the IEC neutral fraction determined by vapor phase osmometry (VPO) in toluene at 60°C (140°F), and  $C_{fg}$  is the polar functional group concentration (mol/L) of the IEC neutral fraction determined by infrared spectrometry. A coefficient of multiple determination of 0.908 was calculated. When the calculated viscosity values are plotted vs. the measured viscosities of the IEC neutral fractions reported in chapter 1, table 1.6, an excellent linear relationship is observed (figure 5.1). The IEC neutral fractions are sufficiently chemically similar so that their viscosities are predictable from their molecular weights and vice versa.

Viscosities of the whole, unfractionated core asphalts measured at 25°C (77°F) do not correlate well with the  $M_n$  values reported for the asphalts (chapter 9, table 9.4), as shown in figure 5.2. The failure to observe linear viscosity-molecular weight relationships for whole asphalts is caused by the presence of different types and amounts of polar molecules in the whole asphalts. Accurate  $M_n$  values cannot be obtained by VPO for materials containing significant amounts of polar, associating molecules (Green, Diehl, and Shay 1991; Storm et al. 1990). Due to involatility of most asphalt polar molecules, it is impossible to obtain true molecular weight range profiles by mass spectrometry, and other

methods are also unsatisfactory. A discussion of the determination of molecular weights by VPO is presented in chapter 9.

For asphalts and mixtures of asphalt fractions containing polar molecules, no simple predictive relationship exists between molecular weight and rheological properties. According to the microstructural model, the total amounts of polar species present in an asphalt and the strengths of their interactions should determine rheological properties. It should therefore be possible to quantify polar content and polar interactions, referred to as total polarity, and develop relationships between total polarity and rheological properties of asphalts.

### **Viscosities of Mixtures of IEC Fractions**

To examine the effects of polarity on viscosities of four core asphalts, mixtures consisting of various combinations of IEC fractions obtained by the three procedures described in chapter 1 were prepared and their viscosities were measured. The first of these three procedures, designated the conventional IEC procedure, separates asphalts into neutral, weak acid, strong acid, weak base, and strong base fractions. The second procedure separates asphalts into neutral, amphoteric, acid, and base fractions. The third procedure, which was not extensively used, separates asphalts into moderate base and moderate base-free fractions.

The viscosities of several of these mixtures and the IEC neutral fractions measured at 25°C (77°F) are plotted vs. the amount of polar components for AAM-1 in figure 5.3 and for AAD-1, AAG-1, AAK-1, and AAM-1 in figure 5.4. Plots for the rest of the core asphalts have the same pattern. Throughout this discussion, the IEC neutrals are arbitrarily considered to be the only nonpolar component. It is noteworthy that the least viscous mixtures in figure 5.3, consisting of neutral, neutral plus acids (isolated after amphoteric and bases have been removed from asphalts), and neutral plus bases do not contain amphoteric. To obtain these fractions, solutions of AAM-1 in the nonpolar solvent cyclohexane were pumped through columns containing either cation or anion resins. When cyclohexane is used as solvent in either IEC separation, all amphoteric species should be adsorbed on whichever resin is used, and no amphoteric should appear in eluates. Even the mixture of neutrals, weak acids, and weak bases contains a small amount of amphoteric. This is because the mixture was obtained by dissolving AAM-1 (or any of the other asphalts) in a mixed solvent (chapter 1) that is more polar than cyclohexane, and then pumping the solution through a pair of columns, the first filled with anion resin and the second with cation resin. Amphoteric with weakly polar functional groups were not adsorbed in this first step of the conventional IEC separation.

The viscosity vs. concentration of polar species curve for those materials that contain no amphoteric has a less steep slope than the curve for the mixtures containing amphoteric. To emphasize this point, mixtures of IEC fractions were prepared in which amphoteric of four core asphalts (AAD-1, AAG-1, AAK-1, and AAM-1) were replaced with the same amount of their own base fractions, and the viscosities of these mixtures were determined to be far lower than those of their parent asphalts (chapter 1). The viscosity vs. percent polar

components of this amphoteric-free mixture of AAD-1 is plotted in figure 5.5, along with the viscosity-polar component curve for AAD-1 shown in figure 5.4. In figure 5.5, the curve for AAD-1 is subdivided into two intersecting straight lines. When viscosity-polar component data for mixtures of IEC fractions of AAD-1 that contain no amphoteric are plotted, the points should fall on the line tangent to the lower part of the curve. When similar data for mixtures containing amphoteric are plotted, the points should fall on the line tangent to the upper part of the curve, which includes the parent asphalt. Without amphoteric, the marked increase in the slope of the curve, and therefore of viscosity as a percent of polar amphoteric, is not observed.

Amphoterics are difunctional or multifunctional and appear to be largely responsible for formation of multiple associative interactions throughout the asphalt matrix. Without amphoteric, the interactions between polar compounds within an asphalt would be greatly reduced in overall effect. The interactions involving amphoteric are speculated to be strong enough that, in their absence, large values of viscosity or elastic moduli would not be observed, and weak enough to be easily broken in part by heat, shear, or dilution in an organic solvent. It is speculated that one reason why the viscosities of asphalts do not correlate well with the molecular weight determined in toluene at 60°C (140°F) is due to breakup of weaker molecular interactions.

## **SEC Separations of Amphoteric and IEC Separations of SEC Fractions**

In the course of the characterization study of the amphoteric fractions (chapter 1), it was decided to further separate amphoteric by means of preparative size exclusion chromatography (PSEC). Solutions of asphalts in toluene are separated into two principal fractions, designated SEC Fraction-I and SEC Fraction-II (chapter 2). The criterion for distinguishing between the two fractions is the onset of constant fluorescence to 350 nm light in collected eluates. Early eluates, consisting of highly associating or high molecular weight materials, are relatively nonfluorescent, due perhaps to quenching caused by associative interactions of molecules. The microstructural model requires that substantial amounts of the amphoteric fraction of an asphalt be found in SEC Fraction-I when a solution of this material is separated by PSEC. Replicate samples of amphoteric of AAD-1 and AAG-1 dissolved in toluene were separated by this technique. Unlike separation of whole asphalts, charges of 16 g were not used. Instead, charges consisting of that portion of 16 g represented by amphoteric (25.5% of 16 g for AAD-1 and 18.5% of 16 g for AAG-1) were used. Results of these SEC separations are reported in table 5.1.

More than 70% of the amphoteric fraction of AAD-1 was isolated in SEC Fraction-I, and about 40% of the amphoteric fraction of AAG-1 was isolated in SEC Fraction-I. The IEC technique separates by means of chemical functionality only. Some amphoteric materials consist of molecules having only weakly interacting polar groups. These materials will not be separated by IEC from more strongly interacting polar species. Weakly interacting polar species would be likely to be found in SEC Fraction-II. There are more of these in AAG-1 than in AAD-1. That portion of the amphoteric found in SEC Fraction-I should constitute the components of asphalts that are the principal viscosity-enhancing components. The same materials should, according to the microstructural model, be the principal contributors



to asphalt elastic properties. Relative absence of these materials in AAG-1 probably causes the lack of elastic properties, indicated by the high  $\tan \delta$  (ratio of viscous modulus  $G''$  to elastic modulus  $G'$ ) value at 25°C (77°F) of this asphalt compared to many of the other asphalts. The amount of amphoteric materials in AAG-1 is relatively small to begin with (chapter 1).

Also, according to the microstructural model, when SEC Fraction-I materials of asphalts are separated by IEC, the amphoteric fraction should be the dominant fraction. This experiment has been performed for SEC Fraction-I of AAD-1 and AAG-1. Cyclohexane was used as the solvent, and charges were reduced proportionally to the mass percentages of SEC Fraction-I in each asphalt. Results of these separations are reported in table 5.2. It is evident that almost all of the SEC Fraction-I materials are either amphoteric or irreversibly adsorb on IEC resins. Only small amounts of neutral, acidic, or basic species not part of amphoteric structures were found in the SEC Fraction-I materials.

Yields of ~80% in IEC experiments are not very satisfactory. Upon inspection, much material from SEC Fraction-I was not desorbed from cation resin by 1-propylamine-benzene and from anion resin by formic acid-benzene. Therefore, each resin was further desorbed by a mixture of toluene, ethanol, and water. This powerful solvent mixture desorbed much more material from ion exchange resins used in these separations than the prescribed solvents. When the additional yields of extracts, as shown in table 5.3, are considered, overall yields in the separations of the SEC Fraction-I materials rise to more than 90% for AAD-1 and AAG-1. According to the microstructural model, SEC Fraction-I should consist of the most polar components, so the results in tables 5.2 and 5.3 are to be expected.

The SEC Fraction-II materials of AAD-1 and AAG-1 were also separated by IEC, and the results are listed in table 5.4. About 10% of the materials are amphoteric. These amphoteric materials are believed to be the weakly interacting polar species. Almost no irreversible adsorption on resins is observed in the IEC separations of the two SEC Fraction-II materials, as indicated by high recovery rates. The IEC separations of SEC Fraction-I and Fraction-II are compared with the IEC separations of their parent asphalts, AAD-1 and AAG-1, in table 5.5. For each IEC fraction, the sum of the yields in the SEC Fraction-I and Fraction-II separations is very close to the yield of the same IEC fraction of its parent asphalt, indicating that the IEC separation is indeed based only on chemical functionality. For IEC separations of neat asphalts, up to 5% of materials are not recovered. This is due to the irreversible adsorption of highly polar species on the IEC resins. The amounts of the irreversibly adsorbed materials seem to be dependent on polarities of the asphalts. For separations of asphalts into amphoteric materials, total bases, and total acids plus neutrals, the highly polar asphalts, AAD-1 and AAK-1 yield average recoveries of 96% and AAG-1 and AAM-1 weakly polar asphalts yield average recoveries of 98%.

Molecular weights of the amphoteric materials of SEC Fraction-I and the SEC Fraction-I component of amphoteric materials were measured and are listed in table 5.6. The molecular weights of these materials are two to three times greater than those of either the corresponding amphoteric materials (table 1.10) or SEC Fraction-I of neat asphalts (table 5.2). By comparing molecular weights measured in toluene and pyridine, degrees of association of these fraction could be

estimated. Because pyridine is a more polar solvent than toluene, it disrupts polar interactions more effectively. Molecular weights measured in pyridine are about 60% of the molecular weights measured in toluene, indicating that these fractions are capable of engaging in associative interactions.

## Estimation of Relative Polarities of Asphalts

Earlier, it was stated that viscosities of nonpolar components of asphalts, as represented by IEC neutral fractions, can be estimated from  $M_n$  values. Because these nonpolar materials comprise the bulk of most asphalts (and are the components of asphalts of lowest apparent molecular weight),  $M_n$  values of whole asphalts are not greatly different from those of their IEC neutral fractions (chapter 9, table 9.4; chapter 1, table 1.4). Viscosities of whole asphalts cannot be estimated from  $M_n$  values of asphalts. The breakdown of the  $M_n$ -viscosity relationship must be due to the presence of polar components in asphalts. Therefore, some estimation of interactions of polar components of asphalts as they influence rheological properties was attempted.

For purposes of calculation of polarities, amphotericics can be classified in four categories: SASB amphotericics having strong acid and strong base functionalities, SAWB amphotericics having strong acid and weak base functionalities, WASB amphotericics having weak acid and strong base functionalities, and WAWB amphotericics having weak acid and weak base functionalities. Other combinations are possible in theory, but they reduce to one of the above categories. Consequently, for the purpose of calculating polarities, an asphalt can be arbitrarily divided into nine "polarity" fractions: the four kinds of amphotericics, strong acids (SA), weak acids (WA), strong bases (SB), weak bases (WB), and neutrals (N).

To quantify the polarities of asphalts, arbitrary numbers are assigned as follows: 1 mass % of weak acid or weak base in asphalt is assigned a polarity factor of 1; 1 mass % of strong acid or base is assigned a polarity factor of 2; likewise, 1 mass % of SASB amphotericics gives two times polarity 2 (i.e., polarity factor 4). These arbitrary values are multiplied by mass percentages of the fractions present in asphalts to calculate total polarities.

To calculate the amounts of the nine fractions, results of three different IEC separations are used: (1) the conventional IEC procedure (chapter 1, table 1.1), (2) the IEC procedure developed to separate amphotericics (chapter 1, table 1.8), and (3) the IEC procedure to separate moderate bases using the mixed solvent and a cation column (chapter 1, supplementary table 1.36). Note that the terms used in this discussion are different from those used for the conventional IEC separation. For example, the strong acids in the conventional IEC consist of strong acids, SASB amphotericics, and SAWB amphotericics and should be differentiated from the amphoteric-free strong acids referred to in this discussion. Similar considerations apply to the strong base and weak acid fractions generated in the conventional IEC separation.

Distribution of the nine polarity fractions among the materials obtained by conventional IEC separation is shown in table 5.7 along with the polarity factors assigned. From the results of all of the above three IEC separations, amounts of strong bases, weak bases,

SASB amphoteric, WASB amphoteric, and neutrals for four core asphalts can be calculated mathematically. For strong acids, weak acids, and SAWB and WAWB amphoteric, only three independent relationships are available, and the exact amounts of the fractions can not be determined unless a different IEC separation procedure is performed or a relationship among them is assumed. Data normalized to 100% yields are used to calculate the amounts of fractions. The calculations for AAD-1, for example, are as follows:

From the conventional IEC procedure,

$$\text{First anion column: } SA + SASB + SAWB = 26.4\% \quad (5.2)$$

$$\text{First cation column: } SB + WASB = 7.8\% \quad (5.3)$$

$$\text{Second anion column: } WA + WAWB = 7.9\% \quad (5.4)$$

$$\text{Second cation column: } WB = 5.7\% \quad (5.5)$$

$$\text{Neutrals: } N = 52.2\% \quad (5.6)$$

From the IEC procedure developed to separate amphoteric,

$$\text{Amphoterics: } SASB + SAWB + WASB + WAWB = 27.0\% \quad (5.7)$$

$$\text{Bases: } SB + WB = 9.9\% \quad (5.8)$$

$$\text{Neutrals plus Acids: } N + SA + WA = 63.1\% \quad (5.9)$$

From the IEC procedure separating moderate bases,

$$\text{Moderate Bases: } SB + SASB + WASB = 23.2\% \quad (5.10)$$

The amounts of WB and N are directly obtained from equations (5.5) and (5.6). From equations (5.5) and (5.8),

$$SB + 5.7 = 9.9, \text{ or } SB = 4.2\% \quad (5.11)$$

From equations (5.3) and (5.11),

$$4.2 + WASB = 7.8, \text{ or } WASB = 3.6\% \quad (5.12)$$

From equations (5.3) and (5.10),

$$SASB + (SB + WASB) = SASB + 7.8 = 23.2, \text{ or } SASB = 15.4\% \quad (5.13)$$

The amounts of SA, WA, SAWB amphoteric, and WAWB amphoteric cannot be determined because only three independent relationships exist among them. These are as follows:

From equations (5.2) and (5.13),

$$SA + SAWB = 11.0\% \quad (5.14)$$

From equations (5.9) and (5.6),

$$SA + WA = 10.9\% \quad (5.15)$$

From equations (5.7), (5.12), and (5.13),

$$SAWB + WAWB = 8.0\% \quad (5.16)$$

Polarity contributions from these four components in neat asphalt AAD-1 are determined by adding fractions multiplied by corresponding polarity factors listed in table 5.7.

$$\text{Polarity} = 3 \times SAWB + 2 \times SA + 2 \times WAWB + WA \quad (5.17)$$

Rearranging terms yields:

$$\begin{aligned} \text{Polarity} &= 2 \times (SAWB + WAWB) + (SA + SAWB) + (SA + WA) \\ &= 2 \times 8.0 + 11.0 + 10.9 \\ &= 37.9 \end{aligned} \quad (5.18)$$

The total polarity of AAD-1 can now be calculated in a straightforward manner:

$$\begin{aligned} \text{Polarity of AAD-1} &= 4 \times SASB + 3 \times WASB + 2 \times SB + WB + (3 \times SAWB + 2 \times SA + 2 \times WAWB + WA) \\ &= 4 \times 15.4 + 3 \times 3.6 + 2 \times 4.2 + 5.7 + 37.9 \\ &= 124.4 \end{aligned} \quad (5.19)$$

For the polarity calculations of various IEC mixtures, as opposed to whole asphalts, some estimates of polarities of each of the four components not directly measured are necessary, so it may be arbitrarily assumed that the amount of SAWB is equal to that of WAWB. Then, for AAD-1, mass fractions can be assigned for the four IEC fractions not directly isolated:

$$\begin{aligned} SAWB &= 4.0\% \\ WAWB &= 4.0\% \\ SA &= 7.0\% \\ WA &= 3.9\% \end{aligned}$$

Based on the composition of the calculated nine fractions, the polarities of all IEC mixtures can be determined. As an example, in the conventional IEC separation, asphalts are dissolved in a mixed solvent (chapter 1) and pumped through a column of anion resin, and then through a column of cation resin. The neutrals, the weak bases, and the combination of weak acids and WAWB amphoteries (this combination of fractions was designated weak acids in chapter 1) are eluted. The polarity of these eluates, which constitute 65.8% of AAD-1, is calculated as follows:

$$\begin{aligned}
 \text{Polarity} &= (3.9 + 5.7 + 2 \times 4.0) \times 100 / (52.2 + 3.9 + 5.7 + 4.0) \\
 &= (17.6) \times (100/65.8) \\
 &= 26.6
 \end{aligned}
 \tag{5.20}$$

The calculated amounts of the nine IEC fractions for four core asphalts are listed in table 5.8. The polarities for these four core asphalts can be mathematically calculated without any assumptions about polarities of their components. In figure 5.6, viscosities of the IEC mixtures at 25°C (77°F) are replotted against their calculated polarities in table 5.8. There are very strong linear relationships. Results of linear regressions are listed in table 5.9. **These regression equations indicate that the viscosity of asphalt is determined by two factors: (1) the intercept, representing the viscosity of the IEC neutral fraction (solvent moiety); and (2) polarity, determined by composition and relative amount of polar components (dispersed moiety).** The slopes of the viscosity-polarity curves in figure 5.6 for AAD-1, AAG-1, and AAK-1 are essentially the same but are different from that of AAM-1, the slope of which is lower. The lower slope of the viscosity-polarity curve for AAM-1 may be due to the high molecular weight of its IEC neutral fraction, which could reduce the effectiveness of viscosity enhancement by the association of the polar materials. Alternatively, AAM-1 also may contain larger amounts of polar components of high true molecular weight. Crude oils are known to contain extended homologous series of various compound types. An example of a homologous series found in some crude oils is that of long-chain monocarboxylic acids. Individual compounds of this series vary from one another in number of methylene (CH<sub>2</sub>) groups (or carbon number), but all contain one carboxylic acid functional group. A monocarboxylic acid of higher carbon number is less polar than a monocarboxylic acid of lower carbon number. Petroleum is composed of a large number of such homologous series. Asphalts relatively enriched in higher molecular weight materials should be somewhat less polar than asphalts having more low molecular weight components.

The viscosities of the amphoteric-free mixture shown in figure 5.5 and the viscosity of whole asphalt AAD-1 are replotted on the viscosity-polarity curve in figure 5.7. In figure 5.7, the dashed line represents a plot of viscosity vs. polarity, which ranges from 0 to 140 on the x-axis. The solid line represents a plot of viscosity vs. mass % IEC polar materials, which range from 0 to 50 on the x-axis. For the whole asphalt, the polar materials consist of natural abundances of amphoterics, bases, and acids. For the amphoteric-free mixture, amphoterics are replaced with bases, so that total mass percentages of polar materials in the mixture and the whole asphalt are identical. Large changes of viscosity in the viscosity-mass %-polar component curve can be explained by polarity change. Replacing amphoterics with their bases, although total amounts of polar components remain the same, decreases the total polarity of the mixture from 124.4 to 70.4. The measured viscosity for this mixture is very close to the viscosity predicted by the viscosity-polarity relationship for a polarity of 70.4. Viscosity predictions based on polarity for the other three amphoteric-free mixtures are also good.

Development of the viscosity-polarity relationship for an asphalt also allows estimation of polarity, which according to the microstructural model should be related to effectiveness for viscosity-enhancement of asphalt fractions containing polar materials, such as SEC fractions, asphaltenes, and maltenes. From figure 5.6 or the regression equations in table

5.9, polarity of any asphalt fraction considered to be the solvent component can be estimated by its viscosity. Since the polarity of whole asphalt and the amounts of the solvent component and the associated component are known, polarity of the associated component can be calculated. For example, AAD-1 SEC Fraction-II, which for many purposes may be considered to be the solvent moiety of an asphalt, comprises 76.6% of whole asphalt and its viscosity is 336.6 Pa·s at 25°C (77°F). From the regression equation for AAD-1 in table 5.9, a polarity of 51.6 for the AAD-1 SEC Fraction-II is obtained. Therefore, the polarity of SEC Fraction-I (to give the total polarity of 124.4 for the whole asphalt) should be 361 ( $361 \times 0.234 + 52 \times 0.766 = 124.4$ ). Polarities calculated in this manner for various fractions of four asphalts are listed in table 5.10. Polarities of a given IEC fraction for the four asphalts are similar, while polarities of fractions obtained by solvent precipitation or SEC separation vary more widely among the four asphalts. Obviously, IEC separates asphalts more efficiently into defined chemical fractions than the other two separation methods. The data in table 5.10 indicate that SEC Fraction-I materials of AAD-1 and AAK-1 are more polar than equivalent materials in AAG-1 and AAM-1. The SEC Fraction-II materials of AAG-1 and AAM-1 are calculated to be more polar than those of AAD-1 and AAK-1. These polarity differences should influence properties of the asphalts.

Asphaltenes are separated based on solubility in n-heptane. Two major factors determining solubility are size and polarity of molecules. In n-heptane, molecules with large size and moderate polarity, small size and high polarity, or extremely large size and low polarity would be precipitated as asphaltenes. As shown in chapter 2, figure 2.1, relatively small amounts of materials having large molecular size are present in AAG-1, but they may exist in fairly significant quantities in AAM-1. Thus, polarity would play a more important role in precipitation of asphaltenes of AAG-1 and molecular size in precipitation of asphaltenes of AAM-1. This might be one reason why asphaltenes of AAG-1 have high polarity and asphaltenes of AAM-1 have low polarity. Because of differing polarities for asphaltenes, chemical separation schemes involving precipitation of asphaltenes, such as Corbett analysis, may not give good correlations between chemical and physical properties.

## Cross-Blending of SEC Fractions

In order to determine the relative influence of asphalt dispersed and solvent moieties (as represented by the two SEC fractions) on rheological properties, a series of cross-blended mixtures of SEC fractions of several asphalts was prepared and viscosities and other rheological properties of the mixtures were measured. The viscosities of the cross-blended mixtures should in theory depend on the total polarities of the mixtures and the  $M_n$  value and chemical composition of the IEC neutrals (which largely constitute the SEC Fraction-II of the mixtures). One basis for preparing the mixtures was the observation that each asphalt is characterized by a unique natural abundance of the two SEC fractions. For example, AAD-1 contains 23.3% nonfluorescent, associating materials (SEC Fraction-I) and 76.7% fluorescent fraction (SEC Fraction-II). AAM-1 contains 30.6% SEC Fraction-I and 69.4% SEC Fraction-II. Four of the core asphalts were chosen for the cross-blending experiments, and four combinations of the asphalts were selected. These are the combinations AAD-1/AAK-1, AAD-1/AAM-1, AAG-1/AAK-1, and AAG-1/AAM-1.

For each combination of asphalts, eight mixtures were prepared. Each mixture comprises a different combination of the two SEC fractions at one of the two natural abundance levels characteristic of the respective asphalts. For ease of reference, the mixtures are coded A through H. Two of the mixtures (A and H) effectively reconstitute the original asphalts and serve as controls, having undergone the same separation and recombination procedures as the other six mixtures. The composition of the mixtures, along with rheological data, are reported in supplementary tables 5.12 through 5.19. In supplementary table 5.12, mixture A contains both SEC Fractions of AAD-1 at their natural abundance levels, reconstituting the asphalt. Mixture B consists of SEC Fraction-I of AAD-1 mixed with SEC Fraction-II of AAK-1, again at the AAD-1 natural abundance level. Mixture C is made up of SEC fractions of AAD-1, but at the AAK-1 natural abundance level. Mixture D contains SEC Fraction-I of AAD-1 and SEC Fraction-II of AAK-1, but combined at natural abundance levels peculiar to AAK-1. Mixtures A through D all contain SEC Fraction-I of AAD-1. Mixtures E through H all contain SEC Fraction-I of AAK-1.

Mixtures A and H correspond to reconstituted AAD-1 and AAK-1, respectively. The viscosities of these mixtures are more than twice as great as the parent asphalts at the temperatures of measurement (supplementary table 5.16). This is not surprising in view of the fact that the mixtures are composed of fractions that were generated by SEC separation followed by removal of solvent. The fractions were then weighed and redissolved in solvent, and the solvent again was removed from the mixtures. Inevitably, some light ends are lost in the process.

At a given temperature of measurement, viscosities and  $\tan \delta$  values reported for the mixtures in supplementary tables 5.12 and 5.16 are not greatly different. Viscosities among the mixtures at each temperature vary by at most a factor of ten. The members of the set of mixtures in which SEC Fraction-II of AAD-1 acts as the solvent moiety (A, C, E, G) tend to be less viscous than the corresponding members of the set of mixtures in which SEC Fraction-II of AAK-1 acts as the solvent moiety (B, D, F, H). These differences are illustrated in supplementary table 5.20, in which averaged viscosities of each mixture at 60°C (140°F) are reported. To determine the relative effectiveness of the SEC Fraction-II materials as solvent components, viscosities of each member of the two sets of mixtures referred to above are compared in the following manner: A is compared with B; C with D; E with F; and G with H. Each of the two paired mixtures contains the same SEC Fraction-I, and the two SEC fractions also are combined in the same proportions for each of the pairs. The difference between each of the pairs in the two sets is the nature of the SEC Fraction-II materials. In supplementary table 5.20, the viscosity of mixture B is greater than that of A; the viscosity of D is greater than that of C; the viscosity of F is greater than that of E; and the viscosity of H is greater than that of G. From these observations, it is speculated that the solvent component of AAD-1, as represented by the SEC Fraction-II of this asphalt, is a more effective solvent than the solvent component of AAK-1.

In a similar manner, the viscosities of the set of mixtures A, B, C, D can be compared with viscosities of the set of mixtures E, F, G, H in order to assess the strengths of interactions among polars (peptizabilities) of the dispersed phases, as represented by SEC Fraction-I materials. The members of the two sets are paired such that the viscosity of A compares with E, B with F, C with G, and D with H. The data listed in supplementary table 5.20

show that the viscosities of the mixtures in the A, B, C, D set are greater than viscosities of paired members of the E, F, G, H set. Therefore, it is speculated that the dispersed component of AAD-1, as represented by the SEC Fraction-I materials, is somewhat more polar (less readily peptized) than the dispersed component of AAK-1.

A third pairing involves materials having the same two SEC fractions as components, but in different natural abundances. The two sets are mixtures A, B, E, F (AAD-1 natural abundance) and mixtures C, D, G, H (AAK-1 natural abundance). Mixture A is paired with C, B with D, E with G, and F with H. Mixtures with the AAK-1 natural abundance have more SEC Fraction-I materials than mixtures with the AAD-1 natural abundance. The mixtures with more SEC Fraction-I materials should be more viscous than corresponding mixtures with less of the SEC Fraction-I materials, and the data listed in supplementary table 5.20 show that this is the case.

Asphalts AAD-1 and AAK-1 are alike in many respects, so mixtures of their SEC fractions at natural abundance levels (which are not greatly different) would be expected to have rheological properties that are similar. From the rheological data for the mixtures of the two SEC fractions of these two asphalts, it was speculated that the dispersed component of AAD-1 (as represented by SEC Fraction-I) is somewhat more polar (less readily peptized) than the dispersed component of AAK-1, and the solvent component of AAD-1 (as represented by SEC Fraction-II) is a somewhat more effective solvent than the solvent component of AAK-1. Because of more strongly interacting polars, poorly peptized dispersed components will form more extensive associations than well peptized dispersed components, resulting in larger viscosities and elastic moduli ( $G'$ ) in the poorly peptized materials, all other factors being equal. A good solvent will tend to suppress extensive associations and hence will also affect rheological behavior. These considerations follow from the microstructural model of asphalts. The conclusions as applied to AAD-1 and AAK-1 find some support from the Heithaus parameters calculated for these two asphalts: AAD-1:  $p_a = 0.61$ ,  $p_o = 1.33$ ; AAK-1:  $p_a = 0.66$ ,  $p_o = 1.25$  (chapter 9, table 9.8), and from polarity calculations in table 5.10. Heithaus parameters are a measure of compatibility of an asphalt. A full discussion of the significance of Heithaus parameters is reserved until chapter 9. Briefly, the parameter  $P$  measures overall compatibility of the maltenes and asphaltenes of an asphalt, which in the Heithaus analysis are presumed to be solvent and dispersed moieties respectively. The parameter  $p_o$  measures maltene solvent power, and the parameter  $p_a$  measures asphaltene peptizability.

Supplementary tables 5.13 and 5.17 report viscosities and  $\tan \delta$  data for mixtures of SEC Fractions-I and -II of AAD-1 and AAM-1 at natural abundance levels characteristic of the two asphalts. The differences in natural abundance levels between AAD-1 and AAM-1 are greater than for AAD-1 and AAK-1. Asphalts AAD-1 and AAM-1 are unlike in many respects. The viscosity and  $\tan \delta$  ranges of the mixtures reported in supplementary tables 5.13 and 5.17 are very large. Supplementary table 5.21 lists average 60°C (140°F) viscosities of the mixtures, arranged in three different sets, in the same manner as was done for the mixtures of AAD-1 and AAK-1 in supplementary table 5.20. At 60°C (140°F), mixture B is much more viscous than A, D is much more viscous than C, F is much more viscous than E, and H is much more viscous than G. The viscosities of these mixtures, which comprise four materials mixed in two different proportions, range from 18 Pa·s to



354,800 Pa·s at 60°C (140°F), a difference of more than four powers of ten! Based on these comparisons, it is speculated that the solvent component of AAD-1 is a much better solvent than the solvent component of AAM-1. Comparison of the mixture pairs A and E, B and F, C and G, and D and H shows that the dispersed component of AAM-1 is much less polar (more readily peptizable) than the dispersed component of AAD-1. Heithaus parameters of the two asphalts are AAD-1:  $p_a = 0.61$ ,  $p_o = 1.33$ ; AAM-1:  $p_a = 0.89$ ,  $p_o = 1.26$  (chapter 9, table 9.8). It is assumed that the Heithaus  $p_a$  value has some relationship to dispersed component peptizabilities, and that the  $p_o$  value relates to solvent power of the solvent components. Polarity calculations in table 5.10 support the Heithaus data.

Data in supplementary table 5.21 also show that mixtures having larger amounts of SEC Fraction-I components (AAM-1 natural abundance) are more viscous than materials that have smaller amounts of SEC Fraction-I components (AAD-1 natural abundance) within each pair of corresponding mixtures.

Supplementary tables 5.14 and 5.18 list viscosities and  $\tan \delta$  values (these are  $\tan \delta$  values measured at constant shear frequency, not the  $\tan \delta_{et}$  values discussed in chapter 2) of mixtures of SEC Fractions-I and -II of asphalts AAG-1 and AAK-1. As for the other mixtures, the SEC fractions were combined in properties equivalent to their natural abundances in the two asphalts. The two asphalts are dissimilar in many ways. Asphalt AAG-1 contains less SEC Fraction-I material than any of the other core asphalts. It also is a highly compatible system, based on asphaltene compatibility index (ACI) value (chapter 9) and Heithaus parameters. Asphalt AAK-1 contains a large SEC Fraction-I component and is classified as a relatively incompatible system. Rheological properties of mixtures of the SEC fractions of the two asphalts cover a wide range of values, as would be expected when components of these dissimilar materials are mixed. The range is not as great as for the mixtures of AAD-1 and AAM-1 SEC fractions (supplementary tables 5.13 and 5.17).

Supplementary table 5.22 compares the averages of two viscosity determinations at 60°C (140°F) of the mixtures of SEC fractions of AAG-1 and AAK-1. The same sets of pairs of mixtures are compared as for the other mixtures of SEC fractions described above. Inspection of the data in supplementary table 5.22 shows that mixture A is more viscous than mixture B; mixture C is more viscous than mixture D; mixture E is more viscous than mixture F, and mixture G is more viscous than mixture H. The viscosity differences are close to an order of magnitude. Therefore, the solvent component of AAK-1 is speculated to be a more effective solvent than the solvent component of AAG-1. To compare the dispersed components, it is observed that the viscosities of the mixtures of E, F, G, and H are somewhat larger than the viscosities of the corresponding members of the set of mixtures A, B, C, and D. Therefore, the dispersed component of AAK-1 is somewhat more polar (less peptizable) than the dispersed component of AAG-1. Viscosities of the set of mixtures characterized by AAK-1 natural abundance of SEC fractions (C, D, G, H) are higher than viscosities of mixtures characterized by AAG-1 natural abundance of SEC fractions (A, B, E, F). In support of the above observations, Heithaus parameters of AAG-1 are  $p_a = 0.78$ ,  $p_o = 1.16$ ; those of AAK-1 are  $p_a = 0.66$ ,  $p_o = 1.25$  (chapter 9, table 9.8). Polarity values (table 5.10) of the SEC fractions also support the above observations.

Asphalts AAG-1 and AAM-1 have the greatest extremes in natural abundances of their SEC fractions. Asphalt AAG-1 consists of 11.8% SEC Fraction-I and 88.2% SEC Fraction-II. Asphalt AAM-1 consists of 30.6% SEC Fraction-I and 69.4% SEC Fraction-II. Viscosities and  $\tan \delta$  values of mixtures of SEC fractions of these asphalts are reported in supplementary tables 5.15 and 5.19. The viscosities and  $\tan \delta$  values in these tables cover a wide range. Supplementary table 5.23 reports comparisons of average viscosities of sets of mixtures of the SEC fractions at 60°C (140°F). From the data in supplementary table 5.23, it is evident that viscosities of the mixtures containing the SEC fractions at the AAM-1 natural abundance are much greater than the viscosities of mixtures containing the SEC fractions at the AAG-1 natural abundance. It is also speculated that the dispersed phase of AAG-1 is more polar (less peptizable) than the dispersed phase of AAM-1 (comparison of viscosities of mixtures A with E, B with F, C with G, and D with H). This conclusion is supported by polarity calculations listed in table 5.10. It is not clear from supplementary table 5.23 which of the two solvent components is the better solvent. While mixture A is more viscous than B, and E is more viscous than F, mixture D is much more viscous than C, and H is more viscous than G. These results imply that at high concentrations of SEC Fraction-I (AAM-1 natural abundance), the AAG-1 solvent component is the better solvent, while at low concentrations of SEC Fraction-I (AAG-1 natural abundance), the solvent phase of AAM-1 is the better solvent.

In the above experiments, viscosities replicated reasonably well. The  $\tan \delta$  values at 25°C (77°F) of the mixtures reconstituting the original asphalts are close to values determined for the tank asphalts.

In the above discussion, the differences in viscosities among the SEC Fraction-II components of the four asphalts were not taken into consideration. The viscosities of these materials are much lower than viscosities of the parent asphalts (chapter 2, table 2.3) at 25°C (77°F), but they vary widely, ranging from 337 Pa·s for SEC Fraction-II of AAD-1 to 62,380 Pa·s for SEC Fraction-II of AAG-1. Viscosities of the SEC Fraction-II materials were not measured on the mechanical spectrometer at higher temperatures because some of them are too fluid. By assuming that SEC Fraction-II components in the mixtures are solvents, relative viscosities ( $\eta_{rel}$ ) can be calculated. The  $\eta_{rel}$  values of the mixtures are numerically equal to the absolute viscosities of the mixtures divided by the absolute viscosities of the SEC Fraction-II materials comprising the solvent moiety of the mixture. The  $\eta_{rel}$  values at 25°C (77°F) of all the mixtures of SEC fractions are listed in supplementary table 5.24. Averages of two determinations of viscosities of each mixture at 25°C (77°F) were used in the calculations.

Comparison of the  $\eta_{rel}$  values of the mixtures accounts for differences in absolute viscosities of the SEC Fraction-II materials. For mixtures of AAD-1 and AAK-1 fractions, these viscosities are not greatly different. The  $\eta_{rel}$  values of the mixtures of SEC fractions of these asphalts vary from 165 to 453. Some mixtures have higher  $\eta_{rel}$  values than either of the reconstituted parent asphalts (mixtures A and H), and some have lower  $\eta_{rel}$  values. The variance in  $\eta_{rel}$  values among these mixtures is not great, so the corresponding SEC fractions of two asphalts appear to be fairly similar in properties.

Relative viscosities of mixtures of AAD-1 and AAM-1 SEC fractions range over several orders of magnitude. Compared with the  $\eta_{rel}$  values of the reconstituted parent asphalts (mixtures A and H;  $\eta_{rel}$  values of the two asphalts differ significantly),  $\eta_{rel}$  values of the other mixtures are much higher, lower, or intermediate. The corresponding SEC fractions of asphalts AAD-1 and AAM-1 therefore are not very much alike.

The  $\eta_{rel}$  values of reconstituted asphalts AAG-1 and AAK-1 (mixtures A and H) vary widely. Other mixtures of the SEC fractions of these asphalts are intermediate in  $\eta_{rel}$ , indicating that the corresponding SEC fractions of the two asphalts are not as different as are the AAD-1 and AAM-1 SEC fractions.

When solvent component, dispersed component, and natural abundance comparisons are made using relative viscosities instead of absolute viscosities, it is found that all mixtures having larger amounts of SEC Fraction-I materials have higher  $\eta_{rel}$  values than equivalent mixtures having smaller amounts of SEC Fraction-I materials, as would be expected. The dispersed materials of AAD-1 are found to be the least peptizable, followed by AAK-1, AAG-1, and AAM-1 in order. This order is in accord with previous conclusions. For the solvent components, in estimating solvent power based on  $\eta_{rel}$  values, AAG-1 is best, followed by AAM-1, AAK-1, and AAD-1. These results are not in accord with some of the previous speculations, and they indicate that the apparently superior solvent power of AAD-1 SEC Fraction-II may be the result of its low absolute viscosity. The comparison of  $\eta_{rel}$  values may provide a more accurate assessment of the true solvent power of an asphalt solvent moiety than merely comparing the  $\eta^*$  values of cross-blended mixtures. It will be shown subsequently that, in ability to accommodate more polar materials produced by oxidation, the solvent moiety of AAG-1 is more effective than the solvent phases of any other asphalt studied (chapter 8).

The variations among the  $\eta_{rel}$  values of the mixtures of SEC fractions are large and in most cases differ significantly from  $\eta_{rel}$  values of reconstituted parent asphalts. These differences are not entirely attributable to differences in relative amounts of SEC fractions that constitute the mixtures. Otherwise, mixtures at a given natural abundance composed of the same SEC Fraction-II but different SEC Fraction-I materials would have similar  $\eta_{rel}$  values. The nature of the two fractions mixed is important in determining rheological properties of mixtures.

The study of rheological properties of the mixtures of SEC fractions shows that asphalt composition profoundly influences asphalt rheological properties. Great differences in rheological properties can be observed by mixing dispersed and solvent components of a pair of asphalts in two different natural abundance levels. This is particularly evident if one asphalt is classified as an incompatible asphalt and the other a compatible asphalt, or if both are compatible. Mixtures of SEC fractions of the two incompatible asphalts (AAD-1 and AAK-1) did not exhibit extremely large differences in rheological properties. It is evident that the solvent moieties of some asphalts effectively disperse large amounts of polar materials, suppressing associative interactions and thereby limiting viscosities of the systems and suppressing elastic properties. Other solvent moieties do not readily suppress associative interactions of polar materials that are not readily peptized, so combinations of poor solvent components with large amounts of dispersed, polar components that are not

readily peptized result in systems that are characterized by high viscosities and low  $\tan \delta$  values. The dispersed components of asphalts vary in their polarity (ease of peptization).

Asphalts AAD-1 and AAK-1 can be characterized as having effective solvent components and large amounts of dispersed components that are strongly polar (difficult to peptize). The effectiveness of the solvent components of these asphalts results mostly from low solvent viscosities, caused by the presence of substantial amounts of molecules of relatively low carbon numbers. These asphalts are classified as incompatible systems. Asphalt AAG-1 can be characterized by a solvent moiety that may not be as effective (based on the high solvent moiety viscosity) as those of AAD-1 and AAK-1, but contains small amounts of dispersed materials of intermediate polarity (peptizability). Asphalt AAM-1 also comprises a relatively poor solvent moiety (again based on its high viscosity) and large amounts of a dispersed component that is not strongly polar (readily peptized). When solvent moieties are ranked corrected for their absolute viscosity differences, the AAG-1 and AAM-1 solvent moieties do not compare as unfavorably with AAD-1 and AAK-1 solvent moieties.

The above results may explain why properties of asphalt blends cannot always be predicted from properties of their components. It can be speculated that other physical properties of the above mixtures may exhibit as much variance as viscosities and  $\tan \delta$  values.

In figures 5.8 through 5.11, viscosities of the mixtures at 25°C (77°F) listed in supplementary tables 5.16 through 5.19 are plotted vs. their polarities. Figure 5.8 illustrates viscosity-polarity relationships for mixtures in which the SEC Fraction-II of AAD-1 is the solvent moiety. Along with the viscosity-polarity plots of the cross-blended mixtures, the viscosity-polarity curve for AAD-1 based on IEC fractions shown in figure 5.6 is overplotted in figure 5.8. Polarity values of the mixtures are calculated by multiplying polarity factors for each SEC fraction in table 5.10 by the mass percent of each SEC fraction in the mixture. As an example, for mixture B in supplementary table 5.16, consisting of 23.4% SEC Fraction-I of AAD-1 and 76.6% SEC Fraction-II of AAK-1, the polarity value is  $(0.234 \times 363) + (0.766 \times 48) = 121.7$ . This data point is plotted in figure 5.10 because the solvent moiety of mixture B is the SEC Fraction-II of AAK-1. Values of polarities of all of the cross-blended mixtures of SEC fractions are listed in supplementary table 5.25. The best fitted lines of cross-blended mixtures are in accord with the polarity-viscosity relationships shown in figure 5.6, with the exception of the AAM-1 SEC-II mixtures. However, the slope of the best fitted line for AAM-1 SEC-II mixtures is almost the same as the rest of the fitted lines. Note also that the viscosities of mixtures containing AAM-1 SEC-I are relatively low compared with the viscosities estimated from the fitted lines for the polarities of the mixtures. This indicates that the polarity of the neat AAM-1 may be somewhat overestimated. If the low concentration of functional groups in IEC fractions of AAM-1 (because of its large molecular size) is assumed, the overestimation of the polarity for AAM-1 could be explained and the slope of the polarity-viscosity relationship for AAM-1 in figure 5.6 would be the same as those of other asphalts. In all cases, SEC Fraction-I of AAD-1 is the most effective viscosity-enhancing material and SEC Fraction-I of AAK-1, AAG-1, and AAM-1 were the next most effective materials in order. This can be predicted from their polarities given in table 5.10. The same conclusion was drawn from the comparisons of viscosities of cross-blended mixtures discussed above.

For prediction of viscosities of cross-blended mixtures, the viscosity-polarity model in the form presented in table 5.9 was used (i.e., logarithm of viscosity of a mixture as a linear function of logarithm of viscosity of IEC neutrals and polarity of the mixture). The regression equation is

$$\text{Log } (V_{\text{mix}}) = 0.041 + 0.732 \text{ Log } (V_n) + 0.0341 (\text{Polarity}) \quad (5.21)$$

where  $V_{\text{mix}}$  is viscosity of a mixture and  $V_n$  is viscosity of IEC neutrals. Multiple linear regression gave the coefficient of determination ( $R^2$ ) of 0.922 with P-value less than 0.0005. The measured and predicted viscosities for the mixtures are shown in figure 5.12.

Another statistical analysis was performed to examine the contributions to viscosity of SEC Fraction -I and -II of four asphalts. The amount of SEC Fraction-I in each mixture was used as the independent variable. The types of asphalts from which SEC Fractions were obtained were used in the regression analysis as dummy variables. The regression equation is

$$\text{Log } (V_{\text{mix}}) = 3.65 + 0.0697 (\% \text{ SEC-I}) + C_{\text{SEC-I}} + C_{\text{SEC-II}} \quad (5.22)$$

$$R^2 = 0.975 \text{ and P-value} = 0.000$$

where

$$C_{\text{SEC-I}} \text{ value} \approx \begin{array}{l} 1.52 \text{ for AAD-1 SEC-I,} \\ 1.04 \text{ for AAG-1 SEC-I,} \\ 1.21 \text{ for AAK-1 SEC-I, and} \\ 0.00 \text{ for AAM-1 SEC-I,} \end{array}$$

and

$$C_{\text{SEC-II}} \text{ value} \approx \begin{array}{l} -1.78 \text{ for AAD-1 SEC-II,} \\ 0.13 \text{ for AAG-1 SEC-II,} \\ -1.38 \text{ for AAK-1 SEC-II, and} \\ 0.00 \text{ for AAM-1 SEC-II.} \end{array}$$

The  $C_{\text{SEC-I}}$  value is a regression constant related to the polarity of the SEC Fraction-I (Table 5.10). The  $C_{\text{SEC-II}}$  value is a regression constant related to the viscosity of the SEC Fraction-II (Table 2.3).

Based on the above regression equation (5.22), average relative contributions to mixture viscosities by four SEC Fraction-I materials and four SEC-II materials are as follows:

for SEC Fraction-I,

$$\text{AAD-1:AAG-1:AAK-1:AAM-1} = 33:11:16:1 \quad (5.23)$$

and for SEC Fraction-II,

$$\text{AAD-1:AAG-1:AAK-1:AAM-1} = 1:82:2.5:60 \quad (5.24)$$

For a given SEC Fraction-II, for example, mixtures containing SEC Fraction-I of AAD-1 should have, on average, 33 times higher viscosities than mixtures containing the same amount of SEC Fraction-I of AAM-1. For a given SEC Fraction-I, mixtures containing SEC Fraction-II of AAG-1 should have viscosities more than 80 times higher than mixtures containing SEC Fraction-II of AAD-1. The measured viscosity ratio for SEC Fraction-II is similar to the ratio of its contribution to viscosity given above and is 1:185:3.3:78 for SEC Fraction-II materials of AAD-1, AAG-1, AAK-1, and AAM-1, respectively.

## **Dielectric Constant, Glass Transition Temperature, and Polarity**

Dielectric constants and glass transition temperatures of the eight core asphalts were determined at The Pennsylvania State University. The dielectric constant is the relative permittivity of a dielectric material in a capacitor. The dielectric constant of an asphalt measures, under a given condition, the degree of polarization or the amount of polarized molecules. Dielectric constants of four core asphalts are plotted against polarities in figure 5.13. As expected, as polarity increases, the dielectric constant increases.

The glass transition temperature is the temperature below which many molecular motions cease because of intramolecular energy barriers. It is known that the glass transition temperature of an amorphous polymer is related to molecular size and somewhat to polarity. As molecular weight or polarity increases, the glass transition temperature increases. However, the glass transition temperatures of the core asphalts show poor correlation with their molecular weights, having a coefficient of determination of 0.32. Instead, they are fairly well correlated with their viscosities at 25°C (77°F) as shown in figure 5.14. Viscosities of asphalts, which are determined by both size of molecules and polarity, should be the better predictor for the glass transition temperature. Relationships of the glass transition temperature with viscosities of various asphalt fractions such as IEC neutrals, SEC Fraction-II, and maltenes, and with retention time of the peak maxima in the fast SEC described in chapter 2, are illustrated in figures 5.15 through 5.18. The best correlation is with the IEC neutral fraction viscosities.

Temperature susceptibilities and glass transition temperatures are important properties of asphalts and are known to be directly related to one another for lubricating oils (Stearns, Duling, and Johnson 1966). Early in this program, viscosities of the eight core asphalts were determined at 25°C (77°F) and 60°C (140°F). When the logarithms of these viscosity values are plotted vs. reciprocals of absolute temperature in a typical Arrhenius plot, the slopes of the lines divided by the gas constant represent activation energies for viscous flow. The activation energy for viscous flow can be used as another measure of viscosity-temperature susceptibility. It also is a measure of non-Newtonian properties. These data are listed in table 5.11. The four asphalts characterized as more compatible systems (AAC-1, AAF-1, AAG-1, and AAM-1) have higher values of energy of activation of viscous flow than the four incompatible asphalts. A full discussion of asphalt compatibility is presented in chapter 9. It is speculated that viscous flow is mostly dependent on asphalt solvent components. For homogeneous polymers, polar materials have much higher energies of activation for viscous flow than nonpolar materials. Compatible asphalts are less polar overall than incompatible asphalts, based on asphaltene contents (chapter 9, table 9.6). However, the solvent components of compatible asphalts may be more aromatic and polar

than solvent components of incompatible asphalts. When activation energies for viscous flow for the eight core asphalts are plotted against glass transition temperatures, a good correlation is observed, as shown in figure 5.19. It is speculated that the contribution to low-temperature cracking from a low activation energy of viscous flow would be small because these asphalts should be better able to relieve strain at low temperatures. This argument pertains only to asphalts which also have low glass transition temperatures.

Effects of temperature on the viscosity-polarity relationship have been studied. As temperature increases from 25°C (77°F) to 45°C (113°F), the viscosity-polarity relationships for AAG-1 and AAM-1 nearly overlap, as shown in figure 5.20. At 60°C (140°F), only the viscosity-polarity curve of AAD-1 differs from that of the other asphalts. In figure 5.21, the curves for all asphalts show changes in rate of viscosity increase with polarity increase around polarity 100. The viscosity-polarity relationships for AAG-1, AAK-1 and AAM-1 up to polarity 110, or polarities of these neat asphalts are almost identical, which means that the viscosity differences among the three neat asphalts at 60°C (140°F) may be determined by the polarity differences among them. As temperature increases, viscosity of a weakly polar asphalt decreases more rapidly than that of highly polar asphalt. Activation energy for viscous flow or temperature susceptibility of four core asphalts decreases as the polarity increases, as shown in figure 5.22.

In chapter 1, table 1.2, ratios of IEC fractions by conventional separation were reported. A discussion of the significance of the ratios was reserved. An attempt was made to correlate the ratios, which serve to characterize some features of the chemical composition of asphalts, with various physical properties. The ratio of total acids to total bases was observed to correlate strongly with polarity ( $R^2 = 0.965$ ,  $P\text{-value} = 0.018$ ). Acids in petroleum tend to be more polar than bases, so this correlation is to be expected. A good correlation of the total acid to total base ratio with dielectric constant also was observed ( $R^2 = 0.723$ ,  $P\text{-value} = 0.007$ ).

The ratio of the sum of weak acids and weak bases to the sum of strong acids to strong bases correlates negatively with polarity ( $R^2 = 0.993$ ,  $P\text{-value} = 0.003$ ) due to a relative deficiency of the more strongly polar species. Large relative amounts of weak acids and weak bases are characteristic of the more compatible asphalts. Consequently, it is not surprising to note that activation energy of viscous flow correlates positively with the value of the ratio of weak acids and weak bases to strong acids and strong bases (figure 5.23). Weak acids and weak bases may largely constitute what are often referred to as resins. Resins are thought to be the components of asphalts that confer solubility in solvent moieties of asphaltene fractions. Therefore, the more resins that are present, the more compatible an asphalt should be.

## Summary

Viscosity of an asphalt at 25°C (77°F) can be reasonably predicted from chemical properties of the asphalt. The viscosity is determined by (1) polarity as determined from IEC separations and (2) viscosity of the IEC neutral fraction, which has a close relationship with its molecular weight. Amphoteric, highly associated very polar materials, are

responsible for most viscosity enhancement. Although amounts of amphoteric range from 19% to 27% of total mass of asphalt, the contribution to polarity ranges from 60% to 75%. As temperature rises, effects of polarity on viscosity become more significant. Consequently, polarity of asphalt determines viscosity temperature susceptibility.

Relative effectiveness on viscosity enhancement of each asphalt fraction obtained from various separation procedures as well as IEC separation can be predicted based on polarity. Viscosities of the blended asphalts or the mixtures of asphalt fractions can be estimated using viscosity-polarity relationships.



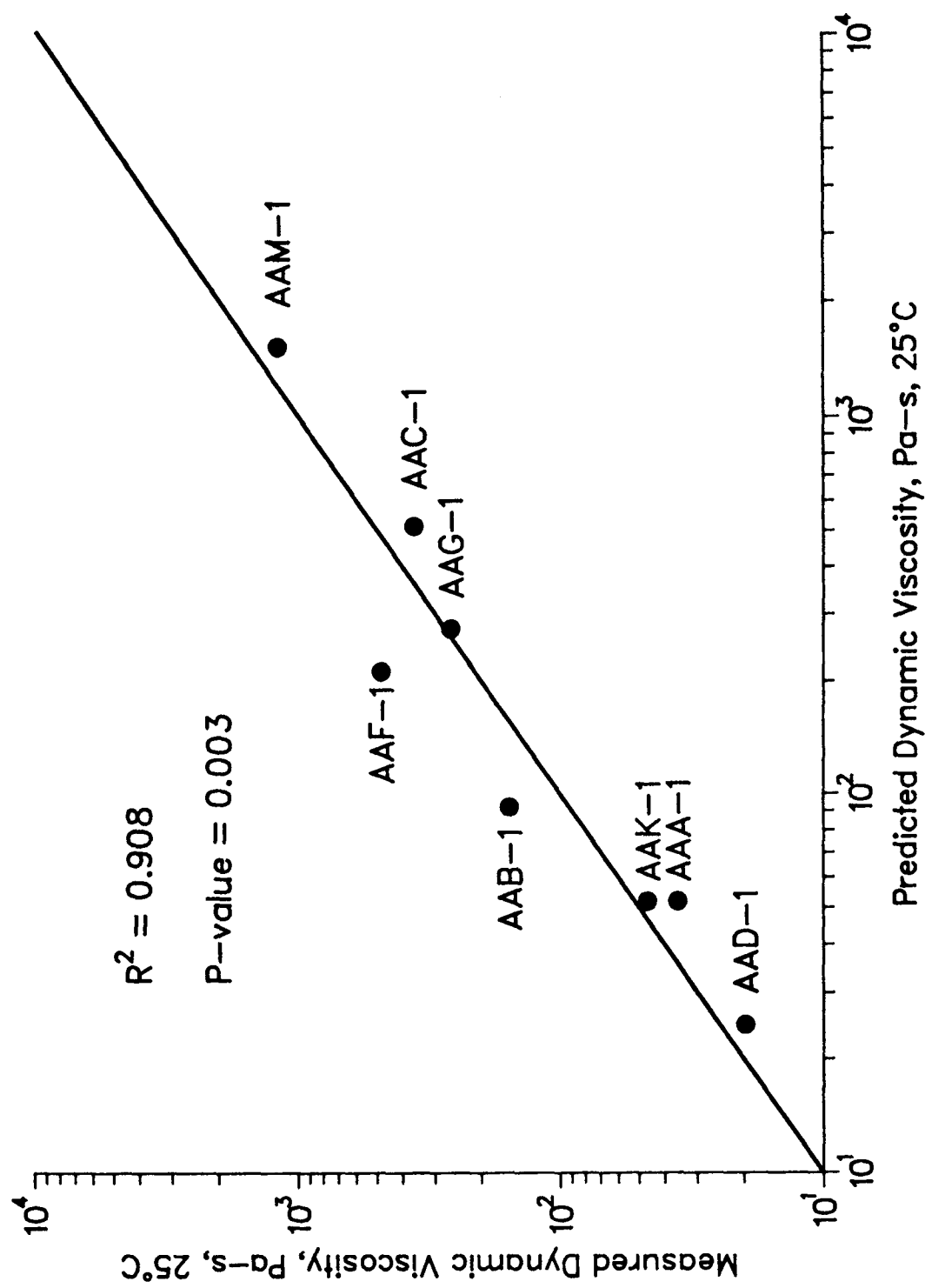


Figure 5.1 Viscosities of Neutrals Measured and Predicted by Molecular Weight and Amount of IR Functional Group

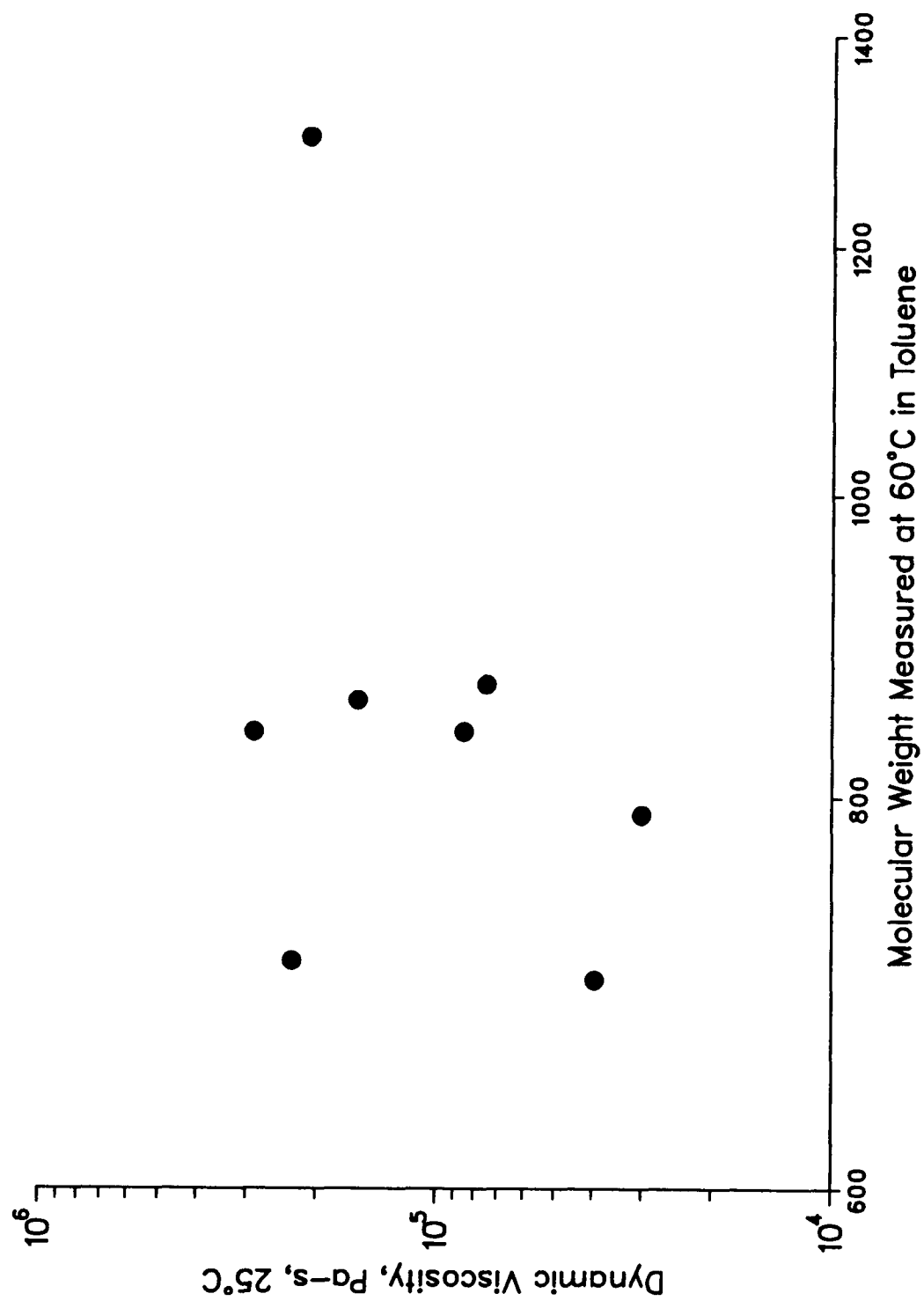


Figure 5.2 Viscosity vs. Molecular Weight for Core Asphalts

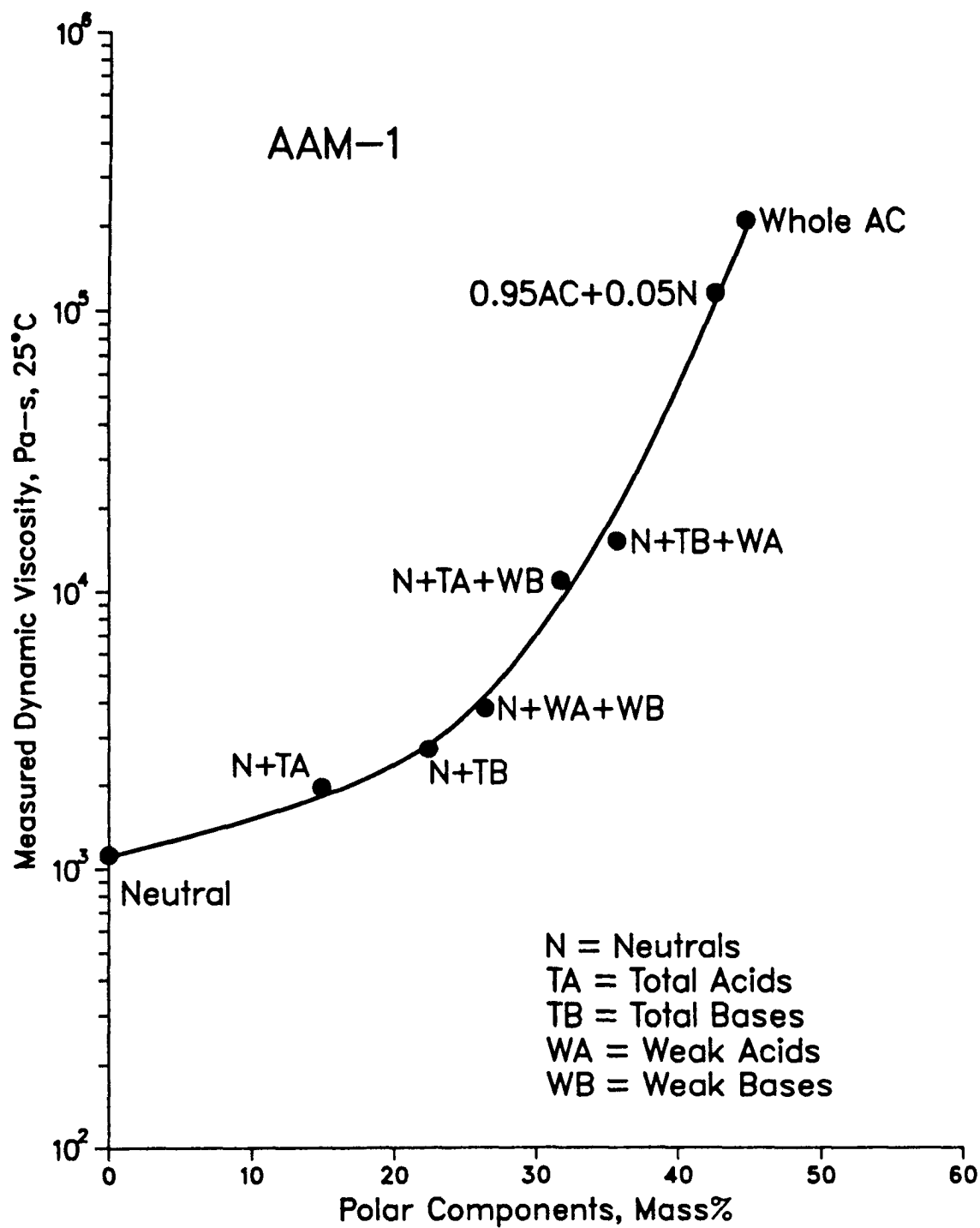


Figure 5.3 Viscosity vs. Amount of Polar Components for AAM-1

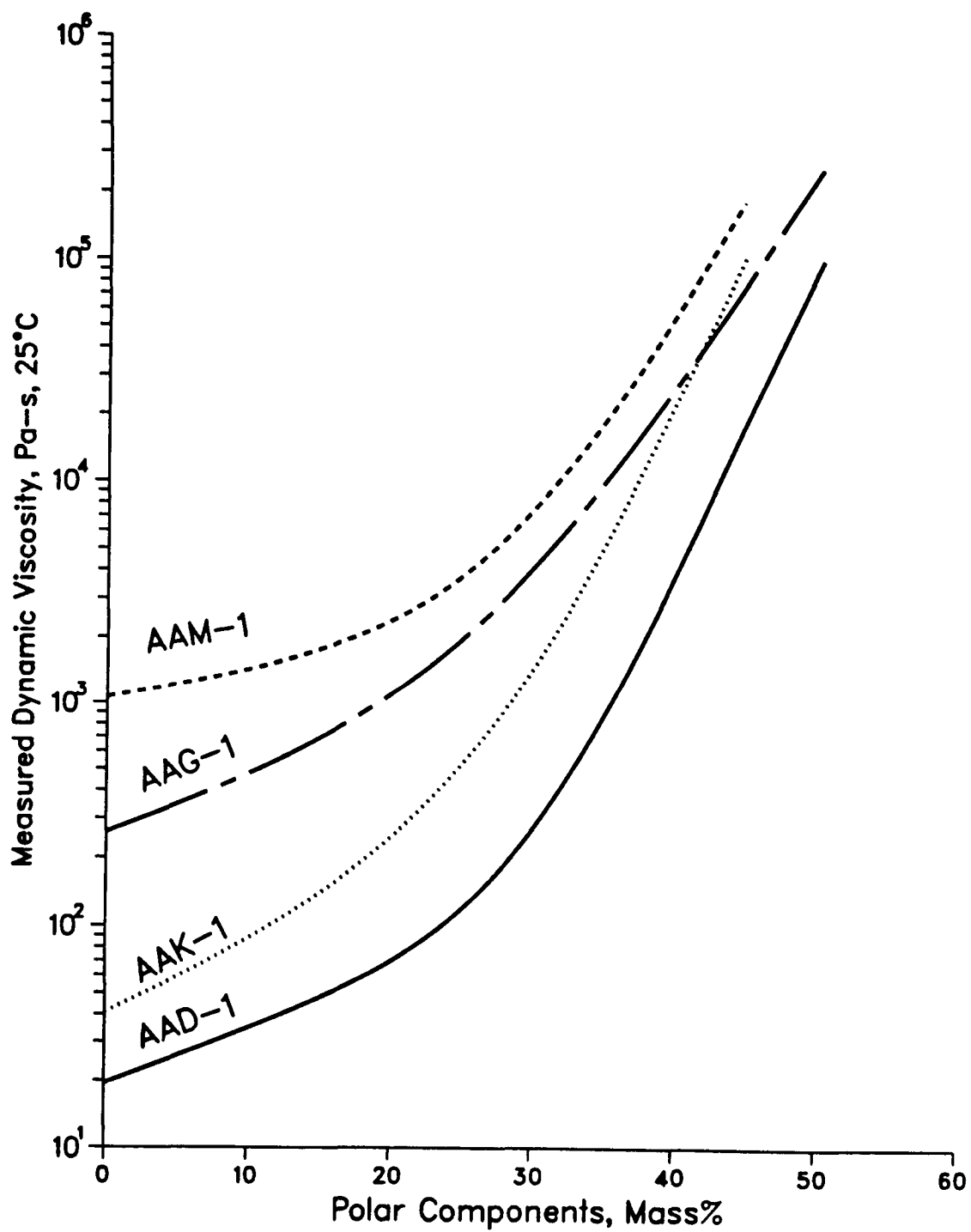


Figure 5.4 Viscosity vs. Amount of Polar Components for Four Core Asphalts

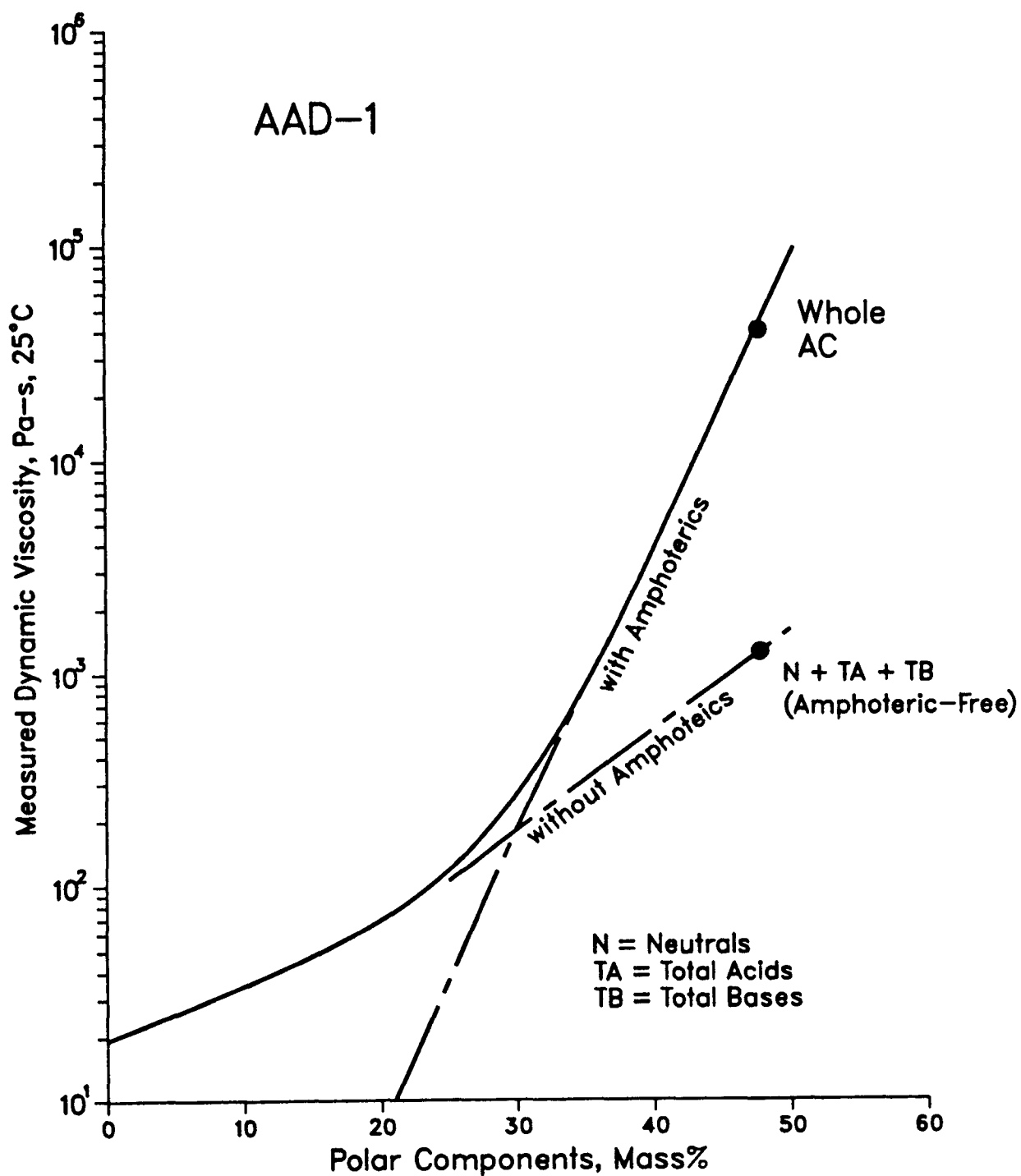


Figure 5.5 Effect of Amphoterics on Viscosity for AAD-1

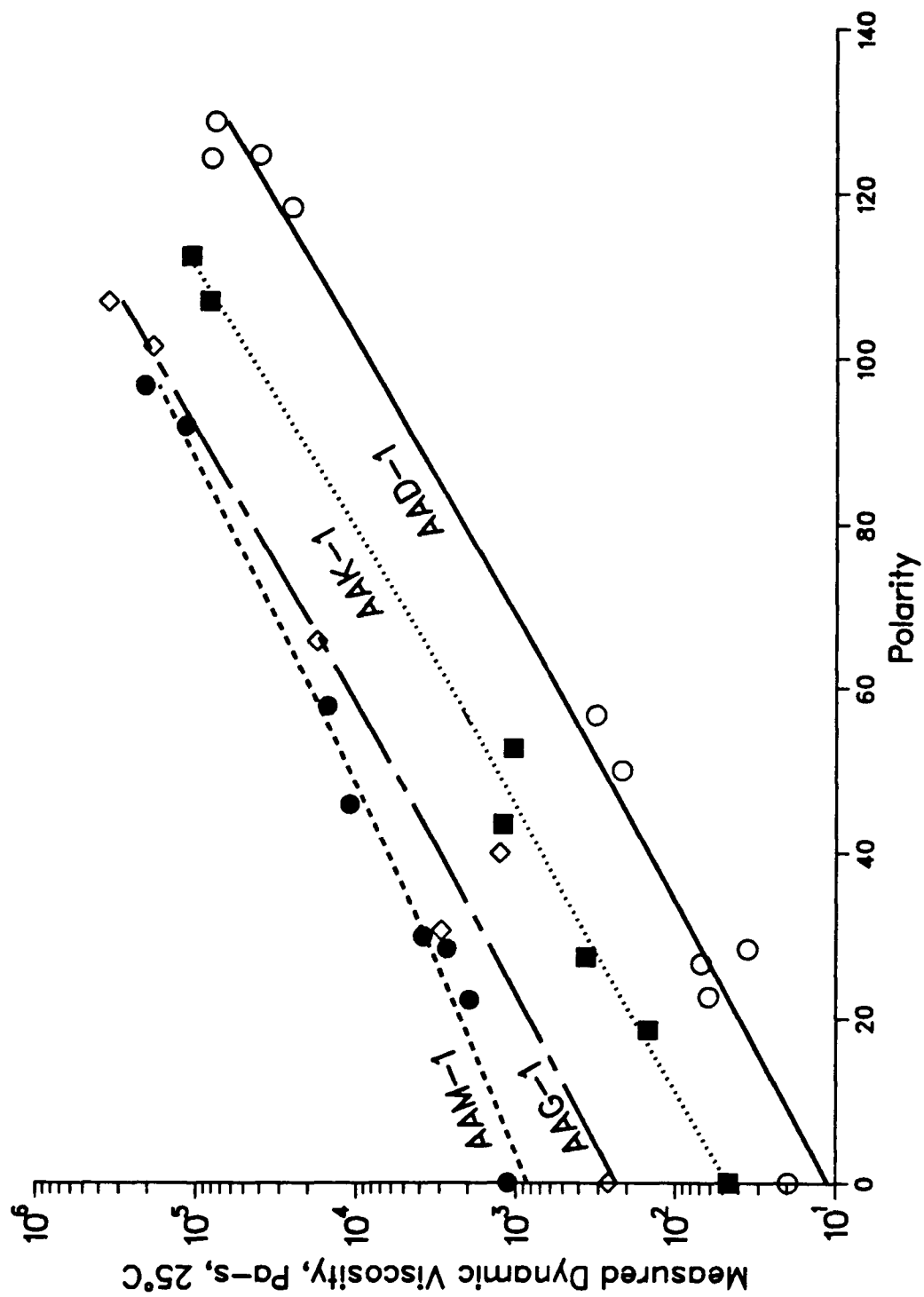


Figure 5.6 Viscosity at 25°C vs. Polarity for Four Core Asphalts

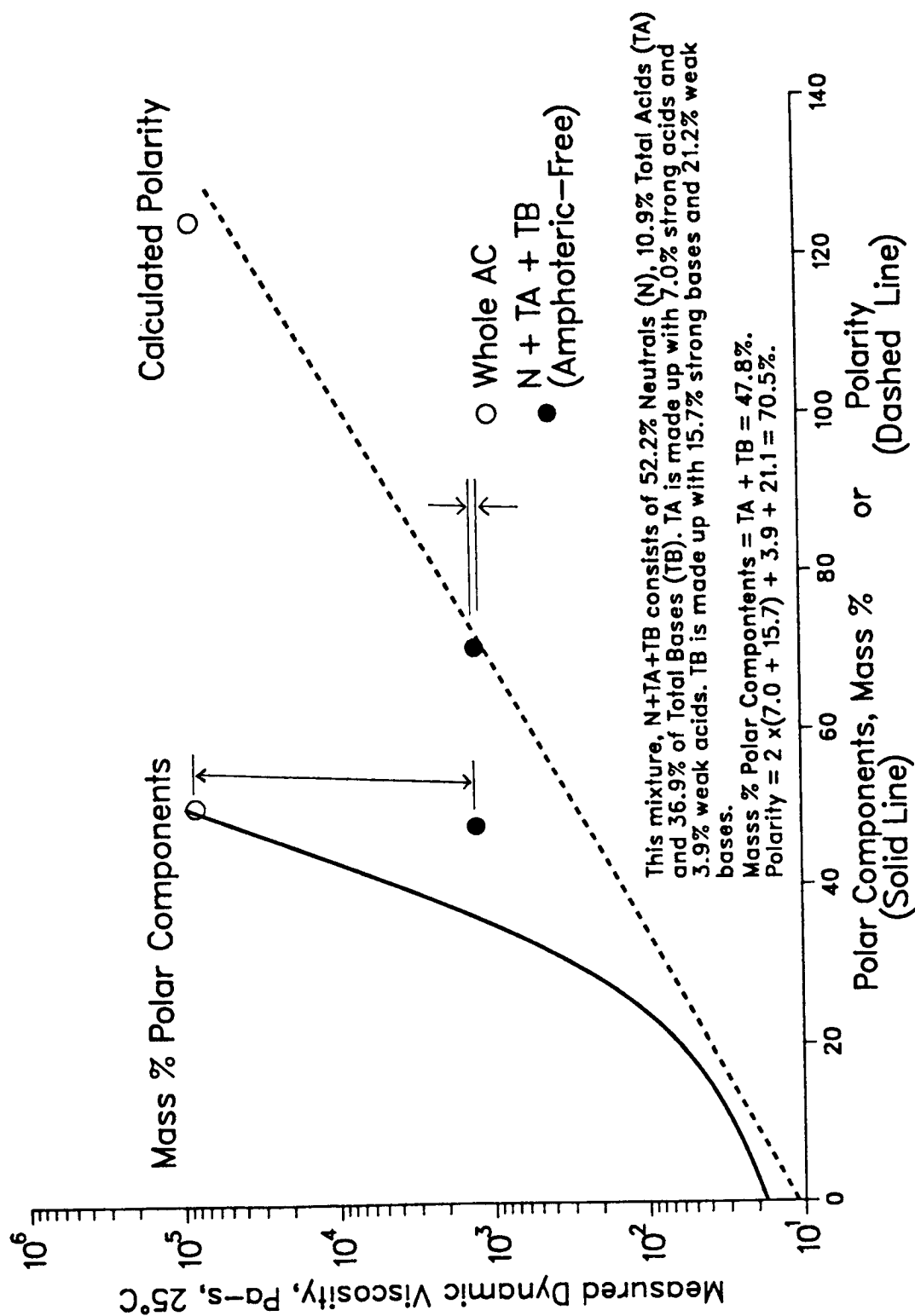


Figure 5.7 Viscosity Prediction of Viscosity--Polarity Relationship for AAD-1

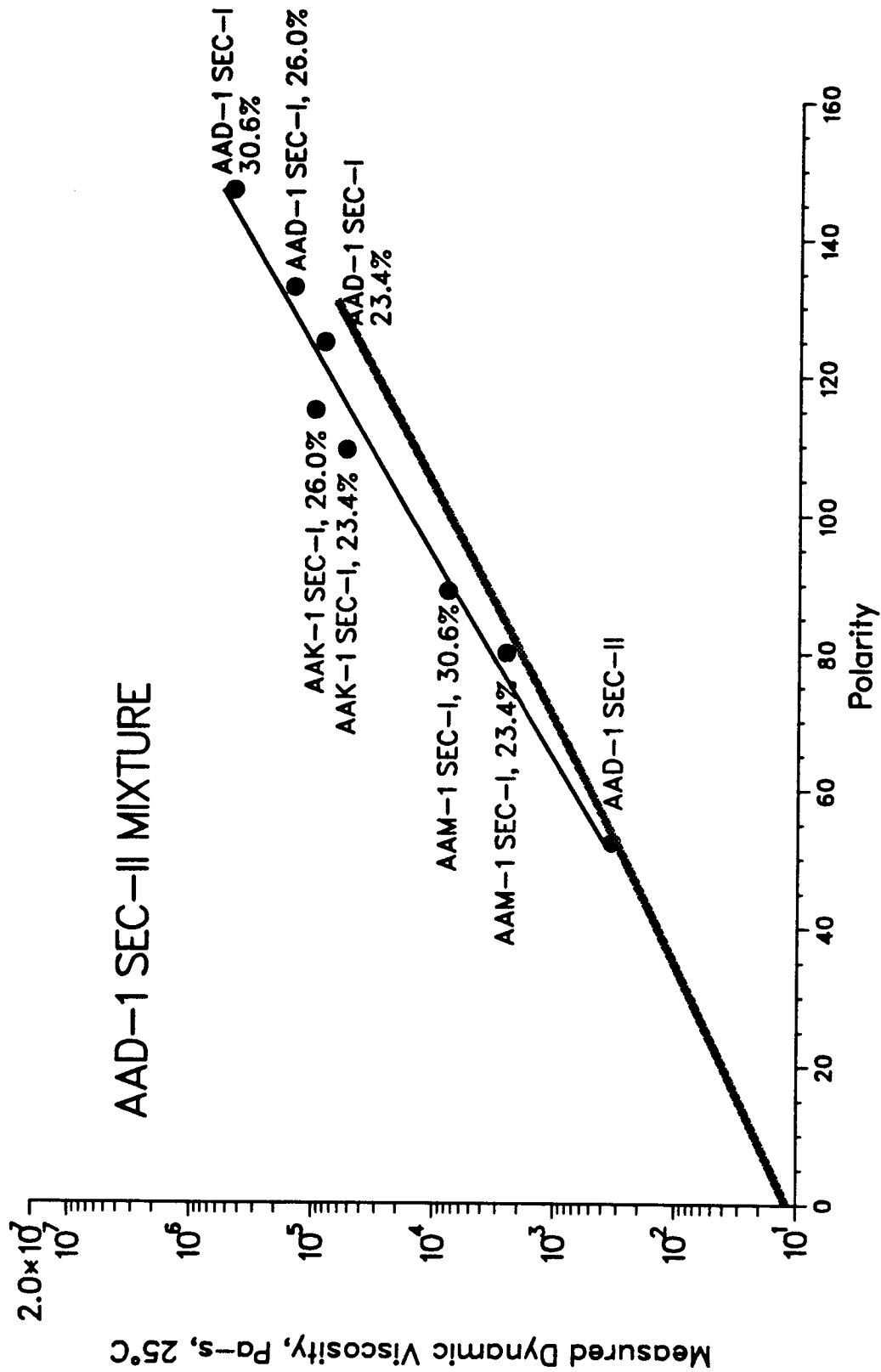


Figure 5.8 Viscosity vs. Polarity for SEC Cross-Blending Mixtures Containing SEC Fraction-II of AAD-1



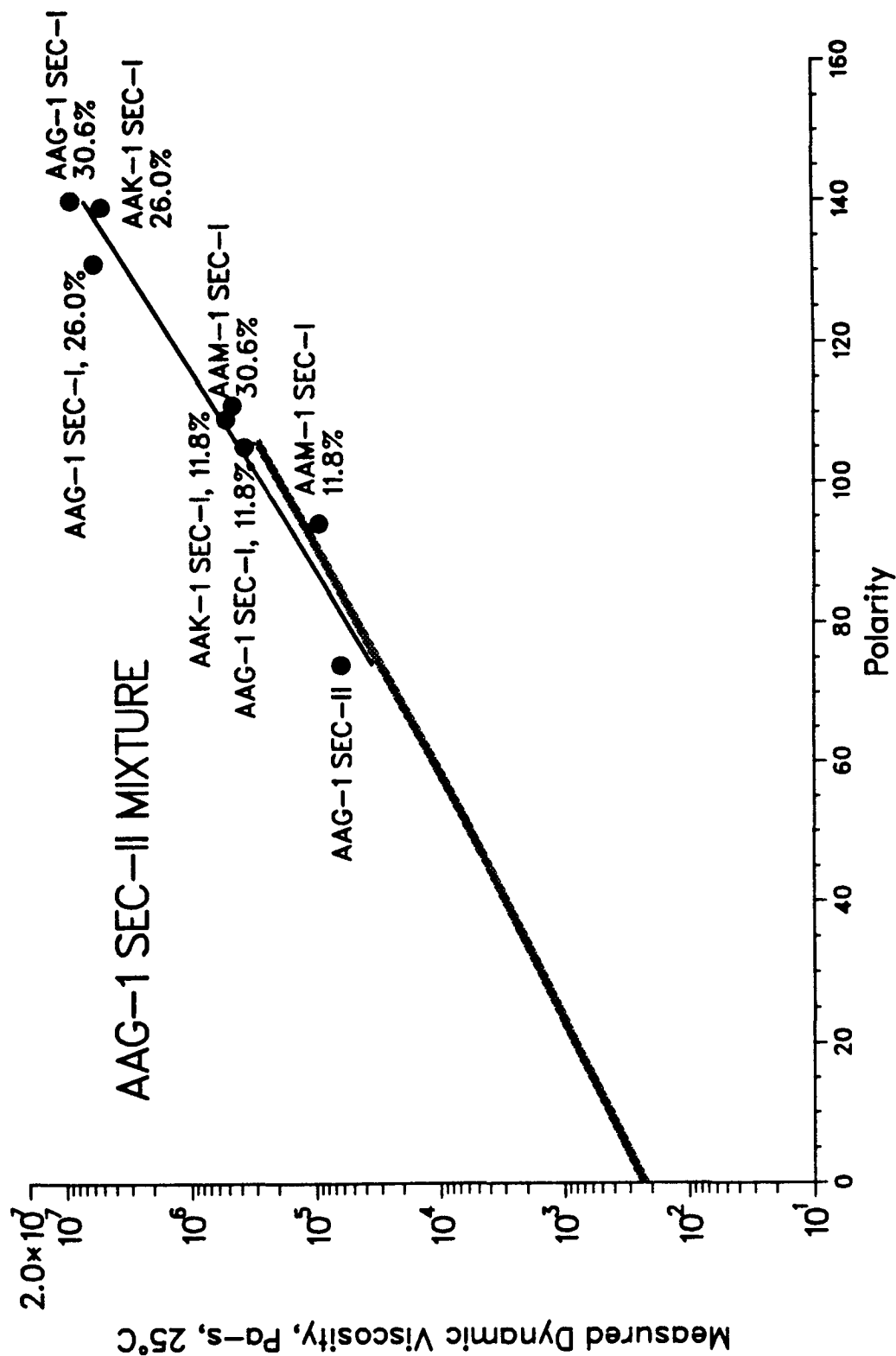


Figure 5.9 Viscosity vs. Polarity for SEC Cross-Blending Mixtures Containing SEC Fraction-II of AAG-1

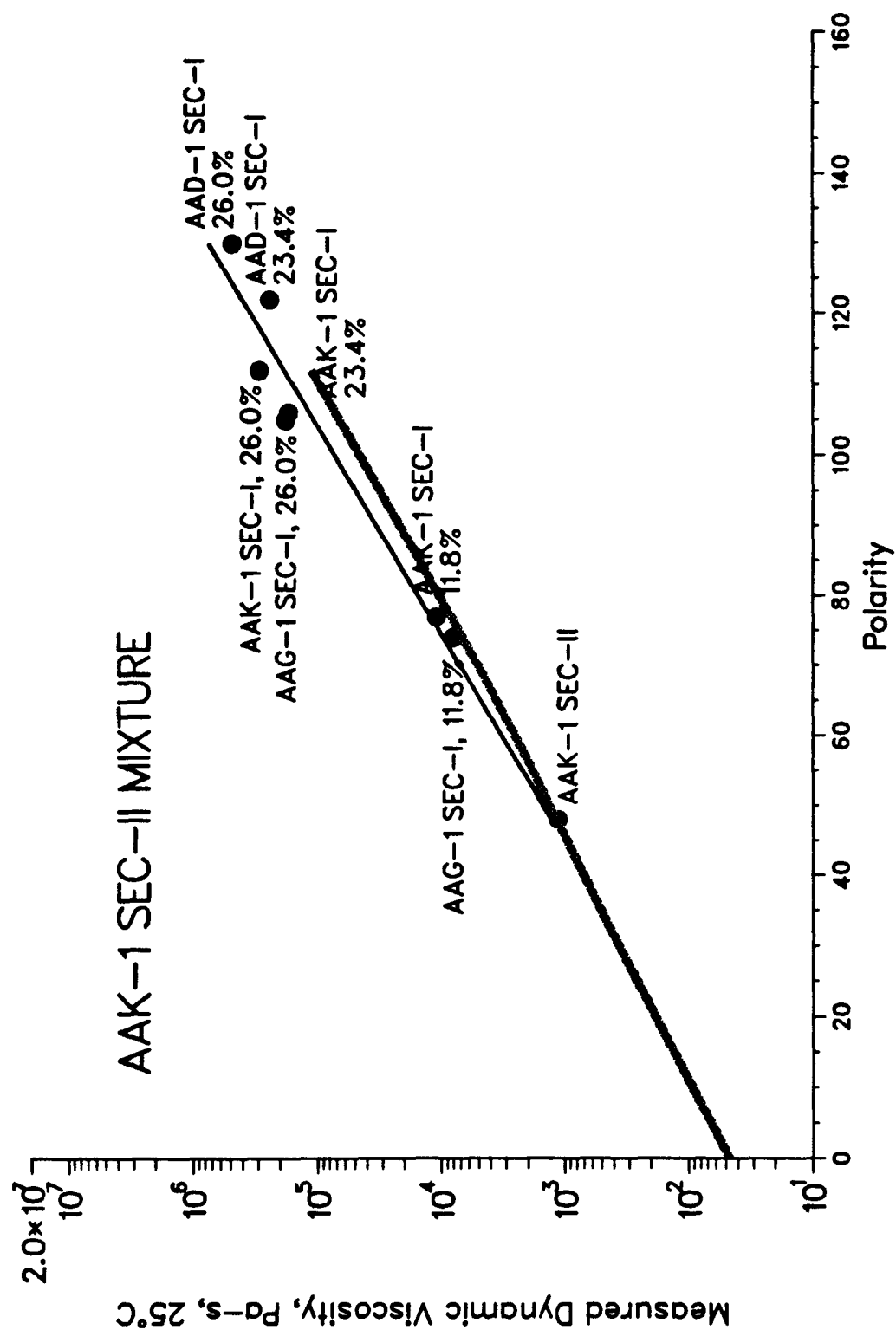


Figure 5.10 Viscosity vs. Polarity for SEC Cross-Blending Mixtures Containing SEC Fraction-II of AAK-1

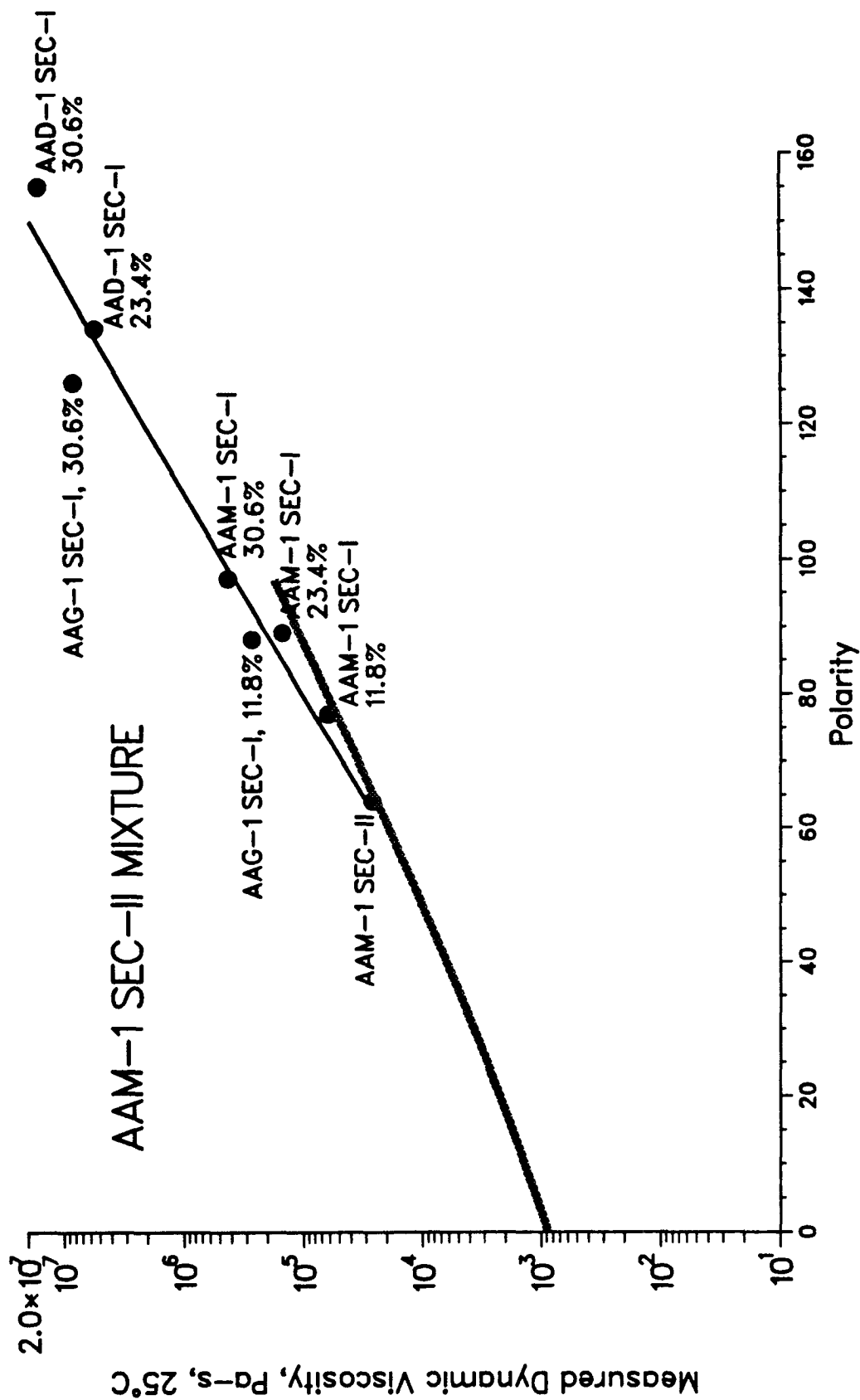


Figure 5.11 Viscosity vs. Polarity for SEC Cross-Blending Mixtures Containing SEC Fraction-II of AAM-1

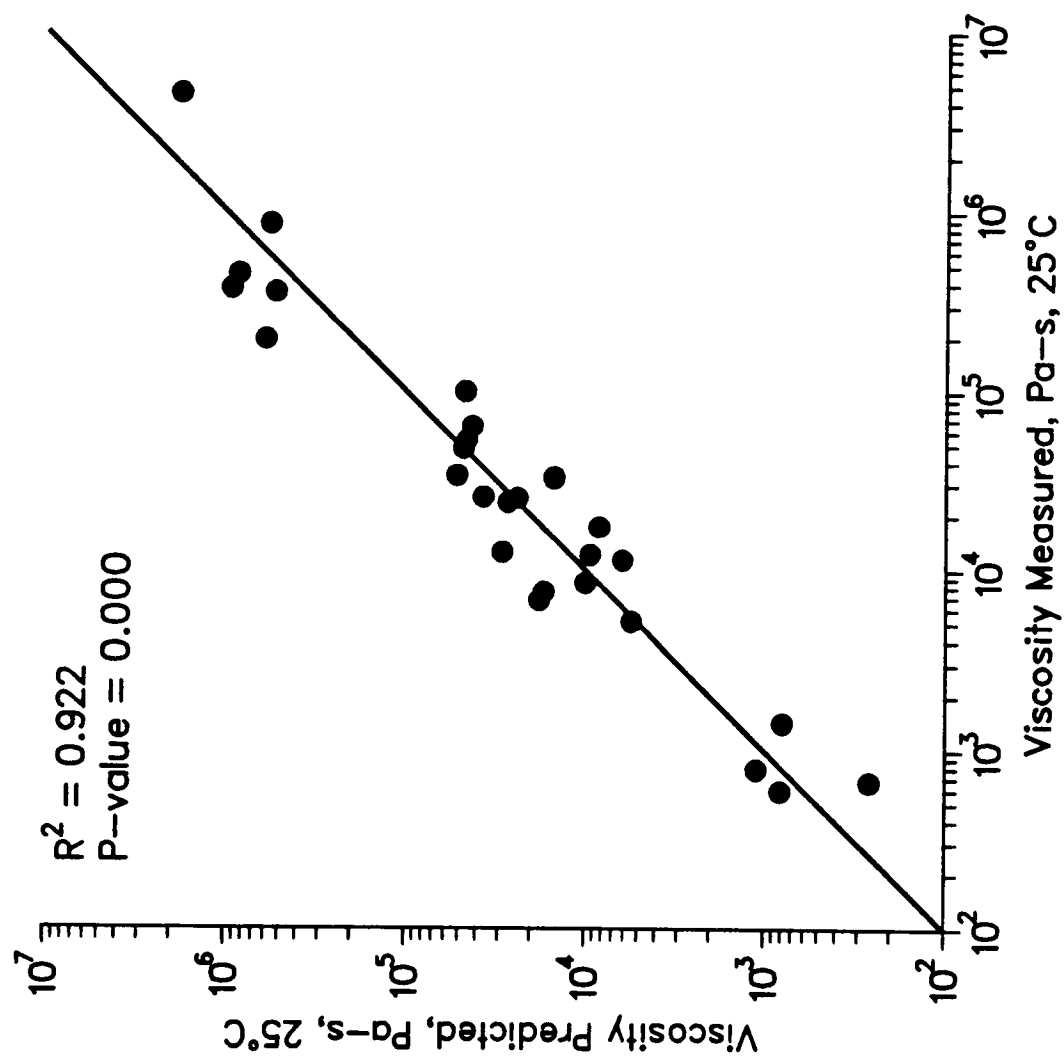


Figure 5.12 Measured and Predicted Viscosities of SEC Cross-Blending Mixtures

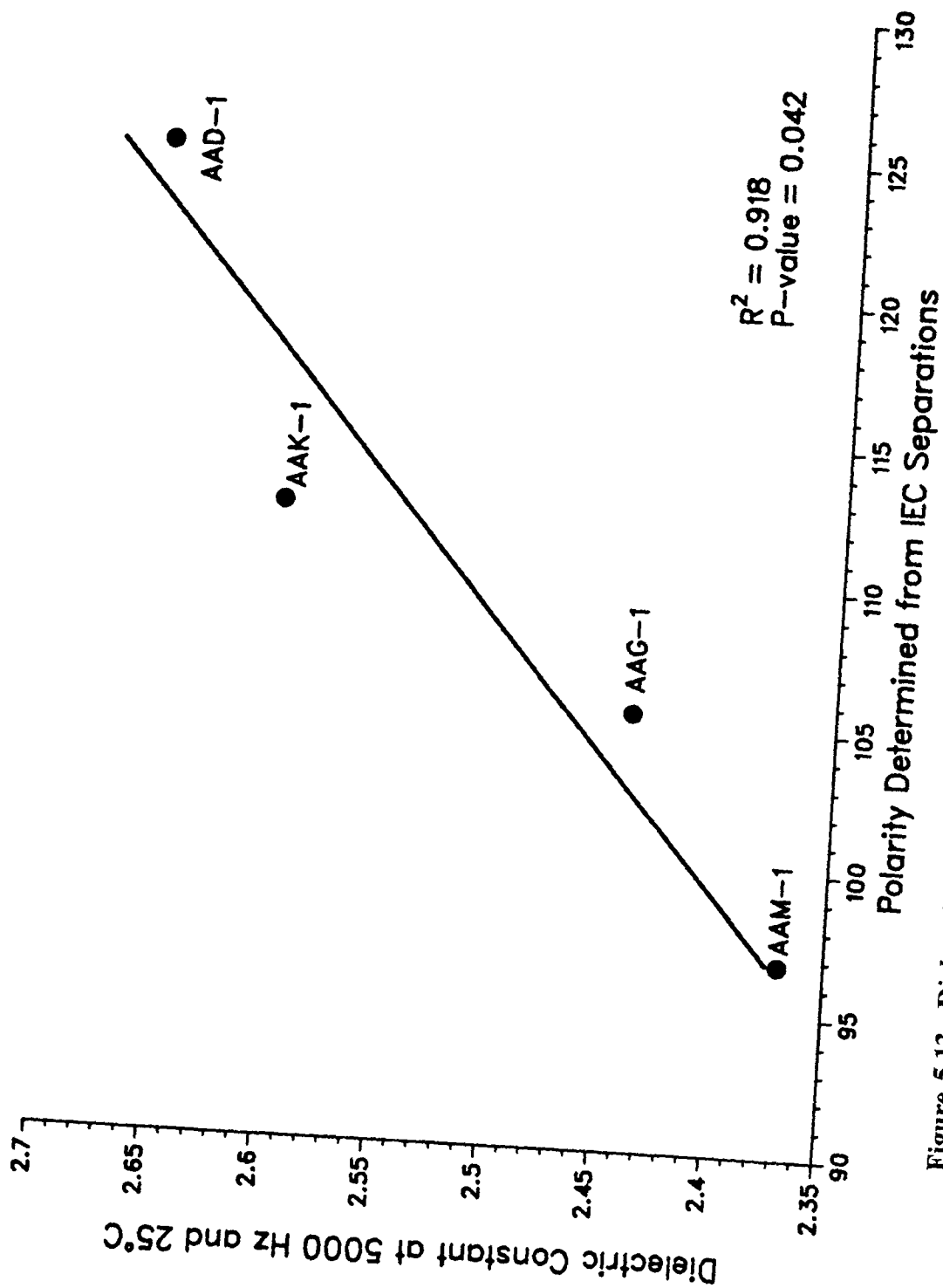


Figure 5.13 Dielectric Constant vs. Polarity

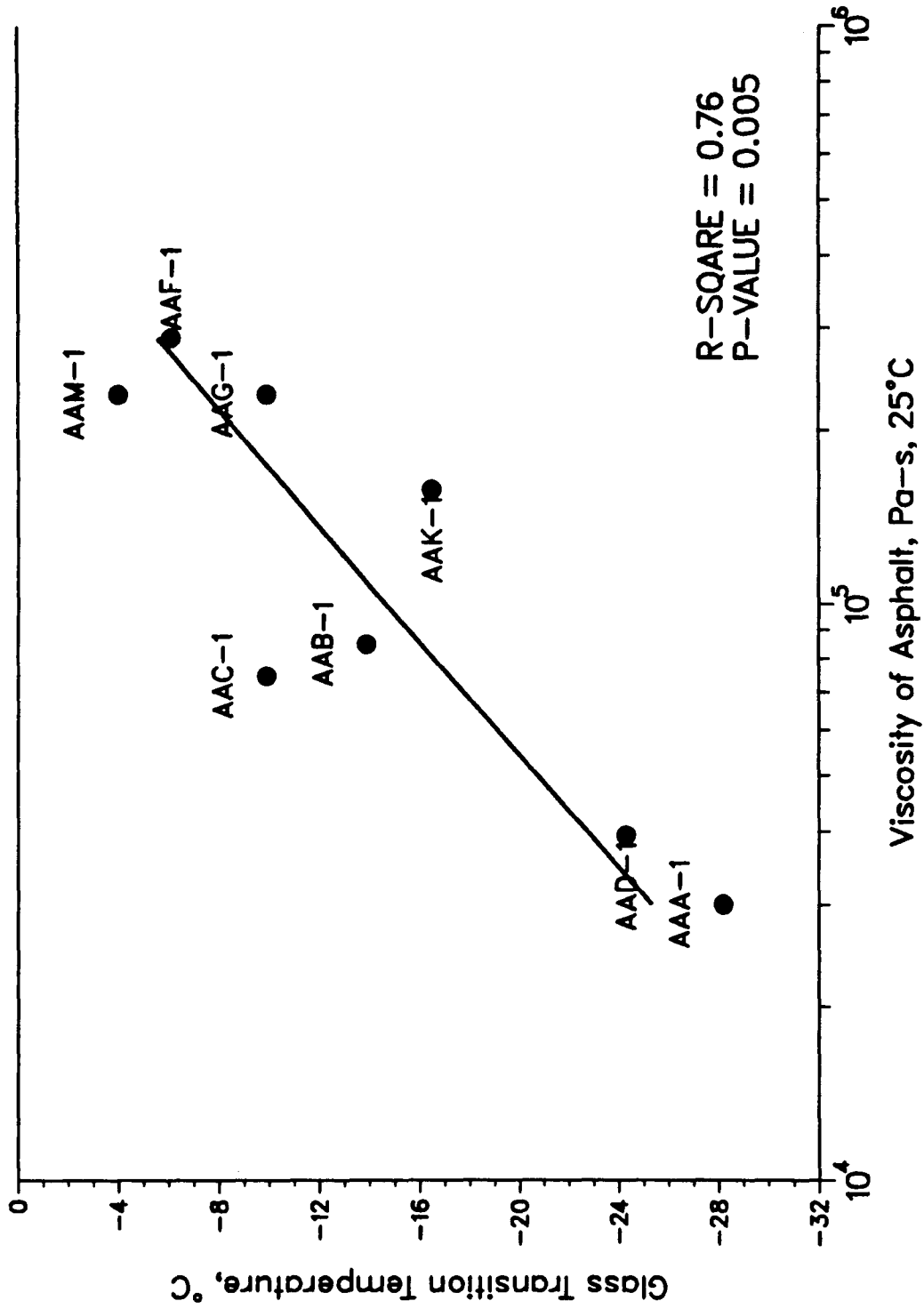


Figure 5.14 Glass Transition Temperature vs. Viscosity of Core Asphalt at 25°C

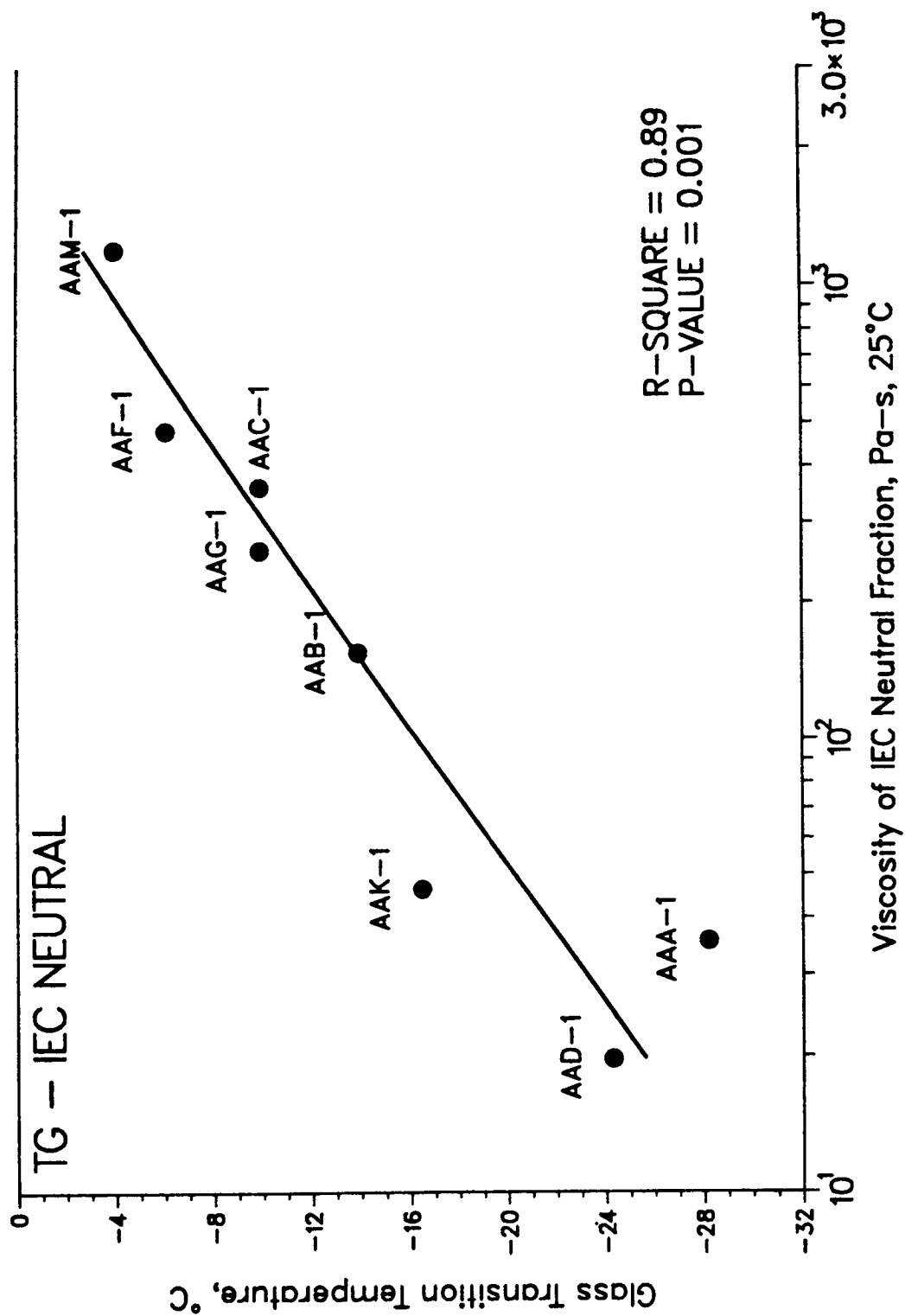


Figure 5.15 Glass Transition Temperature vs. Viscosity of IEC Neutrals at 25°C

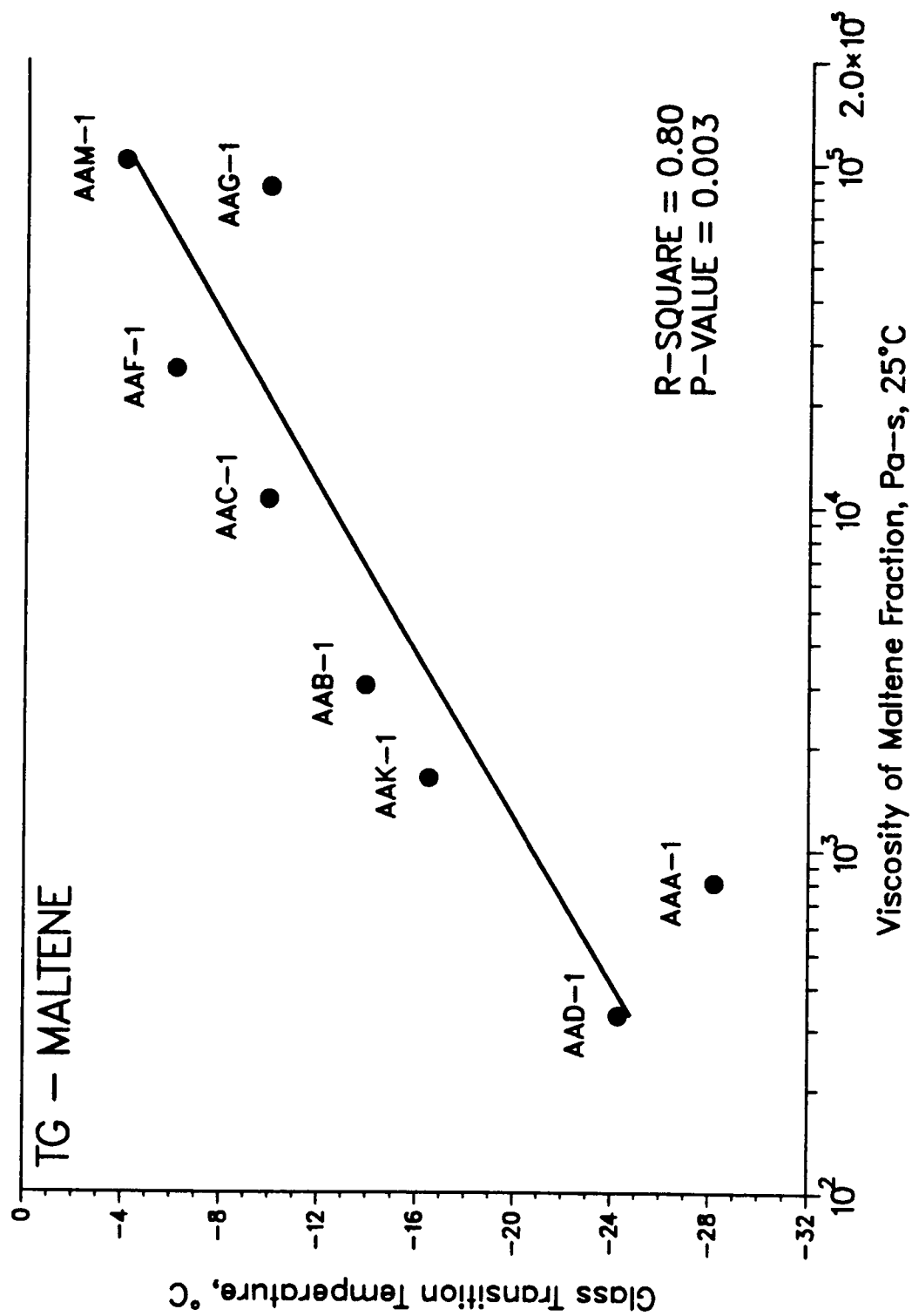


Figure 5.16 Glass Transition Temperature vs. Viscosity of Maltenes at 25°C



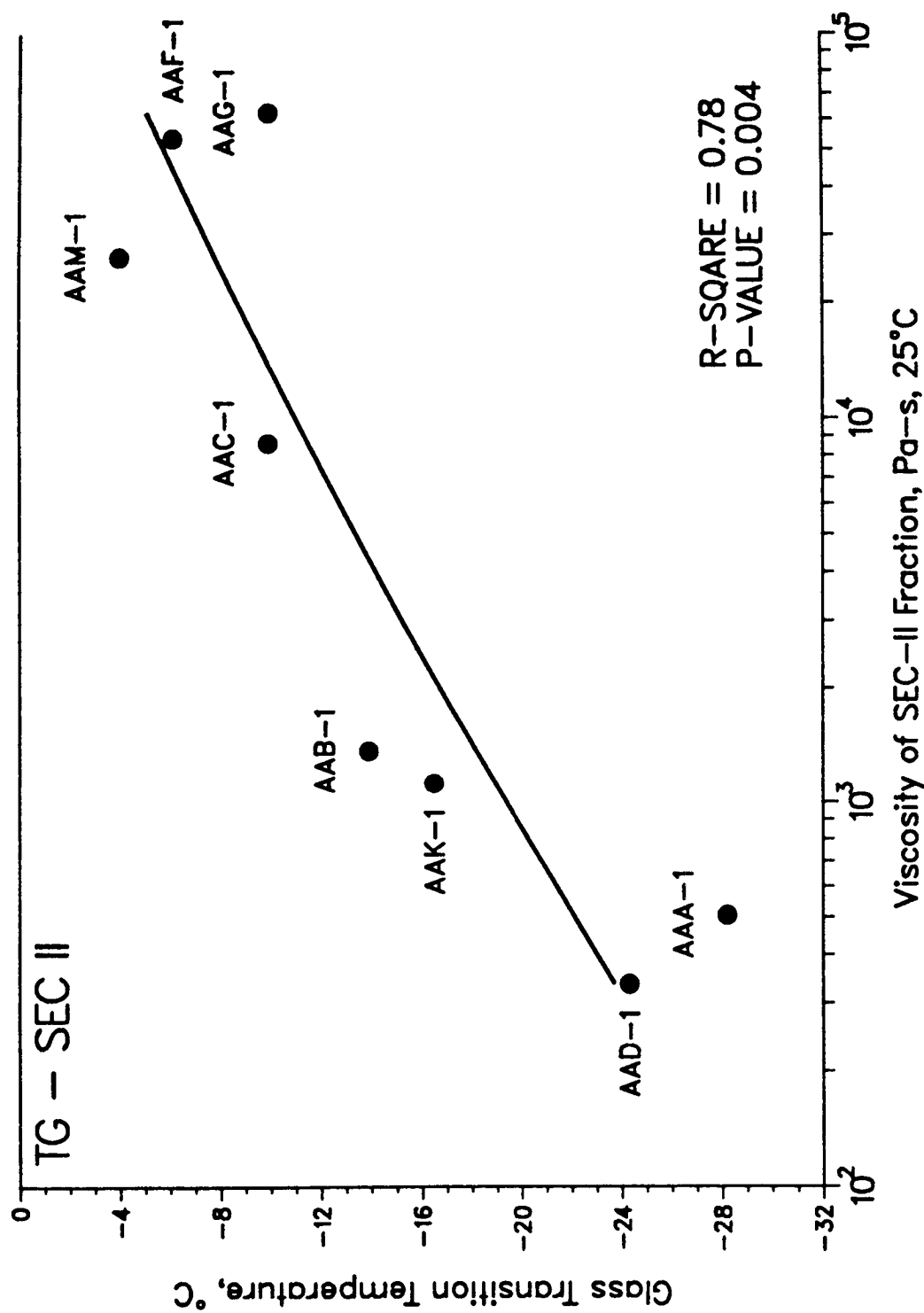


Figure 5.17 Glass Transition Temperature vs. Viscosity of SEC Fraction-II at 25°C

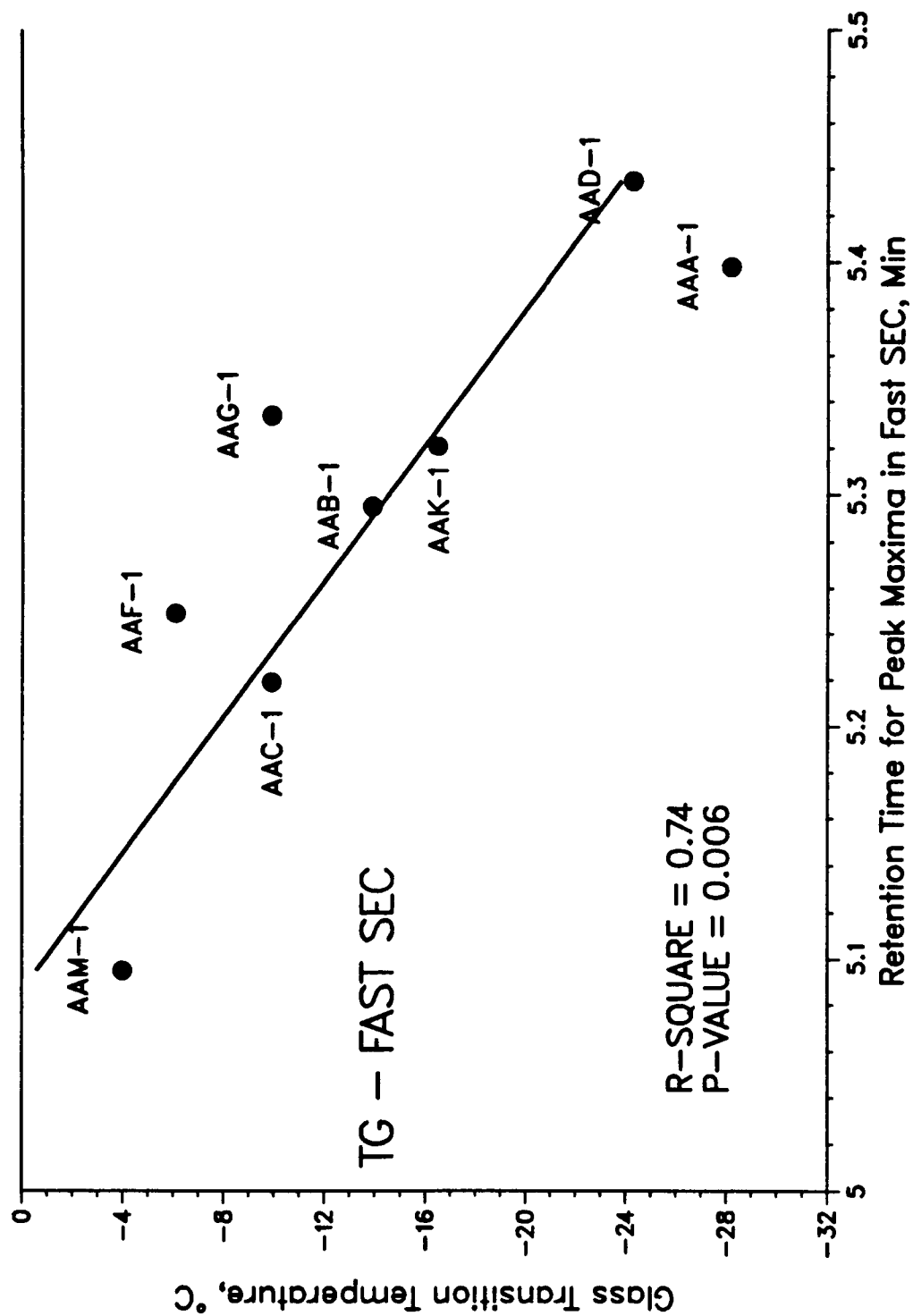


Figure 5.18 Glass Transition Temperature vs. Retention Time for Peak Maxima in Fast SEC.

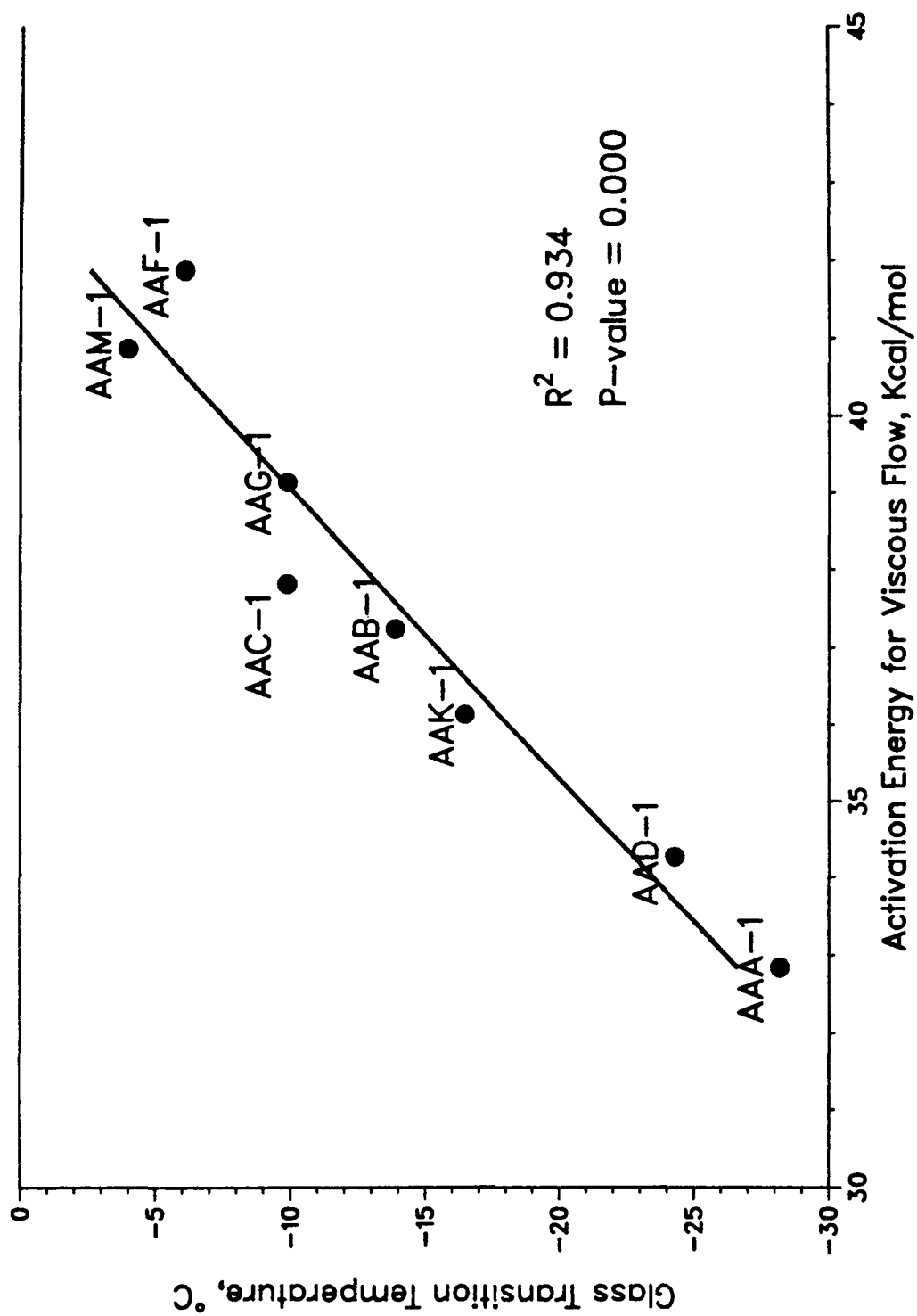


Figure 5.19 Activation Energy for Viscous Flow vs. Glass Transition Temperature

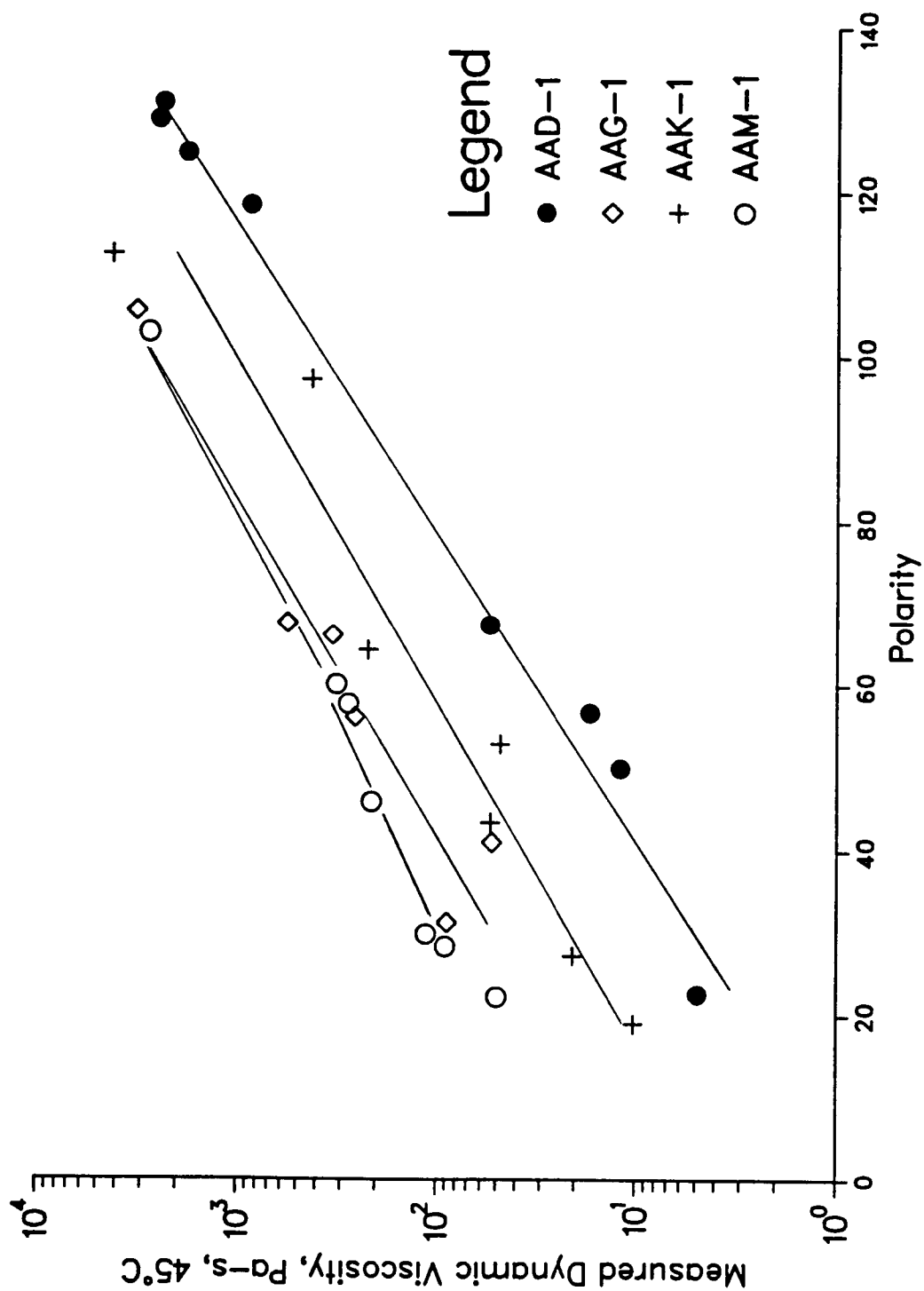


Figure 5.20 Viscosity at 45°C vs. Polarity

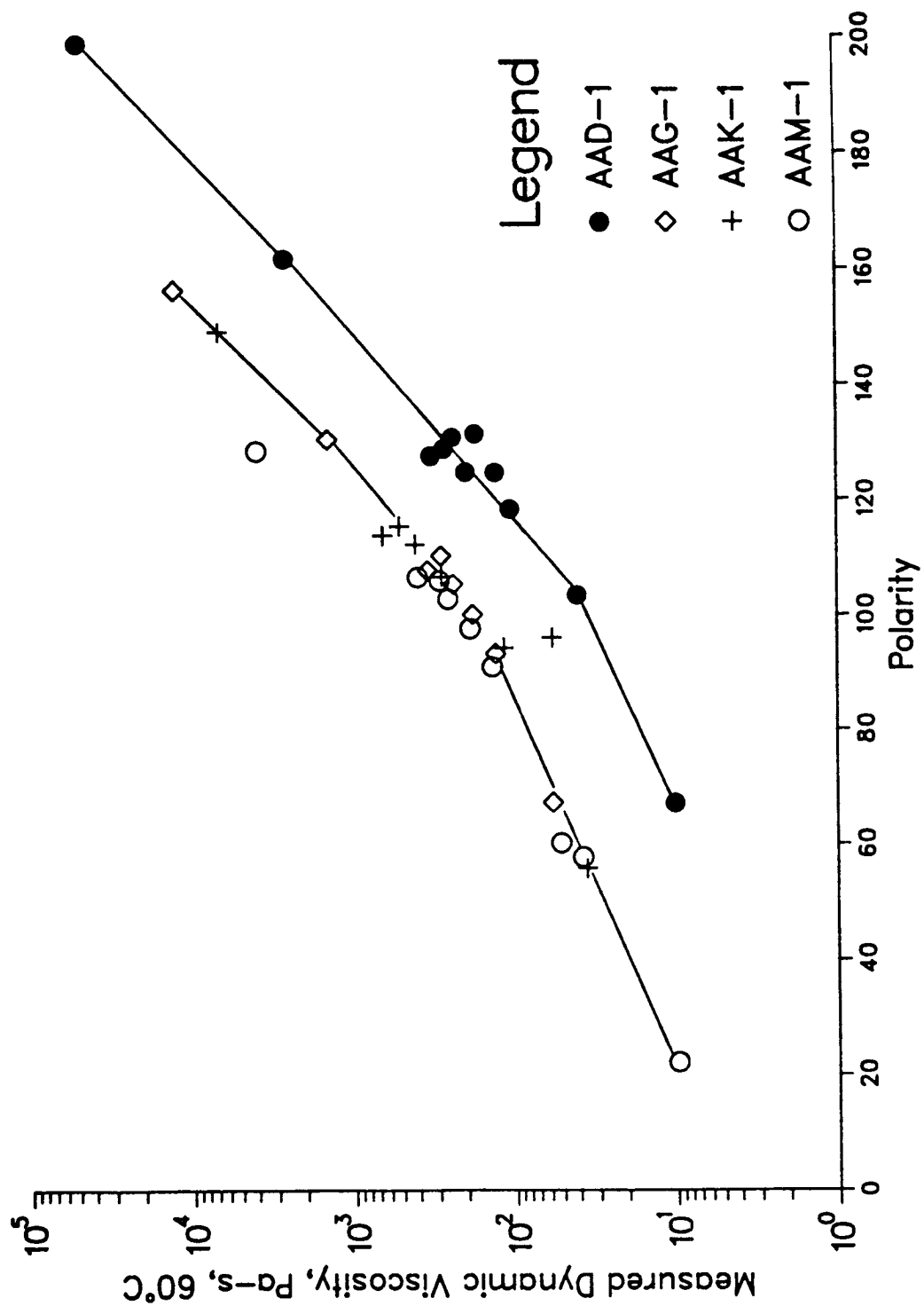


Figure 5.21 Viscosity at 60°C vs. Polarity

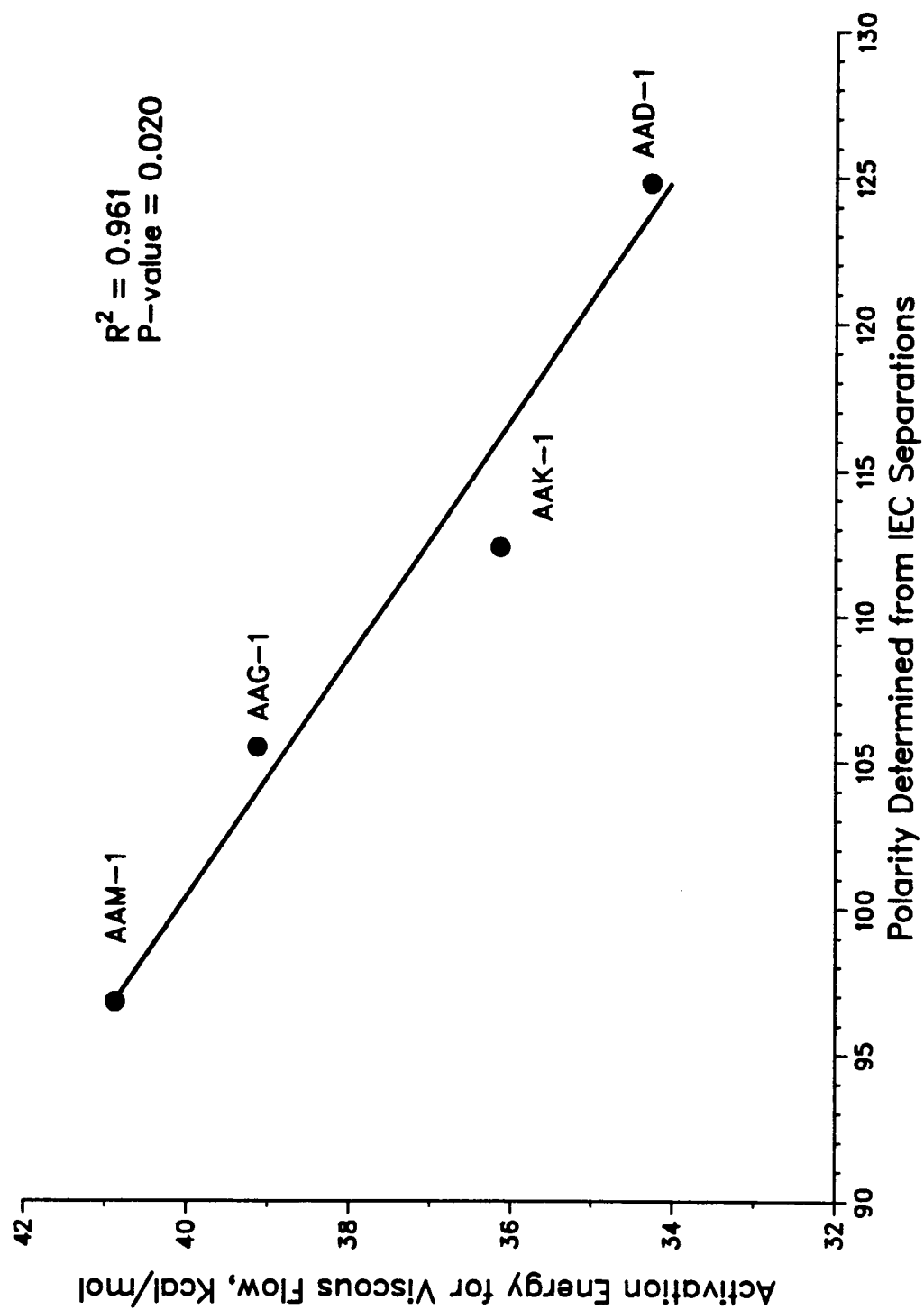


Figure 5.22 Activation Energy for Viscous Flow vs. Polarity

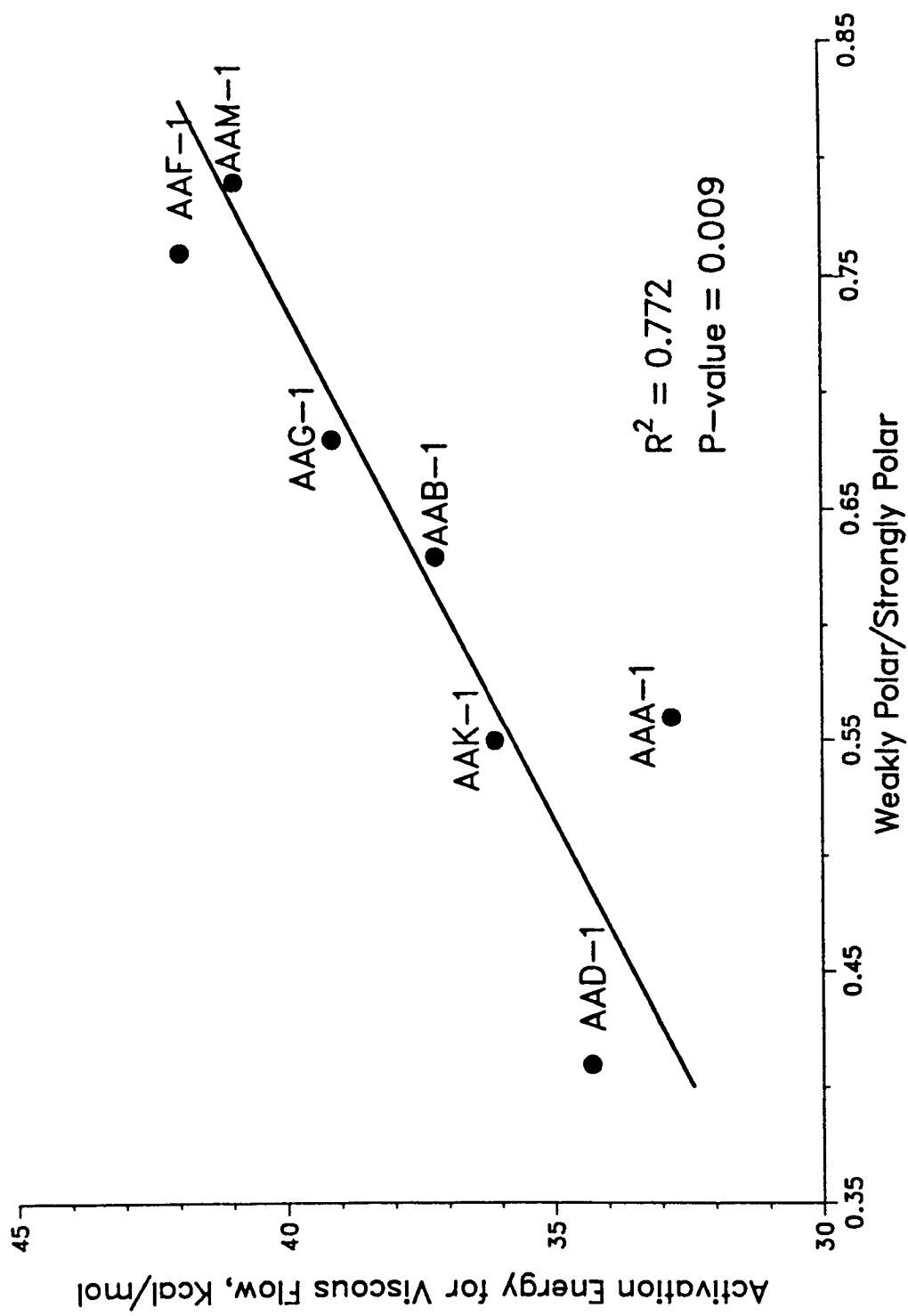


Figure 5.23 Activation Energy for Viscous Flow vs. Ratio of Weakly Polar Fraction to Strongly Polar Fraction Determined from IEC Separations

**Table 5.1 Preparative SEC Separation of IEC Amphoteric Fraction of AAD-1 and AAG-1<sup>1</sup>**

Asphalt	Operator	Yield of SEC Fraction, mass %		Recovery, mass %
		SEC Fraction-I	SEC Fraction-II	
AAD-1	DG	70.8	29.1	99.9
	AG	71.3	29.3	100.6
AAG-1	SK	39.6	62.3	101.9
	DG	38.5	62.3	100.7

<sup>1</sup> Standard deviations (mass %) are: for SEC-I, 0.7; for SEC-II, 0.1; and for Recovery, 0.8.

**Table 5.2 IEC Separation of SEC Fraction-I of AAD-1 and AAG-1<sup>1</sup>**

Asphalt	Operator	Yield of IEC Fraction, mass %			Recovery, mass %
		Neutral Plus Acid	Base	Amphoteric	
AAD-1	DG	2.5	7.7	67.5	77.7
	SK	2.9	5.1	72.6	80.5
AAG-1	DG	16.8	5.6	60.2	82.6
	SK	16.8	3.5	54.6	74.9

<sup>1</sup> Standard deviations (mass %) are: for Neutral plus Acid, 0.2; for Base, 2.1; for Amphoteric, 4.7; and for Recovery, 4.7.



**Table 5.3 Yields of Extracts of IEC Cation and Anion Resins by Toluene, Ethanol, and Water Mixture<sup>1</sup>**

Asphalt	Operator	Amphoteric Plus Base Column, mass % (Cation Resin)	Amphoteric Column, mass % (Anion Resin)	Total Recovery, mass %
AAD-1	DG	12.9	2.7	93.3
	SK	9.4	3.4	93.4
AAG-1	DG	9.1	7.1	98.9
	SK	5.4	14.3	94.6

<sup>1</sup> Standard deviations (mass %) are: for Amphoteric plus Base, 3.2; for Amphoteric, 3.5; and for Total Recovery, 1.9.

**Table 5.4 Separation of SEC Fraction-II of AAD-1 and AAG-1**

Asphalt	Amphoterics, mass %	Base, mass %	Acid plus Neutral, mass %	Recovery, mass %
AAD-1	11.0	10.6	77.3	98.9
AAG-1	10.4	12.3	77.3	100.0

**Table 5.5 IEC Separation of SEC Fractions-I and -II of AAD-1 and AAG-1**

Asphalt	Starting Material	Amphoterics, mass %	Base, mass %	Acid plus Neutral, mass %	Recovery (IEC/SEC), mass %
AAD-1	SEC-I	18.16	1.26	0.71	20.13/25.01
	SEC-II	8.28	8.02	58.28	74.58/75.37
	Total	26.44	9.28	58.99	94.71/100.38
	NEAT (AVG)	25.54	8.76	60.82	95.67
AAG-1	SEC-I	6.30	0.41	1.94	8.65/11.54
	SEC-II	9.20	10.89	68.28	88.37/88.36
	Total	15.50	11.30	70.22	97.02/99.90
	NEAT (AVG)	18.51	12.52	67.58	98.10

**Table 5.6 Molecular Weight of Amphoterics of SEC-I and SEC-I of Amphoterics of AAD-1 and AAG-1**

Asphalt	Fraction	Run No.	Molecular Weight (Daltons)	
			Toluene	Pyridine
AAD-1	Amphoterics of SEC-I	1	9,200	5,700
		2	6,900	3,600
	SEC-I of Amphoterics	1	12,400	7,400
AAG-1	Amphoterics of SEC-I	1	3000	1,800

**Table 5.7 Polarity Fractors of Nine IEC Fractions**

Column	Fraction	Polarity Factor
1st Anion	Strong Acids	2
	SASB Amphoterics	4
	SAWB Amphoterics	3
1st Cation	Strong Bases	2
	WASB Amphoterics	3
2nd Anion	Weak Acids	1
	WAWB Amphoterics	2
2nd Cation	Weak Bases	1
Eluates	Neutrals	0

**Table 5.8 Calculated Polarities of Four Core Asphalts**

Fraction	Asphalt			
	AAD-1, mass %	AAG-1, mass %	AAK-1, mass %	AAM-1, mass %
Strong Acids	7.0	9.35	3.0	3.5
Weak Acids	3.9	9.55	6.2	7.8
Strong Bases	4.2	3.3	2.3	5.2
Weak Bases	5.7	8.9	8.0	9.4
SASB Amphoterics	15.4	6.8	14.0	8.1
SAWB Amphoterics	4.0	1.75	2.7	2.6
WASB Amphoterics	3.6	8.6	6.1	5.6
WAWB Amphoterics	4.0	1.75	2.7	2.6
Neutrals	52.2	50.0	55.0	55.2
Polarity <sup>1</sup>	124.4	105.5	112.6	96.8

<sup>1</sup> Polarities were calculated by multiplying each entry in Table 5.8 by corresponding numerical factors in Table 5.7 and adding.

**Table 5.9 Regression Equations of Viscosity-Polarity Relationship for Four Core Asphalts**

Asphalt	Regression Equations <sup>1</sup>	R <sup>2</sup>	P-value
AAD-1	Log Vis = 1.009 + 0.0294 (Polarity)	0.984	0.000
AAG-1	Log Vis = 2.312 + 0.0296 (Polarity)	0.967	0.000
AAK-1	Log Vis = 1.663 + 0.0294 (Polarity)	0.990	0.000
AAM-1	Log Vis = 2.868 + 0.0242 (Polarity)	0.982	0.000

<sup>1</sup> Viscosity is in Pa · s

**Table 5.10 Polarities of Various Fractions of Four Core Asphalts**

Fraction	Asphalt			
	AAD-1, polarity <sup>1</sup> factor	AAG-1, polarity factor	AAK-1, polarity factor	AAM-1, polarity factor
IEC Fractions				
Total Amphoterics	342	327	344	329
Total Acids	164	149	132	131
Total Bases	142	127	122	136
Asphaltene and Maltene Fractions				
Asphaltenes	391	427	346	279
Maltenes	52	89	53	88
SEC Fractions				
SEC-I	361	266	296	172
SEC-II	52	84	48	64

<sup>1</sup> Polarity factor is reported in dimensionless units

**Table 5.11 Activation Energy of Viscous Flow and Glass Transition Temperatures for Eight Core Asphalts**

Asphalt	Visc at 25 °C, Pa · s	Visc at 60 °C, Pa · s	Ea, Kcal/mol	T <sub>g</sub> , °C
AAA-1	37,020	109	32.8	-28.2
AAB-1	118,600	160	37.2	-13.9
AAC-1	90,100	110	37.8	-9.9
AAD-1	57,280	131	34.3	-24.3
AAF-1	381,700	226	41.9	-6.1
AAG-1	248,900	234	39.1	-9.9
AAK-1	251,700	413	36.1	-16.5
AAM-1	364,400	258	40.9	-4.0

Viscosities were determined at shear rate 0.1 rad/s.

T<sub>g</sub> values were determined at The Pennsylvania State University.

## 6

# Molecular Structuring Studies

### Introduction

The phenomenon of isothermal reversible age-hardening, otherwise known as steric hardening, has long been known to occur in asphalt cement (Traxler 1961). Isothermal reversible age-hardening is distinct from irreversible hardening resulting from oxidative aging and is believed to be a result of reorganization of asphalt microstructural systems to approach an optimum thermodynamic state under a specific set of conditions.

Experimentally, it is observed that, after an asphalt is cooled from a high (e.g., mixplant) temperature to ambient temperatures, the viscosity of the asphalt at room temperature continues to increase from an initial value over extended time periods. This type of viscosity increase can be reduced almost to initial values by reheating the sample and allowing it to cool again. Shortly after the second cooling, an isothermal increase in viscosity of the sample again is observed. Brown, Sparks, and Smith (1957) claimed that the asphaltene component of asphalts governed the phenomenon. When an asphalt is recovered from a pavement using different solvents, a solvent effect on the viscosity of the recovered asphalt is also observed. For a given asphalt, the viscosity of a freshly recovered and dried sample depends on the extraction solvent used. After prolonged isothermal storage, viscosities of samples of a given asphalt extracted by different methods approach the same value. This phenomenon has been related to isothermal reversible age hardening.

Isothermal reversible age hardening is not peculiar to asphalts. Pirela and de Marcano (1985) reported on a similar phenomenon observed in heavy crudes and mixtures of heavy crudes and solvents.

Because of the known dependence of viscosities of solutions of associated molecules on weight-average molecular weights ( $M_w$ ) and shapes of associated species, the weak bonds connecting components of molecular associations must be broken and reformed as asphalt systems approach a preferred thermodynamic state during the process of isothermal viscosity increase. The breaking and reforming of weak bonds (which are much less strong than molecular sigma and pi bonds that are responsible for the stability of molecules) can be referred to as molecular structuring. As the process continues, either  $M_w$  values of associations increase with time or the shapes of the associations change, or both. If the associations that are formed are more ordered than initial states (decrease in entropy), then the enthalpy associated with the process must be substantial.

## Studies of Time-Dependent Isothermal Viscosity Changes

The rheology of isothermal reversible age-hardening of asphalts is not conveniently studied because systems must be disturbed in some way prior to measurement. If investigations are to be performed at low temperatures, asphalts must be heated to load into vessels to perform rheological measurements, which results in a "washing out" of some of the increased viscosity buildup over time. At higher test temperatures, a great deal of molecular structuring is not observed. Consequently, if the phenomenon of age hardening is to be measured accurately, a method must be found to do so without seriously disturbing asphalts in the process. Therefore, a procedure had to be developed to load asphalts into vessels in which they could be stored until ready for rheological measurements, and which could be inserted into the Rheometrics RMS-605 Mechanical Spectrometer. To accomplish this objective, special fixtures were designed by H. Plancher. Various features of the device were perfected over a period of time in consultation with Rheometrics, Inc. Several configurations were tried, each at considerable expense of time, and revisions were made to accommodate early design problems. It proved impossible to employ demountable parallel plates in carefully controlled studies because of the fluidity of asphalts at test temperatures, with the consequent inability to ensure a strictly parallel alignment of the plates once they are taken outside the spectrometer. One fixture has an internal volume of 7.75 mL and is suitable for measuring complex dynamic shear moduli ( $G^*$ ) in the 6,900 to 2,400,000 dyne/cm<sup>2</sup> range using a 50 milliradian motor angular deflection (0.9% strain). With proper compliance allowances for the recording transducer, the fixture can be operated near 1 milliradian motor angular deflection using only 0.018% strain. It is important to use low motor angular deflections in these experiments so that weak molecular associations are not disturbed. Another fixture was manufactured having 4.0 mL internal volume that can be used for aged asphalts. The operational range of this fixture is 63,000 to 22,000,000 dyne/cm<sup>2</sup> ( $G^*$ ) at 50 milliradian motor angular deflection (1.5% strain).

Initial studies of isothermal reversible age hardening were performed on asphalt AAK-1 at 25°C (77°F) over a period of 50 hours. A sample of asphalt was heated and loaded into a special fixture, and the fixture and contents were heated to 110°C (230°F) for 1 hour. The fixture and contents were allowed to cool to 25°C (77°F). The annealing temperature was chosen because it is known that sulfoxides, which are components of aged asphalts, decompose at observable rates at temperatures above 110°C (230°F). It is not desirable to confound the study of what appears to be a physical process with chemical changes. Measurements of annealed AAK-1 then were taken on the spectrometer 2 hours later. Fourteen measurements were taken at 0.1 rad/s over a 25-minute period. After a 10-minute rest period, two more 0.1 rad/s measurements were taken, followed by a frequency sweep from 0.1 rad/s to a frequency corresponding to 1,500 g torque. After another 10 minutes, 14 more measurements were made at 0.1 rad/s.

Molecular structuring leading to isothermal reversible age hardening follows a logarithmic pathway. It is most rapid initially. During the first series of 14 measurements at 0.1 rad/s, the sample viscosity increased from 260,900 Pa·s to 272,800 Pa·s. After 10 more minutes, at the beginning of the frequency sweep, the viscosity of the sample was observed to be 294,100 Pa·s. During the second set of 14 measurements at 0.1 rad/s, the viscosity rose

from 294,800 Pa·s to 296,300 Pa·s. These results show that although there may have been slight loss of stiffness in performing the frequency sweep, the loss during the 0.1 rad/s measurements is negligible. Subsequent measurements in this experiment involve performing a frequency sweep at selected intervals.

Table 6.1 lists rheological data for a sample of AAK-1 annealed at 110°C (230°F) and loaded into a fixture at that temperature. Annealing and loading were performed while the sample was blanketed with an inert gas. The fixture and contents were allowed to cool to 25°C (77°F), and rheological measurements were obtained at time intervals up to 5,138 hours. Loss (viscous) modulus ( $G''$ ), storage (elastic) modulus ( $G'$ ),  $G^*$  values, viscosities, and  $\tan \delta$  values were calculated. These quantities are defined below.

$$G^* = \sqrt{(G')^2 + (G'')^2} \quad (6.1)$$

$$\begin{aligned} \text{dynamic viscosity} &= \eta^* \text{ (poises)} = G^* / \omega \\ \eta^* \text{ (Pa·s)} &= G^* / (\omega \times 10) \end{aligned} \quad (6.2)$$

$$\tan \delta = G'' / G' \quad (6.3)$$

When rheological measurements were not being performed, the fixture and contents were stored under an inert gas atmosphere at 25°C (77°F). Table 6.1 shows that over a 214-day period, the viscosity of the sample increases by about 50%. The elastic modulus increases more than the viscous modulus over the same period of time, which is reflected in the gradual decrease of  $\tan \delta$  values. The rate of molecular structuring is more rapid initially, and then the rate decreases.

Table 6.2 lists rheological data from a similar experiment involving AAM-1. This sample was annealed at 150°C (302°F) for 1 hour. In subsequent work, it was decided to employ the higher annealing temperature because serious doubt arose that 110°C (230°F) was sufficient to break up some molecular associations. It should be borne in mind that at the higher temperature, sulfoxide decomposition will occur in aged asphalts. Except for an anomalous data point at 96 hours, the behavior of AAM-1 is similar to that of AAK-1. An explanation of the anomalous data point at 96 hours is not evident. Most of the molecular structuring of AAM-1 takes place in the first 48 hours of the experiment. Asphalt AAM-1 has a low asphaltene content, so if molecular structuring is associated with asphaltenes, then it is somewhat of a surprise to find that the phenomenon is as pronounced as it is in AAM-1 at 25°C (77°F). As in the case of AAK-1, the elastic modulus ( $G'$ ) increases more over time than the viscous modulus ( $G''$ ), which results in a progressively lower value of  $\tan \delta$ .

Molecular structuring leading to isothermal reversible age hardening of AAB-1 also was measured after annealing at 150°C (302°F) for 1 hour (table 6.3). As was observed for AAK-1 and AAM-1,  $G'$ ,  $G''$ , and viscosities rose rapidly in the first 49 hours of the experiment. These values then were observed to decline in magnitude for the next 800 hours, after which they were observed to rise again. It is believed that the high values of  $G'$ ,  $G''$ , and viscosities at intermediate times in the experiment were due to problems of temperature control with the spectrometer. Nevertheless, after almost 2,000 hours, the



viscosity of AAB-1 at 25°C (77°F) had increased by more than 60%, and  $G'$  had more than doubled.

Asphalt AAM-1 also was loaded into a special fixture and was annealed at 150°C (302°F) for 1 hour and then cooled to 45°C (113°F) and maintained at that temperature for 2,009 hours. During this time, rheological measurements were performed, the results of which are listed in supplementary table 6.4. Based on these measurements at 45°C (113°F), molecular structuring occurs to a greater degree for AAM-1 at that temperature than at 25°C (77°F). The viscosity of AAM-1 more than doubles at 45°C (77°F) over a 2,000-hour period. Unfortunately,  $G'$  could not be measured until the very last determination because the value of this quantity is too low for the operating range of the transducer on the mechanical spectrometer to record.

Another sample of AAM-1 was loaded into a special fixture, annealed at 150°C (302°F) for 1 hour, cooled to 60°C (140°F), and maintained at that temperature for 2,560 hours. Viscosity measurements were performed at the same temperature at periodic intervals, the results of which are listed in supplementary table 6.5. The viscosity of AAM-1 increased by more than 80% in 2,560 hours. These results prove that molecular structuring occurs in AAM-1 at fairly high temperatures, at which only effects on  $G''$  can be measured.

A sample of asphalt AAG-1 was annealed at 150°C (302°F) for 1 hour, cooled to 60°C (140°F), and maintained at that temperature for 2,224 hours. No changes in viscosity were observed after numerous measurements during this time (supplementary table 6.6).

Isothermal reversible age hardening studies also were performed on samples of AAK-1 and AAM-1 that had been subjected to oxidative aging. The aging procedure consisted of a preliminary thin film oven (TFO) treatment followed by oxidation in a pressure air vessel (PAV) at 60°C (140°F) and  $2.07 \times 10^6$  Pa (300 psi) for 144 hours. This aging method is discussed at length in chapter 8. Two samples of aged AAK-1 were annealed at two different temperatures, 110°C (230°F) and 150°C (302°F), for 1 hour in special fixtures. The samples were cooled to 25°C (77°F) and were maintained at that temperature for more than 4,000 hours, during which rheological measurements were performed at selected times. Data are reported in supplementary tables 6.7 and 6.8. Increases in viscosity for both samples were more than 50% after the last measurement was taken. Increases in  $G'$  were about 80%. These are approximately the same percentage increases in these quantities that were observed for unaged AAK-1 (table 6.1). However, it is important to note that the viscosity of aged AAK-1 is much greater than that of neat AAK-1, so the increase in viscosity of the aged material is actually much more than for the neat asphalt. The absolute viscosity increase was approximately 1.1 million Pa·s (11 million poises) over a 7- month period.

Three samples of aged AAM-1 (treated under the same conditions as described for AAK-1 above) were loaded into special fixtures and were annealed at 150°C (302°F) for 1 hour and then cooled to 60°C (140°F), 45°C (113°F), and 25°C (77°F) respectively. The samples were stored at the three temperatures for about 1,800 to 2,400 hours, and rheological measurements were performed at selected intervals. After the last measurements were made, significant increases in viscosities at all three temperatures and  $G'$  values at the two

lower temperatures were observed. These data are listed in supplementary tables 6.9 through 6.11. As was seen for the unaged AAM-1, the greatest percentage increases in viscosity were observed at 45°C (113°F). Of course, the absolute increases in viscosity are much greater at 25°C (77°F) than at 45°C (113°F). Unfortunately, the data obtained in these experiments are erratic, possibly due to problems with temperature control of the mechanical spectrometer or in the loading of the test fixture in the spectrometer.

In order to test the hypothesis that isothermal reversible age hardening is related to asphaltene content, a 1.0 g sample of n-heptane maltenes (chapter 9) from AAM-1 was loaded into a special fixture, annealed at 150°C (302°F) for 1 hour, and cooled to 0°C (32°F). The sample was maintained at this temperature for 2,556 hours, during which rheological measurements were performed at the same temperature at various times. Results are listed in supplementary table 6.12. At 0°C (32°F), the maltenes of AAM-1 exhibit rheological changes over time that are characteristic of molecular structuring. The viscosity of the maltenes is almost three times as large after 2,500 hours as at the beginning of the period. Changes in  $G'$  were even greater than three-fold.

The neutral fractions of asphalts obtained by ion exchange chromatography (IEC) contain few polar materials (chapter 1). Maltenes, although by definition asphaltene-free, contain considerable amounts of polars, which may engage in associations. A sample of IEC neutral fraction of AAM-1 weighing 2.5 g was loaded into a special fixture and was annealed at 150°C (302°F) for one-half hour, and then was cooled to 0°C (32°F). This temperature was maintained for more than 2,500 hours. Periodic rheological measurements were taken during this period, and results are listed in supplementary table 6.13. Evidence for molecular structuring is observed in these materials at 0°C (32°F). Interestingly, the increase in  $G'$  is less than that for  $G''$  or viscosity over 2,500 hours. In chapter 1, it was pointed out that  $\tan \delta$  values increase with rate of shear for IEC neutral fractions, and so these materials also manifest this unusual characteristic during isothermal reversible age hardening.

The above results suggest that isothermal reversible age hardening is a phenomenon characteristic of many asphalt components and is significant at relatively high temperatures. It was therefore decided to measure rheological properties of all core asphalts cured for 45 days at 25°C (77°F) on the mechanical spectrometer but without the use of special fixtures. At the outset of this experiment, each of the core asphalts was annealed at 150°C (302°F) for 6 hours in a glass vial. During this time, the samples were placed in a paint shaker for 5 minutes after 2, 4, and 6 hours of annealing. A small amount of air was in contact with the asphalt samples during the annealing, so minor oxidative reactions took place. Rheological measurements were taken 2 hours after the samples had cooled to 25°C (77°F), and again after 45 days. The samples to be measured were momentarily heated to 60°C (140°F) to allow for loading in the 25 mm-diameter parallel plates, even though rheological measurements were taken at 25°C (77°F). During the 45-day cure time, the samples were stored in vials. As mentioned earlier, it is impossible to store asphalt samples between demountable parallel plates. The measurements were performed at different torque values because of the differences in stiffness among the asphalts. These data are reported in supplementary table 6.14. It is evident that much molecular structuring has occurred in most of the core asphalts in 45 days and is not completely "erased" by heating asphalts to

60°C (140°F) for a short time to load them into the viscometer. Very little molecular structuring appears to have been "erased" from AAM-1 (table 6.2), and not a great deal from AAK-1 (table 6.1). AAG-1 either shows no tendency to engage in molecular structuring, or molecular structuring in this asphalt is "erased" at 60°C (140°F). Thus, isothermal reversible age hardening studies of limited accuracy are possible without specialized fixtures, but such fixtures are required for more rigorous work.

## Summary

This work was of a reconnaissance nature and terminated before replication was performed, so no rigorous statistical analysis is possible. Some of the aberrant observations that were made have not been explained. Nevertheless, the above results show that isothermal reversible age hardening is a significant phenomenon in many asphalts. Viscosity changes are observed in some tank asphalts after prolonged storage that are equivalent to changes brought about by a few degrees of temperature change. Isothermal reversible age hardening does not appear to depend on the presence of asphaltenes. The phenomenon was not observed in one of the asphalts studied (AAG-1), and the unique chemical composition of this material may be a key to a better understanding of isothermal reversible age hardening. Aged asphalts exhibit significant increases in viscosity due to molecular structuring even at relatively high temperatures. Isothermal reversible age hardening may therefore contribute significantly to the approach to failure thresholds for some asphalts.

The microstructural model predicts that polar molecules, which are more abundant in aged than in neat asphalts, would contribute more to enhancing molecular structuring, particularly to interactions involving enhancing  $G'$ , than would nonpolar molecules. The unusual behavior of the IEC neutral fractions discussed above supports this view. It may be that isothermal reversible age hardening involves more than a single process. Mechanisms occurring in nonpolar components of asphalts such as IEC neutral fractions and governing increases in  $G''$  may not be the same as those in polar components, which appear to govern  $G'$ . Because it is observed that aged asphalts undergo isothermal reversible age hardening, the process can hardly be wholly diffusion-controlled, unless some other factor exactly cancels increased viscosity. The existence of the phenomenon of isothermal reversible age hardening is strong evidence for the formation of complex structural units in asphalts that interact to form three-dimensional networks.

**Table 6.1 Viscoelastic Properties of Asphalt AAK-1 After Extended Cure Time at 25°C**

Cure Time, hr.	Elastic Modulus, $G'$ , dyne/cm <sup>2</sup>	Viscous Modulus, $G''$ , dyne/cm <sup>2</sup>	Viscosity <sup>1,2</sup> (Pa · s)	Tan $\delta$ <sup>2</sup>	Torque, g-cm
2	6.204 x 10 <sup>4</sup>	2.190 x 10 <sup>5</sup>	2.276 x 10 <sup>5</sup>	3.529	162.9
6	6.554 x 10 <sup>4</sup>	2.271 x 10 <sup>5</sup>	2.364 x 10 <sup>5</sup>	3.465	169.1
27	7.412 x 10 <sup>4</sup>	2.481 x 10 <sup>5</sup>	2.589 x 10 <sup>5</sup>	3.348	185.2
48	7.277 x 10 <sup>4</sup>	2.442 x 10 <sup>5</sup>	2.548 x 10 <sup>5</sup>	3.356	182.2
72	6.990 x 10 <sup>4</sup>	2.356 x 10 <sup>5</sup>	2.457 x 10 <sup>5</sup>	3.370	175.7
96	7.113 x 10 <sup>4</sup>	2.375 x 10 <sup>5</sup>	2.480 x 10 <sup>5</sup>	3.339	177.3
169	7.256 x 10 <sup>4</sup>	2.399 x 10 <sup>5</sup>	2.506 x 10 <sup>5</sup>	3.306	179.2
545	8.861 x 10 <sup>4</sup>	2.831 x 10 <sup>5</sup>	2.967 x 10 <sup>5</sup>	3.195	211.9
667	8.808 x 10 <sup>4</sup>	2.776 x 10 <sup>5</sup>	2.913 x 10 <sup>5</sup>	3.152	208.1
1,096	9.087 x 10 <sup>4</sup>	2.826 x 10 <sup>5</sup>	2.968 x 10 <sup>5</sup>	3.110	223.2
5,138	1.152 x 10 <sup>5</sup>	3.371 x 10 <sup>5</sup>	3.562 x 10 <sup>5</sup>	2.927	253.8

<sup>1</sup> 0.1 rad/s, 1.8% strain

<sup>2</sup> Five viscosity measurements at 25°C and 1.0 rad/s on the Rheometrics Mechanical Spectrometer were obtained for AAK-1. A standard deviation of 2,000 Pa · s and a coefficient of variance of 2.5% were calculated for this set of measurements. A standard deviation of 0.020 for tan  $\delta$  was calculated.

**Table 6.2 Viscoelastic Properties of Asphalt AAM-1 After Extended Cure Time at 25°C**

Cure Time, hr.	Elastic Modulus, $G'$ , dyne/cm <sup>2</sup>	Viscous Modulus, $G''$ , dyne/cm <sup>2</sup>	Viscosity <sup>1,2</sup> (Pa · s)	Tan $\delta$ <sup>2</sup>	Torque, g-cm
2	$9.00 \times 10^4$	$3.67 \times 10^5$	$3.78 \times 10^5$	4.08	270
6	$1.04 \times 10^5$	$4.02 \times 10^5$	$4.15 \times 10^5$	3.89	296
24	$1.20 \times 10^5$	$4.35 \times 10^5$	$4.51 \times 10^5$	3.63	321
48	$1.26 \times 10^5$	$4.52 \times 10^5$	$4.69 \times 10^5$	3.57	334
72	$1.47 \times 10^5$	$5.07 \times 10^5$	$5.27 \times 10^5$	3.44	375
96	$2.08 \times 10^5$	$6.70 \times 10^5$	$7.01 \times 10^5$	3.22	496
913	$1.52 \times 10^5$	$5.04 \times 10^5$	$5.27 \times 10^5$	3.33	374
2,031	$1.57 \times 10^5$	$5.00 \times 10^5$	$5.24 \times 10^5$	3.19	372

<sup>1</sup> 0.1 rad/s

<sup>2</sup> Four viscosity measurements at 25 °C and 1.0 rad/s on the Rheometrics Mechanical Spectrometer were obtained for AAM-1. A standard deviation of 7,500 Pa · s and a coefficient of variance of 4.7% were calculated. A standard deviation of 0.020 for tan  $\delta$  was calculated.

**Table 6.3 Viscoelastic Properties of Asphalt AAD-1 After Extended Cure Time at 25°C**

Cure Time, hr.	Elastic Modulus, $G'$ , dyne/cm <sup>2</sup>	Viscous Modulus, $G''$ , dyne/cm <sup>2</sup>	Viscosity <sup>1,2</sup> (Pa · s)	Tan $\delta$ <sup>2</sup>	Torque, g-cm
2	$1.89 \times 10^4$	$1.07 \times 10^5$	$1.09 \times 10^5$	5.67	78
6	$2.22 \times 10^4$	$1.21 \times 10^5$	$1.23 \times 10^5$	5.45	88
25	$4.57 \times 10^4$	$2.16 \times 10^5$	$2.20 \times 10^5$	4.71	158
49	$4.96 \times 10^4$	$2.22 \times 10^5$	$2.27 \times 10^5$	4.47	163
73	$4.31 \times 10^4$	$1.97 \times 10^5$	$2.01 \times 10^5$	4.56	144
96	$4.30 \times 10^4$	$1.94 \times 10^5$	$1.99 \times 10^5$	4.52	143
875	$3.37 \times 10^4$	$1.63 \times 10^5$	$1.67 \times 10^5$	4.85	120
1,958	$3.99 \times 10^4$	$1.74 \times 10^5$	$1.79 \times 10^5$	4.37	128

<sup>1</sup> 0.1 rad/s

<sup>2</sup> See footnote 2, Tables 6.1 and 6.2

## 7

# Oxidation Pathways for Asphalt

### Introduction and Background

The pavement engineering community recognized 50 years ago that age hardening and embrittlement of asphalt during service is a primary cause of failure of roads (Welborn 1984) and that oxidation is the major cause of age hardening (Nicholson 1937; Traxler 1961). Oxidative aging is characterized by oxygen uptake, formation of sulfoxide and carbonyl bands in the infrared (IR) spectrum, and marked increases in dynamic viscosity and other rheological properties (Petersen 1984). No chemical changes are observed on heating asphalt at 60°-130°C (140°-266°F) in the absence of oxygen, although small amounts of volatiles may be lost at elevated temperature, causing viscosity increases. Above 150°C (302°F) non-oxidative reactions may begin to cause chemical changes, even without oxygen.

The composition of asphalt as a complex mixture of partly aromatic hydrocarbons leads to a variety of reactions with atmospheric oxygen even at the moderately low temperatures encountered under pavement service conditions. Inspection of elemental analyses for several core asphalts indicates some variability in the heteroatom and trace metal composition, although CHO atomic ratios as well as molecular weights vary by less than a factor of two (chapter 9).

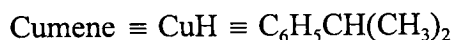
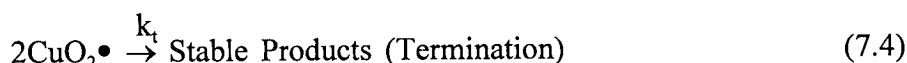
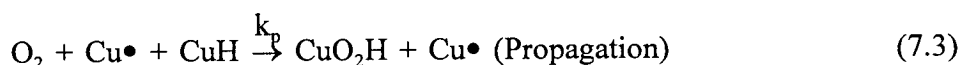
A recent SHRP supported nuclear magnetic resonance (NMR) study of the molecular composition of core asphalts by Jennings et al. (1993) provides a useful focus for molecular pathways for oxidation in asphalt. Examples of NMR-derived structures are shown for AAK-1 and AAG-1 in figure 7.1. The structures are representative, not actual structures; they are composites of the structural features needed in AAG-1 or AAK-1 to be consistent with elemental CHNOS analytical values and with NMR-derived values for ratios of aromatic to aliphatic protons and for different classes of aliphatic protons.

Figure 7.1 illustrates the point that oxidative aging in asphalts is not a single chemical process, but a composite of several independent and concurrent oxidation reactions at several sites in the asphalt structure. These reactions affect families of similar structural units for which a unique molecular identity cannot be provided. Therefore, to understand the process at the molecular level, one must rely for guidance on the behavior of model compounds and model probes. Moreover, the oxidation process is only a part of the

explanation for changes in rheological properties, since it is the interactions of certain oxidation products with each other and with other polar groups in asphalt that lead to large changes in physical properties and affect service life.

The major benefits of understanding the mechanisms of oxidation processes are that producers and users can better evaluate, and then select, asphalts with superior resistance to aging. Users and producers can find improved ways to stabilize those asphalts that oxidize with large changes in properties and can develop new accelerated aging tests that are scientifically, instead of empirically, based.

Reactions of organic compounds with oxygen at moderate temperatures are generally slow, which accounts in part for the relatively long service lives exhibited by many organic materials including asphalts. Most oxidations of hydrocarbons involve free radical intermediates in the form of peroxy ( $\text{RO}_2$ ), alkoxy ( $\text{RO}$ ), or phenoxy ( $\text{PhO}$ ) radicals and usually include a regeneration cycle (chain reaction). The process is exemplified by the classic autoxidation of a benzylic hydrocarbon such as cumene ( $\text{CuH}$ ) (Mill and Hendry 1980), in which  $R_i$  is the rate of initiation (specified by  $k_i$ ) to generate  $\text{X}\bullet$ , which initiates the process;  $k_p$  is the propagation rate constant; and  $k_t$  is the rate constant for all termination reactions.



Reaction (7.1) is the initiation step to generate radicals  $\text{X}\bullet$  with rate  $R_i$ . Reaction (7.3) is a chain cycle, the length of which is defined by the ratio of propagation to initiation or termination rates (kinetic chain length,  $kcl$ ):

$$kcl = k_p(\text{CuH})(R_i/2k_t)^{1/2}/R_i \quad (7.5)$$

$$= k_p(\text{CuH}) / (R_i 2k_t)^{1/2} \quad (7.6)$$

Many factors affect values of  $kcl$ , which rarely exceed 20 to 30 and are often close to one. Figure 7.1 shows that asphalts contain multiple sites for free radical oxidation, and their absolute reactivities are compared below. Phenols and pyrroles are by far the most reactive species by factors of  $10^5$  to  $10^6$ . Functional analyses for phenols, pyrroles, and benzylic CH concentrations (see chapter 3) are shown below, together with first-order rate constants for H-atom transfers by  $\text{RO}_2$  (Hendry et al. 1974).

X-H Bond	Conc., M	$k_p$ , $M^{-1} s^{-1}$	$k_p$ , $s^{-1}$
=N-N(H)-	0.05	<1(4)	<5(2)
PhOH	0.07	1(5)	7(3)
PhCHRR'	10	0.1	1

Studies of the thermal oxidation of asphalt over the past 30 years have almost uniformly concluded that asphalts are not protected from oxidation by addition of most autoxidation inhibitors such as hindered phenols or zinc dithiocarbamates (Martin 1966, 1968). The conclusion is that free radicals do not play a role in the oxidation process. Thus, the process must proceed by some other pathway, perhaps involving complexes of oxygen with aromatics, peroxides reactions with metals, or even spontaneous reaction of oxygen with reactive pyrrole-like structures.

This conclusion is based on a concept of free radical oxidation as it applies to reactive hydrocarbons where oxidation proceeds by way of long chains (reaction 7.3). A phenolic inhibitor added to a long-chain oxidation system intercepts  $RO_2$  before RH reacts with it and inhibits oxidation until the phenol is consumed. The longer the chain before addition of the phenol, the more dramatic the inhibition by small amounts of inhibitor (Mill and Hendry 1980). In the case of asphalt oxidation, native phenol inhibitors already are present (as noted above); therefore, it is not surprising that added phenols have little or no effect. This means that thermal oxidation of asphalt might be caused by nonchain free radical oxidation. Of course, other combinations of oxygen with asphalt components also may occur.

Earlier studies of asphalt oxidation have focused on sulfide oxidation to sulfoxide and on carbonyl formation. Both types of products are readily determined by IR spectroscopy. Sulfoxide forms a prominent single band near  $1030\text{ cm}^{-1}$  and carbonyl forms complex bands near  $1700\text{ cm}^{-1}$  (Petersen 1975; Petersen, Barbour, and Dorrence 1975; Petersen et al. 1981; Petersen 1986). A few studies have examined oxygen uptake in treated asphalt solutions (Knotnerus 1971; van Gooswilligen, Gergh, and de Bats 1985), but no material or oxygen balance studies have been reported. Thus, one cannot judge from these studies whether sulfoxide and (mostly ketonic) carbonyl (Dorrence, Barbour, and Petersen 1974) account for most or all of the absorbed oxygen.

Asphalt contains two major kinds of sulfur. Ruiz et al. (1982) used X-ray photoelectron spectroscopy (ESCA) analysis to distinguish among sulfide, sulfoxide, and sulfone forms of sulfur in asphalt, taking advantage of the large energy shift between sulfide and sulfoxide near 164 eV and sulfone ( $>SO_2$ ) near 170 eV in ESCA spectra. From model compounds and selective oxidations and reduction they concluded that a light Arabian asphalt contained 54% aromatic sulfur, 33% aliphatic sulfur and 13% alicyclic sulfur.

Recently, Green et al. (1992) characterized SHRP asphalt sulfur by chromatographic and IR methods. This detailed study succeeded in separating total sulfide sulfur from thiophenic sulfur and into aliphatic and aromatic sulfides. No sulfonic acids, thiols, or sulfones were detected. Generally, SHRP asphalts have a 40:60 ratio of sulfide:thiophenic sulfur.



Huggins et al. (1992) also characterized asphalt sulfur using X-ray spectroscopy (XANES) to speciate different sulfur types. XANES is inherently less accurate and precise than IR spectroscopy for sulfoxide but much more powerful in separating all types of sulfur. The results from XANES agree qualitatively with the chromatographic methods of Green et al. (1992) and with ESCA spectroscopy for AAA-1 (see below).

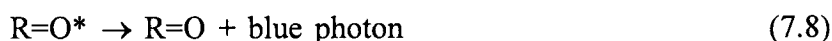
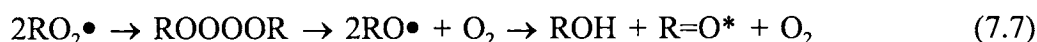
In the following sections of this chapter, an experimental program conducted at SRI International is described that is aimed at enhancing the basic understanding of molecular pathways for absorbing oxygen and distributing it among reactive sites in the asphalt molecular ensemble. The first section focuses on free radical formation and trapping in asphalts. The second section deals with sulfur characterization and oxidation in asphalt and pathways for oxidation. The third section examines oxygen uptake, product formation, oxygen balances, and rates. The last section discusses how these data fit together to give a description of the oxidation process.

## Free Radicals and Inhibitors in Asphalts

### *Chemiluminescence*

Eight to 11  $\mu\text{m}$ -thick films of AAB-1, AAD-1, and AAG-1 asphalts were monitored for chemiluminescence (CL) emission in the near uv/visible region when heated in air or oxygen. Significant CL emissions beyond a background count were observed when each of the films was heated to 140°-150°C (284°-302°F) in air. These counts dropped to nearly background values when air was replaced with nitrogen. AAG-1 is the most emissive asphalt and AAB-1 the least emissive asphalt. These data show that oxidation is accompanied by formation of peroxy radicals.

CL is widely observed in the oxidation of simple organic compounds and polymers and has been shown to be caused by peroxy free radical interactions (Mendenhall 1990):



CL is due to conversion of a carbonyl triplet ( $\text{R}=\text{O}^*$ ) excited state to the ground state with production of a blue photon. Additional emissions also occur in the near IR region from singlet oxygen decay.

Figure 7.2 illustrates photon counting data for several asphalt films and an uncoated wafer over the temperature range in air and nitrogen. The temperature dependencies of the data in figure 7.2 correspond to activation energies of  $15 \pm 3 \text{ kcal/mol}^{-1}$ , which is additional evidence for involvement of a free radical process in asphalt CL: Radical reactions typically have composite activation values in the range of 10-20 kcal/mol, whereas nonradical processes known to cause light emission (such as cleavage of dioxetanes) typically have much higher activation parameters (Mill and Hendry 1980). It is important to emphasize

that, while CL firmly establishes that free radicals are formed by reaction of asphalt with oxygen, it does not define their importance in the overall oxidation process.

CL experiments with asphalt thin films ( $\sim 10 \mu\text{m}$ ) were also conducted to determine the oxygen dependence of CL intensity. These experiments show that substituting pure oxygen for air leads to significant increases (factors of 2.3 to 7) in CL intensities for AAG-1, AAB-1, and AAD-1 films with an approximate half order in oxygen concentration (figure 7.3). AAG-1 films gave the highest CL emissions in air and oxygen, but emissions from AAD-1 increased the most with addition of oxygen instead of air. The intensity of the CL emission diminishes with time for each thin film sample.

The effect of oxygen concentration on CL intensity indicates either that oxygen has a direct role in generating free radicals by reaction with some components of the asphalt or that diffusion of oxygen into the films is rate-controlling. Van Gooswilligen, Bergh, and de Bats (1985) reported similar half-order concentration dependence for rates of oxygen uptake and decreasing oxygen uptake with time for solutions of asphalts in dichlorobenzene at  $60^\circ\text{C}$  ( $140^\circ\text{F}$ ) and  $130^\circ\text{C}$  ( $266^\circ\text{F}$ ) where diffusion control is not likely to be important; half-order dependence in these kinds of experiments ordinarily indicates formation of pairs of free radicals through interaction of oxygen with (in this case) the asphalt.

Films of varying thickness were used to learn if the CL originates only at the asphalt film surface or in bulk asphalt, where oxidation could be important in affecting bulk properties. Several films of 1.4, 6.5, and  $18 \mu\text{m}$  thickness were prepared from AAG-1 on silicon discs and then heated to  $90^\circ\text{C}$  ( $194^\circ\text{F}$ ) in the CL counting instrument for periods of up to 60 min. Intensities under nitrogen typically were 5% to 10% of the intensities under oxygen. The experiments show that film thickness does affect CL intensity, increasing from 440 counts/sec for a  $1.4 \mu\text{m}$  film to 1500 counts/sec for an  $18 \mu\text{m}$  film. Heating the films at  $80^\circ\text{--}90^\circ\text{C}$  ( $176^\circ\text{--}194^\circ\text{F}$ ) for 20 to 30 minutes decreases CL intensity in all films by almost half.

These results are consistent with the ideas that CL originates not only at the surface of the film but also in the bulk, and that self-absorption of the light limits the amount transmitted from thicker films. If it is assumed that oxidation occurs uniformly throughout the bulk film, it would be expected that the  $18 \mu\text{m}$  film would produce almost 13 times the CL intensity of the  $1.4 \mu\text{m}$  film. However, most CL light comes from emission near 450 nm (Mendenhall 1990), where neat asphalt films absorb significant fractions of the transmitted light, depending on their thickness. Thus, a  $2 \mu\text{m}$  film transmits 89% of the 450 nm light, while an  $18 \mu\text{m}$  film transmits only 2% of this light. Thus, the observation that the  $18 \mu\text{m}$  film, which is 13 times thicker than the  $1.4 \mu\text{m}$  film, emits only 4 times as much light is qualitatively consistent with the idea of bulk oxidation.

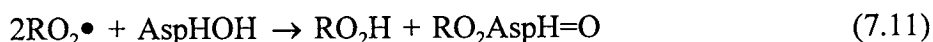
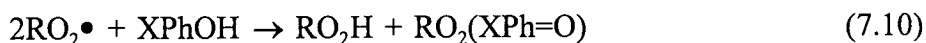
Another experiment with a  $19 \mu\text{m}$  AAG-1 film showed that at  $87^\circ\text{C}$  ( $188.6^\circ\text{F}$ ) the rate of CL intensity declined to less than half the original intensity in 1 hour (2,800 to 1,100 counts/sec) and that reforming the film with toluene (removed under vacuum) barely restored the CL intensity to the final value in the original film. A second restoration of the same film gave the same value as the first, showing that (1) oxidation takes place in the bulk film and the original intensity cannot be restored by redissolving and recasting the

film, and (2) CL intensities in the same film can be measured reproducibly within 10%. Several other samples of thin, medium, and thick AAG-1 films were first heated at 110°C (230°F) for 3 days before CL was measured. These CL intensities were reduced four-fold.

Another sample of AAG-1 was oxidized at 25°C (77°F) with t-butyl hydroperoxide to convert aliphatic sulfides to sulfoxides and then heated in the CL apparatus as a 19 µm film at 87°C (188.6°F). Although a special effort was made to remove residual hydroperoxide from the asphalt by water washing of the asphalt in toluene solution followed by vacuum pumping, the film gave a very large initial CL count of 11,000 counts/sec which declined to only 2,000 counts/sec in 45 minutes at 87°C (188.6°F). The high count rate is almost certainly due to traces of peroxide left in the asphalt that forms oxyradicals detected by the very sensitive CL method.

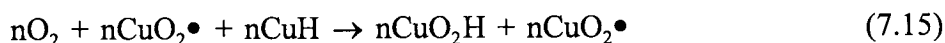
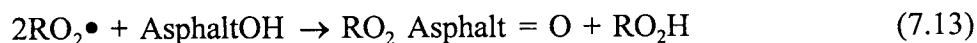
### *Inhibitors*

Western Research Institute (WRI) has reported phenol and pyrrole concentrations in core asphalts using an IR method developed by Petersen (1986). Kinetic methods have been used to measure total free-radical inhibitor concentrations including phenols. One method uses competition between added model phenol and native asphalt phenols and pyrroles toward peroxy radical (RO<sub>2</sub>) generated from a free-radical initiator azobisisobutyronitrile (ABN):



Cooxidation of core asphalt AAA-1 with p-methoxyphenol (MP) or hydroxynaphthoic acid (HNA) and 1 mM ABN at 50°C (122°F), together with an asphalt-free control, gave values for R<sub>o</sub>/R<sub>A</sub> of 8.3 with MP and 1.2 with HNA. This large difference probably was due to the much higher reactivity of HNA in scavenging RO<sub>2</sub> radicals than MP: The difference is equivalent to a 15-fold greater reactivity, a value larger than expected based on other phenol rate constants (Howard and Furimsky 1973).

The inhibiting properties of several asphalts were also measured using the inhibition time for oxidation of cumene (CuH), a well-studied and reactive hydrocarbon (Hendry 1967), as a measure of inhibitor concentration:



The time ( $t_{inh}$ ) required to observe oxygen uptake in cumene oxidized at 50°C (122°F) with ABN as a source of  $RO_2$  radicals and inhibited with small amounts of the asphalts is related to the inhibitor concentration by the relation

$$[\text{Inhibitor}] = t_{inh}/R_i \quad (7.16)$$

where  $R_i$  is the rate of production of  $RO_2$ • radicals (Reaction 7.12). In practice, a known concentration of 2,6-di-*t*-butyl-4-methylphenol (XPhOH) is used to calibrate the oxygen uptake system for  $R_i$ , and the asphalt inhibitor concentration (AOH) is given by

$$[\text{AOH}] = [\text{XPhOH}] \{ (t_{inh}(\text{asphalt})/t_{inh}(\text{XPhOH})) \} \quad (7.17)$$

The XPhOH-inhibited solution gives an oxygen uptake slope equal to the slope for a CuH solution without added inhibitor; asphalt-inhibited CuH solutions give smaller slopes for oxygen uptake corresponding to inhibition by a mixture of inhibitors with a range of reactivities.

Results for core asphalts, summarized in table 7.1, show that inhibitor concentrations in asphalts measured with CuH vary only by a factor of two from 0.053 to 0.100 M with a variability of  $\pm 10\%$ , whereas asphalt phenols measured by NMR (Jennings et al. 1993) have a much larger concentration range, from 0.019 to 0.270 M. The origins of this difference are not known at this time.

Inhibitor content of several asphalt fractions and modified asphalts were also measured. Table 7.2 summarizes results for the permethylated asphalts and maltenes obtained from Montana State University (MSU) and WRI, respectively. According to Dr. W. Jennings of MSU, the permethylated AAA-1 and AAD-1 had been exhaustively methylated to remove all phenols, alcohols, and carboxyl groups, but not amines. These materials had zero inhibition times for CuH oxidations, even when several mg of asphalt were used, clearly demonstrating that phenols are responsible for the observed inhibition. Heptane maltene fractions from AAA-1 and AAB-1 have about two-thirds of the inhibitors present in their parent asphalts, which may account for the lack of any correlation between asphaltene concentration and inhibitor concentration. A vanadium-enriched fraction from AAK-1 was clearly depleted of inhibitors (table 7.2).

## Sulfur Characterization and Oxidation

### *Characterization*

Sulfur oxidation to sulfoxide is easily measured by a single band in the IR near 1,030  $\text{cm}^{-1}$ . Because it is easy to measure, many investigators have used sulfoxide formation as a measure of asphalt aging, but without clear evidence for the role of sulfoxides in the aging process or the relation of this oxidation to other oxidative changes in the asphalt, such as carbonyl formation. There is now some agreement that the highly polar sulfoxide group plays a role in the age hardening process. If true, then understanding how sulfoxide forms

will help in developing better specifications for stable asphalts and for improved methods to retard the oxidation.

The SHRP core asphalts have total sulfur content ranging from 1% to 8% (chapter 9). Thermal oxidation at 50°-100°C (122°-212°F) converts a fraction of the total sulfur to sulfoxide (>SO), corresponding to conversion of aliphatic sulfide (>S) to >SO. Figure 7.4 shows that the concentration of >SO formed in asphalts heated in the TFAAT correlates well ( $r^2 = 0.95$ ) with the original concentration of S, but accounts for only 20-30 mole % of it. Table 7.3 lists the original molar concentrations of S, and molar concentrations of SO formed in the TFOT.

Sulfur K-edge X-ray spectroscopy (XAFS/XANES) spectra are reported for several unoxidized and oxidized SHRP asphalts using the Brookhaven National Laboratory synchrotron light source by Huggins et al. (1992). XANES resolves different oxidation states of sulfur in bulk material in much ESCA spectra characterize surface sulfur species. Eleven asphalt samples were supplied by WRI, three of which were thermally oxidized, and two samples of chemically oxidized asphalt were supplied by SRI. Analysis of the XANES data are summarized in table 7.4. Unoxidized samples of asphalts show the presence of only two kinds of sulfur: aliphatic sulfide and thiophenic sulfur in the ratio of 22:78 to 40:60; among unoxidized asphalts, only AAG-1 and AAM-1 show the presence of any sulfoxide. Comparison of the XANES and ESCA spectral analyses for AAA-1 (see below) shows fairly good agreement in the ratios of sulfide and thiophenic sulfur: XANES gave 40:60, while ESCA gave 34:66.

XANES analyses of thermally oxidized AAA-1, AAG-1, and AAK-1 indicate formation of varying proportions of sulfoxide derived only from sulfide sulfur. About 32% and 14% of AAA-1 and AAK-1 sulfides, respectively, disappear on oxidization, part of which is accounted for by sulfoxide; however, in AAG-1 51% of sulfide oxidizes to give the expected amount of additional sulfoxide. No other oxidized sulfur species was observed with these samples.

The chemically oxidized samples of AAA-1 and AAG-1 provided by SRI International were prepared using t-BuOOH in cyclohexane. The reason sample Y (AAG-1) shows a high proportion of sulfate in the XAFS spectrum is probably because bisulfite ion was used to reduce t-BuOOH in the oxidation of AAG-1 to ensure that no peroxide was entrained with the asphalt during clean up and drying. Apparently no sulfide sulfur is left after oxidation, consistent with the low concentration of sulfide sulfur of 0.13 M in AAG-1. This value also agrees with the observation that thermal oxidation of AAG-1 gives only 0.15 M sulfoxide. Asphalt X (AAA-1) has 10% sulfide left after chemical oxidation, with almost all the difference accounted for by sulfoxide. AAM-1 is especially interesting in having the lowest proportion of sulfide of any sample examined by XANES; on thermal oxidation AAM-1 also shows formation of the smallest amount of sulfoxide, in keeping with the idea that only sulfide sulfur is oxidized.

The data of Green et al. (1992) for AAG-1 indicate that up to 12% of sulfur may be aryl sulfide or disulfide (ArSAr or ArS-SAr). This form of sulfur apparently shows up as thiophenic sulfur by XANES spectroscopy.

The oxidation pathways and speciation of asphalt sulfur compounds were further characterized by photoelectron spectroscopy (ESCA) measurements. The ESCA spectra were prepared by the Surface Science Laboratory in Mountain View, California, on several thin film samples of AAA-1 and a sample of AAA-1 doped with di-n-butyl sulfone. The ESCA spectrum of unoxidized AAA-1 shows only two kinds of sulfide sulfur corresponding to aromatic and aliphatic sulfur in a ratio of 2:1. Thermal oxidation (TTA) at 110°C (230°F) removes part of the aliphatic sulfide with little or no effect on aromatic sulfur. However, the sensitivity of the measurement method prevented observation of sulfoxide formation. Chemical oxidation of AAA-1 at 25°C with t-BuOOH removes all of the aliphatic sulfur and the sulfoxide bands are clearly observed. Figure 7.5 shows these changes in the ESCA spectra of AAA-1.

Comparison of ESCA and XAFS/XANS spectra for AAA-1 in table 7.4 shows good agreement on the proportion of aliphatic sulfide oxidized to >SO. Almost 40% of sulfide was oxidized in 72 hours at 113°C (235°F), in good agreement with results from XANES. The data of Green et al. (1992) data suggest that AAA-1 has 22% ArSAr, 40% total sulfide, and the remainder is presumably thiophenic sulfur. ESCA indicates a similar amount of aliphatic sulfur, all of which oxidizes with t-BuOOH. Ruiz et al. (1982) reported that t-BuOOH does not oxidize aryl sulfides, so it can be concluded that one or another analysis is in error.

Oxidation of the eight core asphalts with t-BuOOH at 25°C (77°F) gives >SO, which accounts on average for 30 mole % of the original sulfur; >SO formed at 113°C (235.4°F) in the TFAAT accounts for ~13 mole % of the sulfur in the same asphalts, and the proportions of >SO formed in the asphalts correlate reasonably well between the chemical and thermal routes of formation of >SO. Figure 7.6 illustrates the >SO IR peak found in each core asphalt oxidized by t-BuOOH. Figure 7.4 plots >SO versus total asphalt S in each core asphalt. These relations support the idea that the same pool of aliphatic sulfur is oxidized by thermal oxidation with oxygen and by t-BuOOH.

## *Oxidation*

The model compounds n-butyl sulfide and dibenzyl sulfide (NBS, DBS) were used to study the case of thermal oxidation of the aliphatic sulfide bond of the kind believed to be thermally and chemically oxidized in asphalts. Green et al. (1992) believe all aliphatic sulfur in asphalt is in the form of cyclic sulfides. Samples of neat NBS or DBS, or NBS in benzene, were sealed under air or pure oxygen and heated at 100°-130°C (212°-266°F) for 3 days. The samples were then analyzed for sulfoxide (>SO) by IR spectra or gas chromatography (GC) and compared with spectra of unheated NBS or DBS and authentic n-Bu<sub>2</sub>SO. No trace of >SO was found in the neat NBS heated in air or oxygen, and less than 0.1 % of >SO was found in the benzene solution. These experiments provide clear evidence that simple sulfides do not form by direct thermal reaction with oxygen. It is concluded that >SO formation in asphalts does not arise from direct reaction of asphalt sulfides with oxygen. Some other structural feature in asphalt must be the primary site of interaction with oxygen.

Peroxide treatment of AAD-1 and AAK-1 gave twice as much >SO as from heating, and in no case was it possible to account for more than 10 to 30 mole % of the total S as >SO, further supporting the conclusion that only the minor aliphatic sulfide is easily oxidized to >SO. Thiophenic sulfide either is not oxidized to >SO at all or (less likely) is rapidly oxidized further to >SO<sub>2</sub> (Kuhnen 1966). Aryl sulfides probably are not oxidized either thermally or with t-BuOOH.

To evaluate the role of O<sub>2</sub> on >SO formation, experiments were conducted with several samples of 50 μm asphalt films coated on Pyrex tubes and either evacuated to .025 to .030 torr microns before sealing or sealed under air and heated at 110°C (230°F) for 3 days. No >SO formed in vacuum, while substantial amounts formed in air.

Neat asphalt samples heated as small lumps in air gave about as much >SO as did thin films cast from solvent. Similar results were found using mixtures of 1:3 asphalt:toluene, indicating that neither solvent nor film thickness in small samples plays a role in the oxidation process, as expected if oxygen diffusion is not rate-controlling. Oxygen uptake measurements (see below) confirmed this result.

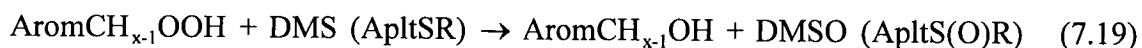
The role of solvent in >SO formation was investigated by heating solutions of 200 mg/mL AAK-1 in toluene at 106°C (222.8°F) for 48 hours. The solution gave 0.23 M >SO while an AAK-1 film gave 0.27 M >SO; these are nearly the same (0.3 M) as reported for >SO formed from AAK-1 in the TFO. Moreover, no significant difference was noted in the growth rate of the 1030 cm<sup>-1</sup> band between dilute or concentrated toluene solutions of AAG-1 or AAK-1. These results point to an intramolecular process involving some oxidant molecularly linked to the sulfide group as responsible for >SO formation (see below).

Dimethyl sulfide (DMS) was added to AAA-1 to probe the pathway for sulfoxide formation from asphalt aliphatic sulfides under conditions where direct oxidation of di-n-butyl or dibenzyl sulfide at 110°C (230°F) in oxygen is not detectable. A mixture of 190 mg DMS and 50 mg AAA-1 was heated for 3 days at 110°C (230°F) in air in a sealed tube; this amount of DMS was needed to leave some liquid phase at 110°C (230°F) (DMS has 7 atm pressure at this temperature). The mixture, stripped of excess DMS, showed a strong band in the IR spectrum at 1000 cm<sup>-1</sup> due to dimethyl sulfoxide (DMSO) corresponding to 0.5 M in the asphalt. DMSO was then stripped out by heating in a .020 torr vacuum at 80°-90°C (176°-194°F) and the IR spectrum retaken to show that almost no AAA-1 sulfoxide had formed. Figure 7.7 shows the IR spectra from the experiment. The result clearly demonstrates that a peroxy intermediate (probably nonsulfur) species that forms with oxygen can be intercepted by DMS.

To corroborate the effect of DMS and better understand it, the original experiment was repeated with 200 mg DMS and 50 mg of either unoxidized (tank) AAA-1 or preoxidized (3 days at 110°C, 230°F in air) AAA-1 at 110°C (230°F) in air in sealed tubes. IR spectra of the resultant mixtures (first stripped of DMS) showed DMSO formation in the tank and preoxidized asphalt samples in amounts similar to those observed in the initial DMS/AAA-1 experiment. The experiment with DMS and preoxidized asphalt shows that even when asphalt aliphatic sulfur is largely oxidized, the reactive oxidation species responsible for oxidizing DMS is still available for oxidation of additional DMS.

In other, non-SHRP supported work, the present authors have shown that n-BU<sub>2</sub>S is oxidized to n-BU<sub>2</sub>SO in oxidizing asphalt thin films and benzene solutions (Mill et al. 1992).

A likely candidate for this reactive oxidation species is a hydroperoxide formed from the most reactive benzyl CH bonds in asphalt:



Purified cumene (isopropylbenzene, CuH) was examined as a model compound for asphalt benzylic CH bonds and a thermal source of hydroperoxide. In a heated sealed tube, 180 mg DMS and 50 mg CuH were heated in the presence of oxygen at 110°C (230°F) for 3 days. The reaction products were analyzed for DMSO using GC. Much less DMSO formed in the reaction mixture (barely above the detection limit) compared with the amounts of DMSO formed in 50 mg AAA-1 (~ 1.60 mg) under the same conditions with air instead of oxygen. This experiment shows that the reactive oxidation centers in asphalt are much more reactive to oxygen than cumene CH bonds.

The effect of oxygen pressure on rates of oxidation in AAA-1 thin films was examined by heating samples in air or oxygen at 100°C (212°F) for 25 hours and comparing the FTIR band for sulfoxide between 1,100 and 960 cm<sup>-1</sup>. The oxygen reaction was clearly faster by a factor of about two. At shorter reaction times, the difference was slightly smaller. For simple first power dependence on oxygen concentration for sulfoxide formation, a factor of five in rate would be expected on going from air to oxygen.

### *Sulfoxide Decomposition*

To help clarify the importance of how sulfoxide decomposition competes with formation, the literature on sulfoxide decomposition kinetics and the kinetics for sulfoxide loss were evaluated by heating air-oxidized samples of AAA-1 and AAK-1 under vacuum at 100°C (212°F), and samples of AAG-1, AAK-1, and DBS under argon at 165°C (329°F) for 40 hours and remeasuring the sulfoxide band by FTIR. The formation of sulfoxide was then modeled using simple first order kinetics to learn how the decomposition of sulfoxide (by elimination) during oxidation would affect the kinetic curves for formation.

Sulfoxides and carbonyls may be thermally unstable under TFO conditions at 165°C (329°F). The rates of cleavage to olefins and sulfenic acids depend on sulfoxide structure (cyclic or alicyclic; substituted, benzylic, or aliphatic) and on solvent polarity (Kingsbury and Cram 1960; Walling and Bollyky 1964; Kice and Campbell 1967). A brief investigation of the decomposition kinetic behavior of sulfoxide formed on oxidation of AAA-1, AAD-1, AAGT, and AAKT (AAGT and AAKT were thin film oxidized in air at 100°C), as well as di-n-butyl sulfoxide (DBSO) dissolved at 0.1 M concentration in unoxidized AAD-1 was conducted to learn whether the sulfoxides are stable and are structurally similar to each other and to a di-primary alkyl sulfoxide like DBSO. Results,



summarized in table 7.5, show that AAD-1 and AAKT are similar in reactivity to DBSO, but AAGT is quite unreactive over 10 hours at 165°C (329°F) under argon.

Only in AAGT does the carbonyl region increase much on heating at 165°C (329°F) under argon. The origins of additional carbonyl may be peroxide decomposition, since AAGT is low in aliphatic sulfide (which can scavenge peroxide), or it may result from a rearrangement or cleavage to form a new carbonyl with stronger IR cross action.

Asphalt AAA-1 heated under vacuum at 100°C (212°F) for 40 hours showed a loss of less than 10% of the original sulfoxide, corresponding to a first order half-life of more than 20 days. This result agrees with the result of modeling the oxidation of asphalt with simple first order kinetics, in which WRI's results on sulfoxide formation at 113°C (235.4°F) in 120 hours can be accurately reproduced using a rate constant derived from the relation

$$k_1 = \ln\{[>\text{SO}]_{\infty}/([>\text{SO}]_{\infty}-[>\text{SO}]_t)\}/t \quad (7.20)$$

where  $[>\text{SO}]_{\infty}$  and  $[>\text{SO}]_t$  are the sulfoxide concentrations at times  $t$  and 120 hours taken from the WRI plots of sulfoxide vs. time at 113°C (235.4°F). When the present authors modeled the same process but introduced a competitive decomposition step for the sulfoxide, the results gave much lower values of sulfoxide >70 hours, indicating that sulfoxide decomposition is not important at 100°-113°C (212°-235.4°F).

The stability of >SO formed in several asphalts under TFO conditions at 165°C (329°F) was also measured by first oxidizing samples at 100°C (212°F) for 20 to 30 hours. Samples were subsequently heated under argon in sealed tubes for 5 to 10 hours at 165°C (329°F). Both samples were then analyzed for >SO by FTIR. Argon heated samples showed about 10 to 58% less >SO than unheated ones, indicating a modest degree of stability for >SO under TFO conditions. These >SO loss rates correspond to half-lives of 8 hours at 165°C (329°F), consistent with half-lives found by Walling and Bollyky (1964) for pyrolysis of long chain aliphatic sulfoxides. This result may account for the smaller amounts of sulfoxide found in TFO treated AAD-1, AAK-1, and AAG-1 on oxidation at 100°C (212°F) (tables 7.6 through 7.8) compared with tank samples of the same asphalts: Sulfoxide formed and decomposed at 165°C (329°F) during this pretreatment may inhibit oxidation by intercepting peroxide intermediates. Table 7.5 summarizes >SO decomposition data.

### *Effect of Sulfoxide Formation on Rheological Properties*

The selective oxidation of asphalt alkyl sulfides to sulfoxides with t-BuOOH was used to examine the possible link between >SO formation and changes in physical properties of AAD-1 and AAM-1 without other oxidative changes that must accompany thermal oxidation. AAD-1 and AAM-1 contain 8.6% and 0.5% sulfur, respectively.

A sample of AAD-1 containing 500 mole % of aliphatic sulfide was oxidized at 25°C (77°F) in methylene chloride. The cleaned up product was sent to WRI for viscosity measurements, and a small sample was retained for FTIR spectrum. The viscosity of the

oxidized AAD-1 was nearly 10 times higher than that of the unoxidized sample (5,802 Pa·s oxidized vs. 523.7 Pa·s TFO), although the IR carbonyl region showed little change.

## Oxygen Uptake and Balances in Oxidized Asphalt

### *Oxygen and Product Balances*

Detailed oxygen uptake and product studies were conducted on the four core asphalts AAD-1, AAG-1, AAK-1 and AAM-1 to evaluate how well the observable products, including >SO and >CO, account for the absorbed oxygen. In each case the oxidation of both the tank asphalt and the TFOT asphalt, which had been heated in air for 5 hours at 165°C (329°F) was examined. (WRI supplied these samples.) These asphalts were designated as AADT, etc. We oxidized several samples of these asphalts as thin films, lumps and in *t*-butylbenzene (TBB) as 300 mg/mL solutions, at 100°C (212°F) in air for as long as 409 hours in one case, but more usually up to 120 hours. Samples were initially in the range of 80 to 100 mg each, but later samples were much larger, 200 to 300 mg, to improve the accuracy of the oxygen uptake and product formation data. Oxygen uptake for each sample was measured at each time point using an improved GC method, and >SO and >CO formation in these samples were quantitatively measured by FTIR to find out how much absorbed oxygen is accounted for by these two classes of products.

Tables 7.6 through 7.10 summarize the oxidation product and rate data. The most important qualitative conclusions are that oxygen balances are generally low (20-60%), that carbonyl forms in low yield in most asphalts but not AAM-1 or AAMT, and that there are no significant differences between tank and TFOT samples, again except for AAM-1 and AAMT. For most asphalts, oxygen uptake and product formation are similar in both kinds of asphalts. The ratio of >SO:>CO is close to 10 in oxidized AAK-1 and AAKT samples, whereas it is closer to 3 or 4 in AAD-1 and AADT. Both asphalts have relatively high total sulfur, but AAD-1 (AADT) has a higher proportion of sulfide sulfur than does AAK-1 (46% vs. 36%). The long-duration AADT experiment in table 7.6 was analyzed for CO and CO<sub>2</sub> formation as well as oxygen uptake, but none could be found under conditions where detection capability was estimated at < 3  $\mu$ moles. Thus, the missing oxygen is still largely in the asphalt or as water.

Oxygen balances are most accurate at longer times but either decrease or remain unchanged at longer times, probably because primary products decompose. The uncertainty in oxygen uptake and product measurements is greatest in the early stages where all of the values are small:  $\pm 20\%$  in O<sub>2</sub>,  $\pm 10\%$  in >SO formation, and possibly as high as  $\pm 100\%$  in >CO are the current best estimates of uncertainty in the absence of more data. The high uncertainty in >CO stems mainly from uncertainty as to which model ketone standard to use for calibration of the FTIR spectrum around 1700 cm<sup>-1</sup>. Valerophenone was chosen as a standard, assuming that any ketones would form at benzylic positions and would be well modeled by valerophenone. However, oxidation of phenols also leads to ketone formation (as cyclohexadienones), which probably have very different IR spectral cross sections from arylphenones such as valerophenone. But even doubling the carbonyl concentrations still

leaves oxygen balances short of the 2:1 stoichiometry for each  $O_2$  to form one  $>SO$  or  $>CO$  and one  $ROH$  or  $H_2O$ .

Sulfoxide concentrations are based on a calibration curve prepared for the IR peak area around  $1050\text{ cm}^{-1}$  for di-n-butyl sulfoxide. Recent studies by Green et al. (1992) suggest that use of a simple model compound sulfoxide leads to an underestimation of  $>SO$  by 30+%. If this is correct, all of the data would show improved oxygen balances.

### *Oxidation and Product Rates*

Tables 7.6 to 7.10 also show the rates of oxygen uptake normalized for time and sample size in  $\mu\text{mol mg}^{-1}\text{ hr}^{-1}$ . The striking feature of these data is the similarity in rates for all of the asphalt samples. With a few exceptions, the rates are close to  $5 \times 10^{-3}\text{ }\mu\text{moles mg}^{-1}\text{ hr}^{-1}$  for oxygen uptake. This is hardly a two-fold difference in rates among all asphalts studied, even though AADT and AAKT have 1.2 M and 0.76 M sulfide sulfur compared with AAGT and AAMT which have only 0.14 M and 0.065 M sulfide.

The most striking rate effect is found between films and t-butylbenzene (TBB) solutions, where consistently higher rates by factors of two to five are observed for solutions. Since asphalt concentrations are lower by 3.3 times, the true rate differences are substantial.

### *Photooxidation of Asphalt Films*

Two AAB-1 asphalt films were cast on 1 cm diameter salt plates; one film was  $3\text{ }\mu\text{m}$  and the other was  $30\text{ }\mu\text{m}$  thick. The films were exposed to simulated sunlight from the filtered output of a xenon-mercury lamp for up to 6 hours in air. The IR spectra taken at 0, 3, and 6 hours show progressive growth of  $1000$  and  $1700\text{ cm}^{-1}$  bands in both films. Growth of the  $1700\text{ cm}^{-1}$  carbonyl band is much greater relative to unchanged bands near  $1700\text{ cm}^{-1}$  in the  $3\text{ }\mu\text{m}$  film than in the  $30\text{ }\mu\text{m}$  film, whereas growth of the  $1050\text{ cm}^{-1}$  sulfoxide band is slower and has about the same proportional rate in both films.

UV spectra of asphalt films show that a  $3\text{ }\mu\text{m}$  film absorbs 99.7% of 300 nm light and 88% of 400 nm light, the wavelengths most likely to cause oxidation. Thus, the relatively smaller growth of the carbonyl band in the  $30\text{ }\mu\text{m}$  film is the result of absorption of all UV light in the top  $10\text{ }\mu\text{m}$ , leading to an oxidative skin effect. In contrast, UV light penetrated throughout the  $3\text{ }\mu\text{m}$  film, leading to a higher proportion of oxidized material. Longer wavelength light  $>400\text{ nm}$  will penetrate deeper and can generate singlet oxygen, a selective oxidant for converting sulfide to  $>SO$ .

The low penetration of UV light into asphalt films precludes a direct role for photooxidation in the failure process for the bulk asphalt. However, if products produced in the thin surface skin migrate into the bulk phase over the long times found under service conditions, photooxidation might play an important indirect role in failure of bulk asphalt by constantly generating oxidation products at the surface that affect bulk performance adversely. Similarly, surface oxidation and embrittlement might lead to microcracks which

propagate through the bulk phase, thereby providing a mechanical mechanism for amplifying photooxidative effects in the bulk phase. Both of these mechanisms deserve careful examination and perhaps experimental tests.

## Model Systems for Asphalt Oxidation<sup>1</sup>

The primary unsolved chemical problem in asphalt oxidation is the chemistry of the reactions of oxygen with reactive sites in asphalt. Bond strengths of phenol OH and benzylic CH bonds typically found in asphalts are too high to allow significant rates of simple H-atom transfer to occur directly with O<sub>2</sub> to form phenoxyl or benzyl radicals. Therefore, if these reactions occur in asphalt with oxygen, they probably involve either concerted reactions or electron transfer, as for example with phenolic anions in polar solvents.

A detailed study of selected model compounds with oxygen using di-n-butyl sulfide (Bu<sub>2</sub>S) has been conducted to detect transient or intermediate oxidants that are capable of oxidizing Bu<sub>2</sub>S to the sulfoxide (Bu<sub>2</sub>SO). By using Bu<sub>2</sub>S to monitor for oxidants similar to those found in oxidizing asphalt (where Bu<sub>2</sub>S is competitively oxidized only to Bu<sub>2</sub>SO), several candidate classes of compounds can be efficiently screened.

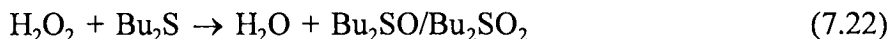
All of the experiments were conducted in benzene at 100°C (212°F) with 1 atm (0.1 MPa) of oxygen. Subsequent analyses of the mixtures were performed using GC to measure Bu<sub>2</sub>S, Bu<sub>2</sub>SO, and Bu<sub>2</sub>SO<sub>2</sub> as well as the parent and oxidized hydrocarbon. Control experiments with 3-4 mM Bu<sub>2</sub>S in pure benzene showed no oxidation in up to 100 hours, a time in which half or more of the Bu<sub>2</sub>S would be oxidized in the presence of 50 mg asphalt/mL solution. Similar experiments were conducted with Bu<sub>2</sub>S in purified cumene (isopropylbenzene, PhCH(Me)<sub>2</sub>), tetralin (tetrahydronaphthalene) and dihydroanthracene (DHA). Despite purification to remove peroxides, trace peroxide appeared to be present in cumene, as shown by prompt formation of Bu<sub>2</sub>SO on mixing Bu<sub>2</sub>S with cumene without heating. The Bu<sub>2</sub>SO did not increase significantly on heating the mixture with oxygen, which was interpreted to mean that cumene-like tertiary benzyl hydrogens are not important in oxidation of asphalt.

Tetralin oxidation for 30 hours resulted in only trace quantities of Bu<sub>2</sub>SO and Bu<sub>2</sub>SO<sub>2</sub>. Tetralin is 10 or more times as reactive (per CH bond) as cumene toward oxy radicals, so failure to find significant induced oxidation of Bu<sub>2</sub>S with tetralin reinforces the conclusion that simple benzylic H-atom transfer to oxygen is not involved in asphalt oxidation.

Dihydroanthracene, dissolved in benzene, readily induces the oxidation of Bu<sub>2</sub>S to Bu<sub>2</sub>SO and then Bu<sub>2</sub>SO<sub>2</sub> when heated at 100° with oxygen. Anthracene (A) is the other major product detected by GC with small amounts of another unidentified product (possibly anthrol or anthraquinone):

---

<sup>1</sup>Supported by a grant from Euron, Milan; work conducted at SRI by E. Canavesi from Euron.



The rapid conversion of DHA to A, a 20% conversion of 50 mM DHA in 16 to 20 hours, is surprisingly fast and is strong evidence for a concerted removal of both H-atoms to form  $\text{H}_2\text{O}_2$  and A. Moreover, this rate is comparable to the rates of oxidation of  $\text{Bu}_2\text{S}$  in asphalts. Also surprising was the rapid conversion of  $\text{Bu}_2\text{SO}$  to  $\text{Bu}_2\text{SO}_2$  such that almost no  $\text{Bu}_2\text{SO}$  was present after even 16 hours, because induced oxidation of  $\text{Bu}_2\text{S}$  in asphalt invariably forms  $\text{Bu}_2\text{SO}$  with only traces of  $\text{Bu}_2\text{SO}_2$ .

In experiments using  $\text{H}_2\text{O}_2$  alone in benzene at  $100^\circ\text{C}$ ,  $\text{Bu}_2\text{S}$  rapidly oxidizes to  $\text{Bu}_2\text{SO}$  and  $\text{Bu}_2\text{SO}_2$  in several hours and excess  $\text{H}_2\text{O}_2$  oxidizes all  $\text{Bu}_2\text{S}$  to  $\text{Bu}_2\text{SO}_2$ . One experiment with 0.2 M  $\text{H}_2\text{O}_2$ , 4 mM  $\text{Bu}_2\text{S}$  and 50 mg/mL AAGT under argon gave equimolar amounts of  $\text{Bu}_2\text{SO}$  and  $\text{Bu}_2\text{SO}_2$  in 2 hours. Longer times gave even higher proportions of  $\text{Bu}_2\text{SO}_2$ . The shift to the sulfone in oxidizing DHA and with  $\text{H}_2\text{O}_2$  alone supports the reaction sequence shown above. However, the change in product composition may signal that DHA oxidation is not the appropriate model for asphalt oxidation, or that  $\text{H}_2\text{O}_2$  formed in asphalt oxidations in low concentrations in the presence of other functional groups is a more selective oxidant for sulfide bonds than in higher concentrations with DHA or alone in benzene.

Experiments now in progress will determine whether similar results are obtained when  $\text{H}_2\text{O}_2$  is introduced into asphalt- $\text{Bu}_2\text{S}$  mixtures at much lower concentrations ( $\sim 0.03$  M) continuously to better simulate conditions in oxidizing asphalt. Induced oxidation of  $\text{Bu}_2\text{S}$  with DHA appears to be a promising approach to understanding not only induced oxidation of sulfide but the whole range of other oxidation processes in asphalt.

## Summary

The data presented here provide the basis for formulating a general pathway for oxidation of asphalt carbon and sulfur, but with some key features still missing or in doubt.

First, detection of CL in asphalts in the presence of oxygen is convincing evidence for the formation of peroxy free radicals in bulk asphalt when heated, even to moderate temperatures. There is no question that peroxy radicals are abundant in asphalt under service conditions. What is not known is whether these radicals play any role in oxidative age hardening. More detailed spectral analyses and time emission studies are required to establish the relationship to oxidative aging and to yield more detailed knowledge of the origins of the radicals. Note that the decline in CL activity with time is consistent with the apparent decline in rates of oxygen uptake (tables 7.6 through 7.10).

Inhibition studies using MP, HNA, and especially CuH oxidation show the presence of significant amounts of free radical inhibitors in all core asphalts, distributed almost equally between maltene and asphaltene fractions. The inhibitors are mostly phenols, as shown by the effect of phenol methylation in removing any inhibition in AAA-1 or AAD-1. The

cumene oxidation technique is a sensitive and reliable measure of oxidative inhibition in asphalts and can be used to probe further the effect of oxidative hardening on inhibitor concentrations.

The presence of the native inhibitors in significant concentrations provides a simple explanation for the general ineffectiveness of added phenolic inhibitors on the oxidative aging process: If oxidation were a chain process capable of being inhibited by phenols, native phenols would probably serve that purpose as well. The present evidence from CL and cumene experiments indicates that oxidation in asphalt is a nonchain process that probably involves radical intermediates at some stage.

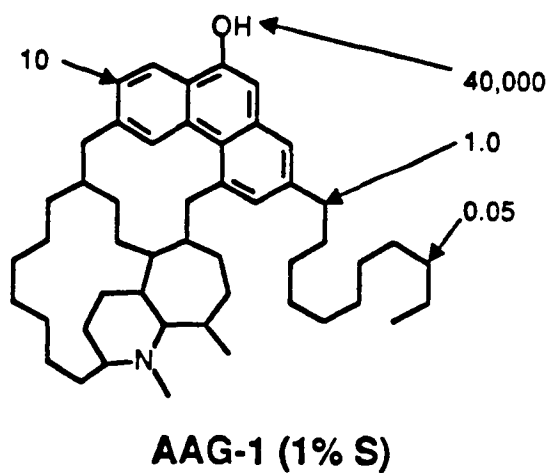
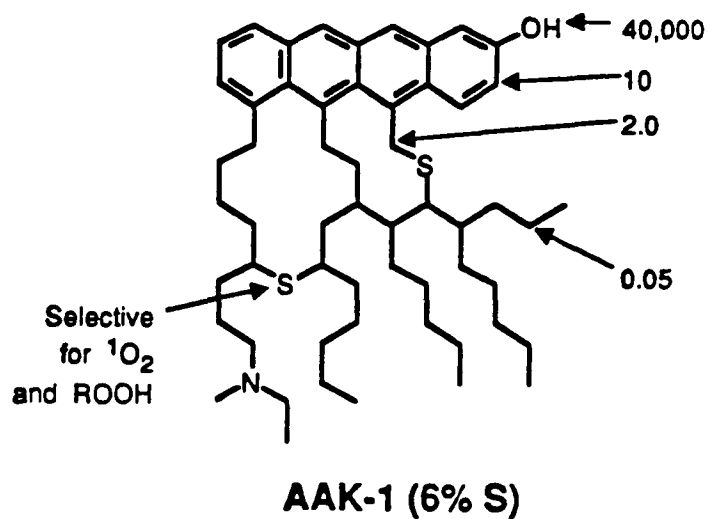
The data from this study using XANES and ESCA spectroscopies clearly show that only aliphatic sulfide sulfur is oxidized during thermal oxidation or mild chemical oxidation by t-BuOOH. Thiophenic sulfur and probably aryl sulfide are not significantly affected during these oxidations. This conclusion, first reached by Ruiz et al. (1982) and by Petersen (1991) for a few kinds of asphalts, has now been extended semi-quantitatively to the SHRP core asphalts and by implication to all other asphalts as well.

With this understanding, it becomes clearer why >SO-time curves for oxidation of different asphalts are so different, and why asphalts with similar total sulfur content but different aliphatic:aromatic distributions of sulfur give different >SO yields. In the case of low sulfur asphalts such as AAG-1 or AAM-1, aliphatic sulfide is rapidly exhausted and formation of >SO almost stops after 30 hours at 100°C (212°F). Asphalts high in aliphatic sulfide sulfur such as AAA-1 or AAD-1, oxidize for longer times to form much higher proportions of >SO.

The effect of added DMS and DBS on the yield of asphalt >SO in the case of AAA-1 and the induced oxidation of DMS and DBS by the oxidizing asphalt both point to the formation of a peroxy intermediate from direct interaction of asphalt with oxygen. Induced oxidation of DMS is found in both preoxidized and tank asphalts, indicating that the source of the peroxy intermediate is both independent of the sulfur and in excess of sulfide sulfur, at least in AAA-1. Oxygen effects on rates of formation of >SO also are in qualitative agreement with this hypothesis. The present authors have not been able to establish the effect of >SO formation on rheological properties, although it is believed that >SO exerts a strong H-bonding affect on other functionalities and effects the visco-elastic properties.

Rates and products in oxidation of core asphalts point to oxygen imbalances in terms of the >SO and >CO products; in some cases the deficits are large. Rates of oxidation show a striking similarity among the four core asphalts even though they differ by 20-fold in sulfide content and almost as much in vanadium and other metal ion contents. Oxidation rates do not appear to be controlled by these components but by other components such as phenols or dihydroaromatic groups, the identities of which are currently under investigation. Other features of the rate and product studies also fit well with the overall concept. AAM-1 or AAMT oxidize rapidly to form >SO, but the oxidation continues after >SO production stops due to exhaustion of the aliphatic sulfide to form much more carbonyl. In that sense sulfide sulfur acts as an internal redox inhibitor to limit >CO formation from the peroxy intermediate.

Figure 7.8 shows a schematic representation of the oxidation process. In this scheme, the peroxy intermediate can oxidize sulfur and form alcohol, but in the absence of the sulfide sulfur, the intermediate may form carbonyl by one of several paths. Alcohols are difficult to detect by IR methods and might account for part of the missing oxygen.

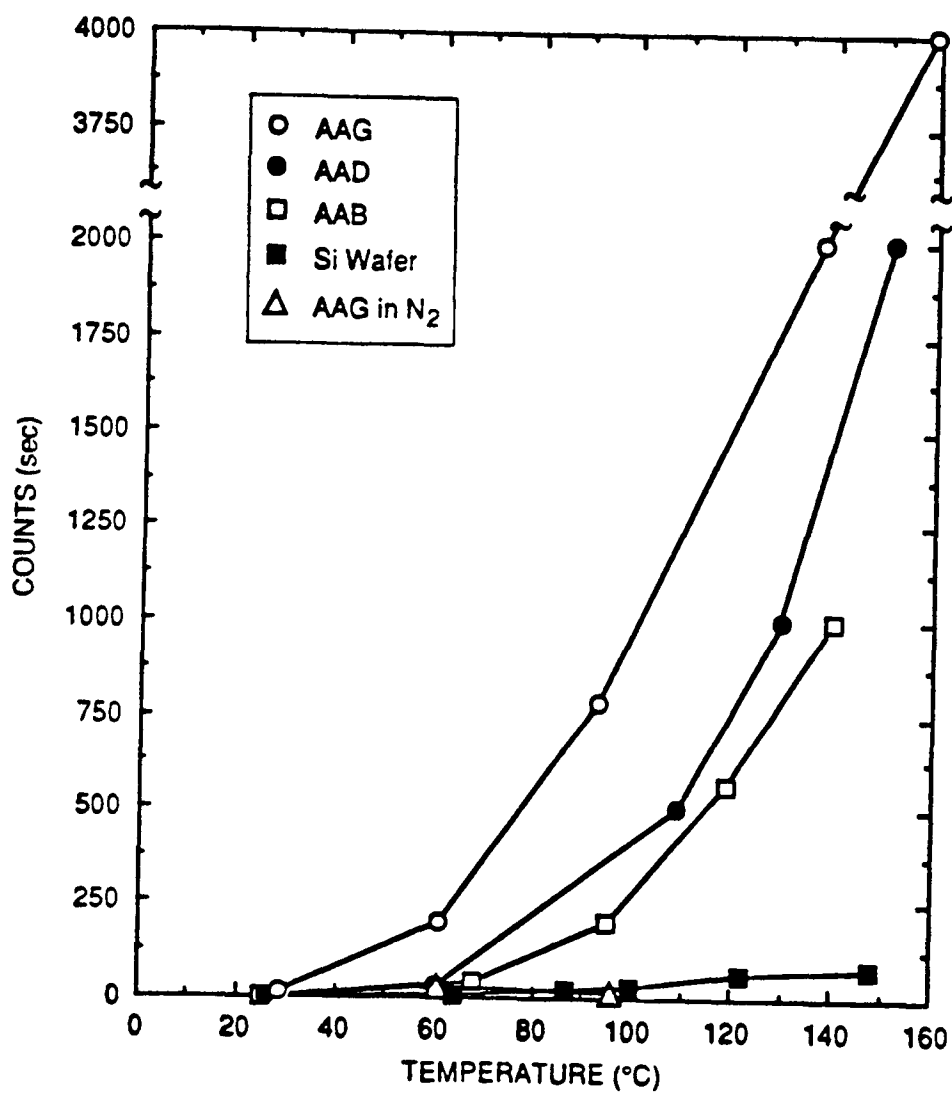


• From P.W. Jennings, Montana State University.

RM-6319-20A

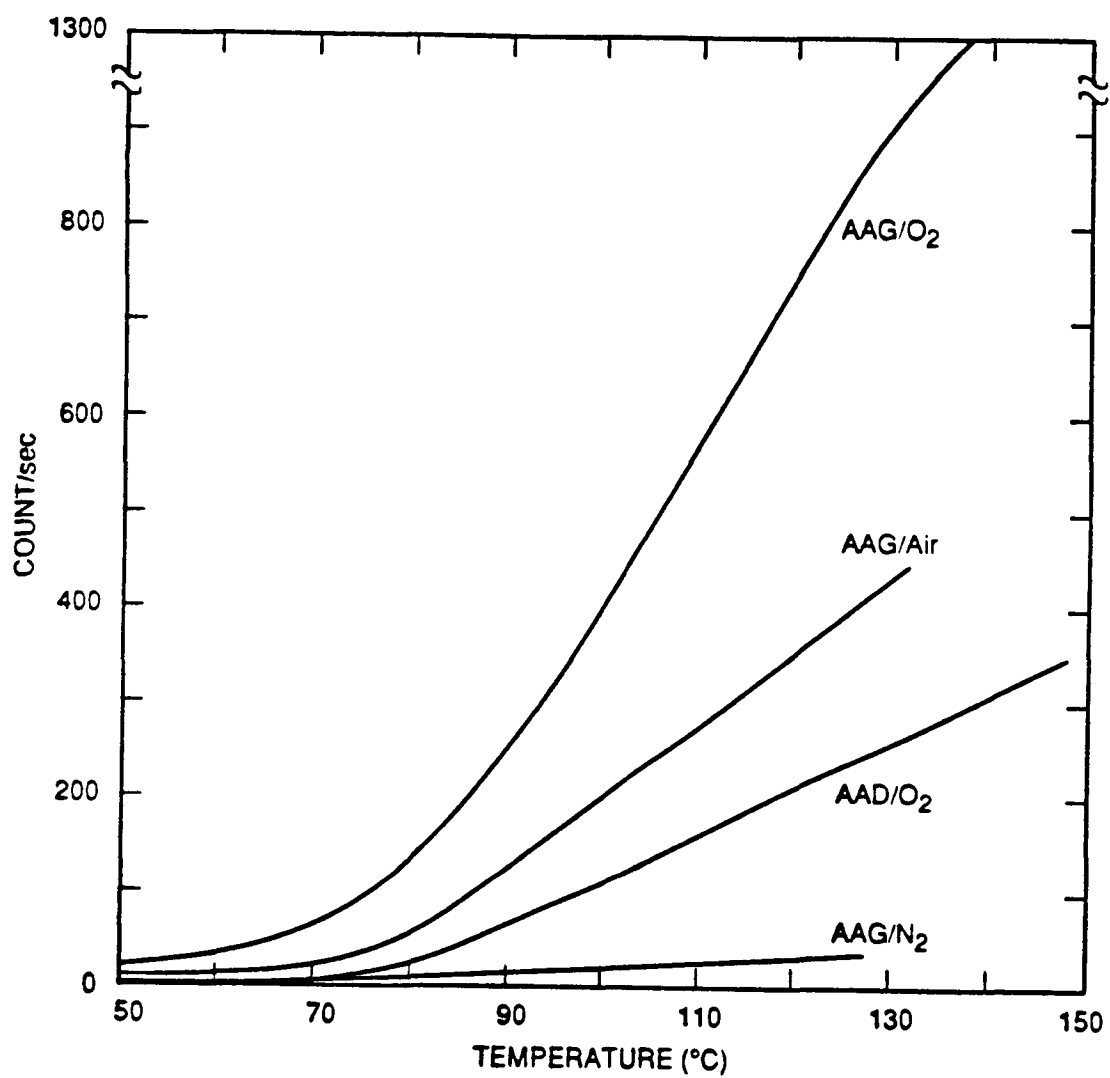
**Figure 7.1 Oxidizable Structures in Representative Asphalt Molecules**





RM-6319-23

Figure 7.2 Relative Chemiluminescence (CL) Intensities in Air



RM-6319-28

Figure 7.3 Effect of Oxygen Concentration on CL

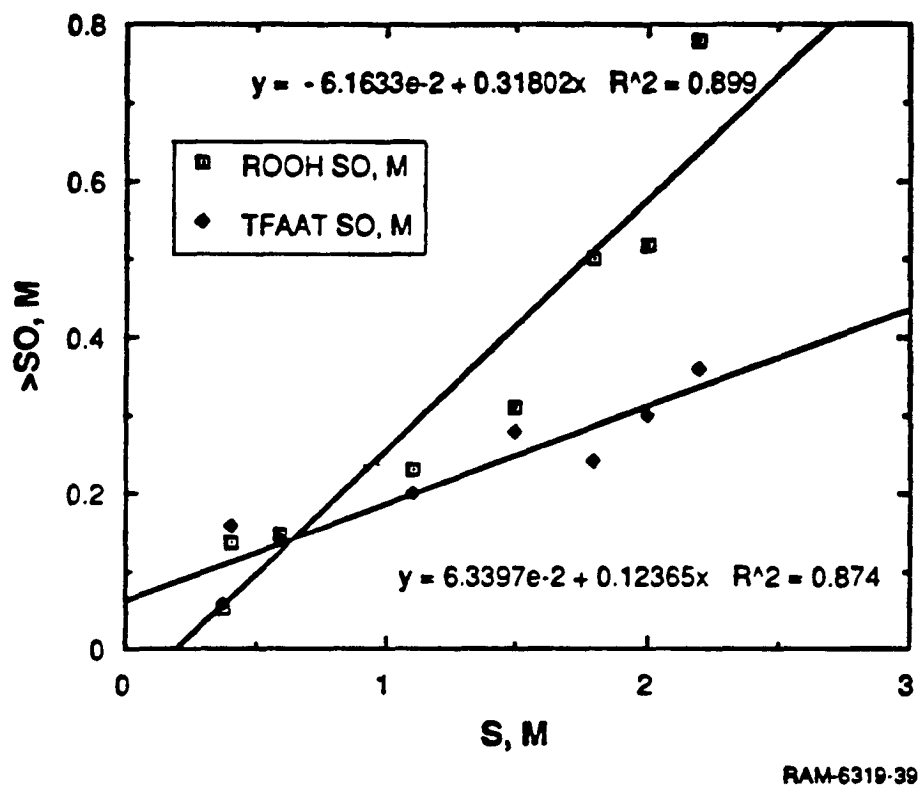
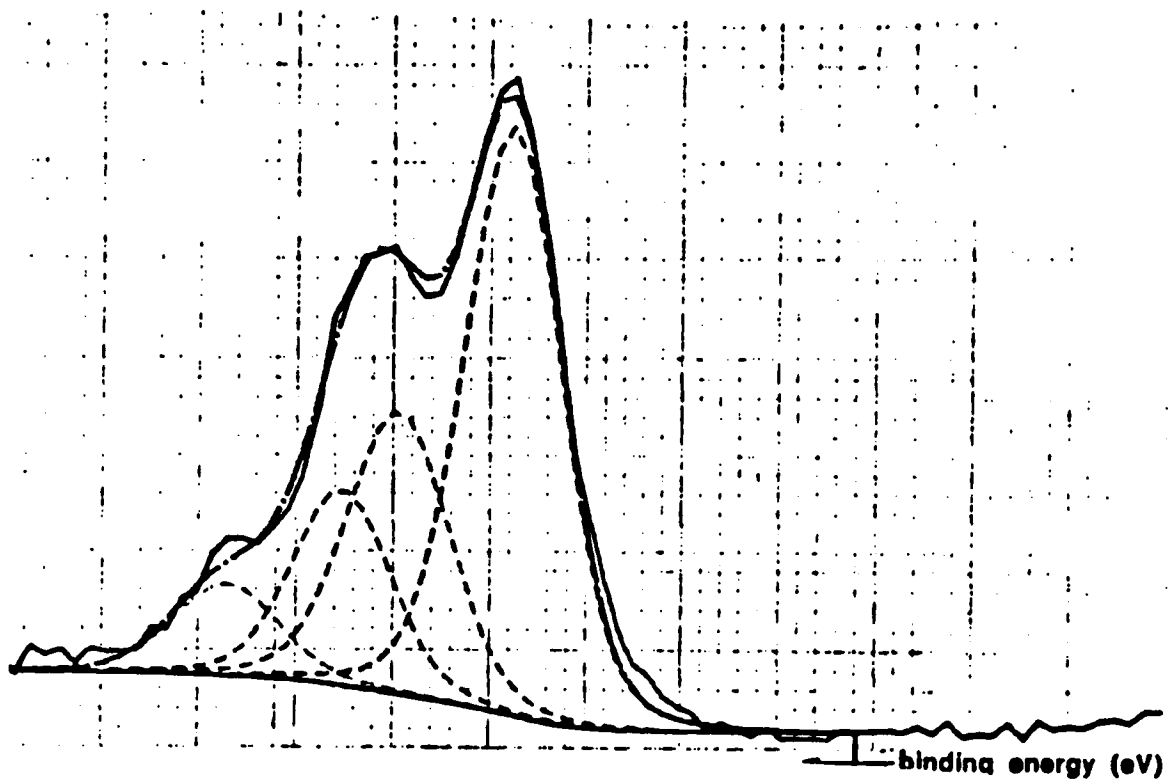
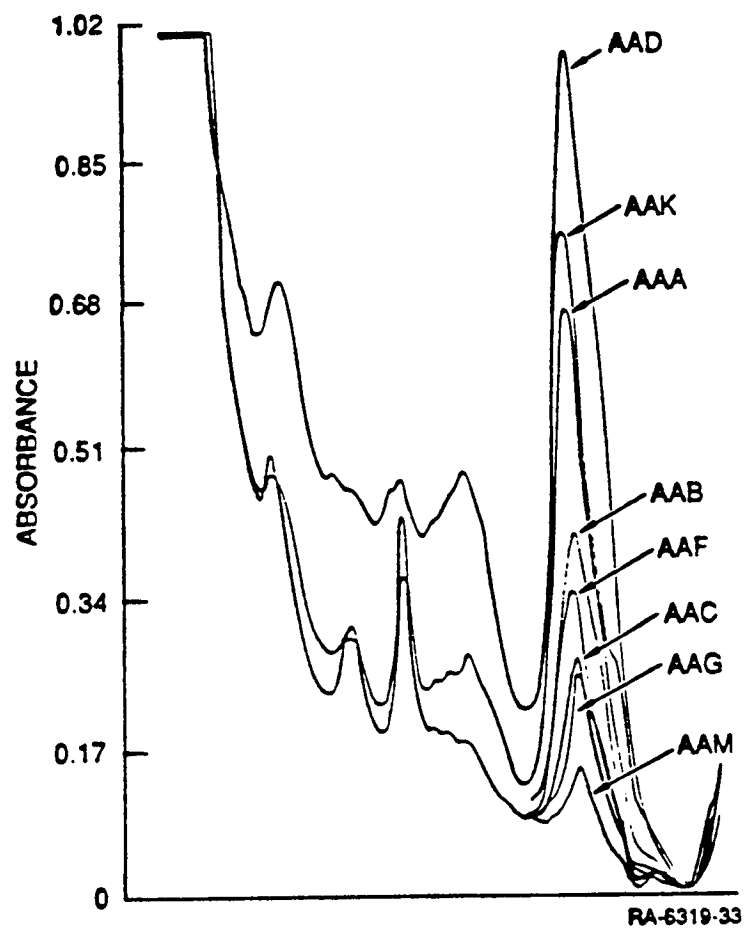


Figure 7.4 Correlation of Sulfoxide with Sulfur in Core Asphalts



**Figure 7.5** X-Ray Photoelectron Spectroscopy (ESCA) Sulfur Spectrum for ROOH-Oxidized AAA-1



**Figure 7.6** Formation of Sulfoxide Band at  $1030\text{ cm}^{-1}$  in Core Asphalts Using  $t\text{-BuOOH}$  in Toluene at  $25^{\circ}\text{C}$

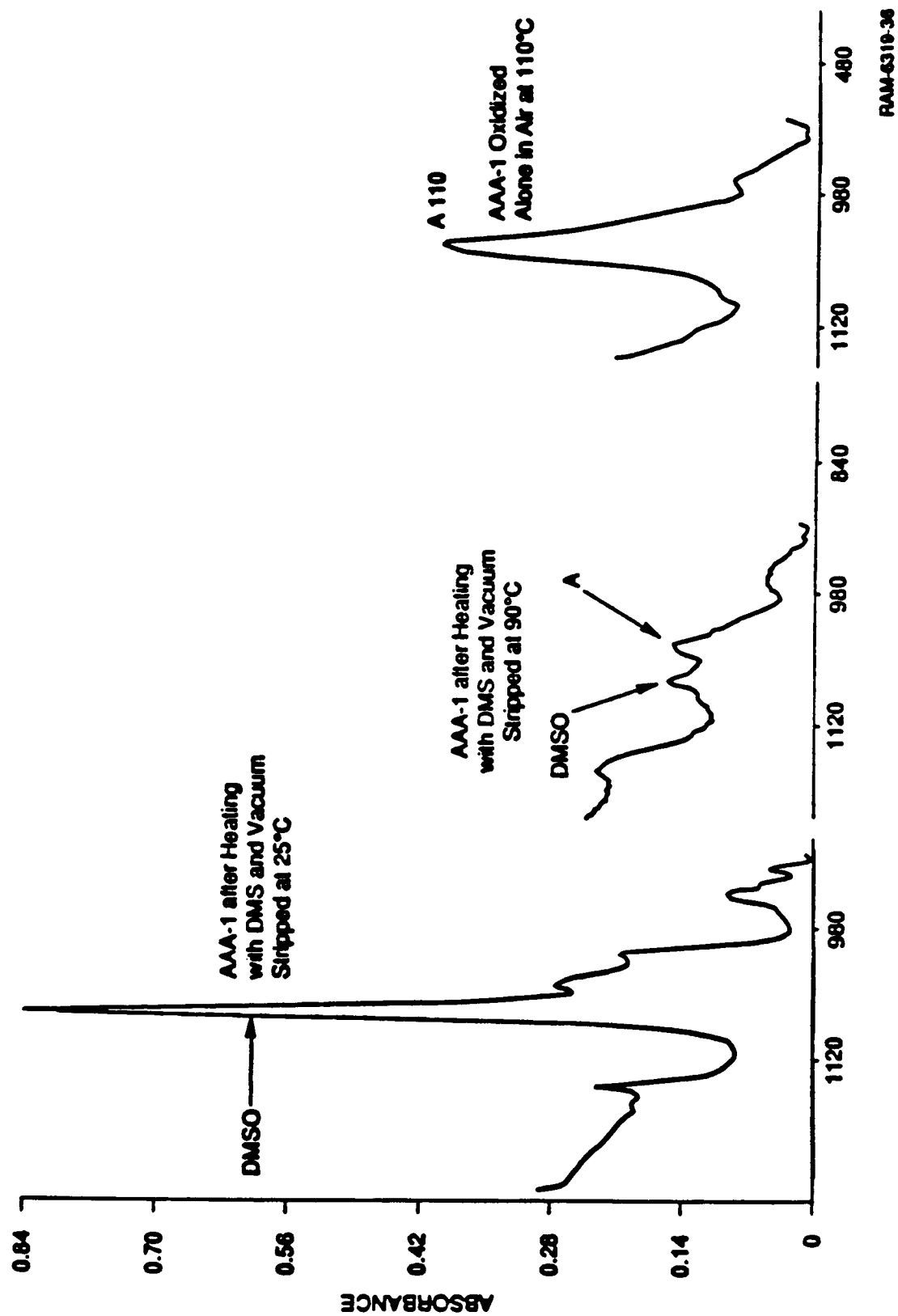
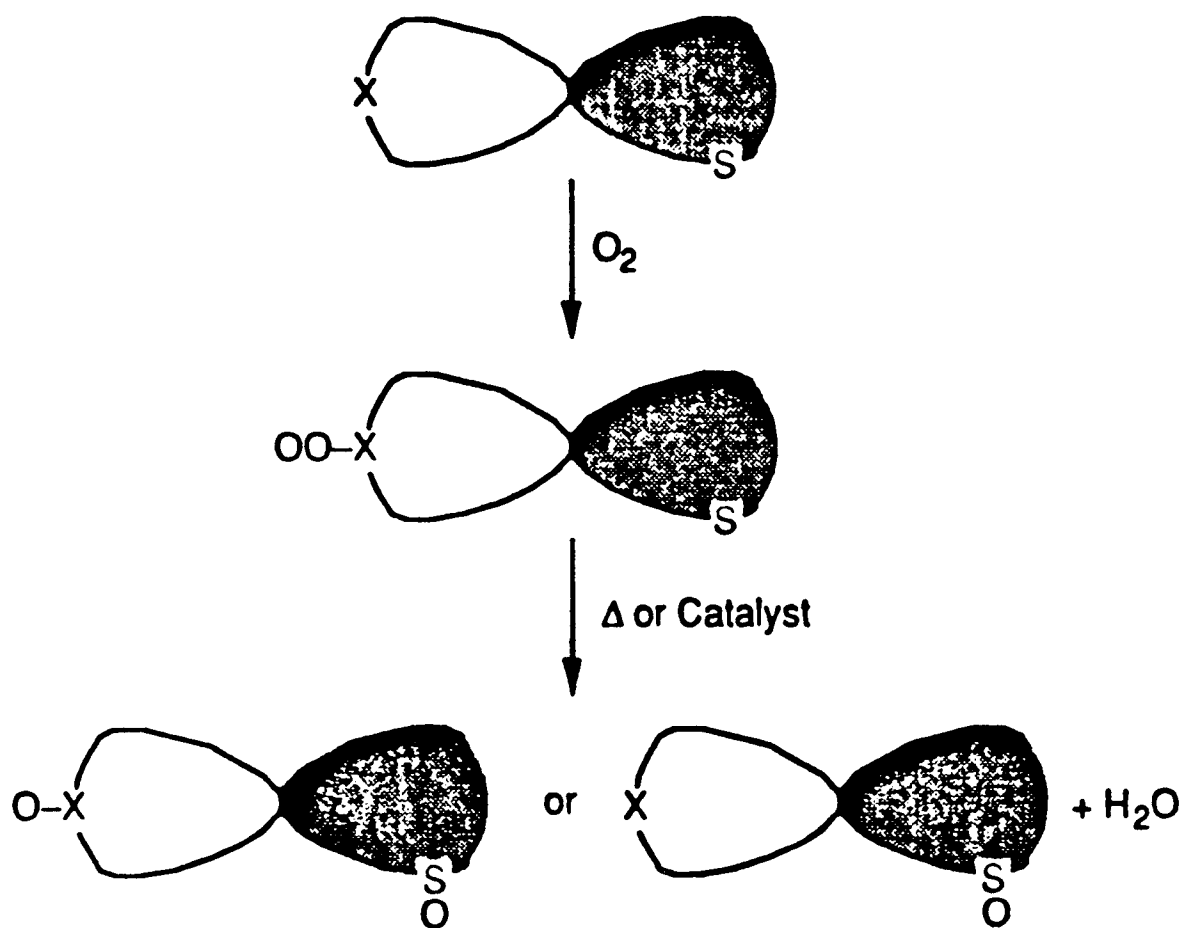


Figure 7.7 Cooxidation of AAA-1 with Dimethyl Sulfide at 110°C, 48 Hours



**Figure 7.8** Possible Pathways for Sulfoxide Formation

**Table 7.1 Concentrations of Phenols in Core Asphalts by Several Methods and Comparison with Asphaltene Content**

Asphalt	MP <sup>a</sup> , mM	NMR <sup>b</sup> , mM	[Inh, CuH] <sup>a</sup> , mM	HA <sup>c</sup> , %
AAA-1	200	55	53	16
AAB-1	43	19	57	17
AAC-1	-	200	55	-
AAD-1	100	68	73	20
AAF-1	-	270	100	-
AAG-1	56	120	92	5
AAK-1	75	120	60	19
AAM-1	72	30	60	4

<sup>a</sup> SRI results.

<sup>b</sup> From P. W. Jennings, Montana State Univ.

<sup>c</sup> From WRI, June Quarterly Report

**Table 7.2 Concentrations of Phenols in Modified Asphalts**

Asphalt	[Inh, CuH], mM
AAA-1 permethyl <sup>a</sup>	0
AAA-1 maltene <sup>b</sup>	41
AAB-1 maltene <sup>b</sup>	36
AAD-1 permethyl <sup>a</sup>	0
AAG-1 oxidized	100
AAK-1 -vanadium enrich <sup>c</sup>	7-19

<sup>a</sup> From P.W.Jennings.

<sup>b</sup> Heptane soluble fraction; from J. Branthaver and J.C. Petersen, WRI.

<sup>c</sup> From weak base fraction.



**Table 7.3 Comparison of Sulfur Contents of Core Asphalts and Sulfoxide Contents in Core Asphalts Oxidized by a Chemical and Two Thermal Methods.**

Asphalt	S, M	(ROOH) <sup>a</sup>	TTA <sup>b</sup>	TFAAT <sup>c</sup>
AAA-1	1.8	0.50	0.29	0.24
AAB-1	1.50	0.31	0.31	0.28
AAC-1	0.6	0.15	0.18	0.14
AAD-1	2.2	0.78	0.31	0.36
AAF-1	1.1	0.23	0.23	0.20
AAG-1	0.41	0.14	0.16	0.16
AAK-1	2.0	0.52	0.35	0.30
AAM-1	0.37	0.05	0.09	0.06

<sup>a</sup> Oxidized with t-BuOOH at 25 °C

<sup>b</sup> Heated at 110 °C for 3 days in air (SRI data)

<sup>c</sup> Heated at 113 °C for 72 hr in air (WRI data)

**Table 7.4 Analysis of Sulfur X-Ray Spectroscopy (XANES) and X-Ray Photoelectron Spectroscopy (ESCA) Spectra of Asphalt Samples<sup>ab</sup>**

Sample	%Sulfide(M)	(DS) <sup>c</sup>	%Thiophene	>SO Sulfoxide	(D>SO) <sup>d</sup>	% S (M)
AAA-1	40[34] <sup>e</sup>	-	60 (66) <sup>e</sup>	-	-	7.3 (2.3)
AAA-1 oxid <sup>f</sup>	27[24] <sup>e</sup>	13	67	6	-7	7.3
AAB-1	31	-	69	-	-	5.6 (1.75)
AAC-1	25	-	75	-	-	2.7 (0.84)
AAD-1	46 (1.2)	-	54	-	-	8.6 (2.7)
AAF-1	28	-	72	-	-	3.5 (1.1)
AAG-1	33 (0.14)	-	59	8	-	1.3 (0.41)
AAG-1 oxid <sup>f</sup>	15	18	60	25	-1	1.3
AAK-1	36 (0.76)	-	64	-	-	6.6 (2.1)
AAK-1 oxid <sup>f</sup>	31	5	62	7	+2	6.6
AAM-1	17 (0.065)	-	78	5	-	1.2 (0.38)
Asph-X						
(AAA-1 oxid) <sup>g</sup>	10	30	63	27	-3	7.3
Asph-Y						
(AAG-1 oxid) <sup>g</sup>	0	33	53	17	+23	1.3

<sup>a</sup> Data from G. P. Huffman et al., Univ. Kentucky.

<sup>b</sup> Samples from WRI except X and Y from SRI.

<sup>c</sup> Change in sulfide.

<sup>d</sup> Difference between DS and >SO.

<sup>e</sup> ESCA spectra taken at SRI.

<sup>f</sup> Oxidized by heating at 113 °C for 120 hr.

<sup>g</sup> Oxidized with t-BuOOH in cyclohexane at 25°C.

**Table 7.5 Thermal Changes in Sulfoxide and Carbonyl in Preoxidized Asphalts in Argon at 165°C**

Asphalts ( $\geq$ SO M)	Times, hr	% Change >SO	% Change >CO
DRSO (0.29 M)	5	-58	-
AAD	7	-38	-
AAGT (0.19 M)	5	-7	+44
AAGT (0.19 M)	10	-7	+60
AAK-1 (0.37 M)	5	-48	+12
AAK-1 (0.37 M)	10	-54	+7

**Table 7.6 Oxidation of AAD-1 and AADT<sup>a</sup>**

Sample	Times, hr	Wt Sample (mg)	Products, $\mu$ moles				$10^3$ Oxid Rate $\mu$ mol/mg hr
			$\Delta O_2$	>SO	>CO (M)	%OB <sup>b</sup>	
AAD-1	10	75	9.6	5.6	1.3	35	13
AAD-1	20	82	12	7.1	1.7	36	7.3
AAD-1	114	79	38	13	4.1	23	4.2
AADT	10	74	7 (5)	5.5	1.2	26	9.4
AADT	20	80	12	7	1.3	34	7.5
AADT	114	79	13	6.4	1.1	29	1.4
AADT	234	87	55	25	11	32	2.7
AADT	409	100	105	37	7	22	2.6

<sup>a</sup> Oxidized in air as thin films at 100°C

<sup>b</sup> OB = oxygen balance =  $[(>SO + >CO) / 2\Delta O_2] \times 100$ .

**Table 7.7 Oxidation of AAG-1 and AAGT<sup>a</sup>**

Sample	Times, hr	Wt Sample (mg)	Products, $\mu$ moles				$10^3$ Oxid Rate $\mu$ mol/mg hr
			$\Delta O_2$	>SO	>CO (M)	%OB <sup>b</sup>	
AAG-1	10	139	14	13			10
AAG-1	30	111	21	7.5			6.3
AAG-1	30	113	14	13			4.2
AAG-1	30	135	-	14			-
AAGT	10	127	11	7.9			8.7
AAGT	30	131	21	11			5.3
AAGT	30 <sup>c</sup>	160	23	8.9			4.8
AAGT	30	107	-	8.7			-
AAGT	140	184	61	34	24	48	2.3

<sup>a</sup> Oxidized in air as thin films at 100°C

<sup>b</sup> OB = oxygen balance =  $[(>SO + >CO) / 2\Delta O_2] \times 100$ .

<sup>c</sup> Small lump, not a film

**Table 7.8 Oxidation of AAK-1 and AAKT<sup>a</sup>**

Sample	Times, hr	Wt Sample (mg)	Products, $\mu$ moles				$10^3$ Oxid Rate $\mu$ mol/mg hr
			$\Delta O_2$	>SO	>CO (M)	%OB <sup>b</sup>	
AAK-1	7	89	7	7.2	0.8	57	11
AAK-1	14	82	9	8.0	0.9	49	7.8
AAK-1	24	86	7	13	1.0	100	3.4
AAKT	7	80	5	1.3	0	9	8.9
AAKT	14	117	14	5.1	0.7	20	8.5
AAKT	24	85	13	6.4	1.1	28	6.4
AAKT	140	392	79	141	32	108	2.5

<sup>a</sup> Oxidized in air as thin films at 100°C

<sup>b</sup> OB = oxygen balance =  $[(>SO + >CO) / 2\Delta O_2] \times 100$ .

<sup>c</sup> Small lump, not a film.

**Table 7.9 Long Term Oxidation of Asphalts<sup>a</sup>**

Sample	Times, hr	Wt Sample (mg)	Products, $\mu$ moles				$10^3$ Oxid Rate $\mu$ mol/mg hr
			$\Delta O_2$	>SO	>CO (M)	%OB <sup>b</sup>	
AADT	234	87	55	25	11	32	2.7
AADT	409	100	105	37	7	22	2.5
AAGT	140	184	61	34	12	38	2.3
AAKT	140	392	79	141	32	108	1.5

<sup>a</sup> Oxidized in air as thin films at 100°C

<sup>b</sup> OB = oxygen balance =  $[(>SO + >CO) / 2\Delta O_2] \times 100$ .

**Table 7.10 Oxidation of AAM-1 and AAMT<sup>a</sup>**

Sample	Times, hr	Wt Sample (mg)	Products, $\mu$ moles				$10^3$ Oxid Rate $\mu$ mol/mg hr
			$\Delta O_2$	>SO	>CO (M)	%OB <sup>b</sup>	
AAM-1	30	304	198	25	-	-	22
AAM-1	120	276	172	28	-	-	5.2
AAMT	30	316	34	28	88	170	3.6
AAMT	120	290	83	26	44	42	2.4

<sup>a</sup> Oxidized in air as thin films at 100°C

<sup>b</sup> OB = oxygen balance =  $[(>SO + >CO) / 2\Delta O_2] \times 100$ .

## 8

# Aging Studies of Asphalt

### Introduction

Oxidation of asphalt in asphaltic pavements is a reaction that begins during the hot-mix process and continues throughout the lifetime of the pavement. The role of oxidation in the performance of asphaltic pavements is important because it results in stiffening or hardening of the binder. Some of the first work on prediction of asphalt oxidation and/or aging involved extrapolation of results obtained from the thin-film oven (TFO) test (ASTM D 1754). The TFO test simulates the chemical and physical property changes in asphalt binders during mix-plant operations (Lewis and Welborn 1940), but it is not a good predictor of long-term durability (Pauls and Welborn 1952; Schmidt and Santucci 1969; Schmidt 1973). The TFO test is conducted in an oven in which an open pan containing a sample of asphalt is heated for 5 hours at hot-mix temperature ( $163^{\circ}\text{C}/325^{\circ}\text{F}$ ). The result of this treatment is a combination of loss of volatiles in addition to some oxidation. The rolling thin-film oven (RTFO) test (ASTM D 2872) also simulates mix-plant conditions and is used mainly in California. In this test, asphalt samples are weighed into special bottles and placed into a rotating rack in an oven at hot-mix temperature for 85 minutes. A fresh surface of asphalt is continually exposed to air by the rotation of the rack, which accelerates oxidation and volatile loss. Two drawbacks to the RTFO test are the large film thickness of asphalt and the high temperature of the test relative to pavement temperature.

It became apparent that when used for extended times the high temperature of the TFO and RTFO tests caused excessive loss of volatiles and that the tests were unrealistic for predicting pavement aging at lower temperatures. Consequently, the California Highway Department investigated several modifications of the RTFO test. One modification was to lower the temperature to  $113^{\circ}\text{C}$  ( $235^{\circ}\text{F}$ ) and age the asphalt for 7 days. This test is referred to as the extended RTFO test (Kemp and Predoehl 1981). It was also apparent that the film thickness in the TFO and RTFO tests was unrealistically large. Therefore, another modification was developed in which 0.5 g of asphalt dissolved in a solvent was added to an RTFO bottle to produce a  $20\mu\text{m}$ -thick asphalt film after solvent removal. The test temperature was reduced to  $98.9^{\circ}\text{C}$  ( $210^{\circ}\text{F}$ ), but because the loss of volatiles was still excessive, Schmidt (1973) restricted the bottle opening using a cork pierced by a capillary to mimic the levels of oxidation and volatile loss that actually occur during pavement aging. This modification of the RTFO test is known as the RMF-C test. Schmidt (1973) compared results from asphalts aged by the RMF-C test with results from field aging for various

California road tests and found fairly good correlations. A limitation of the RMF-C test is the small amount of aged sample (0.5 g) available for additional testing.

Petersen (1989) modified the RMF-C test to provide enough sample (4 g) for subsequent chemical and physical property characterizations. This test, known as the thin-film accelerated-aging test (TFAAT), is also run in a standard RTFO oven using an RTFO bottle with a capillary in the cork covering the bottle mouth, as in the RMF-C test. The test temperature is 113°C (235°F). Petersen (1989) suggested that asphalts aged using the TFAAT exhibit property changes comparable to about 5-10 years of pavement aging, with the caveat that construction and uncontrollable environmental conditions may affect the correlation between laboratory and field results. A principal objective of SHRP research was to develop a laboratory aging test that more closely simulated or predicted pavement aging than tests developed in the past.

## **Changes in Asphalts Caused by Oxidation**

The major products of asphalt oxidation resulting from oxygen incorporation are carbonyl and sulfoxide chemical functionalities. The carbonyl functionalities consist mainly of ketones, with much smaller amounts of carboxylic acids and carboxylic acid anhydrides. Structures of these compounds are illustrated in figure 9.1 (chapter 9). The ketones produced in asphalt during oxidation result largely from the oxidation of benzylic carbon atoms in the asphalt molecules, because benzylic positions are highly sensitive to air oxidation. Benzylic positions are abundant in asphalts because of the presence of large numbers of aromatic species having aliphatic side chains. Aromatization and chain scission reactions may also occur during oxidation, but do not result in oxygen incorporation.

At temperatures below about 130°C (266°F), oxidation of asphalt molecules tends to increase their polarity because more oxygen is retained in the molecules as ketones, sulfoxides, and possibly other oxygen-containing functionalities. The stiffening of an asphalt oxidized below 130°C (266°F) compared with the original asphalt therefore results from increased molecular association caused by the increased amount of polar functional groups formed. The degree of stiffening that occurs is thus a result of the total associating polarity formed in the asphalt, the strength of the associations of the polar molecules, and the dispersing power of the nonassociating components. An asphalt may exhibit a large amount of oxidation as measured by increases in oxygen-containing products, but the oxidized species may form rather weak polar associations. The nonassociating components may be very effective in dispersing polar species, resulting in a highly oxidized asphalt that does not show a large change in stiffness. Conversely, an asphalt may undergo a rather small amount of oxidation as measured by increases in oxygen-containing products, but the additional oxidized species might increase the strength and amount of the polar associations because of the poor dispersing power of the nonassociating components. This would result in an asphalt that does not oxidize to a large degree but exhibits a large increase in stiffness. Obviously, the large number of possible combinations of these important factors gives rise to the spectrum of oxidation-related differences observed in properties of petroleum asphalts used for asphalt paving purposes.

Ketones and sulfoxides, the two dominant oxidation products formed in petroleum asphalts, are weak bases. When the ion exchange chromatography (IEC) procedure developed to obtain the amphoteric fraction of asphalts is applied to aged asphalts, there is an observed increase in the amount of the base fraction and the amphoteric fraction compared with parent asphalts for four of the core asphalts tested (chapter 1). The relationship of the increase in the amphoteric fraction to increased stiffness can be rationalized as follows. Oxidation often converts monofunctional molecules to polyfunctional molecules. Molecules with the ability to form polar associations at two or more different sites on the same molecule can engage in more extensive and possibly three-dimensional interactions compared with molecules that have only one site of possible polar interaction. Some polyacidic or polybasic molecules also may form during oxidation, and these products might also engage in three-dimensional structuring. As stated above, other factors such as component compatibility are also involved that affect the degree of stiffening.

Since oxidation of asphalts results in an increased amphoteric fraction, which in turn leads to increased stiffness because of more polar interactions, the increased polar associations should be detectable using size exclusion chromatography (SEC). This technique separates molecules according to molecular size (chapter 2), and experimental conditions can be designed to minimally disrupt the polar associations in asphalt. Therefore, the associated species may be separated from the nonassociated components of asphalts based on their larger apparent molecular size. When SEC is performed on the oxidized asphalts, an increase in the SEC Fraction I (associated materials) compared with parent asphalts is in fact observed. This is strong evidence that increased polar associations caused by oxidation increase the stiffness of asphalts.

The temperature of the asphalt oxidation reaction is an important factor. An increase in temperature can affect both the rate of formation of oxidized species and the nature of the oxidized species formed, as previously described. Rheological measurements of asphalts at different temperatures indicate that increasing temperature increasingly disrupts the polar molecular associations. Therefore, higher temperatures disrupt the microstructures formed by associations, allowing molecules to react with oxygen that would not do so at lower temperatures because of incorporation in polar associations.

## **Factors Involved in Designing Aging Tests**

Simulation in the laboratory of asphalt oxidative aging in the field involves compressing many years of time into just a few hours or days. It has been established that the TFOT (ASTM D 1754) approximates the oxidative aging that occurs during the hot-mix process, but not the much greater amount that occurs during many years of service. To be practical, an aging test must be completed in a timely manner and provide accurate, reproducible measurements of changes in selected binder properties that approximate changes in the same properties during several years of service.

Four approaches can be used to design such an aging test. An aging test can be accelerated by using temperatures higher than pavement service temperatures, at pressures greater than ambient pressure, at reduced film thickness, or with the addition of chemical accelerants.



All of these methods pose difficulties in test development. Increased-temperature aging tests offer the advantage of requiring comparatively simple equipment. However, as previously discussed, if the temperature is raised too high, the kinetics of oxidative hardening may be quite different from the kinetics observed at pavement service temperatures. Test methods using increased oxygen partial pressure and lower temperatures involve the use of high-pressure equipment that is not commonly found in most highway department laboratories. There are also perceived hazards associated with high-pressure experiments. Chemical accelerants may change the mechanism(s) of oxidation of asphalts. Tests using small samples of asphalts in very thin films often do not produce enough sample for physical testing. Accelerating oxidative aging for laboratory or predictive use always involves a tradeoff in potential detrimental effects caused by the particular technique employed.

Considerable prior data in the literature and prior work at Western Research Institute (WRI) suggest that temperature sensitive physical factors strongly influence the rate of asphalt oxidation. The data indicate that when asphalts oxidize (age) at the lower temperatures near pavement service temperatures, many of the more inherently chemically reactive molecular species (polar aromatics and asphaltenes) are more tightly bound in microstructure formation. The molecular immobilization caused by these polar associations greatly reduces their reactivity with oxygen.

A classic example of the reduction of oxidation from molecular immobilization comes from polymer chemistry. Isotactic polypropylene is a solid plastic at ambient temperature and consists of a mixture of crystallized and uncrystallized polymer. If this polymer is oxidized at ambient temperatures, further analysis shows that the solid polypropylene molecules that were immobilized in the crystalline structure remain virtually unoxidized, while the polypropylene molecules of similar chemical composition in the amorphous, more mobile region eventually oxidize sufficiently to free the crystallites because of oxidative chain scission in the amorphous region. In another example of the effect of molecular immobilization on chemical reactivity, Kowanko, Branthaver, and Sugihara (1978) treated heavy crude oils with elemental fluorine at room temperature and did not observe particularly vigorous reactions. Fluorine is much more reactive than oxygen, and crude oils contain molecules inherently reactive with fluorine. Crude oils dissolved in a solvent of alkanes were found to be more reactive than were the raw crudes. These results suggest that molecular association of the potential reactive polar, aromatic components in the crudes is inactivated by association in the raw crude.

If the above model of the effect of molecular association and microstructuring on asphalt oxidative aging kinetics is correct, then it follows as a pragmatic consequence that the commonly used high-temperature aging tests, in which oxidation is relatively uninhibited by molecular association, may not mimic what happens in many asphalts during low-temperature pavement aging in which increasing molecular association may significantly reduce the rate of oxidation as the oxidation proceeds. One of the major objectives of the Binder Characterization and Evaluation Program was to develop a realistic laboratory asphalt aging test that would mimic as closely as possible the chemical changes and age-hardening kinetics that exist during pavement aging.

## Chemistry and Kinetics of Asphalt Oxidative Age Hardening

A literature review strongly suggested that a test to reliably simulate pavement aging in the laboratory should be conducted near pavement temperatures. Modification of a test procedure developed by Lee (1968, 1972, 1973) appeared to offer such a test method. The slowing of the rates of reaction caused by lowering the temperature to a realistic value is offset in Lee's method by increasing the oxygen pressure. Lee conducted his test at 65.6°C (150°F); however, the temperature of 60°C (140°F) was chosen for initial investigations in the Binder Characterization and Evaluation Program because this is the temperature at which numerous physical properties of asphalt have been evaluated in the past. This allowed oxidative aging to be conducted and physical property measurements to be made at the same temperature. It also provided the opportunity to compare new physical property data obtained in the SHRP program with physical property data in the literature obtained at this same temperature. The temperature of 60°C (140°F) is also in the pavement temperature range. To increase the oxidation reaction rate at lower temperatures, Lee used pure oxygen instead of air. Oxygen also was chosen in the initial work of the Binder Characterization and Evaluation Program.

Before being aged in a pressure vessel, some asphalt samples were first aged using the familiar TFOT (ASTM D 1754) to simulate changes that occur in a hot mix plant. The TFO test was followed by pressure oxygen vessel (POV) aging using 300 psi ( $2.07 \times 10^6$  Pa) pressure of oxygen at a temperature of 60°C (140°F). Under these conditions the pressure (concentration) of the reactant, oxygen, is increased about 100-fold over its pressure in ambient air at standard conditions. In those experiments in which pressure vessel aging using oxygen is preceded by a TFO treatment, the whole procedure is referred to as the TFO-POV procedure. To summarize, the advantages of the TFO-POV procedure are that (1) a relatively large quantity of asphalt (50 g) spread as a thick film (1/8 in. [3.175 mm]) can be oxidized in a single run, (2) the procedure is performed in the pavement service temperature range, and (3) no solvent is used that may adversely affect physical property measurements.

Lee's data and early reconnaissance experiments in the SHRP program suggested the possibility that on a molecular level there may be significant physical effects on the kinetics of low temperature oxidative aging. It was noted that the kinetic plots of changes in viscosity during low temperature oxidation were not readily explained by the inherent chemical reactivity of the asphalt molecules alone. It has been well documented that (1) the polar components of asphalt (largely the asphaltene and polar aromatic fractions) are the components that are the most chemically reactive with oxygen, and (2) these polar components are also those components that participate in molecular association leading to the formation of a microstructure. Molecular association should reduce the mobility of the most chemically reactive molecules, thus reducing their ability to react with oxygen. Because the equilibrium between the associated and unassociated molecules shifts toward increased dissociation with increasing temperatures, it follows that increasing the temperature of oxidative aging should lead to an increase in the "effective" concentration of the most reactive species by converting them from a more immobile, associated state to a more mobile and reactive dissociated state.

The oxidation of asphaltenes at low and high temperatures is a classic example of the molecular immobilization phenomenon. When a powdered asphaltene sample is aged as a dry powder at ambient temperature, it is virtually inert to oxidation. However, when asphaltenes are oxidized above their softening point as a thin film at 130°C (266°F) for 24 hours, they are the most chemically reactive fraction in asphalt, producing more than 1.8 mol/L ketones (Petersen, Barbour, and Dorrence 1974).

In the early phases of the Binder Characterization and Evaluation Program, the core asphalts were pressure oxidized using the POV method with and without prior TFO aging. In these experiments, a series of TFO pans containing the asphalt were oxidized as a function of time at 60°C (140°F) and at 300 psi ( $2.07 \times 10^6$  Pa) oxygen pressure for up to 1,000 hours. An example of the change in viscosity during POV aging with and without TFO aging is plotted in figure 8.1 from kinetic data in table 8.1. In this example using core asphalt AAD-1, the samples were annealed at 110°C (230°F) for 1 hour followed by a resting period of 2 days at room temperature prior to making viscosity measurements. This standard annealing procedure was used to minimize the known effects of time-dependent structuring on the reproducibility of the rheological measurements.

Parenthetically, results of the TFO test alone on asphalt AAD-1 and the remaining seven core asphalts are reported in supplementary table 8.37. These results show that the asphalts undergo moderate age hardening during the TFO test as measured by the aging index. The aging index is the ratio of viscosity after aging divided by the viscosity of the unaged asphalt. The viscosity increase upon TFO aging is known to result from both volatile loss and oxidation. The relative amount that each factor contributes to the total hardening is dependent on the volatility and reactivity of the asphalts.

Three observations can be made about the plots in figure 8.1. First, the plots are parabolic in form. Second, examination of the kinetic data shows that the rate of viscosity increased very rapidly during the first 100 hours, then decreased rapidly during the next 100 hours or so, and finally reached a "steady state" rate of increase for the remainder of the 1,000 hours. Third, the viscosity-time plots are virtually identical but are displaced from each other by the amount of viscosity change during the TFO test. The significance of these results will be discussed later.

During evaluation of the AAD-1 kinetic experiment, the hypothesis was suggested that during the course of the oxidation reaction additional molecular structuring might be taking place from the reaction of polar molecules with oxygen and their subsequent immobilization. This molecular immobilization would then reduce the reactivity of these polar molecules with oxygen. It was reasoned that such a sequence of events might contribute to the rapid decrease in the rate of viscosity rise as shown by the hump in the plot that occurs between 100 and 200 hours of aging, just prior to the plateau region of the plot.

To test this hypothesis, asphalts with 400 hours of POV aging were removed from the POV and treated at 110°C (230°F) to "break up" association of polar, reactive molecules. The thermal treatment was followed by a rapid cooling of the samples to room temperatures to "freeze" the asphalt matrix in a dissociated, metastable state. The thermally treated,

"quenched" asphalts were reintroduced into the POV for a second series of oxidations up to an additional 400 hours. Kinetic data for the experiment are reported in tables 8.1 and 8.2 and plotted in figures 8.2 and 8.3.

The figures show that the thermal treatment of the 400-hour samples did indeed increase their rate of reactivity for the first 200 hours, as indicated by the plot. These results suggest that associated, reactive components were made available for reaction by the thermal treatment.

Another hypothesis may explain why the kinetic curve of the thermally treated asphalt converged with the curve of the nontreated asphalt after the additional 400 hours of POV aging. Because only the physical state (morphology) of the asphalt, and not its chemical composition, was altered by the thermal treatment, it follows that the additional oxidation produced in the thermally treated asphalt (compared with the nontreated asphalt) during the initial stages of the second 400 hours of POV aging should give the thermally treated asphalt additional polar "quenching" power as the restructuring moves toward a new thermal equilibrium. That this appears to be happening is seen by comparing the plots of the thermally treated and nontreated asphalts. These plots converge to virtually the same viscosity at the end of the second 400-hour POV aging period. Although the effect of the thermal treatment was not large, it appears real because of the fit of the data. The data are not scattered and hence are statistically significant. Further, if it is assumed that the production of polar oxidation products is the primary factor responsible for viscosity increase on oxidation (this will be shown later to be true), and that polar oxidation products reduce the asphalt chemical reactivity through molecular association, then it follows that the thermally treated and nontreated asphalts should eventually reach the same level of oxidation and viscosity.

Additional data give support to the above hypothesis. Data in table 8.3 show the ability of thermal treatment to disrupt molecular association in asphalt AAD-1. Both the TFO-treated and the non-TFO-treated asphalt showed a significant reduction in viscosity by raising the temperature from 70°C (158°F) to 110°C (230°F). Also, the value of  $\tan \delta$  ( $G''/G'$ ) was increased from 6.8 to 10.9 and from 4.6 to 5.9 for the non-TFO-treated and the TFO-treated asphalts, respectively. This is direct evidence of the breaking up of molecular association since the shear storage (elastic) modulus decreased at a faster rate than the shear loss (viscous) modulus on thermal treatment. It has been demonstrated in many prior "steric hardening" and "mixture setting" studies that asphalt, once thermally dissociated, usually takes days to reassociate and approach its viscosity before the thermal treatment. Because the time-dependent association, or structuring process, is an exponential function of viscosity with respect to time, the major portion of the viscosity recovery typically occurs during the first day or so at ambient temperatures. If one accepts the hypothesis that thermal treatment mobilizes reactive asphalt molecules, making them more reactive with oxygen, and that subsequent "quenching" of the oxidation reaction results from association of reactive molecules containing the oxidation products, then the phenomenon demonstrated in figures 8.2 and 8.3 for the second 400 hours of POV aging does not seem sufficient to account for the initial large increase in viscosity followed by the rapid decrease in rate of viscosity rise during the first 200 hours of aging.

To help assess the effects of chemical changes on the kinetics of the oxidation reaction, the major chemical functionalities formed on oxidation (ketones and sulfoxides) were monitored using quantitative IR spectra obtained using carbon disulfide ( $\text{CS}_2$ ) solutions of the asphalts. The relative concentration of ketones was measured using the intensity of their IR absorption peak at about  $1700\text{ cm}^{-1}$ . It has been demonstrated by past research that ketones account for more than 95% of the increase in this band on oxidation. The remaining trace amounts of nonketone carbonyl are accounted for by small amounts of dicarboxylic anhydrides and carboxylic acids produced. The  $1700\text{ cm}^{-1}$  peak height, rather than peak area as used in the functional group analysis (FGA) was used to determine ketones because of its greater precision. Relative peak heights are adequate to display kinetic data and can be converted to concentration in mol/L using a nomograph (Volume IV, chapter 6). Also, determination of peak height is much more rapid. Sulfoxide concentrations were determined by measuring the area of the IR band at about  $1030\text{ cm}^{-1}$ .

Changes in the ketone and sulfoxide concentrations for asphalt AAD-1 during the POV aging experiment described above are represented by the data in table 8.4. These data are further supplemented by the data in table 8.5, which presents kinetic data obtained on asphalt AAD-1 in separate kinetic experiments. It can be seen that the chemical and physical property data collected at the nominal  $60^\circ\text{C}$  ( $140^\circ\text{F}$ ) temperature have only slightly lower values than those for the  $70^\circ\text{C}$  ( $158^\circ\text{F}$ ) data. This discrepancy undoubtedly reflects incorrect temperature setting for the experiments; however, the fit of the kinetic data are good, indicating good control of the temperatures during the experiments. The data are thus valid for this application.

Further examination of the data in tables 8.4 and 8.5 shows that the concentration of measured oxidation products formed in both the original (no prior TFO) samples and the prior TFO samples are virtually the same at the same POV aging condition. This is true even though their viscosity kinetic plots are displaced by the amount of the TFO viscosity increase on aging. Unlike the earlier experiment, where the kinetic curve was disrupted by a reversible thermal treatment and returned to the same curve as the untreated sample on further aging, the TFO-displaced kinetic curve always remains at a higher viscosity level than the curve for the sample not receiving prior TFO treatment. It is proposed that this displacement is a result of irreversible compositional changes in the asphalt sample. These irreversible changes result from both oxidation and volatile loss; usually it is largely volatile loss.

The mass and viscosity changes upon TFO aging are cited for the core asphalts in table 8.6 and displayed in figure 8.4. In figure 8.4, the mass change on TFO testing is displayed vs. the log viscosity increase during the testing. At zero mass change, the mass decrease from volatile loss exactly offsets the mass gain from oxygen incorporation on oxidation. The zero point for both mass and viscosity change is the point of origin for no oxidation or mass change. Lines to the right of the zero mass change point indicate that the effects of volatile loss were greater than the effects of oxidation on viscosity increase, and vice versa. It is apparent from the figure that, except for asphalt AAM-1, change attributed to volatile mass loss was greater than change attributed to oxidative mass increase. It is significant, however, that there was significant viscosity increase for asphalts AAM-1, AAB-1, and AAF-1 in which mass gain and mass loss nearly offset each other. This mass increase can

only come from oxidation, yet many examples of IR data indicate that the quantities of sulfoxides and ketones remaining in the asphalt after TFO aging are very low, much lower than the quantities necessary to account for the mass gains shown in figure 8.4. It is proposed that the significant increase in viscosity during TFO aging without significant mass change results from the formation of sulfoxides and their subsequent rapid thermal decomposition to form oxygen-containing sulfoxide decomposition products. Significant amounts of ketones are probably not formed from hydrocarbon moieties during TFO aging because the oxygen that is able to diffuse into the TFO sample is rapidly scavenged by the much more reactive sulfides in the asphalt to form the sulfoxides that subsequently decompose.

The above hypothesis regarding changes during TFO aging is not without precedent. It was shown in an earlier study of sulfoxide thermal decomposition kinetics (Petersen 1982) that a major portion of the sulfoxide in oxidized Boscan asphalt containing 0.42 mol/L sulfoxides was thermally decomposed during the first few hours of nonoxidative thermal treatment at the TFO test temperature of 163°C (325°F). Also, in a study of the kinetics of sulfoxide formation during air aging at 130°C (266°F) (Petersen et al. 1981), it was shown that the same overall concentration of sulfoxides was formed in a Boscan asphalt, whether or not the asphalt was spiked with 37% by weight of dibenzylsulfide, a readily oxidizable sulfide. Any oxidation of the dibenzylsulfide was correspondingly offset by the nonreaction of normally present sulfides that would have normally reacted in the asphalt. In the same study it was shown that for a group of six asphalts with sulfur contents ranging from 0.99% to 5.43%, the amount of sulfoxides formed during the standard 130°C (266°F) oxidation was nearly inversely proportional to the percentage of sulfur in the asphalt. These latter two observations strongly support the earlier proposal that during 163°C (325°F) TFO oxidation, any oxygen diffusing into the sample is rapidly scavenged by reaction with asphalt sulfides, and that the rate of sulfide oxidation is largely controlled by the rate of diffusion of oxygen into the asphalt.

It has previously been shown (Epps et al. 1986; Lau et al. 1992) that for a given asphalt, the concentration of ketones formed on oxidation correlates well with the log viscosity change. Such a plot was constructed in figure 8.5 from the carbonyl and viscosity data in tables 8.3, 8.4, and 8.5 for asphalt AAD-1. The scatter in the data are significant but are within the limits expected from the analytical techniques used at the time. Sufficient data points are present to define two distinct data plots with the same slope, displaced from each other by the amount of hardening that occurred during the TFO aging. These results again provide strong evidence that the TFO test produces irreversible compositional changes in the asphalt that increase viscosity. The oxidation chemistry and reaction kinetics remain the same for the prior TFO aged asphalt; the reactions just take place in a higher viscosity asphalt. The results also indicate that the viscosity change during low temperature oxidation is controlled primarily by the formation of oxidation products, and that this formation is relatively independent of the initial viscosity of the asphalt.

These results have significant pragmatic implications. They suggest that age hardening in asphalt that occurs in the mix plant (simulated by TFO aging) is added to the subsequent hardening that occurs in the pavement. Because the change in viscosity in the TFO test (and in the hot-mix plant) is influenced greatly by volatile loss, it would appear that there is

further reason to believe that volatile loss during pavement mixing could be detrimental to the subsequent aging characteristics of the pavement mixture.

Figure 8.6, based on the data in table 8.7, shows a plot of the dynamic shear viscosity vs. aging time for the eight SHRP core asphalts. The aging was conducted at 60°C (140°F) with 300 psi ( $2.07 \times 10^6$  Pa) oxygen, with and without prior TFO aging. It can be seen that the displacement of the zero time viscosity from the TFO aging varies considerably among the asphalts (e.g., AAK-1 and AAD-1 show large displacements, and AAM-1 shows a small displacement). The general shapes of their kinetic curves are quite similar.

Additional evidence that the oxidation kinetics are similar in asphalts before and after TFO aging is also shown by the data in table 8.7. Within the error of the experimental techniques, the final carbonyl and sulfoxide concentrations for each of the eight asphalts were virtually identical whether or not the asphalts had prior TFO aging. Again, this occurred even though the prior TFO-treated asphalts began and ended the aging period at a significantly higher viscosity. The data further support the proposal that the formation of oxidation products largely dominates the reaction kinetics.

Kinetic data for the eight core asphalts aged by the thin-film oven followed by the pressure air vessel (TFO-PAV) method at 60°C (140°F) and 300 psi ( $2.07 \times 10^6$  Pa) air are shown in table 8.8 and figure 8.7. Data for the expanded set of asphalts aged by the TFO-PAV method at 60°C (140°F) are shown in supplementary table 8.38. The precision of these data are better than that of the older POV data because of a modification made in the logistics of the pressure vessel aging procedure. Note that, as with the POV-aged asphalts, the PAV-aged asphalts show a significant increase in viscosity during the PAV aging, the magnitude of which is unique for each individual asphalt. Note also that the slope of the viscosity curves past the plateau region is less steep for the PAV-aged than the POV-aged asphalts. This undoubtedly occurs because the partial pressure of oxygen is more than five times greater in the POV than in the PAV, thus increasing the "steady state" rate of reaction.

In asphalt AAG-1, there is a striking difference between the slope of the viscosity curve during POV aging (figure 8.6) and the slope of the curve during PAV aging (figure 8.7) with respect to the behavior of the other asphalts. During PAV aging, the slope in the plateau region for AAG-1 is similar to the other asphalts; during POV aging, however, it has more nearly the same slope as during PAV aging while the other asphalts show an increase in slope. This is believed to be a result of AAG-1's much lower sensitivity to the oxidation products formed; this phenomenon will be discussed in detail later. Also of significance is that during PAV aging, the slope of the kinetic curve in the plateau region is virtually the same for all asphalts and is nearly linear. A possible explanation for this phenomenon is that the more highly reactive components of the asphalts have either reacted or have been immobilized by polar interactions, and that a slower hydrocarbon oxidation reaction that is very similar for all asphalts is occurring in the plateau region. If this is true, then generic hydrocarbon moieties in the less polar, dissociated fractions of the asphalts are quite similar.

The difference in the sensitivities of the different asphalts to viscosity increase from the formation of oxidation products is explicitly demonstrated in figures 8.8 and 8.9, which are plots of the data in table 8.8. In these figures the relative amounts of carbonyl compounds (primarily ketones) that are formed during TFO and subsequent PAV aging at 60°C (140°F) for aging times of 48, 96, 144, and 400 hours are plotted against viscosity increase. There is a good correlation between the viscosity increase on oxidative aging and ketone formation for each asphalt; however, each asphalt has its own sensitivity to the oxidation products formed, as indicated by the individually different slopes of their plots. Again, the data points for the asphalts having no prior TFO treatment do not fall on the line for the TFO-aged asphalts. As previously discussed, this is probably a result of composition changes that took place during the TFO test.

A model that rationalizes the data in figures 8.8 and 8.9 is as follows. On a molecular level, asphalt consists of a collection of molecules ranging from very nonpolar, nonassociated molecules to highly polar and strongly associated molecules. Components that constitute these two extremes are kept in a state of dispersion by molecules exhibiting a polarity gradient between these two extremes, thus creating a microgradient from weakly to strongly associated molecular agglomerates of unknown morphology. It is believed that the most strongly associated agglomerates, particularly those containing the highly aromatic molecules, assemble into more ordered or structured formations. The more strongly associated and structured component is commonly referred to as the dispersed moiety, and the weakly associated or unstructured component is referred to as the dispersing moiety. There are probably no discrete boundaries between moieties, but rather a continuum of materials having various degrees of interaction. For an asphalt like AAK-1 (figure 8.8), which possesses a rather high level of molecular association, the products formed on oxidation probably interact with larger, more associated species already present, thus having a large effect on viscosity increase. On the other hand, in asphalts like AAG-1 that are believed to be highly dispersed and initially possess little interacting microstructure, the oxidation products formed become well dispersed and have a lesser effect on viscosity increase.

The rates of ketone and sulfoxide formation during PAV aging at 60°C (140°F) are shown in figure 8.10 for five of the SHRP core asphalts. There is no apparent relationship between the relative amounts of ketones and sulfoxides formed in the asphalts. For example, asphalt AAD-1 and asphalt AAK-1 form ketones at the lowest rate and sulfoxides at the highest rate among the five asphalts.

Significant evidence has been presented thus far to suggest that the molecular association of polar components naturally present or formed on oxidation plays a major role in determining the aging characteristics of asphalt. Because it is well known that the degree of molecular association is highly sensitive to temperature, it becomes obvious that the kinetics of aging must be examined as a function of temperature. The importance of such an examination is underlined by the results of the field aging study of Kemp and Predoehl (1981) in which pavement mixtures were aged in four different California climates. Although the void content of a pavement mixture is well known to correlate with oxidative hardening, the California study showed that the tendency for the pavement mixtures to age harden was much more dependent on the climate temperature than on the void content. For



example, the recovered viscosity of a Santa Maria asphalt after 50 months of pavement mixture aging increased from about 3.3 to 6,000 kPa in the hot Indigo desert climate, while the recovered viscosity of the same asphalt aged for the same period in the cooler Fort Bragg coastal climate increased from only about 3.3 to 18 kPa. Thus it appears that an understanding of the kinetics of asphalt aging as a function of temperature is critical to the design of a realistic aging test.

To study in the laboratory a representative number of SHRP asphalts through a wide temperature range, a more rapid test and one more suited to higher temperatures than the POV method was needed. The TFAAT was therefore chosen to examine how temperature affected aging kinetics. Procedural information for the TFAAT method was briefly described in the introductory material of this chapter. It seemed desirable to obtain representative aging data through the temperature range of 60°C (140°F) to 130°C (266°F). To justify the use of the TFAAT aging method, kinetic data obtained at 65°C (149°F) using the method were compared with kinetic data from the POV and PAV methods at 60°C (140°F). The temperature of 65°C (149°F) rather than 60°C (140°F) was used for the TFAAT method because of equipment limitations. The POV and PAV aging data for asphalts AAD-1 and AAG-1 are shown in table 8.9 and the TFAAT aging data in table 8.10. The data for the PAV and POV oxidations were corrected for the incremental increase in viscosity during prior TFO aging so that the kinetics of PAV and POV could be graphed for comparison with data from the TFAAT method, which did not use asphalts with prior TFO aging. Data thus corrected are also shown in table 8.9.

In figure 8.11, kinetic data for POV and PAV aging at 60°C (140°F) and TFAAT aging at 65°C (149°F) are shown. Asphalts AAD-1 and AAG-1 were used for comparison because they represent compatibility extremes: Asphalt AAG-1 is highly dispersed with limited thermally reversible structuring, and asphalt AAD-1 possesses a rather high level of thermally reversible structuring. The kinetic data using the three methods are strikingly similar. Final viscosities for the POV-aged asphalts are higher than those for the PAV- and TFAAT-aged asphalts, undoubtedly because 100% oxygen rather than air was used in the POV method.

Kinetic data for the SHRP core asphalts aged by the TFAAT method at 85°C (185°F) for 400 hours are reported in table 8.11. Viscosity data for these asphalts are shown in figure 8.12. As expected, the TFAAT age hardening rate for asphalts AAD-1 and AAG-1 was greater at 85°C (185°F) than at 65°C (149°F). There is, however, a striking difference between the absolute levels of age hardening reached by the two asphalts at the two temperatures. Although both reached about the same level at 65°C (149°F), AAD-1 reached a significantly higher level at 85°C (185°F). A postulate was presented earlier while evaluating the PAV data at 60°C (figure 8.7) that the hydrocarbon oxidation chemistry appeared similar for all asphalts once the plateau region of the parabolic curve was reached. The difference in the viscosity kinetic plots of AAD-1 and AAG-1 at 85°C (185°F) suggests that additional reactive components were mobilized in asphalt AAD-1 from thermal disruption of molecular association.

The aging characteristics of the core asphalts at an even higher temperature of 113°C (235°F) are listed in table 8.12. The corresponding viscosity plots are shown in figure 8.13.

It is apparent that the asphalts rank differently at 113°C (235°F) (figure 8.13) than they do at 85°C (185°F) (figure 8.12). For example, the kinetic plots of AAC-1 and AAG-1 have exchanged places and AAC-1 has moved considerably higher than AAG-1. Note also that AAB-1, which was considerably below AAF-1 at 85°C (185°F), is considerably above AAF-1 at 113°C (235°F). Again, it is proposed that the disrupting of thermally reversible molecular association, which is different for each asphalt, is the primary factor responsible for this change in viscosity kinetic behavior as the temperature is increased. Finally, note the disparity between the ketones formed at 113°C (235°F) and 120 hours for asphalts AAD-1 and AAG-1 (table 8.12). Asphalt AAG-1 showed the lowest viscosity increase of all asphalts, and the viscosity increase of AAD-1 was next to largest. However, asphalt AAG-1 had the highest level of carbonyl oxidation products and AAD-1 the lowest.

The TFAAT aging data for the core asphalts at 130°C (266°F) are shown in table 8.13 and figure 8.14. At this temperature, it is noted that several of the asphalts achieve a higher viscosity after 36 hours than the corresponding asphalt aged at 113°C (266°F) for 120 hours.

Besides having pragmatic value for interpreting asphalt aging data and designing laboratory aging tests, the kinetic data as a function of temperature are very informative with regard to comparing the differences in component compatibility of the different asphalts.

While the kinetic data for TFAAT aging as a function of temperature are instructive, similar data using TFO-PAV aging would be highly desirable within the pavement temperature range, since the TFO-PAV aging procedure was chosen by SHRP for implementation. However, kinetic TFO-PAV data are only available at 60°C (140°F). Nonetheless, the TFO-PAV kinetic data obtained at 60°C (140°F) shown in table 8.8, together with single point data in tables 8.14 and 8.15 for aging at 70°C (158°F) and 80°C (176°F) after 144 hours, are sufficient to tentatively assess the PAV aging kinetics from 60°C (140°F) to 80°C (176°F). Data from the tables were used to construct the plots in figure 8.15.

Because the purpose of these plots is to estimate the kinetic data during PAV aging, the zero time point is taken after prior TFO aging. From comparison of complete PAV kinetic curves determined at 60°C (140°F) and with changes in the shape of the kinetic curves for TFAAT aging between 65°C (149°F) and 85°C (185°F), one can estimate the kinetic plots for the PAV aging at 70°C (158°F) and 80°C (185°F) using the respective zero and 144-hour time points for the PAV aging at these temperatures. This was done to construct figure 8.15. It is apparent from the examination of the plots that the change in the rate of viscosity increase with increasing temperatures is significantly greater for asphalt AAD-1 than AAG-1.

To visually examine the relative changes in viscosity with temperature for the core asphalts, PAV aging index data obtained after 144 hours are displayed in the plot in figure 8.16. The aging index data were calculated by dividing the viscosity of the asphalts at zero time after TFO aging into the viscosity reached after 144 hours of PAV aging (tables 8.14 and 8.15). Although the lines connecting the points for each asphalt do not constitute true kinetic plots, the data graphically illustrate the problem of attempting to assess the aging characteristics of an asphalt at one temperature from a single point determination obtained at a different temperature. Single point data at 70°C (158°F) and 80°C (176°F) using the

TFO-PAV method were also obtained for the expanded set of asphalts (supplementary tables 8.39 and 8.40, respectively) and support the preceding statement. Asphalt aging is a dynamic, time-dependent process. No single point determination can describe the entire aging process, which varies substantially among asphalts.

A plot comparable to figure 8.16 but including TFO aging in the aging index is shown in figure 8.17. It is apparent in the figure that asphalts AAD-1 and AAM-1 have exchanged places and asphalt AAK-1 is substantially higher compared with figure 8.16. Again, it is evident that a single point determination cannot describe the entire aging process among different asphalts, especially when two distinctly different processes like TFO and PAV are involved.

The 80°C (185°F) aging index values plotted in figures 8.16 and 8.17 are plotted vs. each other in figure 8.18. It is very evident by the scatter in the plot that there is no relationship between the aging index calculated including TFO and the aging index calculated excluding TFO. Note that the line drawn on the plot is a regression line of the data and not a line of equal aging for the two calculation methods. Asphalts AAK-1 and AAM-1 have about the same aging index at 80°C (185°F), 144 hours, when TFO is included, but are vastly different when TFO is excluded. Similarly, asphalts AAD-1 and AAM-1 have about the same aging index at 80°C (185°F), 144 hours, when TFO is excluded but are greatly different when TFO is included.

If the aging characteristics of the asphalts were evaluated based on their aging index at 60°C (140°F), a different evaluation would be obtained for several of the asphalts from aging index data at 80°C (176°F). For example, at 60°C (140°F) asphalt AAC-1 shows nearly the same age hardening as asphalt AAK-1. At 70°C (158°F) asphalt AAK-1 has a slightly greater aging index. At 80°C (176°F) the aging index of AAK-1 is significantly greater than that of AAC-1. This disparity becomes very great at 113°C (235°F) based on TFAAT aging for 120 hours. Although at 60°C (140°F) asphalt AAC-1 has about the same aging index as asphalt AAK-1, at 113°C (235°F), 120 hours, asphalt AAK-1 exhibits a viscosity increase nearly two orders of magnitude greater than AAC-1.

It can be concluded that for a single point predictive aging test, the further the aging test temperature is removed from the actual pavement aging temperature, the less reliable will be the ability of the test to predict aging characteristics. It is further evident that the rate of widening of this disparity grows increasingly greater with increasing temperature.

The data showing the changing aging characteristics as a function of temperature (figure 8.16) reveal important information about the molecular morphology (state of dispersion) of the different asphalts. Asphalts such as AAG-1 show nearly a linear relationship with temperature as a result of the high state of dispersion of the polar components and the ability of the asphalt to disperse the oxidation products formed. On the other hand, the increasing slope of the connecting lines with increasing temperature for such asphalts as AAK-1 and AAD-1 results from the effect of increased dispersion of polar components with increasing temperature. When analyzing the kinetic data, one should keep in mind that although the oxidation occurred at different temperatures, measurements of the rheological

properties of the oxidized asphalts were all made at 60°C (140°F) and reflect the morphological state of the asphalt at this temperature.

After examination of the kinetic data presented thus far in this chapter, it is apparent that the rate of measured viscosity increase is greater during the initial stages of oxidation and later levels off to form a parabolic curve in the pavement temperature range. The log of this viscosity change, for a given asphalt, was also shown to correlate well with the increase in carbonyl (ketone) concentration during oxidation. However, the change in sulfoxides does not show such a correlation with viscosity change. Examination of the data presented in the tables shows that at lower temperatures, higher levels of sulfoxides are formed and that at higher temperatures, the concentration of sulfoxides is generally lower for a given level of ketone formation and rapidly reaches a pseudo "steady state" that remains the same for the balance of the oxidation time. This steady state phenomenon has been shown (Petersen et al. 1981) to result from the net effect of the reaction of oxygen with the sulfur compounds in the asphalt to form sulfoxides (which is dependent upon the rate of diffusion of oxygen into the asphalt) and the subsequent thermal decomposition of the sulfoxides formed (which is dependent only on temperature).

Because the kinetics of the front end of the oxidation viscosity curve had not been examined in detail, a reconnaissance experiment was conducted by aging asphalt AAG-1 at 113°C (235°F) using the TFAAT method. Asphalt AAG-1 and the use of a relatively high temperature were chosen so that the physical effects of molecular association on the kinetics of the chemical reaction could be very nearly eliminated. Data for the experiment are shown in table 8.16 and figure 8.19. As seen in the figure, the measured concentration of sulfoxides increased very rapidly during the first 5 hours or so and then rapidly arrived at a steady state concentration thereafter. The ketone concentration also initially formed very rapidly and then tapered off after about 5 hours to a steady rate of formation with time.

Apparently, several factors largely control the shape of these concentration curves during the first few hours of oxidation. The asphalt probably contains small amounts of "hot" or relatively more reactive components that scavenge oxygen rapidly during its initial diffusion through the asphalt. This would result in a more rapid formation of ketones and sulfoxides during the early stages of the reaction. Because the sulfides in asphalts are more reactive than the hydrocarbon moieties, sulfides would scavenge a greater proportion of the oxygen during the initial period of the oxidation prior to the time when the oxygen diffusion reaches a near equilibrium concentration through the sample thickness. Once the more reactive hydrocarbons and sulfides are consumed and the oxygen diffusion reaches pseudo equilibrium, the kinetic curve bends over. The ketones then reach a more or less steady rate of formation and the sulfoxides reach a pseudo steady state concentration based on the balance of their rate of formation and their rate of decomposition, as previously discussed.

At typical pavement temperatures, however, the oxidation kinetics of most asphalts are probably heavily dominated by the physicochemical effects of molecular association as previously discussed. Therefore, the slope of the viscosity kinetic plot after the "steady state" condition described above has been reached is probably heavily dominated by the physicochemical effects of molecular association. Asphalts possessing a greater degree of

molecular association will exhibit a greater degree of reduction in the slope of their viscosity kinetic plots following the plateau region than asphalts with greater component compatibility.

The above asphalt aging model is based on the oxidation of asphalt using the TFAAT method, in which a rather thin film (160  $\mu\text{m}$ ) of asphalt is oxidized. It is instructive to consider how the model might be altered when asphalt is oxidized as a 1/8-in. (3.175-mm) film at 300 psi ( $2.07 \times 10^6$  Pa) air, as proposed for the SHRP asphalt aging test. It was shown by Lee (1968) that when a 1/8-in. (3.175-mm) film of asphalt was aged in a TFO pan at 65.6°C (150°F), the viscosity near the top and the bottom of the sample reached nearly the same value after about 240 hours of oxidation at 29 psig ( $2.00 \times 10^5$  Pa) oxygen, and after about 48 hours of oxidation at 132 psi ( $9.11 \times 10^5$  Pa) oxygen. Prior to this point the viscosity near the top of the sample was found to be higher than the viscosity near the bottom of the sample. Unpublished kinetic oxidation data obtained by WRI in 1989 (during POV aging of a Diamond Shamrock AC-10) showed that after 96 hours of POV aging at 60°C (140°F), the top and bottom of a 1/8-in. (3.175-mm) sample of asphalt had a dynamic viscosity of  $8.1 \times 10^2$  and  $7.6 \times 10^2$  Pa·s at 60°C (140°F) respectively, compared with an initial viscosity of  $1 \times 10^1$  Pa·s for the original asphalt. This 96-hour point was found to be midway through the "hump" in the parabolic viscosity kinetic plot.

A comparison of POV and PAV aging data after 144 hours at 300 psi ( $2.07 \times 10^6$  Pa), 60°C (140°F) is shown in table 8.17. Although PAV aging produces a lower level of age hardening than POV aging after 144 hours, as expected, the levels of carbonyl compounds and sulfoxides are virtually the same both near the top and bottom of the sample. This finding confirms that the sample is uniformly oxidized throughout its thickness. It can be argued that bubbles formed in the asphalt after decompression of the PAV or POV at the end of the aging test is further evidence that in the plateau region of the kinetic curve, the asphalt is saturated with oxygen as a reactant. The aging time of 144 hours for the POV and PAV aging of asphalts in the SHRP studies was chosen to ensure that the viscosity kinetic curve had reached the plateau region. Because it is believed that the rapid increase in viscosity during the initial stages of POV and PAV aging is the result of diffusion- and chemical reactivity-related factors, it is believed undesirable to take measurements for a predictive laboratory aging test until the plateau region of the kinetic viscosity curve has been reached.

To conclude this discussion of the chemistry and kinetics of asphalt oxidative hardening, the relationship between the carbonyls (ketones) formed on oxidative aging and viscosity increase are further defined by additional oxidation data using the TFAAT aging method. The data were collected over the temperature range of 85°C (185°F) through 130°C (266°F). The carbonyl absorbance and dynamic viscosity data in tables 8.11, 8.12, and 8.13 were used to construct the plots of dynamic viscosity vs. relative carbonyl concentration shown in figures 8.20 and 8.21. The correlations shown are good. Each asphalt has its own slope on the plots, which (as explained earlier) is primarily a result of the physicochemical state of the asphalt. Note again that the highly compatible, dissociated state of the polar components in asphalt AAG-1 make it highly insensitive (as measured by dynamic viscosity increase) to the oxidation products formed. On the other hand, the

viscosities of asphalts AAD-1 and AAK-1, in which the least amount of carbonyls were formed, were most affected by the formation of the oxidation products.

A final significant, and also pragmatic, conclusion can be drawn from the plots in figures 8.20 and 8.21. Since the data plotted represent all the kinetic data for the TFAAT aging of asphalts at 85°C (185°F), 113°C (235°F), and 130°C (266°F), and since all the data fall on a line with the same slope for each asphalt, it can be concluded that the nature of the hydrocarbon oxidation reaction in asphalt is virtually the same within this temperature range. This confirms a similar conclusion arrived at by Petersen, Plancher, and Miyake (1983). In that study, the ratio of ketones to anhydrides formed on aging using the TFAAT method at 130°C (266°F) was found to be nearly the same as that found in asphalts recovered from field-aged pavements.

### **Additional Factors to Consider in the Design of a Realistic Laboratory Aging Test**

The previous section provided information about the physicochemical factors that should be considered in the design of a realistic laboratory aging test to predict pavement aging. Physical factors different from those of PAV aging and unique to pavement aging must also be considered for the proper interpretation and correlation of laboratory PAV aging data with pavement aging data.

Coons and Wright (1968) investigated the level of age hardening in pavements as a function of depth within the pavement and pavement age. They found, using 13 different pavements of different ages in Georgia, that there were large differences between the level of oxidative hardening of the asphalt near the surface of the pavement and asphalt within the interior. In a collection of eight pavements between the ages of 4 and 24 months, oxidative hardening had proceeded on average to a depth of only 1/2 in. (12.70 mm) from the surface of the pavement. The asphalt viscosity gradient measured at 25°C (77°F) within this top 1/2 in. (12.70 mm) of pavement dropped from about 2.0 MPa·s for the first 1/4 in. (6.35 mm) of pavement to about 1.4 MPa·s in the section of pavement from 3/8 in. (9.53 mm) to 5/8 in. (15.88 mm) from the surface. Below this point the viscosity of the asphalt remained at 1.4 MPa·s as a function of depth. The viscosity below 1/2 in. (12.70 mm) from the surface was thus the viscosity of the asphalt when it left the mix plant. These data show that, on the average, viscosity increase from atmospheric aging had not proceeded beyond the first 1/2 in. (12.70 mm) of pavement in 2 years. These results suggest that the mixture was rather impermeable to air, because if readily permeable void space had existed through the thickness of the pavements, pavement age hardening should probably have been found below 1/2 in. (12.70 mm) in the pavements. In a separate group of five pavements ranging from 47 to 151 months in age, the same type of analysis showed an average viscosity at 25°C (77°F) of about 2.8 MPa·s at the surface, 1.6 MPa·s at 1/2 in. (12.70 mm) from the surface, 1.0 MPa·s at 1 in. (25.40 mm) from the surface, and 0.7 MPa·s at 1 1/2 in. (38.10 mm) from the surface. Beyond 1 1/2 in. (38.10 mm) the viscosity was still decreasing with depth although at a much slower rate. The viscosities in the two sets of pavements approached different viscosity values as a function of depth because the

eight pavements with short term field exposure were prepared from AC-6 asphalts and the five with longer term exposure were prepared from AC-8 asphalts. During the longer term aging, the atmospheric oxygen proceeded much deeper into the pavement, but a large viscosity gradient still remained through the first 1 1/2 in. (38.10 mm) of pavement thickness.

These results are important to the interpretation of POV and PAV laboratory test results as they relate to asphalts aged in pavements. As might be expected, the level of asphalt aging was much greater at the pavement surface, and several years were necessary before significant oxidation occurred at a significant depth within a pavement. It is proposed that the reaction of oxygen through these pavements was largely diffusion controlled, and that the parabolic shape of the viscosity kinetic curve of asphalts recovered from many pavement cores results from the changing oxidation gradient as oxidation moves down through the depth of the pavement layer. Because the amount of oxidation that can occur is largely diffusion controlled, it proceeds more rapidly in the first few years of pavement aging and proceeds progressively lower as the pavement ages because of a longer diffusion path and the increased viscosity of the asphalt through which the oxygen must diffuse. Thus, cores recovered early in a pavement's life contain only a small amount of highly oxidized material near the surface; hence the recovered asphalt, being an average of the properties of the asphalt through the pavement thickness, is primarily composed of relatively unoxidized asphalt. This accounts for the relatively small observed viscosity increase. Because diffusion of oxygen can occur more rapidly through the thinner surface sections of pavement, the rate of "averaged" viscosity increase with time increases more rapidly during the first few years of aging; as the oxygen must diffuse further to reach the most reactive components, the averaged viscosity increase slows down, producing the parabolic pavement aging curve.

During POV and PAV aging, however, factors other than diffusion appear to control the shape of the age hardening kinetic curve. As discussed earlier, Lee (1968, 1972, and 1973) showed that at 66°C (150°F) the viscosity had nearly reached the same value at both the top and bottom of the POV aged sample after 240 hours at 29 psig ( $2.00 \times 10^5$  Pa) and after 48 hours at 132 psi ( $9.11 \times 10^5$  Pa). In the Binder Characterization and Evaluation Program, 300 psi ( $2.07 \times 10^6$  Pa) oxygen was used, thus the level of oxidation must be nearly uniform throughout the sample thickness within a time significantly less than 48 hours. Yet during POV aging more than 100 hours elapse before the hump in the parabolic aging curve is reached. These data suggest that the shape of the parabolic curve in pressure vessel aging is dominated by the oxidation reaction, as discussed previously in connection with the kinetics of sulfoxide and ketone formation (table 8.16, figure 8.17). Thus, it becomes apparent that samples of the same asphalt aged in a pressure vessel and in the pavement probably arrive at their viscosity plateau region by different mechanisms. The pressure vessel asphalt is uniformly oxidized through its thickness in the plateau region, while the asphalt recovered from pavement might arrive at its plateau region by the mixing of more highly oxidized asphalt near the pavement surface with asphalt having little oxidation from the interior of the pavement.

Because the viscosity reached at the plateau region of the kinetic curve during laboratory aging has been shown to be highly dependent on temperature, the viscosity gradient of the

asphalt in the pavement may be even further widened because the maximum temperature reached with the pavement is a function of distance from the surface.

The uniform oxidation of an asphalt through its thickness during POV aging and the nonuniform oxidation of an asphalt in a pavement through its thickness helps explain why Lee (1973) observed that the plateau region for the POV-aged asphalts occurred at a much higher viscosity than did the plateau region of the same asphalts recovered from pavements after 5 years of service.

From the above discussion, it follows that one should never expect to reach the same viscosity in asphalt recovered from pavement cores as in the PAV test. It also follows that the difference between the viscosity reached in the plateau region of the recovered pavement asphalt will be highly dependent on the air permeability of the pavement. An asphalt recovered from a pavement with high voids and permeability will reach the plateau region of its kinetic curve sooner and have a higher averaged viscosity than the same asphalt recovered from a pavement of low voids and permeability. Thus, air permeability of the pavement mixture becomes an important variable in the equation when attempting to correlate pressure vessel and field aging. For some pavement failure modes (e.g., fatigue cracking from asphalt oxidative hardening), one needs to consider whether the whole pavement core or only the surface portion should be analyzed for correlation with laboratory aging data.

This discussion illustrates some of the complex factors that must be considered when correlating laboratory and field aging data. However, based on data developed in the chemistry and kinetics section of this report, it is believed that the PAV aging test will effectively rank asphalts according to their inherent tendency to age harden in the field if the test is conducted as near as possible to the maximum pavement temperature expected and if measurements are not taken until the asphalt has reached a viscosity as near as practical to the plateau region of the viscosity kinetic curve. It is also believed important to know the aging characteristics of an asphalt being selected for pavement service as a function of temperature so that the asphalt can be properly matched with the climate in which it will be used.

A control experiment was also conducted using the TFO-PAV method. The identical procedure was used, except that the pressure vessel was pressurized with high purity argon gas instead of air. The pressure vessel was flushed several times with argon prior to pressurization to ensure that no oxygen remained in the vessel. The eight core asphalts were heated for 144 hours at 60°C (140°F). After 144 hours the asphalts were removed and viscosity, carbonyl, and sulfoxide measurements were performed. The results in table 8.18 show that no oxidation took place beyond what occurred in the TFO. This experiment conclusively showed that the pressure alone of 300 psi ( $2.07 \times 10^6$  Pa) had no lasting effect on the properties of the asphalts, and that the effects observed in the normal TFO-PAV are those of oxidation and molecular structuring and not of pressure. The results also demonstrate that there is no labile oxygen source inherent in the asphalt that causes significant carbonyl and sulfoxide formation during pressure vessel aging.



## Statistical Analysis of Aging Data

Statistical analysis of the aging data with other chemical and physical property data indicated that there are group relationships. Dr. Leon Borgman, Project Statistician, has supervised a study of factors important in asphalt aging by principal component analysis. Seven eigenvectors were constructed from a number of variables. No obvious correlations with aging were found involving any gross properties of asphalts. This result is hardly surprising, as such a correlation would have been discovered long ago. Aging is dependent on a subtle interplay among many factors, as has been previously shown. Some correlations in the sixth and seventh eigenvectors were noted. For example, aging indices correlate with the following combination of factors: aromatic carbon content, nitrogen content, asphaltene (n-heptane) content, molecular weight of SEC Fraction-I, and response of viscosity to addition of model compounds. Because aging is a combination of oxidation, loss of volatiles, and response of the system to the first two factors, such a complicated dependence is to be expected. Stepwise regression analyses identified weak correlations of aging with certain individual factors. Among these are aromatic carbon and hydrogen contents, vanadium content, and responses of  $\tan \delta$  to addition of model compounds. It was noted that each asphalt seems to be characterized by a response to one predominant factor, which differed among asphalts.

## Metal-Catalyzed Oxidation Using Vanadyl Acetylacetonate

Metal complex catalyzed oxidation experiments using vanadyl acetylacetonate (bis-2,4-pentanedionato-oxovanadium IV) as the catalyst were conducted as adaptations of the standard RTFO test (ASTM D 2872) without air injection. Two different experiments were performed using two different levels of catalyst (0.25% and 0.50%) in the standard 85-minute test. A third experiment was performed using 0.50% vanadyl acetylacetonate (VO AcAc) with the temperature lowered to 130°C (266°F) and the time extended to 4 hours. Results of the dynamic viscosity measurements and the IR analysis of oxidation products of the catalysis experiments on the core asphalts are shown in tables 8.19 and 8.20, respectively. Also shown in the tables are the corresponding results from the 144-hour 60°C (140°F) TFO-PAV and 144-hour 80°C (176°F) TFO-PAV experiments for comparison. The rankings of the asphalts by aging index using the various methods are as follows:

0.25% VO(AcAc) 163°C (325°F) G<C<B<F<A<M<K<D

0.50% VO(AcAc) 163°C (325°F) G<C<B<F<M<A<K<D

0.50% VO(AcAc) 130°C (266°F) G<C<F<B<A<M<K<D

144 Hours 60°C (140°F) TFO-PAV G<A<C<B<K<M<F<D

144 Hours 80°C (176°F) TFO-PAV G<C<B<A<F<K<M<D

Based on viscosity measurements, catalytic oxidation proceeds differently in different asphalt. Doubling catalyst concentration from 0.25% to 0.50% in the 85-minute aging experiments at 163°C (325°F) results in a near doubling of the aging indices of asphalts AAA-1 and AAD-1. Other asphalts are affected to a greater (e.g., AAK-1) or lesser extent when doubling the catalyst concentration. Reducing the temperature of the catalytic oxidation to 130°C (266°F) and increasing reaction time to 4 hours affects asphalts nonuniformly. The rankings of the aging tendencies of the asphalts determined by the TFO-PAV method at 80°C (176°F) for 144 hours correlate well with rankings determined by the catalytic method using 0.25% VO (AcAc) at 163°C (325°F) for 85 minutes; however, the viscosities of the aged products in the catalytic method are much lower.

The results of the IR analysis of the same series of tests are listed in table 8.20. The most notable observation from IR analysis is that when asphalts are catalytically aged with vanadyl acetylacetonate, relatively little sulfoxide tends to form compared with the TFO-PAV procedure. Doubling the catalyst concentration tended to approximately double the carbonyl concentration in aged asphalts, but it also resulted in decreased sulfoxide concentrations. Since all sulfoxide levels are so low, the lower amounts of sulfoxide with increased catalyst are probably insignificant or within the error of the analysis.

Comparison of the 0.25% VO(AcAc) with the 0.50% VO(AcAc) at 163°C (325°F) indicates that the two levels of vanadium generally rank the asphalts the same with respect to oxidative age hardening as measured by aging indices, except that asphalts AAA-1 and AAM-1 switch positions in rank. The values of the aging indices of all three catalyzed RTFO tests are in the range of the 60°C (140°F) TFO-POV aging indices and roughly about 20% of the 80°C (176°F) TFO-POV aging indices, so the level of aging is not excessive.

In summary, vanadyl acetylacetonate was used effectively to catalyze oxidation of the core asphalts to levels of aging comparable to those attained in the lower temperature TFO-PAV and TFAAT tests. However, the data indicate that the catalyzed oxidation proceeds by a somewhat different pathway than the pressure oxidation, at least for six of the asphalts. The catalyzed oxidation method still holds possibilities for rapid screening of asphalts. However, more work needs to be performed to establish proper conditions.

## **Asphalt-Aggregate Aging Experiments**

In order to investigate the effect of aggregate properties on binder aging, asphalt-aggregate aging experiments were conducted by coating 5 mass % asphalt on 95 mass % 20-35 mesh aggregate particles. Sized Teflon® particles were used in the experiments as the control, or relatively inert aggregate, for comparison purposes. After mixing the hot asphalt and hot aggregate together, one-half of the mixture was extracted immediately while the second half was aged in the pressure vessel using 300 psi ( $2.07 \times 10^6$  Pa) air at 60°C (140°F) for 144 hours. The aged mixture was then extracted. Data from the half of the mixture extracted immediately after mixing were used as the zero-hour data point. Results from all of the asphalt-aggregate aging experiments are contained in SHRP Database B (appendix B). The results indicate that there is no predictable pattern of influence of aggregate on aging of

asphalt. There were no observable cases where there was a large influence of the aggregate on the aging or oxidation properties of the core asphalts. However, there are phenomena observed in asphalt aging on aggregate that differ from aging of neat asphalt. The viscosity determinations on each asphalt after aging on different aggregates tended to have considerable scatter even though the oxidation levels (table 8.21) were nearly identical. This result caused some concern, and the cause was proposed to be differential disruption of the microstructure by the solvent extraction and subsequent solvent removal of the aged asphalt. Previous experience at WRI had shown the solvent effect on recovery of aged material to be significant. It was also shown that a substantial amount of time was necessary for the recovered asphalts to reattain microstructural equilibrium at room temperature. Previous work at WRI had also shown that the time period necessary to reach microstructural equilibrium could be shortened by heating the recovered asphalts to a rather high temperature (140°C/284°F) for several hours under inert gas followed by a slow cooling rate (e.g., 2°C/hr [3.6°F/hr]) to near ambient temperature.

A thermal annealing experiment was then performed under the above conditions to remeasure the viscosities of some of the recovered aged asphalts. The aged asphalts selected represented all eight core asphalts that had been aged on aggregates RD, RL, and Teflon®. Samples of neat asphalt that had undergone the 144-hour 60°C (140°F) TFO-PAV test were also included for comparison purposes. The results of the thermal annealing experiment are listed in table 8.22. The results show that there was very little effect of the aggregates tested on aging of some asphalts. However, there was a measurable effect in certain combinations. For example, there appears to be significant difference between aggregates for asphalts AAK-1 and AAM-1. Since the neat asphalts used for comparison had undergone TFO oxidation prior to the PAV oxidation and the asphalts used in asphalt-aggregate mixtures did not undergo TFO oxidation prior to mixing with aggregate, it would be assumed that the neat asphalts after TFO-PAV would have a higher viscosity than the recovered asphalts. However, this is not necessarily the case. Asphalts AAG-1, AAC-1, and AAF-1 are more viscous after aging on aggregate than after TFO-PAV aging. These asphalts, especially AAG-1 and AAC-1, are characterized by their small viscosity changes during almost all aging tests, but become relatively more viscous after aging on aggregate. On the other hand, recovered asphalts AAD-1, AAK-1, and AAB-1 exhibit viscosities much lower than those of the same TFO-PAV aged asphalts. For AAD-1, AAK-1, and AAB-1, the magnitude of the decrease between the recovered asphalts and the TFO-PAV asphalts is greater than can be accounted for by the viscosity change that occurs in the TFO test alone (supplementary table 8.37). These three asphalts are characterized by rather large increases in viscosity upon oxidation when aged neat. It is proposed that the aggregate surface induces structuring in the asphalt. This structuring reduces the amount of viscosity increase that occurs upon oxidation compared with the neat asphalt, resulting in lower viscosity of the asphalts recovered from the aggregate surface. This idea is consistent with the microstructural model of asphalt, and the data shown here support this model. It is possible that some minerals occurring in some aggregates may have more profound effects (more "catalytic") on asphalt oxidation (stiffening), but none were found in this study.

## Other Analytical Techniques Used to Measure Oxidation

### *Size Exclusion Chromatography (SEC) of Aged Asphalts*

SEC was performed on core and noncore asphalts aged according to several different protocols. Two SEC procedures were used: (1) PSEC and (2) streamlined preparative SEC (SPSEC). Both procedures use gravimetric detection but differ in scale and are described in chapter 2. The aging protocols include:

1. TFAAT at 130°C (266°F) for 4 hours
2. TFAAT at 130°C (266°F) for 12 hours
3. TFO-PAV at 60°C (140°F) and 300 psi for 144 hours
4. TFO-PAV at 100°C (212°F) with a 1.6 mm (1/16 in.) film thickness for 24 hours
5. TFO-PAV at 113°C (235°F) with a 1.6 mm (1/16 in.) film thickness for 24 hours
6. ASTM thin film oven test
7. TFO-PAV at 100°C (212°F) with a 3.2 mm (1/8 in.) film thickness for 20 hours.

Aging using protocols 1 through 3 was performed at WRI, and the rest were performed at Penn State.

The PSEC separation can be performed to yield two fractions, nonfluorescent (SEC Fraction-I; molecular associations) materials and fluorescent (SEC Fraction-II) materials. PSEC can also be performed to yield nine fractions, which allows diagraming of a more detailed chromatogram. SEC Fraction-I mass data for the core asphalts aged using protocols 1 through 5 and then separated using the two-fraction procedure are listed in table 8.23 along with mass data for the unaged core asphalts. SEC Fraction-I content is increased over that of the unaged asphalt for every aging protocol. The smallest amount of increase resulted from protocol 3, 144 hours at 60°C (140°F), and the largest increase resulted from protocol 5, 24 hours at 113°C (235°F). IR data on sulfoxide and ketone concentrations listed in table 8.24 corroborate that protocol 5 produces more aging than protocol 4 where the conditions are the same except for temperature; that is, other things being equal, the higher temperature (as expected) yields the most aging. It is significant that increasing the temperature by only 13°C (23°F) results in increases in SEC Fraction-I content, sulfoxide content, and ketone content, all of which are relatively easy to measure. The increase in SEC Fraction-I content in asphalt AAM-1 for protocols 4 and 5 was so large that the ability of the PSEC column to separate that fraction apparently was affected. This problem is indicated by the values for SEC Fraction-I for AAM-1 for protocol 4. For a 16 g sample, the value for Fraction-I was 49.3%, and for a 6 g sample the value was 39.4%. This result indicates that the column may have been overloaded at the 16 g charge level.

Asphalts AAD-1, AAG-1, AAK-1, and AAM-1 aged to two different temperatures each according to protocols 4 and 5 were separated using the nine-fraction PSEC procedure. Data are listed in table 8.25 for these separations. It can be seen that the increase in SEC Fraction-I (fraction 1 in the table), in general, comes at the expense of materials in fractions 2 through 4. That is, larger molecules or molecular associations are produced through

chemical reactions of smaller molecules with oxygen that yield molecules that then associate.

Data in table 8.26 result from aging experiments performed using protocols 4 through 7. These data include PSEC and SPSEC data for core and noncore asphalts. The data for protocol 7 represent baseline data because that is the protocol selected for future aging experiments. The SPSEC data show good agreement with the PSEC data, indicating that the more rapid SPSEC procedure can be used when substantial amounts of SEC fraction material are not needed for further analysis.

Data are listed in supplementary table 8.41 for viscosities and mass fractions of SEC Fraction-II materials aged according to protocols 1 and 2. These data show that there is no significant increase in viscosity of SEC Fraction-II materials for all core asphalts except AAC-1 and AAG-1 after 4 hours TFAAT at 130°C (266°F). The data also show that, for asphalts AAA-1, AAB-1, AAD-1, and AAK-1, there is no significant change in SEC Fraction-II viscosity after 12 hours TFAAT at 130°C (266°F), while for asphalts AAC-1 and AAG-1 there is an increase. However, for AAF-1 and AAM-1 there is a decrease in SEC Fraction-II viscosity. Data in supplementary table 8.42 show apparent molecular weights for SEC Fraction-I materials for the unaged core asphalts and for the core asphalts TFAAT-aged for 12 hours at 130°C (266°F). These data show that for all asphalts but AAG-1 there is an increase in the apparent molecular weight in these materials after aging, as predicted by the model. For AAG-1, the apparent molecular weights of the aged and unaged SEC Fraction-I materials are within experimental error.

Data in supplementary tables 8.43 through 8.45 list results of analysis of the core asphalts aged according to protocol 3, TFO-PAV for 144 hours at 60°C (140°F). Supplementary table 8.43 shows the results of IR analysis of SEC Fraction-I and -II. These data show that carbonyl content does not vary greatly from one asphalt to another or from one fraction to another. Sulfoxide content shows variations reflecting the difference in sulfur content between the asphalts but, except for AAD-1 and AAC-1, does not differ much between fractions of the same asphalt. These data show that oxidation occurs throughout asphalt systems, including the dispersed and dispersing components, or that the products of oxidation equilibrate between the two moieties. Supplementary table 8.44 lists mass fraction and molecular weight data for SEC Fraction-I and -II for the unaged core asphalts and the protocol 3 aged asphalts. These data show the expected decrease in SEC Fraction-II materials due to oxidation. The decrease varies from asphalt to asphalt, reflecting the differences in chemical makeup between the asphalts. The molecular weight data do not always show the expected increase in molecular weight of SEC Fraction-I. This suggests that, although the amount of SEC Fraction-I increases, the size of the molecular associations does not necessarily increase. Both factors can be expected to influence the rheological properties of asphalts. Supplementary table 8.45 reports yields and viscosities of SEC Fraction-II materials of these same aged asphalts. SEC Fraction-II materials in these aged asphalts are somewhat more viscous than the SEC Fraction-II materials in correspondingly unaged asphalts.

Examination of these and previously presented data lead to the conclusion that while TFO-PAV aging causes an increase in the viscosity of the SEC Fraction-II materials, the increase

in asphalt viscosity cannot be accounted for by the increase in viscosity of the SEC Fraction-II materials. The increase in viscosity in asphalts upon aging results from an increase in associations, as reflected in SEC Fraction-I buildup, and a decrease in the amount of SEC Fraction-II.

Data for core asphalts aged according to protocols 4 and 5, TFO-PAV for 24 hours at either 100°C (212°F) or 113°C (235°F), are listed in supplementary table 8.24 and in tables 8.27 and 8.28. Supplementary table 8.24 contains IR data on the aged asphalts that corroborate conclusions discussed earlier. Table 8.27 lists mass fraction and molecular weight data for SEC Fraction-I for the unaged and aged asphalts. The data show the expected increase in the amount of SEC Fraction-I materials on aging for these asphalts, except for AAM-1. However, the molecular weights do not always show the expected increase on aging. Table 8.28 lists molecular weight data for SEC Fraction-I for the two temperatures for asphalts AAD-1, AAG-1, and AAK-1 and also for SEC Fraction-II 113°C (235°F) aged AAD-1 and AAG-1 in toluene and pyridine. Toluene is believed to have a solubility parameter similar to that of the solvent moieties of asphalts and therefore would not be expected to dissociate molecular associations in asphalts. Pyridine, on the other hand, is more polar and would be expected to break up at least some of the associations. The molecular weights of SEC Fraction-I materials are, in every case, smaller when determined in pyridine than in toluene. The SEC Fraction-II materials, however, within experimental error, have the same molecular weight in both solvents. This suggests that SEC Fraction-II materials do not engage in strong molecular associations at the temperature at which the molecular weights are determined.

In addition, it is evident that when asphalts AAD-1 and AAK-1 are aged at the higher temperature, more SEC Fraction-I material is generated than when these asphalts are aged at the lower temperature (table 8.27). The number-average molecular weights of the SEC Fraction-I materials measured in toluene are greater for the materials aged at the higher temperature. The molecular weights in pyridine, however, are lower for SEC Fraction-I materials for AAD-1 and AAK-1 samples aged at the higher temperature than for those aged at the lower temperature. This suggests that as aging conditions become more severe, associating units in these asphalts tend to be smaller (based on molecular weights in pyridine) while associations tend to be larger (based on molecular weights in toluene).

### *Potentiometric Titration of Oxidized Asphalts*

Each of the core asphalts was subjected to PAV aging at 100°C (212°F) for 24 hours, and these aged samples were analyzed by nonaqueous potentiometric titration to determine changes in base concentrations. This procedure was discussed in chapter 4. Each of the core asphalts contains relative amounts of moderately strong and weak bases unique to the asphalt. Asphalt AAG-1 contains an unusually large amount of bases, some of which are more than moderately strong (table 4.1). When the core asphalts were aged according to the TFO-POV (asphalts were aged in an oxygen atmosphere) method at 60°C (140°F) for 1,000 hours (table 4.4), it was observed that total base concentrations increased significantly

for all of the asphalts. This increase was caused by a large increase in weak bases, because for most of the asphalts, aging resulted in decreases in amounts of moderately strong bases.

The same trend is observed for core asphalts TFO-PAV aged at 100°C (212°F) for 20 hours at Penn State (table 8.29). There are differences among the asphalts, as would be expected for two different aging methods. Compared with the 60°C (140°F) aging for 1,000 hours, the 100°C (212°F) aging results in more total bases for AAG-1, about the same for AAM-1, and somewhat less for the other six core asphalts.

Samples of members of the expanded set of asphalts were aged by the TFO and TFO-PAV methods at 100°C (212°F) for 20 hours at Penn State. These aged samples were analyzed for base concentrations by means of nonaqueous potentiometric titration (chapter 4). Some of the members of the expanded set of asphalts (unaged) were titrated, and their base concentrations are listed in supplementary table 4.7. The TFO-treated samples (table 8.30) have base concentrations that differ very little from the unaged parent asphalts. In the TFO-PAV-treated asphalts, with the exception of AAJ, moderately strong bases are observed to be less abundant than in TFO-treated asphalts, but weak bases and total titratable bases are more abundant. Based on these data and data for the core asphalts (chapter 4), this trend appears to be a general one, the exception being AAJ.

### *Asphaltene Determinations of Oxidized Asphalts*

In addition to determining elemental compositions, and  $M_n$  values and performing IR-FGA analyses on aged asphalts, samples of aged asphalts were investigated by other classical methods discussed in chapter 9. It has long been known that aged asphalts have larger asphaltene concentrations than parent asphalts. Three core asphalts were aged by the TFAAT method for 72 hours at 113°C (235.4°F). Asphaltenes were prepared from these aged asphalts by n-heptane precipitation, as described in Volume IV (chapter 6) of this report. Yields of asphaltenes and maltenes from these aged asphalts are reported in table 8.31. The asphaltene yields of two of the three aged core asphalts are more than double the yields from the parent asphalts, and asphalt AAD-1 is nearly double.

### *Heithaus Parameters of Oxidized Asphalts*

Heithaus parameters were determined for seven core asphalts aged by the TFAAT method for 72 hours at 113°C (235.4°F). These data, along with Heithaus parameters of unaged asphalts, are reported in tables 8.32 through 8.34. In all cases but one, the Heithaus P value, measuring total peptizability of an asphalt, decreases on aging. For AAM-1, results were too scattered to provide reliable values. The  $p_a$  value, which purports to measure asphaltene peptizability, decreases significantly for all the asphalts except AAM-1. This result indicates that asphaltenes, which are more abundant in aged than in unaged asphalts, are also less dispersible. The  $p_o$  value, measuring solvent power of maltenes, tends to increase on aging, with the exception of AAD-1 and possibly AAF-1. Unfortunately, data for this parameter exhibit much scatter. It is, however, reasonable that a more polar maltene fraction resulting from aging would be more compatible with a much more polar asphaltene fraction.

### *Reduced Specific Viscosity Measurements on Oxidized Asphalts*

The reduced specific viscosity technique was selected as a definitive method for studying molecular associations. In this application of the technique, the asphaltene fraction was used as the solute and the maltene fraction as the solvent. This allowed the study of the asphalt in the absence of a solvent, thus eliminating the uncertainty in interpreting results because a solvent would alter the physical state of molecular association. Asphaltenes were separated from maltenes by n-heptane precipitation; mixtures of maltenes and asphaltenes in various proportions, which included proportions less than and greater than the natural abundance level, were then prepared. Dynamic viscosities of these mixtures were measured at 25°C (77°F), 45°C (113°F), and/or 60°C (140°F), and reduced specific viscosities  $\langle \eta \rangle$  were calculated. The viscosities of the maltenes were taken to be the viscosities of the solvent (chapter 9).

Asphalts AAD-1 and AAG-1 were chosen for detailed evaluation using the reduced specific viscosity technique because they are believed to represent extremes in asphalt component compatibility. Data obtained at 45°C (113°F) for these asphalts unaged and TFAAT-aged at 113°C (235°F) for 72 hours are shown in table 8.35 and plotted in figure 8.22. The natural abundance level of asphaltenes is also indicated in the figure. The reduced specific viscosity measurements are interpreted as follows.

The reduced specific viscosity is a relative measure of the apparent molecular weight of the asphaltene fraction dispersed in its natural solvent phase: the maltenes. A larger value for the reduced specific viscosity means a larger apparent molecular weight. Because there are no molecular condensation reactions between asphaltenes as their concentration is changed in the maltenes, any increase in the reduced specific viscosity with increasing asphaltene content arises from an increase in the apparent molecular weight of the asphaltenes. This can only occur through molecular association to form microstructure in the asphalts. It should be remembered when relating these data with the kinetic aging model that these associations are thermally reversible.

It is apparent from the reduced specific viscosity measurements made on unaged asphalt AAG-1 (figure 8.22) that up to its natural abundance level of asphaltenes, there was virtually no significant increase in the self-association of asphaltenes with increasing asphaltene concentration. This implies that the maltene fraction had sufficient solvent power to effectively disperse the asphaltenes in the asphalt up to their natural abundance concentration. Beyond this point, increased self-association to produce asphaltene agglomerates of higher apparent molecular weight occurs very slowly as the concentration of asphaltenes is increased. This behavior further confirms the high degree of component compatibility of asphalt AAG-1. The component compatibility of this asphalt remains quite high even after TFAAT oxidation, as indicated by the modest increase in reduced specific viscosity with increasing asphaltene content. The behavior of asphalt AAD-1, on the other hand, is quite different than that of asphalt AAG-1. Note that even for the unaged asphalt, the reduced specific viscosity increased rapidly with increasing asphaltene content before the natural abundance level was reached. This indicates that, unlike asphalt AAG-1, the asphaltenes in neat, unaged asphalt AAD-1 are highly associated at 45°C (113°F). After



TFAAT oxidation, the asphaltenes associate to a much greater extent, as shown by the reduced specific viscosity measurements. The apparent molecular weight of asphaltene agglomerates or microstructure in asphalt AAD-1 is several orders of magnitude larger, on the average, than in asphalt AAG-1. These reduced specific viscosity measurements confirm that (1) polar asphalt molecules associate to form microstructure in asphalt, (2) the size or degree of microstructure varies greatly as a function of asphalt source, and (3) the oxidation of asphalt increases the level of microstructure.

This reduced specific viscosity study thus provides additional confirmation of the microstructural aging model of asphalt developed in the previous section of this chapter. Data in table 8.36 and figure 8.23 illustrate this point. In this experiment, the highly dispersed asphalt AAG-1 and the highly associated asphalt AAD-1 were aged using the TFAAT method at 113°C (235°F) up to 72 hours and the PAV method at 60°C (140°F) up to 400 hours. Samples were analyzed as a function of time to determine the viscosity kinetic plots. The time scale for the 60°C (140°F) PAV aging of AAG-1 was shifted to offset the reduced rate of oxidation at the lower temperature. The same offset scale was then used for asphalt AAD-1 so that the kinetic data for the two asphalts could be compared.

Examination of the kinetic data for AAG-1 shows that the kinetic plots for this asphalt at both temperatures are quite similar. Because reduced specific viscosity measures the apparent average size of the molecular agglomerates, which did not change greatly on oxidation (figure 8.22), these kinetic data strongly support the conclusion drawn in the earlier chemical and kinetic studies that the polar molecules are nearly as highly dissociated at 60°C (140°F) as they are at 113°C (235°F). The data also imply that immobilization of these molecules through association during oxidation within the temperature range of 60°C (140°F) to 113°C (235°F) is not a significant factor dominating aging kinetics. Putting it another way, the physicochemical states of AAG-1 at 60°C (140°F) and 113°C (235°F) are quite similar. However, this is not true for asphalt AAD-1. When AAD-1 was PAV-aged at 60°C (140°F), its viscosity aging characteristics appeared quite similar to those of AAG-1. At the higher 113°C (235°F) temperature, the rate of viscosity increase is much greater than that of AAG-1. These results again support the earlier conclusions that at lower temperatures, many of the reactive components in asphalt AAD-1 are rendered much less reactive by molecular association. However, at the higher temperature of 113°C (235°F), the reactive polar molecules become dissociated and more mobile, thus in effect increasing the concentration of the more oxygen-reactive species.

The fact that the kinetic data for asphalt AAG-1 are similar at both 60°C (140°F) and 113°C (235°F) reveals important additional information on the aging mechanism. The sharp decreases in the rates of age hardening at the humps of the kinetic curves suggest that the same (or similar) components are available for oxidation at both temperatures. This is different from most asphalts, again suggesting that oxidation of most asphalts is controlled by a microstructure.

An important practical conclusion from this experiment with regard to a realistic aging test is this: The more removed the temperature of a laboratory test is from pavement temperature, the greater the chance for invalid predictive information. Based on the data in

figure 8.23, if asphalts AAG-1 and AAD-1 were aged by the TFAAT test for 72 hours at 113°C (235°F), AAD-1 would be judged more susceptible to age hardening than AAG-1. If they were aged by the PAV test for 400 hours at 60°C (140°F), asphalts AAD-1 and AAG-1 would be judged similar. However, if the tests were run at the same temperatures but for only about 50 hours in the PAV and about 10 hours in the TFAAT test, the single point measurement would classify these two asphalts as having nearly the same aging characteristics as determined by viscosity change on aging. The results of this experiment illustrate not only the importance of temperature in designing a practical laboratory aging test, but also the importance of aging time for the test to ensure that the single point determination is on the plateau region of the viscosity kinetic curve.

Reduced specific viscosity studies also were performed for seven TFAAT-aged core asphalts (113°C/235.4°F, 72 hours). Reduced specific viscosity determinations for unaged core asphalts are described in chapter 9. Reduced specific viscosities at various concentrations of asphaltenes for aged asphalts are listed in supplementary tables 8.46 through 8.52. These data are plotted in figures 8.24 through 8.30. Figures 8.24 through 8.30 can be compared with figures 9.2 through 9.8 in chapter 9. The slopes of the plots of  $\langle\eta\rangle$  vs. concentration for the aged asphalts are steeper than the slopes of similar plots for the unaged asphalts, with the exception of AAG-1. This means that the aged asphalts are less compatible systems than their parent asphalts, again with one exception. The behavior of AAG-1 is aberrant in many respects because of its markedly different state of dispersion, as has been pointed out previously. The amount of chemical oxidation observed in AAG-1 is large, but this does not greatly affect compatibility (as measured by classical methods) nor cause great viscosity increases because its polar components and oxidation products are much more easily solubilized or dispersed.

Additionally, figure 8.24 shows that the intrinsic viscosity (increased y-intercept of curve) of AAA-1 increases markedly on aging, which was not observed for the other aged asphalts. This observation indicates that the  $M_n$  value of AAA-1 TFAAT-aged asphaltenes should be much higher than  $M_n$  for asphaltenes from the unaged AAA-1.

## Summary

The microstructural model of asphalt predicts that as oxidation of asphalt occurs, the polarity of the molecules increases causing an increase in the polarity of the whole asphalt. The stiffening of asphalt that occurs upon oxidation is a result of increased structuring caused by an increased amount of polar molecules. Oxidation also produces polyfunctional molecules that promote three-dimensional structuring to a larger degree than do molecules with only one functional group.

Temperature of the oxidation reaction of asphalt is a very important factor that determines the rate of oxidation, the amount of oxidation, and the resultant stiffness of the asphalt. The microstructural model predicts that as temperature is increased, some of the polar associations (microstructure) are disrupted, allowing more molecules to react with oxygen; added to this is the effect of temperature on the rate of reaction with oxygen. Pressure vessel and oven aging (oxidation) tests ranging in temperature from 60°C (140°F) to 130°C

(266°F) produced results that support the microstructural model of asphalt. Higher temperature tests produced more oxidation and more stiffening of the asphalts than did lower temperature tests. Results from oxidative aging tests also showed that physical effects in the asphalt (structuring) play a key role in "quenching" the oxidation process, which occurs before there is a limitation of reactive species. Results also showed that aging tests conducted at temperatures substantially higher than service temperatures can produce oxidation and stiffening in some asphalts that may not be representative of the aging that occurs at field conditions.

The results of the TFO-PAV aging conducted at temperatures of 60°, 70°, and 80°C (140°, 158°, and 176°F) indicated that the maximum temperature to which the pavement is exposed is an important factor in determining the eventual hardening of the pavement. The results showed that asphalts have widely ranging responses to rather small changes in temperature that occur in the pavement service temperature range. An aging test used to predict long-term durability of an asphalt or pavement must take into consideration the climate to which the pavement will be exposed.

PAV aging of asphalt-aggregate mixtures indicated that the aggregates tested did not have a large effect on asphalt aging, but in some cases there was a measurable effect. Asphalts that tended to form larger amounts of associations were those asphalts that tended to harden slightly less when coated on an aggregate. This phenomenon is probably due to aggregate-induced structuring of the asphalt, limiting the availability of reactive species.

Several analytical techniques were also used to evaluate the properties of aged asphalts. These techniques included SEC, both preparative and streamlined preparative; potentiometric titration; asphaltene determinations (n-heptane); Heithaus parameters; and reduced specific viscosity measurements. The results of these techniques also supported the microstructural model of asphalt. The SEC analyses showed that an increased amount of SEC Fraction-I (the associated components) was formed after aging compared with parent asphalts. Potentiometric titrations found increased amounts of total bases in the aged asphalts. The largest increase occurred in the weak base fraction, as would be expected by the formation of ketones and sulfoxides upon oxidation. Asphaltene determinations on the aged asphalts showed an increased amount of asphaltenes in aged asphalts compared with parent asphalts. Values of Heithaus parameters  $P$  and  $p_a$  decreased in the aged asphalts compared with the parent asphalts. The decrease in the  $P$  values indicates that an asphalt is less peptizable after oxidation, and the decrease in the  $p_a$  values indicates that the asphaltenes are less dispersible after oxidation. Values of Heithaus parameter  $p_o$  increased for the aged asphalts compared with the parent asphalts. The increase in the  $p_o$  values for the aged asphalts is reasonable because oxidation in the maltene fraction produces a more polar maltene fraction that has more dispersing power compared with the parent asphalt maltene fraction. The reduced specific viscosity measurements also indicate that aged asphalts are, in general, less compatible than parent asphalts.

Statistical analysis of chemical and physical property data was performed on parent asphalts and on aged asphalts was performed. The statistical analysis involved a study of significant factors in asphalt aging by principal component analysis. Seven eigenvectors were constructed from a number of variables. No obvious correlations with aging were found

involving any gross properties of all asphalts. It was also found that aging for each asphalt seems to be characterized by a response to one predominant factor, which differed among asphalts. This was not surprising because aging is a combination of oxidation, loss of volatiles, and response of the system to the first two factors. At present, the finding of the statistical analysis is that aging of asphalt will probably have to be measured and can not be predicted by simple methods.

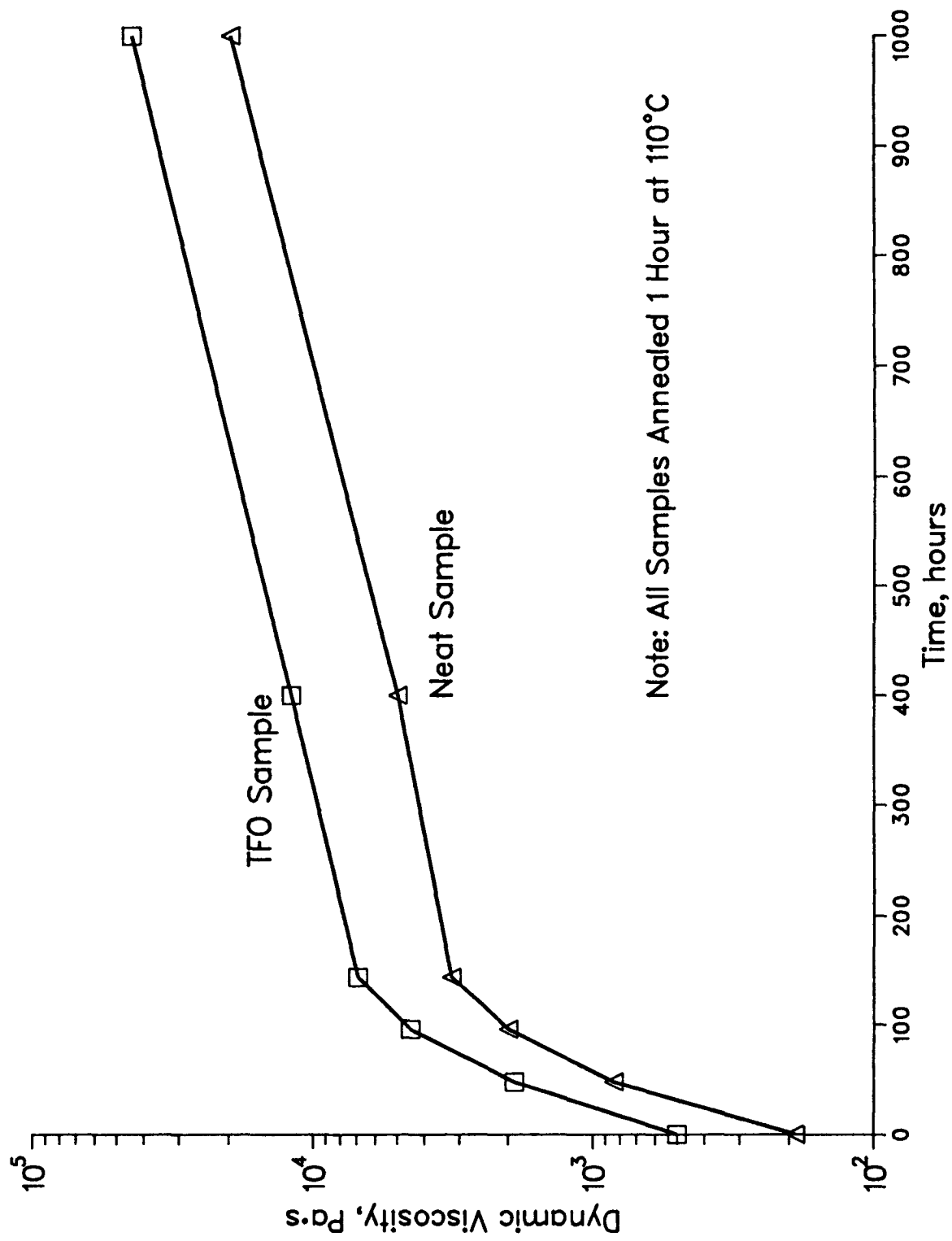


Figure 8.1 Pressure Oxidation Vessel (POV) Oxidation of Core Asphalt AAD-1 With and Without Thin-Film Oven (TFO) Test

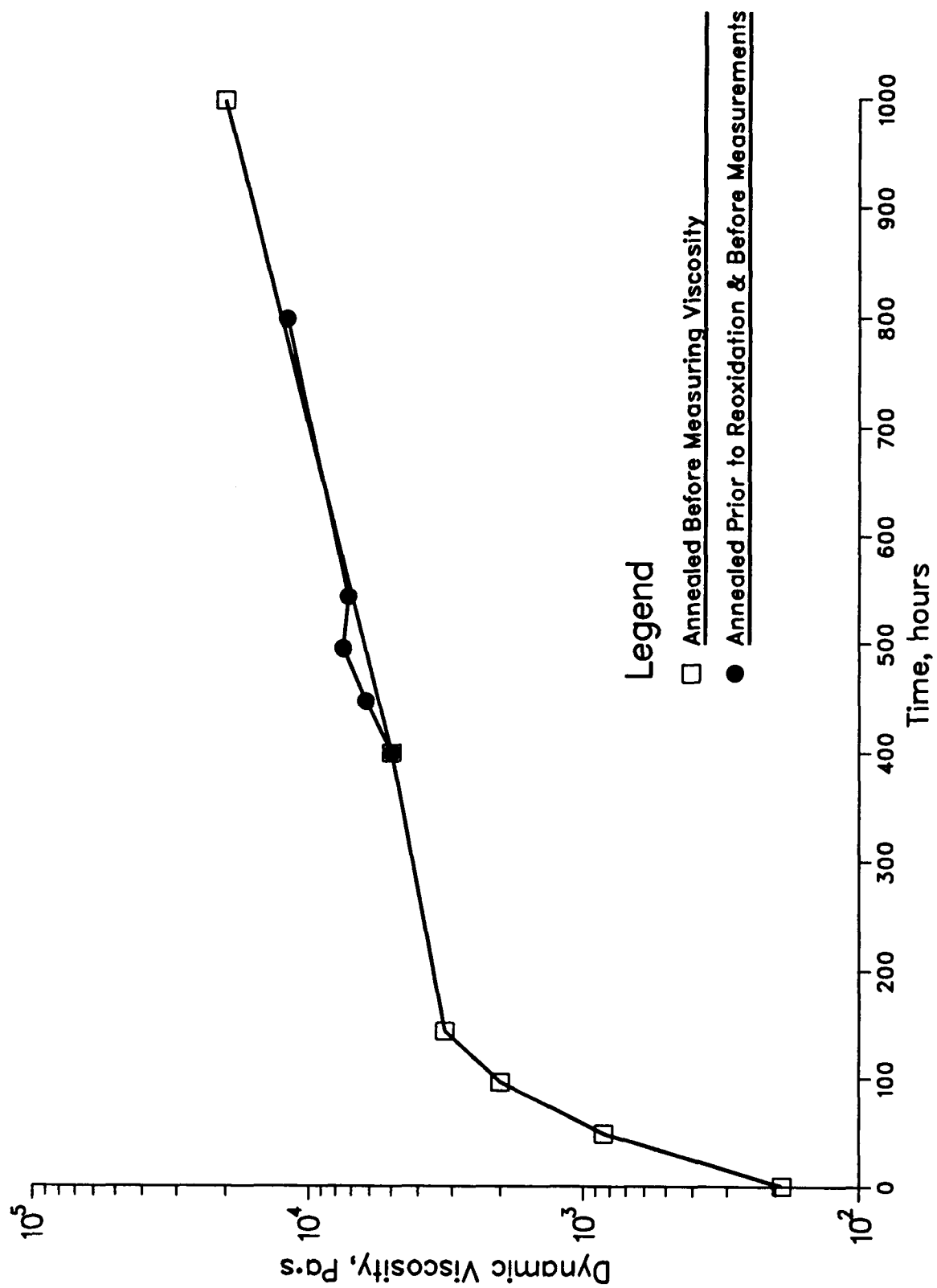


Figure 8.2 POV Oxidation of Core Asphalt AAD-1

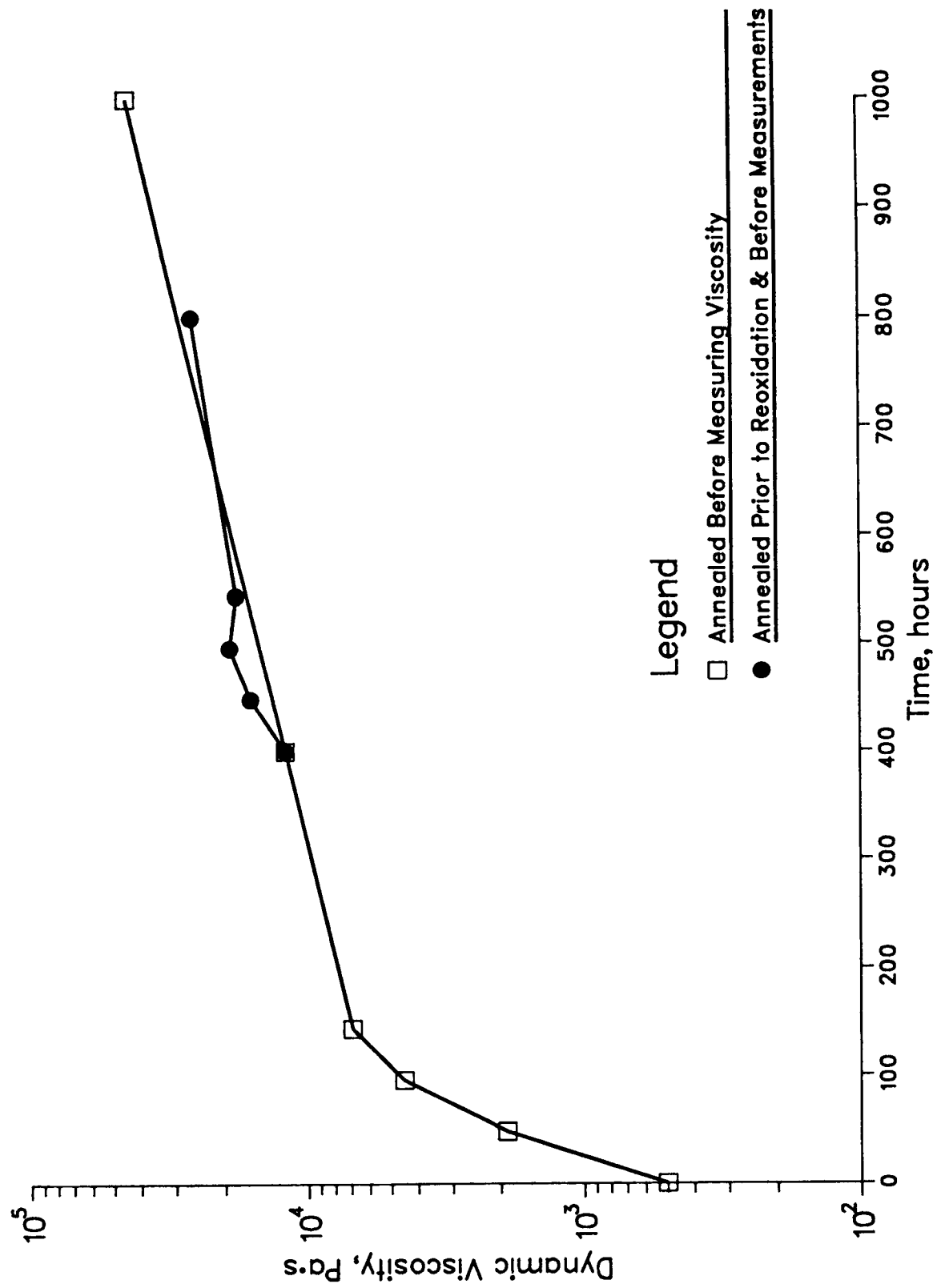


Figure 8.3 POV Oxidation of Core Asphalt AAD-1 After TFO Test

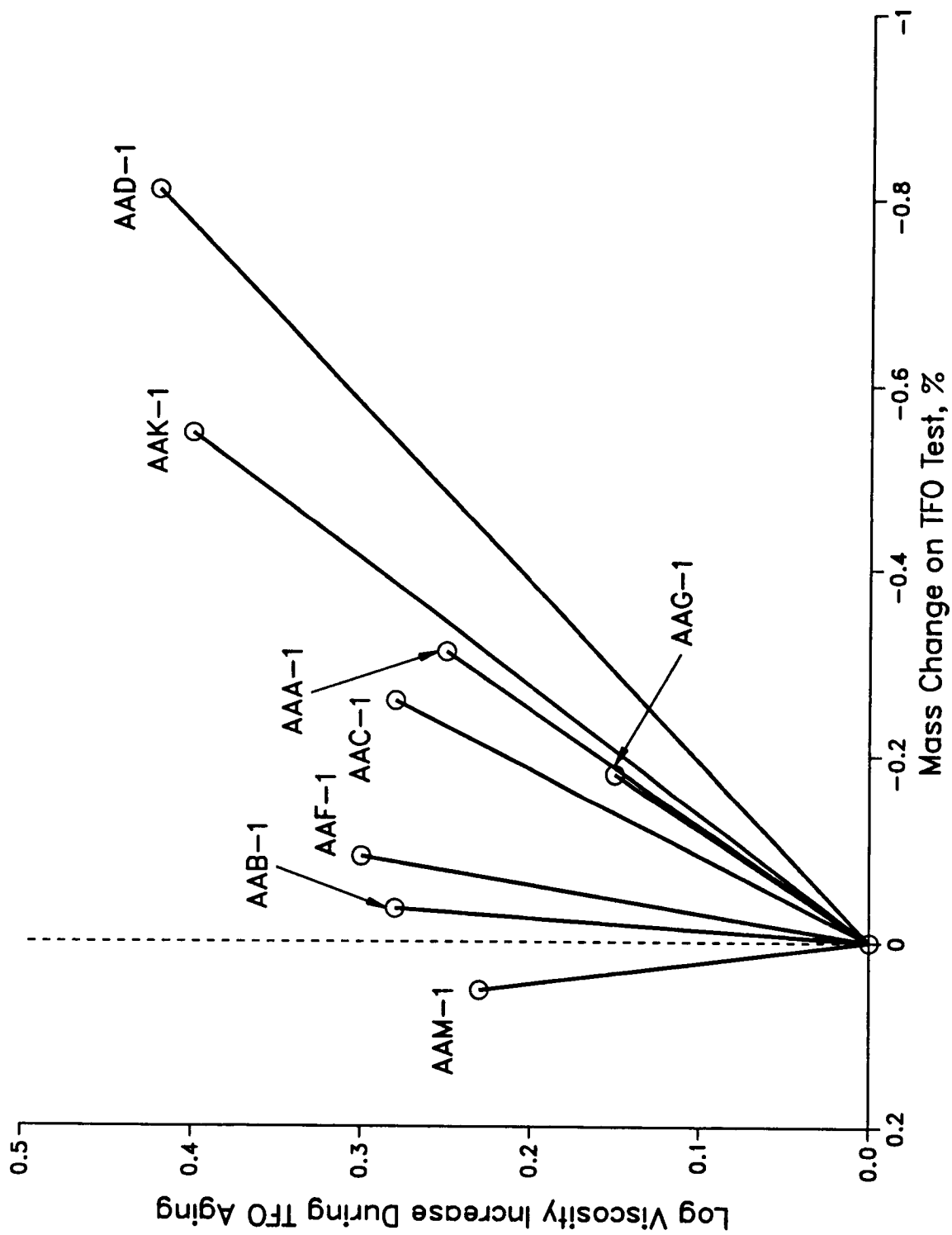


Figure 8.4 Mass Change vs. Log Viscosity Increase During TFO Aging



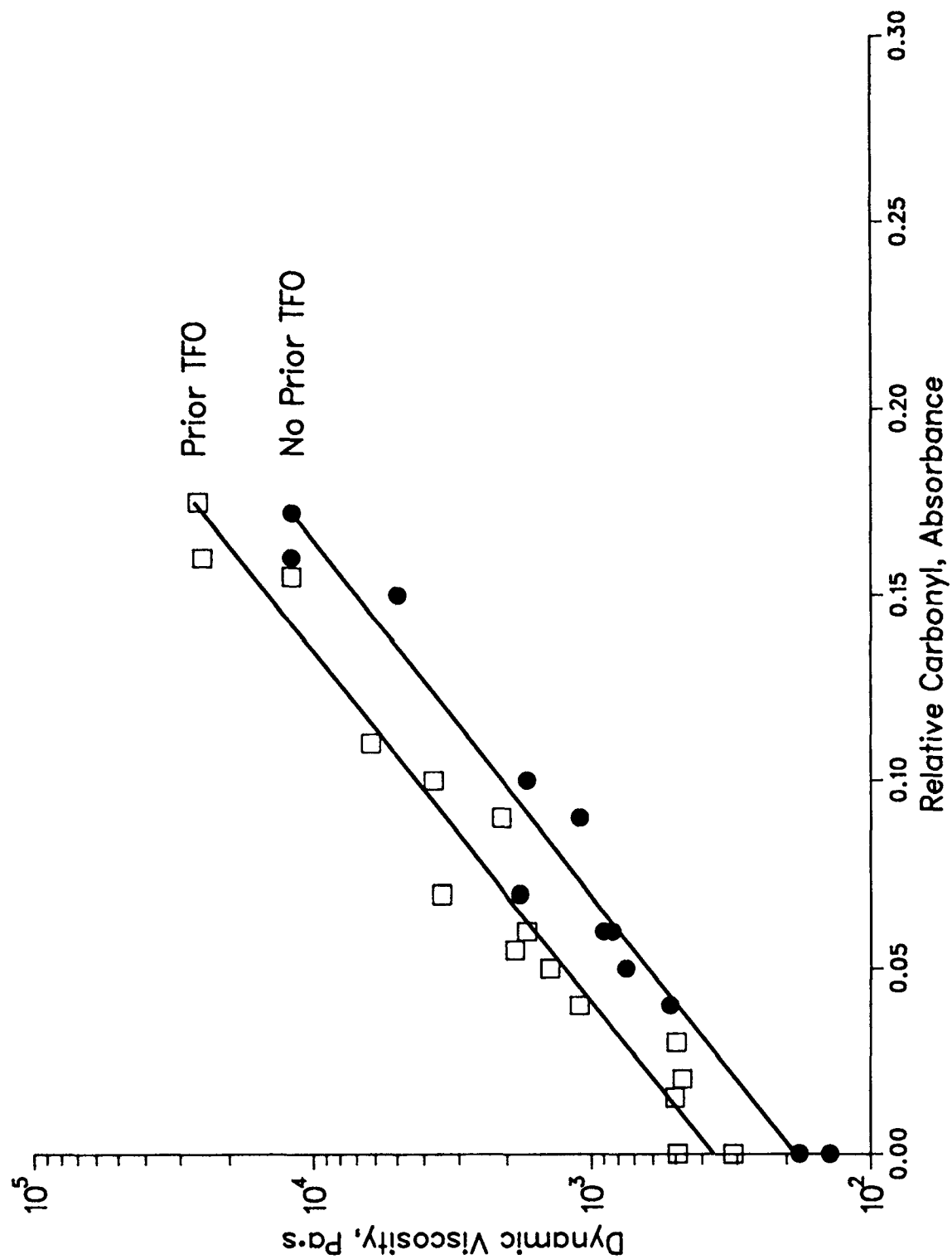


Figure 8.5 Relationship Between Viscosity Change and Carbonyl (Ketone) Formation on POV Oxidation of Asphalt AAD-1 With and Without Prior TFO Oxidation

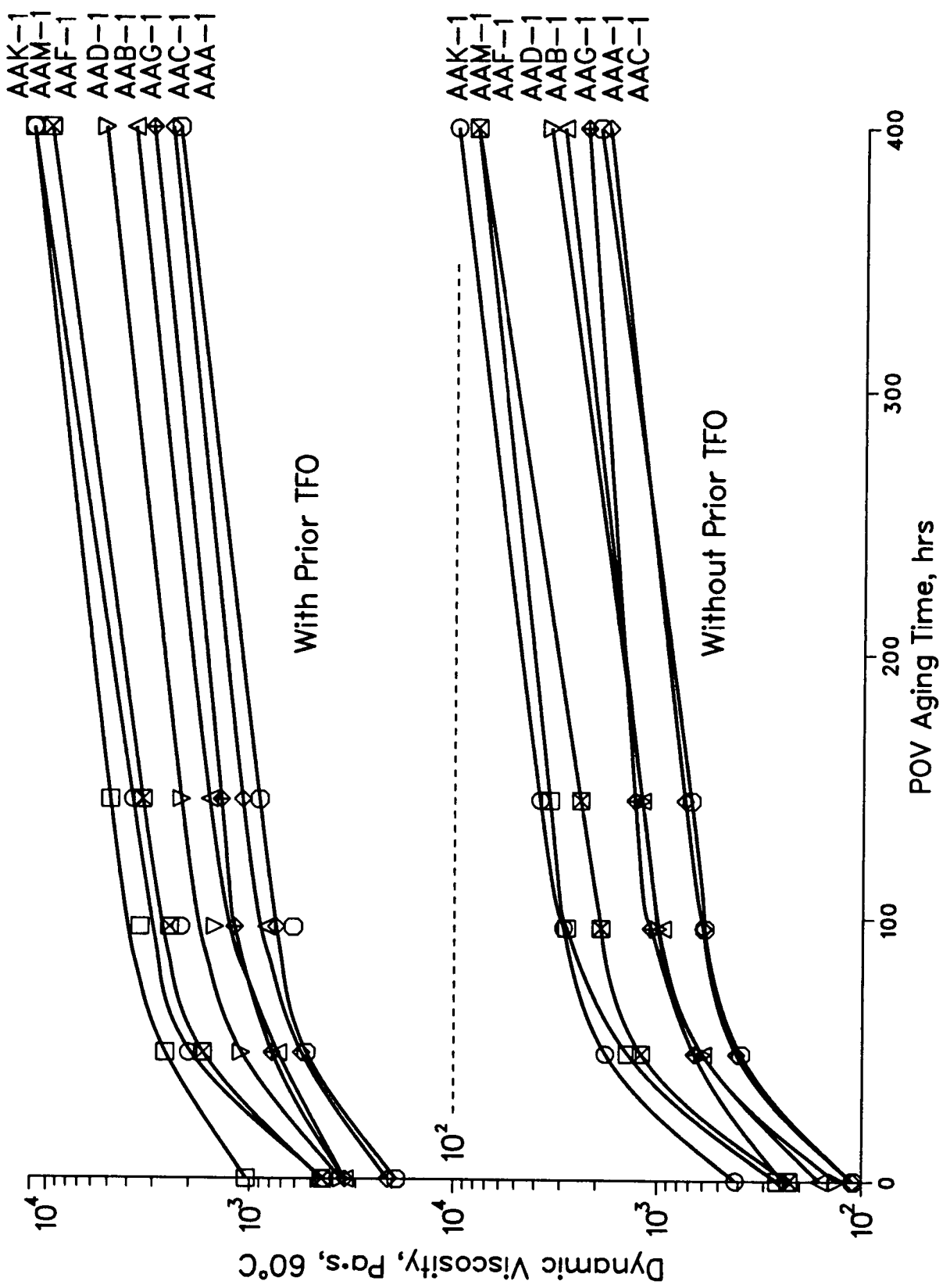


Figure 8.6 Kinetic Plots of POV Aging of Core Asphalts at 2.07 MPa Oxygen, 60°C

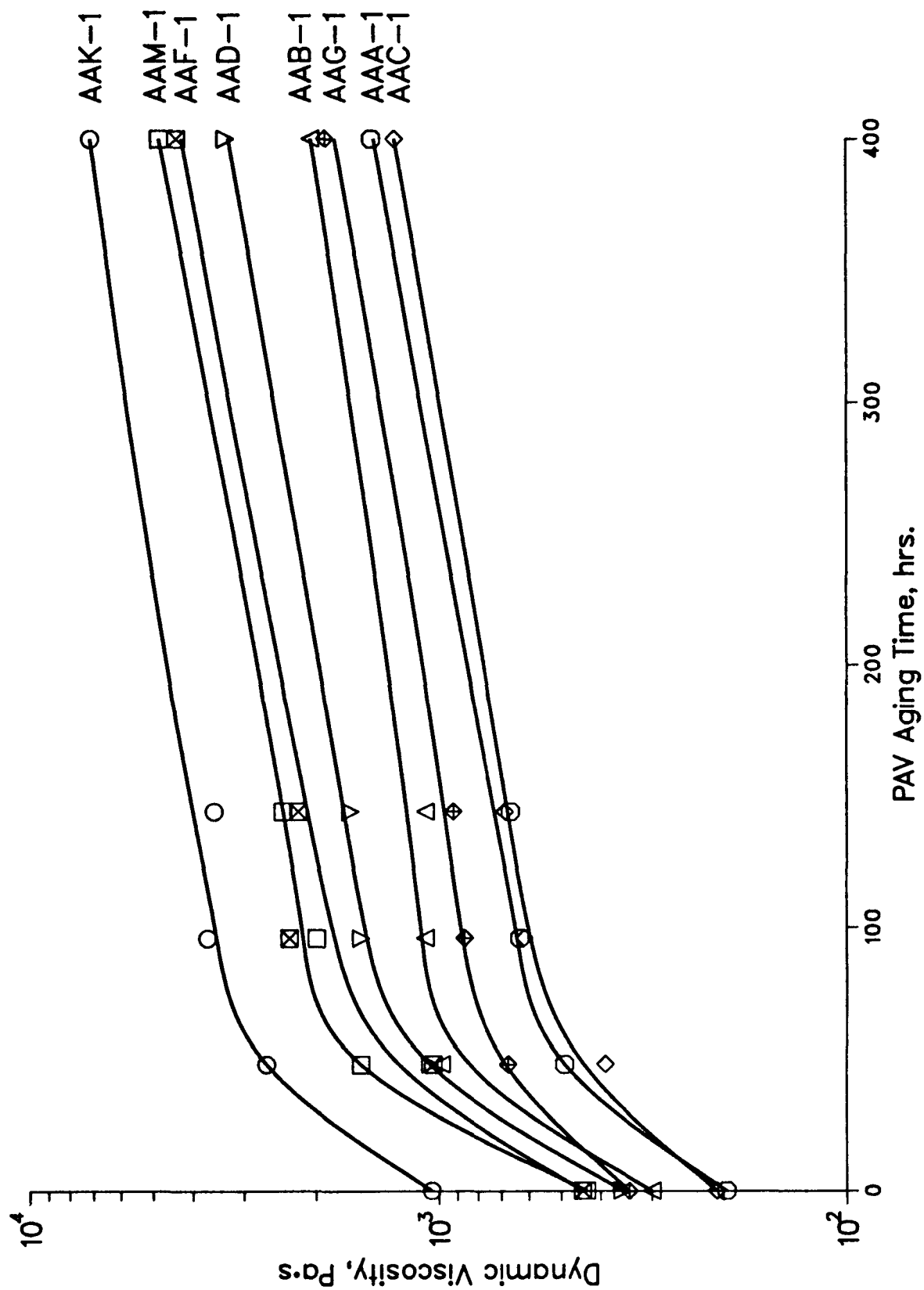


Figure 8.7 Kinetic Aging Plot of Core Asphalts Using the Pressure Air Vessel (PAV)  
Method at 2.07 MPa, 60°C

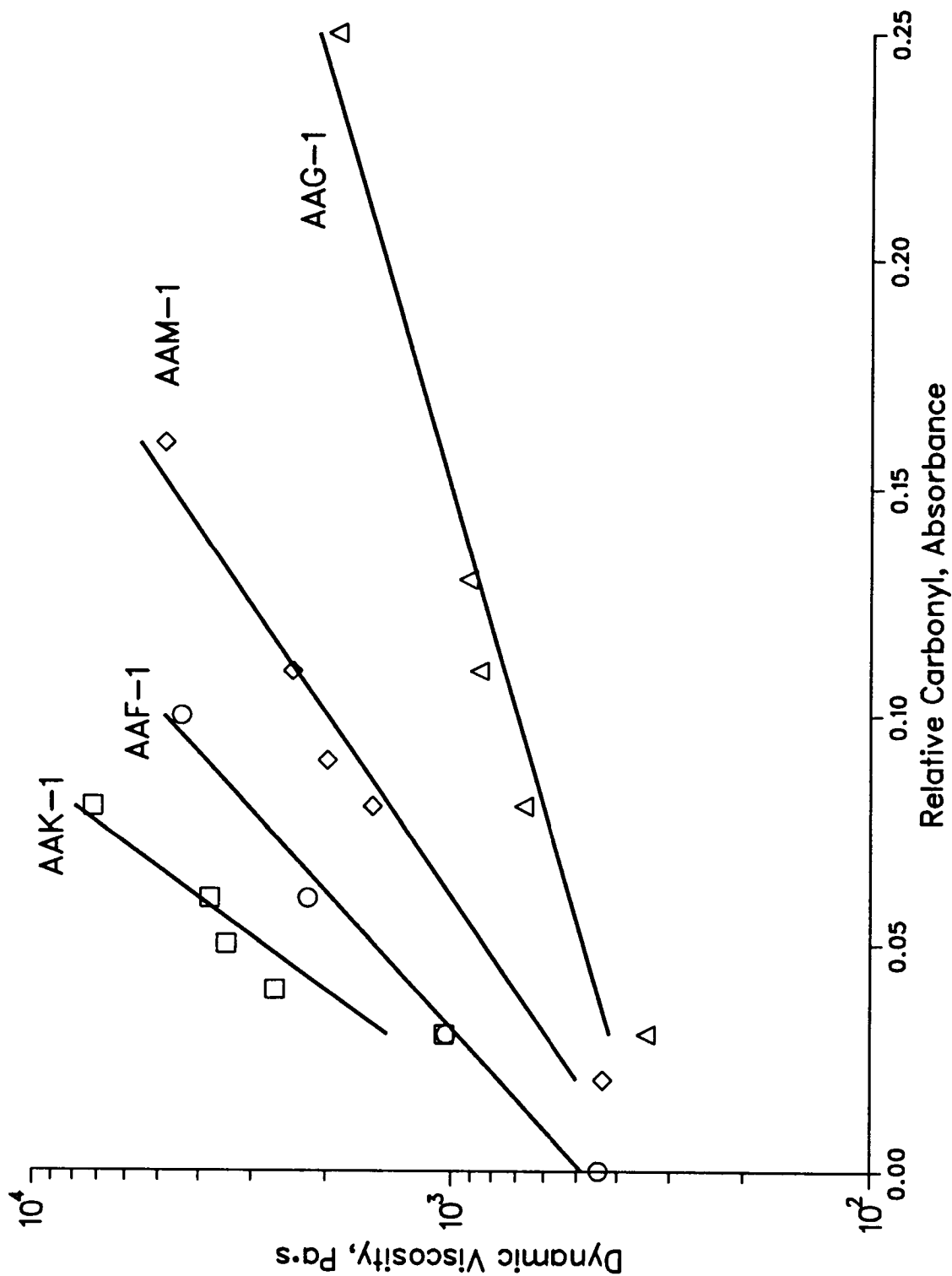


Figure 8.8 Sensitivity of Core Asphalts AAF-1, AAG-1, AAK-1, and AAM-1 to Carbonyl (Ketone) Produced During PAV Aging at 2.7 MPa, 60°C

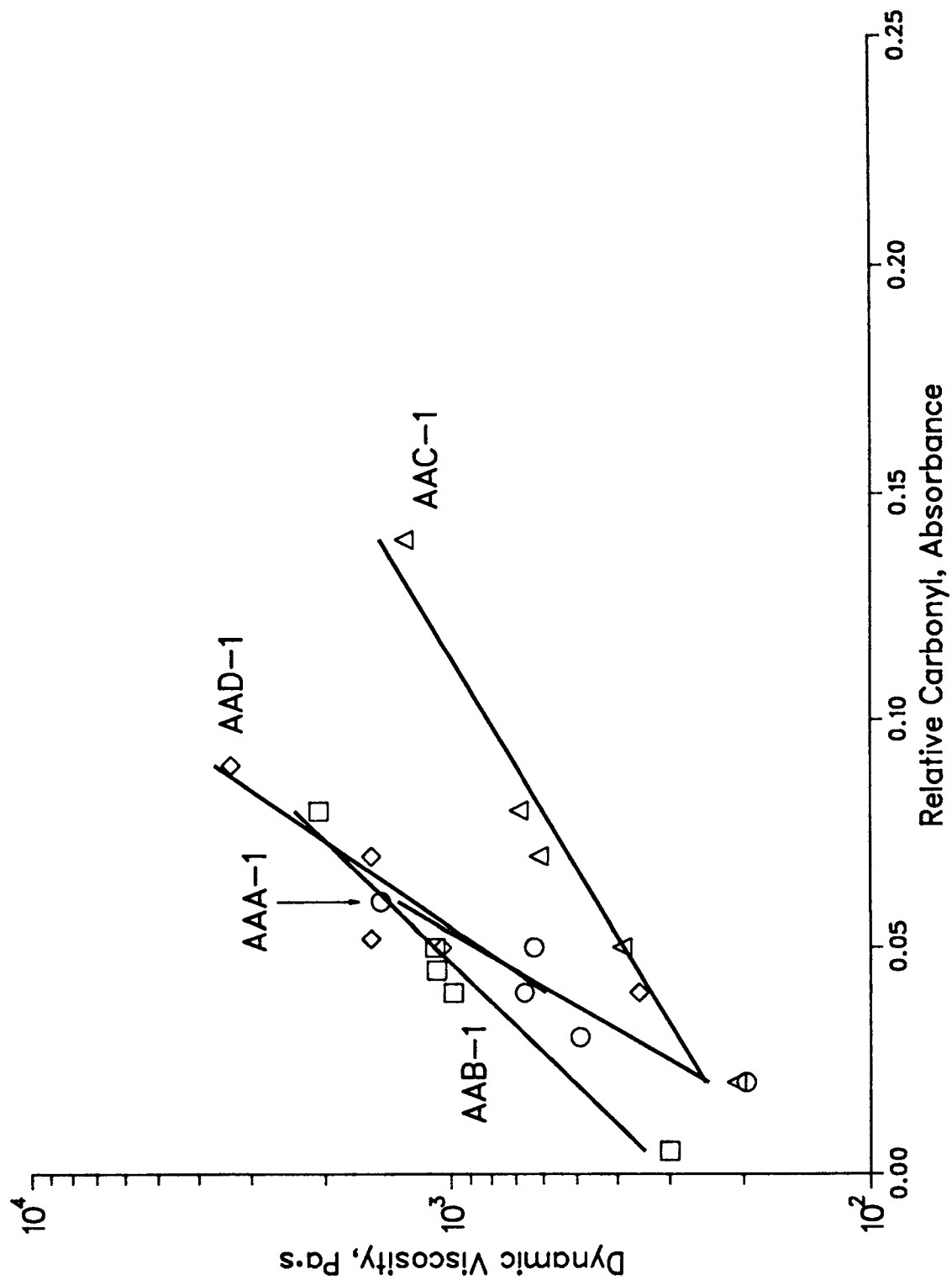
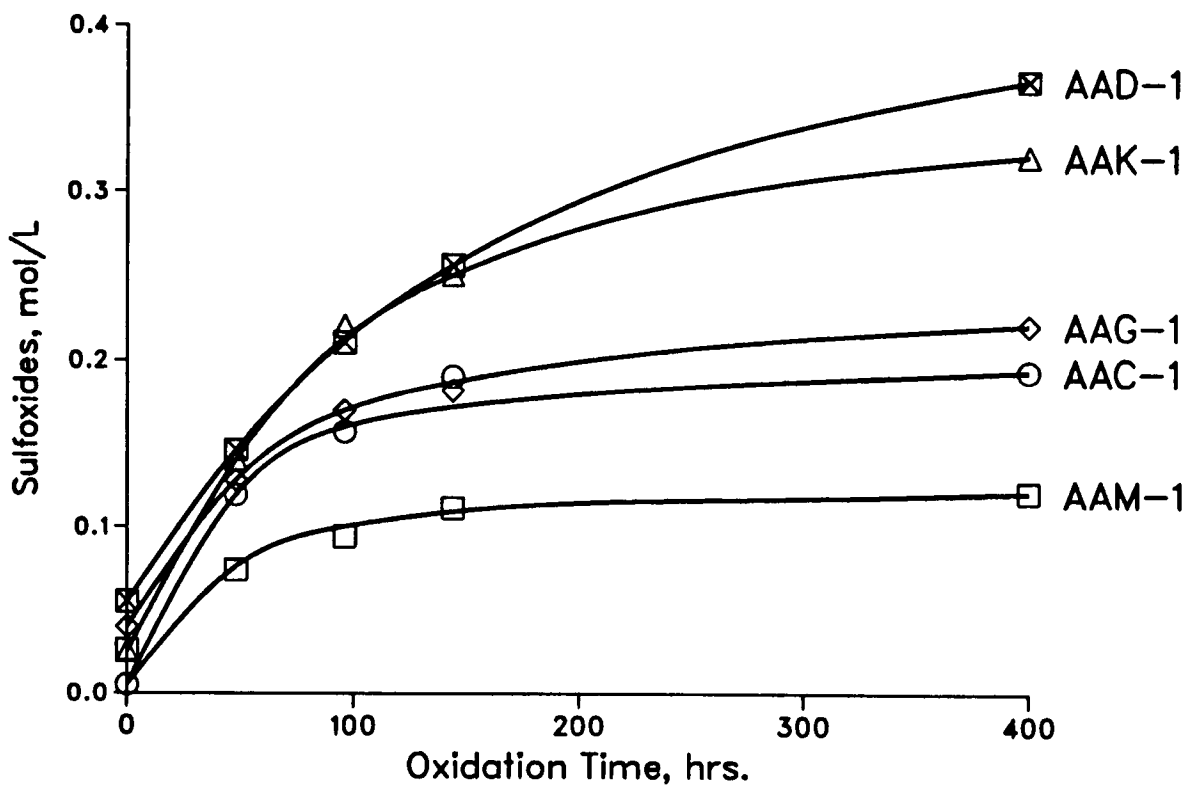
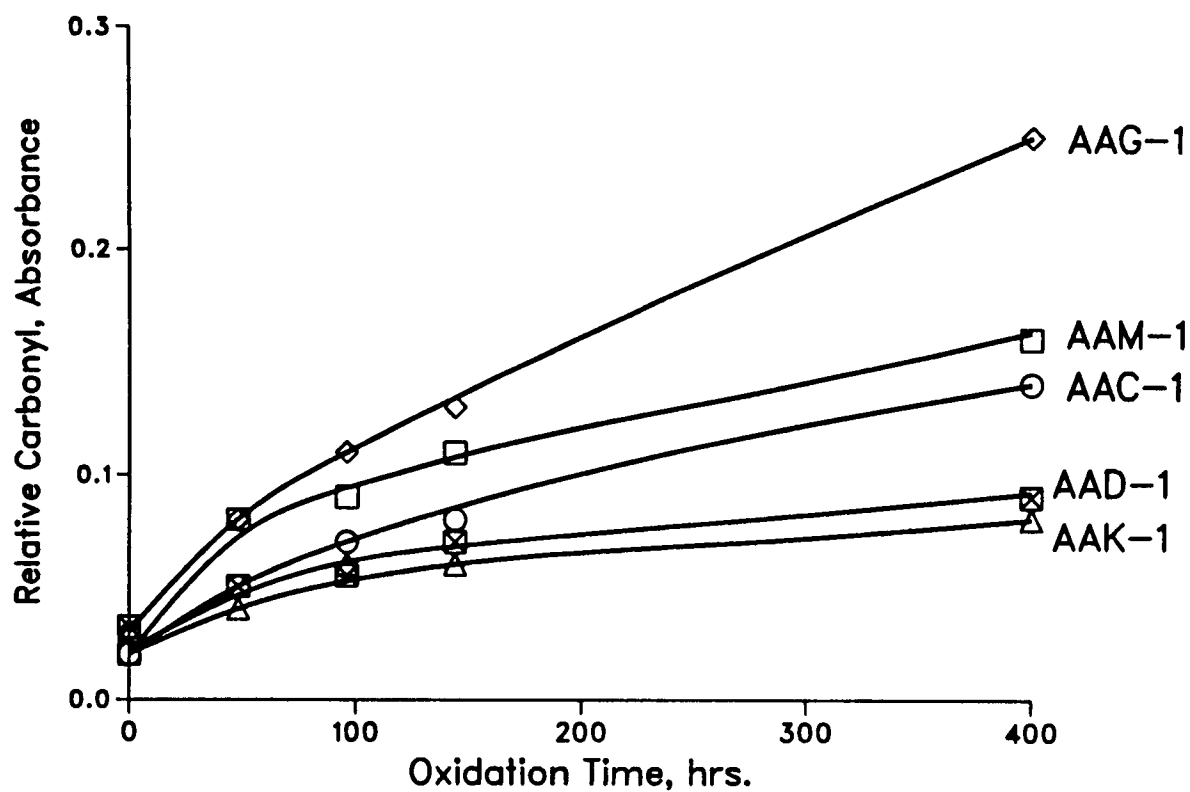


Figure 8.9 Sensitivity of Core Asphalts AAA-1, AAB-1, AAC-1, and AAD-1 to Carbonyl (Ketone) Produced During PAV Aging at 2.7 MPa, 60°C



**Figure 8.10** Oxidation Products Formed in Selected Core Asphalts as a Function of Time During PAV Aging at 60°C

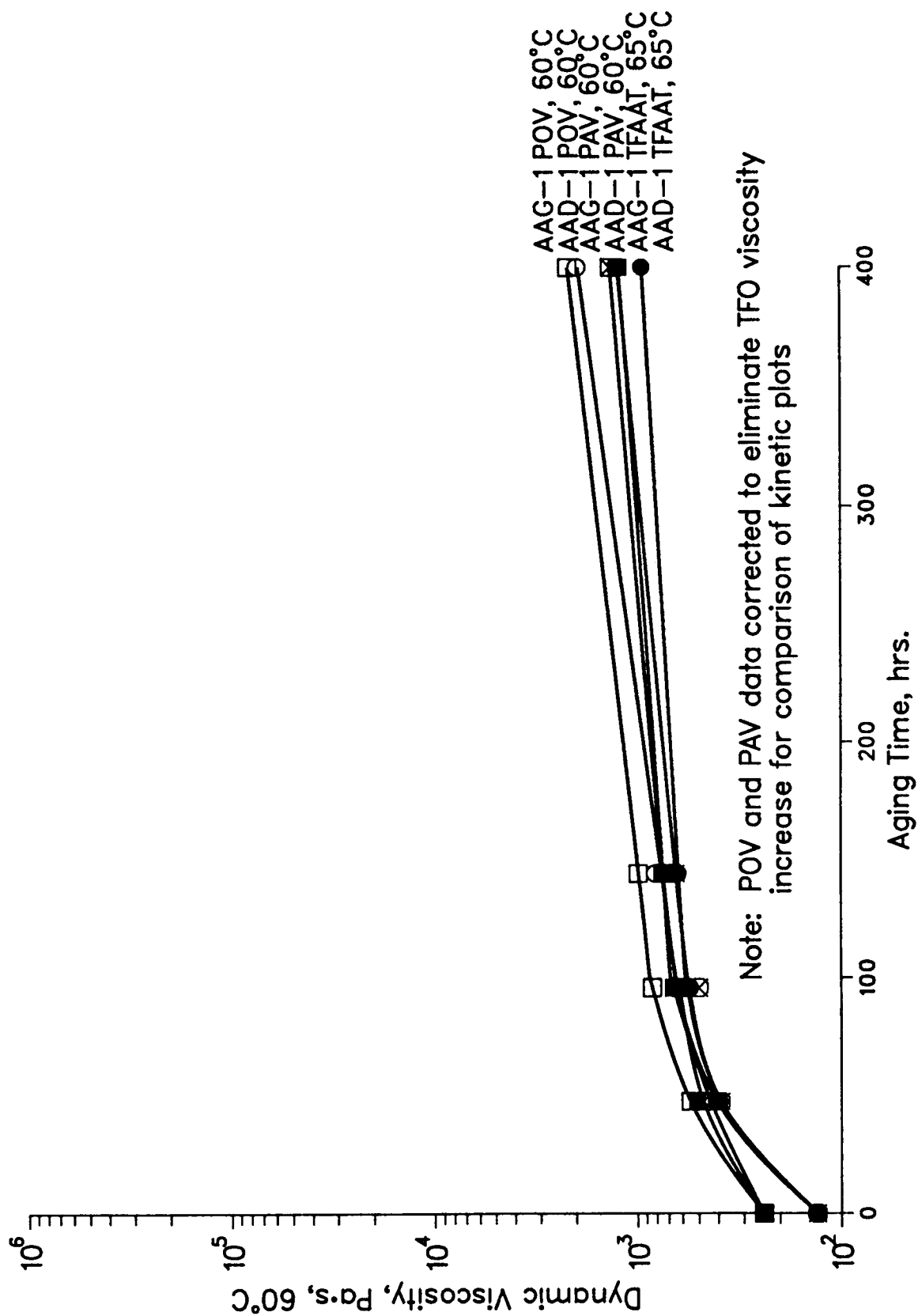


Figure 8.11 Comparison of Low-Temperature Aging Kinetics of Asphalts AAD-1 and AAG-1 Using the POV, PAV, and TFAAT Methods

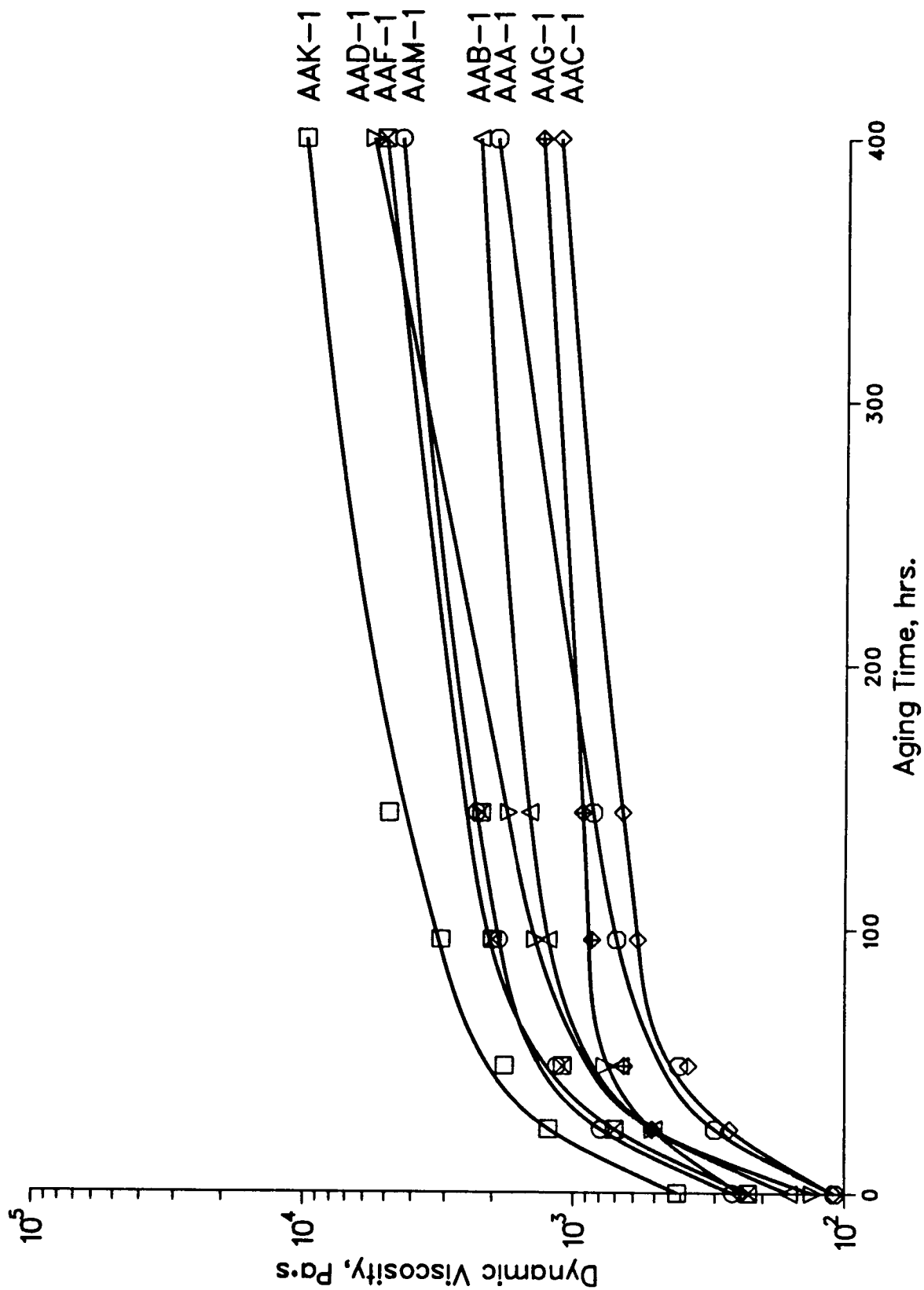


Figure 8.12 Aging Kinetics of Core Asphalts Using the TFAAT Method at 85°C



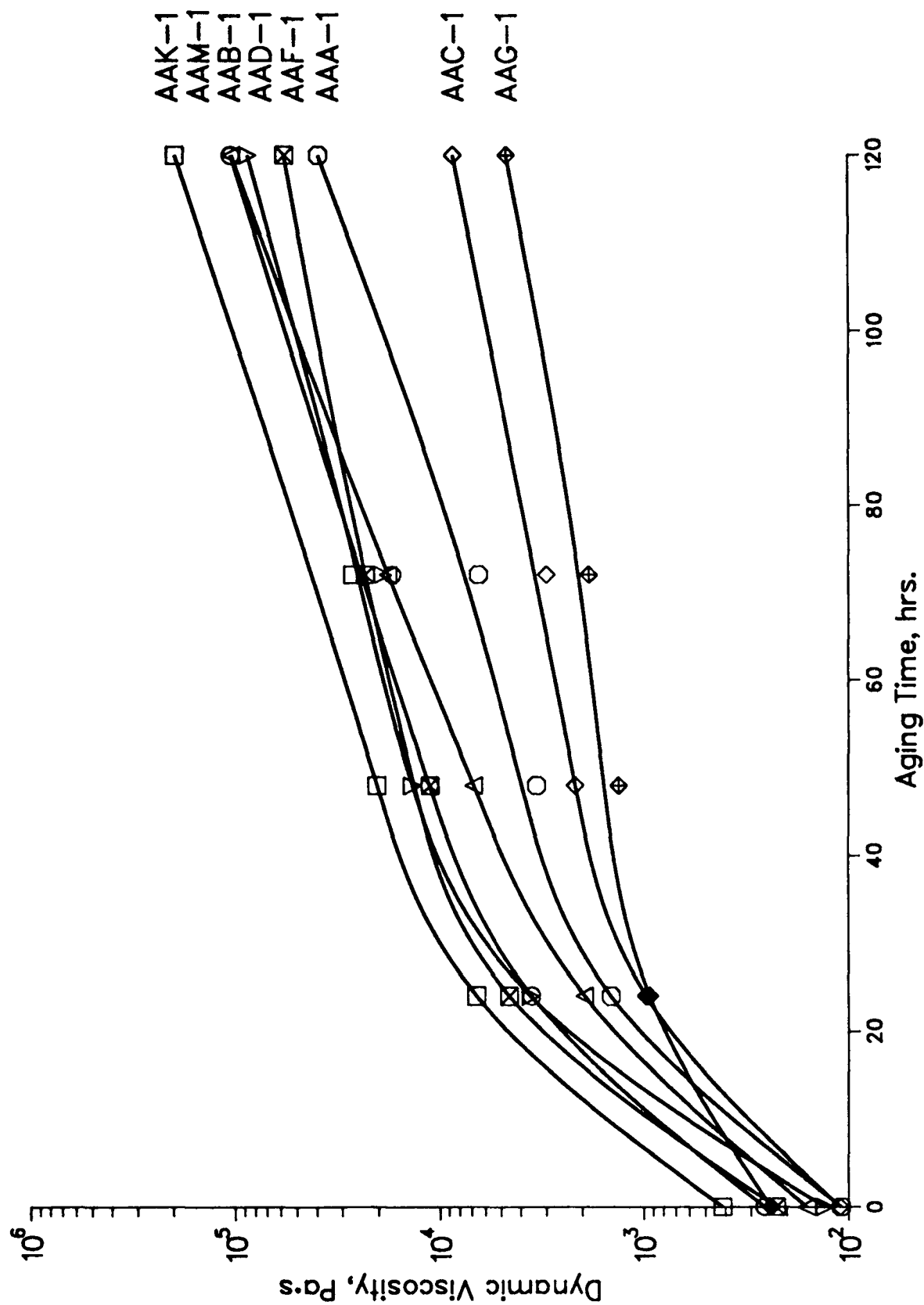


Figure 8.13 Aging Kinetics of Core Asphalts Using the TFAAT Method of 113°C

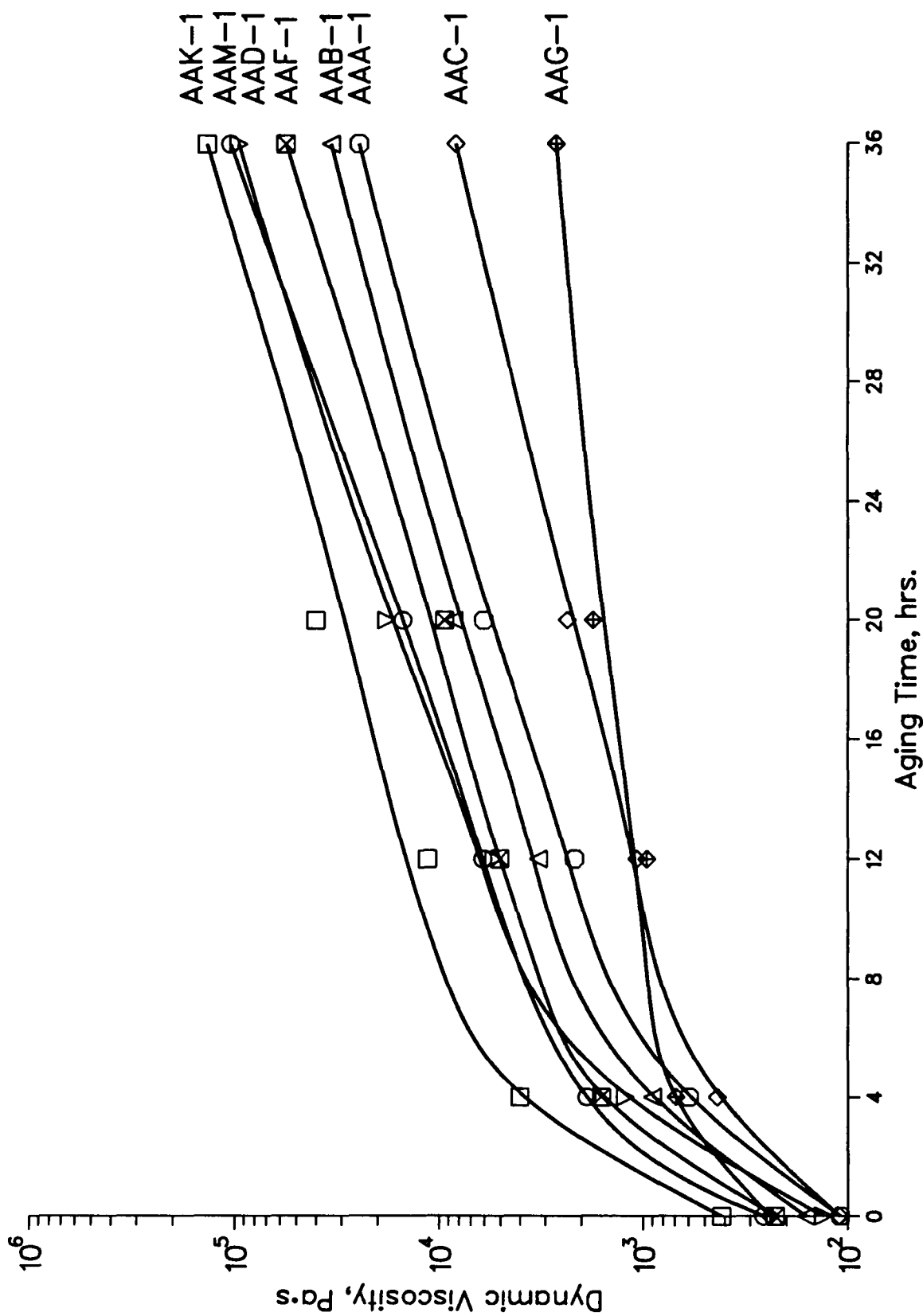
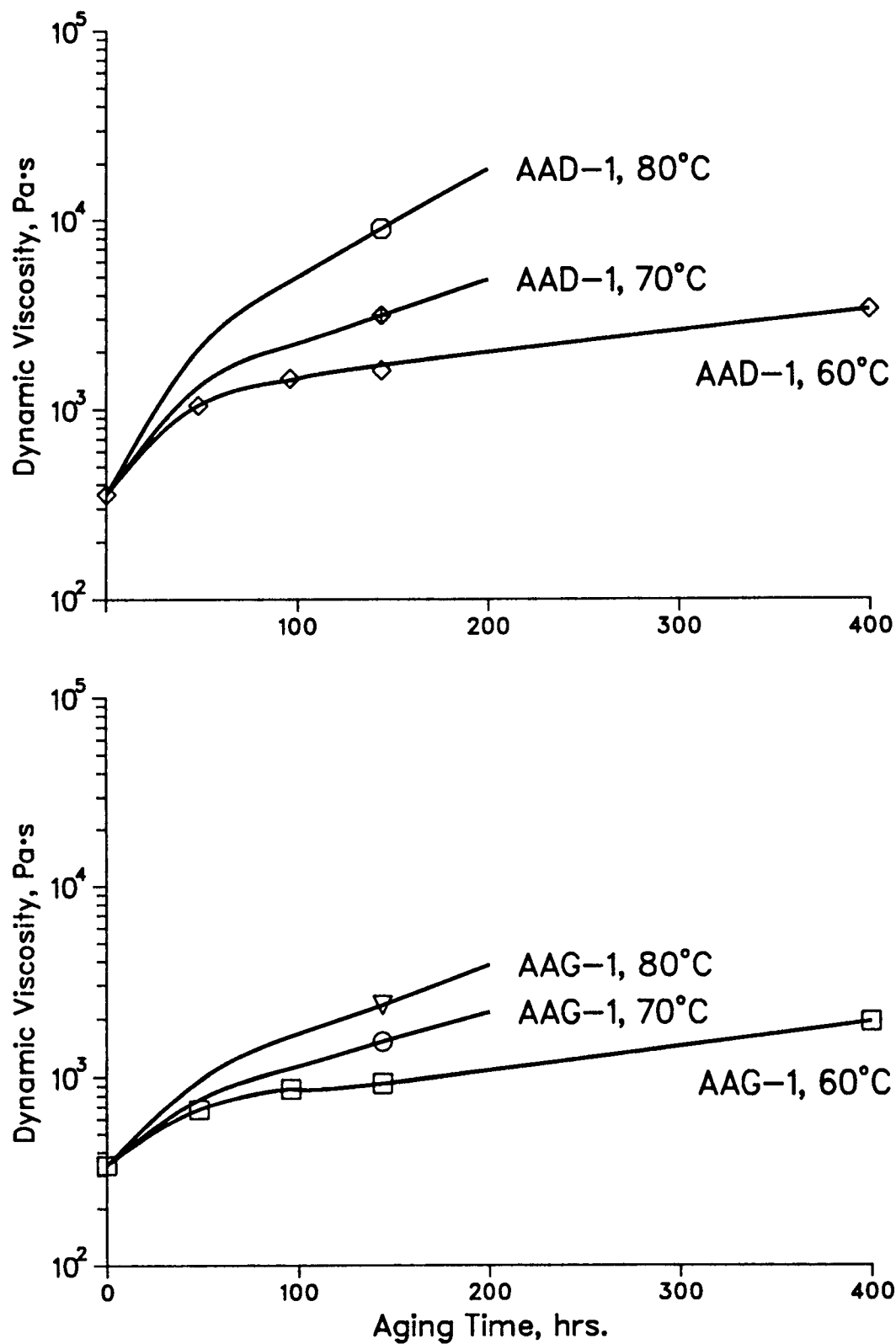


Figure 8.14 Aging Kinetics of Core Asphalts Using the TFAAT Method at 130°C



**Figure 8.15 PAV Aging of Selected Prior TFO-Aged Core Asphalts at Different Temperatures**

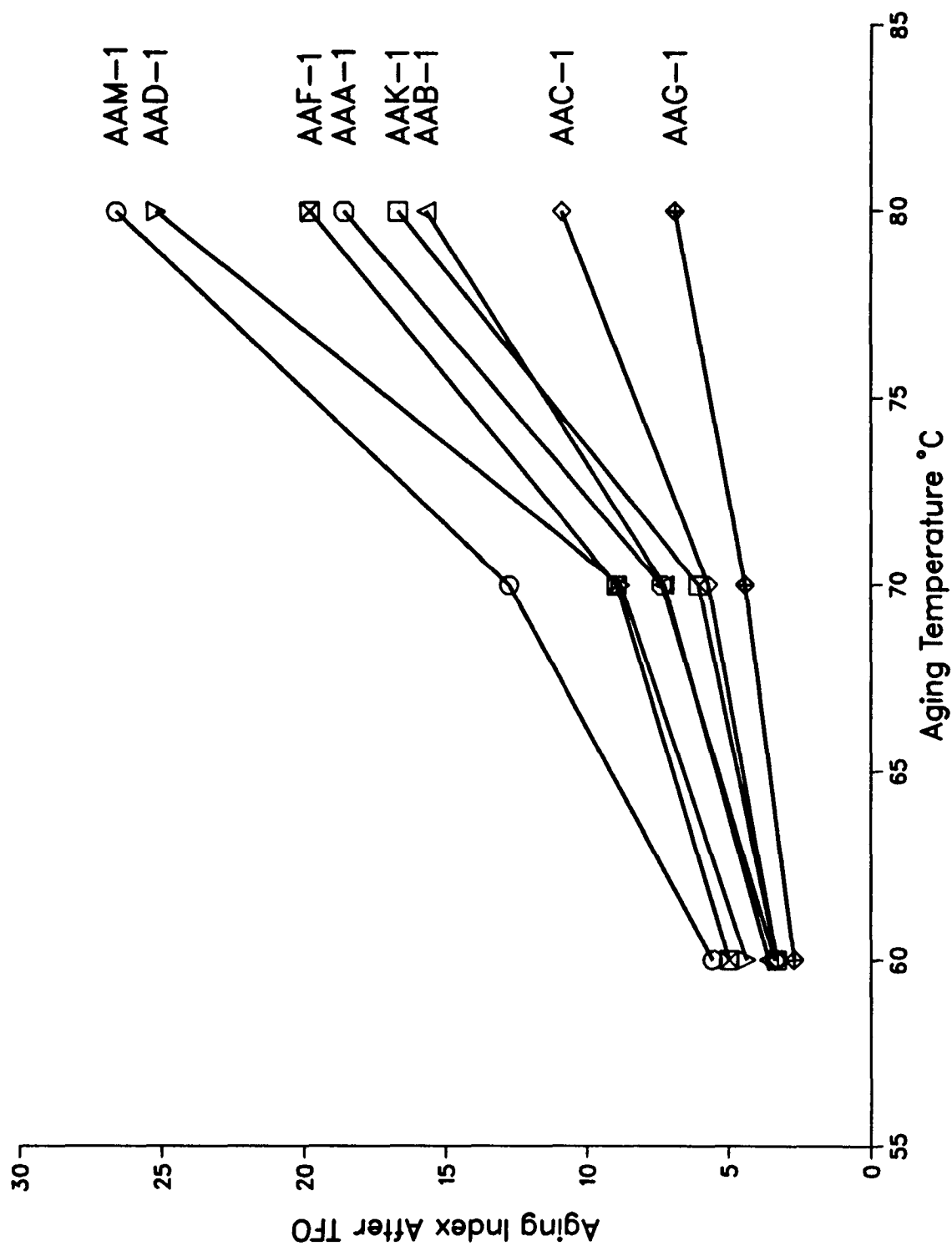


Figure 8.16 Aging Indices After TFO of Core Asphalts Aged by the PAV Method at Different Temperatures

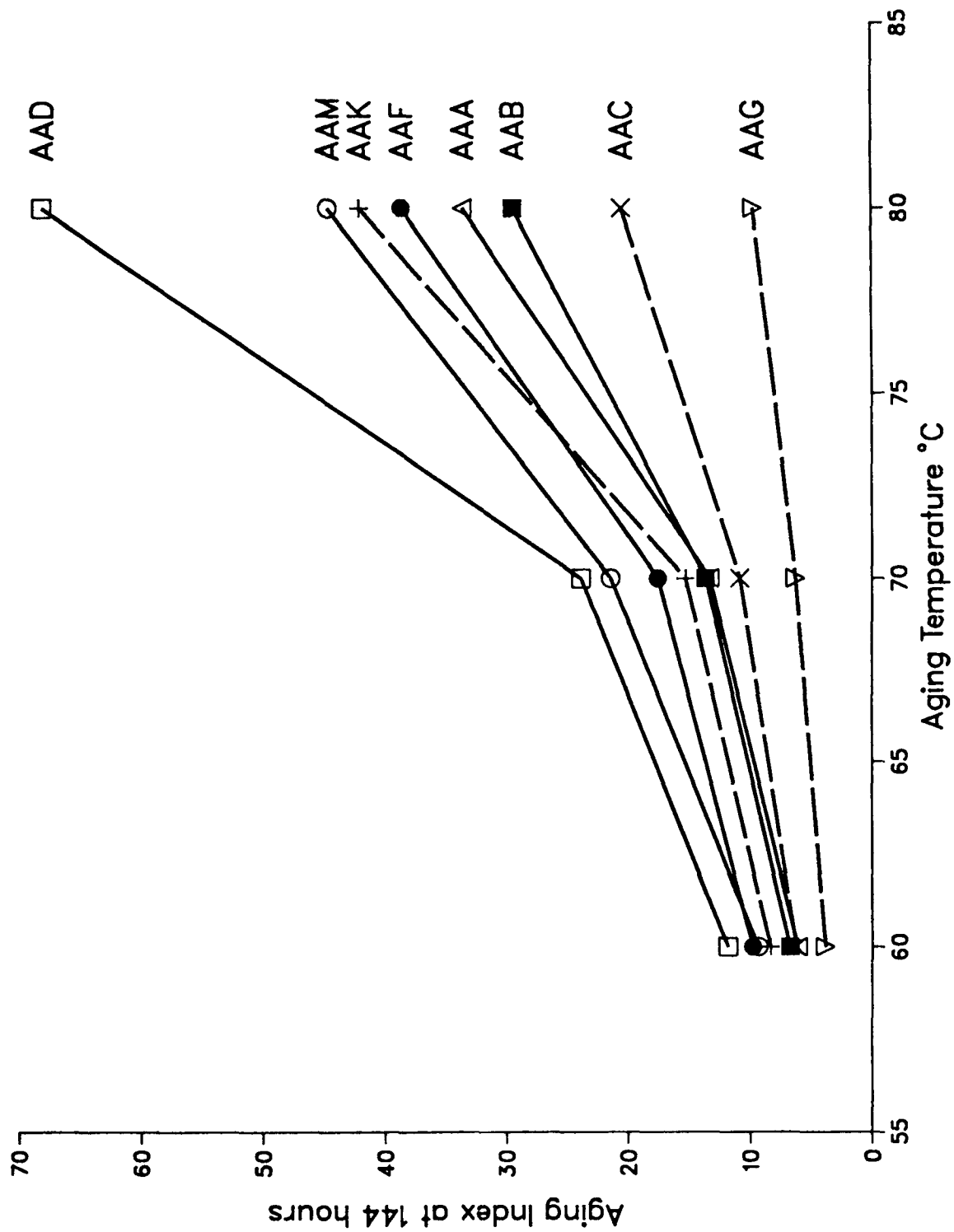


Figure 8.17 Core Asphalt 144-Hour Aging Indices at Three Temperatures

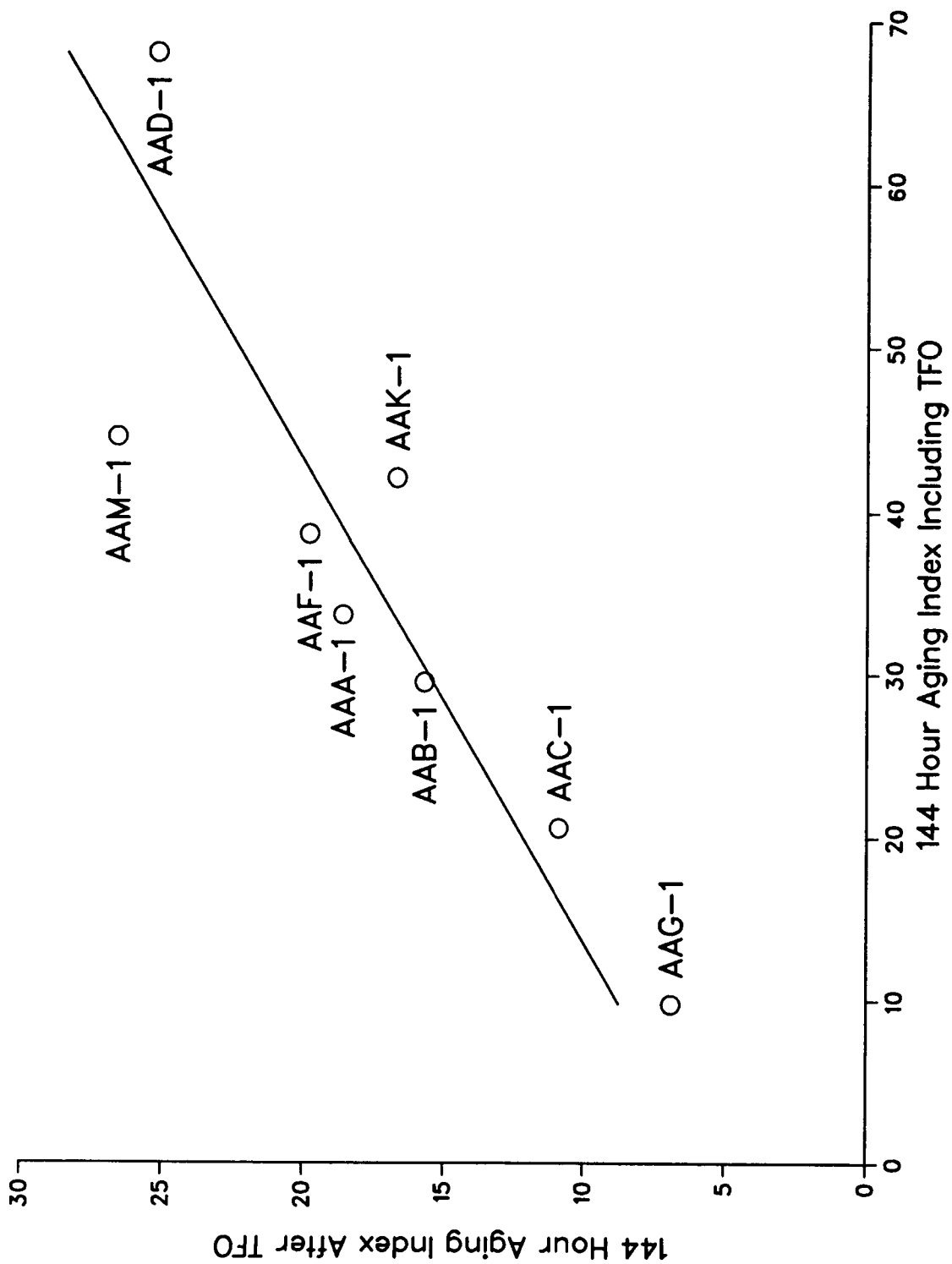


Figure 8.18 Comparison of 80°C PAV 144-Hour Aging Indices, Including and Excluding TFO Aging

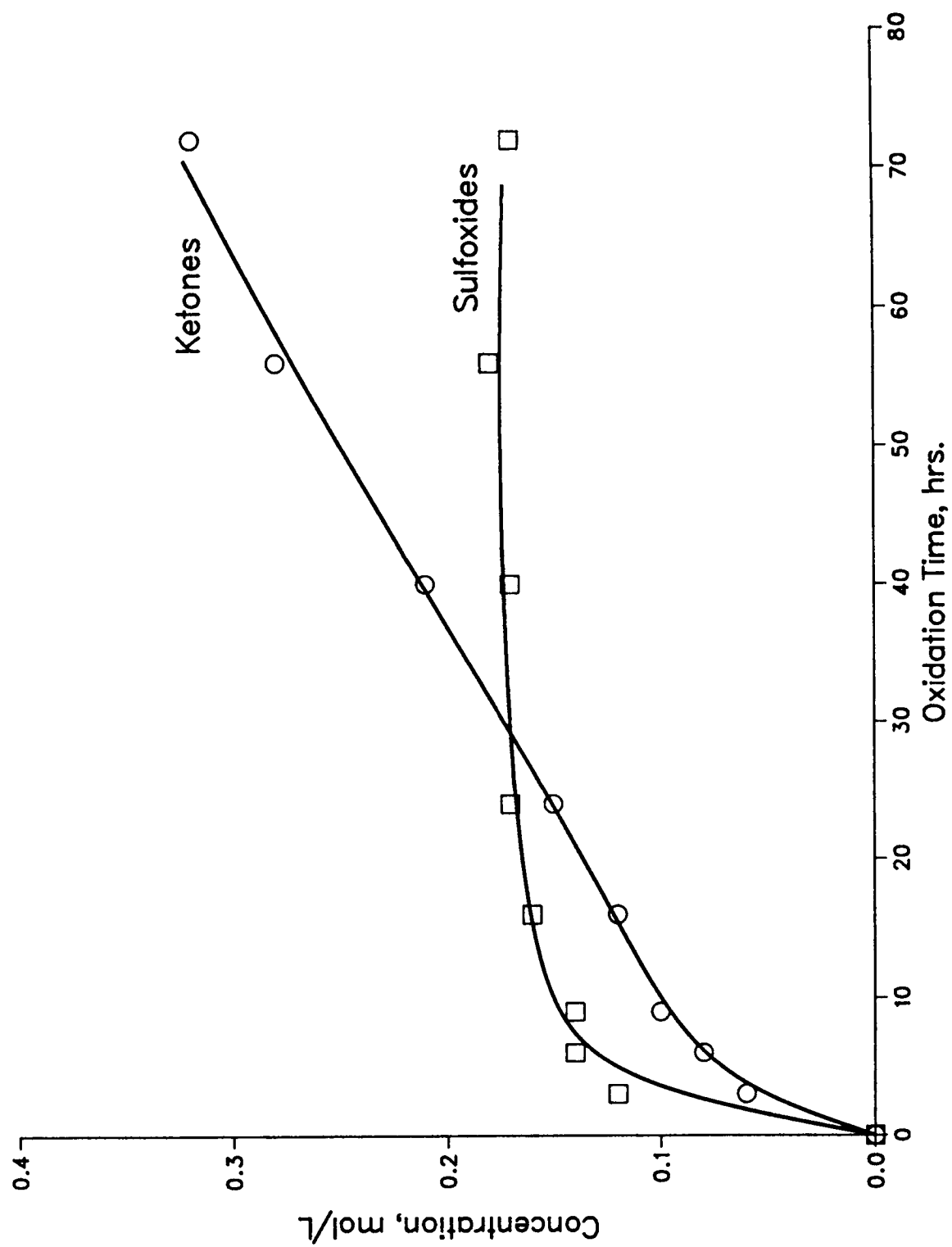
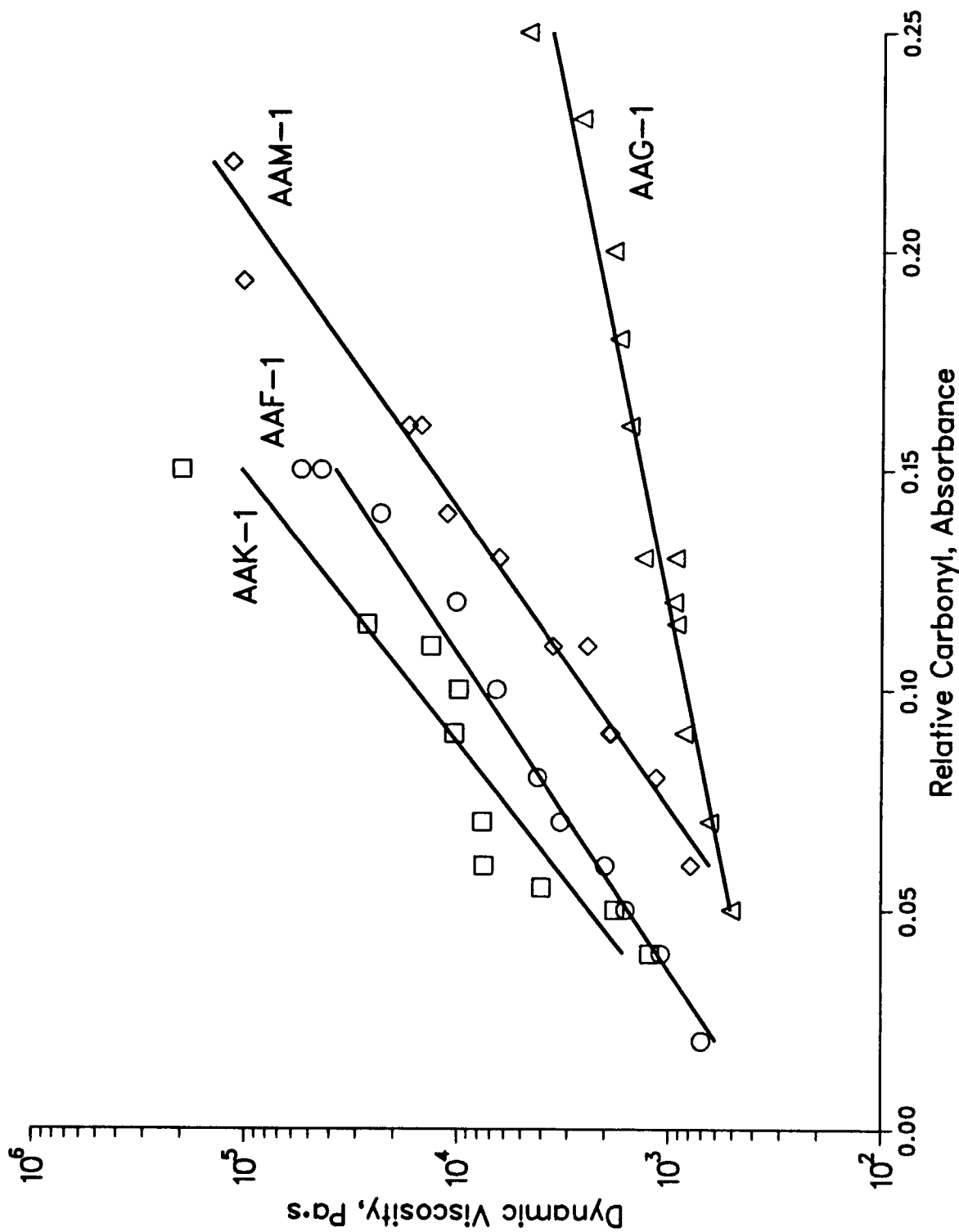


Figure 8.19 TFAAT Oxidation of Asphalt AAG-1 at 113°C



**Figure 8.20** Relationship Between Carbonyls Formed and Dynamic Viscosity Increase Using the TFAAT Method at 85°, 113°, and 130°C for Core Asphalts AAF-1, AAG-1, AAK-1, and AAM-1



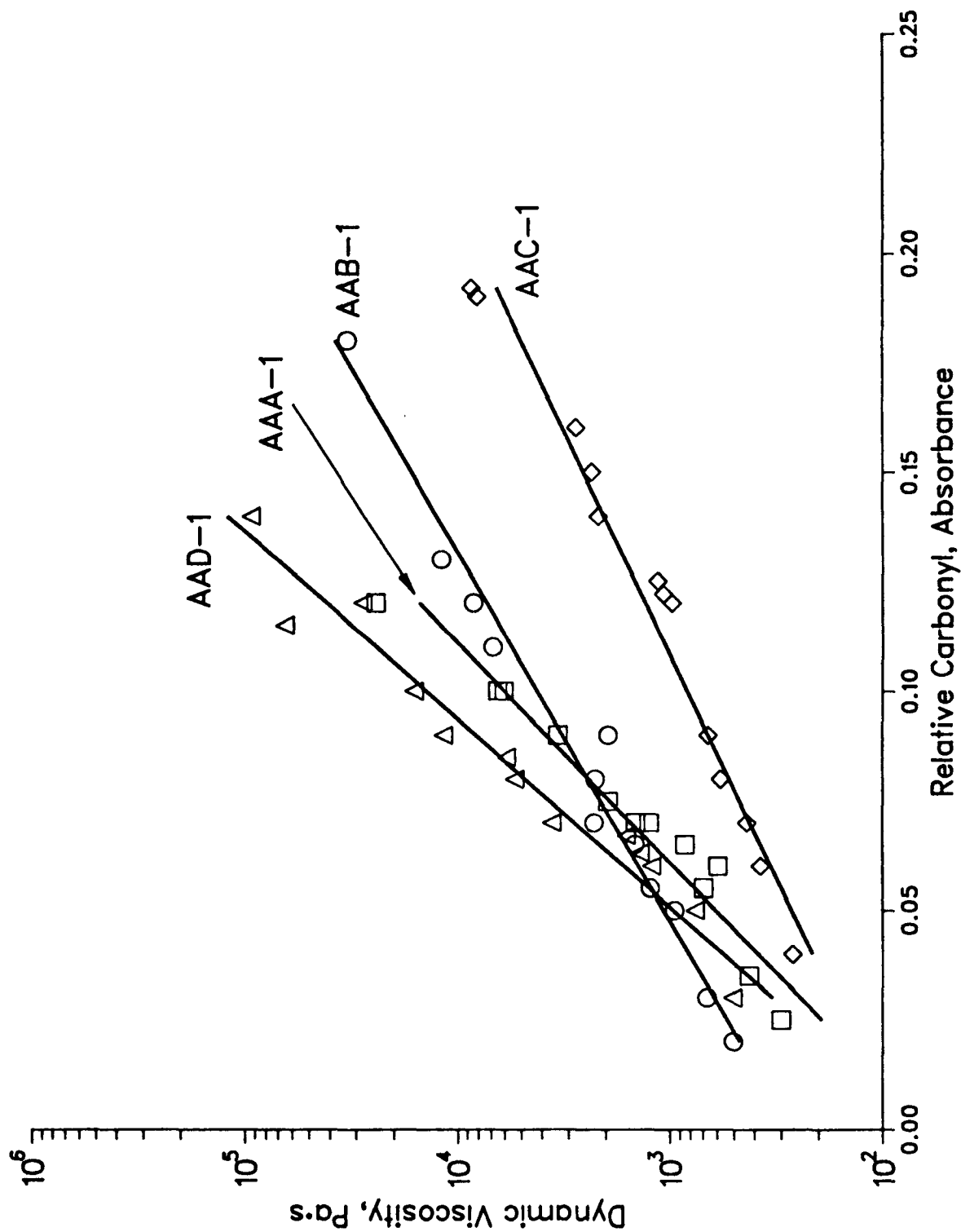


Figure 8.21 Relationship Between Carbonyls Formed and Dynamic Viscosity Increase Using the TFAAT Method at 85°, 113°, and 130°C for Core Asphalts AAA-1, AAB-1, AAC-1, and AAD-1

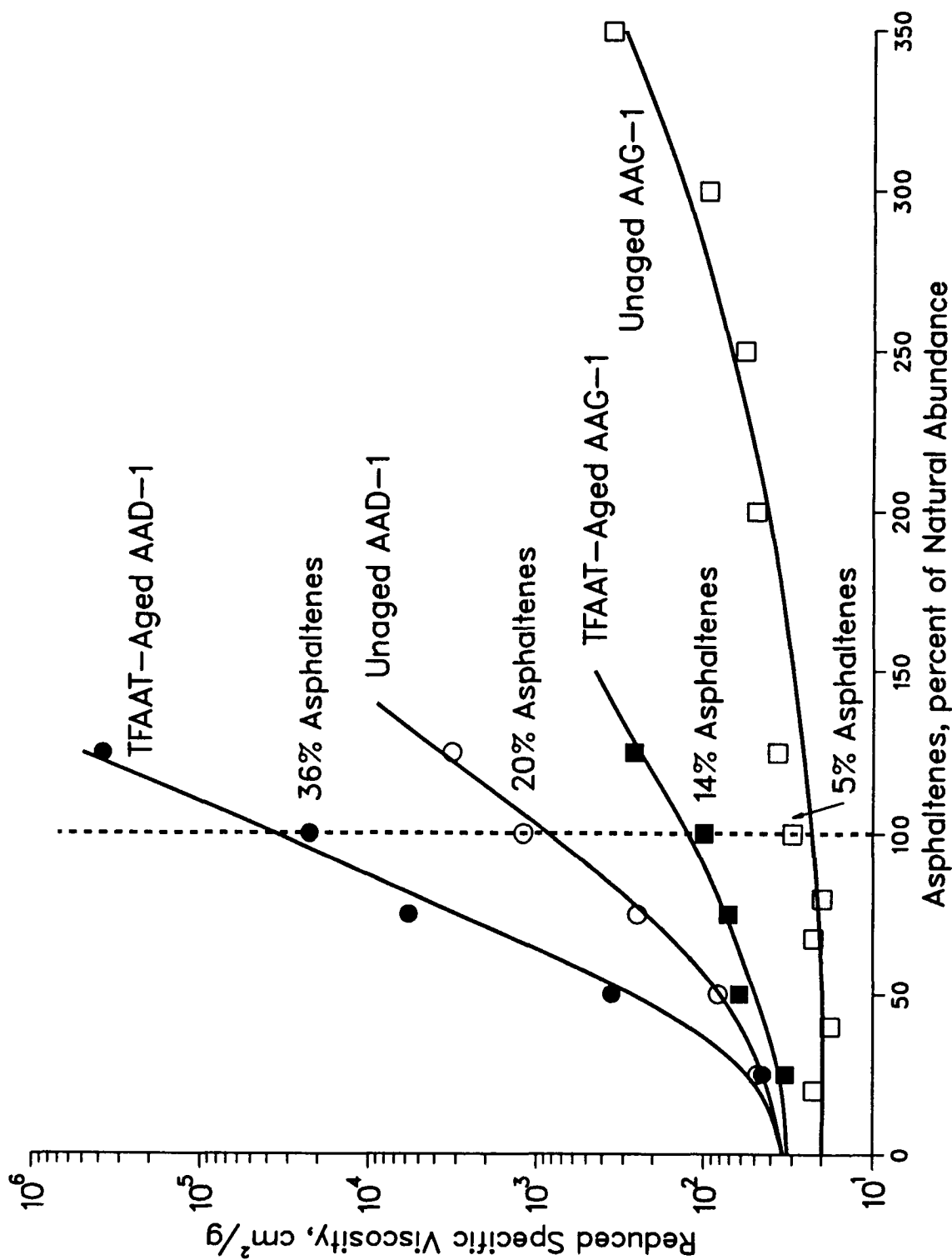


Figure 8.22 Reduced Specific Viscosity Measurements at 45°C for Asphalts AAD-1 and AAG-1 Before and After TFAAT Aging at 113°C, 72 hours

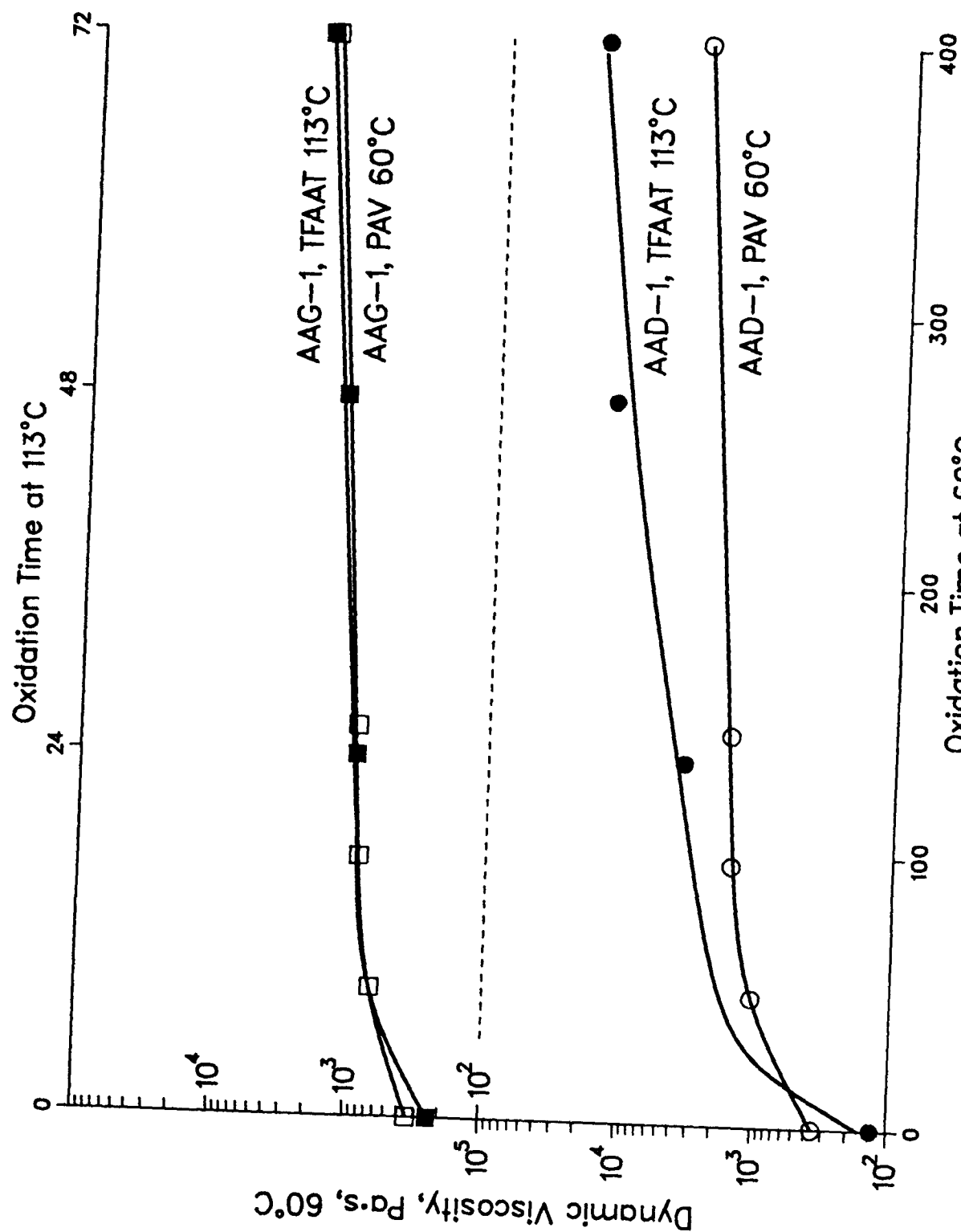
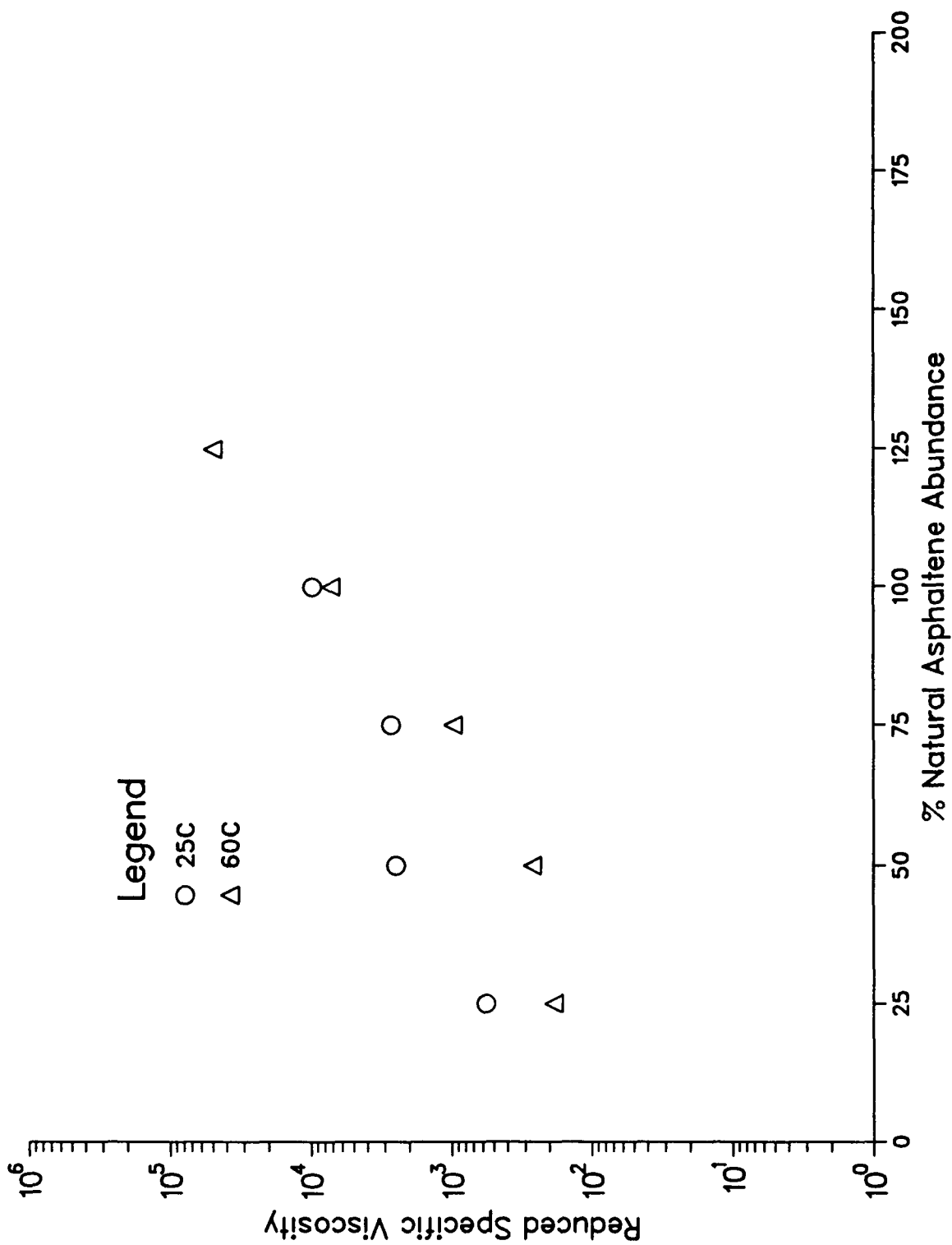


Figure 8.23 Effects of Temperature on the Aging Characteristics of Asphalts AAG-1 and AAD-1



Legend

○ 25C

△ 60C

Figure 8.24 Reduced Specific Viscosities at Two Temperatures for TFAAT-Aged AAA-1

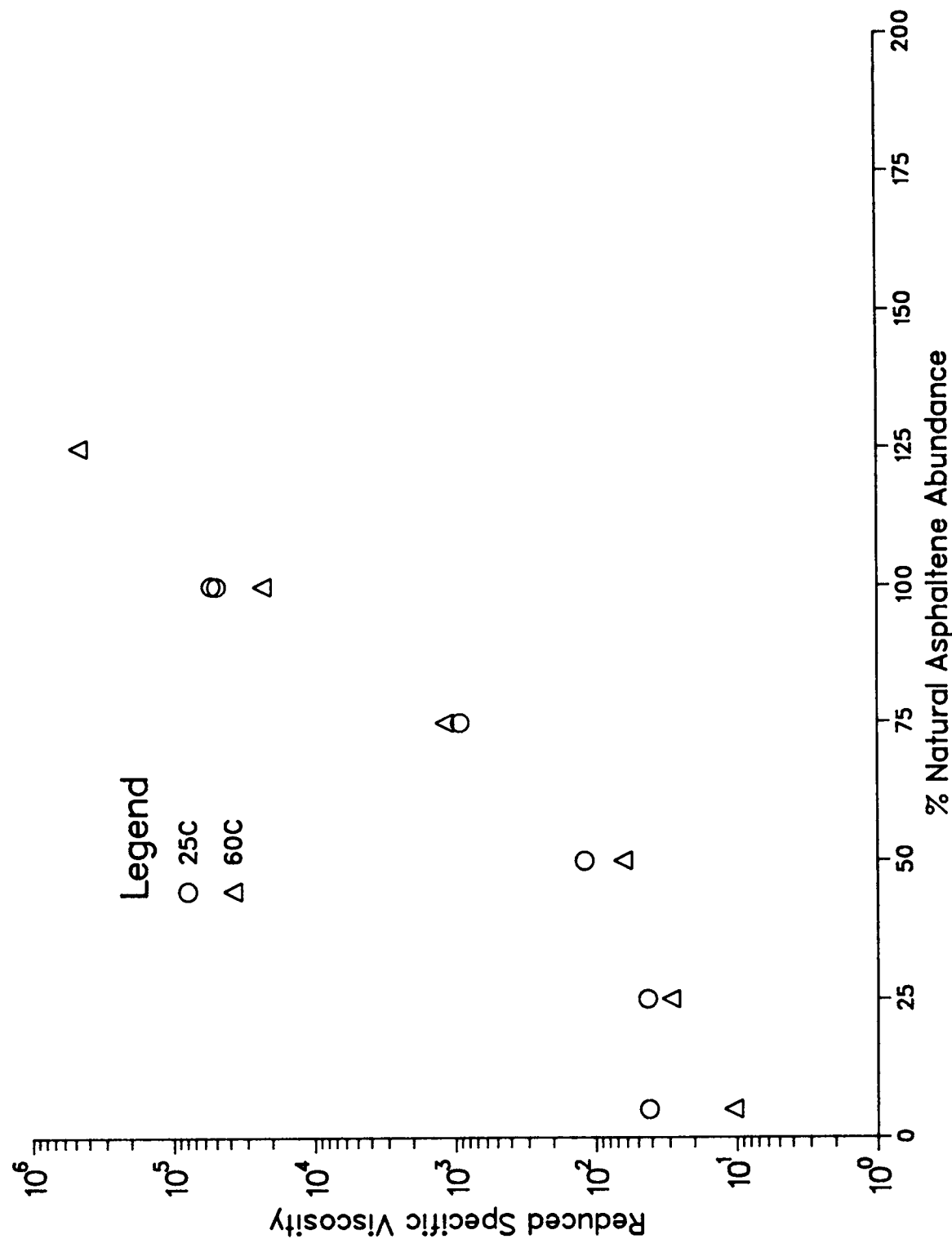


Figure 8.25 Reduced Specific Viscosities at Two Temperatures for TFAAT-Aged AAB-1

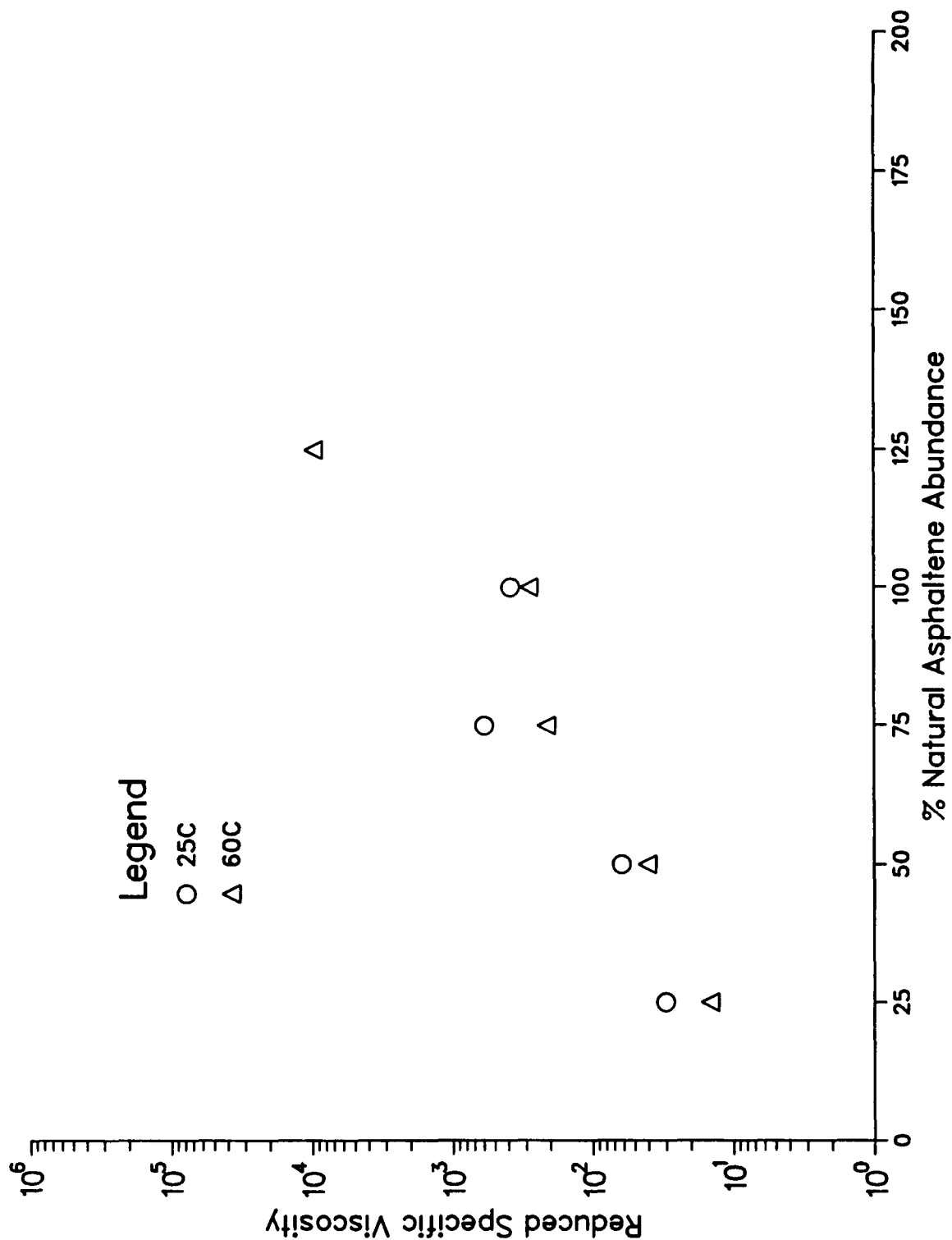


Figure 8.26 Reduced Specific Viscosities at Two Temperatures for TFAAT-Aged AAC-1

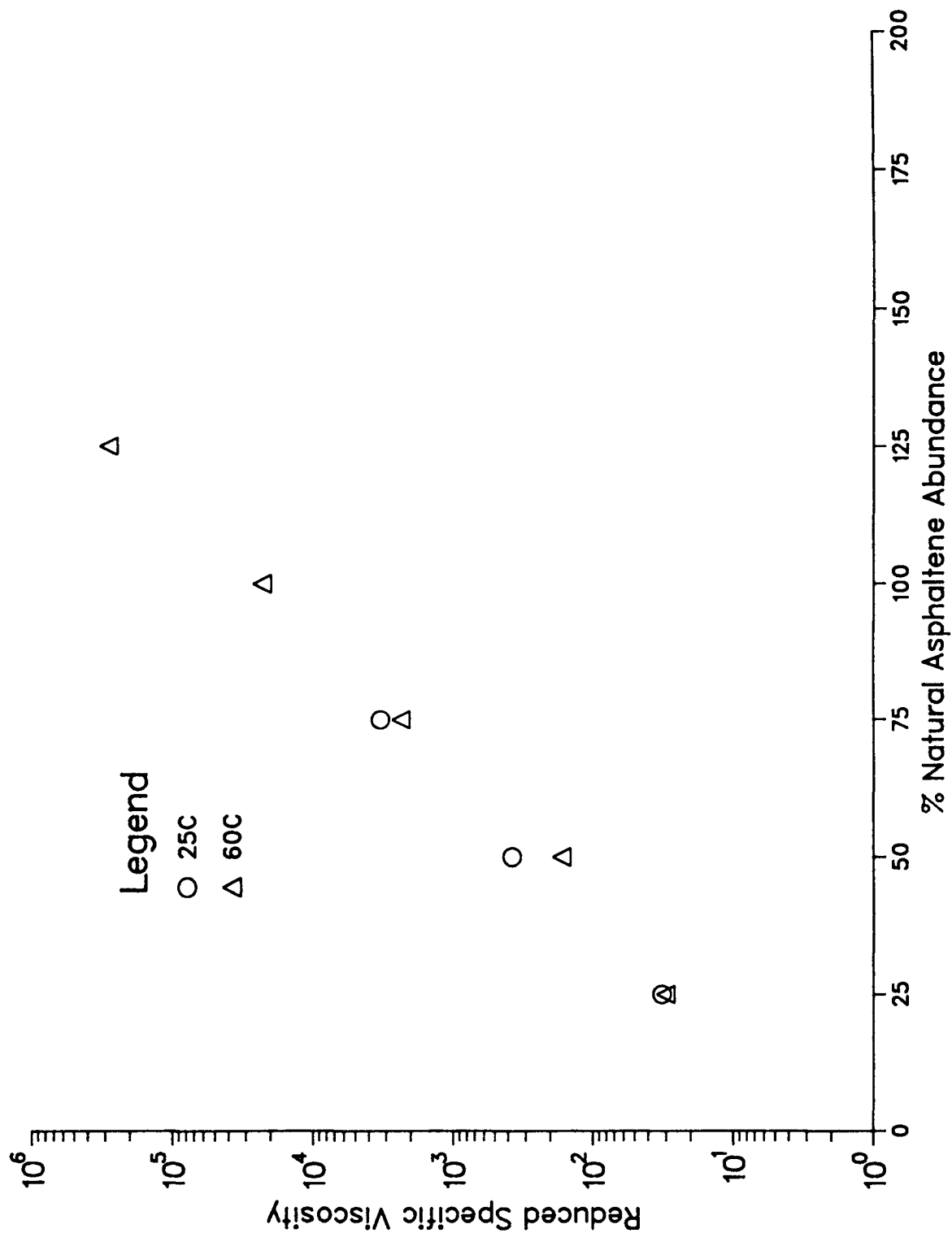


Figure 8.27 Reduced Specific Viscosities at Two Temperatures for TFAAT-Aged AAD-1

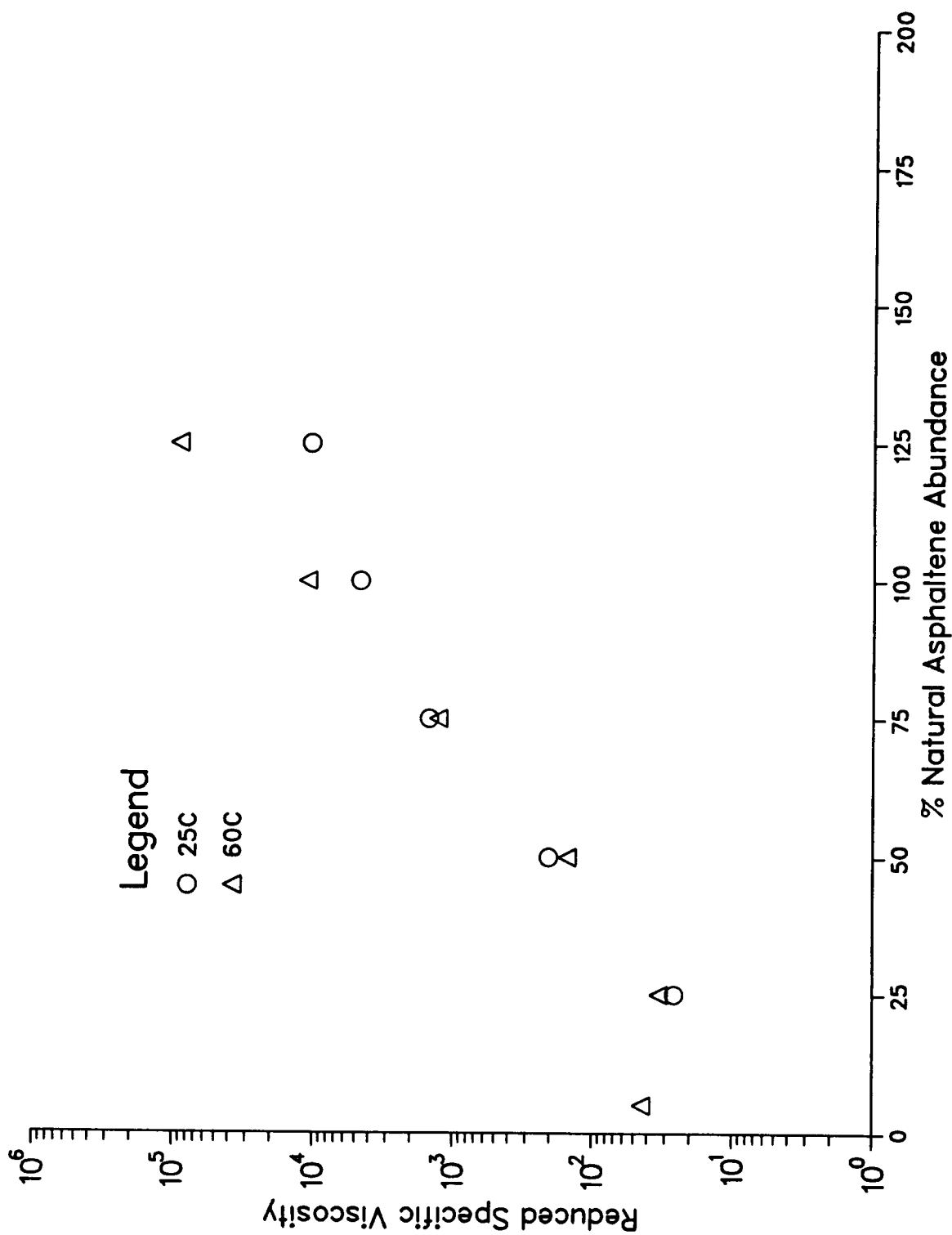


Figure 8.28 Reduced Specific Viscosities of Two Temperatures for TFAAT-Aged AAF-I



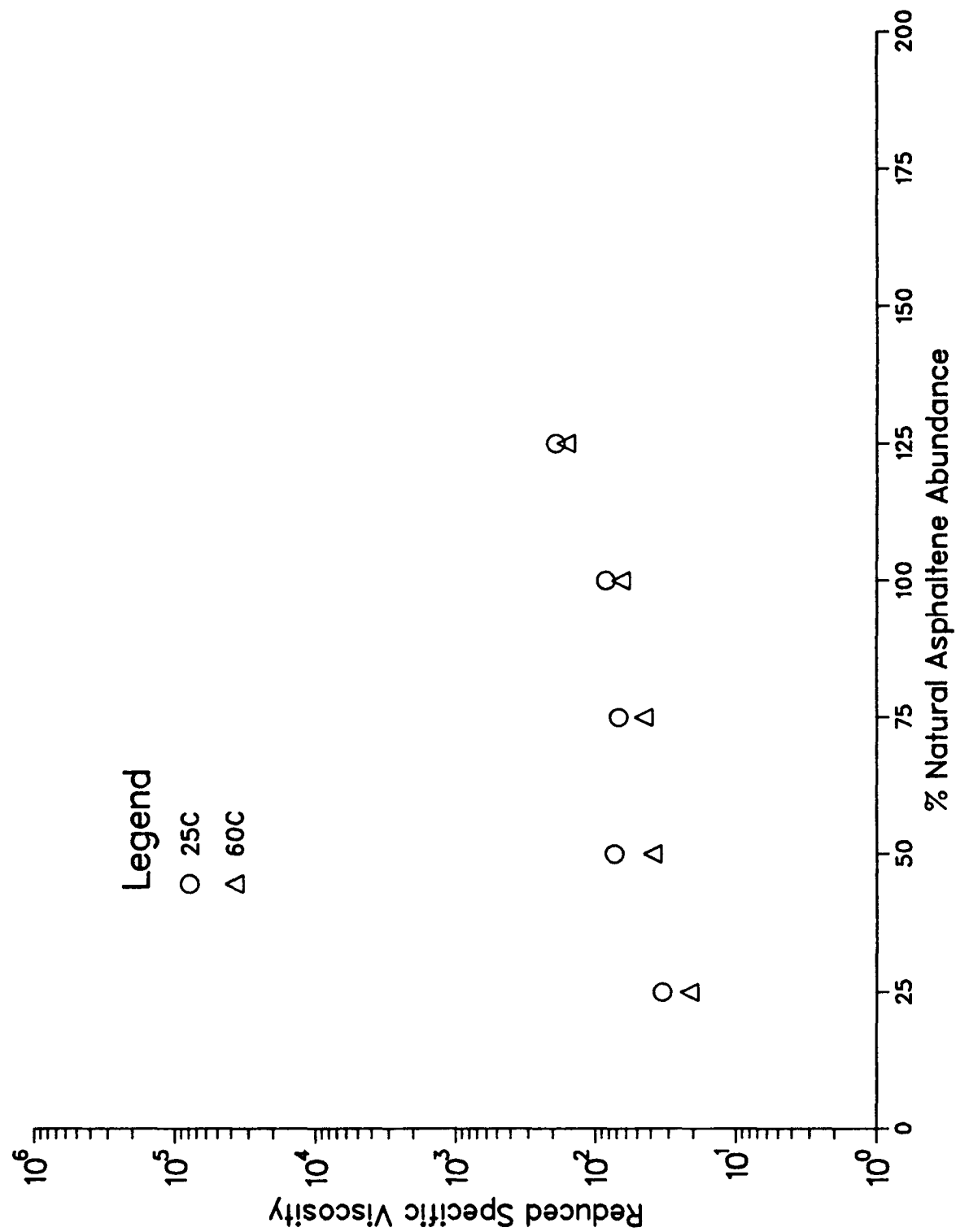


Figure 8.29 Reduced Specific Viscosities at Two Temperatures for TFAAT-Aged AAG-1

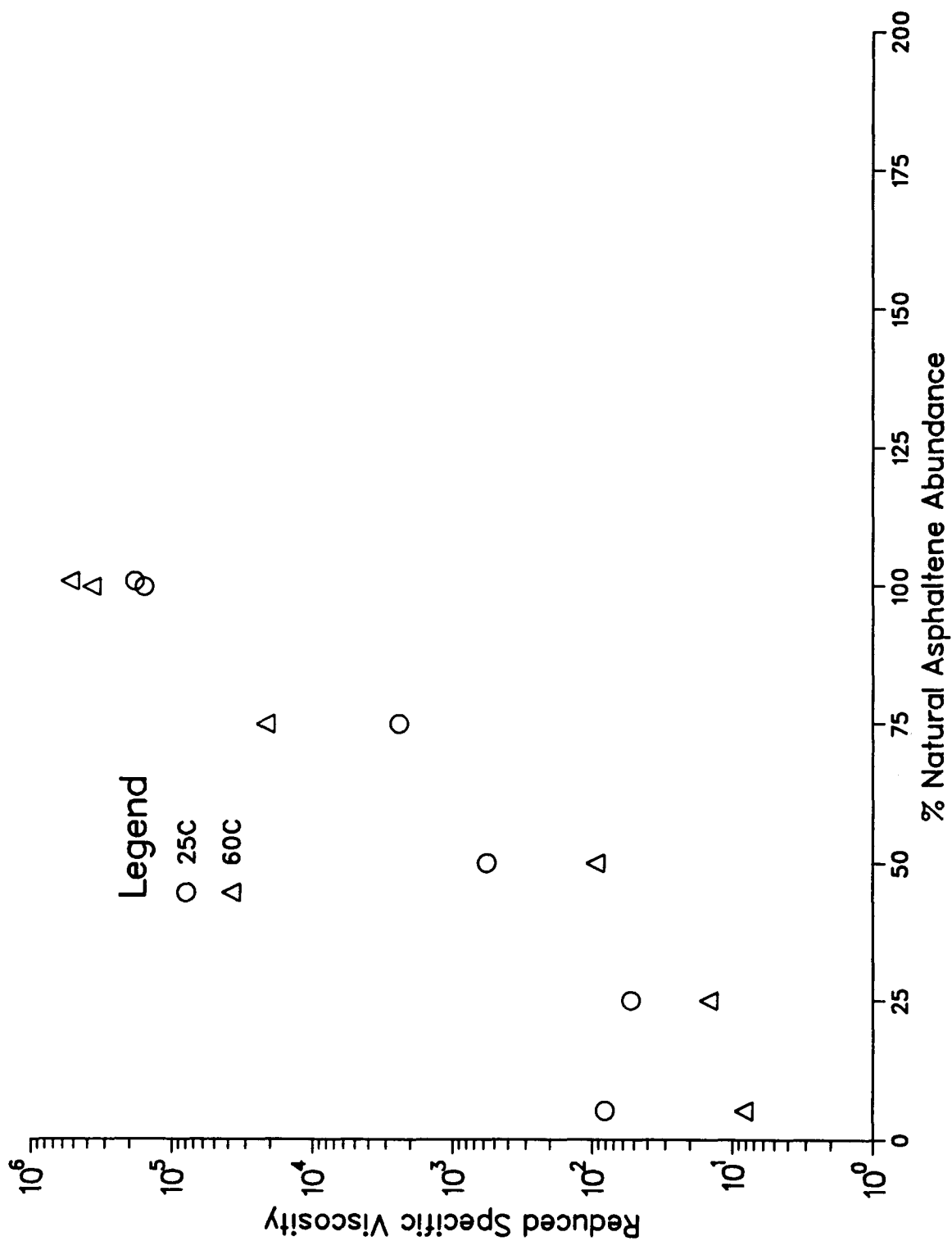


Figure 8.30 Reduced Specific Viscosities at Two Temperatures for TFAAT-Aged AAK-1

**Table 8.1    Change in Dynamic Shear Viscosity With Time During Aging of Asphalt AAD-1 and TFO-Oxidized AAD-1 in Oxygen Pressure Vessel at 60 °C, 300 psi**

Prior Treatment	Aging Time in Pressure Vessel, hr	Dynamic Shear Viscosity, <sup>1,2</sup> Pa · s, 60 °C, 0.1 rad/s
None	0	$1.3 \times 10^2$
	48	$8.4 \times 10^2$
	96	$2.0 \times 10^3$
	144	$3.2 \times 10^3$
	400	$5.0 \times 10^3$
	1000	$2.0 \times 10^4$
TFO-Aged at 163 °C	0	$5.0 \times 10^2$
	48	$1.9 \times 10^3$
	96	$4.5 \times 10^3$
	144	$6.9 \times 10^3$
	400	$1.2 \times 10^4$
	1000	$4.5 \times 10^4$

<sup>1</sup> After aging in pressure vessel, sample was heated to 110 °C for 1 hour, then let stand for 2 days at room temperature before loading in rheometer to measure viscosity.

<sup>2</sup> Viscosity measurements on the Rheometrics Mechanical Spectrometer are estimated to have an error bar of  $\pm 10\%$ .

**Table 8.2    Changes in Dynamic Shear Viscosity With Time During Aging of Annealed, 400-Hour Pressure Oxidized Asphalt AAD-1 With and Without TFO Aging Prior to Initial Pressure Oxidation**

Prior Treatment Before Second Pressure Oxidation	Aging Time, Second Pressure Oxidation, hr	Dynamic Shear Viscosity, <sup>1,2</sup> Pa · s, 60 °C, 0.1 rad/s, Annealed Prior to Measurement
Original Asphalt	0	$5.0 \times 10^3$
Aged 400 hr. in O <sub>2</sub>	48	$6.2 \times 10^3$
at 60 °C, 300 psig	96	$7.5 \times 10^3$
Followed by 110 °C	144	$7.2 \times 10^3$
Thermal Treatment	400	$1.2 \times 10^4$
TFO-Aged Asphalt,	0	$1.2 \times 10^4$
Aged 400 hr in O <sub>2</sub>	48	$1.6 \times 10^4$
at 60 °C, 300 psig	96	$1.9 \times 10^4$
Followed by 110 °C	144	$1.8 \times 10^4$
Thermal Treatment	400	$2.6 \times 10^4$

<sup>1</sup> Sample annealed after second aging in pressure vessel at 110 °C for 1 hour and measurement made after standing 2 days at room temperature.

<sup>2</sup> Viscosity measurements on the Rheometrics Mechanical Spectrometer are estimated to have an error bar of  $\pm 10\%$ .

**Table 8.3 Effect of Thermal Treatment to Disrupt Molecular Structuring on the Rheological Properties at 60°C of Low-Temperature, Pressure-Oxidized (300 psi) Asphalt AAD-1**

Oxidation Conditions	Thermal Treat After Oxidation	Shear Storage Modulus, $G'$ , dynes/cm <sup>2</sup>	Shear Loss Modulus, $G''$ , dynes/cm <sup>2</sup>	Dynamic Shear Viscosity, <sup>5</sup> Pa · s	Tan $\delta$
300 psig O <sub>2</sub> , 400 hr, 60°C	~70°C <sup>1</sup>	$9.655 \times 10^2$	$6.594 \times 10^3$	$6.664 \times 10^3$	6.83
	110°C <sup>2</sup>	$4.616 \times 10^2$	$5.012 \times 10^3$	$5.033 \times 10^3$	10.86
	110°C <sup>3</sup>	$4.951 \times 10^2$	$5.228 \times 10^3$	$5.251 \times 10^3$	10.56
	110°C <sup>4</sup>	$4.596 \times 10^2$	$5.000 \times 10^3$	$5.021 \times 10^3$	10.88
TFO Followed by 300 psig O <sub>2</sub> , 400 hr, 60°C	~70°C <sup>1</sup>	$2.925 \times 10^3$	$1.356 \times 10^4$	$1.387 \times 10^4$	4.63
	110°C <sup>2</sup>	$2.026 \times 10^3$	$1.192 \times 10^4$	$1.209 \times 10^4$	5.88

<sup>1</sup> Heated to 70°C while loading rheometer

<sup>2</sup> One hour 110°C thermal treat in TFO pan in air

<sup>3</sup> One hour 110°C thermal treat in open tube in air

<sup>4</sup> One hour 110°C thermal treat in sealed tube under vacuum

<sup>5</sup> Viscosity measurements on the Rheometrics Mechanical Spectrometer are estimated to have an error bar of  $\pm 10\%$ .

**Table 8.4 Chemical Functionality Formed On Oxidative Aging of AAD-1**

Aging Time in O <sub>2</sub> at 60°C, 300 psig, hr	Relative Carbonyl <sup>3</sup> Peak Height, Abs. Units		Sulfoxide Concentration, <sup>3</sup> mol/L	
	Original <sup>1</sup>	Prior TFO <sup>2</sup>	Original	Prior TFO
0	<0.005	0.015	<0.03	0.06
48	0.060	0.055	0.35	0.35
400	0.150	0.155	0.69	0.67
400 hr Annealed Sample Aged an Additional 144 hrs.	0.17	0.175	0.75	0.72

<sup>1</sup> Original Asphalt aged in pressure vessel.

<sup>2</sup> Original Asphalt subjected to TFO oxidation before aging in pressure vessel.

<sup>3</sup> Based on prior experience with asphalts, standard deviations are (mol/L): sulfoxides, 0.027; ketones, 0.006.

Table 8.5 Changes in Rheological and Chemical Properties with POV-Aging of Asphalt AAD-1 at Different Temperatures

Nominal Aging Temp., °C	Aging Time, hr.	Dynamic Viscosity <sup>1</sup> Pa·s, 60°		Relative Carbonyl, <sup>2</sup> absorbance units		Sulfoxides, <sup>2</sup> mol/L	
		No Prior TFO	Prior TFO	No Prior TFO	Prior TFO	No Prior TFO	Prior TFO
50	0	1.8 x 10 <sup>2</sup>	4.9 x 10 <sup>2</sup>	<0.005	0.03	<0.03	0.07
	48	5.2 x 10 <sup>2</sup>	1.1 x 10 <sup>3</sup>	0.04	0.04	0.19	0.19
	96	7.5 x 10 <sup>2</sup>	1.4 x 10 <sup>3</sup>	0.05	0.05	0.28	0.25
	144	9.0 x 10 <sup>2</sup>	1.7 x 10 <sup>3</sup>	0.06	0.06	0.28	0.28
	400	1.8 x 10 <sup>2</sup>	3.5 x 10 <sup>3</sup>	0.07	0.07	0.39	0.39
60	0	1.3 x 10 <sup>2</sup>	5.0 x 10 <sup>3</sup>	<0.005	0.02	<0.03	0.06
	48	8.4 x 10 <sup>2</sup>	1.9 x 10 <sup>4</sup>	0.06	0.06	0.35	0.35
	96	2.0 x 10 <sup>3</sup>	4.5 x 10 <sup>4</sup>	-	-	-	-
	144	3.2 x 10 <sup>3</sup>	6.9 x 10 <sup>4</sup>	-	-	-	-
	400	5.0 x 10 <sup>3</sup>	1.2 x 10 <sup>4</sup>	0.150	0.155	0.69	0.67
70	0	1.4 x 10 <sup>2</sup>	3.1 x 10 <sup>2</sup>	<0.005	0.05	<0.03	0.05
	48	1.1 x 10 <sup>3</sup>	2.1 x 10 <sup>3</sup>	0.09	0.09	0.37	0.35
	96	1.7 x 10 <sup>3</sup>	3.7 x 10 <sup>3</sup>	0.10	0.10	0.44	0.41
	144	2.9 x 10 <sup>3</sup>	6.2 x 10 <sup>4</sup>	0.12	0.11	0.52	0.53
	400	1.2 x 10 <sup>4</sup>	2.5 x 10 <sup>4</sup>	0.16	0.16	0.70	0.68

<sup>1</sup> Viscosity measurements on the Rheometrics Mechanical Spectrometer are estimated to have an error bar of ± 10%.

<sup>2</sup> Based on prior experience with asphalts, standard deviations are (mol/L): sulfoxides, 0.027; ketones, 0.006.

**Table 8.6 Relationship of Weight Loss to Log Viscosity Increase During TFO Test**

Asphalt	Weight Change During TFO Test, <sup>1</sup> %	Log Viscosity Change During TFO Test, %
AAA-1	-0.311	0.25
AAB-1	-0.036	0.28
AAC-1	-0.259	0.28
AAD-1	-0.810	0.42
AAF-1	-0.092	0.30
AAG-1	-0.180	0.15
AAK-1	-0.548	0.40
AAM-1	+0.052	0.23

<sup>1</sup> Weight change data from MRL Data Base

Table 8.7 Changes in Rheological and Chemical Properties of SHRP Core Asphalts during POV Aging at 60 °C, 300 psi

Asphalt	Aging Time, hr.	Dynamic Viscosity <sup>1</sup> Pa · s, 60 °C		Relative Carbonyl <sup>2</sup> absorbance units		Sulfoxides <sup>2</sup> mol/L	
		No Prior TFO	Prior TFO	No Prior TFO	Prior TFO	No Prior TFO	Prior TFO
AAA-1	0	1.1 x 10 <sup>2</sup>	1.9 x 10 <sup>2</sup>	0.02	0.03	0.03	0.07
	48	3.9 x 10 <sup>2</sup>	5.3 x 10 <sup>2</sup>	0.05	0.05	0.21	0.21
	96	-	6.2 x 10 <sup>2</sup>	-	0.08	-	0.23
	144	6.9 x 10 <sup>2</sup>	9.1 x 10 <sup>2</sup>	0.10	0.10	0.32	0.30
	400	2.0 x 10 <sup>3</sup>	2.3 x 10 <sup>3</sup>	0.14	0.13	0.47	6.46
AAB-1	0	1.6 x 10 <sup>2</sup>	3.4 x 10 <sup>2</sup>	0.00	0.00	0.06	0.12
	48	6.0 x 10 <sup>2</sup>	7.3 x 10 <sup>2</sup>	0.05	0.04	0.25	-
	96	-	8.4 x 10 <sup>2</sup>	-	0.09	-	0.28
	144	1.2 x 10 <sup>3</sup>	1.6 x 10 <sup>3</sup>	0.11	0.15	0.33	0.34
	400	3.0 x 10 <sup>3</sup>	3.8 x 10 <sup>3</sup>	0.16	0.15	0.43	0.41
AAC-1	0	1.1 x 10 <sup>2</sup>	2.1 x 10 <sup>2</sup>	0.02	0.00	0.03	0.06
	48	4.1 x 10 <sup>2</sup>	5.6 x 10 <sup>2</sup>	0.09	0.10	0.17	0.16
	96	-	7.5 x 10 <sup>2</sup>	-	0.13	-	0.19
	144	7.4 x 10 <sup>2</sup>	1.1 x 10 <sup>3</sup>	0.16	0.17	0.20	0.23
	400	1.8 x 10 <sup>3</sup>	2.5 x 10 <sup>3</sup>	0.21	0.24	0.20	0.23
AAD-1	0	1.3 x 10 <sup>2</sup>	9.6 x 10 <sup>2</sup>	0.00	0.09	0.04	0.09
	48	6.0 x 10 <sup>2</sup>	1.1 x 10 <sup>3</sup>	0.08	0.04	0.23	0.27
	96	-	1.5 x 10 <sup>3</sup>	-	0.09	-	0.32
	144	1.2 x 10 <sup>3</sup>	2.2 x 10 <sup>3</sup>	0.10	0.11	0.35	0.36
	400	3.5 x 10 <sup>3</sup>	5.3 x 10 <sup>3</sup>	0.16	0.16	0.61	0.59
AAF-1	0	2.3 x 10 <sup>1</sup>	4.4 x 10 <sup>2</sup>	0.00	0.00	<0.02	0.06
	48	1.2 x 10 <sup>3</sup>	1.7 x 10 <sup>3</sup>	0.06	0.06	0.02	0.24
	96	-	2.5 x 10 <sup>3</sup>	-	0.10	-	0.28
	144	2.4 x 10 <sup>3</sup>	3.4 x 10 <sup>3</sup>	0.13	0.12	0.29	0.31
	400	8.0 x 10 <sup>3</sup>	9.8 x 10 <sup>3</sup>	0.17	0.19	0.36	0.35

Continued on next page



Table 8.7 Continued

AAG-1	0	$2.4 \times 10^2$	$5.6 \times 10^2$	0.00	0.11	0.05	0.12
	48	$6.6 \times 10^2$	$7.8 \times 10^2$	0.13	0.16	0.19	0.22
	96	$1.0 \times 10^3$	$1.2 \times 10^3$	-	0.22	-	0.19
	144	$1.3 \times 10^3$	$1.4 \times 10^3$	0.24	0.23	0.22	0.21
	400	$2.3 \times 10^3$	$3.1 \times 10^3$	6.25	0.26	0.21	0.23
AAK-1	0	$4.1 \times 10^2$	$1.0 \times 10^3$	0.03	0.04	0.03	0.07
	48	$1.6 \times 10^3$	$2.6 \times 10^3$	0.06	0.06	0.21	0.18
	96	-	$3.5 \times 10^3$	-	0.10	-	0.25
	144	$3.8 \times 10^3$	$4.9 \times 10^3$	0.11	0.10	0.38	0.32
	400	$1.0 \times 10^4$	$1.2 \times 10^4$	0.17	0.15	0.55	0.52
AAM-1	0	$2.6 \times 10^2$	$4.3 \times 10^2$	0.01	0.02	0.02	0.03
	48	$1.4 \times 10^3$	$2.0 \times 10^3$	0.10	0.10	0.08	0.07
	96	-	$2.1 \times 10^3$	-	0.09	-	0.09
	144	$3.4 \times 10^3$	$3.8 \times 10^3$	0.17	0.17	0.11	0.11
	400	$8.0 \times 10^3$	$1.2 \times 10^4$	0.21	0.22	0.11	0.12

<sup>1</sup> Viscosity measurements on the Rheometrics Mechanical Spectrometer are estimated to have an error bar of  $\pm 10\%$ .

<sup>2</sup> Based on prior experience with asphalts, standard deviations are (mol/L): sulfoxides, 0.027; ketones, 0.006.

**Table 8.8 Changes in Rheological and Chemical Properties During Thin-Film Oven Aging Followed by 60°C PAV (300 psi) Oxidation of SHRP Core Asphalts**

Asphalt	Oxidation Time, hrs	Dynamic Viscosity ( $\eta^*$ ) <sup>1</sup> 60°C, Pa·s	Carbonyl Absorbance <sup>2</sup> Units	Sulfoxide <sup>2</sup> mol/L	Aging Index Including TFO	Aging Index Excluding TFO
AAA-1	0	1.09 x 10 <sup>2</sup>	0.015	0.037	6.11	3.38
	TFO	1.97 x 10 <sup>2</sup>	0.02	0.04		
	48	4.90 x 10 <sup>2</sup>	0.03	0.15		
	96	6.31 x 10 <sup>2</sup>	0.05	0.23		
	144	6.66 x 10 <sup>2</sup>	0.04	0.234		
	400	1.47 x 10 <sup>3</sup>	0.06	0.33		
AAB-1	0	1.60 x 10 <sup>2</sup>	<0.005	0.064	6.75	3.60
	TFO	3.00 x 10 <sup>2</sup>	<0.005	0.067		
	48	9.85 x 10 <sup>2</sup>	0.04	0.199		
	96	1.08 x 10 <sup>3</sup>	0.04	0.233		
	144	1.08 x 10 <sup>3</sup>	0.05	0.249		
	400	2.07 x 10 <sup>3</sup>	0.08	0.37		
AAC-1	0	1.10 x 10 <sup>2</sup>	0.02	0.029	6.24	3.30
	TFO	2.08 x 10 <sup>2</sup>	0.02	0.04		
	48	3.89 x 10 <sup>2</sup>	0.05	0.119		
	96	6.15 x 10 <sup>2</sup>	0.07	0.157		
	144	6.87 x 10 <sup>2</sup>	0.08	0.19		
	400	1.29 x 10 <sup>3</sup>	0.14	0.193		
AAD-1	0	1.31 x 10 <sup>2</sup>	0.025	0.036	11.83	4.38
	TFO	3.54 x 10 <sup>2</sup>	0.04	0.055		
	48	1.05 x 10 <sup>3</sup>	0.05	0.146		
	96	1.55 x 10 <sup>3</sup>	0.05	0.21		
	144	1.55 x 10 <sup>3</sup>	0.07	0.256		
	400	3.35 x 10 <sup>3</sup>	0.09	0.365		
AAF-1	0	2.26 x 10 <sup>2</sup>	<0.005	0.05	9.79	4.99
	TFO	4.43 x 10 <sup>2</sup>	0.00	0.06		
	48	1.03 x 10 <sup>3</sup>	0.03	0.167		
	96	2.52 x 10 <sup>3</sup>	-	-		
	144	2.21 x 10 <sup>3</sup>	0.06	0.263		
	400	4.43 x 10 <sup>3</sup>	0.10	0.289		
AAG-1	0	2.40 x 10 <sup>2</sup>	0.01	0.046	3.84	2.70
	TFO	3.41 x 10 <sup>2</sup>	0.03	0.05		
	48	6.74 x 10 <sup>2</sup>	0.08	0.128		
	96	8.64 x 10 <sup>2</sup>	0.11	0.17		
	144	9.21 x 10 <sup>2</sup>	0.13	0.182		
	400	1.91 x 10 <sup>3</sup>	0.25	0.22		

Continued on next page

Table 8.8 Continued

AAK-1	0	$4.13 \times 10^2$	0.03	0.022		
	TFO	$1.04 \times 10^3$	0.03	0.025		
	48	$2.64 \times 10^3$	0.04	0.14		
	96	$3.78 \times 10^3$	0.06	0.22		
	144	$3.45 \times 10^3$	0.05	0.212	8.34	3.32
	400	$7.19 \times 10^3$	0.08	0.32		
AAM-1	0	$2.58 \times 10^2$	0.01	0.023		
	TFO	$4.33 \times 10^2$	0.02	0.026		
	48	$1.55 \times 10^3$	0.08	0.074		
	96	$1.99 \times 10^3$	0.09	0.094		
	144	$2.41 \times 10^3$	0.11	0.111	9.33	5.57
	400	$4.88 \times 10^3$	0.16	0.12		

<sup>1</sup> Viscosity measurements on the Rheometrics Mechanical Spectrometer are estimated to have an error bar of  $\pm 10\%$ .

<sup>2</sup> Based on prior experience with asphalts, standard deviations are (mol/L): sulfoxides, 0.027; ketones, 0.006.

**Table 8.9 Correction of Viscosities for Prior-TFO Aged Asphalts Subsequently Aged by POV and PAV Method for TFO Aging**

Asphalt	Aging Method	Aging Time, hrs	Dynamic Viscosity <sup>1</sup> Pa · s, 60 °C	Log Viscosity	Log Viscosity Minus Log Δ TFO	Corrected Dynamic Viscosity
AAD-1	POV	0	1.31 x 10 <sup>2</sup>	2.12		
				Δ Log TFO = 0.43		
		0-TFO	3.54 x 10 <sup>2</sup>	2.55	2.12	1.31 x 10 <sup>2</sup>
		48	1.1 x 10 <sup>3</sup>	3.04	2.61	4.08 x 10 <sup>2</sup>
		96	1.5 x 10 <sup>3</sup>	3.18	2.75	5.57 x 10 <sup>2</sup>
		144	2.2 x 10 <sup>3</sup>	3.34	2.91	8.17 x 10 <sup>2</sup>
AAG-1	POV	400	5.3 x 10 <sup>3</sup>	3.72	3.29	1.97 x 10 <sup>3</sup>
		0	2.40 x 10 <sup>2</sup>	2.38		
				Δ Log TFO = 0.15		
		0-TFO	3.41 x 10 <sup>2</sup>	2.53	2.38	2.40 x 10 <sup>2</sup>
		48	7.8 x 10 <sup>2</sup>	2.89	2.74	5.50 x 10 <sup>2</sup>
		96	1.2 x 10 <sup>3</sup>	3.08	2.93	8.51 x 10 <sup>2</sup>
AAD-1	PAV	144	1.4 x 10 <sup>3</sup>	3.15	3.00	1 x 10 <sup>3</sup>
		400	3.1 x 10 <sup>3</sup>	3.49	3.34	2.19 x 10 <sup>3</sup>
		0	1.31 x 10 <sup>2</sup>	2.12		
				Δ Log TFO = 0.43		
		0-TFO	3.54 x 10 <sup>2</sup>	2.55	2.12	1.32 x 10 <sup>2</sup>
		48	1.05 x 10 <sup>3</sup>	3.02	2.59	3.89 x 10 <sup>2</sup>
AAG-1	PAV	96	1.55 x 10 <sup>3</sup>	3.19	2.76	5.75 x 10 <sup>2</sup>
		144	1.55 x 10 <sup>3</sup>	3.19	2.76	5.75 x 10 <sup>2</sup>
		400	3.55 x 10 <sup>3</sup>	3.55	3.12	1.32 x 10 <sup>3</sup>
		0	2.40 x 10 <sup>2</sup>	2.38		
				Δ Log TFO = 0.15		
		0-TFO	3.41 x 10 <sup>2</sup>	2.53	2.38	2.40 x 10 <sup>2</sup>
AAG-1	PAV	48	6.74 x 10 <sup>2</sup>	2.83	2.68	4.79 x 10 <sup>2</sup>
		96	8.64 x 10 <sup>2</sup>	2.94	2.79	6.17 x 10 <sup>2</sup>
		144	9.21 x 10 <sup>2</sup>	2.96	2.81	6.46 x 10 <sup>2</sup>
		400	1.91 x 10 <sup>3</sup>	3.28	3.13	1.35 x 10 <sup>3</sup>

<sup>1</sup> Viscosity measurements on the Rheometrics Mechanical Spectrometer are estimated to have an error bar of ± 10%.

**Table 8.10 Changes in Rheological and Chemical Properties of Selected SHRP  
Asphalts During TFAAT Aging at 65 °C**

Asphalt	Aging Time, hrs	Weight Change, %	Dynamic Viscosity <sup>1</sup> Pa · s, 60 °C	Relative Carbonyl, <sup>2</sup> absorbance	Sulfoxides, <sup>2</sup> mol/L
AAD-1	0	0.0	$1.31 \times 10^2$	0.025	0.036
	48	+0.42	$3.94 \times 10^2$	0.06	0.20
	96	+0.39	$5.69 \times 10^2$	0.06	0.25
	144	+0.20	$6.28 \times 10^2$	0.07	0.27
	400	+0.49	$9.39 \times 10^2$	0.09	0.39
AAG-1	0	0.0	$2.40 \times 10^2$	0.01	0.046
	48	+0.92	$5.08 \times 10^2$	0.07	0.21
	96	+0.39	$5.66 \times 10^2$	0.08	0.24
	144	+0.54	$6.47 \times 10^2$	0.10	0.25
	400	+0.51	$1.22 \times 10^2$	0.17	0.30

<sup>1</sup> Viscosity measurements on the Rheometrics Mechanical Spectrometer are estimated to have an error bar of  $\pm 10\%$ .

<sup>2</sup> Based on prior experience with asphalts, standard deviations are (mol/L): sulfoxides, 0.027; ketones, 0.006.

**Table 8.11 Changes in Rheological and Chemical Properties of SHRP Core Asphalts During TFAAT Aging at 85°C**

Asphalt	Aging Time, hrs	Weight Change, %	Dynamic Viscosity <sup>1</sup> Pa · s, 60°C	Relative Carbonyl, <sup>2</sup> absorbance	Sulfoxides, <sup>2</sup> mol/L
AAA-1	0	0.0	$1.09 \times 10^2$	0.015	0.037
	24	+0.34	$2.94 \times 10^2$	0.03	0.15
	48	+0.40	$3.89 \times 10^2$	0.04	0.20
	96	+0.21	$6.45 \times 10^2$	0.05	0.25
	144	+0.38	$8.56 \times 10^2$	0.06	0.25
	400	+0.63	$1.96 \times 10^3$	0.07	0.34
AAB-1	0	0.0	$1.60 \times 10^2$	<0.0005	0.064
	24	+0.72	$5.04 \times 10^2$	0.02	0.19
	48	+0.82	$6.68 \times 10^2$	0.03	0.23
	96	+0.68	$1.24 \times 10^3$	0.05	0.25
	144	+0.38	$1.54 \times 10^3$	0.07	0.29
	400	+0.76	$2.27 \times 10^3$	0.06	0.33
AAC-1	0	0.0	$1.10 \times 10^2$	0.01	0.029
	24	+0.49	$2.65 \times 10^2$	0.04	0.15
	48	+0.55	$3.76 \times 10^2$	0.06	0.19
	96	+0.40	$5.79 \times 10^2$	0.08	0.17
	144	-	$6.78 \times 10^2$	0.09	0.18
	400	+0.81	$1.14 \times 10^3$	0.12	0.23
AAD-1	0	0.0	$1.31 \times 10^2$	0.02	0.036
	24	+0.35	$5.07 \times 10^2$	0.03	0.14
	48	+0.20	$7.60 \times 10^2$	0.05	0.19
	96	+0.38	$1.38 \times 10^3$	0.06	0.24
	144	+0.32	$1.71 \times 10^3$	0.05	0.26
	400	+0.79	$5.90 \times 10^3$	0.06	0.36
AAF-1	0	0.0	$2.26 \times 10^2$	<0.005	0.05
	24	+0.54	$7.08 \times 10^2$	0.02	0.21
	48	+0.62	$1.21 \times 10^3$	0.04	0.26
	96	+0.66	$1.92 \times 10^3$	0.06	0.30
	144	+0.55	$2.19 \times 10^3$	0.05	0.25
	400	+0.68	$5.05 \times 10^3$	0.13	0.35
AAG-1	0	0.0	$2.40 \times 10^2$	0.01	0.046
	24	0.61	$5.10 \times 10^2$	0.05	0.13
	48	0.69	$6.47 \times 10^2$	0.05	0.13
	96	0.44	$8.53 \times 10^2$	0.09	0.15
	144	0.88	$9.28 \times 10^2$	0.11	0.16
	400	0.62	$1.33 \times 10^3$	0.13	0.21

Continued on next page

Table 8.11 Continued

AAK-J	0	0.0	$4.13 \times 10^2$	0.02	0.022
	24	-	$1.23 \times 10^3$	0.04	0.13
	48	+0.40	$1.80 \times 10^3$	0.05	0.15
	96	+0.20	$3.10 \times 10^3$	0.07	0.22
	144	+0.53	$3.68 \times 10^3$	0.07	0.25
	400	+0.59	$9.94 \times 10^3$	0.10	0.42
AAM-1	0	0.0	$2.58 \times 10^2$	<0.005	0.023
	24	+0.37	$7.91 \times 10^2$	0.06	0.07
	48	+0.23	$1.15 \times 10^3$	0.08	0.08
	96	+0.25	$1.91 \times 10^3$	0.09	0.08
	144	+0.56	$2.37 \times 10^3$	0.12	0.10
	400	+0.72	$4.40 \times 10^3$	0.13	0.10

<sup>1</sup> Viscosity measurements on the Rheometrics Mechanical Spectrometer are estimated to have an error bar of  $\pm 10\%$ .

<sup>2</sup> Based on prior experience with asphalts, standard deviations are (mol/L): sulfoxides, 0.027; ketones, 0.006.

**Table 8.12 Changes in Rheological and Chemical Properties of SHRP Core Asphalts During TFAAT Aging at 113°C**

Asphalt	Aging Time, hrs	Weight Change, %	Dynamic Viscosity <sup>1</sup> Pa · s, 60°C	Relative Carbonyl, <sup>2</sup> absorbance	Sulfoxides, <sup>2</sup> mol/L
AAA-1	0	0.0	$1.09 \times 10^2$	0.015	0.037
	24	+0.57	$1.61 \times 10^3$	0.07	0.21
	48	+0.82	$5.63 \times 10^3$	0.11	0.24
	72	+1.10	$2.52 \times 10^4$	0.13	0.27
	120	+0.95	$1.79 \times 10^5$	0.16	0.23
AAB-1	0	0.0	$1.60 \times 10^2$	<0.005	0.064
	24	+0.67	$2.32 \times 10^3$	0.09	0.21
	48	+0.96	$1.10 \times 10^4$	0.12	0.25
	72	+1.29	$3.04 \times 10^4$	0.17	0.27
	120	+1.39	$1.56 \times 10^5$	0.21	0.28
AAC-1	0	0.0	$1.10 \times 10^2$	0.01	0.029
	24	+0.28	$1.09 \times 10^3$	0.12	0.12
	48	+0.39	$2.74 \times 10^3$	0.17	0.13
	72	+0.79	$5.29 \times 10^3$	0.20	0.13
	120	+0.62	$3.00 \times 10^4$	0.24	0.13
AAD-1	0	0.0	$1.31 \times 10^2$	0.02	0.036
	24	+0.28	$4.07 \times 10^3$	0.08	0.21
	48	+0.85	$1.92 \times 10^4$	0.11	0.30
	72	+1.02	$7.58 \times 10^4$	0.13	0.31
	120	+1.18	$3.36 \times 10^5$	0.13	0.35
AAF-1	0	0.0	$2.26 \times 10^2$	<0.005	0.05
	24	+0.62	$4.56 \times 10^3$	0.11	0.18
	48	+0.30	$1.02 \times 10^4$	0.15	0.19
	72	+0.89	$5.01 \times 10^4$	0.17	0.19
	120	+0.76	$1.15 \times 10^5$	0.22	0.21
AAG-1	0	0.0	$2.40 \times 10^2$	0.01	0.046
	24	+0.72	$1.12 \times 10^3$	0.15	0.14
	48	+0.84	$1.97 \times 10^3$	0.24	0.15
	72	+0.61	$3.62 \times 10^3$	0.32	0.13
	120	+0.99	$8.66 \times 10^3$	0.39	0.14
AAK-1	0	0.0	$4.13 \times 10^2$	0.02	0.022
	24	+0.59	$9.28 \times 10^3$	0.08	0.21
	48	+0.74	$4.77 \times 10^4$	0.11	0.26
	72	+0.34	$1.89 \times 10^5$	0.14	0.26
	120	+1.32	$1.35 \times 10^6$	0.21	0.33

Continued on next page



Table 8.12 Continued

AAM-1	0	0.0	$2.58 \times 10^2$	<0.005	0.023
	24	+0.56	$4.63 \times 10^3$	0.12	0.05
	48	+0.76	$2.14 \times 10^4$	0.21	0.07
	72	+0.94	$6.03 \times 10^4$	0.27	0.06
	120	+1.13	$1.99 \times 10^5$	0.25	0.06

---

<sup>1</sup> Viscosity measurements on the Rheometrics Mechanical Spectrometer are estimated to have an error bar of  $\pm 10\%$ .

<sup>2</sup> Based on prior experience with asphalts, standard deviations are (mol/L): sulfoxides, 0.027; ketones, 0.006.

**Table 8.13 Changes in Rheological and Chemical Properties of SHRP Core Asphalts During TFAAT Aging at 130°C**

Asphalt	Aging Time, hrs	Weight Change, %	Dynamic Viscosity <sup>1</sup> Pa · s, 60 °C	Relative Carbonyl, <sup>2</sup> absorbance	Sulfoxides, <sup>2</sup> mol/L
AAA-1	0	0.0	$1.09 \times 10^2$	0.015	0.037
	4	+0.49	$5.95 \times 10^2$	0.06	0.16
	12	+0.80	$4.30 \times 10^3$	0.10	0.22
	20	+0.93	$2.75 \times 10^4$	0.12	0.19
	36	+1.11	$1.97 \times 10^6$	0.17	0.21
AAB-1	0	0.0	$1.60 \times 10^2$	<0.005	0.064
	4	+0.81	$9.00 \times 10^2$	0.05	0.17
	12	+0.79	$6.40 \times 10^3$	0.11	0.21
	20	+0.88	$2.60 \times 10^4$	0.16	0.22
	36	+1.16	$2.64 \times 10^5$	0.20	0.22
AAC-1	0	0.0	$1.10 \times 10^2$	0.01	0.029
	4	+0.25	$4.34 \times 10^2$	0.07	0.11
	12	-	$1.87 \times 10^3$	0.14	0.14
	20	+0.28	$6.34 \times 10^3$	0.18	0.14
	36	-	$5.41 \times 10^4$	0.25	0.14
AAD-1	0	0.0	$1.31 \times 10^2$	0.02	0.036
	4	+0.42	$1.22 \times 10^3$	0.06	0.14
	12	+0.68	$1.04 \times 10^4$	0.09	0.21
	20	+0.68	$6.23 \times 10^4$	0.12	0.27
	36	+1.05	$4.63 \times 10^5$	0.15	0.30
AAF-1	0	0.0	$2.26 \times 10^2$	<0.005	0.05
	4	-	$1.60 \times 10^3$	0.05	0.17
	12	-	$8.28 \times 10^3$	0.10	0.18
	20	+0.35	$2.59 \times 10^4$	0.14	0.18
	36	+0.57	$3.16 \times 10^5$	0.24	0.19
AAG-1	0	0.0	$2.40 \times 10^2$	0.01	0.046
	4	+0.70	$6.90 \times 10^2$	0.10	0.10
	12	+0.83	$1.49 \times 10^3$	0.19	0.12
	20	+1.10	$2.50 \times 10^3$	0.25	0.13
	36	+0.95	$1.02 \times 10^4$	0.34	0.12
AAK-1	0	0.0	$4.13 \times 10^2$	0.02	0.022
	4	+0.38	$4.01 \times 10^3$	0.07	0.14
	12	+0.43	$2.10 \times 10^4$	0.10	0.21
	20	+0.76	$9.08 \times 10^4$	0.13	0.24
	36	+0.39	$7.58 \times 10^5$	0.17	0.26

Continued on next page

Table 8.13 Continued

AAM-1	0	0.0	$2.58 \times 10^2$	<0.005	0.023
	4	0.40	$1.88 \times 10^3$	0.09	0.06
	12	0.60	$1.16 \times 10^4$	0.17	0.06
	20	0.82	$3.71 \times 10^4$	0.22	0.06
	36	0.98	$2.65 \times 10^5$	0.30	0.06

<sup>1</sup> Viscosity measurements on the Rheometrics Mechanical Spectrometer are estimated to have an error bar of  $\pm 10\%$ .

<sup>2</sup> Based on prior experience with asphalts, standard deviations are (mol/L): sulfoxides, 0.027; ketones, 0.006.

**Table 8.14 Changes in Rheological and Chemical Properties During Thin-Film Oven Aging Followed by 70°C PAV (300 psi) Oxidation of SHRP Asphalts**

Asphalt	Oxidation Time, hrs	Dynamic Viscosity ( $\eta^*$ ) <sup>1</sup> 60°C, Pa·s	Carbonyl Absorbance <sup>2</sup> Units	Sulfoxide <sup>2</sup> mol/L	Aging Index Including TFO	Aging Index Excluding TFO
AAA-1	0	$1.09 \times 10^2$	0.015	0.037	13.30	7.36
	TFO	$1.97 \times 10^2$	-	-		
	144	$1.45 \times 10^3$	0.065	0.288		
AAB-1	0	$1.60 \times 10^2$	<0.005	0.064	13.63	7.27
	TFO	$3.00 \times 10^2$	-	-		
	144	$2.18 \times 10^3$	0.07	0.286		
AAC-1	0	$1.10 \times 10^2$	0.02	0.029	10.83	5.72
	TFO	$2.08 \times 10^2$	-	-		
	144	$1.19 \times 10^3$	0.13	0.167		
AAD-1	0	$1.31 \times 10^2$	0.025	0.036	23.85	8.81
	TFO	$3.54 \times 10^2$	-	-		
	144	$3.12 \times 10^3$	0.085	0.337		
AAF-1	0	$2.26 \times 10^2$	<0.005	0.05	17.54	8.95
	TFO	$4.43 \times 10^2$	-	-		
	144	$3.965 \times 10^3$	0.095	0.256		
AAG-1	0	$2.40 \times 10^2$	0.01	0.046	6.29	4.43
	TFO	$3.41 \times 10^2$	-	-		
	144	$1.51 \times 10^3$	0.18	0.175		
AAK-1	0	$4.13 \times 10^2$	0.03	0.022	15.28	6.07
	TFO	$1.04 \times 10^3$	-	-		
	144	$6.31 \times 10^3$	0.07	0.301		
AAM-1	0	$2.58 \times 10^2$	0.01	0.023	21.42	12.77
	TFO	$4.33 \times 10^2$	-	-		
	144	$5.53 \times 10^3$	0.14	0.09		

<sup>1</sup> Viscosity measurements on the Rheometrics Mechanical Spectrometer are estimated to have an error bar of  $\pm 10\%$ .

<sup>2</sup> Based on prior experience with asphalts, standard deviations are (mol/L): sulfoxides, 0.027; ketones, 0.006.

**Table 8.15 Changes in Rheological and Chemical Properties During Thin-Film Oven Aging Followed by 80°C PAV (300 psi) Oxidation of SHRP Asphalts**

Asphalt	Oxidation Time, hrs	Dynamic Viscosity ( $\eta^*$ ) <sup>1</sup> 60°C, Pa·s	Carbonyl Absorbance <sup>2</sup> Units	Sulfoxide <sup>2</sup> mol/L	Aging Index Including TFO	Aging Index Excluding TFO
AAA-1	0	1.09 x 10 <sup>2</sup>	0.015	0.037	33.67	18.6
	TFO	1.97 x 10 <sup>2</sup>	-	-		
	144	3.67 x 10 <sup>3</sup>	0.10	0.336		
AAB-1	0	1.60 x 10 <sup>2</sup>	<0.005	0.064	29.50	15.7
	TFO	3.00 x 10 <sup>2</sup>	-	-		
	144	4.72 x 10 <sup>3</sup>	0.11	0.317		
AAC-1	0	1.10 x 10 <sup>2</sup>	0.02	0.029	20.55	10.9
	TFO	2.08 x 10 <sup>2</sup>	-	-		
	144	2.26 x 10 <sup>3</sup>	0.165	0.169		
AAD-1	0	1.31 x 10 <sup>2</sup>	0.025	0.036	68.10	25.2
	TFO	3.54 x 10 <sup>2</sup>	-	-		
	144	8.92 x 10 <sup>3</sup>	0.11	0.424		
AAF-1	0	2.26 x 10 <sup>2</sup>	<0.005	0.05	38.76	19.8
	TFO	4.43 x 10 <sup>2</sup>	-	-		
	144	8.76 x 10 <sup>3</sup>	0.13	0.278		
AAG-1	0	2.40 x 10 <sup>2</sup>	0.01	0.046	9.75	6.9
	TFO	3.41 x 10 <sup>2</sup>	-	-		
	144	2.34 x 10 <sup>3</sup>	0.235	0.17		
AAK-1	0	4.13 x 10 <sup>2</sup>	0.03	0.022	42.13	16.7
	TFO	1.04 x 10 <sup>3</sup>	-	-		
	144	1.74 x 10 <sup>4</sup>	0.115	0.413		
AAM-1	0	2.58 x 10 <sup>2</sup>	0.01	0.023	44.57	26.6
	TFO	4.33 x 10 <sup>2</sup>	-	-		
	144	1.15 x 10 <sup>4</sup>	0.175	0.075		

<sup>1</sup> Viscosity measurements on the Rheometrics Mechanical Spectrometer are estimated to have an error bar of  $\pm 10\%$ .

<sup>2</sup> Based on prior experience with asphalts, standard deviations are (mol/L): sulfoxides, 0.027; ketones, 0.006.

**Table 8.19 Results of Vanadyl Acetylacetonate Catalyzed Oxidation of Core Asphalts Using the Rolling Thin-Film Oven (RTFO) Method**

Asphalt	0.25% VO(AcAc) 163 °C, 85 min.		0.50% VO(AcAc) 163 °C, 85 min.		0.50% VO(AcAc) 130 °C, 4 hours		60 °C TFO-POV 144 hours	80 °C TFO-POV 144 hours
	$\eta^*$ , Pa·s	AI <sup>1</sup>	$\eta^*$ , Pa·s	AI <sup>1</sup>	$\eta^*$ , Pa·s	AI <sup>1</sup>	Aging Index	Aging Index
AAA-1	417	3.82	815	7.48	660	6.05	6.11	33.67
AAB-1	543	3.39	948	5.92	854	5.34	6.75	29.50
AAC-1	327	2.97	429	3.90	458	4.16	6.24	20.56
AAD-1	1,646	12.56	3,500	26.71	1,520	11.60	11.83	68.15
AAF-1	850	3.75	1,350	5.96	1,000	4.42	9.79	38.69
AAG-1	453	1.89	694	2.89	553	2.30	3.84	9.75
AAK-1	2,957	7.16	7,840	18.98	2,780	6.73	8.34	42.16
AAM-1	988	3.83	1,560	6.05	1,610	6.24	9.34	44.77

<sup>1</sup> AI = Aging Index = Aged Viscosity/Unaged Viscosity at 60 °C

**Table 8.20 Infrared Spectroscopic Analysis Results of Vanadyl Acetylacetonate Catalyzed Oxidation of SHRP Asphalts**

Asphalt	0.25% V (AcAc) 163 °C, 85 min.		0.50% V (AcAc) 163 °C, 85 min.		0.50% V (AcAc) 130 °C, 4 hours		60 °C TFO-POV 144 hours		80 °C TFO-POV 144 hours	
	Carbonyl <sup>1</sup> Abs. Units	Sulfoxide <sup>1</sup> Mol/L	Carbonyl <sup>1</sup> Abs. Units	Sulfoxide <sup>1</sup> Mol/L	Carbonyl <sup>1</sup> Abs. Units	Sulfoxide <sup>1</sup> Mol/L	Carbonyl <sup>1</sup> Abs. Units	Sulfoxide <sup>1</sup> Mol/L	Carbonyl <sup>1</sup> Abs. Units	Sulfoxide <sup>1</sup> Mol/L
AAA-1	0.04	0.029	0.05	0.017	0.06	0.025	0.04	0.22	0.10	0.33
AAB-1	0.03	0.044	0.03	0.028	0.03	0.031	0.05	0.25	0.11	0.32
AAC-1	0.04	0.044	0.07	0.027	0.06	0.029	0.09	0.19	0.17	0.17
AAD-1	0.05	0.027	0.08	0.018	0.05	0.022	0.07	0.24	0.11	0.42
AAF-1	0.03	0.050	0.05	0.047	0.04	0.035	0.07	0.25	0.13	0.28
AAG-1	0.05	0.049	0.07	0.041	0.06	0.041	0.12	0.18	0.23	0.17
AAK-1	0.04	0.034	0.06	0.032	0.06	0.036	0.05	0.21	0.12	0.41
AAM-1	0.04	0.031	0.07	0.016	0.10	0.027	0.11	0.10	0.18	0.075

<sup>1</sup> Based on prior experience with asphalts, standard deviations are (mol/L): sulfoxides, 0.027; ketones, 0.006.

**Table 8.21 Results of Infrared Analysis of Extracted Asphalts from Asphalt-Aggregate PAV Aging, 144 Hours, 60°C**

Sample	Carbonyl <sup>1</sup> Absorbance Units	Sulfoxide <sup>1</sup> Concentration, mL
AAA/ RD	0.06	0.23
RL	0.05	0.23
Teflon	0.06	0.24
TFO-PAV	0.05	0.23
AAB/ RD	0.06	0.26
RL	0.05	0.23
TFO-PAV	0.05	0.25
AAC/ RD	0.13	0.18
RL	0.12	0.12
TFO-PAV	0.08	0.19
AAD/ RD	0.08	0.27
RL	0.08	0.27
Teflon	0.08	0.28
TFO-PAV	0.07	0.26
AAF/ RD	0.09	0.29
RL	0.09	0.26
TFO-PAV	0.06	0.26
AAG/ RD	0.19	0.18
RL	0.20	0.20
Teflon	0.20	0.19
TFO-PAV	0.13	0.18
AAK/ RD	0.05	0.25
RL	0.06	0.27
Teflon	0.06	0.26
TFO-PAV	0.05	0.21
AAM/ RD	0.14	0.08
RL	0.14	0.07
TFO-PAV	0.11	0.11

<sup>1</sup> Based on prior experience with asphalts, standard deviations are (mol/L): sulfoxides, 0.027; ketones, 0.006.



**Table 8.22 Results from Thermal Annealing Experiments on Extracted Asphalts from Asphalt-Aggregate PAV Aging**

Sample	Annealed Viscosity, <sup>1</sup> Pa · s	Original Viscosity, <sup>1</sup> Pa · s
AAA/ RD	606.4	545.0
RL	602.7	398.0
Teflon	601.5	507.0
TFO-PAV	654.2	601.0
AAB/ RD	959.2	612.0
RL	998.4	703.0
TFO-PAV	1241.0	1090.0
AAC/ RD	858.0	723.0
RL	710.6	605.0
TFO-PAV	678.6	658.0
AAD/ RD	1566.0	1197.0
RL	1453.0	723.0
Teflon	1386.0	1005.0
TFO-PAV	1912.0	1690.0
AAF/ RD	2661.0	2598.0
RL	2788.0	2521.0
TFO-PAV	2232.0	2210.0
AAG/ RD	1375.0	902.0
RL	1607.0	1127.0
Teflon	1452.0	1153.0
TFO-PAV	1219.0	922.0
AAK/ RD	2976.0	1670.0
RL	3395.0	2893.0
Teflon	3461.0	2081.0
TFO-PAV	5092.0	3380.0
AAM/ RD	2651.0	2281.0
RL	3070.0	2745.0
TFO-PAV	3150.0	2410.0

<sup>1</sup> Viscosity measurements on the Rheometrics Mechanical Spectrometer are estimated to have an error bar of  $\pm 10\%$ .

**Table 8.23**    **Preparative Size Exclusion Fraction-I Data for Aged<sup>1</sup> Core Asphalts, Mass %<sup>1</sup>**

Asphalt	Unaged	mass % SEC Fraction-I				
		TFAAT, 130°C <sup>2</sup>		TFO-PAV, 60°C <sup>2</sup>	TFO-PAV, 24 hr <sup>3</sup>	
		4 hr	12 hr	144 hr, 300 psi	100°C	113°C
AAA-1	21.6 ± 0.5	25.6	26.7	24.1	ND <sup>4</sup>	ND
AAB-1	20.9 ± 0.7	25.0	27.0	24.6	ND	ND
AAC-1	13.6 ± 0.1	17.0	18.5	16.7	ND	ND
AAD-1	23.4 ± 0.2	27.3	29.4	27.0 ± 0.2	33.8	36.2
AAF-1	13.9 ± 18.4	18.4	20.6	18.2	ND	ND
AAG-1	11.9 ± 0.4	14.7	16.2	14.4 ± 0.2	18.0	19.2
AAK-1	25.8 ± 0.3	28.7	31.5	27.8	34.7	39.9
AAM-1	30.8 ± 0.5	34.5	35.6	34.5	49.3; 39.4 <sup>5</sup>	47.1

<sup>1</sup> Standard deviations are given where 3 or more runs were done. For others, a standard deviation of ± 0.8 has been estimated.

<sup>2</sup> Aged at Western Research Institute

<sup>3</sup> Aged at The Pennsylvania State University

<sup>4</sup> ND = Not determined

<sup>5</sup> This run was done with a 6 g sample; all others were done with 16 g samples.

**Table 8.24 Carbonyl Absorbance and Sulfoxide Concentrations of PSU Aged Asphalts**

Asphalt	Aging <sup>1</sup> Temperature, °C	Sulfoxide <sup>2</sup> Concentration, mol/L	Ketones, <sup>2</sup> Absorbance Units
AAD-1	100	0.25	0.11
	113	0.32	0.15
AAG-1	100	0.15	0.19
	113	0.14	0.26
AAK-1	100	0.26	0.10
	113	0.30	0.17
AAM-1	100	0.08	0.15
	113	0.06	0.22

<sup>1</sup> Aged at The Pennsylvania State University

<sup>2</sup> Based on prior experience with asphalts, standard deviations are (mol/L): sulfoxides, 0.027; ketones, 0.006.

**Table 8.25 Preparative Size Exclusion Chromatography of Aged<sup>1</sup> Core Asphalts, Mass %<sup>2</sup>**

Fraction Number	AAD-1		AAG-1		AAK-1		AAM-1	
	100°C	113°C	100°C	113°C	100°C	113°C	100°C	113°C
1	33.8	36.2	18.0	19.2	34.7	39.9	49.3	47.1
2	8.4	7.6	10.0	10.1	10.9	10.2	21.1	22.2
3	11.7	9.9	19.7	18.3	14.0	~14.0 <sup>3</sup>	15.8	16.5
4	18.7	16.6	26.3	26.1	18.5	17.5	8.9	8.9
5	19.3	19.3	18.1	18.1	15.2	13.4	3.7	4.0
6	6.8	8.7	7.1	7.1	5.7	4.4	1.2	1.3
7	1.1	1.5	1.2	1.2	1.0	0.7	0.1	0.2
8	0.1	0.1	0.1	0.1	<0.1	<0.1	<0.1	<0.1
9	0	<0.1	<0.1	<0.1	<0.1	<0.1	<0.1	<0.1

<sup>1</sup> Aged at The Pennsylvania State University

<sup>2</sup> One run only, see Chapter 5, Table 5.1 for an estimate of the standard deviations per fraction.

<sup>3</sup> Estimated by subtracting sum from other fractions from 100.

**Table 8.26 Comparison of PSEC and SPSEC Fraction-I Data for Aged<sup>1</sup> Asphalts**

Asphalt	Aging Protocol <sup>2</sup>	PSEC, <sup>3</sup> mass %	SPSEC, mass %
AAA-1	A	ND <sup>4</sup>	27.8 ± 0.5
AAB-1	A	ND	26.2 ± 0.7
AAC-1	A	ND	18.1 ± 0.2
AAD-1	B	33.8	31.0 ± 0.4
AAD-1	A	ND	27.8 ± 0.8
AAD-1	C	36.2	34.6 ± 0.4
AAF-1	A	ND	20.6 ± 0.4
AAG-1	B	18.0	17.7 ± 0.8
AAG-1	A	ND	15.2 ± 1.0
AAG-1	C	19.2	19.6 ± 0.4
AAK-1	B	34.7	33.0 ± 0.6
AAK-1	A	ND	29.9 ± 0.3
AAK-1	C	39.9	37.0 ± 0.3
AAM-1	B	49.3	42.3 ± 1.6
AAM-1	A	ND	38.2 ± 1.4
AAM-1	C	47.1	47.3 ± 0.6
AAE	A	32.5	ND
AAE	D	~28.5	ND
AAN	A	24.6	24.5 ± 0.8
AAN	D	22.6	21.5 ± 1.0
AAS-1	D	26.4	ND

<sup>1</sup> Aged at The Pennsylvania State University

<sup>2</sup> Aging protocols:

A = Thin-film oven test followed by pressure air vessel aging at 100 °C (212 °F) for 20 hr with a 3.2 mm (1/8") film thickness

B = Thin-film oven test followed by pressure air vessel aging at 100 °C (212 °F) for 24 hr with a 1.6 mm (1/16") film thickness

C = Thin-film oven test followed by pressure air vessel aging at 113 °C (235 °F) for 24 hr with a 1.6 mm (1/16") film thickness

D = Thin-film oven test (ASTM D 1754)

<sup>3</sup> These PSEC results are for one run only. A study of the results from PSEC runs of unaged asphalts gives a standard deviation of 0.8

<sup>4</sup> ND = Not determined

Table 8.27 Mass Fractions of SEC Fraction-I of PSU Aged Asphalts

Asphalt	Mass Fraction, % SEC Fraction-I		Molecular Weight, SEC Fraction-I (Daltons) <sup>2</sup>			
	Unaged Asphalt	Asphalt Aged <sup>1</sup> at 100°C	Asphalt Aged <sup>1</sup> at 113°C	Unaged Asphalt	Asphalt Aged at 100°C	Asphalt Aged at 113°C
AAD-1	24.6	33.8	36.2	7,000	10,600	17,400
AAG-1	11.8	18.0	19.1	7,900	7,220	8,400
AAK-1	26.0	34.7	39.9	10,000	8,800	10,100
AAM-1	31.8	49.3	47.1	4,600	3,960	4,800

<sup>1</sup> Aged at The Pennsylvania State University<sup>2</sup> Molecular weights were determined in toluene at 60°C by vapor phase osmometry. At these levels, error bars are  $\pm 10\%$ .

**Table 8.28 Molecular Weights in Toluene and Pyridine of SEC Fractions of Aged Asphalts**

Asphalt	Aging <sup>1</sup> Temperature, °C	SEC Fraction	M <sub>n</sub> <sup>2</sup>	
			Toluene	Pyridine
AAD-1	100	I	10,600	5,660
	113	I	17,400	4,840
	113	II	571	601
AAG-1	100	I	7,220	3,690
	113	I	8,400	3,970
	113	II	679	712
AAK-1	100	I	8,820	6,470
	113	I	10,100	5,130
AAM-1	100	I	3,960	insol
	113	I	4,800	insol

<sup>1</sup> Aged at The Pennsylvania State University

<sup>2</sup> Determined by vapor phase osmometry at 60 °C. Error bars ± 10%

**Table 8.29 Potentiometric Titration of Bases in Core Asphalts TFO-PAV Aged at 100°C**

Aged Asphalt <sup>1</sup>	Run No.	Strong Bases (meq/g)	Moderately Strong Bases (meq/g)	Weak Bases (meq/g)	Total Titratable Bases (meq/g)
AAA-1	1		0.04	0.21	0.25
	2		0.05	0.21	0.26
	3		<u>0.04</u>	<u>0.21</u>	<u>0.25</u>
	Avg. + Std. Dev.		0.04 ± 0.01	0.21 ± 0	0.25 ± 0.01
AAB-1	1		0.08	0.22	0.30
	2		0.08	0.23	0.31
	3		<u>0.08</u>	-	-
	Avg. + Std. Dev.		0.08 ± 0	0.23	0.31
AAC-1	1		0.10	0.17	0.27
	2		<u>0.09</u>	<u>0.16</u>	<u>0.25</u>
	Avg.		0.10	0.17	0.26
AAD-1	1		0.09	0.34	0.43
	2		<u>0.10</u>	<u>0.31</u>	<u>0.41</u>
	Avg.		0.10	0.33	0.42
AAF-1	1		0.06	0.24	0.30
	2		0.06	0.20	0.26
	3		<u>0.05</u>	<u>0.23</u>	<u>0.28</u>
	Avg. + Std. Dev.		0.06 ± 0.01	0.22 ± 0.02	0.28 ± 0.02
AAG-1	1	0.13	0.17	0.26	0.56
	2	0.14	0.17	0.28	0.59
	3	0.15	0.15	0.26	0.56
	4	<u>0.16</u>	<u>0.14</u>	<u>0.24</u>	<u>0.54</u>
	Avg. + Std. Dev.	0.15 ± 0.01	0.16 ± 0.02	0.26 ± 0.02	0.56 ± 0.02
AAK-1	1		0.08	0.23	0.30
	2		<u>0.08</u>	<u>0.22</u>	<u>0.30</u>
	Avg.		0.08	0.23	0.30
AAM-1	1		0.07	0.11	0.18
	2		<u>0.08</u>	<u>0.11</u>	<u>0.19</u>
	Avg.		0.08	0.11	0.19

<sup>1</sup> Aged at The Pennsylvania State University

**Table 8.30 Potentiometric Titration of Bases in TFO and TFO-PAV Aged Asphalts**

Aged Asphalt <sup>1</sup>	Aging Method	Moderately Strong Bases (meq/g)	Weak Bases (meq/g)	Total Titratable Bases (meq/g)
AAE	TFO	0.05	0.11	0.16
	TFO-PAV	0.03	0.20	0.23
AAH	TFO	0.08	0.11	0.19
	TFO-PAV	0.06	0.22	0.28
AAJ	TFO	0.10	0.12	0.22
	TFO-PAV	0.09	0.14	0.23
AAL	TFO	0.07	0.14	0.21
	TFO-PAV	0.04	0.20	0.24
AAN	TFO	0.06	0.11	0.17
	TFO-PAV	0.04	0.21	0.25
AAO	TFO	0.05	0.09	0.14
	TFO-PAV	0.03	0.17	0.20
AAP	TFO	0.08	0.10	0.18
	TFO-PAV	0.09	0.15	0.24
AAR	TFO	0.08	0.14	0.22

<sup>1</sup> Aged at The Pennsylvania State University



**Table 8.31 Asphaltene and Maltene Yields from TFAAT-Aged Core Asphalts**

Asphalt	Run No.	Yield (mass %)	
		Maltenes	Asphaltenes
AAA-1	1	83.4	16.8
AAA-1, Aged <sup>1</sup>	1	70.0	30.3
AAD-1	1	80.0	20.0
AAD-1, Aged <sup>1</sup>	1	64.1	35.9
AAD-1, Aged <sup>1</sup>	2	64.4	35.7
AAG-1	1	95.0	5.0
AAG-1, Aged <sup>1</sup>	1	86.0	14.0
AAG-1, Aged <sup>1</sup>	2	84.9	15.0

<sup>1</sup> Aging conditions were 113 °C, 72 hours.

**Table 8.32 Heithaus P (State of Peptization) for Unaged and TFAAT Aged Core Asphalts**

Asphalt	Unaged			TFAAT Aged		
	1 <sup>1</sup>	2 <sup>2</sup>	Avg. ± Std. Dev.	1 <sup>1</sup>	2 <sup>2</sup>	Avg. ± Std. Dev.
AAA-1	3.44	3.45	3.44 ± 0.01	2.73	2.93	2.83 ± 0.14
AAB-1	3.50	3.55	3.52 ± 0.04	2.50	3.46	2.98 ± 0.68
AAC-1	-	-	-	-	-	-
AAD-1	3.30	3.37	3.34 ± 0.05	2.66	2.42	2.54 ± 0.17
AAF-1	3.52	3.09	3.30 ± 0.30	2.84	2.93	2.88 ± 0.06
AAG-1	5.46	4.82	5.14 ± 0.45	4.91	4.23	4.57 ± 0.48
AAK-1	3.75	3.71	3.73 ± 0.03	3.13	3.24	3.18 ± 0.08
AAM-1	12.77	10.50	12.51 ± 2.57	-	9.95	17.0 ± 10.0
	14.85	9.40	-	-	24.10	-
	15.06	9.27 <sup>3</sup>	-	-	-	-
	15.69	-	-	-	-	-

<sup>1</sup> Operator 1

<sup>2</sup> Operator 2

<sup>3</sup> Operator 3

**Table 8.33 Heithaus  $p_a$  (Peptizability of Asphaltenes) for Unaged and TFAAT Aged Core Asphalts**

Asphalt	Unaged			TFAAT Aged		
	1 <sup>1</sup>	2 <sup>2</sup>	Avg. $\pm$ Std. Dev.	1 <sup>1</sup>	2 <sup>2</sup>	Avg. $\pm$ Std. Dev.
AAA-1	0.68	0.64	0.66 $\pm$ 0.03	0.58	0.56	0.57 $\pm$ 0.01
AAB-1	0.67	0.63	0.65 $\pm$ 0.03	0.57	0.52	0.54 $\pm$ 0.04
AAC-1	-	-	-	-	-	-
AAD-1	0.63	0.60	0.62 $\pm$ 0.02	0.48	0.49	0.48 $\pm$ 0.01
AAF-1	0.62	0.63	0.62 $\pm$ 0.01	0.57	0.56	0.56 $\pm$ 0.01
AAG-1	0.80	0.74	0.77 $\pm$ 0.04	0.69	0.69	0.69 $\pm$ 0.00
AAK-1	0.67	0.64	0.66 $\pm$ 0.02	0.54	0.53	0.54 $\pm$ 0.01
AAM-1	0.92	0.86; 0.86	0.89 $\pm$ 0.04	0.92	0.89	0.90 $\pm$ 0.02

<sup>1</sup> Operator 1

<sup>2</sup> Operator 2

**Table 8.34 Heithaus  $p_o$  (Peptizing Power of Maltenes) for Unaged and TFAAT Aged Core Asphalts**

Asphalt	Unaged			TFAAT Aged		
	1 <sup>1</sup>	2 <sup>2</sup>	Avg. $\pm$ Std. Dev.	1 <sup>1</sup>	2 <sup>2</sup>	Avg. $\pm$ Std. Dev.
AAA-1	1.10	1.24	1.17 $\pm$ 0.17	1.16	1.30	1.23 $\pm$ 0.10
AAB-1	1.17	1.31	1.24 $\pm$ 0.10	1.07	1.64	1.36 $\pm$ 0.40
AAC-1	-	-	-	-	-	-
AAD-1	1.23	1.36	1.30 $\pm$ 0.09	1.37	1.25	1.31 $\pm$ 0.08
AAF-1	1.33	1.14	1.24 $\pm$ 0.13	1.23	1.30	1.26 $\pm$ 0.05
AAG-1	1.07	1.25	1.16 $\pm$ 0.13	1.51	1.32	1.42 $\pm$ 0.13
AAK-1	1.23	1.32	1.28 $\pm$ 0.06	1.43	1.51	1.47 $\pm$ 0.06
AAM-1	1.28	1.48; 1.14	1.30 $\pm$ 0.17	1.99	1.06	1.52 $\pm$ 0.66

<sup>1</sup> Operator 1

<sup>2</sup> Operator 2

**Table 8.35 Reduced Specific Viscosity of Selected SHRP Asphalts Before and After Aging at 45°C as a Function of Percent Natural Abundance of Asphaltenes**

Asphalt	Percent Natural Abundance of Asphaltenes	Reduced Specific Viscosity, cm <sup>2</sup> /gm	
		Unaged	Aged <sup>1</sup>
AAD-1	0	-	-
	25	4.8 x 10 <sup>1</sup>	3.8 x 10 <sup>1</sup>
	50	8.2 x 10 <sup>1</sup>	3.09 x 10 <sup>2</sup>
	75	2.52 x 10 <sup>2</sup>	5.86 x 10 <sup>3</sup>
	100	1.12 x 10 <sup>3</sup>	2.33 x 10 <sup>4</sup>
	125	3.17 x 10 <sup>3</sup>	3.76 x 10 <sup>5</sup>
AAG-1	0	-	-
	20	2.2 x 10 <sup>1</sup>	-
	25	-	3.3 x 10 <sup>1</sup>
	40	1.8 x 10 <sup>1</sup>	-
	50	-	6.4 x 10 <sup>1</sup>
	60	2.2 x 10 <sup>1</sup>	-
	75	-	7.1 x 10 <sup>1</sup>
	80	2.0 x 10 <sup>1</sup>	-
	100	3.0 x 10 <sup>1</sup>	1.01 x 10 <sup>2</sup>
	125	3.7 x 10 <sup>1</sup>	2.60 x 10 <sup>2</sup>
	200	5.0 x 10 <sup>1</sup>	
	250	2.08 x 10 <sup>2</sup>	
	300	9.57 x 10 <sup>2</sup>	
	350	3.57 x 10 <sup>3</sup>	

<sup>1</sup> Oxidative aging performed using the TFAAT method, 113°C, 72 hrs.

**Table 8.36 Kinetic Data for Comparison of 113°C TFAAT and 60°C PAV (Corrected for TFO)**

Asphalt	Aging Conditions	Aging Time, hrs	Dynamic Viscosity <sup>1</sup> Pa · s, 60 °C
AAD-1	113 °C, TFAAT	0	$1.31 \times 10^2$
		24	$4.07 \times 10^3$
		48	$1.92 \times 10^4$
		72	$7.58 \times 10^4$
AAG-1	113 °C, TFAAT	0	$2.40 \times 10^2$
		24	$1.12 \times 10^3$
		48	$1.97 \times 10^3$
		72	$3.62 \times 10^3$
AAD-1	60 °C, PAV	0	$1.31 \times 10^2$
		TFO	$3.54 \times 10^2$
		48	$1.05 \times 10^3$
		96	$1.55 \times 10^3$
		144	$1.55 \times 10^3$
		400	$3.55 \times 10^3$
AAG-1	60 °C, PAV	0	$2.40 \times 10^2$
		TFO	$3.41 \times 10^2$
		48	$6.74 \times 10^2$
		96	$8.64 \times 10^2$
		144	$9.21 \times 10^2$
		400	$1.91 \times 10^3$

<sup>1</sup> Viscosity measurements on the Rheometrics Mechanical Spectrometer are estimated to have an error bar of  $\pm 10\%$ .

## 9

# Characterization of Asphalts by Classical Methods

### Introduction

To make possible comparisons with data from historical studies, it was decided to analyze asphalts investigated during the Binder Characterization and Evaluation Program by selected classical chemical characterization techniques. The techniques chosen were elemental analysis for carbon, hydrogen, nitrogen, oxygen, sulfur, and metals; number-average molecular weight ( $M_n$ ) determined by vapor phase osmometry (VPO) in pyridine and toluene; infrared functional group analysis (IR-FGA); asphaltene content determined by precipitation with n-heptane and iso-octane; and measurement of Heithaus parameters. Additionally, rheological measurements were performed as part of the chemistry program. Elemental analyses, molecular weight determinations, and IR studies have long been used by chemists and are routinely performed in investigations of organic materials. These methods provide information about overall polarity, aromaticity, and molecular size, which are important properties of any substance. Measurements of asphaltene content are usually performed during the analyses of crude oils and their heavier fractions. For these materials, asphaltene content provides a measure of compatibility or state of dispersion of the system. The Heithaus titration method also is a measure of compatibility.

Many prior studies of asphalt chemistry have reported data using the above analytical methods. They are reasonably rapid to perform, are not unusually expensive, and for the most part are reliable. Unfortunately, the global parameters derived from these classical analyses are not sufficient for accurate prediction of asphalt performance-related properties, although they do serve as a basis for some general characterization of asphalts. At the outset of the Binder Characterization and Evaluation program, it was hoped that the parameters derived from classical analysis could be combined with other kinds of data to provide useful predictive chemical indices.

Nuclear magnetic resonance (NMR) spectroscopy is another technique commonly used in the analysis of fossil fuels. The NMR studies sponsored by SHRP were performed in another program, designated Binder Characterization and Evaluation by NMR Spectroscopy (Jennings et al. 1993). Separation of asphalts into saturates, naphthene aromatics, and polar aromatics by the Corbett procedure, another classical method of asphalt analysis, was performed and the data were provided by the A-001 contractor. Measurement of wax

content is a standard method in the analysis of crude oils. Dr. F. Fleitas of INTEVEP performed wax determinations for the SHRP asphalts.

Other classical methods of analysis were not performed because of the emphasis in the Binder Characterization and Evaluation Program on novel approaches to the study of asphalt chemistry.

All analyses reported below were performed at Western Research Institute (WRI) with the exception of some carbon, hydrogen, and nitrogen analyses, which were performed at Wyoming Analytical Laboratories (WAL).

## **Elemental Composition of Core Asphalts**

Table 9.1 lists elemental analyses of the eight core asphalts for carbon and hydrogen. Carbon and hydrogen values were obtained by two different laboratories using standard methods, which are described in Volume IV, chapter 6. The ratios of hydrogen to carbon vary from 1.38 to 1.49, which does not represent a great difference in aromaticities among the eight asphalts. A low value of the atomic hydrogen-to-carbon (H/C) ratio indicates that a material is relatively aromatic (e.g., H/C ratios for coals are nearly unity). A high H/C value indicates that a material is aliphatic (e.g., kerosines, in which H/C is nearly 2).

Nitrogen, oxygen, sulfur, vanadium, and nickel values for the eight core asphalts are listed in tables 9.2 and 9.3. Standard methods, described in Volume IV, chapter 6, were employed to obtain these data. Nitrogen determinations were performed at two different laboratories. Asphalts AAC-1, AAG-1, and AAM-1 are characterized by low sulfur concentrations (<2.0%), whereas asphalts AAD-1 and AAK-1 are high in sulfur (>5.0%). Asphalt AAG-1 is high in nitrogen compared with the other seven core asphalts. Oxygen values, for which only single determinations were performed, range from 0.5 (AAM-1) to 1.1 (AAF-1 and AAG-1) mass %. Asphalts AAF-1, AAG-1, and AAM-1 are characterized by low metal concentrations. Both vanadium and nickel concentrations are less than 100 ppm in these three asphalts. The two high sulfur asphalts (AAD-1 and AAK-1) are rich in vanadium, AAK-1 particularly so. Asphalt AAG-1, while low in sulfur and metal content, has large amounts of nitrogen and oxygen. Asphalt AAM-1 is low in heteroatom (nitrogen, oxygen, sulfur), vanadium, and nickel content. Some other metal analyses were performed to determine whether any unusual concentrations were present. Except for a large (255 ppm) iron concentration in AAM-1, none was observed. The complete data set can be found in SHRP Database B (appendix B).

## **Molecular Weight Determinations of Core Asphalts**

Number-average molecular weights ( $M_n$ ) of the asphalts were determined in toluene and pyridine at 60°C (140°F) by VPO (table 9.4), using the standard ASTM method (ASTM D 2503). Calibrations were performed using benzil as standard in both toluene and pyridine.

Molecular weights of asphalt fractions reported earlier in this volume and later in this chapter were determined in the same manner. For seven of the core asphalts,  $M_n$  values range from 710 to 850 daltons and are essentially the same in pyridine as in toluene. The  $M_n$  value of AAM-1 is much larger than those of the other core asphalts. Due to the reconnaissance nature of these experiments and the expense of molecular weight determinations, very few replications were performed. However, some of the specific values cited were derived from triplicate measurements of individual samples. Additionally, determinations of standard materials were occasionally run. In all cases, single point determinations of solutions of asphalts and asphalt fractions in toluene or pyridine at the 1.0 mass % level were performed. At lower concentrations, good readings cannot be obtained for solutions of higher molecular weight materials. At higher concentrations, associations of molecules become important for materials containing polar components. Measurements of solutions at several levels of concentration were not performed for the above reasons and because of the expense involved.

It has long been recognized that the standard ASTM method D 2503 commonly used to determine "true"  $M_n$  values of petroleum and petroleum derived materials is not entirely satisfactory (Moschopedis, Fryer, and Speight 1976). The method appears to give good "true" molecular weights for those materials that do not have large amounts of strongly polar components. Recently Green, Diehl, and Shay (1991) reported results of an investigation of ion exchange chromatography (IEC) fractions of Cerro Negro crude and its distillation fractions. "True" molecular weights were determined by mass spectrometry (MS) and titrimetry. Even these methods posed problems for some of the fractions that were studied. Involatile materials cannot be studied by MS. Different compound types in mixtures also are characterized by different MS sensitivities. Considering these difficulties, Green et al. concluded that for polar materials, VPO molecular weights can be much higher than "true" molecular weights due to molecular associations and interactions with solvent molecules. Storm et al. (1990) determined upper bounds on  $M_n$  values of petroleum asphaltenes by other methods and also concluded that ASTM D 2503 yielded higher values than the "true"  $M_n$  values.

Obviously, the determination of accurate molecular weights of asphalts would be a project in itself. The standard ASTM (D 2503) VPO method was chosen at the outset of the Binder Characterization and Evaluation Program partly because the literature reported a large amount of molecular weight data on asphalts and their fractions obtained using the method. The method is fairly rapid and much less expensive than other methods that may give results closer to "true" molecular weights. Additionally, relatively nonpolar materials were measured for which the method should provide fairly accurate data. The  $M_n$  values obtained by the VPO method may, however, more accurately reflect effective (apparent)  $M_n$  values of materials that contain polar components and tend to associate.

## **Infrared Functional Group Analysis of Core Asphalts**

IR-FGA, a method developed at WRI (Petersen 1986), was performed on all of the core asphalts. Various chemical functional groups of interest in tank and aged asphalts can be quantified by this technique, and the structures of these functional groups are illustrated in

figure 9.1. The IR-FGA method of analysis provides more information when applied to aged asphalts and polar fractions of asphalts than tank asphalts. Results are listed in table 9.5. The IR-FGA analysis shows that carboxylic acids are sufficiently abundant in AAA-1, AAD-1, and AAK-1 to be detected in IR spectra of the whole asphalts. Asphalt AAG-1 contains carboxylic acid salts, and it is known that the asphalt has been lime treated. The highly polar 2-quinolone compounds are found in all of the asphalts. Asphalt AAG-1 contains large amounts of pyrroles and phenols. Asphalts AAF-1 and AAK-1 are deficient in phenols. Again, because of the reconnaissance nature of this study, the analyses were not replicated.

## Asphaltene Contents of Core Asphalts

Asphaltene yields of heavy crudes and asphalts provide a measure of compatibility. Additionally, asphaltene and maltenes are required for intrinsic viscosity studies (see below). Asphaltene yields were determined by mixing samples of asphalts with 40 volumes of n-heptane. The experimental details are described in Volume IV, chapter 6. The precipitated heptane asphaltene ( $H_A$ ) were separated from the dissolved maltenes and were dried and weighed, and then solvent was removed from the maltenes. The maltenes then were treated with 40 volumes of iso-octane, which caused more precipitation. After solvent removal and drying, iso-octane maltenes and iso-octane asphaltene ( $I_A$ ) were weighed. Yields of both types of asphaltene are listed in table 9.6. A parameter designated the Asphaltene Compatibility Index (ACI) was calculated by multiplying by 10 the ratio of the iso-octane asphaltene yield ( $I_A$ ) to the sum of the yields of both types of asphaltene ( $I_A + H_A$ ). The parameter serves as an index of compatibility of asphalt systems and can always be obtained, even when Heithaus parameters (discussed below) cannot.

For all asphalts except AAG-1 and AAK-1, heptane asphaltene yields are much higher than iso-octane asphaltene yields. Asphaltene contents of AAD-1 and AAK-1 are high. For AAM-1, yields are unusually low. Elemental analyses and molecular weight data for the asphaltene are listed in table 9.7. Replications were not performed due to the reconnaissance nature of this study. All the asphaltene are aromatic (low atomic H/C ratios), the heptane asphaltene more so than the iso-octane asphaltene. Except for AAF-1, all heptane asphaltene conform to the well-known rule of thumb that the H/C atomic ratio is  $1.15 \pm 0.05$ . In most cases, the heteroatoms nitrogen, oxygen, and sulfur are more abundant in the heptane asphaltene. The  $M_n$  values of the heptane asphaltene in toluene are much larger than those of the iso-octane asphaltene. These values range from 10,000 daltons (AAM-1) to 4,500 daltons (AAF-1) for the heptane asphaltene, and from 7,200 daltons (AAM-1) to 2,600 daltons (AAF-1) for the iso-octane asphaltene. The  $M_n$  values in pyridine for both kinds of asphaltene are lower than the corresponding  $M_n$  values in toluene. These data show that the asphaltene interact in toluene to form associations, which are broken up to some extent in pyridine.

The ACI values range from 1.04 to 5.93. Based on this parameter, asphalts AAM-1 and AAG-1 are compatible systems in the classical sense as defined by Pfeiffer and Saal (1940). In these asphalts, dispersed materials are effectively solubilized. Asphalts AAA-1, AAB-1, AAD-1, AAF-1, and AAK-1 are less compatible systems. Asphalt AAC-1 is intermediate.



## Heithaus Titrations

The Heithaus test (Heithaus 1962) has long been used to measure asphalt compatibility. The method is based on the hypothesis that asphalts consist of polar asphaltene peptized, or dispersed, in a solvent consisting of maltenes. In the Heithaus test, solutions of asphalts in varying amounts of toluene are titrated with n-heptane, and the amount of n-heptane required to effect flocculation is measured. Experimental details, including improvements in the procedure developed during the Binder Characterization and Evaluation Program, are described in Volume IV, chapter 6. From these data, three parameters are calculated:  $P$ , measuring the overall compatibility of the asphalt;  $p_a$ , measuring asphaltene peptizability; and  $p_o$ , measuring solvent power of the maltenes. Table 9.8 lists Heithaus parameters for seven core asphalts. Asphalt AAC-1 was too waxy to be measured, and it was difficult to obtain satisfactorily reproducible data for AAM-1. According to their Heithaus  $P$  values, AAM-1 and AAG-1 are the most compatible systems, in line with their ACI values. Again, asphalts AAA-1, AAB-1, AAD-1, AAF-1, and AAK-1 are incompatible systems based on their Heithaus  $P$  values. The low  $p_a$  values of these asphalts indicate that their asphaltenes are not readily peptizable. The  $p_o$  values do not vary much but indicate that the AAD-1 maltenes have the highest solvent power of the seven maltenes.

## Results of Classical Analyses of Core Asphalts

The classical chemical techniques provide a basis for a classification of the eight asphalts. One asphalt (AAM-1) is quite different from the other seven. This asphalt contains the smallest amounts of heteroatoms (oxygen, nitrogen, sulfur) and metals, has the lowest asphaltene content, and has by far the highest  $M_n$  and Heithaus  $P$  values.

Asphalt AAG-1 also differs from the other asphalts; it is high in nitrogen and oxygen, is low in metals, sulfur, and asphaltene content, and also has a high Heithaus  $P$  value. This asphalt is unique in having been lime treated, which is manifest in the large amounts of carboxylic acid salts detected by IR-FGA. The asphaltenes of this asphalt also are of low  $M_n$ .

The other six asphalts resemble one another more than they resemble the other two. All six have moderate to high concentrations of sulfur and asphaltenes and have low Heithaus  $P$  values ( $P$  for AAC-1 was not determined). They can be described as less compatible systems than AAM-1 or AAG-1.

## Classical Analyses of Other SHRP Asphalts

Some of the same chemical analyses were performed on the expanded set of asphalts with the exception of some viscosity grades of the same asphalts. These data are listed in supplementary table 9.11. Note that AAE is air-blown AAA-1, and ABD is the same material as AAG-1 before lime treatment. Two of the expanded set of asphalts have  $M_n$  values above 1,000 daltons, and AAS-1, AAX, and AAZ have  $M_n$  values nearly that high. Asphalt ABD has a high nitrogen content, as does the lime-treated asphalt from the same

crude, AAG-1. Asphalts AAE, AAH, AAL, AAX, and AAC-2 have high oxygen contents. This would be expected for the air-blown asphalt AAE. Of the expanded set of asphalts, only ABC is particularly high in sulfur content. Low-sulfur asphalts are AAJ, AAP, ABD, and AAC-2. Asphalt ABC is unusual in that it is a high-sulfur asphalt which contains very little vanadium. Of the asphalts in supplementary table 9.11, only AAY contains large amounts of vanadium. Some other metal determinations (Fe, Mn, Mo) were performed, but no large concentrations were found in any of the expanded set of asphalts. These data are in SHRP Database B (appendix B).

IR-FGA analysis of many members of the expanded set of asphalts was performed (supplementary table 9.12). Although air-blown, AAE does not contain significant amounts of sulfoxides or ketones, as is typical for asphalt oxidized at high temperatures. Only AAP contains measurable amounts of ketones, indicative of some degree of oxidation. Carboxylic acids are fairly abundant in AAE, AAL, and ABD. The highly polar 2-quinolones are observed in all of the asphalts whose IR-FGA analyses are listed in supplementary table 9.12. Compared with the core asphalts, only AAW and ABD contain large amounts of phenols.

Asphaltene contents and ACI values were determined for selected members of the expanded set of asphalts, including some different viscosity grades of the core asphalts. These data are listed in supplementary table 9.13. Air-blown asphalt AAE has an extremely low ACI value, indicating that it is a highly incompatible system. Based on the data in supplementary table 9.13, the more compatible asphalts are AAJ, AAV, AAX, AAZ, ABD, and AAM-2. Some comparisons of asphaltene yields of asphalts derived from the same crude oils but different viscosity grades are listed in supplementary table 9.14. In each related pair of asphalts, asphaltene yields and ACI values are nearly identical.

A few Heithaus titrations were performed on some of the expanded set of asphalts. These data are listed in supplementary table 9.15. With the exception of AAE, whose Heithaus P value indicates that it is not a particularly incompatible material, the Heithaus P values are in accord with the ACI values. Both AAJ and AAV are identified as compatible asphalts by each method of measurement.

## Viscosity Measurements

In the course of the chemistry studies of the asphalts at WRI, numerous viscosity determinations were performed. Most of this work was done on a Rheometrics Mechanical Spectrometer, which measures dynamic viscosity, viscous (loss) modulus ( $G''$ ), elastic (storage) modulus ( $G'$ ), and  $\tan \delta$ , the ratio of the values of viscous to elastic moduli. Temperatures of measurement usually were 25°C (77°F), 45°C (113°F), and 60°C (140°F). Protocols for viscosity measurements are discussed in Volume IV, chapter 12.

A few viscosity measurements were obtained on a Brabender Rheotron Viscometer, which determines static (apparent) viscosities. Viscosities determined on this viscometer compare with dynamic viscosities measured at about 0.1 rad/s. Table 9.9 lists viscosity determinations of the eight core asphalts at 60°C (140°F). With the exception of AAA-1

and AAK-1, viscosities determined by the two instruments are very close. Table 9.10 lists viscosities of the eight core asphalts determined on the mechanical spectrometer at 25°C (77°F) and of four of the core asphalts determined on the viscometer at 25°C (77°F). These values agree fairly well with the dynamic viscosity determinations at 0.1 rad/s. The duplicate viscosity determinations at 1.0 rad/s for AAA-1, AAB-1, AAD-1, and AAK-1 were measured after different annealing procedures, but the viscosities measured are within the error bars of measurement on the mechanical spectrometer. The viscosity determinations on the mechanical spectrometer in tables 9.9 and 9.10 have been used in a number of calculations in earlier chapters of this volume.

Viscosity determinations of the core asphalts at 45°C (113°F) are reported in supplementary table 9.16. Except for AAB-1, the viscosities determined on the mechanical spectrometer agree fairly closely with viscosities determined on the viscometer.

Viscosity determinations at 60°C (140°F) for members of the expanded set of asphalts are listed in supplementary table 9.17. These values have been used in a large number of calculations in earlier chapters in this report.

## **Intrinsic Viscosity Studies on Core Asphalts**

The study of reduced specific viscosities of solutions as a function of concentration has long been used to gain information about the nature and magnitude of polar associations. The reduced specific viscosity  $\langle \eta \rangle$  of a solution is defined as:

$$\langle \eta \rangle = (\eta - \eta_o) / (\eta_o * c) \quad (9.1)$$

where  $\eta$  = absolute viscosity of the solution  
 $\eta_o$  = absolute viscosity of the solvent  
 $c$  = concentration of solvent.

For asphalts, it may be arbitrarily assumed that the maltene fraction obtained by n-heptane precipitation of asphaltenes represents the solvent, and the asphaltenes are the solute. The reduced specific viscosity of an asphalt at a given asphaltene concentration is related to the size of associations in asphaltene microstructural units by a constant, the magnitude of which will be asphalt-dependent and must be determined by other means. The value of the reduced specific viscosity extrapolated to zero asphaltene concentration, known as the intrinsic viscosity, is related to actual sizes of asphaltene microstructural units in asphalts.

Asphaltenes and maltenes were prepared by the n-heptane precipitation method for each of the core asphalts, as described earlier. Viscosities of the dried maltene fractions were determined at three temperatures. These viscosities are the  $\eta_o$  values in equation (9.1) and are listed in supplementary table 9.18. Mixtures formulated for reduced specific viscosity measurements were prepared in two different ways. In one method, neat asphalts were diluted with maltenes, and the combined materials were heated until uniform mixtures were obtained. This method could not be used for mixtures containing more than natural abundances of asphaltenes. To make asphaltene-rich mixtures, asphaltenes and maltenes

were combined directly, and the whole mixture was dissolved in dichloromethane. The solvent then was removed. By the two procedures, mixtures were formulated containing varying amounts of asphaltenes and maltenes. Reduced specific viscosities  $\langle\eta\rangle$  at 25°C (77°F) and 60°C (140°F) are plotted versus percent asphaltene content based on asphaltene natural abundances in figures 9.2 through 9.9. The data on which these graphs are based are listed in supplementary tables 9.19 through 9.26. The  $\langle\eta\rangle$  values are dimensionless, because the concentrations used to calculate  $\langle\eta\rangle$  are in grams of asphaltenes per gram of asphalt. In figures 9.2 through 9.9, the 100% asphaltene natural abundance entry corresponds to the neat asphalt. Asphaltene contents vary markedly among the asphalts, ranging from 3.7 mass % (AAM-1) to 20.2 mass % (AAD-1). Figures 9.2 through 9.9 show that intrinsic viscosities of each asphalt (which can be roughly estimated by extrapolation of the curves to the y-axes) are lower at 60°C (140°F) than at 25°C (77°F). This must be so if association phenomena occur in asphalts. The intrinsic viscosities estimated for most of the asphalts are similar to values determined by Storm, Barresi, and DeCanio (1991) for several vacuum residua.

The intrinsic viscosities of AAM-1 at the two temperatures of measurement are much greater than those of the other asphalts at the same temperature. It can be concluded that AAM-1 is more compatible than the other asphalts (this is confirmed by high Heithaus P values and ACI values) and that the  $M_n$  value of the AAM-1 asphaltenes is much larger than  $M_n$  values of asphaltenes of the other asphalts. Table 9.7 verifies this observation. Unfortunately, the curves in figures 9.2 through 9.9 are not smooth. Measurements of  $\langle\eta\rangle$  at low asphaltene concentrations proved to be extremely variable. Occasionally, viscosity values were measured that were lower than maltene viscosities. Attempts at repeating the measurements did not improve matters (supplementary table 9.24). Thus, intrinsic viscosities of the core asphalts other than AAM-1 cannot be estimated with any certainty. Viscosity measurements are most variable at the asphaltene concentration levels that are of greatest importance. The problem may be due to molecular structuring with time, a factor not fully understood at the beginning of the Binder Characterization and Evaluation Program. Or it may be that different asphaltene and maltene preparations of the same asphalt are not reproducible enough for the purposes of this study. Mixtures were allowed to stand for variable lengths of time before rheological properties were measured. It was hoped that annealing would erase effects of structuring, particularly for samples having low asphaltene contents.

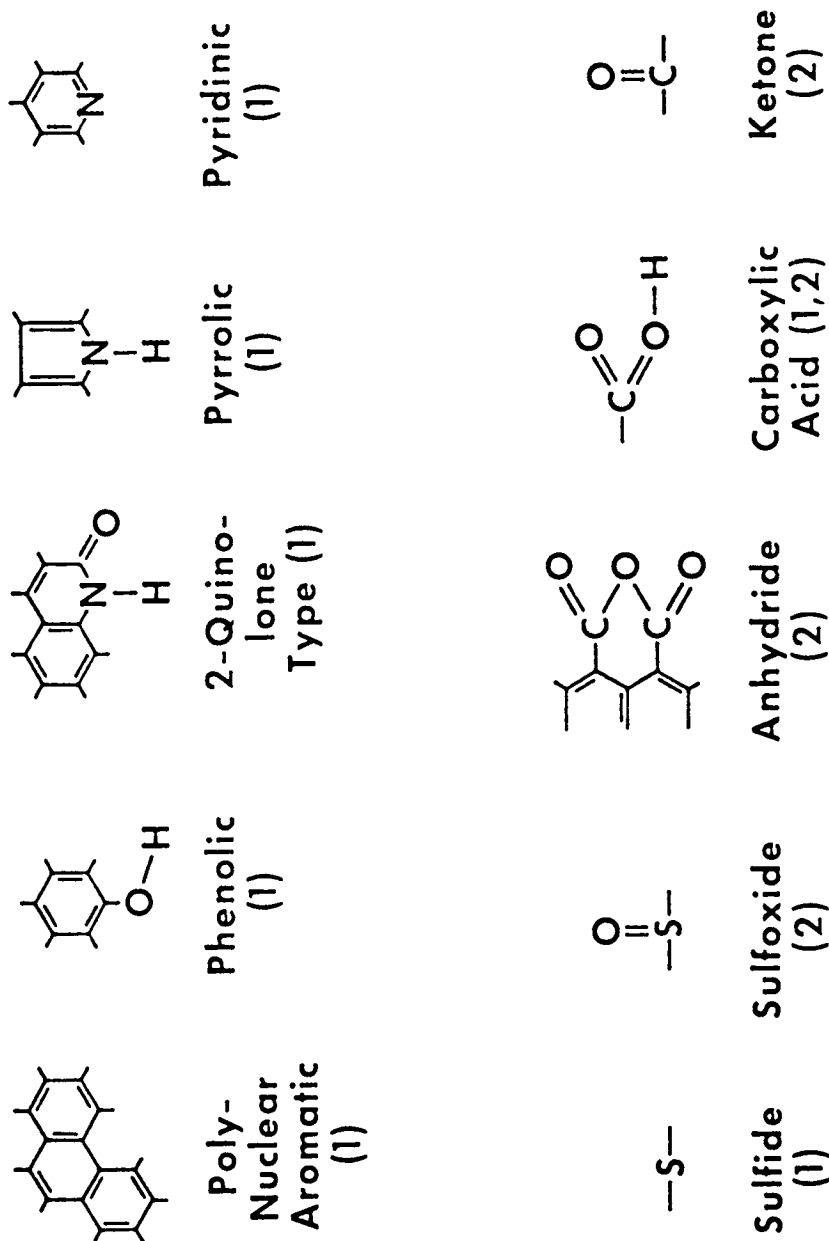
Taking all these difficulties into consideration, the shapes of the curves in figures 9.2 through 9.9 are informative. For asphalts AAA-1, AAB-1, AAD-1, and AAK-1, the concentration vs.  $\langle\eta\rangle$  curves are relatively steep. For asphalts AAG-1 and AAM-1, curves are almost parallel to the x-axis. Thus AAG-1 and AAM-1 are identified as compatible, and the other four asphalts much less so. Asphalts AAC-1 and AAF-1 are intermediate. These results are in accordance with Heithaus titration data and ACI determinations.

If the microstructural model is correct, oxidatively aged asphalts should be characterized by asphaltene concentration versus  $\langle\eta\rangle$  curves that are steeper than those of parent asphalts. In chapter 8, a study of reduced specific viscosities of aged asphalts was discussed.

## Summary

The classical methods of analysis serve to characterize asphalts according to compatibility. Compatibility has been correlated with asphalt physical properties (Traxler 1961). It has long been known that asphalts characterized by high viscosity maltenes and low asphaltene contents differ in physical properties from asphalts characterized by low viscosity maltenes and high asphaltene contents. Asphalts with high asphaltene contents usually have high sulfur contents.

The core asphalts were characterized by classical chemical methods. Two of the asphalts were determined to be compatible and differ greatly from the other six in most properties. Differences among the six less compatible asphalts are less pronounced as determined by classical methods. In general, the results of the classical methods correspond with the other methods used to study asphalts in the SHRP Binder Characterization and Evaluation Program.



(1) Naturally Occurring  
(2) Formed on Oxidative Aging

Figure 9.1 Functional Groups in Neat and Aged Asphalts Measured by IR  
Functional Group Analysis

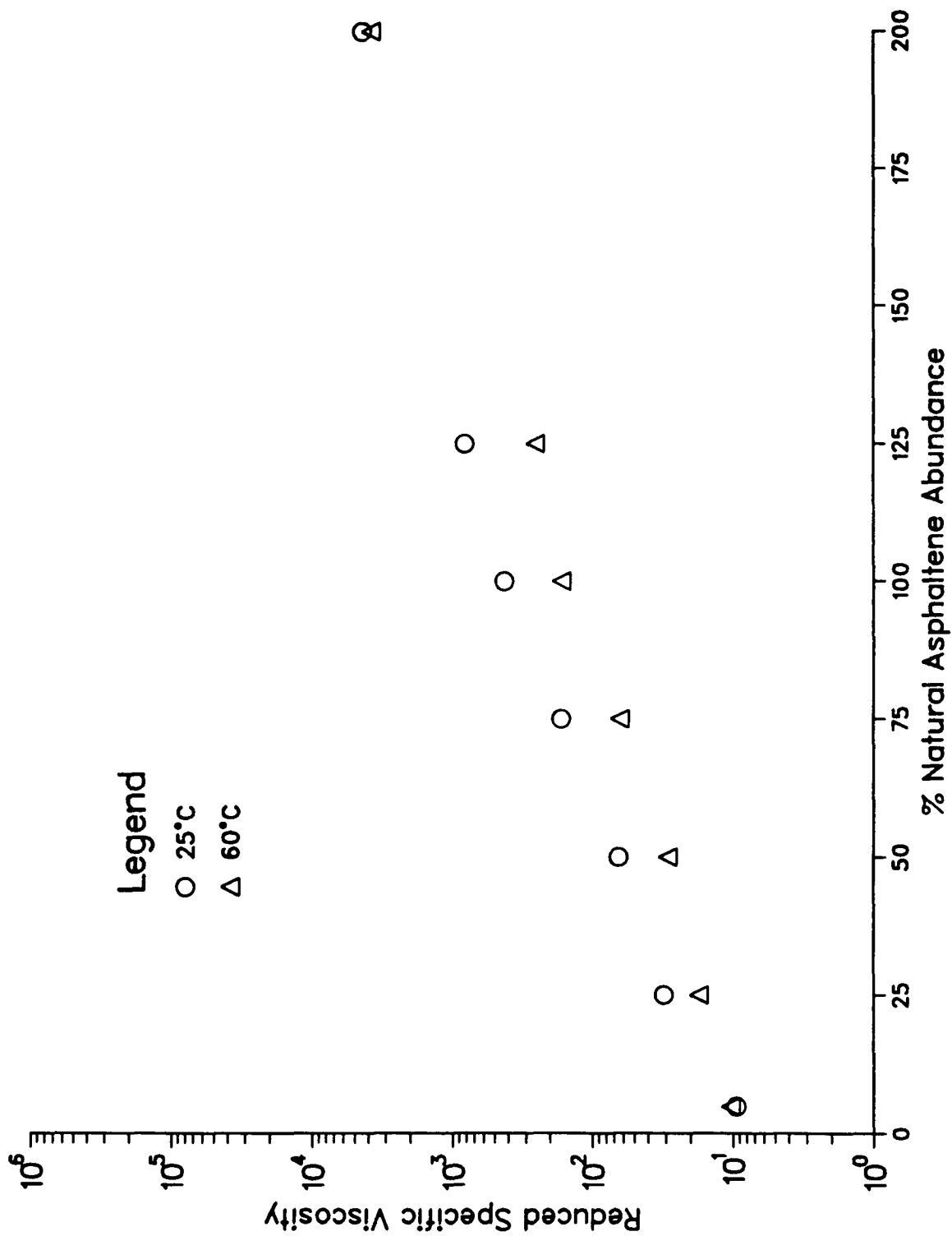


Figure 9.2 Reduced Specific Viscosities at Two Temperatures for Unaged AAA-1

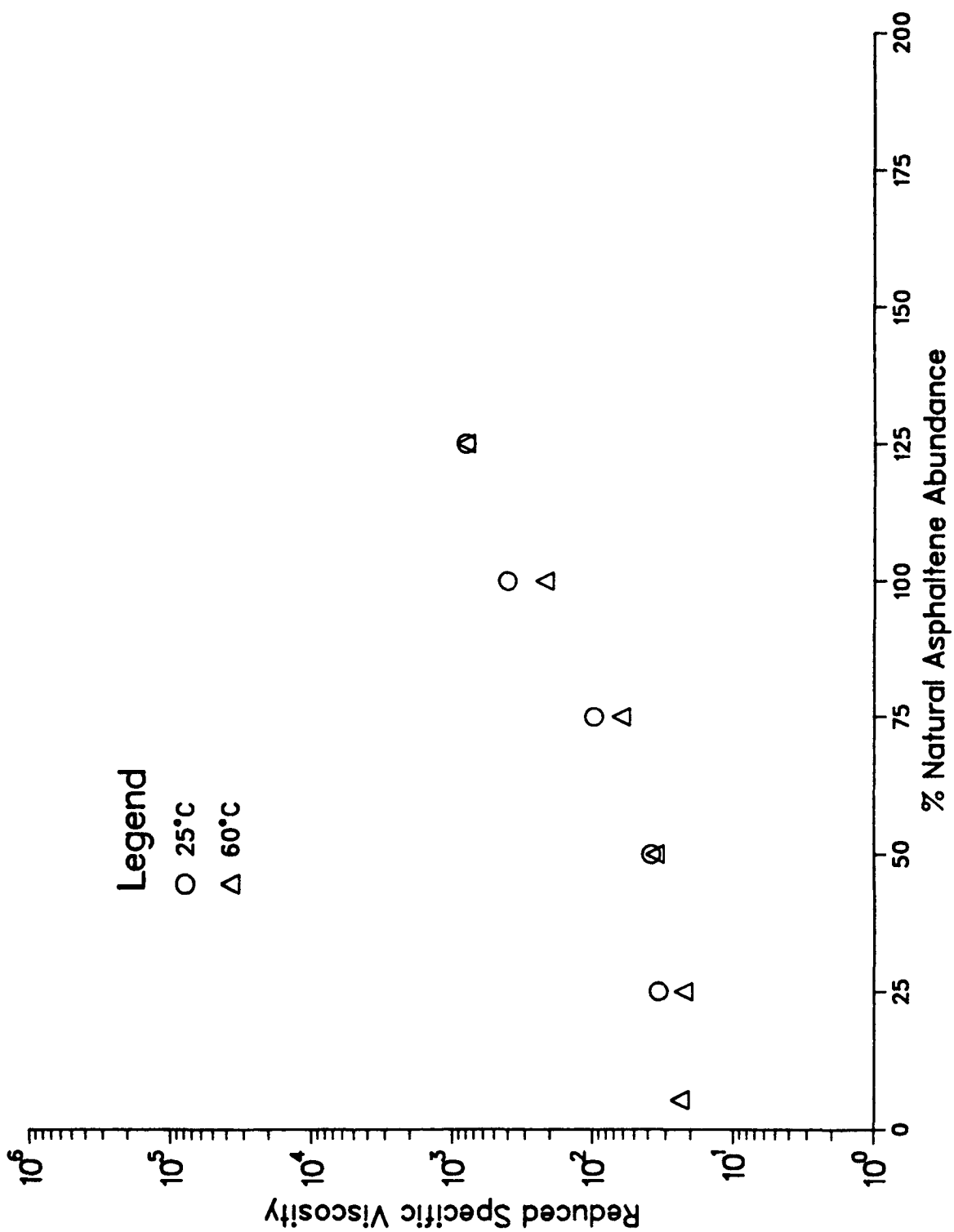


Figure 9.3 Reduced Specific Viscosities at Two Temperatures for Unaged AAB-1



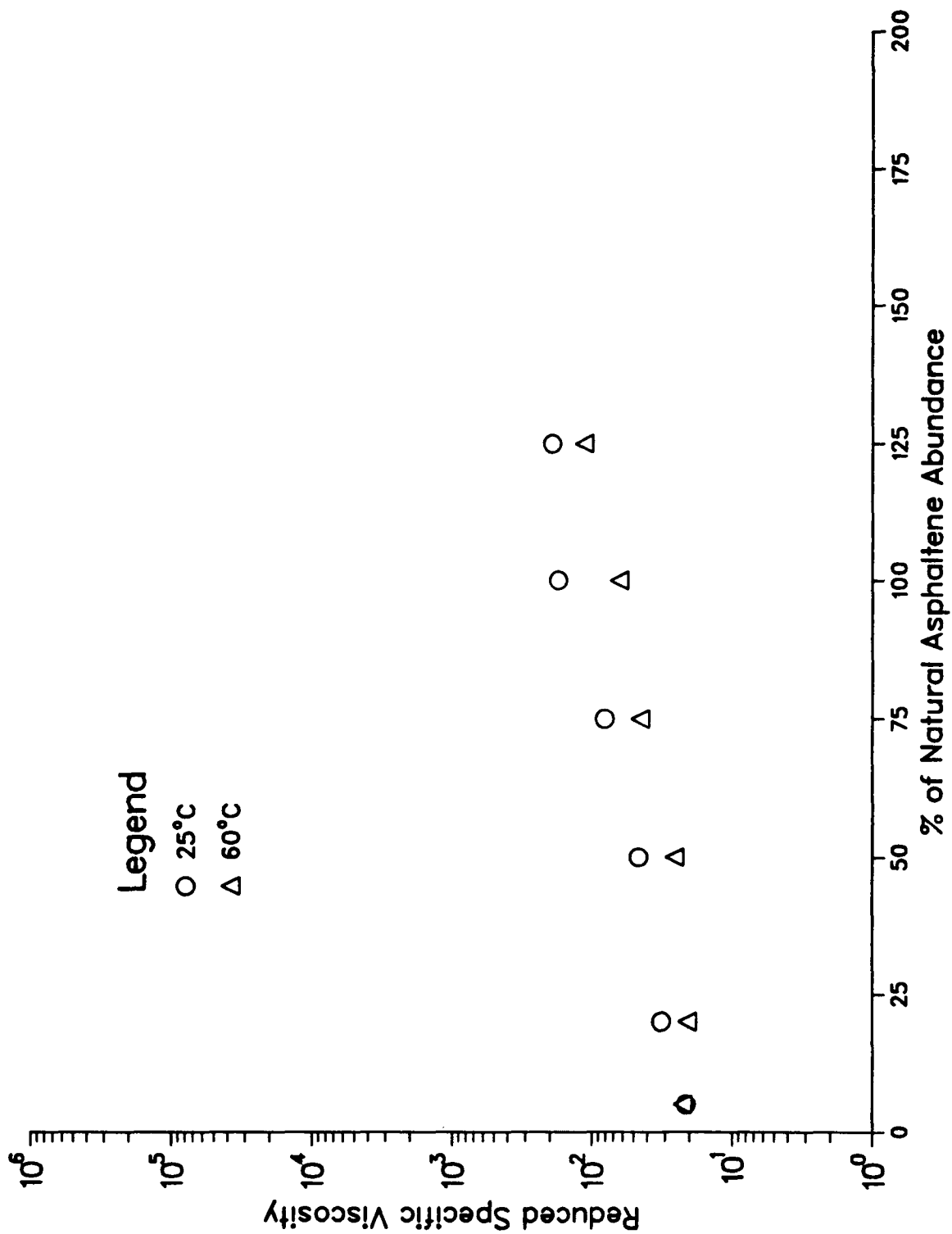


Figure 9.4 Reduced Specific Viscosities at Two Temperatures for Unaged AAC-1

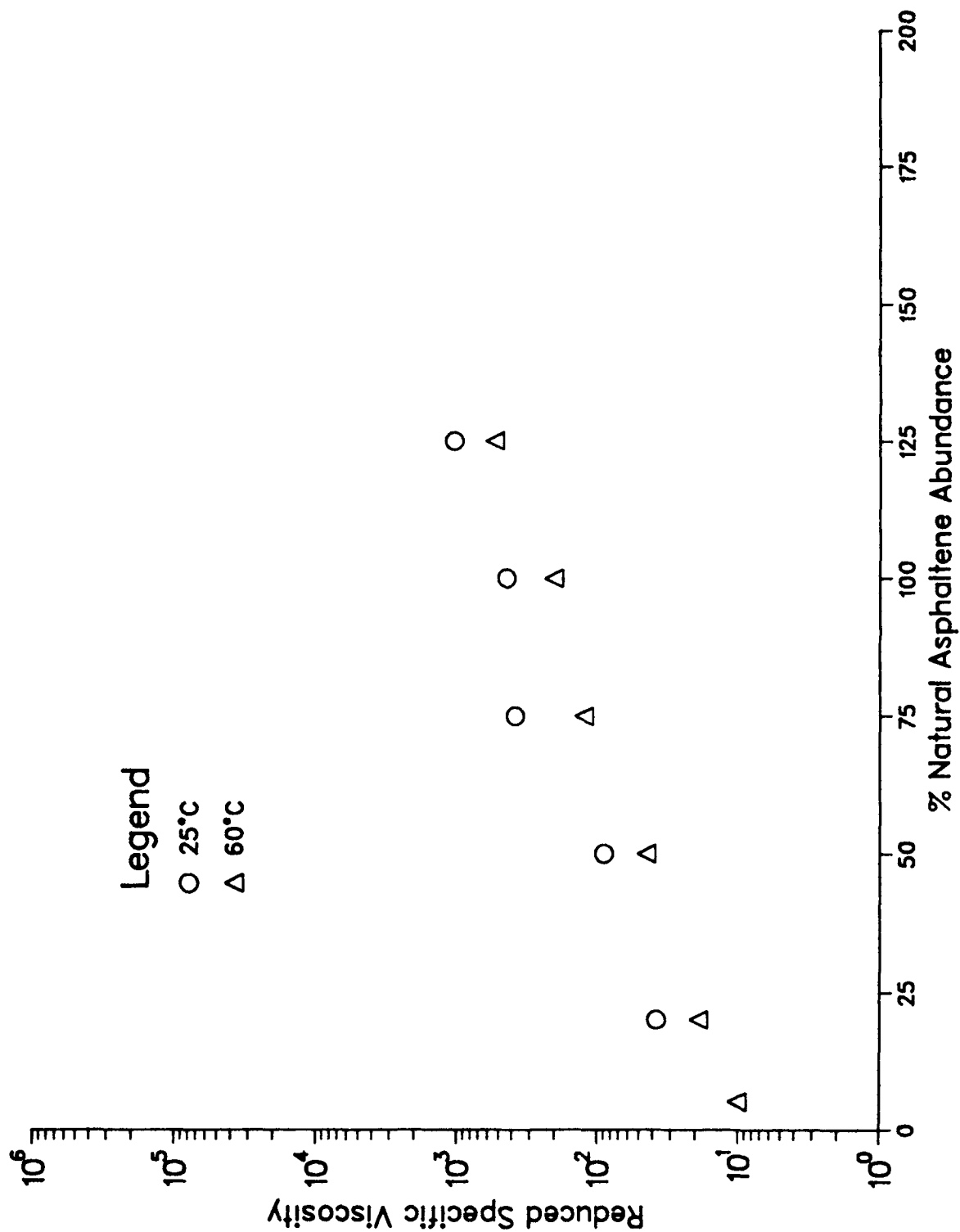


Figure 9.5 Reduced Specific Viscosities at Two Temperatures for Unaged AAD-1

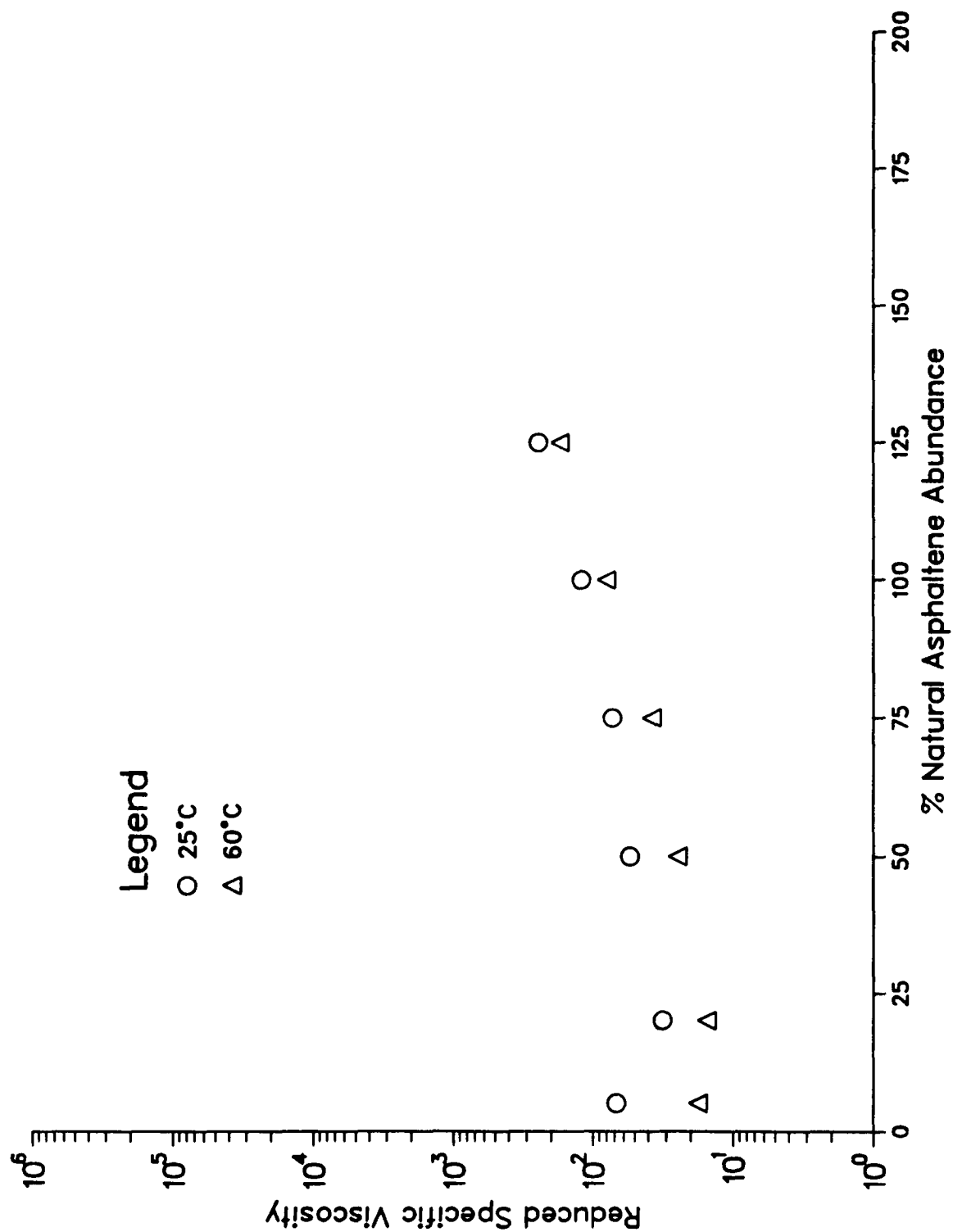


Figure 9.6 Reduced Specific Viscosities at Two Temperatures for Unaged AAF-1

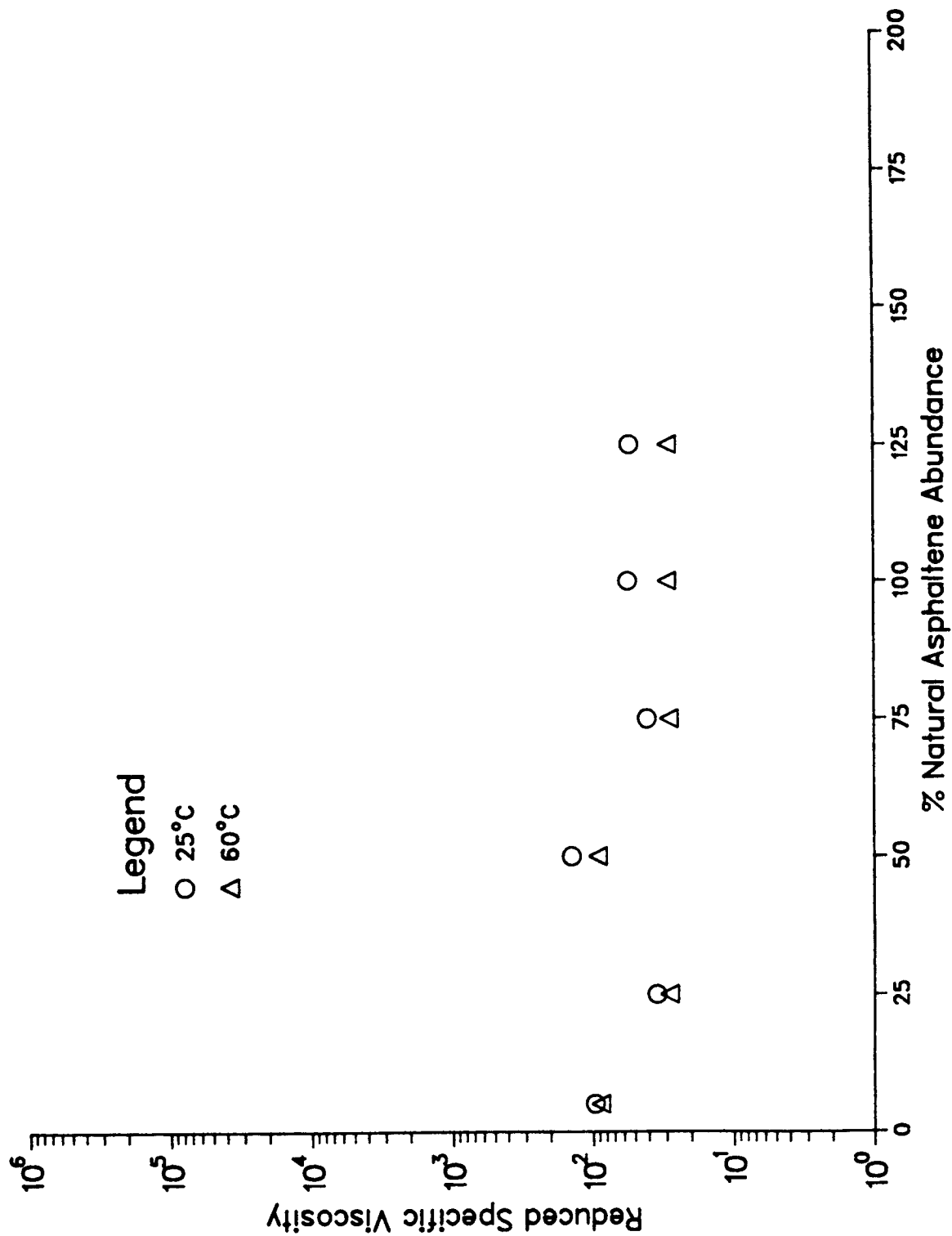


Figure 9.7 Reduced Specific Viscosities at Two Temperatures for Unaged AAG-1

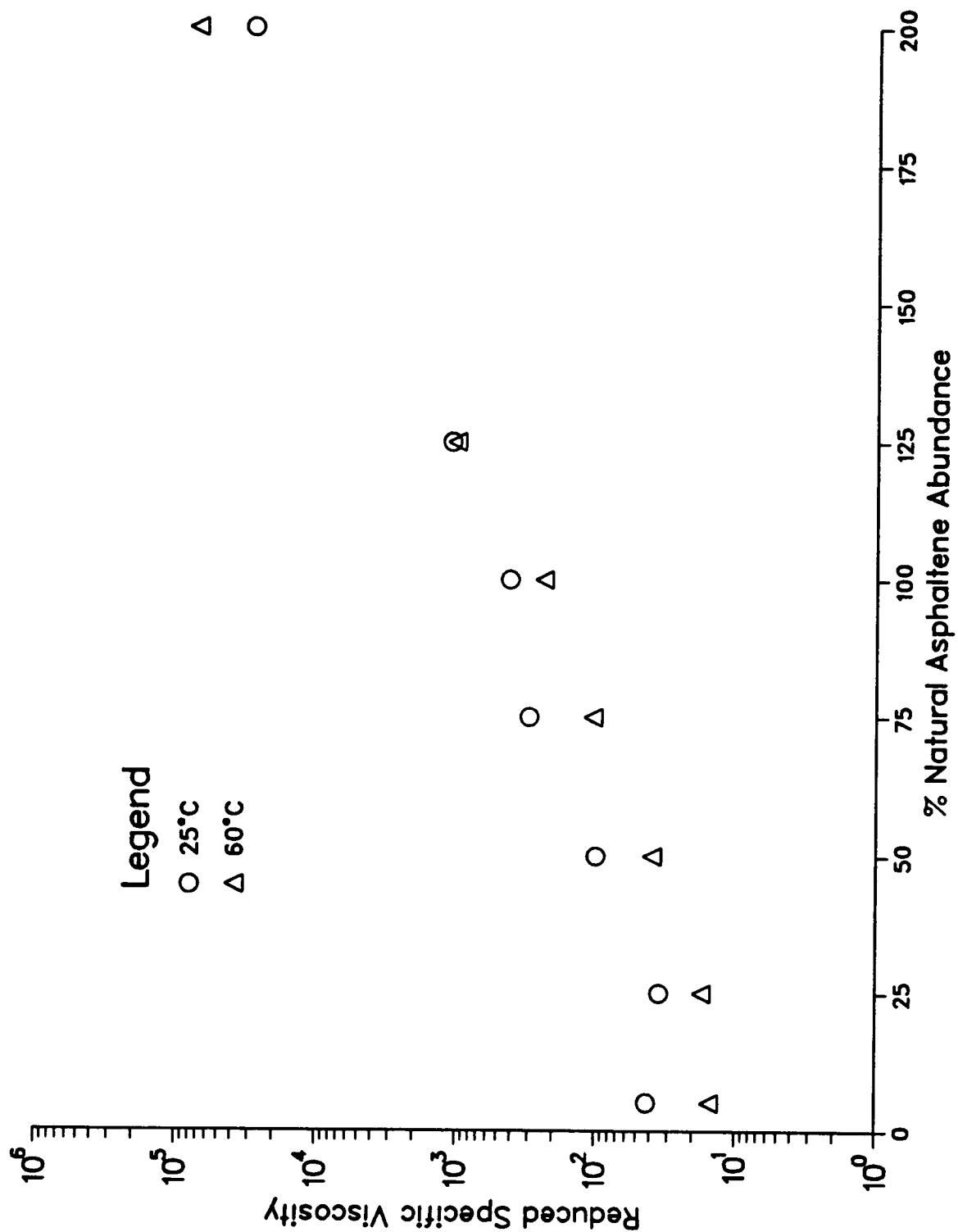


Figure 9.8 Reduced Specific Viscosities at Two Temperatures for Unaged AAK-1

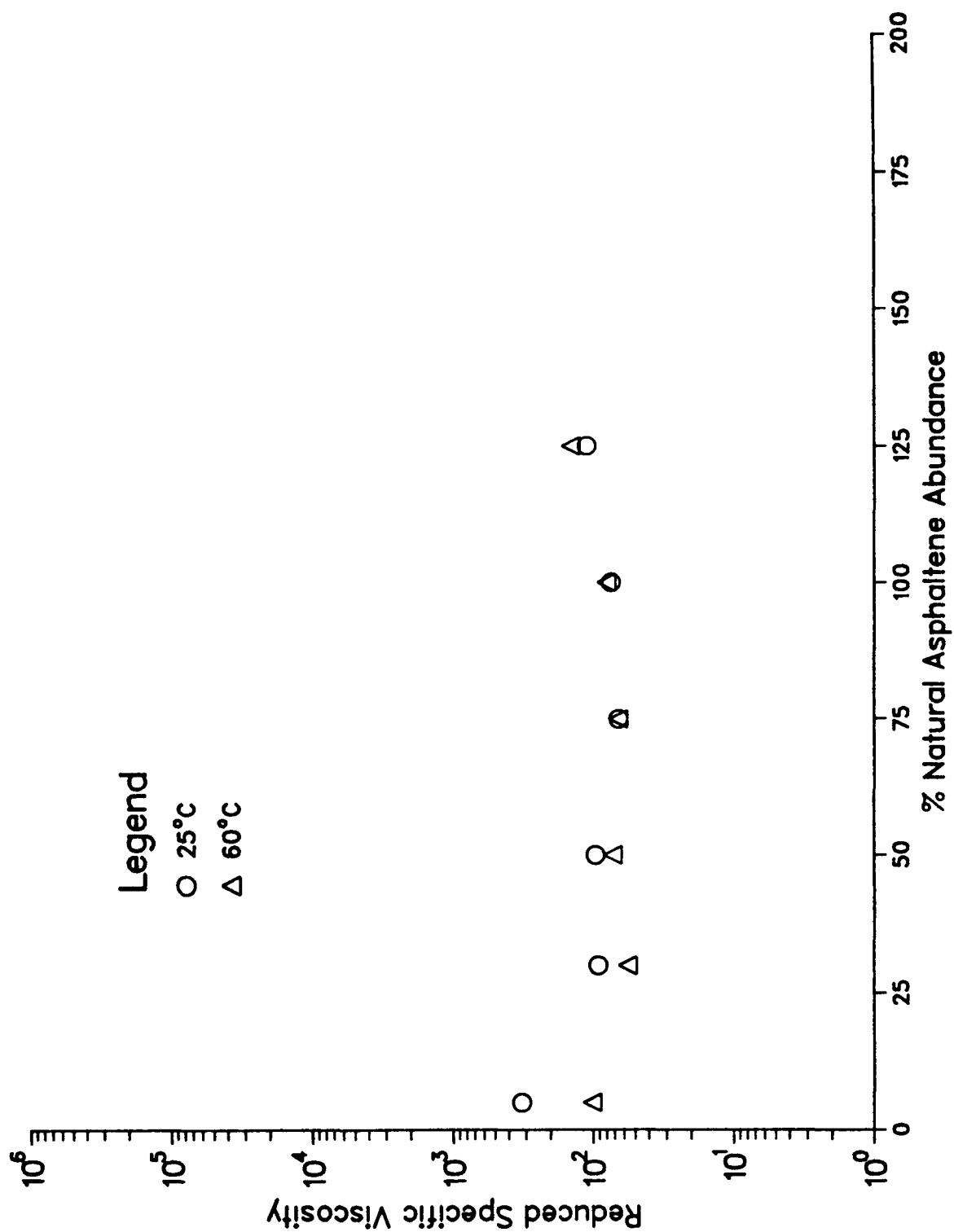


Figure 9.9 Reduced Specific Viscosities at Two Temperatures for Unaged AAM-1

Table 9.1 Carbon and Hydrogen Analyses of Core Asphalts Performed by Two Analytical Laboratories

Asphalt	Element, mass %						H/C, Atomic Ratio (Calculated from Avg.)
	Carbon			Hydrogen			
	Laboratory		Avg. + Std. Dev. <sup>2</sup>	Laboratory		Avg. + Std. Dev. <sup>2</sup>	
	WRI <sup>1</sup>	WAL <sup>1</sup>		WRI <sup>1</sup>	WAL <sup>1</sup>		
AAA-1	84.2,83.2	84.9,83.9	84.1 ± 0.6	10.5,9.9	10.4, 9.3	10.0 ± 0.5	1.42
AAB-1	82.3,82.7	85.1	83.4 ± 1.2	10.6,9.3	10.2	10.0 ± 0.5	1.43
AAC-1	83.5,86.5	86.5	85.5 ± 1.4	10.1,11.3	10.5	10.6 ± 0.5	1.48
AAD-1	81.4,79.3,81.4	82.3	81.1 ± 1.1	10.8,9.3,9.9	10.5	10.1 ± 0.6	1.48
AAF-1	81.2,84.4,83.7	85.5	83.7 ± 1.6	9.2,10.4,10.0	9.1	9.7 ± 0.5	1.38
AAG-1	85.6,85.3	86.2	85.7 ± 0.4	10.5,9.7	9.4	9.9 ± 0.5	1.38
AAK-1	80.7,80.1	82.3	81.0 ± 0.9	10.2,9.2	9.3	9.6 ± 0.4	1.41
AAM-1	86.7,86.6	86.6	86.6 ± 0.1	11.4,10.6	10.3	10.8 ± 0.5	1.49

<sup>1</sup> WRI = Western Research Institute; WAL = Wyoming Analytical Laboratories

<sup>2</sup> Analyses for carbon and hydrogen were performed using standard methods. Based on experience with a large number of fossil fuel samples, standard deviations are: carbon, 0.36; hydrogen, 0.20. Standard deviations reported above are calculated for the numbers in the table.

**Table 9.2 Determination of Nitrogen, Oxygen, and Sulfur in Eight Core Asphalts**

Asphalt	Nitrogen, mass %		Avg. + Std. Dev. <sup>2</sup>	Oxygen, <sup>2</sup> mass %	Sulfur, <sup>2</sup> mass %	Avg. <sup>3</sup>
	Laboratory WRI <sup>1</sup>	WAL <sup>1</sup>				
AAA-1	0.5,0.5	0.8,0.5	0.58 ± 0.13	0.6	5.7,5.3	5.5
AAB-1	0.6,0.5	0.6	0.57 ± 0.05	0.8	4.7,4.7	4.7
AAC-1	0.6,0.7	0.8	0.7 ± 0.08	0.9	1.8,2.0	1.9
AAD-1	0.8,0.7	0.8	0.77 ± 0.05	0.9	6.9,6.9	6.9
AAF-1	0.6,0.5	0.7	0.60 ± 0.08	1.1	3.5,3.4	3.4
AAG-1	1.1,1.1	1.0	1.07 ± 0.05	1.1	1.4,1.2	1.3
AAK-1	0.7,0.7	0.8	0.73 ± 0.05	0.8	6.5,6.4	6.4
AAM-1	0.6,0.6	0.6	0.60 ± 0.0	0.5	1.3,1.1	1.2

<sup>1</sup> WRI = Western Research Institute; WAL = Wyoming Analytical Laboratories

<sup>2</sup> Analyses for nitrogen, oxygen, and sulfur were performed using standard methods. Based on experience with a large number of fossil fuel samples, standard deviations are: nitrogen, 0.09; oxygen, 0.41; sulfur, 0.36. Standard deviations reported above are calculated for numbers in the table.

<sup>3</sup> A value of the standard deviation of 0.133 is estimated by multiplying the average of the ranges of the sulfur determinations by 0.886.

**Table 9.3 Determination of Vanadium and Nickel in Eight Core Asphalts**

Asphalt	Vanadium, ppm	Avg. + Std. Dev. <sup>1</sup>	Nickel, ppm	Avg. + Std. Dev. <sup>1</sup>
AAA-1	177,174,170	173.7 ± 2.9	89,85,84	86 ± 2.2
AAB-1	235,220,211	222 ± 9.9	61,55,55	57 ± 2.8
AAC-1	149,150,146,145	147.5 ± 2.1	64,65,62,62	63.3 ± 1.3
AAD-1	325,300,298	307.7 ± 12.3	155,135,134	141.3 ± 9.7
AAF-1	84,94,95	91 ± 5.0	33,38,38	36.3 ± 2.4
AAG-1	39,36,36	37 ± 1.4	103,92,91	95.3 ± 5.4
AAK-1	1,580;1,464;1,450	1498 ± 58.3	152,134,137	141 ± 7.9
AAM-1	56,59,59	58 ± 1.4	30,40,42	37.3 ± 5.2

<sup>1</sup> Based on experience with other fossil fuel samples, standard deviations are: vanadium, 18.4; nickel, 14.7. The high vanadium content of AAK-1 is near the upper limit for which the same level of accuracy can be claimed as for the other asphalts by the method employed.



**Table 9.4 Number-Average Molecular Weights ( $M_n$ ) of Core Asphalts by Vapor Phase Osmometry at 60 °C**

Asphalt	$M_n$ (Daltons)	
	Solvent	
	toluene	pyridine
AAA-1	790	810
AAB-1	840	850
AAC-1	870;870	N.D.
AAD-1	700	710
AAF-1	840;840	N.D.
AAG-1	710	700
AAK-1	860	820
AAM-1	1,300	insoluble

Errors are estimated to be  $\pm 5.0\%$  at the 700-1,000 Dalton level and  $\pm 10.0\%$  at the 1,000 Dalton level or higher for this technique. These estimates are based on a large number of determinations of tar sand bitumens and heavy oils.

**Table 9.5 Infrared Functional Group Analysis of Neat SHRP Core Asphalts**

Sample	Functional Group (Moles/L)						
	Sulfoxide	Ketone	Carboxylic Acid	Carboxylic Acid Salt	2-Quinolone	Pyrrolic N-H	Phenolic O-H
AAA-1	0.037	<0.005	0.015	<0.005	0.011	0.12	0.08
AAB-1	0.064	<0.005	<0.005	<0.005	0.012	0.14	0.06
AAC-1	0.029	<0.005	0.010	<0.005	0.011	0.22	0.04
AAD-1	0.036	<0.005	0.015	<0.005	0.027	0.19	0.13
AAF-1	0.050	<0.005	<0.005	<0.005	0.007	0.14	0.01
AAG-1	0.046	<0.005	<0.005	0.055	0.010	0.38	0.14
AAK-1	0.022	<0.005	0.012	<0.005	0.014	0.12	0.03
AAM-1	0.023	<0.005	<0.005	<0.005	0.013	0.17	0.07

Based on prior experience with asphalts, standard deviations are (mol/L): sulfoxides, 0.027; ketones, 0.006; carboxylic acids, 0.005; 2-quinolones, 0.002. The analyses for N-H and O-H are qualitative.

**Table 9.6 Asphaltene Yields and Asphaltene Compatibility Indices of Core Asphalts**

Asphalt	Operator (Initials)	Heptane Asphaltenes (H <sub>A</sub> ), mass %	Iso-octane Asphaltenes (I <sub>A</sub> ), mass %	ACI, [I <sub>A</sub> / (H <sub>A</sub> + I <sub>A</sub> )] x 10
AAA-1	MS	15.1	3.8	1.77
	MC	<u>16.6</u>	<u>3.0</u>	
	Average	15.8	3.4	
AAB-1	MC	17.1	2.2	1.04
	MC	<u>17.6</u>	<u>1.8</u>	
	Average	17.3	2.0	
AAC-1	MC	9.8	3.1	2.45
	AG	<u>10.1</u>	<u>3.5</u>	
	Average	9.9	3.3	
AAD-1	MC	19.7	3.6	1.44
	SP	<u>20.8</u>	<u>3.3</u>	
	Average	20.2	3.4	
AAF-1	MC	13.2	2.7	1.88
	JW	<u>13.7</u>	<u>3.5</u>	
	Average	13.4	3.1	
AAG-1	MS	4.9	3.4	3.97
	MC	<u>5.1</u>	<u>3.3</u>	
	Average	5.0	3.3	
AAK-1	MS	19.2	3.4	1.22
	MC	<u>20.9</u>	<u>2.3</u>	
	Average	20.1	2.8	
AAM-1	MC	3.4	4.6	5.93
	SP	<u>4.1</u>	<u>6.2</u>	
	Average	3.7	5.4	

Standard deviations were calculated by multiplying the averages of the ranges in each column by 0.886. These values are: Heptane asphaltenes, 0.78; Iso-octane asphaltenes, 0.64; ACI, 0.27.

Table 9.7 Elemental Analyses and Molecular Weights of Core Asphalt Asphaltenes

Asphalt	Asphaltene Type	Element (mass %) <sup>1</sup>					H/C atomic ratio	Molecular Weight (Daltons) <sup>2</sup>	
		C	H	N	S	O		Toluene	Pyridine
AAA-1	Heptane	80.6	7.8	1.2	8.5	1.5	1.15	8,000	5,800
	Iso-octane	80.8	8.3	0.9	8.2	1.8	1.22	4,500	3,700
AAB-1	Heptane	84.9	7.4	1.4	5.2	1.2	1.04	6,500	4,600
	Iso-octane	83.9	7.7	1.1	5.9	1.5	1.09	4,500	3,400
AAC-1	Heptane	86.4	7.6	1.4	3.4	1.1	1.05	5,000	4,400
	Iso-octane	86.6	8.1	1.2	3.1	1.2	1.11	2,800	2,800
AAD-1	Heptane	79.9	8.1	1.8	8.8	1.9	1.21	7,400	4,600
	Iso-octane	79.8	8.8	1.4	8.1	2.0	1.31	3,500	2,600
AAF-1	Heptane	84.1	7.1	1.0	6.4	1.6	1.01	4,500	3,600
	Iso-octane	84.9	8.0	0.8	5.4	1.6	1.12	2,600	2,300
AAG-1	Heptane	82.7	7.8	2.2	1.5	2.9	1.12	5,500	3,100
	Iso-octane	84.4	8.2	2.2	1.2	2.4	1.16	3,000	2,100
AAK-1	Heptane	80.9	7.9	1.7	6.7	1.5	1.16	7,900	-
	Iso-octane	81.0	8.4	1.3	7.6	1.6	1.24	4,500	3,900
AAM-1	Heptane	85.6	8.1	1.1	2.4	1.4	1.13	10,000	-
	Iso-octane	86.9	8.6	1.0	1.9	1.1	1.18	7,200	-

<sup>1</sup> Analysis for C, H, N, S, O are standard methods and their standard deviations are (mass %): carbon, 0.36; hydrogen, 0.20; nitrogen, 0.09; oxygen, 0.41; sulfur, 0.36.

<sup>2</sup> The MW data was obtained by a vapor phase osmometry method at 60°C in toluene. For these values, error bars are ± 5%. It is the nature of the method that for the error increases as MW's increase.

Table 9.8 Heithaus Parameters for Seven Asphalts

Asphalt	Run Number	P (Compatibility)	P <sub>a</sub> (Asphaltene Peptizability)	P <sub>o</sub> (Maltene Solvent Power)
AAA-1	1	3.29	0.69	1.02
	2	3.50	0.68	1.12
	3	3.56	0.68	1.14
	4	3.26	0.65	1.14
	5	<u>3.42</u>	<u>0.64</u>	<u>1.23</u>
	Avg. + Std. Dev.	3.41 ± 0.12	0.67 ± 0.02	1.13 ± 0.07
AAB-1	1	3.30	0.67	1.09
	2	3.65	0.66	1.24
	3	3.62	0.63	1.34
	4	<u>3.49</u>	<u>0.63</u>	<u>1.29</u>
	Avg. + Std. Dev.	3.51 ± 0.14	0.65 ± 0.02	1.24 ± 0.09
AAD-1	1	3.42	0.62	1.30
	2	3.50	0.62	1.33
	3	3.47	0.62	1.32
	4	3.40	0.60	1.36
	5	<u>3.38</u>	<u>0.60</u>	<u>1.35</u>
	Avg. + Std. Dev.	3.43 ± 0.04	0.61 ± 0.01	1.33 ± 0.02
AAF-1	1	3.55	0.62	1.35
	2	3.39	0.62	1.29
	3	3.53	0.62	1.34
	4	3.27	0.63	1.21
	5	<u>3.17</u>	<u>0.64</u>	<u>1.14</u>
	Avg. + Std. Dev.	3.38 ± 0.15	0.63 ± 0.01	1.27 ± 0.08
AAG-1	1	5.30	0.80	1.06
	2	5.80	0.80	1.16
	3	5.50	0.80	1.10
	4	4.65	0.74	1.21
	5	<u>4.96</u>	<u>0.74</u>	<u>1.29</u>
	Avg. + Std. Dev.	5.24 ± 0.40	0.78 ± 0.03	1.16 ± 0.08
AAK-1	1	3.73	0.67	1.23
	2	3.79	0.67	1.24
	3	3.56	0.68	1.14
	4	3.60	0.65	1.26
	5	<u>3.66</u>	<u>0.65</u>	<u>1.28</u>
	Avg. + Std. Dev.	3.67 ± 0.08	0.66 ± 0.01	1.25 ± 0.05
AAM-1	1	15.87	0.92	1.27
	2	14.87	0.92	1.19
	3	14.62	0.92	1.17
	4	10.50	0.86	1.47
	5	10.57	0.86	1.48
	6	9.58	0.88	1.15
	7	<u>9.33</u>	<u>0.88</u>	<u>1.12</u>
	Avg. + Std. Dev.	12.19 ± 2.59	0.89 ± 0.03	1.26 ± 0.14

**Table 9.9 Viscosities of Core Asphalts Determined at 60 °C**

Asphalt	Viscosity Grade	Viscosity (Pa · s) <sup>1</sup>	
		Mechanical Spectrometer, 0.1 rad/s	Brabender
AAA-1	150/120 pen	109	152
AAB-1	AC-10	160	167
AAC-1	AC-8	111	127
AAD-1	AR-4000	131	142
AAF-1	AC-20	226	-
AAG-1	AR-4000	240	235
AAK-1	AC-30	413	567
AAM-1	AC-20	258	263

<sup>1</sup> Viscosities were measured after argon annealing. Error bars are estimated to be ± 10% on the Rheometrics Mechanical Spectrometer.

**Table 9.10 Viscosities of Core Asphalts at 25 °C**

Asphalt	Viscosity (Pa · s) <sup>1</sup>		
	Mechanical Spectrometer		Brabender
	0.1 rad/s	1.0 rad/s	
AAA-1	37,021 -	30,070 35,000	-
AAB-1	118,600 -	85,020 95,000	-
AAC-1	90,100	74,710	-
AAD-1	57,280 -	39,440 42,800	45,200 -
AAF-1	381,700	287,900	-
AAG-1	248,900	230,300	210,000
AAK-1	251,700 -	157,900 150,000	234,000 -
AAM-1	364,400	230,000	356,000

<sup>1</sup> For the 0.1 rad/s determinations and the topmost entries of the 1.0 rad/s determinations, the samples were annealed at 150 °C. For the bottom entries in the 1.0 rad/s determinations, the samples were annealed at 110 °C. A standard deviation of 2,000 Pa · s and a coefficient of variance of 2.5% were calculated for AAK-1 at 25 °C based on five separate measurements. A standard deviation of 7,500 Pa · s and a coefficient of variance of 4.7% were calculated for AAM-1 at 25 °C based on four separate measurements.

## References

- Ali, M.F., and M.A. Ali (1988). Nonaqueous Potentiometric Titration and Elemental Analysis of High-Boiling Distillates of Saudi Arabian Crude Oils. Fuel Sci. Tech. Int'l., 6, 663-685.
- Altgelt, K.H., and E. Hirsch (1970). GPC Separation and Integrated Structural Analysis of Petroleum Heavy Ends. Separation Sci., 5, 855-862.
- ASTM D 1754-87 (1991). Standard Test Method for Effect of Heat and Air on Asphaltic Materials (Thin-Film Oven Test). In *Annual Book of ASTM Standards*, Am. Soc. Test. Mat'l, 04.03, Philadelphia.
- ASTM D 2503-88 (1985). Test Method for Molecular Weight (Relative Molecular Mass) of Hydrocarbons by Thermoelectric Measurement of Vapor Pressure. In *Annual Book of ASTM Standards*, Am. Soc. Test. Mat'l, 05.02, Philadelphia.
- ASTM D 2872-88 (1991). Standard Test Method for Effect of Heat and Air on a Moving Film of Asphalt (Rolling Thin-Film Oven Test). In *Annual Book of ASTM Standards*, Am. Soc. Test. Mat'l, 04.03, Philadelphia.
- Beazley, P.M., L.E. Hawsey, and M.A. Plummer (1987). Size Exclusion Chromatography and Nuclear Magnetic Resonance Techniques for Predicting Asphalt Yields and Viscosities from Crude Oil Analyses. Trans. Res. Rec., 1115, 46-50.
- Bishara, W.W., R.L. McReynolds, and E.R. Lewis (1991). The Interrelationship Between Performance-Related Properties of Asphalt Cement and Their Correlation with Molecular Size Distribution (MSD). Trans. Res. Rec., 1323, 1-9.
- Boduszynski, M.M., B.R. Chadha, and T.S. Pochopien (1977). Investigations on Romashkino Asphaltic Bitumen. 3. Fractionation of Asphaltenes Using Ion Exchange Chromatography. FUEL, 56, 432-436.

- Brown, A.B., J.W. Sparks, and F.M. Smith (1957). Steric Hardening of Asphalts. Proc. Assoc. Asph. Pav. Technol., 26, 486-494.
- Brule, B., G. Raymond, and C. Such (1986). Relationships Between Composition, Structure, and Properties of Road Asphalts: State of Research at the French Public Works Central Laboratory. Trans. Res. Rec., 1096, 22-34.
- Buell, B.E. (1967a). Differential Titration of Acids and Very Weak Acids in Petroleum with Tetrabutylammonium Hydroxide and Pyridine-Benzene Solvent. Anal. Chem., 39, 762-764.
- Buell, B.E. (1967b). Nonaqueous, Differential Titration Applied to a Classification of Basic and Very Weak Basic Nitrogen Compounds in Petroleum. Anal. Chem., 39, 756-761.
- Bynum, D., and R.N. Traxler (1970). Gel Permeation Chromatography Data on Asphalts Before and After Service in Pavements. Proc. Assoc. Asph. Pav. Technol., 39, 683-702.
- Coons, R.F., and P.H. Wright (1968). An Investigation of the Hardening of Asphalt Recovered From Pavements of Various Ages. Proc. Assoc. Asph. Pav. Technol., 37, 510-528.
- Donaldson, G.R., M.W. Hlalinka, J.A. Bullin, C.J. Glover, and R.R. Davison (1988). The Use of Toluene as a Carrier Solvent for Gel Permeation Chromatography Analyses of Asphalt. Liq. Chromat., 11, 749-765.
- Dorrence, S., F. Barbour, and J.C. Petersen (1974). Direct Evidence of Ketones in Oxidized Asphalts. Anal. Chem., 46, 2242-2244.
- Dutta, P.K., and R.J. Holland (1984). Acid-Base Characteristics of Petroleum Asphaltenes as Studied by Non-aqueous Potentiometric Titrations. FUEL, 63, 197-201.
- Dutta, P.K., and R.J. Holland (1983). Acidic Groups in Coal and Coal-Derived Materials. FUEL, 62, 732-737.
- Epps, J., J.C. Petersen, T.W. Kennedy, D.A. Anderson, and R. Haas (1986). Chemistry, Rheology, and Engineering Properties of Manganese. Trans. Res. Rec., 1096, 106-119.
- Giraudeau, A., M. El. Meray, M. Gross, C. Piechocki, and M. Bernard (1991). Redox Behavior of Phthalocyanines Bearing Aliphatic and Polyethylene Oxide Chain. Anal. Chim. Acta., 251, 39-46.



- Gratzfeld-Husgen, A. (1989). Simultaneous Determination of Porphyrins, Aromatics, and Olefins in Crude Oil by Gel Permeation Chromatography and Multiple Signal Detection. LC-GC, 7, 836-845.
- Green, J.B., S.K.-T. Yu, C.D. Pearson, and J.W. Reynolds (1992). Analysis of Sulfur Compound Types in Asphalt (Final Report NIPER B06251-1) Natl. Inst. Petrol. Energy Res., Bartlesville, OK.
- Green, J.B., B.H. Diehl, and J.Y. Shay (1991). Effects of Composition and Boiling Range on the Accuracy of Average Molecular Weight of Petroleum Fractions Determined by Vapor Pressure Osmometry. Proc. 5th Unitar Intl. Conf. on Heavy Crude & Tar Sands, 4, 133-142.
- Green, J.B., J.A. Green, S.K.-T. Yu, and P.L. Grizzle (1989). Detailed Separation and Analysis of Basic Compounds. In Analysis of Heavy Oils: Method Development and Application to Cerro Negro Heavy Petroleum (U.S. DOE Report NIPER 452, Volume 2). by J.A. Green, J.B. Green, R.D. Grigsby, C.D. Pearson, J.W. Reynolds, J.Y. Shay, G.P. Sturm, Jr., J.S. Thomson, J.W. Vogh, P.P. Vrana, S.K.-T. Yu, B.H. Diehl, P.L. Grizzle, D.E. Hirsch, K.W. Hornung, S.-Y. Tang, L. Carbognani, M. Hazos, and V. Sanchez.
- Green, J.B., R.J. Hoff, P.W. Woodward, and L.L. Stevens (1984). Separation of Liquid Fossil Fuels into Acid, Base, and Neutral Concentrates. 1. An Improved Nonaqueous Ion Exchange Method. FUEL, 63, 1290-1301.
- Haley, G.M. (1975). Changes in Chemical Composition of a Kuwait Short Residue During Air Blowing. Anal. Chem., 47, 2432-2438.
- Heithaus, J.J. (1962). Measurement of Significance of Asphaltene Peptization. Instit. of Petrol., 48, 45-53.
- Hendry, D.G. (1967). Rate Constants for Oxidation of Cumene. Am. Chem. Soc., 89, 5433-5438.
- Hendry, D.G., T. Mill, L. Piskiewicz, J.A. Howard, and H.K. Eigenmann (1974). A Critical Review of H-Atom Transfer in the Liquid Phase. Phys. Chem. Ref. Data., 3, 937-978.
- Howard, J.A., and E. Furimsky (1973). Arrhenius Parameters for Reaction of t-Butylperoxy Radicals with Some Hindered Phenols and Aromatic Amines. Can. J. Chem., 51, 3738-3745.

- Huggins, F., S.V. Vaidya, G.P. Huffman, T. Mill, and J. Youtcheff (1992). Analysis of Sulfur Forms in Asphalts Using Sulfur K-Edge XAFS Spectroscopy. Preprints, Am. Chem. Soc., Div. Fuel Chem., 37, 1376-1382.
- Huynh, H.K., T.D. Khong, S.L. Malhotra, and L.P. Blanchard (1978). Effect of Molecular Weight and Composition on the Glass Transition Temperatures of Asphalts. Anal. Chem., 50, 976-979.
- Jennings, P.W., J.A. Pribanic, M.F. Raub, J.A. Smith, and T.M. Mendes. 1993. Advanced High Performance Gel Permeation Chromatography Methodology (SHRP-A-630.) National Research Council, Washington D.C.
- Jennings, P.W., J.A. Pribanic, B. Fanconi, and D.L. VanderHart (1993). Binder Characterization and Evaluation by NMR Spectroscopy. (SHRP-A-335.) National Research Council, Washington, D.C.
- Jennings, P.W., J.A. Pribanic, J. Smith, and T.M. Mendes (1988). Predicting the Performance of Montana Test Sections by Physical and Chemical Testing. Trans. Res. Rec., 1171, 59-65.
- Kemp, G.R., and N.H. Predoehl (1981). A Comparison of Field and Laboratory Environments on Asphalt Durability. Proc. Assoc. Asph. Pav. Technol., 50, 492-531.
- Kice, J.L., and J.D. Campbell (1967). Effect of Ring Size on the Rate of Pyrolysis of Cycloalkyl Phenyl Sulfoxides. Org. Chem., 32, 1631-1632.
- Kingsbury, C.A., and D.J. Cram (1960). Elimination of Sulfoxides. Am. Chem. Soc., 82, 1810-1819.
- Kircher, C.C. (1991). Separations and Characterizations of Fractions from Mayan, Heavy Arabian, and Hondo Crude Oils. Fuel Sci. Tech. Int'l., 9, 379-395.
- Knotnerus, J. (1971). Oxygen Uptake by Bitumen Solutions as a Potential Measure of Bitumen Durability. Preprint. Am. Chem. Soc. Div. Petrol. Chem., Los Angeles Meeting. D37-D57.
- Kowanko, N., J.F. Branthaver, and J.M. Sugihara (1978). Direct Liquid-Phase Fluorination of Petroleum. FUEL, 57, 769-774.
- Kuhnen, L. (1966). Oxidation of Sulphoxides with Hydroperoxides. Angew. Chemie (English Ed.), 5, 893.
- Labib, M.L., and P.J. Zanzucchi (1991). Evaluation of Donor-Acceptor Properties of Asphalt and Aggregate Materials and Relationship to Asphalt Composite Performance. End of Phase II Report, Strategic Highway Research Program, National Research Council, Washington, D.C.

- Langhals, H., S. Demming, and T. Potrawa (1991). The Relation between Packing Effects and Solid State Fluorescence of Dyes. J. f. Prakt. Chemie. Band, 333, 733-748.
- Lau, C.K., K.M. Lunsford, C.J. Glover, R.R. Davidson, and J.A. Bullin (1992). Reaction Rates and Hardening Susceptibilities as Determined from Pressure Oxygen Vessel Aging of Asphalts. Trans. Res. Rec., 1342, 50-57.
- Lee, D.Y. (1973). Asphalt Durability Correlation in Iowa. Highway Res. Rec., 468, 43-60.
- Lee, D.Y. (1972). Development of a Durability Test for Asphalts. (Final Report, ERI Project 7175 and 8285). Engineering Research Institute, Iowa State University.
- Lee, D.Y. (1968). Development of a Laboratory Durability Test for Asphalts. Highway Res. Rec., 231, 34-49.
- Lewis, R.H., and J.Y. Welborn (1940). Report on the Physical and Chemical Properties of Petroleum Asphalts of the 50-60 and 85-100 Penetration Grades. Proc. Assoc. Asph. Pav. Technol., 11, 86-157.
- Martin, K.G. (1968). Laboratory Evaluation of Antioxidants for Bitumen. Fourth Conf. A.R.R.B., 1-14.
- Martin, K.G. (1966). Influence of Stabilizers on Bitumen Durability. Appl. Chem., 16, 198-201.
- McKay, J.F., J.H. Weber, and D.R. Latham (1976). Characteristics of Nitrogen Bases in High-Boiling Petroleum Distillates. Anal. Chem., 48, 891-898.
- McKay, J.F., T.E. Cogswell, J.H. Weber, and D.R. Latham (1975). Analysis of Acids in High-Boiling Petroleum Distillates. FUEL, 54, 50-61.
- Mendenhall, G.D. (1990). Chemiluminescence in Free Radical Oxidations. Angew. Chemie (English Ed.), 158, 48-72.
- Mill, T., D.S. Tse, B. Loo, CC.D. Yao, and E. Canaresi (1992). Oxidation Pathways for Asphalt. Preprints, Am. Chem. Soc., Div. Fuel Chem., 37, 1367-1375.
- Mill, T., and D.G. Hendry (1980). Kinetics and Mechanism of Free Radical Oxidation of Alkanes and Olefins in the Liquid Phase. In Comprehensive Chemical Kinetics, C.H. Bamford and C.F.H. Tipper (Eds.), Elsevier Amsterdam, 16, 1-83.
- Moschopedis, S.E., J.F. Fryer, and J.G. Speight (1976). Investigation of Asphaltene Molecular Weights. FUEL, 55, 227-232.

- Nicholson, V. (1937). A Laboratory Oxidation Test for Bitumens. Proc. Assoc. Asph. Pav. Technol., 9, 208-213.
- Pauls, R.H., and J.Y. Welborn (1952). Studies of the Hardening Properties of Asphaltic Materials. Proc. Assoc. Asph. Pav. Technol., 21, 48-75.
- Petersen, J.C. (1991). Private communication of several unpublished studies of sulfoxide formation and decomposition conducted prior to 1987.
- Petersen, J.C. (1989). A Thin-Film Accelerated-Aging Test for Evaluating Asphalt Oxidative Aging. Proc. Assoc. Asph. Pav. Technol., 58, 220-237.
- Petersen, J.C. (1986). Quantitative Functional Group Analysis of Asphalts Using Differential Infrared Spectrometry and Selective Chemical Reactions - Theory and Application. Trans. Res. Rec. 1096, 1-11.
- Petersen, J.C. (1984). Chemical Composition of Asphalt as Related to Asphalt Durability: State of the Art. Trans. Res. Rec., 999, 13-30.
- Petersen, J.C., H. Plancher, and G. Miyake (1983). Chemical Reactivity and Flow Properties of Asphalt Modified by Metal Complex-Induced Reaction with Atmospheric Oxygen. Proc. Assoc. Asph. Pav. Technol., 52, 32-60.
- Petersen, J.C. (1982). Oxidation of Sulfur Compounds in Petroleum Residues: Reactivity-Structural Relationships and Reaction Kinetics. Confab 82 on Fossil Fuel Chem. Ener., Saratoga, WY.
- Petersen, J.C., S.M. Dorrence, M. Nazir, H. Plancher, and F.A. Barbour (1981). Oxidation of Sulfur Compounds in Petroleum Residues: Reactivity-Structural Relationships. Div. Petrol. Chem., Am. Chem. Soc. Meeting, New York, N.Y.
- Petersen, J.C. (1975). Quantitative Method Using Differential Infrared Spectrometry for the Determination of Compound Types Absorbing in the Carbonyl Region in Asphalts. Anal. Chem., 47, 112-117.
- Petersen, J.C., F.A. Barbour, and S.M. Dorrence (1975). Identification of Dicarboxylic Anhydrides in Oxidized Asphalts. Anal. Chem., 47, 107-111.
- Petersen, J.C., F.A. Barbour, and S.M. Dorrence (1974). Catalysis of Asphalt Oxidation by Mineral Aggregate Surfaces and Asphalt Components. Proc. Assoc. Asph. Pav. Technol., 43, 162-177.
- Petersen, J.C., R.V. Barbour, S.M. Dorrence, F.A. Barbour, and R.V. Helm (1971). Molecular Interactions of Asphalt: Tentative Identification of 2-Quinolones in Asphalt and Their Interaction with Carboxylic Acids Present. Anal. Chem., 43, 1491-1496.

- Pfeiffer, J.P.H., and R.N.J. Saal (1940). Asphaltic Bitumen as Colloidal System. Phys. Chem., 44, 139-149.
- Pirela, L., and N.C. de Marcano (1985). Influence of Time on the Viscosity of Heavy Crude Oils and Heavy Crude Oil-Solvent Mixtures. Preprint, 3rd Int'l Conf. Heavy Crude and Tar Sands, 2, 22-31, Long Beach, CA.
- Preece, S.C., J.F. Branthaver, and S.S. Kim (1992). Separation of a Quinolone-Enriched Fraction From SHRP Asphalts. Am. Chem. Soc., Div. Fuel Chem., 37, 1342-1349.
- Reerink, H., and J. Lijzenga (1975). Gel-Permeation Chromatography Calibration Curve for Asphaltene and Bituminous Resins. Anal. Chem., 47, 2160-2167.
- Ruiz, J.M., B.M. Carden, L.J. Laura, and E.-J. Vincent (1982). Determination of Sulfur in Asphalt by Selective Oxidation and Photoelectron Spectroscopy for Chemical Analysis. Anal. Chem., 54, 688-691.
- Schmidt, R.J. (1973). Laboratory Measurement of the Durability of Paving Asphalts. ASTM STP, 532, 79-99.
- Schmidt, R.J., and L.E. Santucci (1969). The Effect of Asphalt Properties on the Fatigue Cracking of Asphalt Concrete on the Zaca-Wigmore Test Project. Proc. Assoc. Asph. Pav. Technol., 38, 39-64.
- Selucky, M.L., S.S. Kim, F. Skinner, and O.P. Strausz (1981). Structure Related Properties of Athabasca Asphaltenes and Resins as Indicated by Chromatographic Separation. In "Chemistry of Asphaltenes," J.W. Bunger, Ed., Am. Chem. Soc., Washington, DC, (Advances in Chemistry Series, 195, Chapter 6).
- Sköld, R.O., and M.A.R. Tunius (1992). Self-Association of 1,10-Decanedicarboxylates in Aqueous Solution. Colloid Interface Sci., 152, 183-196.
- Stearns, R.S., I.N. Duling, and R.H. Johnson (1966). The Relationship of the Glass Transition Temperature to the Viscosity-Temperature Characteristics of Lubricants. Preprints, Am. Chem. Soc. Div. Petrol. Chem., 11 (1), 5-19.
- Storm, D.A., R.J. Barresi, and S.J. DeCanio (1991). Colloidal Nature of Vacuum Residue. FUEL, 70, 779-782.
- Storm, D.A., S.J. DeCanio, M.M. DeTar, and V.P. Nero (1990). Upper Bound on Number Average Molecular Weight of Asphaltenes. FUEL, 69, 735-738.
- Traxler, R.N. (1961). Asphalt, Its Composition, Properties and Uses. Reinhold, NY.

- van Gooswilligen, G., H. Bergh, and F. Th. de Bats (1985). Oxidation of Bitumen in Various Tests. European Bitumen Conference.
- Walling, C., and L. Bollyky (1964). The Addition of Dimethylsulfoxide Anion to Olefins and Pyrolysis of Sulfoxides. Org. Chem., 29, 2699-2703.
- Welborn, J.Y. (1984). Physical Properties as Related to Asphalt Durability: State of the Art. Trans. Res. Rec., 999, 31-37.

## **Appendix A**

### **Supplementary Figures and Tables**

Supplementary Table 1.18 Separation of Seven Asphalts by IEC

Asphalt	Operator Initials and Run Number	IEC Fraction (mass %)					Total Recovery (mass %)
		Strong Acid	Strong Base	Weak <sup>1</sup> Acid	Weak <sup>1</sup> Base	Neutral <sup>1</sup>	
AAA-1	MC6	17.5	6.3	8.6	5.2	59.5	97.0
	MC7	17.3	6.5	8.7	4.8	59.7	97.0
	MC8	18.9	-	-	-	-	97.8
	SP1	17.7	5.9	-	-	-	96.2
	MC9	18.8	6.2	-	-	-	97.8
	Avg. + Std. Dev.	18.0 ± 0.7	6.2 ± 0.2	8.7	5.0	59.6	97.2 ± 0.6
AAB-1	MC10	14.8	9.2	8.2	7.8	57.1	97.1
	MC11	15.2	9.1	9.0	5.7	56.7	95.8
	MC12	15.5	8.9	-	-	-	96.8
	MC13	15.9	-	-	-	-	96.1
	Avg. + Std. Dev.	15.4 ± 0.4	9.1 ± 0.1	8.6	6.8	56.9	96.5 ± 0.5
AAD-1	MC14	26.1	7.8	7.7	5.5	51.4	98.5
	MC15	26.0	7.7	7.9	5.6	51.9	98.9
	MC16	23.1	7.5	-	-	-	95.7
	MC17	25.3	-	-	-	-	97.9
	Avg. + Std. Dev.	25.1 ± 1.2	7.7 ± 0.1	7.8	5.6	51.7	97.8 ± 1.2
AAF-1	SP2	15.4	6.1	9.8	8.5	56.7	96.5
	MC18	17.0	6.1	10.0	6.8	56.9	96.9
	MC19	17.0	6.4	-	-	-	98.0
	MC20	18.0	-	-	-	-	99.5
	Avg. + Std. Dev.	16.9 ± 0.9	6.2 ± 0.1	9.9	7.7	56.8	97.7 ± 1.2

Continued on next page



Supplementary Table 1.18 continued

AAG-1	MC21	17.4	11.9	11.0	9.4	50.4	100.1
	SP3	18.7	12.2	11.8	8.7	50.4	101.8
	MC22	17.3	12.3	-	-	-	97.5
	MC23	19.0	-	-	-	-	100.0
	Avg. + Std. Dev.	18.1 ± 0.8	12.1 ± 0.2	11.4	9.1	50.4	99.9 ± 1.5
AAK-1	MC24	17.7	8.6	8.8	7.5	51.0	93.6
	MC25	19.7	7.4	8.3	7.6	53.5	96.4
	SP4	20.9	9.2	-	-	-	95.7
	MC26	21.3	8.2	-	-	-	96.7
	MC27	21.9	-	-	-	-	97.2
	MC28	20.9	-	-	-	-	97.3
	DG7	22.1	7.6	7.8	8.0	52.2	97.7
	Avg. + Std. Dev.	20.6 ± 1.4	8.2 ± 0.7	8.3 ± 0.4	7.7 ± 0.2	52.2 ± 1.0	96.4 ± 1.3
AAM-1	MC29	13.9	9.8	10.1	8.8	53.1	95.7
	MC30	13.5	11.1	10.0	9.4	53.7	97.6
	Avg. + Std. Dev.	13.7	10.4	10.1	9.1	53.4	96.7

<sup>1</sup> For the weak acid, weak base, and neutral fractions, for which there are pairs of determinations, standard deviations were calculated by multiplication of the average of the ranges by 0.886. These values are: weak acids, 0.32; weak bases, 0.83; neutrals, 0.28.

**Supplementary Table 1.19 Separation of Asphalt AAC-1 by IEC**

Run	IEC Fraction (mass %)			Total Recovery (mass %)
	Total Acids	Total Bases	Neutrals	
1	22.7	13.9	60.7	97.3
2	24.2	13.2	59.6	97.1
3	<u>22.8</u>	<u>-</u>	<u>-</u>	<u>97.3</u>
Avg. + Std. Dev.	23.2 ± 0.7	13.6	60.2	97.2 ± 0.1

**Supplementary Table 1.20 Quantitative IR Analyses of IEC Fractions of AAB-1**

Fraction	Functional Group (Moles/L) <sup>1</sup>					
	Sulfoxides	Ketones	Carboxylic Acid	2-Quinolones	Pyrrolic N-H	Phenolic O-H
<b>Strong Acid</b>						
Run 1	0.10	<0.01	0.03	0.05	0.31	0.44
Run 2	0.08	<0.01	0.04	0.06	0.31	0.32
<b>Strong Base</b>						
Run 1	0.08	0.02	<0.01	<0.01	0.12	--
Run 2	0.05	0.02	<0.01	<0.01	0.10	0.06
<b>Weak Acid</b>						
Run 1	0.07	<0.01	<0.01	<0.01	0.69	0.10
Run 2	0.05	0.15	0.02	0.01	0.56	0.22
<b>Weak Base</b>						
Run 1	0.31	0.23	<0.01	<0.01	0.13	<0.1
Run 2	0.11	0.22	<0.01	<0.01	0.11	0.05
<b>Neutral</b>						
Run 1	<0.01	<0.01	<0.01	<0.01	<0.1	<0.1
Run 2	<0.01	<0.01	<0.01	<0.01	<0.1	<0.1

<sup>1</sup> Based on prior experience with asphalts, standard deviations are (Moles/L): sulfoxides, 0.027; ketones, 0.006; carboxylic acids, 0.005; 2-quinolones, 0.002. The analyses for pyrroles and phenols are qualitative.

**Supplementary Table 1.21 Quantitative IR Analyses of IEC Fractions of AAD-1**

Fraction	Functional Group (Moles/L) <sup>1</sup>					
	Sulfoxides	Ketones	Carboxylic Acid	2-Quinolones	Pyrrolic N–H	Phenolic O–H
Strong Acid						
Run 1	0.09	<0.01	0.05	0.06	0.51	0.22
Run 2	0.07	<0.01	0.05	0.08	0.31	0.40
Strong Base						
Run 1	0.20	0.05	<0.01	0.01	0.17	0.09
Run 2	0.21	0.09	<0.01	0.01	0.27	0.07
Weak Acid						
Run 1	0.07	0.17	0.01	0.02	1.02	0.02
Run 2	0.08	0.14	0.02	0.02	0.09	0.18
Weak Base						
Run 1	0.18	0.38	<0.01	<0.01	0.27	0.03
Run 2	0.18	0.33	<0.01	<0.01	0.30	0.06
Neutral						
Run 1	<0.01	<0.01	<0.01	<0.01	<0.1	<0.1
Run 2	<0.01	<0.01	<0.01	<0.01	<0.1	<0.1

<sup>1</sup> Based on prior experience with asphalts, standard deviations are (Moles/L): sulfoxides, 0.027; ketones, 0.006; carboxylic acids, 0.005; 2-quinolones, 0.002. The analyses for pyrroles and phenols are qualitative.

**Supplementary Table 1.22 Quantitative IR Analyses of IEC Fractions of AAF-1**

Fraction	Functional Group (Moles/L) <sup>1</sup>					
	Sulfoxides	Ketones	Carboxylic Acid	2-Quinolones	Pyrrolic N–H	Phenolic O–H
<b>Strong Acid</b>						
Run 1	0.07	0.05	0.01	0.03	0.30	0.29
Run 2	0.07	0.03	0.02	0.03	0.21	0.38
<b>Strong Base</b>						
Run 1	0.03	0.04	<0.01	<0.01	0.05	<0.01
Run 2	0.07	0.04	<0.01	<0.01	0.07	<0.01
<b>Weak Acid</b>						
Run 1	0.03	0.17	<0.01	<0.01	0.46	0.05
Run 2	0.05	0.20	<0.01	<0.01	0.51	0.06
<b>Weak Base</b>						
Run 1	0.07	0.13	<0.01	<0.01	0.07	<0.1
Run 2	0.15	0.20	<0.01	<0.01	0.07	<0.1
<b>Neutral</b>						
Run 1	0.11	<0.01	<0.01	<0.01	<0.01	<0.1
Run 2	0.02	<0.01	<0.01	<0.01	<0.01	<0.1

<sup>1</sup> Based on prior experience with asphalts, standard deviations are (Moles/L): sulfoxides, 0.027; ketones, 0.006; carboxylic acids, 0.005; 2-quinolones, 0.002. The analyses for pyrroles and phenols are qualitative.

**Supplementary Table 1.23 Quantitative IR Analyses of IEC Fractions of AAG-1**

Fraction	Functional Group (Moles/L) <sup>1</sup>					
	Sulfoxides	Ketones	Carboxylic Acid	2-Quinolones	Pyrrolic N-H	Phenolic O-H
<b>Strong Acid</b>						
Run 1	0.05	0.16	0.255	0.09	0.83	0.20
Run 2	0.05	<0.01	0.186	0.15	0.68	0.47
<b>Strong Base</b>						
Run 1	0.08	0.15	<0.01	0.011	0.31	0.07
Run 2	0.07	0.08	<0.01	0.019	0.24	0.21
<b>Weak Acid</b>						
Run 1	0.11	<0.01	0.076	<0.01	0.55	0.58
Run 2	0.12	<0.01	0.145	<0.01	0.76	0.61
<b>Weak Base</b>						
Run 1	0.21	0.35	<0.01	<0.01	0.45	0.10
Run 2	0.18	0.43	<0.01	<0.01	0.38	0.25
<b>Neutral</b>						
Run 1	0.04	<0.01	<0.01	<0.01	0.11	0.01
Run 2	0.03	<0.01	<0.01	<0.01	0.11	0.13

<sup>1</sup> Based on prior experience with asphalts, standard deviations are (Moles/L): sulfoxides, 0.027; ketones, 0.006; carboxylic acids, 0.005; 2-quinolones, 0.002. The analyses for pyrroles and phenols are qualitative.

**Supplementary Table 1.24 Quantitative IR Analyses of IEC Fractions of AAK-1**

Fraction	Functional Group (Moles/L) <sup>1</sup>					
	Sulfoxides	Ketones	Carboxylic Acid	2-Quinolones	Pyrrolic N-H	Phenolic O-H
<b>Strong Acid</b>						
Run 2	0.08	<0.01	0.05	0.04	0.34	0.08
Run 3	0.05	<0.01	0.09	0.05	0.24	0.26
<b>Strong Base</b>						
Run 2	0.49	0.07	<0.01	0.01	0.17	0.04
Run 3	0.04	0.04	<0.01	0.01	0.16	0.03
<b>Weak Acid</b>						
Run 2	0.08	0.02	0.05	0.01	0.61	0.08
Run 3	0.09	0.27	0.06	0.02	0.51	0.05
<b>Weak Base</b>						
Run 2	0.40	0.20	<0.01	<0.01	0.15	0.01
Run 3	0.16	0.21	<0.01	<0.01	0.19	0.03
<b>Neutral</b>						
Run 1	<0.01	<0.01	<0.01	<0.01	<0.1	<0.1
Run 2	<0.01	<0.01	<0.01	<0.01	<0.1	<0.1

<sup>1</sup> Based on prior experience with asphalts, standard deviations are (Moles/L): sulfoxides, 0.027; ketones, 0.006; carboxylic acids, 0.005; 2-quinolones, 0.002. The analyses for pyrroles and phenols are qualitative.

**Supplementary Table 1.25 Quantitative IR Analyses of IEC Fractions of AAM-1**

Fraction	Functional Group (Moles/L) <sup>1</sup>					
	Sulfoxides	Ketones	Carboxylic Acid	2-Quinolones	Pyrrolic N-H	Phenolic O-H
<b>Strong Acid</b>						
Run 1	0.03	<0.01	0.02	0.02	0.38	0.17
Run 2	0.05	<0.01	0.03	0.02	0.41	0.17
<b>Strong Base</b>						
Run 1	0.03	0.14	<0.01	0.01	0.12	0.05
Run 2	0.04	0.07	<0.01	0.01	0.13	0.04
<b>Weak Acid</b>						
Run 1	0.05	0.16	0.01	0.01	0.54	0.11
Run 2	0.04	0.29	0.04	0.01	0.60	0.10
<b>Weak Base</b>						
Run 1	0.07	0.19	<0.01	<0.01	0.12	0.03
Run 2	0.08	0.16	<0.01	<0.01	0.12	0.05
<b>Neutral</b>						
Run 1	<0.01	<0.01	<0.01	<0.01	<0.1	<0.1
Run 2	<0.01	<0.01	<0.01	<0.01	<0.1	<0.1

<sup>1</sup> Based on prior experience with asphalts, standard deviations are (Moles/L): sulfoxides, 0.027; ketones, 0.006; carboxylic acids, 0.005; 2-quinolones, 0.002. The analyses for pyrroles and phenols are qualitative.

**Supplementary Table 1.26 Elemental Analyses of IEC Strong Base Fractions of Seven Core Asphalts<sup>1</sup>**

Parent Asphalt	Run No.	Element (mass %)					Total (mass %)	H/C
		C	H	N	O	S		
AAA-1	1	82.5	8.6	1.2	1.2	5.9	99.4	1.24
	2	82.4	8.3	1.3	-	-	-	-
AAB-1	1	84.8	8.3	1.3	0.9	4.6	99.9	1.17
	2	83.9	8.3	1.5	-	-	-	1.18
AAD-1	1	81.0	8.7	2.0	1.6	5.9	99.2	1.28
AAF-1	1	84.1	8.5	1.6	1.1	3.8	99.1	1.20
AAG-1	1	84.7	9.3	2.3	1.0	1.1,1.1	98.4	1.31
AAK-1	1	81.2	8.7	1.7	1.5	5.8	98.9	1.29
	2	81.5	8.6	1.7	-	-	-	1.26
AAM-1	1	86.3	9.7	1.2	0.9	1.2	99.3	1.34

<sup>1</sup> Standard deviations for the elemental analyses are estimated to be (mass %): carbon, 0.36; hydrogen, 0.20; nitrogen, 0.09; oxygen, 0.41; sulfur, 0.36.

**Supplementary Table 1.27 Elemental Analyses of IEC Weak Acid Fractions of Seven Core Asphalts<sup>1</sup>**

Parent Asphalt	Element (mass %)					Total (mass %)	H/C
	C	H	N	O	S		
AAA-1	83.7	9.1	1.1	1.9,2.0	5.4	101.2	1.30
AAB-1	84.1	9.0	1.2	2.4	4.1	100.8	1.28
AAD-1	81.4	9.3	1.7	2.3	5.6	100.3	1.36
AAF-1	85.3	9.0	1.0	1.9	3.5	100.7	1.26
AAG-1	81.1	8.8	1.8	8.7	0.8	101.2	1.29
AAK-1	80.2	9.0	1.5	4.9	5.2	100.8	1.34
AAM-1	87.1	10.0	0.7	1.9	1.1	100.8	1.37

<sup>1</sup> Standard deviations for the elemental analyses are estimated to be (mass %): carbon, 0.36; hydrogen, 0.20; nitrogen, 0.09; oxygen, 0.41; sulfur, 0.36.



**Supplementary Table 1.28 Elemental Analyses of IEC Weak Base Fractions of Seven Core Asphalts<sup>1</sup>**

Parent Asphalt	Run No.	Element (mass %)					Total (mass %)	H/C
		C	H	N	O	S		
AAA-1	1	82.7	9.5	1.1	1.5	6.2	101.0	1.37
AAB-1	1	83.1	9.5	1.0	1.4	5.4	100.4	1.36
	2	82.3	9.5	1.0	-	5.2	-	1.38
AAD-1	1	80.2	10.1	1.4	1.9	6.5	99.1	1.50
	2	79.9	10.3	1.5	2.1	6.4	100.2	1.54
AAF-1	1	84.5	9.0	0.9	1.5,1.5	4.6	100.5	1.27
AAG-1	1	86.1	10.0	1.8	1.7	1.5	101.1	1.38
AAK-1	1	80.9	9.9	1.2	1.7	7.0	100.7	1.46
	2	80.1	10.0	1.1	1.7	6.5	99.4	1.49
	3	80.0	9.8	1.5	1.4	6.7	99.4	1.46
AAM-1	1	86.5	10.9	0.8	0.9	1.6	100.7	1.50
	2	86.5	11.0	0.9	0.8	1.3	100.5	1.52

<sup>1</sup> Standard deviations for the elemental analyses are estimated to be (mass %): carbon, 0.36; hydrogen, 0.20; nitrogen, 0.09; oxygen, 0.41; sulfur, 0.36.

**Supplementary Table 1.29 Metal and Porphyrin Contents of IEC Fractions of Asphalt AAD-1<sup>1</sup>**

IEC Fraction	Run No.	Yield, (mass %)	Metal concentration, ppm		Porphyrin Concentration, $\mu\text{M}/\text{gram}$
			V	Ni	
Whole Asphalt	1	100	300	135	3.4
Strong Acid	1	23.3	534.5	256	0.8
	2	23.8	530.0	259.5	-
Strong Base	1	7.1	219.5	129	2.0
	2	7.0	229.5	136	1.8
Weak Acid	1	8.1	664.5	123	5.6
	2	7.5	611.5	115	4.9
Weak Base	1	5.8	430	415	14.9
	2	6.1	516.5	358	21.2
Neutral	1	50.0	3.0	14.8	0
	2	49.2	1.2	13.3	0

<sup>1</sup> Based on experience with other fossil fuel samples, standard deviations are: vanadium, 18.4; nickel, 14.7. Porphyrin analyses are qualitative.

**Supplementary Table 1.30 Rheological Data for Six Core Asphalt IEC Neutral Fractions at 25 °C, 50 mm Parallel Plates**

Parent Asphalt	Run No.	Rad/s	Viscosity <sup>1</sup> (Pa · s)	G' (dynes/cm <sup>2</sup> )	G'' (dynes/cm <sup>2</sup> )	tan δ
AAA-1	1	1.0	35.2	2.4	352.4	147.7
		10.0	34.0	86.3	3,398.0	39.38
		100.0	32.8	55.9	32,830.0	586.7
	2	1.0	36.0	0.8	359.9	432.0
		10.0	35.3	33.7	4,448.0	131.9
		100.0	34.3	24.9	34,250.0	1,374.0
AAB-1	1	1.0	142.3	159.8	1,413.0	8.8
		10.0	104.5	734.2	10,430.0	14.2
		100.0	80.9	2,888.0	80,870.0	28.0
	2	1.0	168.4	266.9	1,663.0	6.3
		10.0	109.7	1,116.0	10,910.0	9.8
		100.0	81.7	4,004.0	82,630.0	20.4
AAD-1	1	1.0	19.7	20.8	195.5	9.4
		10.0	14.4	83.8	1,442.0	17.2
		100.0	12.7	264.7	12,680.0	47.9
	2	1.0	15.8	6.7	158.0	23.6
		10.0	13.8	35.0	1,377.0	39.3
		100.0	12.7	265.5	12,720.0	47.9
AAG-1	1	1.0	282.1	30.6	2,820.0	92.1
		10.0	282.5	58.5	28,250.0	482.9
		100.0	279.4	---	221,900.0	---
	2	1.0	238.9	25.5	2,383.0	9.4
		10.0	239.3	---	23,920.0	---
		100.0	231.2	---	231,100.0	---
AAK-1	1	1.0	46.7	14.1	467.0	33.2
		10.0	45.4	143.0	4,540.0	31.8
		100.0	40.6	540.8	40,560.0	75.0
	2	1.0	46.0	17.5	459.5	26.2
		10.0	40.9	38.6	4,092.0	106.1
		100.0	36.5	610.7	36,520.0	59.8
AAM-1	1	1.0	1,448.0	3,039.0	14,160.0	4.7
		10.0	942.0	13,060.0	93,280.0	7.1
		100.0	678.1	50,850.0	676,000.0	13.3
	2	1.0	934.0	1,304.0	9,248.0	7.1
		10.0	705.7	7,015.0	70,210.0	10.0
		100.0	548.5	33,110.0	547,300.0	16.5

<sup>1</sup> Viscosities measured on the Rheometrics Mechanical Spectrometer are estimated to have an error bar of ± 10%.

**Supplementary Table 1.31 Rheological Data for IEC Neutral Fractions of Asphalt  
AAC-1 and AAF-1, 25 °C and 45 °C, 50 mm Parallel Plates**

Parent Asphalt	Run No.	Temperature °C	Rad/s	Viscosity <sup>1</sup> (Pa · s)	G' (dynes/cm <sup>2</sup> )	G'' (dynes/cm <sup>2</sup> )	tan δ
AAC-1	1	25	0.1	480.3	90	472	5.2
			1.0	349.1	440	3,463	7.9
			10.0	268.1	2,092	26,730	12.8
			100.0	221.7	10,130	221,400	21.9
	2	25	0.1	505.1	91	497	5.5
			1.0	371.0	576	3,664	6.6
			10.0	259.0	2,634	25,760	9.8
			100.0	208.6	11,780	208,200	17.7
AAC-1	1	45	0.1	19.6	11.3	16	1.4
			1.0	16.2	12.2	161	13.2
			10.0	13.4	35.2	1,337	38.0
			100.0	11.3	361.2	11,250	31.1
	2	45	0.1	49.0	12.8	47.3	3.7
			1.0	26.7	41.9	263.8	6.3
			10.0	14.2	96.0	1,413	14.7
			100.0	12.3	614.3	12,310	20.0
AAF-1	1	25	0.1	629.6	86	624	7.2
			1.0	446.7	534	4,435	8.3
			10.0	330.3	2,217	22,950	14.9
	2	25	0.1	762.6	159	746	4.7
			1.0	512.4	664	5,080	7.6
			10.0	367.9	2,429	36,700	15.1
	1	45	0.1	19.9	19.9	1.5	0.1
			1.0	16.2	10.4	162	15.5
			10.0	13.6	41.4	1,357	36.7
			100.0	11.7	317.3	11,660	36.7
AAF-1	2	45	0.1	33.4	8.4	32.3	3.8
			1.0	21.2	32.8	209.6	6.4
			10.0	15.4	110.3	1,539	14.0
			100.0	12.3	425.5	12,250	28.8

<sup>1</sup> Viscosities measured on the Rheometrics Mechanical Spectrometer are estimated to have an error bar of ± 10%.

**Supplementary Table 1.32 Rheological Data for IEC Neutral Fractions at 0 °C, 10% Strain, 25 mm Parallel Plates**

Parent Asphalt	Run No.	Rad/s	Viscosity <sup>1</sup> (Pa · s)	G' (dynes/cm <sup>2</sup> )	G'' (dynes/cm <sup>2</sup> )	tan $\delta$
AAB-1	1	1.0	13,420	14,630	133,300	9.1
		10.0	10,520	71,770	1,049,000	14.6
		100.0	8,173	343,000	5,144,000	15.0
	2	1.0	11,970	16,470	118,500	7.2
		10.0	8,928	80,740	884,000	11.0
		100.0	5,965	41,930	594,800	14.2
AAD-1	1	1.0	4,388	14,530	41,480	2.8
		10.0	2,190	35,550	216,100	6.1
		100.0	1,412	131,000	1,406,000	10.7
	2	1.0	5,411	20,000	50,250	2.5
		10.0	2,481	44,690	244,000	5.5
		100.0	1,485	166,600	1,476,000	8.9
AAK-1	1	1.0	14,620	25,710	143,900	5.6
		10.0	9,683	108,100	96,200	8.9
		100.0	6,154	630,300	6,120,000	9.7
	2	1.0	10,350	19,410	101,600	5.2
		10.0	7,012	74,970	697,000	9.3
		100.0	4,807	426,900	4,787,000	11.2

<sup>1</sup> Viscosities measured on the Rheometrics Mechanical Spectrometer are estimated to have an error bar of  $\pm 10\%$ .

**Supplementary Table 1.33 Viscosities (Pa · s) of Mixtures of Core Asphalts (95 wt %) with Their Own IEC Neutral Fractions (5 wt %) Compared with Original Asphalt Viscosities at 25 °C and 60 °C, 1.0 rad/s**

Asphalt	25 °C		60 °C	
	Viscosity <sup>1</sup> of Mixture	Viscosity of Asphalt	Viscosity of Mixture	Viscosity of Asphalt
AAA-1	19,190	30,070	86	124
AAB-1	60,650	85,020	116	151
AAC-1	65,870	74,710	99	119
AAD-1	25,360	57,280	106	164
AAF-1	216,400	381,700	179	289
AAG-1	187,800	248,900	182	300
AAK-1	83,220	251,700	283	470
AAM-1	116,200	364,400	188	276

<sup>1</sup> Viscosities measured on the Rheometrics Mechanical Spectrometer are estimated to have an error bar of ± 10%.

**Supplementary Table 1.34 Viscosities (Pa · s) of Mixtures of Asphalt AAD-1 with Its IEC Fractions, 25 °C, 45 °C, 60 °C, 1.0 rad/s**

Mixture	Viscosity <sup>1</sup>		
	25 °C	45 °C	60 °C
Control	60,220	1,798	199
95% AAD-1 + 5% IEC Neutral Fraction	25,080	870	106
95% AAD-1 + 5% IEC Strong Base Fraction	81,220	2,377	240
98% AAD-1 + 2% IEC Strong Acid Fraction	76,330	2,496	272

<sup>1</sup> Viscosities measured on the Rheometrics Mechanical Spectrometer are estimated to have an error bar of ± 10%.

**Supplementary Table 1.35 Viscosities (Pa·s) of Neutral Plus Acid Fractions of Four Asphalts at 25°C and 45°C, 1.0 rad/s**

Asphalt	Run No.	Viscosity <sup>1</sup> of Neutrals plus Acids, Pa·s, 1.0 rad/s	
		25 °C	45 °C
AAD-1	1	26	-
	2	44	-
AAG-1	1	1,269	48
	2	1,676	57
AAK-1	1	157	11
	2	140	9
AAM-1	1	1,961	46
	2	2,340	53

<sup>1</sup> Viscosities measured on the Rheometrics Mechanical Spectrometer are estimated to have an error bar of ± 10%.

**Supplementary Table 1.36  $G^*/\sin \delta$  (dynes/cm<sup>2</sup>) Values of Mixtures of Four Core Asphalts with Their IEC Amphoteric, Base, Acid, or Neutral Fractions at 60°C and 1.0 rad/s**

Asphalt	$G^*/\sin \delta$ of Asphalt + Amphoterics <sup>1</sup>	$G^*/\sin \delta$ of Asphalt + Bases <sup>1</sup>	$G^*/\sin \delta$ of Asphalt + Acids <sup>1</sup>	$G^*/\sin \delta$ of Asphalt + Neutrals <sup>1</sup>
AAD-1	26,707	3,275	1,743	404
AAG-1	14,400	3,461	2,853	1,311
AAK-1	69,990	6,574	5,176	1,168
AAM-1	40,215	3,993	2,922	1,373

<sup>1</sup> These values were calculated by Dr. David Jones.

**Supplementary Table 1.37 Yields of Moderate Base Fractions and Moderate Base-Free Fractions by IEC Separation of Five Core Asphalts**

Asphalt	Run No.	Fraction and Yield, mass %		% Recovery	Viscosity (Pa · s), <sup>1</sup> 25 °C, 1.0 rad/s	M <sub>n</sub> (Daltons) <sup>2</sup>
		Moderate Base-Free	Moderate Bases		Moderate Base-Free Fraction	Moderate Base Fraction
AAA-1	1	81.8	17.2	99.0	941	3,900
	2	81.8	17.4	99.2	841	3,900
AAD-1	1	74.5	22.6	97.1	314	3,500
	2	74.0	22.4	96.5	306	-
AAG-1	1	79.2	18.2	97.4	1,291	-
AAK-1	1	76.0	22.3	98.3	1,209	4,200
	2	75.9	21.7	97.6	-	-
AAM-1	1	80.3	19.2	99.4	11,200	3,600
	2	80.6	18.2	98.8	8,480	-

<sup>1</sup> Viscosities measured on the Rheometrics Mechanical Spectrometer are estimated to have an error bar of ± 10%.

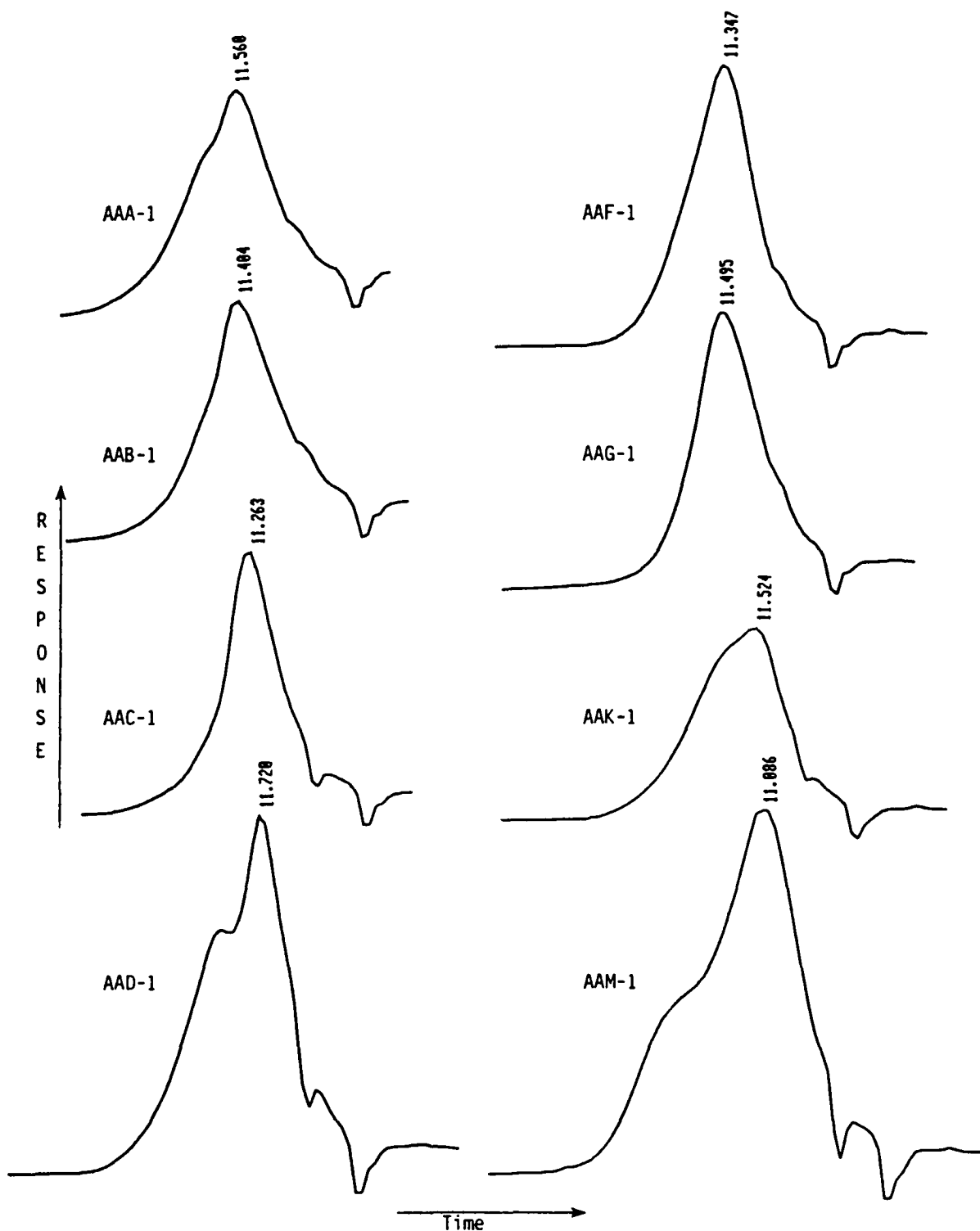
<sup>2</sup> ASTM Method D 2503 is estimated to have an error bar of ± 10% in this molecular weight range.



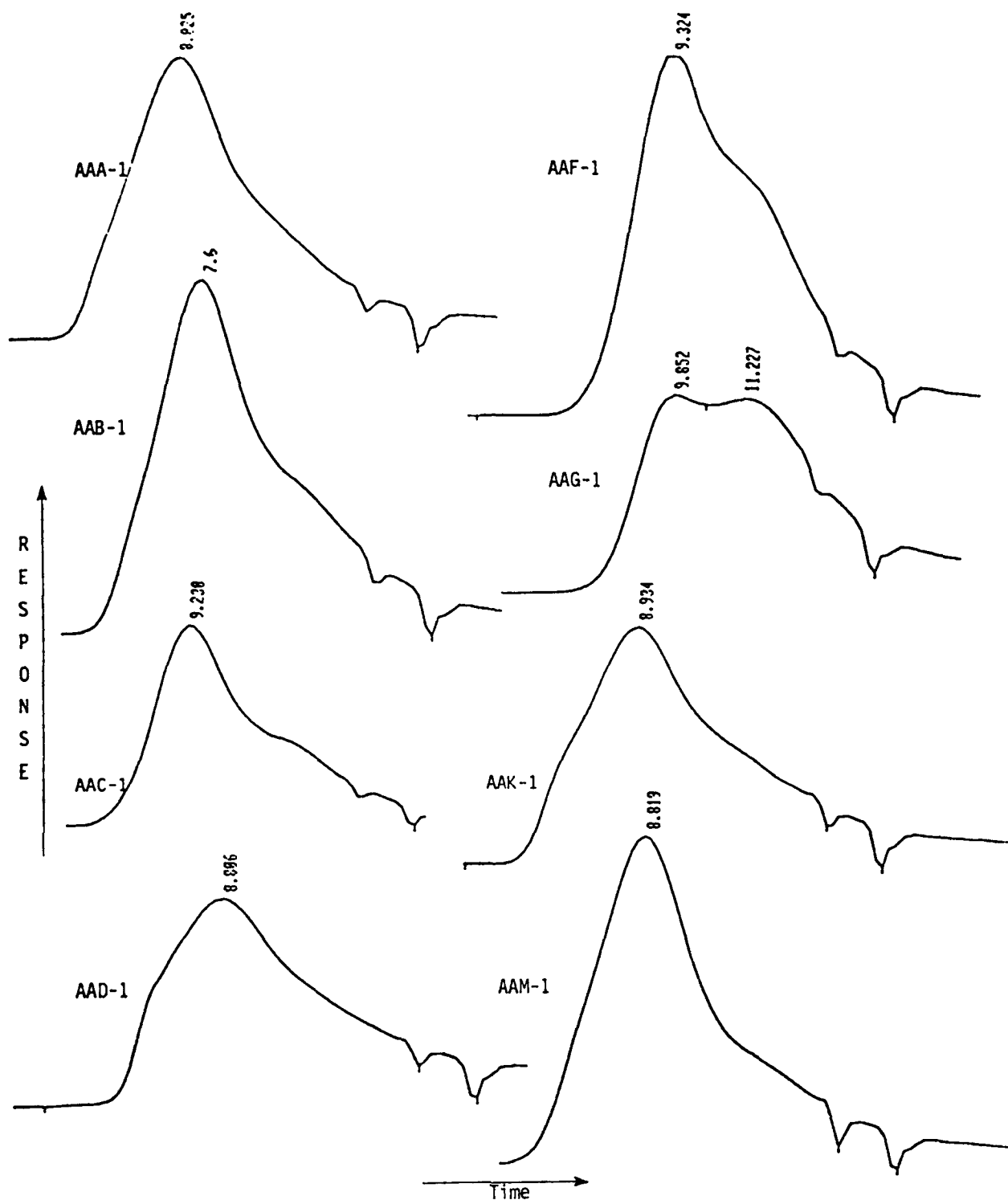
**Supplementary Table 1.38 Molecular Weights of IEC Amphoteric and Base Fractions of TFO-POV Aged (60 °C; 144 hr) Asphalts**

Asphalt	Run No.	Fraction	Molecular Weight (Daltons) <sup>1</sup>	
			Toluene	Pyridine
AAD-1	1	Amphoteric	2,900	1,910
	1	Base	836	873
AAG-1	1	Amphoteric	1,610	1,250
	1	Base	819	875
AAK-1	1	Amphoteric	2,920	1,820
	1	Base	1,050	1,100
	2	Amphoteric	3,490	2,540
	2	Base	1,030	1,060
AAM-1	1	Amphoteric	3,140	insoluble
	1	Base	1,510	insoluble
	2	Amphoteric	3,000	insoluble
	2	Base	1,600	insoluble

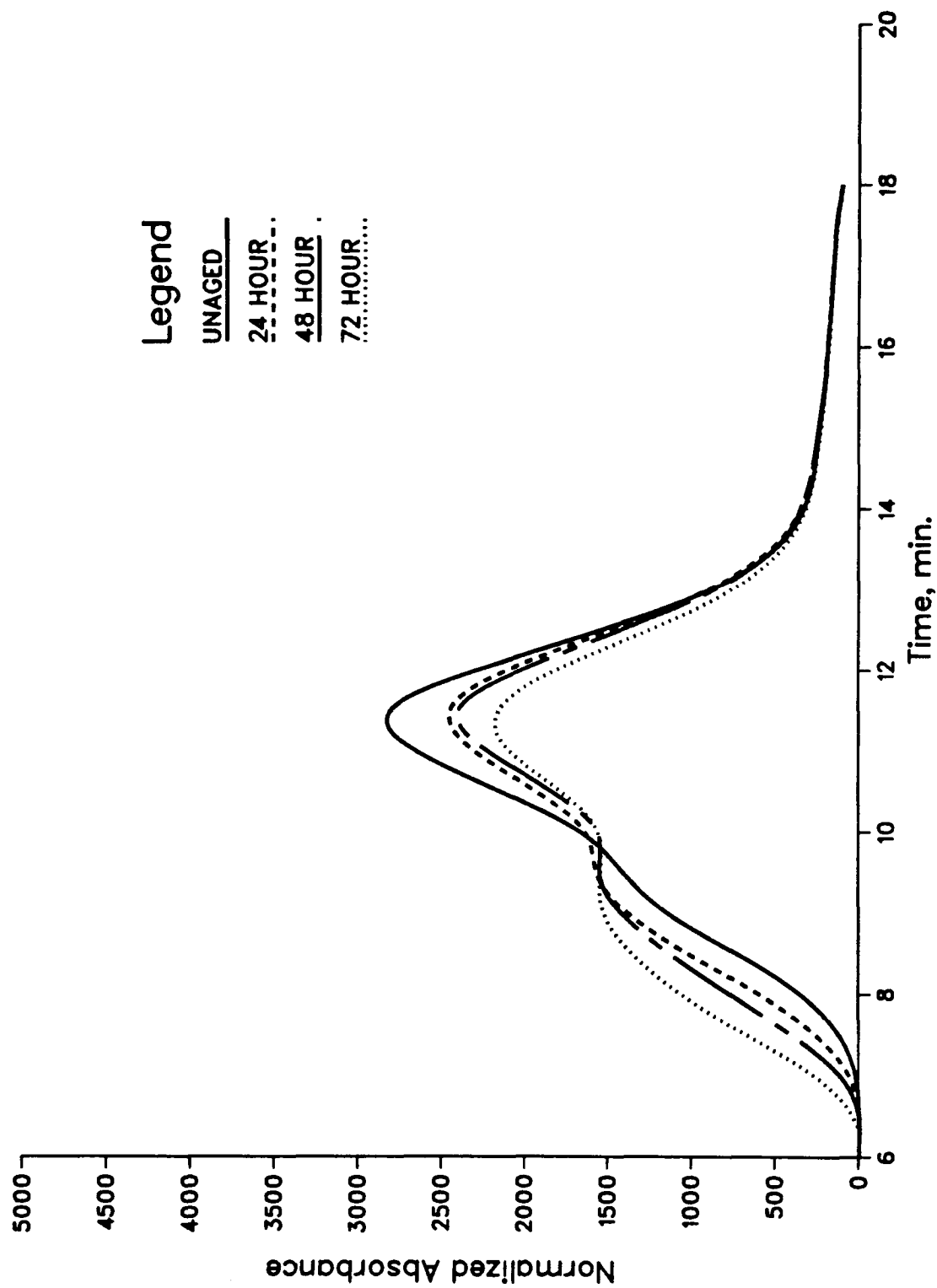
<sup>1</sup> These analyses were performed by vapor phase osmometry at 60 °C, and the results are number-average molecular weights. Error bars are estimated to be ± 5% below 1,000 Daltons, increasing to ± 10% at higher values.



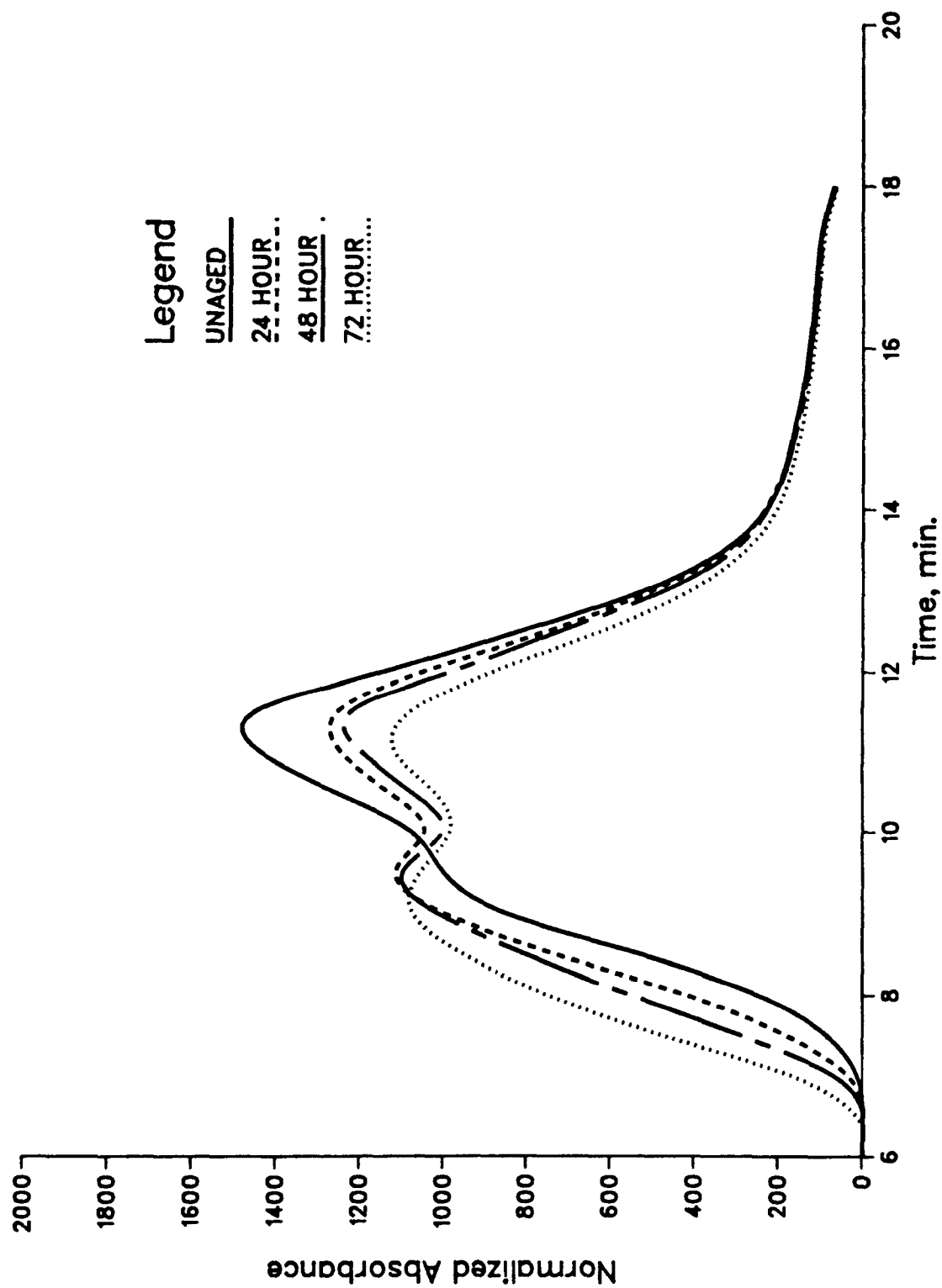
**Supplementary Figure 2.11** Fast SEC Refractive Index Chromatograms for Maltenes from Unaged Core Asphalts, Toluene Carrier,  $10^4$  Å and  $10^3$  Å Columns in Series (Retention Times for Peak Maxima are given in Minutes)



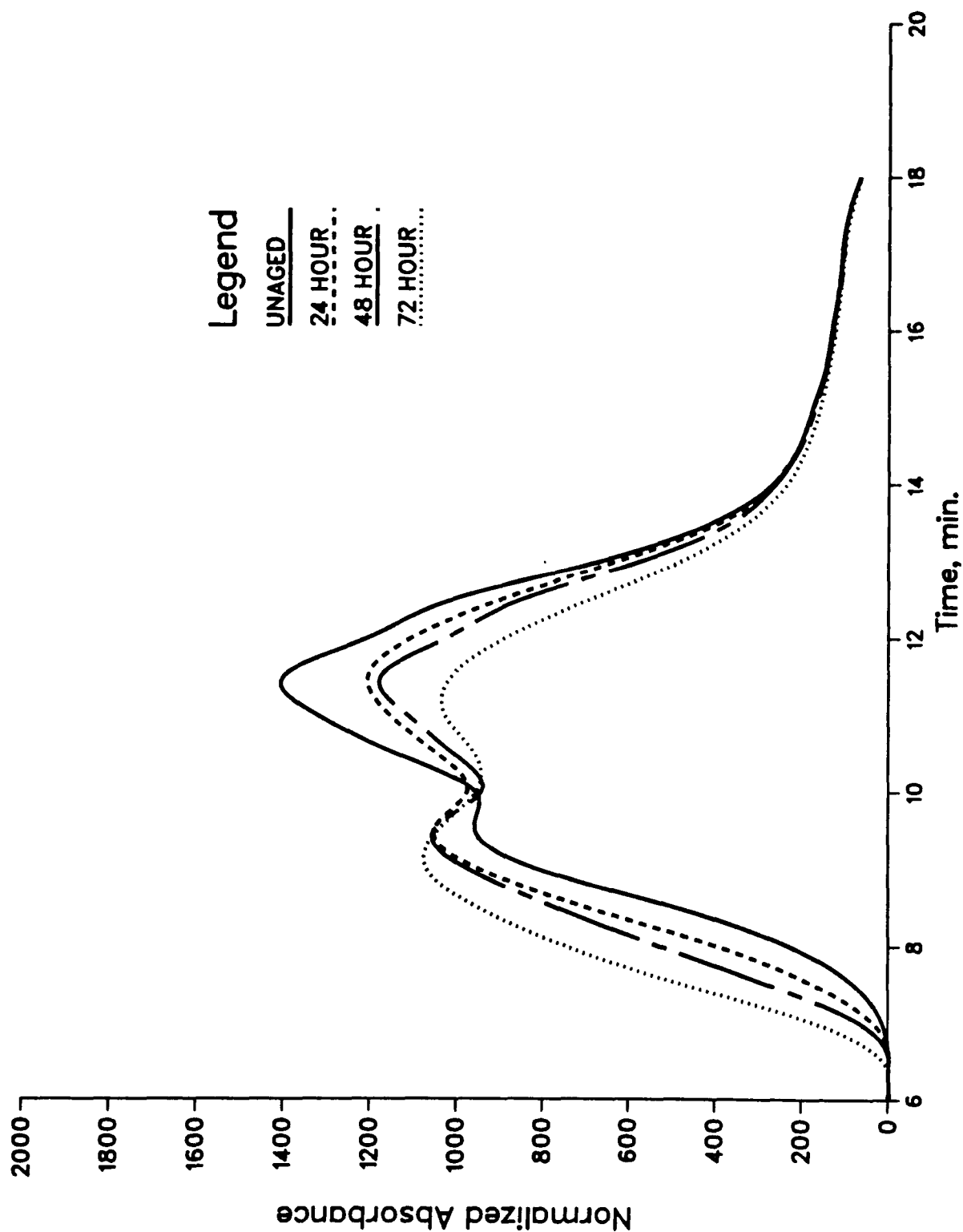
**Supplementary Figure 2.12** Fast SEC Refractive Index Chromatograms for Asphaltenes from Unaged Core Asphalts, Toluene Carrier,  $10^4$  Å and  $10^3$  Å Columns in Series (Retention Times for Peak Maxima are given in Minutes)



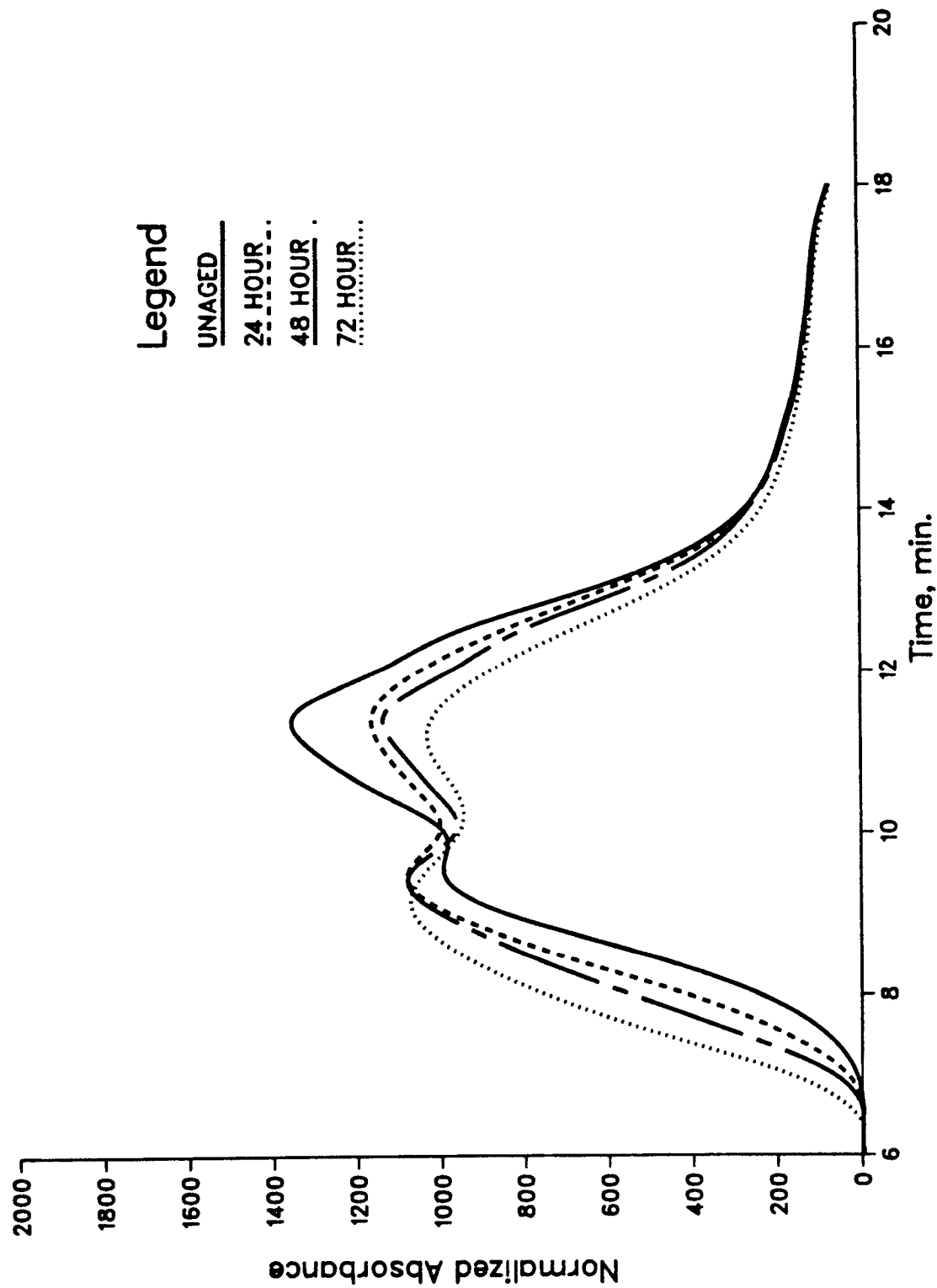
Supplementary Figure 2.13 Fast SEC of AAK-1, TFAAT Aged 0, 24, 48, & 72 hrs, Scanned at 340 nm



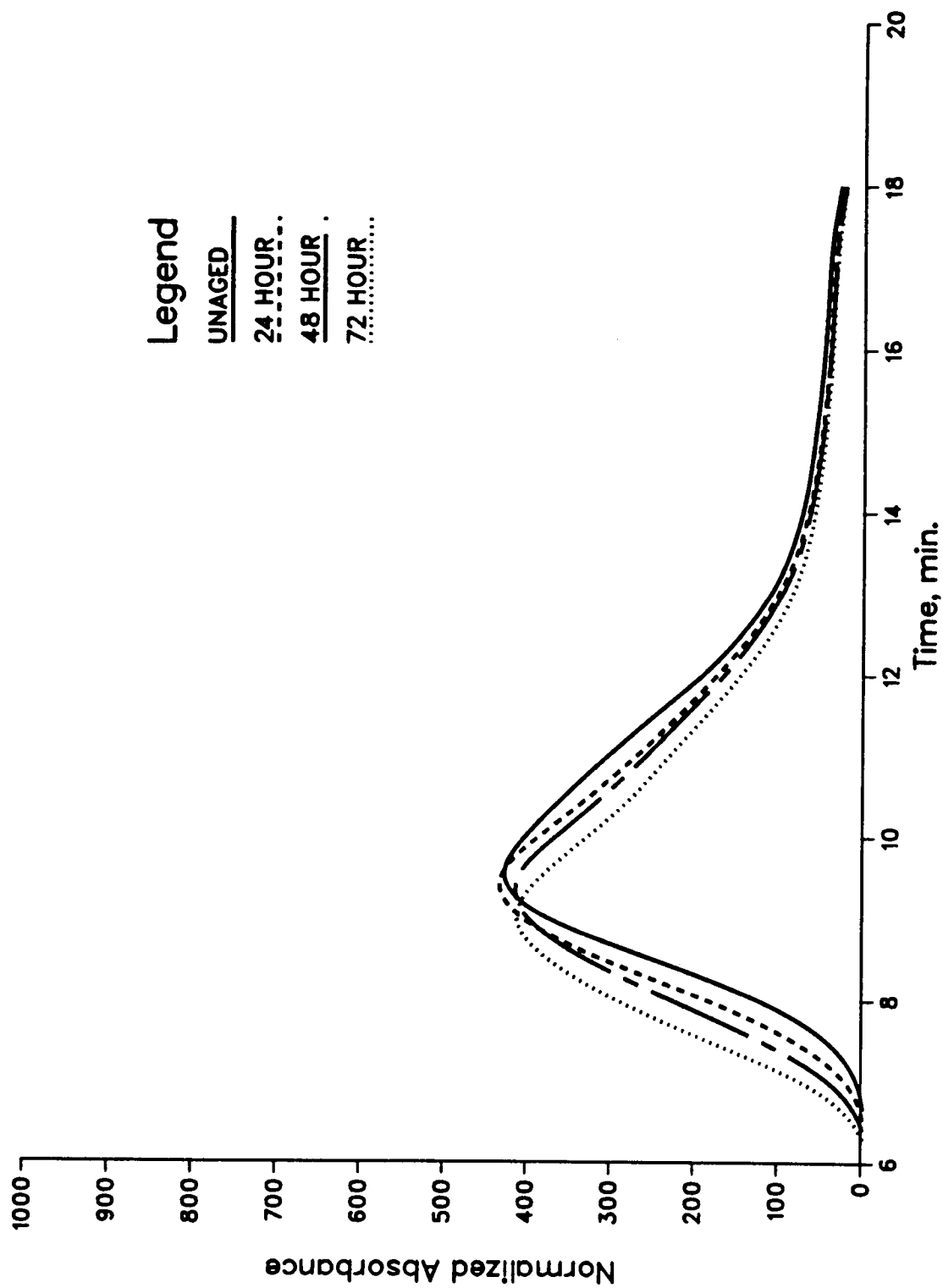
Supplementary Figure 2.14 Fast SEC of AAK--1, TFAAT Aged 0, 24, 48, & 72 hrs, Scanned at 380 nm



Supplementary Figure 2.15 Fast SEC of AAK-1, TFAAT Aged 0, 24, 48, & 72 hrs, Scanned at 410 nm

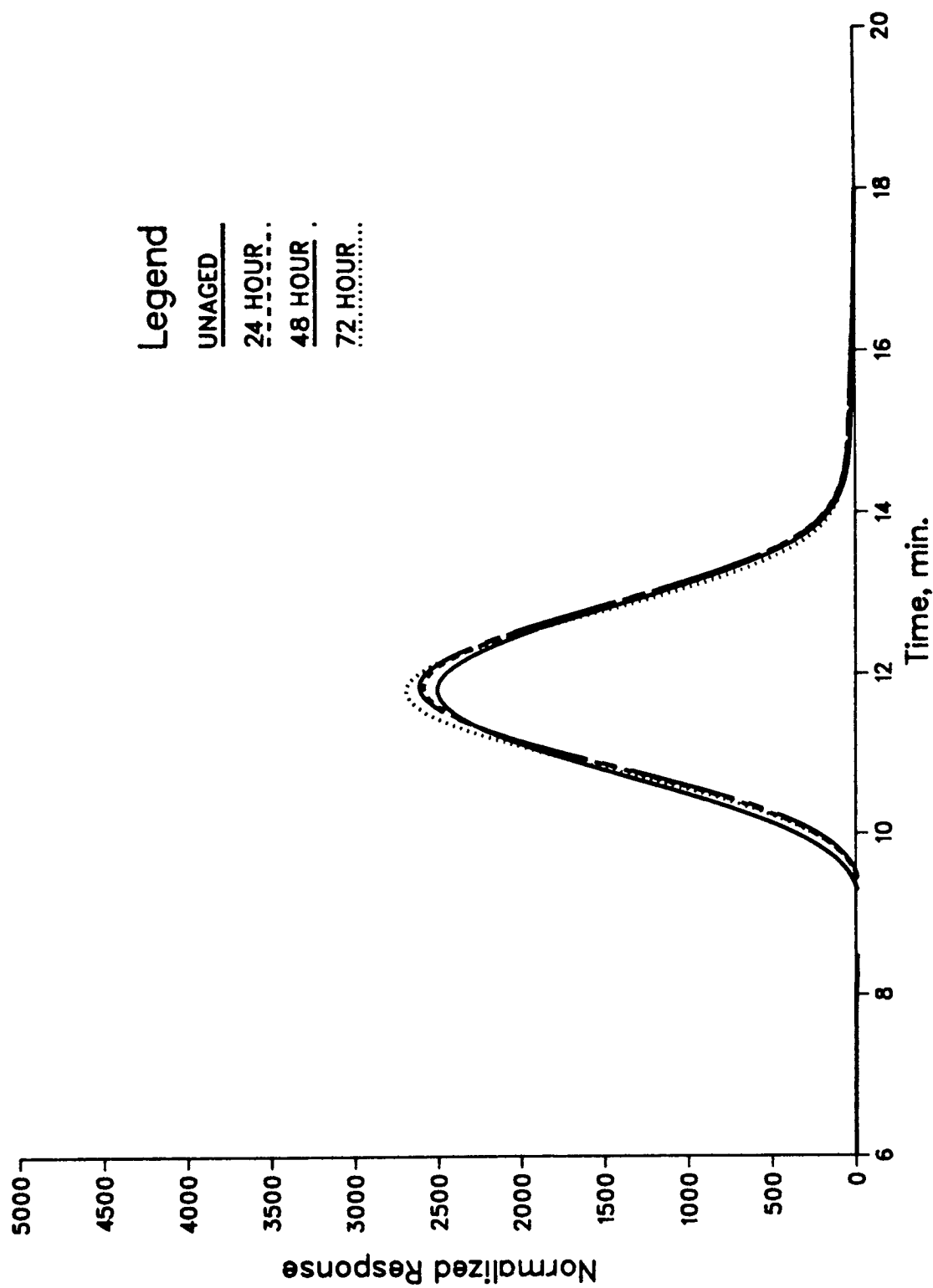


Supplementary Figure 2.16 Fast SEC of AAK-1, TFAAT Aged 0, 24, 48, & 72 hrs, Scanned at 420 nm

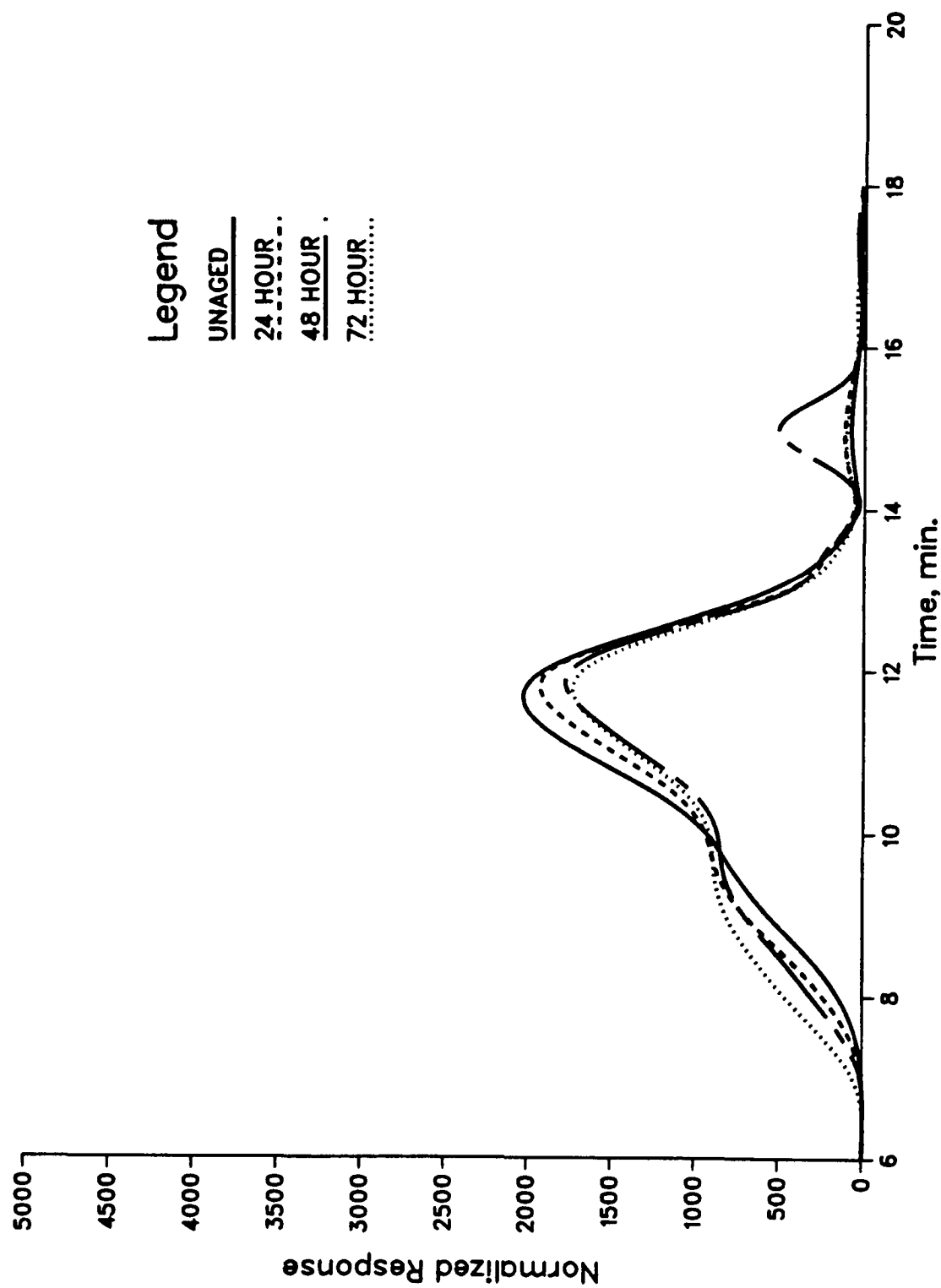


Supplementary Figure 2.17 Fast SEC of AAK-1, TFAAT Aged 0, 24, 48, & 72 hrs, Scanned at 500 nm

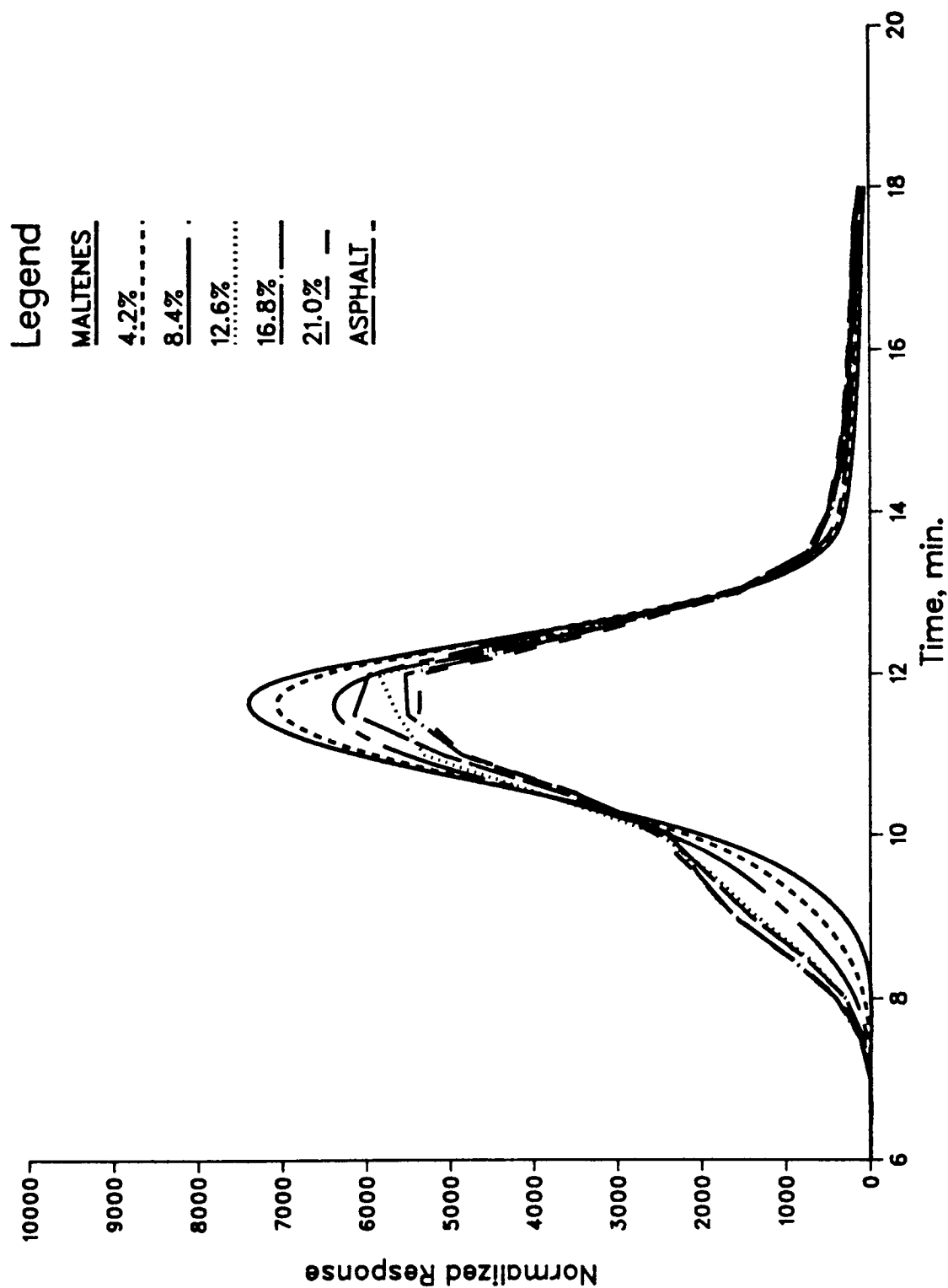




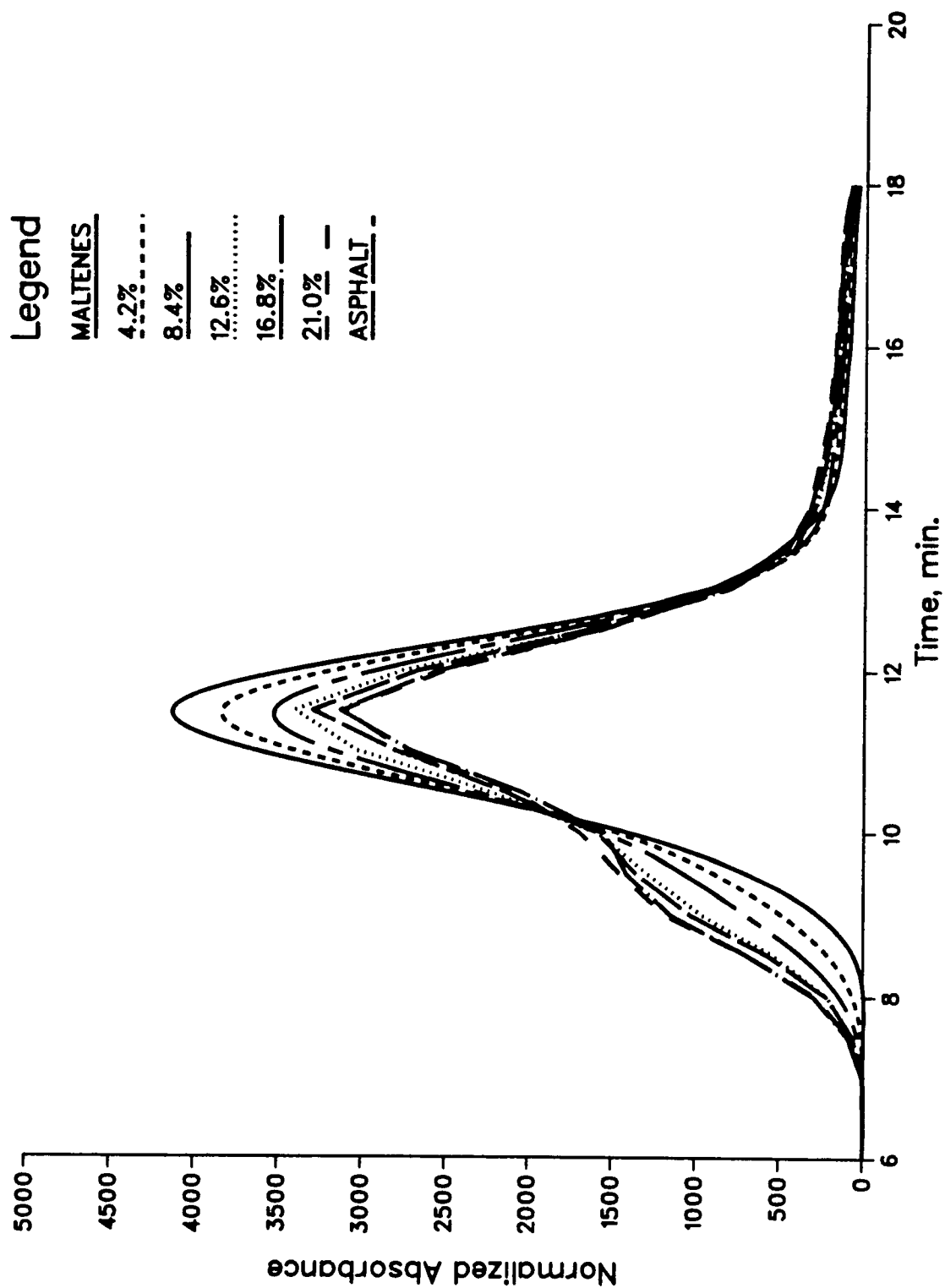
Supplementary Figure 2.18 Fast SEC of AAK-1, TFAAT Aged 0, 24, 48, & 72 hrs, by Fluorescence Detector



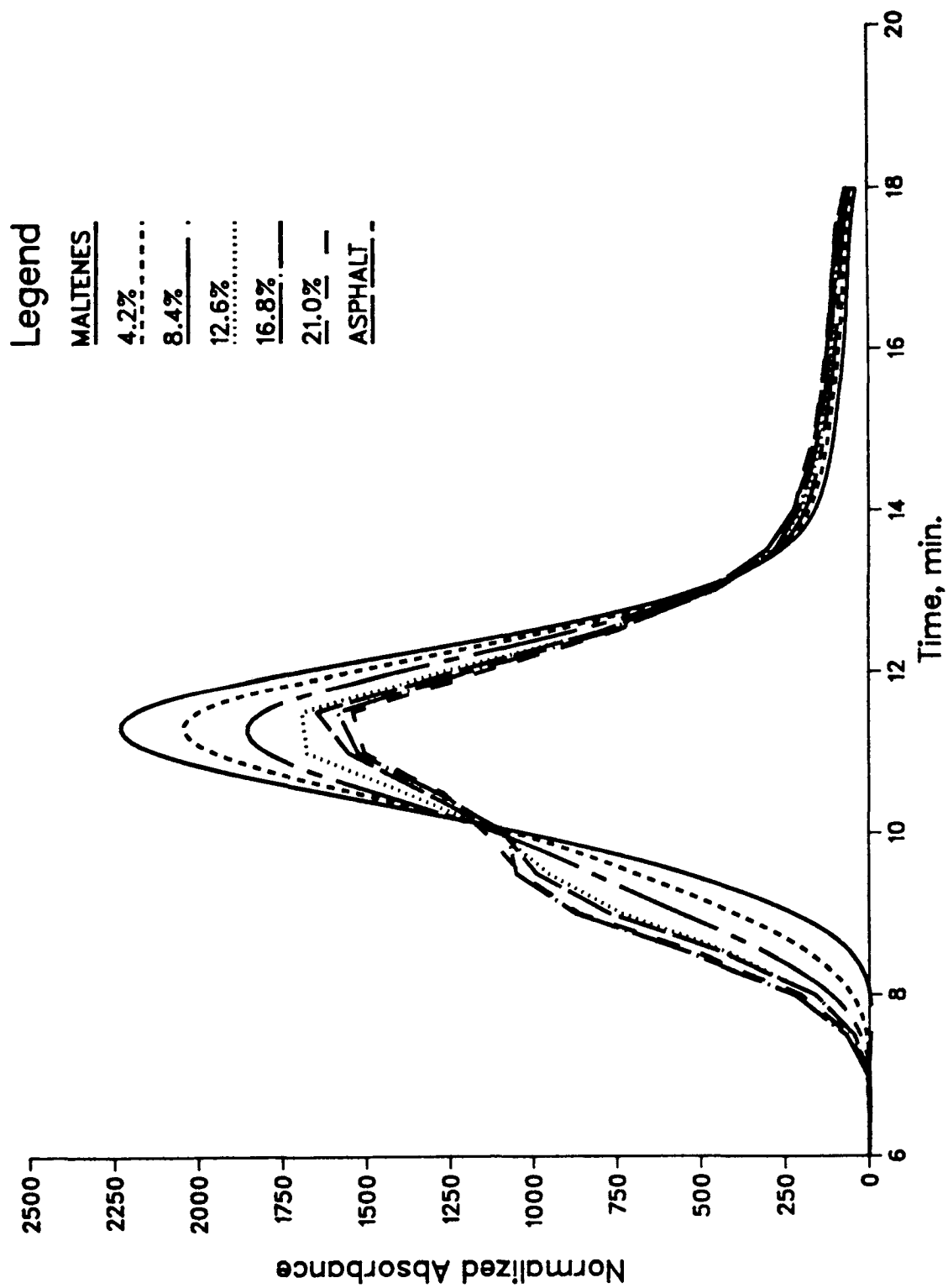
Supplementary Figure 2.19 Fast SEC of AAK-1, TFAAT Aged 0, 24, 48, & 72 hrs, by DRID



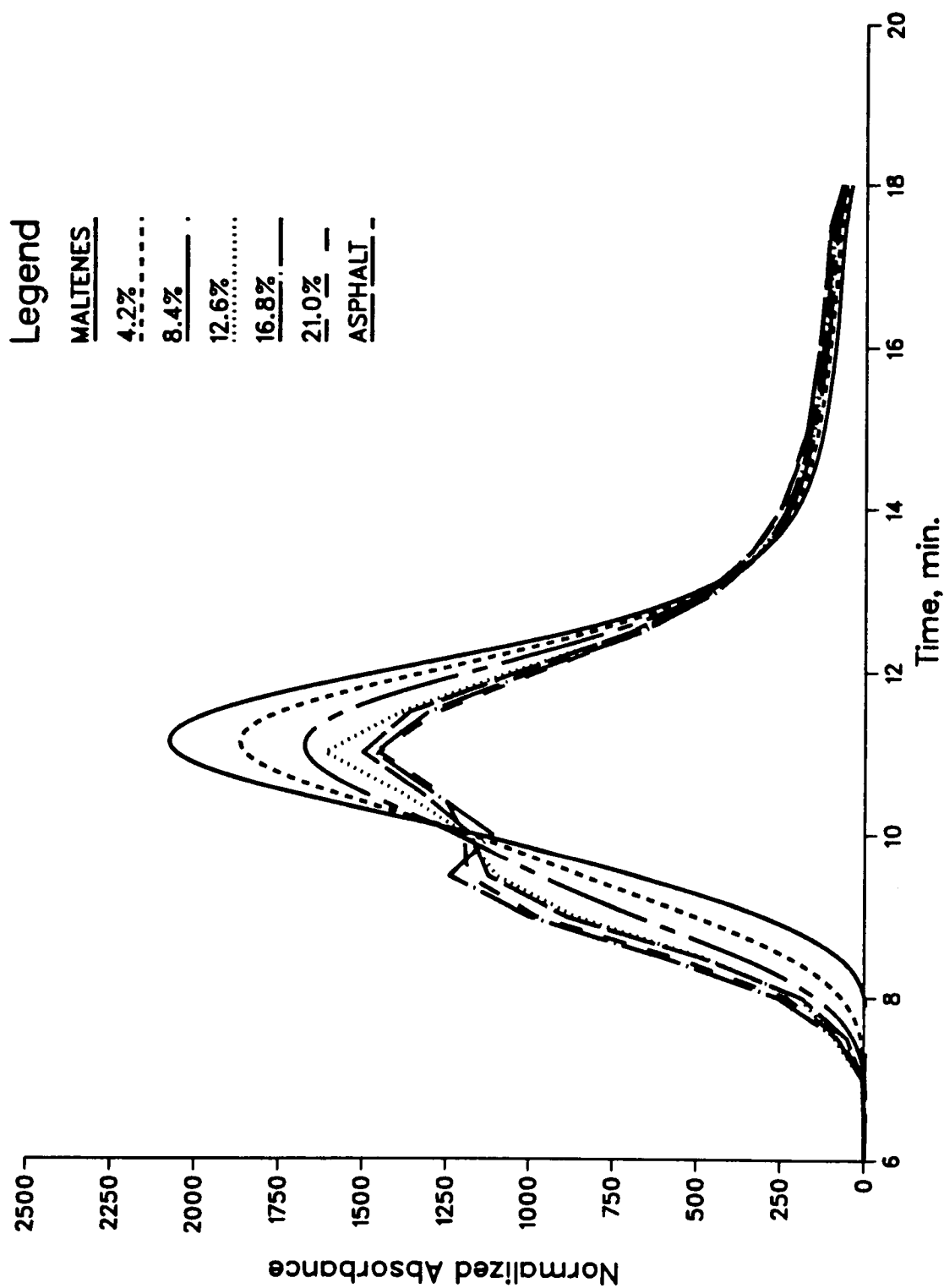
Supplementary Figure 2.20 Fast SEC of Blends of Asphaltenes/Maltenes of AAA-1, Scanned at 300 nm



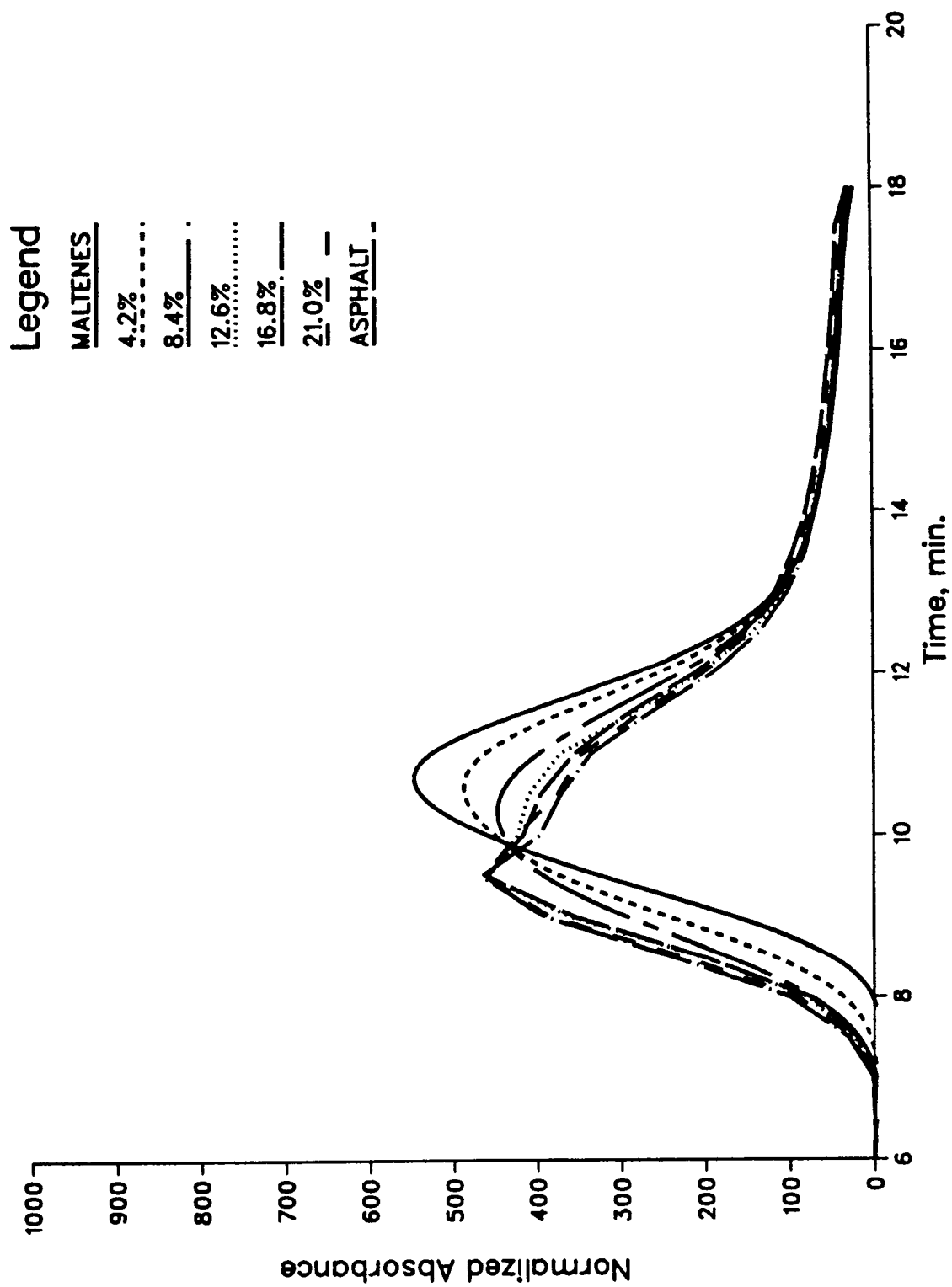
Supplementary Figure 2.21 Fast SEC of Blends of Asphaltenes/Maltenes of AAA-1, Scanned at 340 nm



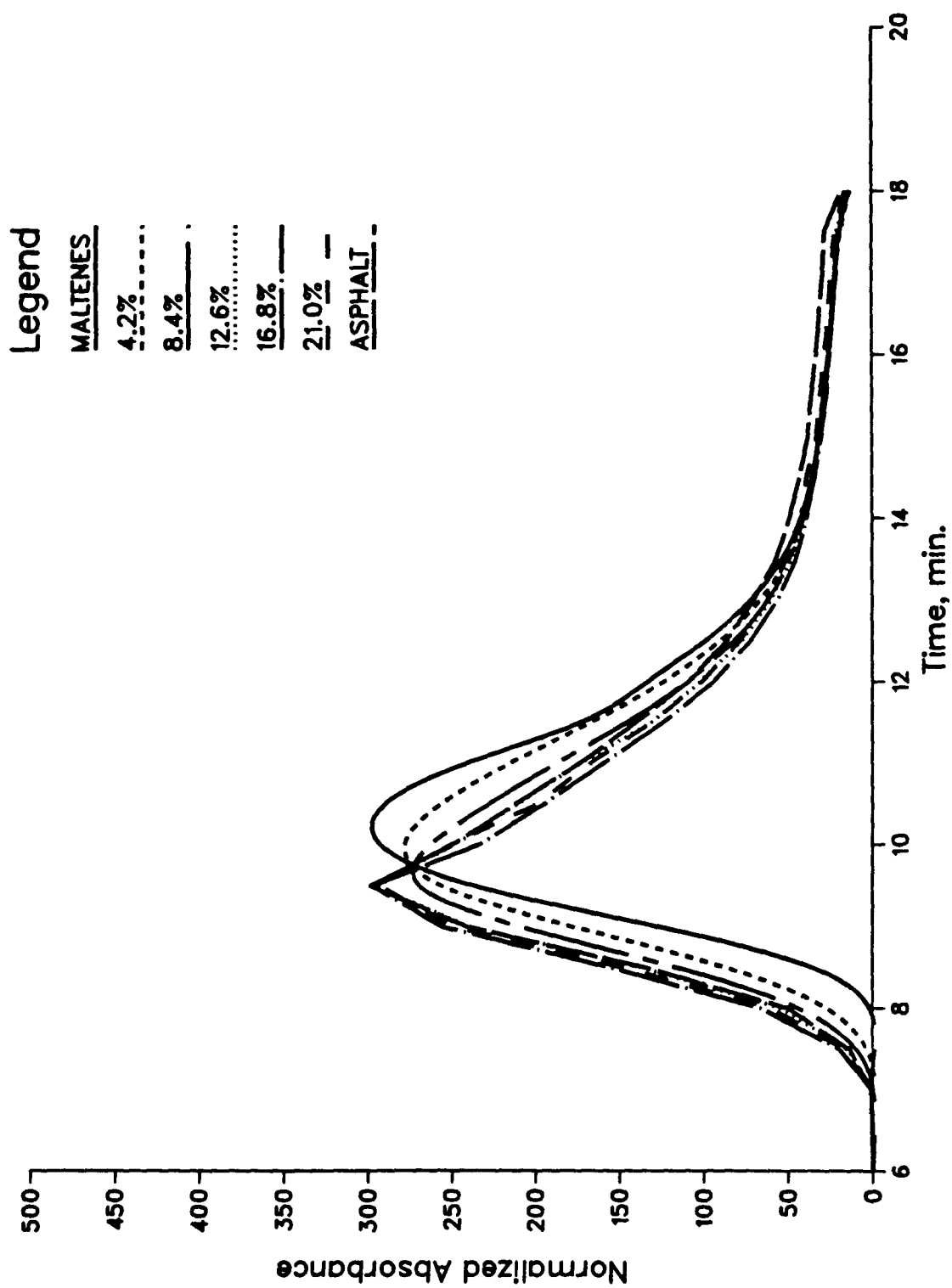
Supplementary Figure 2.22 Fast SEC of Blends of Asphaltenes/Maltenes of AAA-1, Scanned at 380 nm



Supplementary Figure 2.23 Fast SEC of Blends of Asphaltenes/Maltenes of AAA-1, Scanned at 420 nm

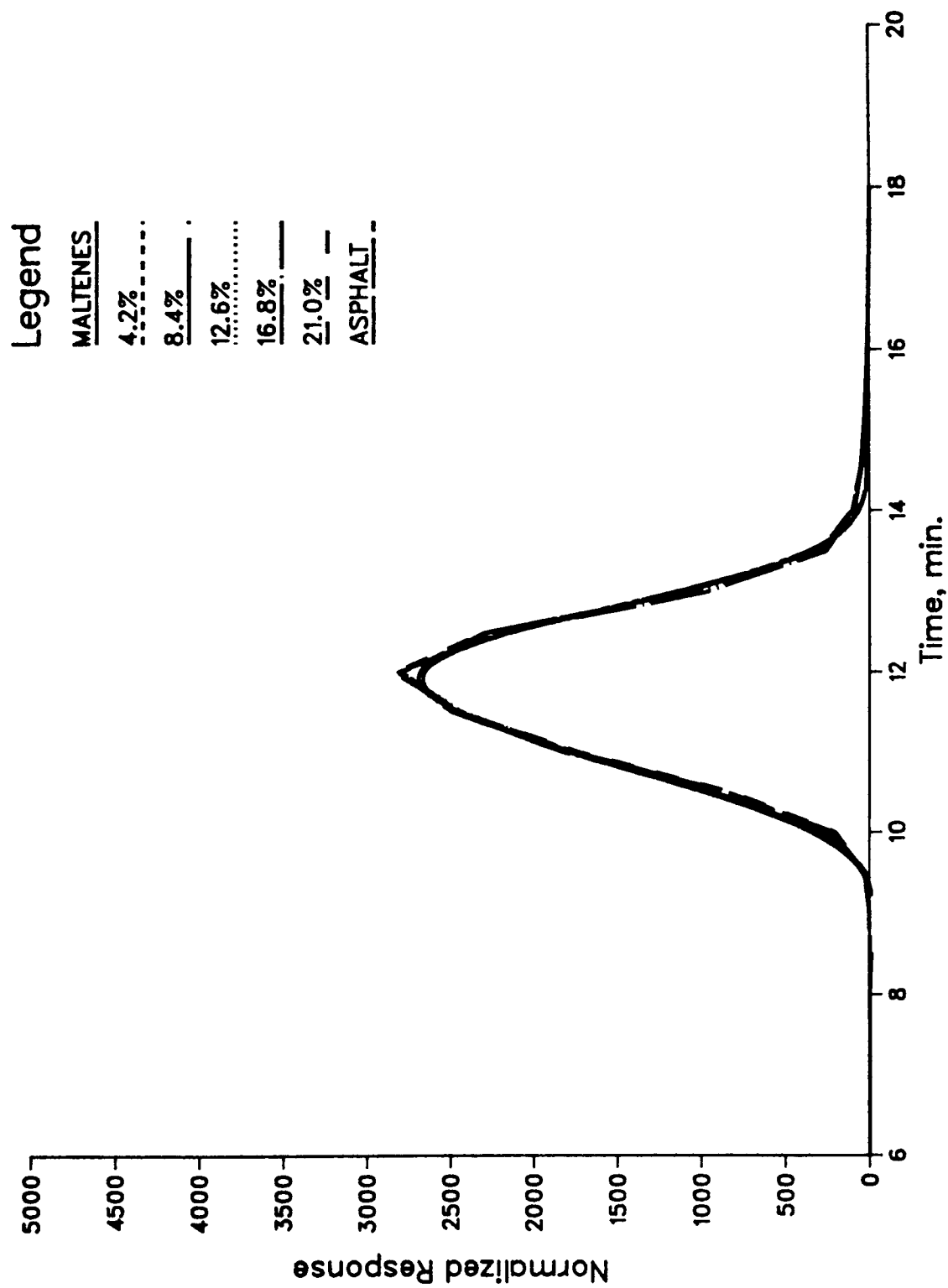


Supplementary Figure 2.24 Fast SEC of Blends of Asphaltenes/Maltenes of AAA-1, Scanned at 500 nm

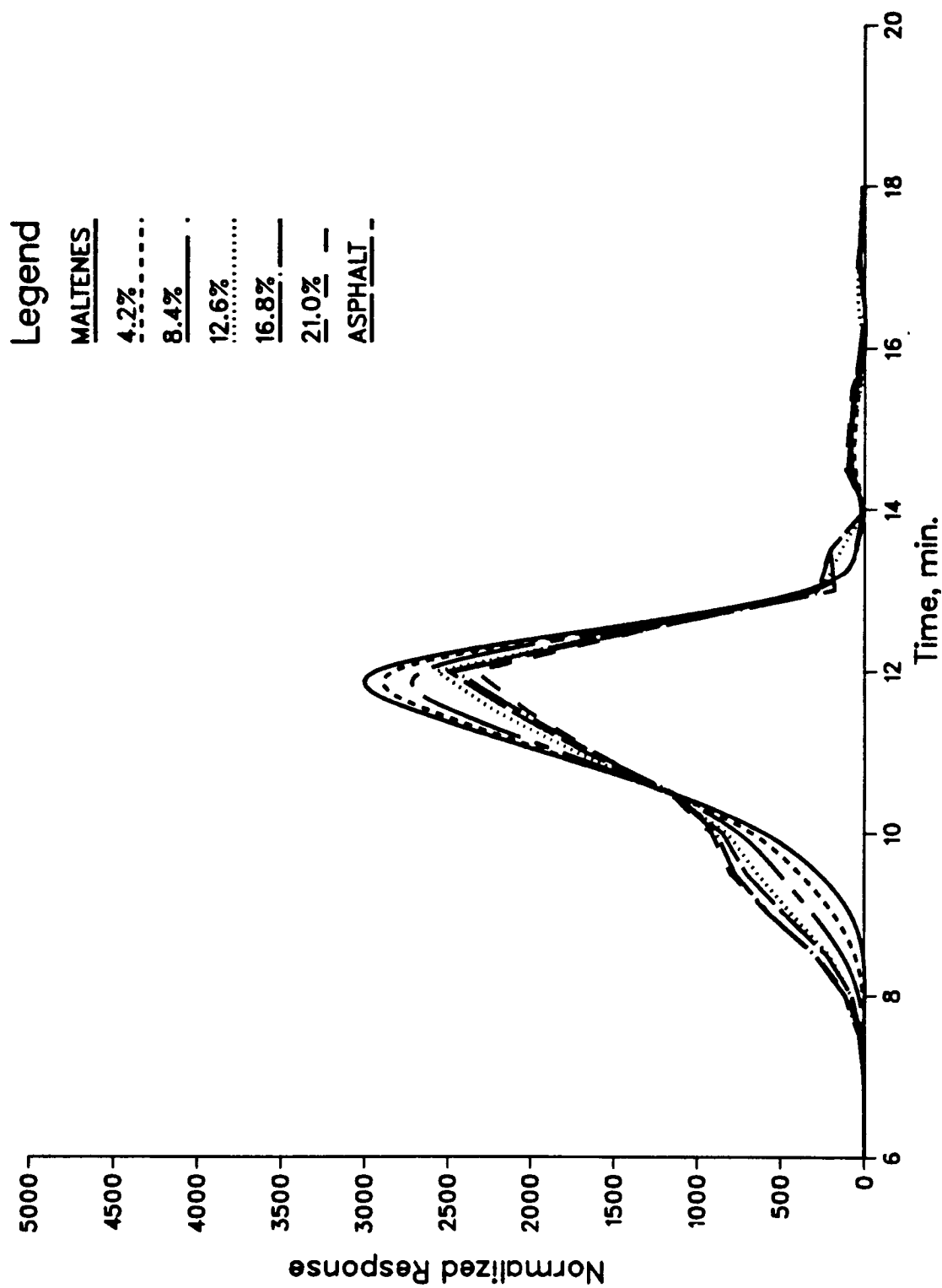


Supplementary Figure 2.25 Fast SEC of Blends of Asphaltenes/Maltenes of AAA-1, Scanned at 575 nm

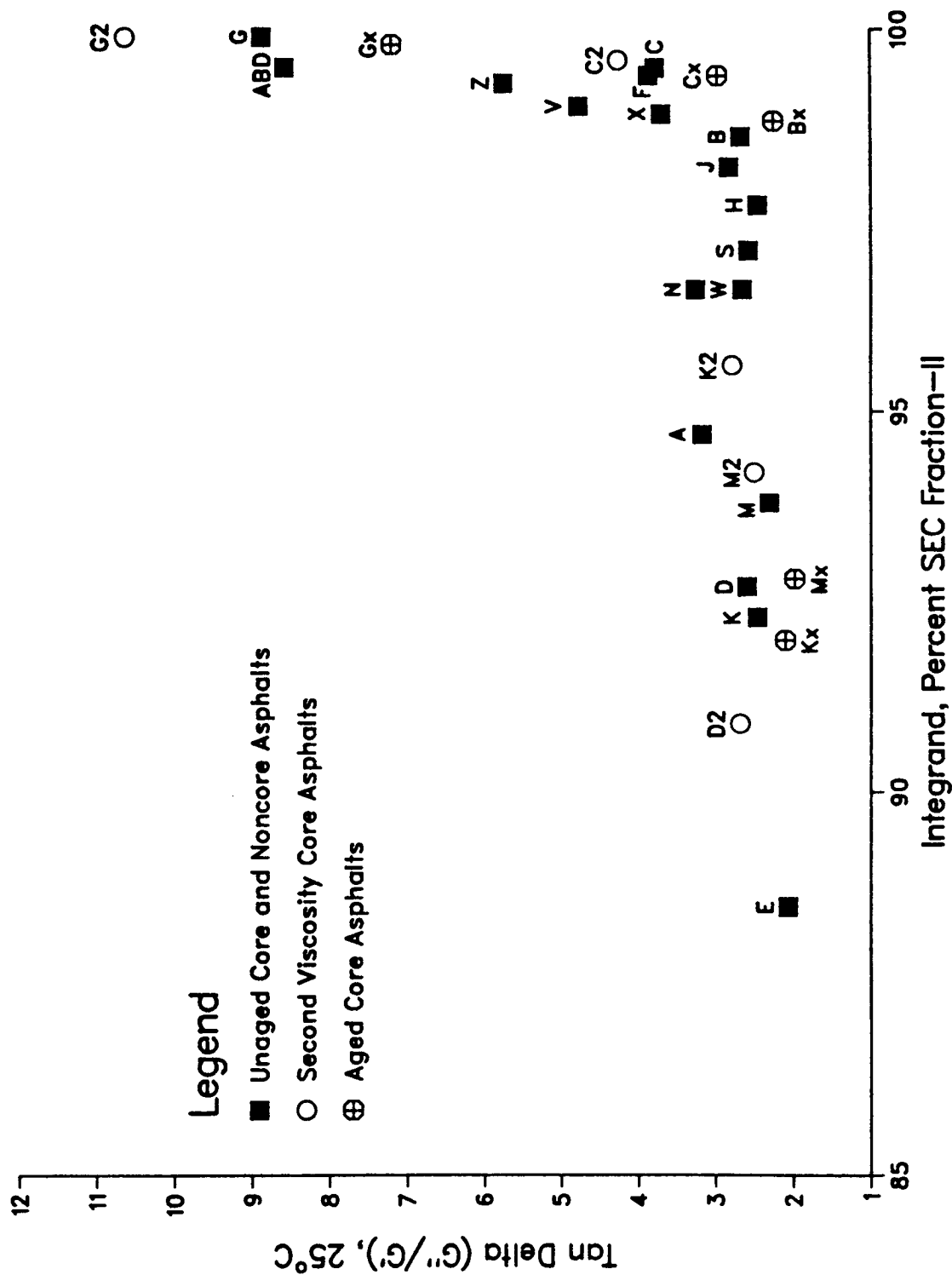




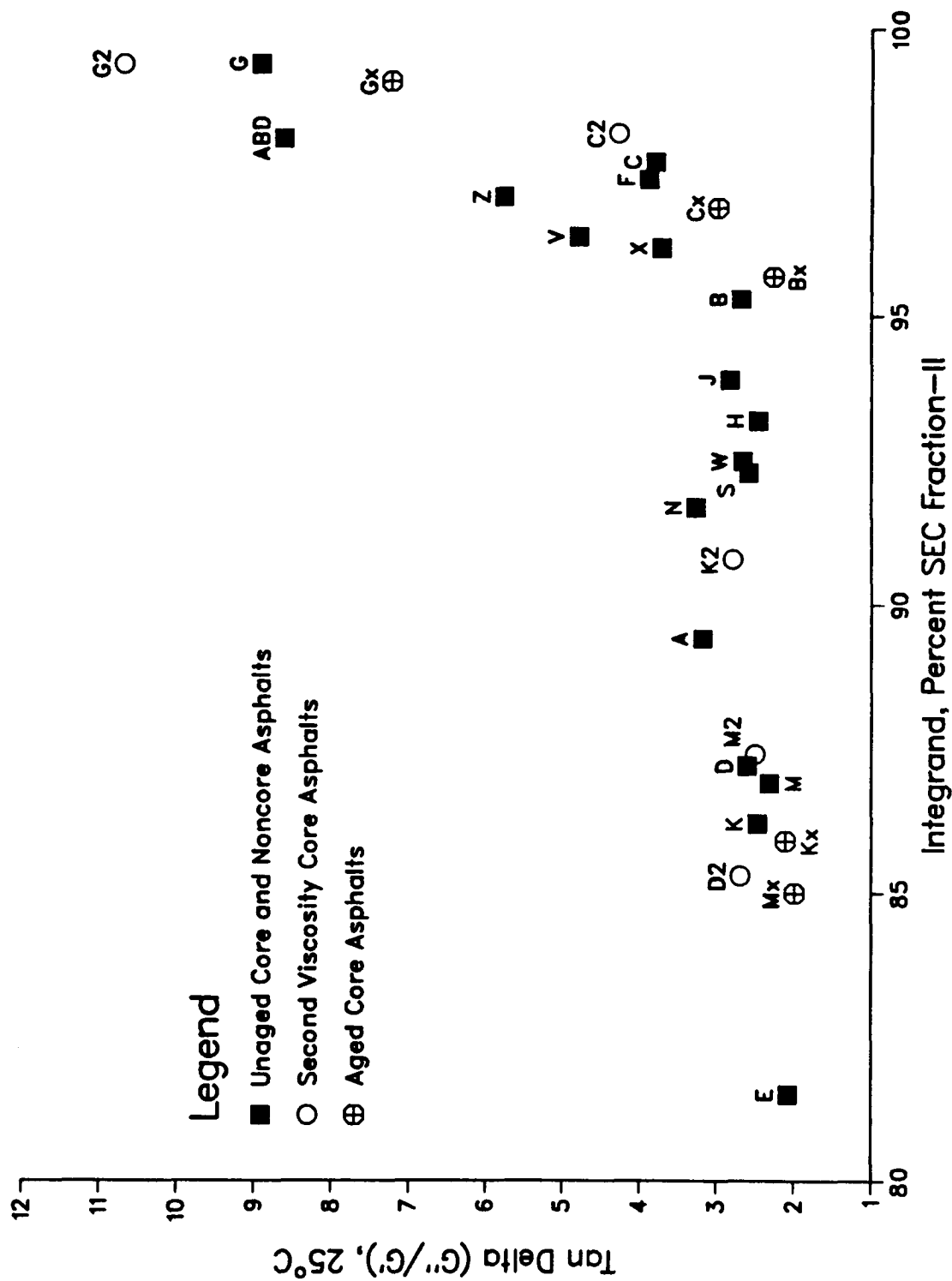
Supplementary Figure 2.26 Fast SEC of Blends of Asphaltenes/Maltenes of AAA-1, Fluorescence Detector



Supplementary Figure 2.27 Fast SEC of Blends of Asphaltenes/Maltenes of AAA-1, DRID

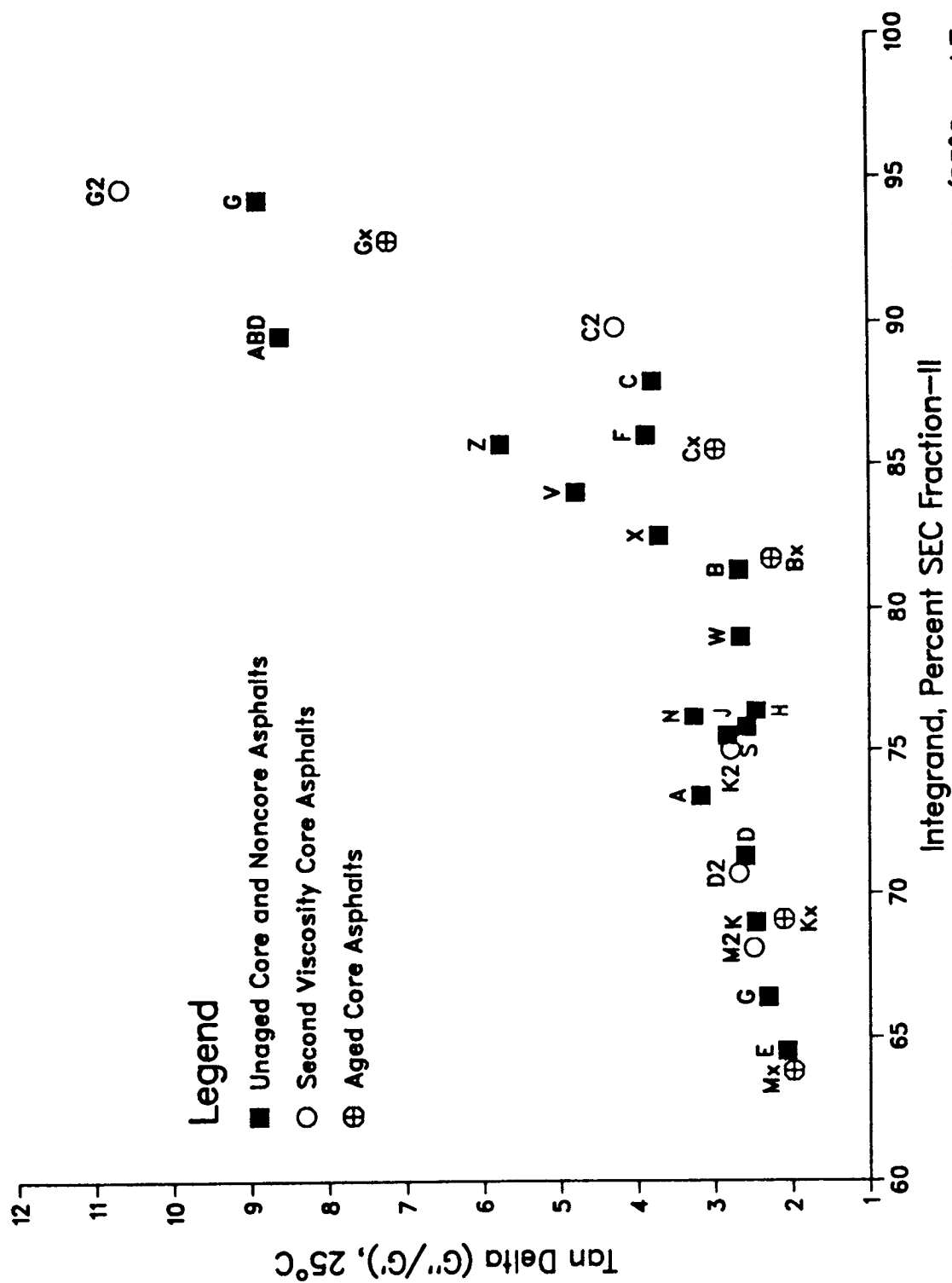


Supplementary Figure 2.28 Relationship Between SEC Fraction—II and Tan Delta (25°C and Torque at 400 g-cm) for the Refractive Index Detector at 9 min into the Run

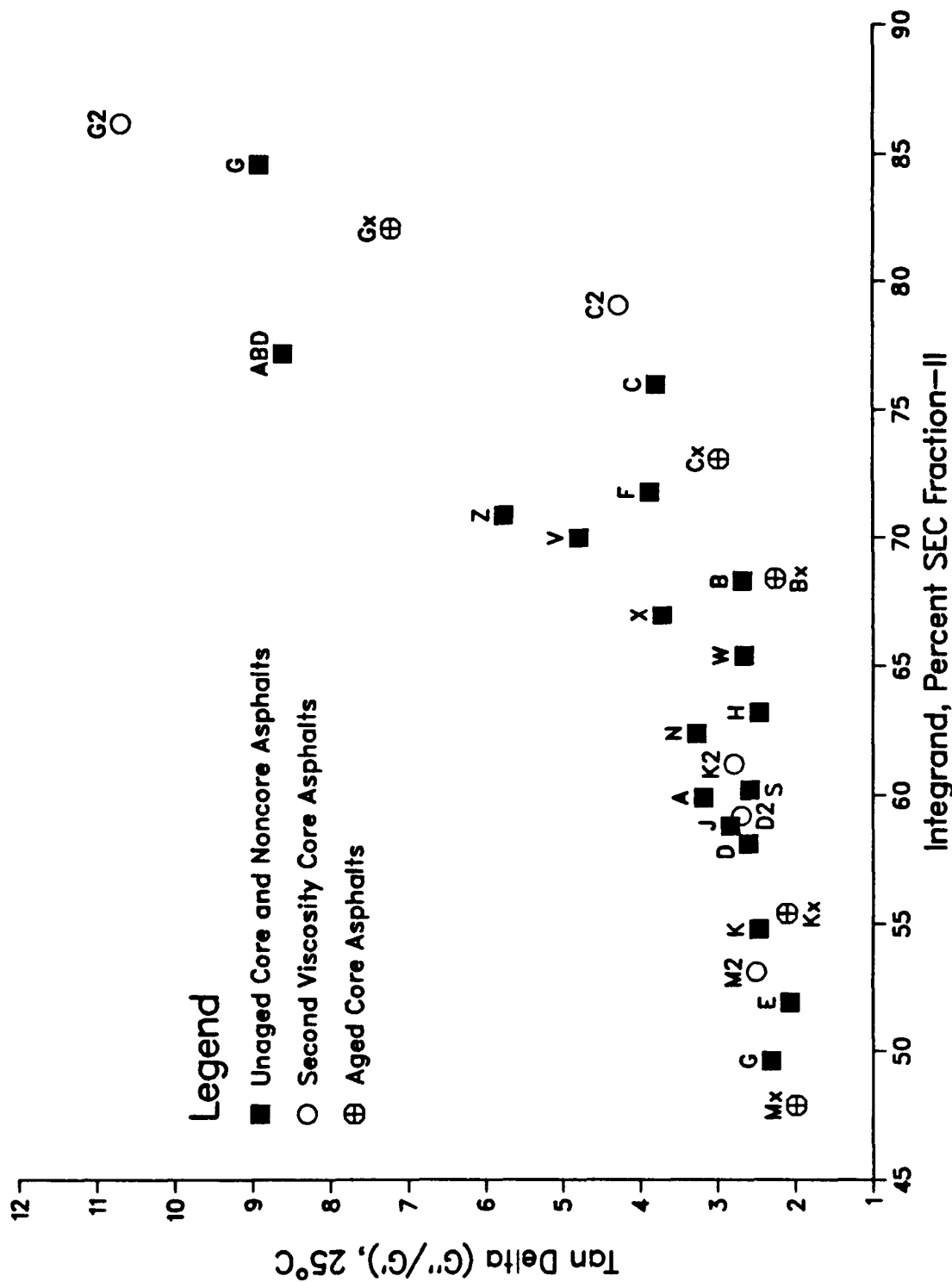


Integrant, Percent SEC Fraction-II

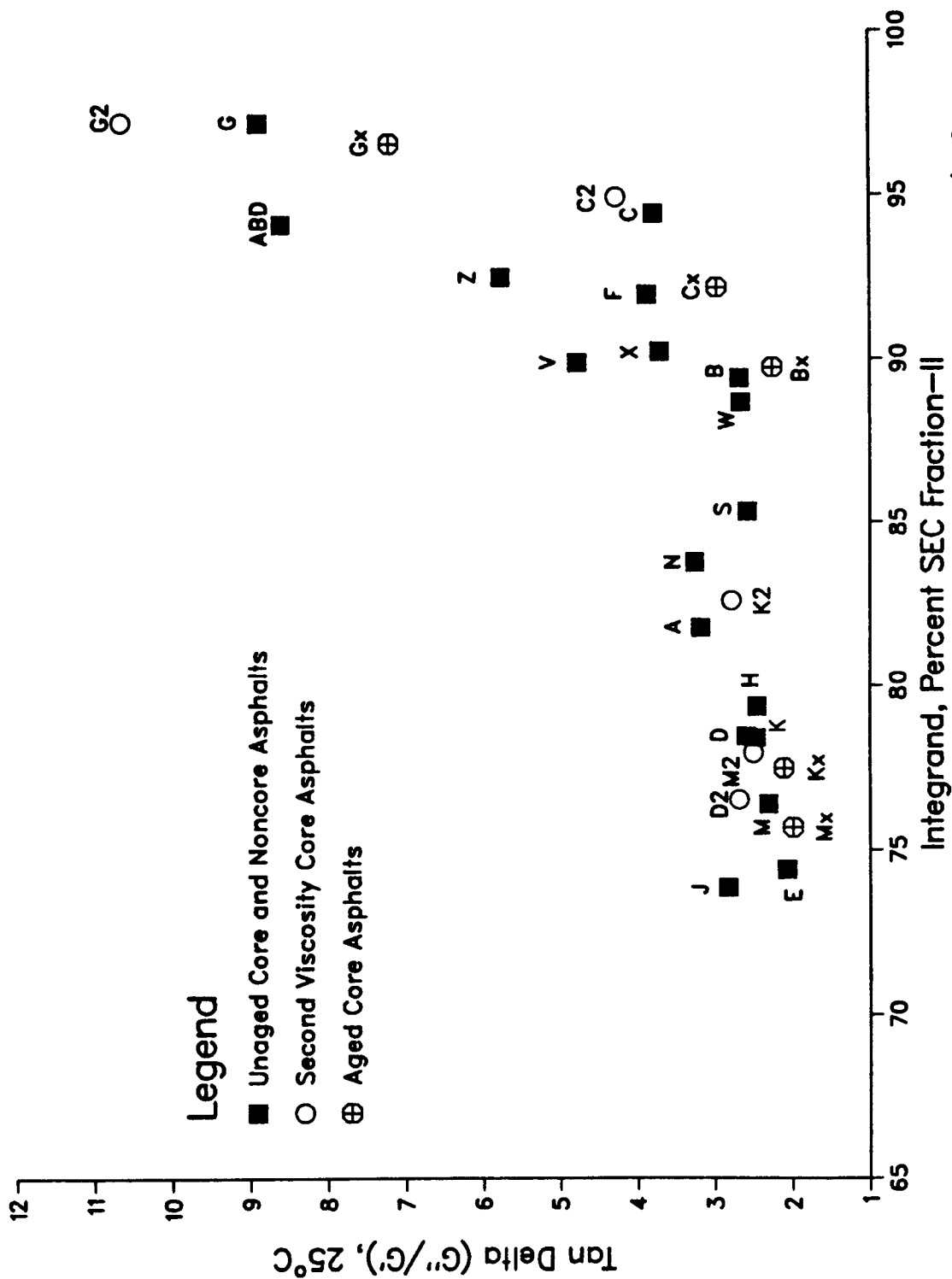
Supplementary Figure 2.29 Relationship Between SEC Fraction-II and Tan Delta (25°C and Torque at 400 g-cm) for Refractive Index Detector at 9.5 min into Run



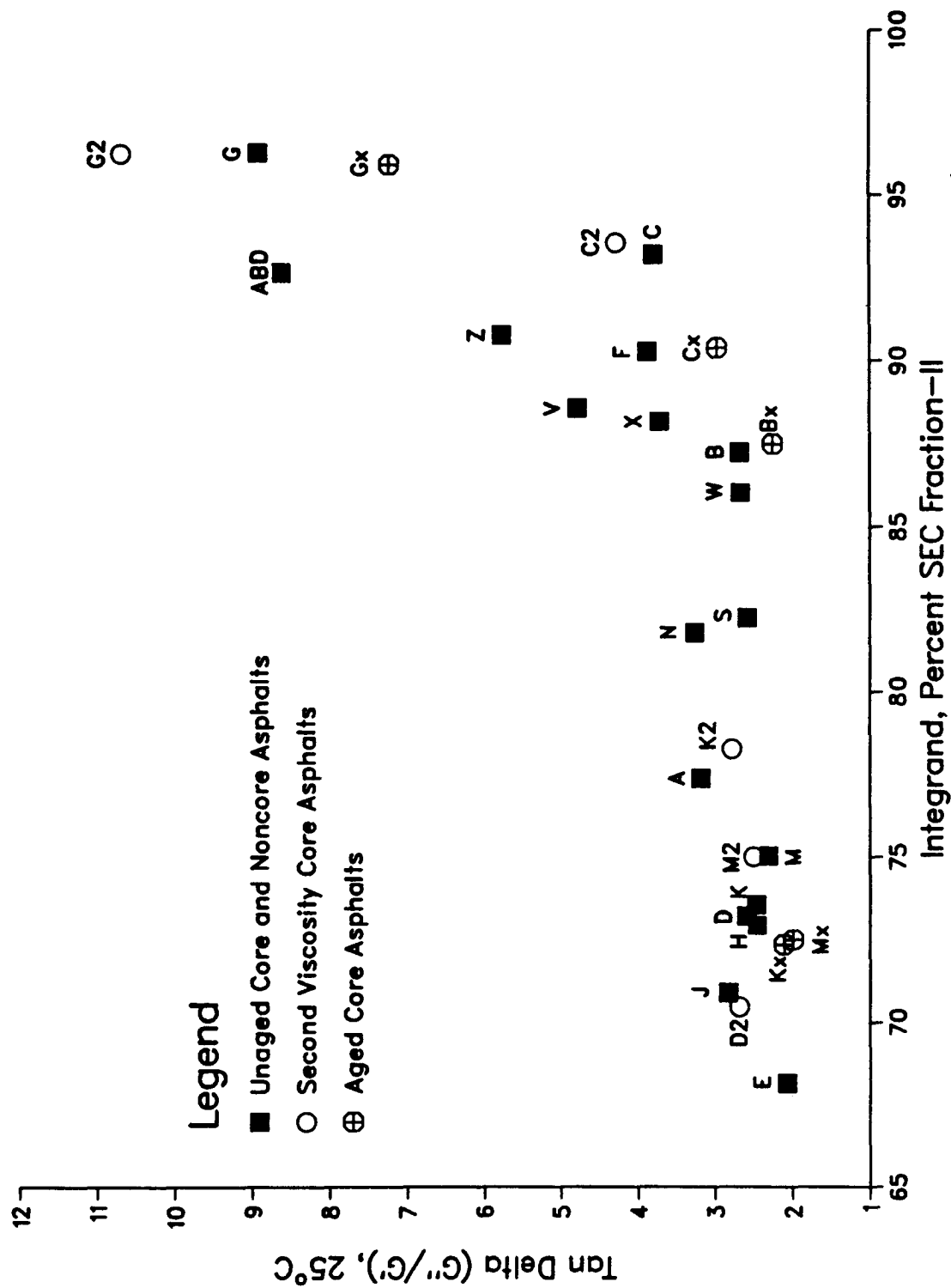
Supplementary Figure 2.30 Relationship Between SEC Fraction II and Tan Delta (25°C and Torque at 400 g-cm for the Refractive Index Detector at 10.5 min into Run)



Supplementary Figure 2.31 Relationship Between SEC Fraction-II and Tan Delta (25°C and Torque at 400 g-cm for the Refractive Index Detector at 11 min into Run)

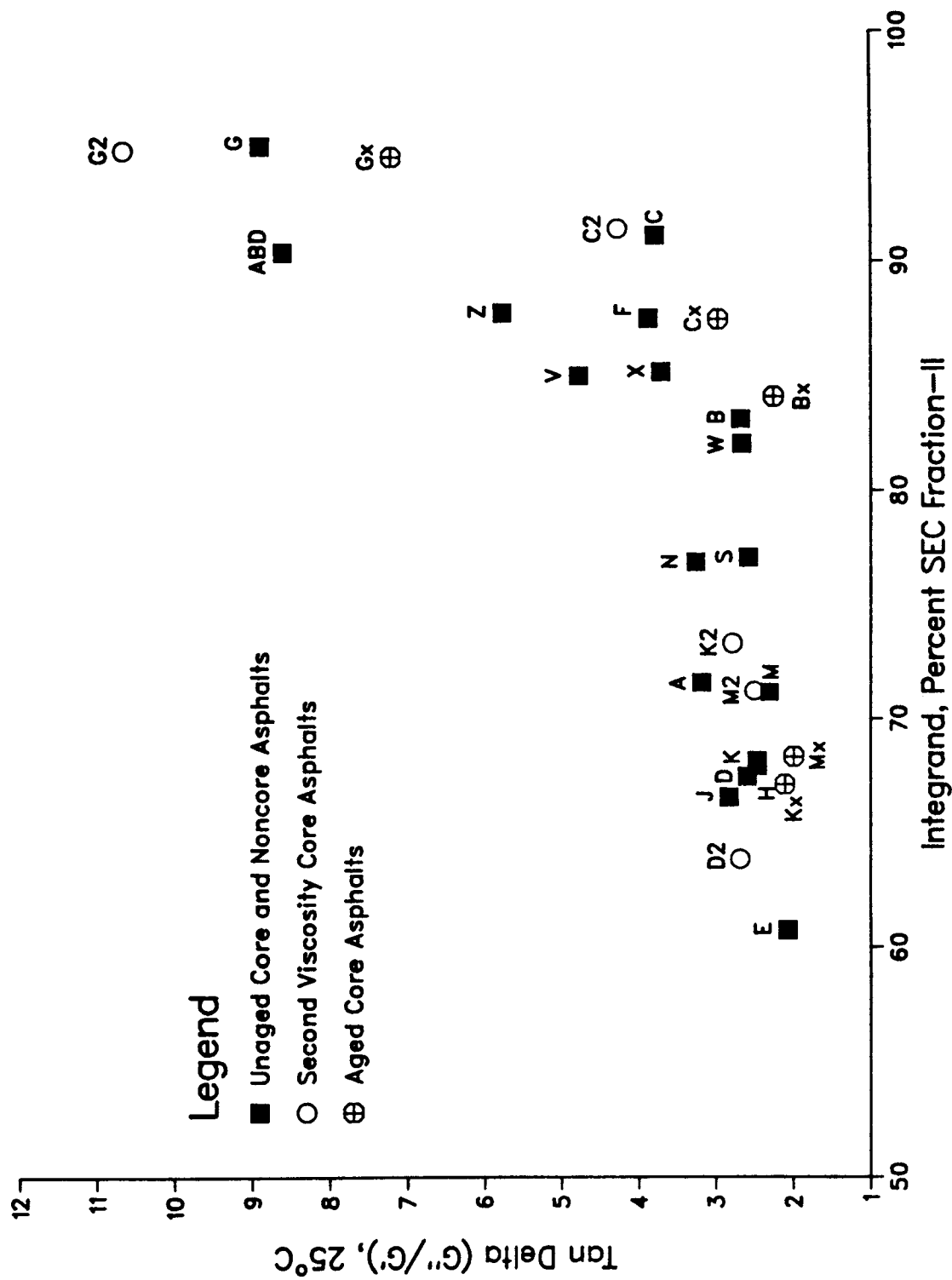


Supplementary Figure 2.32 Relationship Between SEC Fraction-II and Tan Delta (25°C and Torque at 400 g-cm) at 305 nm and 10 min into Run

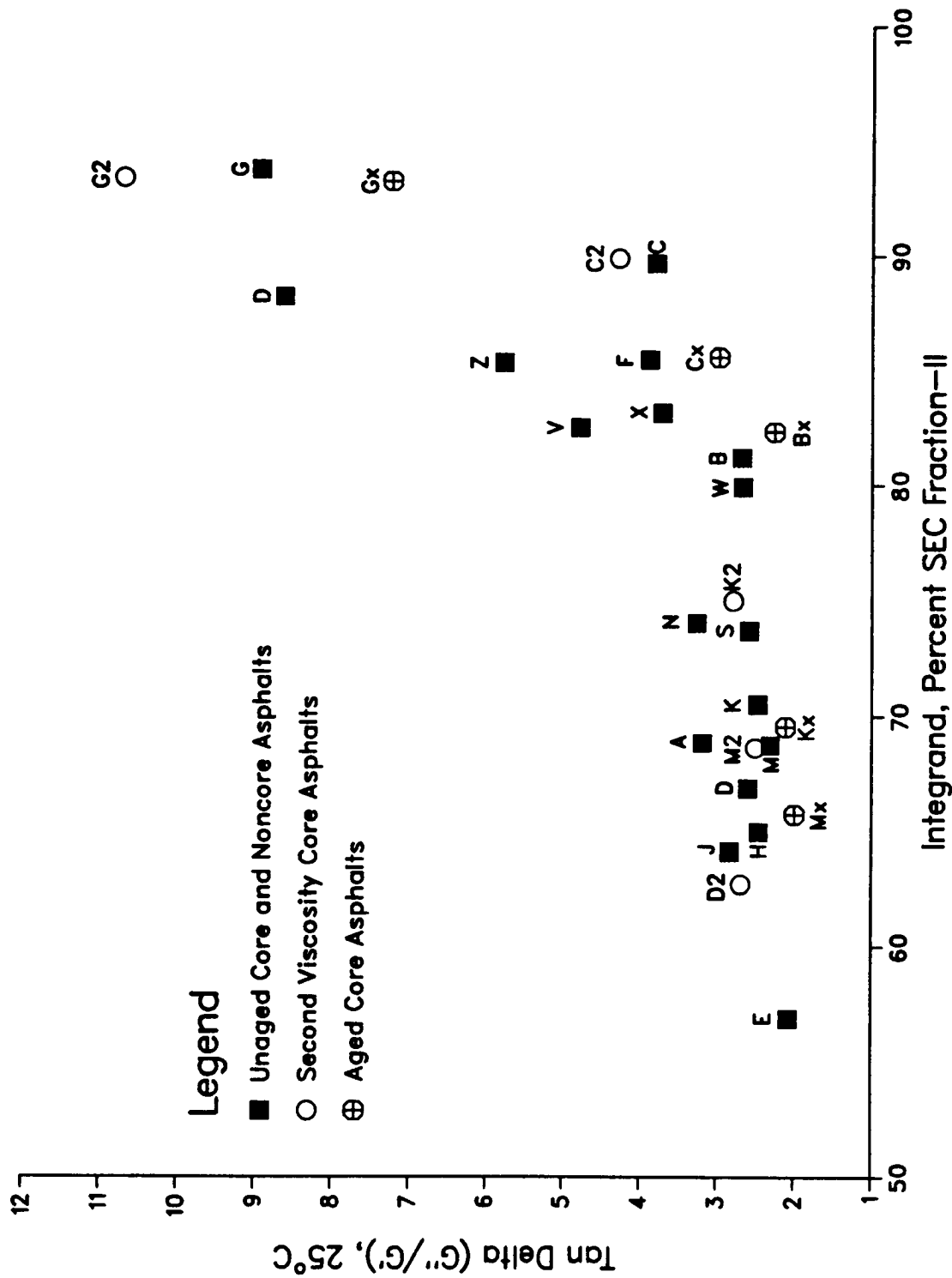


Supplementary Figure 2.33 Relationship Between SEC Fraction-II and Tan Delta (25°C and Torque at 400 g-cm) at 340 nm and 10 min into Run



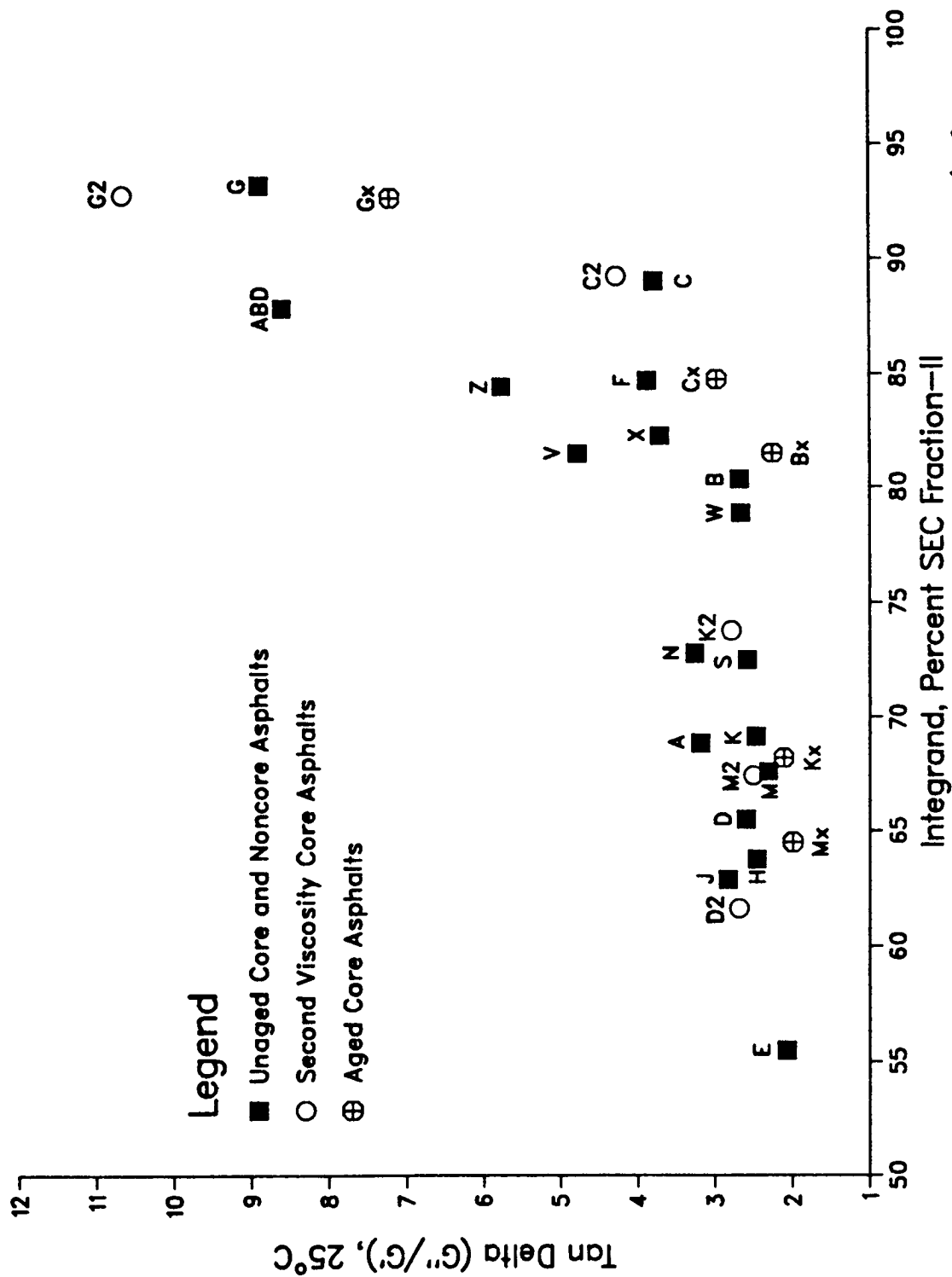


Supplementary Figure 2.34 Relationship Between SEC Fraction-II and Tan Delta (25°C and Torque at 400 g-cm) at 380 nm and 10 min into Run

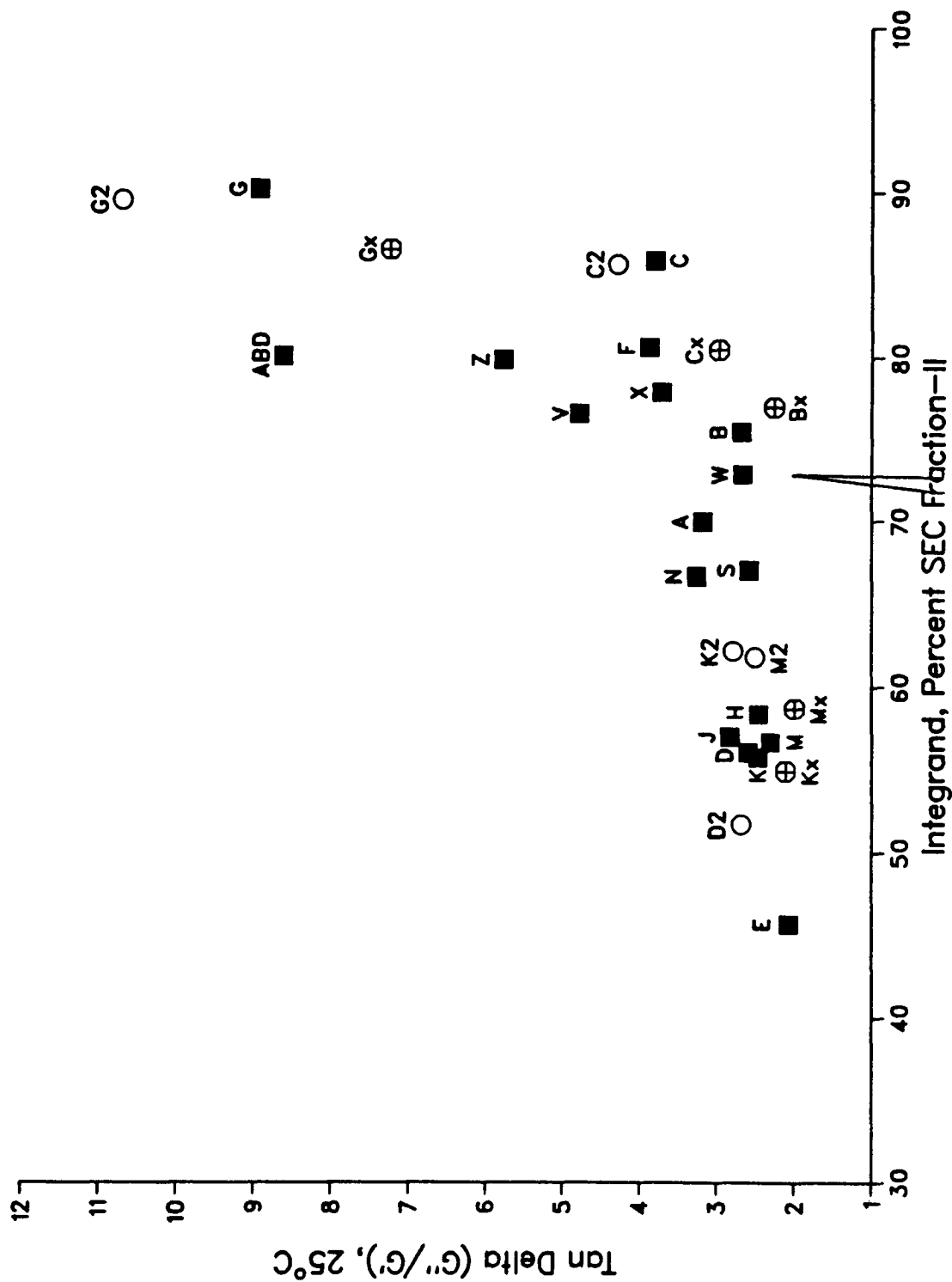


Integrant, Percent SEC Fraction-II

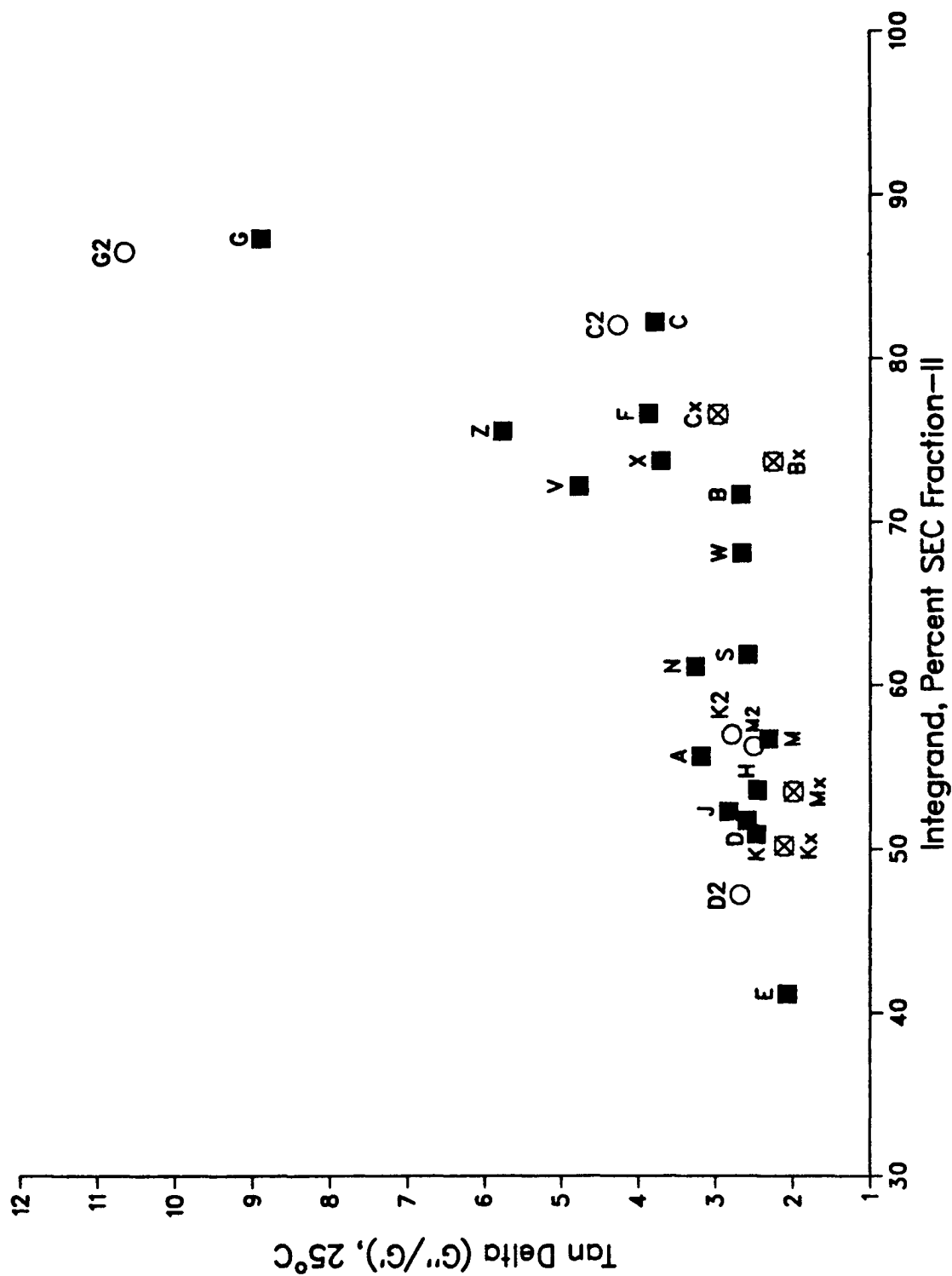
Supplementary Figure 2.35 Relationship Between SEC Fraction-II and Tan Delta (25°C and Torque at 400 g-cm) at 410 nm and 10 min into Run



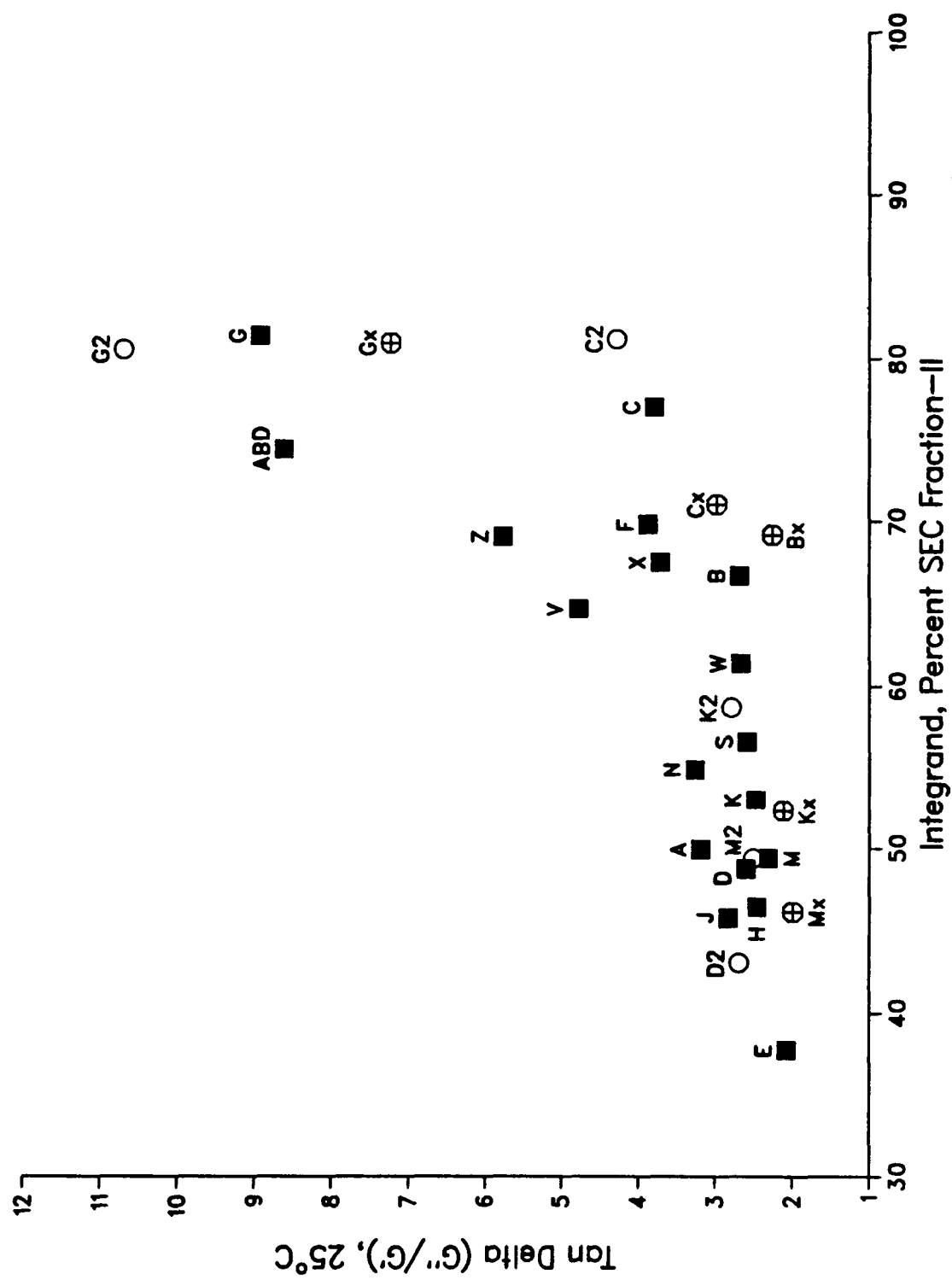
Supplementary Figure 2.36 Relationship Between SEC Fraction-II and Tan Delta (25°C and Torque at 400 g-cm) at 420 nm and 10 min into Run



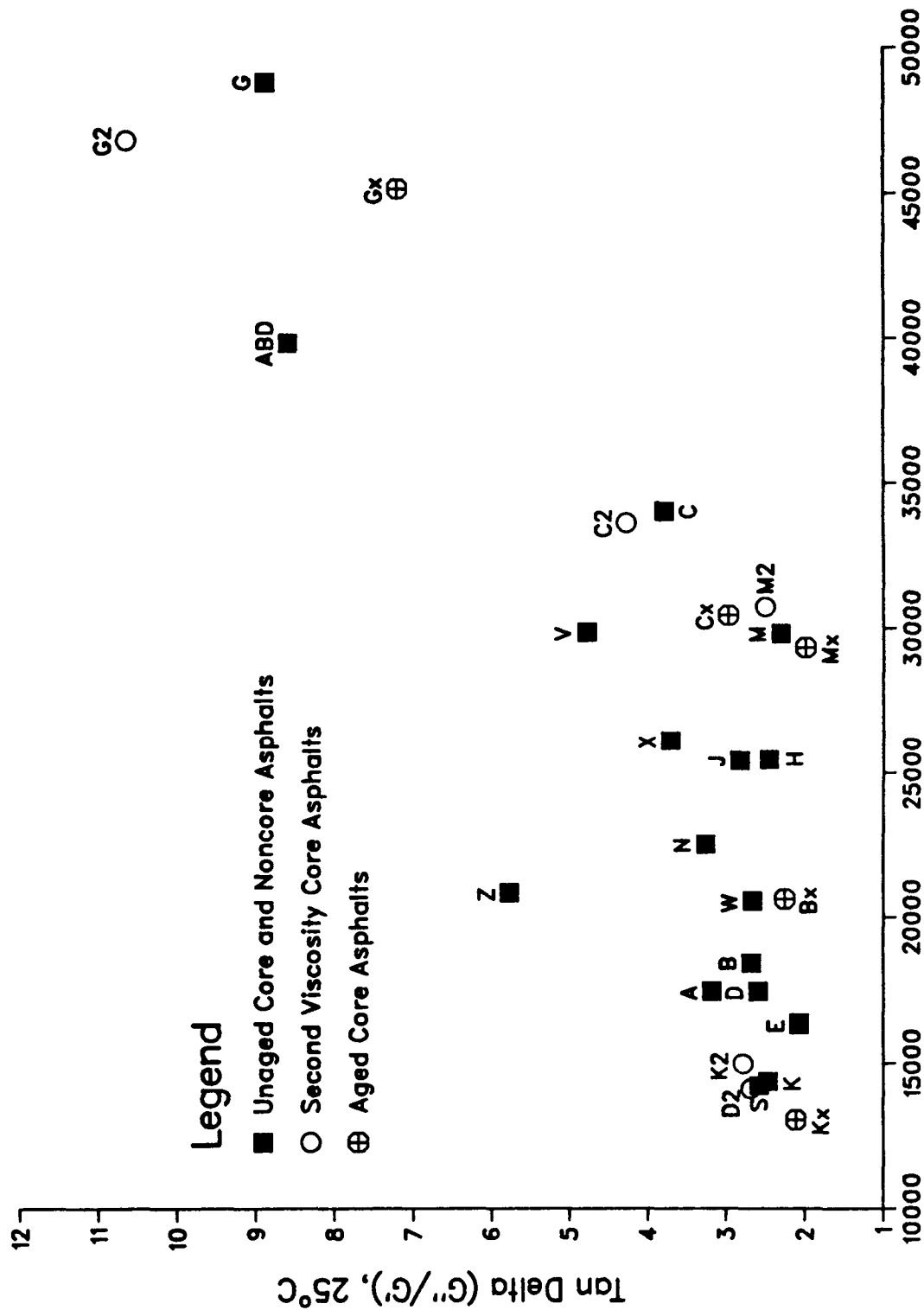
Supplementary Figure 2.37 Relationship Between SEC Fraction-II and Tan Delta (25°C and Torque at 400 g-cm) at 460 nm and 10 min into Run



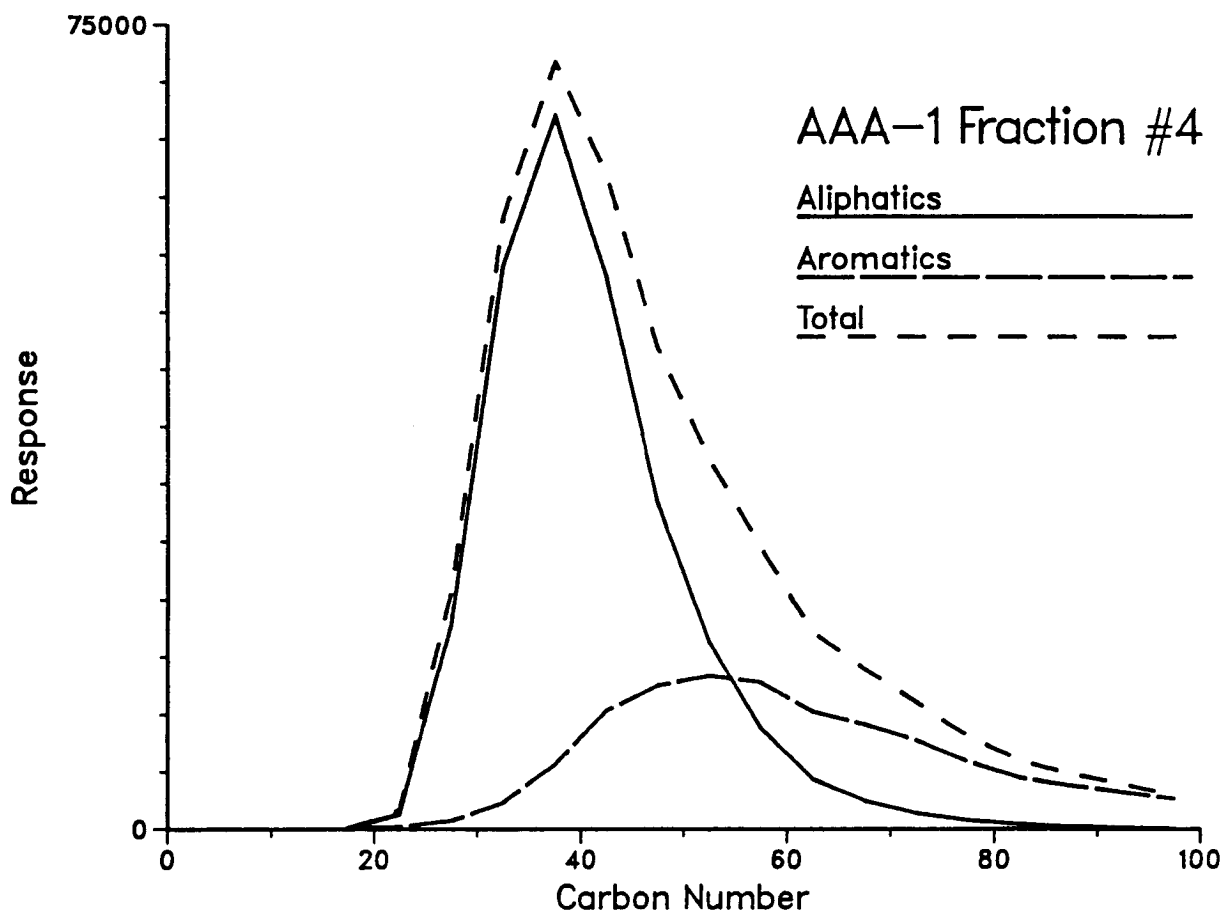
Supplementary Figure 2.38 Relationship Between SEC Fraction-II and Tan Delta (25°C and Torque at 400 g-cm) at 500 nm and 10 min into Run



Supplementary Figure 2.39 Relationship Between SEC Fraction-II and Tan Delta (25°C and Torque at 400 g-cm) at 575 nm and 10 min into Run

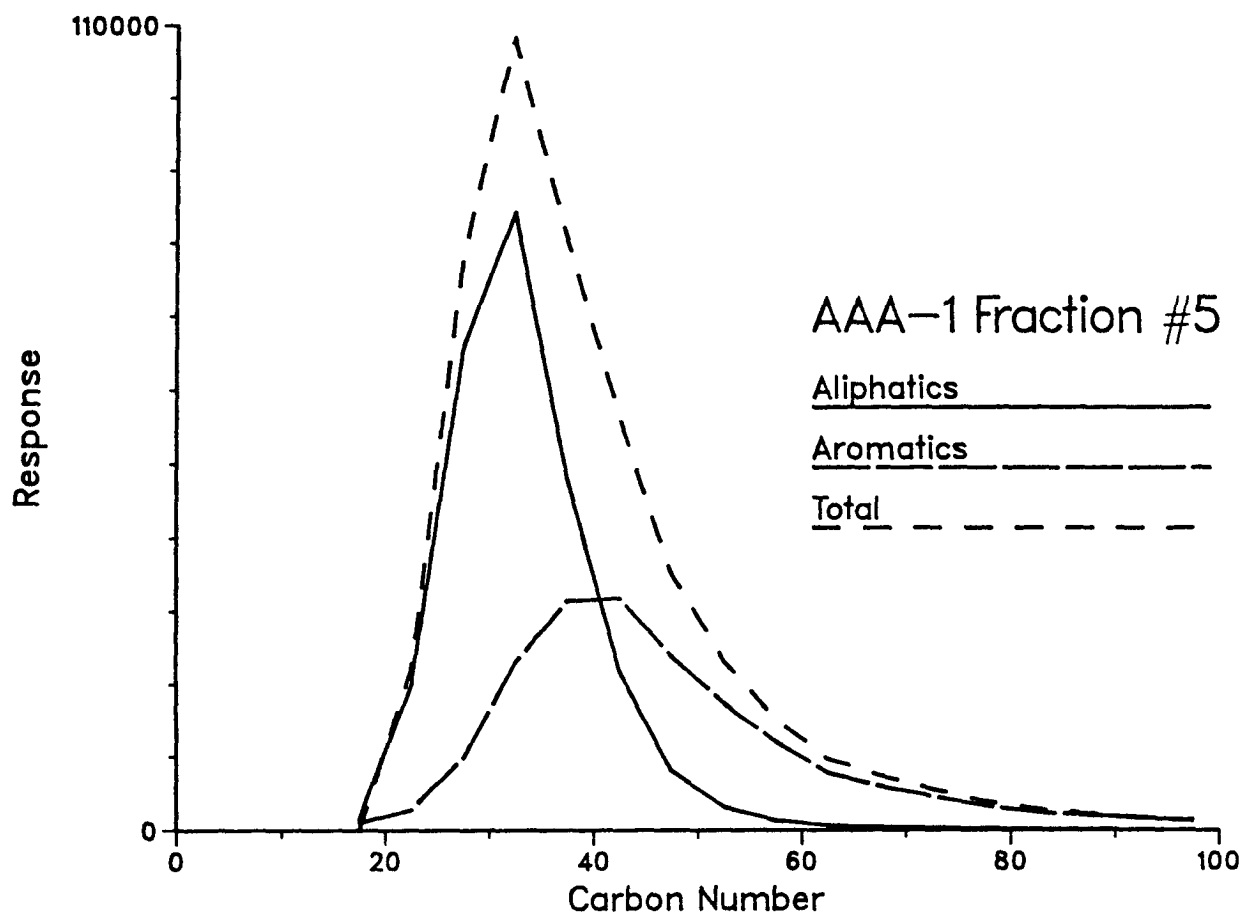


Integrand of SEC Fraction—II by Fluorescence Detector  
 Supplementary Figure 2.40 Relationship Between Total Response of the Fluorescence Detector at 10 min into Run and Tan Delta (25°C and Torque at 400 g-cm)



**Supplementary Figure 2.41** SFC Chromatograms of Aliphatic and Aromatic Components of AAA-1 Size Exclusion Chromatography Fraction Number 4





**Supplementary Figure 2.42** SFC Chromatograms of Aliphatic and Aromatic Components of AAA-1 Size Exclusion Chromatography Fraction Number 5

Supplementary Table 2.13 Quantitative IR Analyses of SEC Fractions of AAD-1

Fraction Number	Functional Group (mol/L)							
	Sulfoxides	Ketones	Carboxylic Acids		Carboxylic Acids		Hydrolyzable Carbonyls <sup>1</sup>	2-Quinolones
			Free	Salts	Anhydrides	Acids		
1	0.07	0	0.009	0	0	0	0	0.041
2	0.05	0.04	0.007	0	0	0	0	0.035
3	0.10	0.08	0.014	0	0	0	0	0.025
4	<0.01	0.05	0.022	0	0	0	0	0.017
5	<0.01	0.04	0.014	0	0	0	0	0.011
6	0.10	0.06	0.005	0	0	0	0	0.013
								0.0160
								0.065
								0.105
								0.089
								0.076
								0.351
								0.261
								0.392
								0.194
								0.016
								0.051
								0.089
								0.076
								0.351
								0.261
								0.392
								0.194
								0.016
								0.051
								0.089
								0.076
								0.351
								0.261
								0.392
								0.194
								0.016
								0.051
								0.089
								0.076
								0.351
								0.261
								0.392
								0.194
								0.016
								0.051
								0.089
								0.076
								0.351
								0.261
								0.392
								0.194
								0.016
								0.051
								0.089
								0.076
								0.351
								0.261
								0.392
								0.194
								0.016
								0.051
								0.089
								0.076
								0.351
								0.261
								0.392
								0.194
								0.016
								0.051
								0.089
								0.076
								0.351
								0.261
								0.392
								0.194
								0.016
								0.051
								0.089
								0.076
								0.351
								0.261
								0.392
								0.194
								0.016
								0.051
								0.089
								0.076
								0.351
								0.261
								0.392
								0.194
								0.016
								0.051
								0.089
								0.076
								0.351
								0.261
								0.392
								0.194
								0.016
								0.051
								0.089
								0.076
								0.351
								0.261
								0.392
								0.194
								0.016
								0.051
								0.089
								0.076
								0.351
								0.261
								0.392
								0.194
								0.016
								0.051
								0.089
								0.076
								0.351
								0.261
								0.392
								0.194
								0.016
								0.051
								0.089
								0.076
								0.351
								0.261
								0.392
								0.194
								0.016
								0.051
								0.089
								0.076
								0.351
								0.261
								0.392
								0.194
								0.016
								0.051
								0.089
								0.076
								0.351
								0.261
								0.392
								0.194
								0.016
								0.051
								0.089
								0.076
								0.351
								0.261
								0.392
								0.194
								0.016
								0.051
								0.089
								0.076
								0.351
								0.261
								0.392
								0.194
								0.016
								0.051
								0.089
								0.076
								0.351
								0.261
								0.392
								0.194
								0.016
								0.051
								0.089
								0.076
								0.351
								0.261
								0.392
								0.194
								0.016
								0.051
								0.089
								0.076
								0.351
								0.261
								0.392
								0.194
								0.016
								0.051
								0.089
								0.076
								0.351
								0.261
								0.392
								0.194
								0.016
								0.051
								0.089
								0.076
								0.351
								0.261
								0.392
								0.194
								0.016
								0.051
								0.089
								0.076
								0.351
								0.261
								0.392
								0.194
								0.016
								0.051
								0.089
								0.076
								0.351
								0.261
								0.392
								0.194
								0.016
								0.051
								0.089
								0.076
								0.351
								0.261
								0.392
								0.194
								0.016
								0.051
								0.089
								0.076
								0.351
								0.261
								0.392
								0.194
								0.016
								0.051
								0.089
								0.076
								0.351
								0.261
								0.392
								0.194
								0.016
								0.051
								0.089
								0.076
								0.351
								0.261
								0.392

<sup>1</sup> Reported as esters

**Supplementary Table 2.15 Carbon Number Distribution for AAG-1 Saturate/  
Aromatic Fractions**

Sample	Mass Fraction	Carbon		
		Initial	Mid	Final
SEC-3 Saturates	52	22	62	100
SEC-3 Aromatics	42	42	80	>100
SEC-4 Saturates	51	17	47	80
SEC-4 Aromatics	44	22	62	>100
SEC-5 Saturates	39	17	37	60
SEC-5 Aromatics	57	20	50	95

**Supplementary Table 2.16 Carbon Number Distributions of Saturate Fractions  
Compared with Aromatic Fractions by SFC, Asphalt  
AAA-1**

Sample	Mass Fraction	Carbon		
		Initial	Mid	Final
SEC Fraction 4, Saturates	53	17	39	80
SEC Fraction 4, Aromatics	40	22	58	>100
SEC Fraction 5, Saturates	49	17	33	60
SEC Fraction 5, Aromatics	45	20	43	95

**Supplementary Table 3.3 Rheological Data of Mixtures of Model Compounds (1 mass % ) with AAA-1 at 25 °C<sup>1</sup>**

Model Compound	Rad/s	Viscosity (Pa · s)	G' , dynes/cm <sup>2</sup>	G'' , dynes/cm <sup>2</sup>	Tan δ
None	1.0	27,540	57,310	269,300	4.7
	10.0	19,170	544,000	1,838,000	3.4
	100.0	11,670	4,163,000	10,900,000	2.6
Dodecane	1.0	16,690	33,070	163,600	4.9
	10.0	11,540	324,000	1,107,000	3.4
	100.0	7,064	2,461,000	6,620,000	2.7
Lauric acid	1.0	26,400	54,640	258,300	4.7
	10.0	18,240	517,300	1,748,000	3.4
	100.0	11,110	3,955,000	10,380,000	2.6
1-Dodecanol	1.0	15,020	25,260	148,100	5.9
	10.0	11,050	267,900	1,072,000	4.0
	100.0	7,258	2,268,000	6,893,000	3.0
12-Amino-Lauric Acid	1.0	32,550	69,160	318,100	4.6
	10.0	22,520	647,000	2,157,000	3.3
	100.0	13,580	4,875,000	12,680,000	2.6
Dodecanedioic Acid	1.0	34,900	78,470	340,000	4.3
	10.0	23,430	703,800	2,234,000	3.2
	100.0	13,690	5,107,000	12,690,000	2.5
1,12 Diamino-Dodecane	1.0	24,000	47,780	235,200	4.9
	10.0	16,840	461,800	1,619,000	3.5
	100.0	10,520	3,654,000	9,867,000	2.7
5-Phenyl-Valeric acid	1.0	15,780	27,890	155,300	5.6
	10.0	11,620	292,400	1,124,000	3.8
	100.0	7,468	2,401,000	7,069,000	2.9
Tetrastearoyl-Pentaerythritol	1.0	21,870	42,240	214,500	5.1
	10.0	15,560	419,200	1,498,000	3.6
	100.0	9,600	3,237,000	9,034,000	2.8

<sup>1</sup> 3% Strain, 25 mm PP

**Supplementary Table 3.4 Rheological Data of Mixtures of Model Compounds (1 mass %) with AAA-1 at 60 °C<sup>1</sup>**

Model Compound	Rad/s	Viscosity (Pa·s)	G', dynes/cm <sup>2</sup>	G'', dynes/cm <sup>2</sup>	Tan $\delta$
None	1.0	124	0	1,240	$\infty$
	10.0	118	769	11,740	15.3
	100.0	98	11,560	97,580	8.4
Dodecane	1.0	75	25	746	29
	10.0	73	304	7,333	24
	100.0	64	6,517	64,110	9.8
Lauric Acid	1.0	83	15	826	54
	10.0	81	3220	8,058	25
	100.0	72	7,069	71,440	10
1-dodecanol	1.0	72	0	719	$\infty$
	10.0	72	290	7,202	25
	100.0	63	5,948	63,000	10
12-Amino-Lauric Acid	1.0	119	12	1,194	97
	10.0	113	545	11,300	21
	100.0	97	10,690	96,220	9
Dodecanedioic Acid	1.0	149	21	1,488	72
	10.0	134	863	13,050	15
	100.0	105	12,470	104,400	8
1,12 Diamino-Dodecane	1.0	95	29	950	3
	10.0	91	356	9,086	25
	100.0	79	8,115	78,650	9.7
Tetrastearoyl-Pentaerythritol	1.0	89	36	892	2.5
	10.0	88	360	892	2.5
	100.0	74	7,977	73,390	9.2

<sup>1</sup> 50% Strain, 25 mm PP

**Supplementary Table 3.5 Rheological Data of Mixtures of Model Compounds (1 mass %) with AAB-1 at 25 °C<sup>1</sup>**

Model Compound	Rad/s	Viscosity (Pa · s)	G', dynes/cm <sup>2</sup>	G'', dynes/cm <sup>2</sup>	Tan δ
None	1.0	112,500	346,500	1,070,000	3.1
	10.0	63,850	2,544,000	5,856,000	2.3
Dodecane	1.0	52,780	138,400	509,300	3.7
	10.0	32,800	1,169,000	3,064,000	2.6
	100.0	16,780	7,480,000	15,010,000	2.0
Lauric acid	1.0	56,860	142,600	550,400	3.9
	10.0	35,570	1,210,000	3,344,000	2.8
	100.0	18,500	7,952,000	16,700,000	2.1
1-Dodecanol	1.0	61,860	166,100	595,800	3.6
	10.0	37,850	1,358,000	3,532,000	2.6
12-Amino-Lauric Acid	1.0	105,000	319,300	1,000,000	3.1
	10.0	59,740	2,336,000	5,497,000	2.4
Dodecanedioic Acid	1.0	98,230	295,800	936,600	3.2
	10.0	56,330	2,205,000	5,182,000	2.4
1,12 Diamino-Dodecane	1.0	65,230	172,200	629,100	3.7
	10.0	40,050	1,413,000	3,747,000	2.7
5-Phenyl-Valeric acid	1.0	92,530	270,400	884,800	3.3
	10.0	53,960	2,061,000	4,986,000	2.4
Tetrastearoyl-Pentaerythritol	1.0	109,400	348,100	1,037,000	3.0
	10.0	60,530	2,481,000	5,520,000	2.2

<sup>1</sup> 3% Strain, 25 mm PP

**Supplementary Table 3.6 Rheological Data of Mixtures of Model Compounds (1 mass %) with AAB-1 at 60 °C<sup>1</sup>**

Model Compound	Rad/s	Viscosity (Pa · s)	G', dynes/cm <sup>2</sup>	G'', dynes/cm <sup>2</sup>	Tan $\delta$
None	1.0	151	37	1,506	40.2
	10.0	139	712	13,900	19.5
Dodecane	1.0	106	0	1,059	$\infty$
	10.0	100	429	9,998	23.3
Lauric Acid	1.0	112	12	1,121	93
	10.0	104	433	10,400	24
1-Dodecanol	1.0	118	7	1,184	174
	10.0	114	391	11,420	29
12-Amino-Lauric Acid	1.0	201	60	2,012	34
	10.0	179	1,077	17,840	17
Dodecanedioic Acid	1.0	190	52	1,895	36
	10.0	167	985	16,650	17
1,12 Diam-inododecane	1.0	106	15	1,056	70
	10.0	99	435	9,886	23
5-Phenyl-Valeric Acid	1.0	135	35	1,347	38
	10.0	124	736	12,360	17

<sup>1</sup> 90% Strain, 25 mm PP



**Supplementary Table 3.7 Rheological Data of Mixtures of Model Compounds (1 mass %) with AAC-1 at 25 °C<sup>1</sup>**

Model Compound	Rad/s	Viscosity (Pa · s)	G', dynes/cm <sup>2</sup>	G'', dynes/cm <sup>2</sup>	Tan δ
None	1.0	94,540	152,500	932,900	6.1
Dodecane	1.0	49,640	74,740	490,050	6.6
Lauric Acid	1.0	58,910	98,340	580,800	5.9
	10.0	43,250	1,107,000	4,180,000	3.8
1-Dodecanol	1.0	43,840	64,400	433,600	6.7
	10.0	33,400	762,100	3,252,000	4.3
12-Amino-Lauric Acid	1.0	104,300	211,100	1,022,000	4.8
	10.0	69,830	2,069,000	6,668,000	3.2
Dodecanedioic Acid	1.0	101,700	219,400	992,700	4.5
	10.0	65,860	2,038,000	6,261,000	3.1
1,12 Diam-inododecane	1.0	65,390	99,380	646,300	6.5
5-Phenyl-Valeric Acid	1.0	77,000	123,400	760,000	6.2
Tetrastearoyl-Pentaerythritol	1.0	69,240	10,590	684,000	6.5

<sup>1</sup> 3% Strain, 25 mm PP

**Supplementary Table 3.8 Rheological Data of Mixtures of Model Compounds (1 mass % ) with AAC-1 at 60°C<sup>1</sup>**

Model Compound	Rad/s	Viscosity (Pa · s)	G' , dynes/cm <sup>2</sup>	G'' , dynes/cm <sup>2</sup>	Tan $\delta$
None	1.0	119	9	1,194	139
	10.0	118	201	11,790	39
Dodecane	1.0	82	2	821	335
	10.0	81	21	8,103	391
Lauric Acid	1.0	98	15	983	66
	10.0	97	261	9,738	37
1-Dodecanol	1.0	77	14	770	55
	10.0	74	156	7,409	48
12-Amino-Lauric Acid	1.0	131	25	1,312	53
	10.0	126	307	12,640	41
Dodecanedioic Acid	1.0	123	0	1,233	$\infty$
	10.0	126	546	12,030	22
1,12 Diam-inododecane	1.0	89	6	889	155
	10.0	90	168	9,018	54
5-Phenyl-Valeric Acid	1.0	104	3	1,039	382
	10.0	103	212	10,280	49
Tetrastearoyl-Pentaerythritol	1.0	99	10	986	102
	10.0	99	267	9,856	37

<sup>1</sup> 50% Strain, 25 mm PP

**Supplementary Table 3.9 Rheological Data of Mixtures of Model Compounds (1 mass % ) with AAD-1 at 25 °C<sup>1</sup>**

Model Compound	Rad/s	Viscosity (Pa · s)	G', dynes/cm <sup>2</sup>	G'', dynes/cm <sup>2</sup>	Tan $\delta$
None	1.0	40,570	120,600	387,300	3.2
	10.0	25,580	918,300	2,387,000	2.6
Dodecane	1.0	25,540	71,570	245,100	3.4
	10.0	15,770	541,300	1,481,000	2.7
Lauric Acid	1.0	29,890	77,080	288,700	3.7
	10.0	191,000	618,300	1,806,000	2.9
1-Dodecanol	1.0	24,580	62,610	237,600	3.8
	10.0	15,800	508,500	1,495,000	2.9
12-Amino-Lauric Acid	1.0	44,440	128,600	425,400	3.3
	10.0	27,260	947,100	2,555,000	2.7
Dodecanedioic Acid	1.0	47,810	144,500	455,700	3.2
	10.0	28,860	1,036,000	2,693,000	2.6
1,12 Diam-inododecane	1.0	43,940	128,700	420,000	3.3
	10.0	26,860	954,100	2,510,000	2.6
5-Phenyl-Valeric Acid	1.0	32,220	86,080	310,400	3.6
	10.0	20,500	671,200	1,937,000	2.9
Tetrastearoyl-Pentaerythritol	1.0	32,980	91,510	316,800	3.5
	10.0	20,520	697,600	1,930,000	2.8

<sup>1</sup> 3% Strain, 25 mm PP

**Supplementary Table 3.10 Rheological Data of Mixtures of Model Compounds (1 mass %) with AAD-1 at 60 °C<sup>1</sup>**

Model Compound	Rad/s	Viscosity (Pa · s)	G', dynes/cm <sup>2</sup>	G'', dynes/cm <sup>2</sup>	Tan $\delta$
None	1.0	164	52	1,643	31
	10.0	152	1,326	15,190	11
Dodecane	1.0	110	40	1,099	28
	10.0	104	878	10,330	12
Lauric Acid	1.0	99	0	987	$\infty$
	10.0	100	713	9,948	14
1-Dodecanol	1.0	93	69	932	14
	10.0	92	62	9,144	15
12-Amino-Lauric Acid	1.0	158	26	1,578	61
	10.0	146	1,112	14,570	13
Dodecanedioic Acid	1.0	162	53	1,621	30
	10.0	151	1,406	15,080	10
1,12 Diam-inododecane	1.0	135	15	1,354	88
	10.0	126	544	12,580	23
5-Phenyl-Valeric Acid	1.0	119	65	1,184	18
	10.0	113	817	11,320	14
Tetrastearoyl-Pentaerythritol	1.0	129	0	1,295	$\infty$
	10.0	123	923	12,230	13

<sup>1</sup> 50% Strain, 25 mm PP

**Supplementary Table 3.11 Rheological Data of Mixtures of Model Compounds (1 mass %) with AAF-1 at 25 °C<sup>1</sup>**

Model Compound	Rad/s	Viscosity (Pa · s)	G', dynes/cm <sup>2</sup>	G'', dynes/cm <sup>2</sup>	Tan $\delta$
None	1.0	307,800	744,900	2,986,000	4.0
Dodecane	1.0	261,300	619,700	2,538,000	4.1
	10.0	161,200	5,635,000	15,100,000	2.7
Lauric Acid	1.0	199,700	410,400	1,955,000	4.7
	10.0	131,600	4,157,000	12,480,000	3.0
1-Dodecanol	1.0	157,800	289,000	1,551,000	5.3
	10.0	109,100	3,147,000	10,440,000	3.3
12-Amino-Lauric Acid	1.0	333,500	739,200	3,252,000	4.4
Dodecanedioic Acid	1.0	236,700	529,800	2,306,000	4.4
	10.0	150,000	5,169,000	14,070,000	2.7
1,12 Diam-inododecane	1.0	226,900	472,300	2,219,000	4.7
	10.0	147,200	4,747,000	13,930,000	2.9
5-Phenyl-Valeric Acid	1.0	236,600	527,700	2,307,000	4.4
	10.0	148,900	4,982,000	14,030,000	2.8
Tetristearoyl-Pentaerythritol	1.0	209,200	450,200	2,043,000	4.5
	10.0	134,500	4,569,000	12,650,000	2.8

<sup>1</sup> 3 % Strain, 25 mm PP

**Supplementary Table 3.12 Rheological Data of Mixtures of Model Compounds (1 mass %) with AAF-1 at 60 °C<sup>1</sup>**

Model Compound	Rad/s	Viscosity (Pa · s)	G', dynes/cm <sup>2</sup>	G'', dynes/cm <sup>2</sup>	Tan $\delta$
None	1.0	289	37	2,892	77
	10.0	280	830	2,804	34
Dodecane	1.0	216	2.6	2,162	822
	10.0	211	240	21,110	88
Lauric Acid	1.0	181	18.8	1,810	96
	10.0	182	462	18,200	39.4
1-Dodecanol	1.0	155	15.5	1,547	97
	10.0	153	688	15,270	22
12-Amino-Lauric Acid	1.0	251	6.9	2,511	365
	10.0	246	366	24,570	67
Dodecanedioic Acid	1.0	238	0	2,381	$\infty$
	10.0	231	60	23,050	38
1,12 Diam-inododecane	1.0	186	456	1,862	4
	10.0	178	2,067	17,840	8.6
5-Phenyl-Valeric Acid	1.0	208	48	2,083	43
	10.0	202	313	20,240	64
Tetrastearoyl-Pentaerythritol	1.0	230	34	2,297	68
	10.0	222	61	22,210	36

<sup>1</sup> 50% Strain, 25 mm PP

**Supplementary Table 3.13 Rheological Data of Mixtures of Model Compounds (1 mass %) with AAG-1 at 25 °C<sup>1</sup>**

Model Compound	Rad/s	Viscosity (Pa · s)	G', dynes/cm <sup>2</sup>	G'', dynes/cm <sup>2</sup>	Tan δ
None	1.0	354,000	417,700	3,515,000	8.4
Dodecane	1.0	109,900	80,640	1,095,000	13.6
	10.0	94,330	1,463,000	9,317,000	6.4
Lauric acid	1.0	233,700	223,100	2,326,000	10.4
1-Dodecanol	1.0	164,500	139,500	1,639,000	11.7
	10.0	146,700	2,635,000	14,430,000	54.8
12-Amino-Lauric Acid	1.0	330,100	356,700	3,281,000	9.2
Dodecanedioic Acid	1.0	308,900	352,100	3,068,000	8.7
1,12 Diamino-Dodecane	1.0	200,000	176,400	1,992,000	11.3
	10.0	170,200	3,069,000	16,740,000	5.5
5-Phenyl-Valeric acid	1.0	292,400	340,300	2,904,000	1.0
Tetrastearoyl-Pentaerythritol	1.0	231,900	225,100	2,308,000	10.3

<sup>1</sup> 3% Strain, 25 mm PP

**Supplementary Table 3.14 Rheological Data of Mixtures of Model Compounds (1 mass %) with AAG-1 at 60°C<sup>1</sup>**

Model Compound	Rad/s	Viscosity (Pa · s)	G', dynes/cm <sup>2</sup>	G'', dynes/cm <sup>2</sup>	Tan δ
None	1.0	300	0	2,998	∞
	10.0	298	0	29,760	∞
	100.0	208	6,449	208,200	32.3
Dodecane	1.0	153	12	1,530	125
	10.0	149	423	14,850	35.2
	100.0	134	3,209	134,100	41.8
Lauric acid	1.0	228	57	2,280	40.2
	10.0	236	0	23,570	∞
	100.0	195	5,532	194,500	35.2
1-Dodecanol	1.0	187	46	1,873	40.1
	10.0	187	142	18,730	132
	100.0	169	4,110	168,800	41.1
12-Amino-Lauric Acid	1.0	228	0	2,281	∞
	10.0	224	51	22,430	444
	100.0	181	5,367	180,500	33.6
Dodecanedioic Acid	1.0	306	57	3,058	53.2
	10.0	291	497	29,090	58.5
	100.0	209	6,336	209,300	33.0
1,12 Diamino-Dodecane	1.0	177	36	1,769	48.8
	10.0	172	124	17,240	139
	100.0	162	3,650	161,600	44.3
5-Phenyl-Valeric acid	1.0	269	66	2,693	41.1
	10.0	258	132	25,820	195
	100.0	203	7,229	202,800	28.1
Tetrastearoyl-Pentaerythritol	1.0	239	0	2,390	∞
	10.0	233	0	23,340	∞
	100.0	206	5,431	205,500	37.8

<sup>1</sup> 50% Strain, 25 mm PP



**Supplementary Table 3.15 Rheological Data of Mixtures of Model Compounds (1 mass %) with AAK-1 at 25 °C<sup>1</sup>**

Model Compound	Rad/s	Viscosity (Pa·s)	G', dynes/cm <sup>2</sup>	G'', dynes/cm <sup>2</sup>	Tan δ
None	1.0	107,700	353,600	1,018,000	2.9
	10.0	62,350	2,425,000	5,743,000	2.4
Dodecane	1.0	96,420	331,100	905,500	2.7
	10.0	54,940	2,177,000	5,043,000	2.3
Lauric acid	1.0	90,510	287,500	858,100	3.0
	10.0	53,790	1,991,000	4,996,000	2.5
1-Dodecanol	1.0	71,610	225,500	679,700	3.0
	10.0	42,550	1,575,000	3,951,000	2.5
12-Amino-Lauric Acid	1.0	191,700	700,100	1,784,000	2.5
	10.0	101,200	4,220,000	9,196,000	2.2
Dodecanedioic Acid	1.0	161,800	581,500	1,510,000	2.6
	10.0	89,580	3,710,000	8,151,000	2.2
1,12 Diamino-Dodecane	1.0	134,500	463,600	1,263,000	2.7
	10.0	74,840	3,024,000	6,844,000	2.3
5-Phenyl-Valeric acid	1.0	104,500	344,000	986,600	2.9
	10.0	59,160	2,252,000	5,470,000	2.4
Tetrastearoyl-Pentaerythritol	1.0	115,000	394,200	1,081,000	2.7
	10.0	65,420	2,591,000	6,005,000	2.3

<sup>1</sup> 3% Strain, 25 mm PP

**Supplementary Table 3.16 Rheological Data of Mixtures of Model Compounds (1 mass %) with AAK-1 at 60 °C<sup>1</sup>**

Model Compound	Rad/s	Viscosity (Pa · s)	G', dynes/cm <sup>2</sup>	G'', dynes/cm <sup>2</sup>	Tan $\delta$
None	1.0	470	271	4,697	17.3
	10.0	396	5,239	39,250	7.5
	100.0	101	19,340	99,260	5.1
Dodecane	1.0	404	240	4,034	16.8
	10.0	348	4,452	34,550	7.8
	100.0	100	19,230	97,960	5.1
Lauric acid	1.0	346	117	3,460	3.0
	10.0	300	3,176	29,870	9.4
	100.0	92	16,470	90,740	5.5
1-Dodecanol	1.0	310	138	3,101	22.4
	10.0	269	3,289	26,700	8.1
	100.0	82	15,090	80,330	5.3
12-Amino-Lauric Acid	1.0	621	460	6,197	13.5
	10.0	493	7,356	48,790	6.6
	100.0	116	23,760	113,900	4.8
Dodecanedioic Acid	1.0	563	377	5,618	14.9
	10.0	460	6,715	45,520	6.8
	100.0	106	21,200	103,800	4.9
1,12 Diamino-Dodecane	1.0	434	213	4,331	20.3
	10.0	371	4,870	36,800	7.6
	100.0	107	20,130	104,800	5.2
5-Phenyl-Valeric acid	1.0	370	204	3,695	18.1
	10.0	323	4,099	32,050	7.8
	100.0	91	16,780	89,060	5.3
Tetrastearoyl-Pentaerythritol	1.0	439	248	4,387	17.7
	10.0	375	5,252	37,090	7.1
	100.0	96	17,940	94,520	5.3

<sup>1</sup> 50% Strain, 25 mm PP

**Supplementary Table 3.17 Rheological Data of Mixtures of Model Compounds (1 mass %) with AAM-1 at 25 °C<sup>1</sup>**

Model Compound	Rad/s	Viscosity (Pa · s)	G', dynes/cm <sup>2</sup>	G'', dynes/cm <sup>2</sup>	Tan $\delta$
None	1.0	112,300	425,600	1,039,000	2.4
	10.0	57,140	2,694,000	5,038,000	1.9
Dodecane	1.0	84,830	296,900	794,600	2.7
	10.0	44,930	2,043,000	4,001,000	2.0
Lauric acid	1.0	267,800	1,049,000	2,464,000	2.4
	10.0	128,600	6,264,000	11,230,000	1.8
1-Dodecanol	1.0	114,300	354,100	1,087,000	3.1
	10.0	61,550	2,504,000	5,621,000	2.2
12-Amino-Lauric Acid	1.0	284,900	1,133,000	2,614,000	2.3
	10.0	132,600	6,525,000	11,540,000	1.8
Dodecanedioic Acid	1.0	322,600	1,320,000	2,943,000	2.2
	10.0	148,600	7,449,000	12,850,000	1.7
1,12 Diamino-Dodecane	1.0	205,600	720,000	1,926,000	2.7
	10.0	105,700	4,728,000	9,451,000	2.0
5-Phenyl-Valeric acid	1.0	160,000	564,600	1,497,000	2.7
	10.0	83,120	3,701,000	7,441,000	2.0
Tetrastearoyl-Pentaerythritol	1.0	167,900	564,100	1,581,000	2.8
	10.0	87,520	3,773,000	7,896,000	2.1

<sup>1</sup> 3% Strain, 25 mm PP

**Supplementary Table 3.18 Rheological Data of Mixtures of Model Compounds (1 mass % ) with AAM-1 at 60 °C<sup>1</sup>**

Model Compound	Rad/s	Viscosity (Pa · s)	G' , dynes/cm <sup>2</sup>	G'' , dynes/cm <sup>2</sup>	Tan δ
None	1.0	276	95	2,759	28.8
	10.0	257	1,673	25,660	15.3
	100.0	59	6,211	58,400	9.4
Dodecane	1.0	202	72	2,015	27.9
	10.0	189	1,288	18,840	14.6
	100.0	58	6,347	58,130	9.2
Lauric Acid	1.0	207	55	2,069	27.7
	10.0	189	827	18,910	16.3
	100.0	70	6,988	69,610	10.0
1-Dodecanol	1.0	176	19	1,761	90.1
	10.0	166	770	16,610	21.6
	100.0	51	4,654	50,630	10.9
12-Aminolauric Acid	1.0	367	171	3,667	21.4
	10.0	327	2,943	32,560	11.1
	100.0	72	8,655	71,460	8.3
Dodecanedioic Acid	1.0	308	73	3,084	42.2
	10.0	276	2,170	27,540	12.7
	100.0	70	8,272	69,790	8.4
1,12 Diamino Dodecane	1.0	224	39	2,243	57.8
	10.0	209	1,273	20,820	16.3
	100.0	71	7,362	70,450	9.6
5-Phenylvaleric Acid	1.0	222	49	2,220	45.1
	10.0	202	1,443	20,160	14.0
	100.0	68	7,283	67,480	9.3

<sup>1</sup> 50% Strain, 25 mm PP

**Supplementary Table 3.19 Rheological Data for Mixtures of Model Compounds (2 mass %) with AAA-1 at 25 °C and 60 °C<sup>1</sup>**

Model Compound	Temperature, °C	Viscosity (Pa · s)	Visc 25/Visc 60
None	25	42,910	296
	60	145	
Dodecane	25	13,290	213
	60	62	
Lauric Acid	25	16,080	223
	60	72	
1-Dodecanol	25	11,340	221
	60	51	
12-Aminolauric Acid	25	44,940	310
	60	145	
Dodecanedioic Acid	25	37,020	269
	60	138	
1,12-Diaminododecane	25	19,760	254
	60	78	
5-Phenyl-Valeric Acid	25	18,720	240
	60	78	

<sup>1</sup> 1.0 rad/s; at 25 °C, 3% strain, 25 mm PP; at 60 °C, 50% strain, 25 mm pp

**Supplementary Table 3.20 Rheological Data for Mixtures of Model Compounds (2 mass %) with AAB-1 at 25 °C and 60 °C<sup>1</sup>**

Model Compound	Temperature, °C	Viscosity (Pa · s)	Visc 25/Visc 60
None	25	176,300	771
	60	229	
Dodecane	25	48,510	521
	60	92	
Lauric Acid	25	53,840	487
	60	110	
1-Dodecanol	25	30,420	487
	60	62	
12-Aminolauric Acid	25	124,100	626
	60	198	
Dodecanedioic Acid	25	108,000	656
	60	165	
1,12-Diaminododecane	25	41,920	541
	60	77	
5-Phenyl-Valeric Acid	25	50,660	580
	60	87	

<sup>1</sup> 1.0 rad/s; at 25 °C, 3% strain, 25 mm PP; at 60 °C, 50% strain, 25 mm PP

**Supplementary Table 3.21 Rheological Data for Mixtures of Model Compounds (2 mass %) with AAC-1 at 25 °C and 60 °C<sup>1</sup>**

Model Compound	Temperature, °C	Viscosity (Pa · s)	Visc 25/Visc 60
None	25	126,000	978
	60	129	
Dodecane	25	33,340	571
	60	58	
Lauric Acid	25	48,320	731
	60	66	
1-Dodecanol	25	20,810	426
	60	49	
12-Aminolauric Acid	25	102,300	868
	60	118	
Dodecanedioic Acid	25	109,500	919
	60	119	
1,12-Diaminododecane	25	39,460	698
	60	56	
5-Phenyl-Valeric Acid	25	57,070	748
	60	76	

<sup>1</sup> 1.0 rad/s; at 25 °C, 3% strain, 25 mm PP; at 60 °C, 50% strain, 25 mm PP

**Supplementary Table 3.22 Rheological Data for Mixtures of Model Compounds (2 mass %) with AAD-1 at 25 °C and 60 °C<sup>1</sup>**

Model Compound	Temperature, °C	Viscosity (Pa · s)	Visc 25/Visc 60
None	25 60	54,730 177	310
Dodecane	25 60	20,280 92	221
Lauric Acid	25 60	24,530 89	274
1-Dodecanol	25 60	19,320 86	225
12-Aminolauric Acid	25 60	55,960 185	302
Dodecanedioic Acid	25 60	56,020 146	383
1,12-Diaminododecane	25 60	29,590 96	309
5-Phenyl-Valeric Acid	25 60	27,240 91	299

<sup>1</sup> 1.0 rad/s; at 25 °C, 3% strain, 25 mm PP; at 60 °C, 50% strain, 25 mm PP



**Supplementary Table 3.23 Rheological Data for Mixtures of Model Compounds (2 mass %) with AAF-1 at 25 °C and 60 °C<sup>1</sup>**

Model Compound	Temperature, °C	Viscosity (Pa · s)	Visc 25/Visc 60
None	25	461,300	1380
	60	334	
Dodecane	25	91,210	740
	60	123	
Lauric Acid	25	151,000	1010
	60	149	
1-Dodecanol	25	89,870	889
	60	101	
12-Aminolauric Acid	25	342,700	1200
	60	285	
Dodecanedioic Acid	25	279,100	1100
	60	254	
1,12-Diaminododecane	25	134,100	1045
	60	128	
5-Phenyl-Valeric Acid	25	124,600	933
	60	134	

<sup>1</sup> 1.0 rad/s; at 25 °C, 3% strain, 25 mm PP; at 60 °C, 50% strain, 25 mm PP

**Supplementary Table 3.24 Rheological Data for Mixtures of Model Compounds (2 mass %) with AAG-1 at 25 °C and 60 °C<sup>1</sup>**

Model Compound	Temperature, °C	Viscosity (Pa · s)	Visc 25/Visc 60
None	25	376,000	1,282
	60	293	
Dodecane	25	43,830	527
	60	83	
Lauric Acid	25	253,700	1,016
	60	250	
1-Dodecanol	25	92,310	794
	60	116	
12-Aminolauric Acid	25	442,400	1,245
	60	355	
Dodecanedioic Acid	25	325,400	1,270
	60	256	
1,12-Diaminododecane	25	155,700	1,111
	60	140	
5-Phenyl-Valeric Acid	25	224,000	1,272
	60	176	

<sup>1</sup> 1.0 rad/s; at 25 °C, 3% strain, 25 mm PP; at 60 °C, 50% strain, 25 mm PP

**Supplementary Table 3.25 Rheological Data for Mixtures of Model Compounds (2 mass %) with AAK-1 at 25 °C and 60 °C<sup>1</sup>**

Model Compound	Temperature, °C	Viscosity (Pa · s)	Visc 25/Visc 60
None	25	162,600	282
	60	577	
Dodecane	25	64,230	219
	60	293	
Lauric Acid	25	75,100	263
	60	285	
1-Dodecanol	25	47,810	229
	60	209	
12-Aminolauric Acid	25	163,900	277
	60	591	
Dodecanedioic Acid	25	139,000	282
	60	494	
1,12-Diaminododecane	25	79,680	298
	60	267	
5-Phenyl-Valeric Acid	25	76,210	283
	60	270	

<sup>1</sup> 1.0 rad/s; at 25 °C, 3% strain, 25 mm PP; at 60 °C, 50% strain, 25 mm PP

**Supplementary Table 3.26 Rheological Data for Mixtures of Model Compounds (2 mass %) with AAM-1 at 25 °C and 60 °C<sup>1</sup>**

Model Compound	Temperature, °C	Viscosity (Pa · s)	Visc 25/Visc 60
None	25	380,600	778
	60	489	
Dodecane	25	105,800	596
	60	177	
Lauric Acid	25	118,200	641
	60	184	
1-Dodecanol	25	102,100	629
	60	162	
12-Aminolauric Acid	25	435,300	813
	60	535	
Dodecanedioic Acid	25	274,700	801
	60	343	
1,12-Diaminododecane	25	133,300	867
	60	154	
5-Phenyl-Valeric Acid	25	141,300	784
	60	180	

<sup>1</sup> 1.0 rad/s; at 25 °C, 3% strain, 25 mm PP; at 60 °C, 50% strain, 25 mm PP

**Supplementary Table 3.27 Rheological Data for Mixtures of Model Compounds with AAA-1 at 25 °C and 60 °C<sup>1</sup>**

Model Compound	Run No.	Mass % Compound in Mixture	Temperature, °C	Viscosity (Pa · s)	Tan $\delta$	Visc 25/Visc 60
None	1	0	25	50,530	4.0	313
			60	161	38.0	
	2	0	25	34,980	4.5	289
			60	121	78.0	
Hexadecane	1	1	25	23,800	4.9	245
			60	97	$\infty$	
	1	2	25	13,980	5.3	204
			60	68	76.2	
	2	1	25	14,680	5.4	193
			60	76	29.9	
	2	2	25	10,110	6.2	189
			60	53	161.0	
1-hexadecanol	1	1	25	22,000	5.2	231
			60	95	$\infty$	
	1	2	25	11,890	5.9	180
			60	66	$\infty$	
	2	1	25	16,220	6.0	213
			60	76	118.6	
	2	2	25	11,720	6.7	202
			60	58	47.4	
Palmitic Acid	1	1	25	29,660	4.7	310
			60	96	78.3	
	1	2	25	17,330	5.7	234
			60	74	$\infty$	
	2	1	25	18,490	5.4	219
			60	85	30.8	
	2	2	25	13,870	6.5	207
			60	67	$\infty$	
Thapsic Acid	1	1	25	37,380	4.4	240
			60	156	33.5	
	1	2	25	43,570	4.2	242
			60	180	32.5	
	2	1	25	25,480	4.9	212
			60	120	130.1	
	2	2	25	33,820	4.9	264
			60	128	68.9	

<sup>1</sup> 1.0 rad/s; at 25 °C, 3% strain, 25 mm PP; at 60 °C, 50% strain, 25 mm PP

**Supplementary Table 3.28 Rheological Data for Mixtures of Model Compounds with AAB-1 at 25 °C and 60 °C<sup>1</sup>**

Model Compound	Run No.	Mass % Compound in Mixture	Temperature, °C	Viscosity (Pa · s)	Tan $\delta$	Visc 25/Visc 60
None	1	0	25	195,500	2.7	731
			60	267	32.9	
	2	0	25	148,500	2.8	742
			60	200	59.9	
Hexadecane	1	1	25	87,900	3.1	541
			60	162	170.8	
	1	2	25	44,170	3.8	426
			60	104	28.4	
	2	1	25	63,150	3.4	556
			60	113	$\infty$	
	2	2	25	30,670	4.3	407
			60	75	$\infty$	
	1	1	25	63,220	3.7	514
			60	123	$\infty$	
1-hexadecanol	1	2	25	37,880	4.3	403
			60	94	42.5	
	2	1	25	46,060	4.0	402
			60	114	3,139	
	2	2	25	27,550	4.8	363
			60	76	$\infty$	
	1	1	25	72,480	3.5	514
			60	141	37.6	
	1	2	25	53,070	4.1	579
			60	111	35.4	
Palmitic Acid	2	1	25	59,160	3.8	499
			60	119	146.9	
	2	2	25	44,590	4.2	450
			60	99	120.5	
	1	1	25	128,200	3.0	662
			60	194	64.5	
	1	2	25	166,600	2.4	503
			60	331	12.6	
Thapsic Acid	2	1	25	118,600	2.9	672
			60	176	61.5	
	2	2	25	122,400	2.7	575
			60	213	66.6	

<sup>1</sup> 1.0 rad/s; at 25 °C, 3% strain, 25 mm PP; at 60 °C, 50% strain, 25 mm PP

**Supplementary Table 3.29 Rheological Data for Mixtures of Model Compounds with AAC-1 at 25 °C and 60 °C<sup>1</sup>**

Model Compound	Run No.	Mass % Compound in Mixture	Temperature, °C	Viscosity (Pa · s)	Tan $\delta$	Visc 25/Visc 60
None	1	0	25	66,250	4.3	409
			60	162	48.8	
	2	0	25	88,050	4.9	679
			60	130	85.2	
Hexadecane	1	1	25	58,120	5.5	630
			60	92	$\infty$	
	1	2	25	26,810	6.7	415
			60	64	$\infty$	
	2	1	25	47,950	5.8	542
			60	88	63.0	
	2	2	25	20,890	7.7	409
			60	51	66.6	
1-hexadecanol	1	1	25	60,140	5.8	611
			60	98	85.4	
	1	2	25	30,230	7.4	506
			60	60	48.2	
	2	1	25	51,880	6.2	598
			60	87	44.9	
	2	2	25	26,690	7.2	442
			60	60	$\infty$	
Palmitic Acid	1	1	25	73,190	5.4	726
			60	101	87.9	
	1	2	25	47,050	6.3	579
			60	81	15.9	
	2	1	25	63,480	5.4	664
			60	96	54.3	
	2	2	25	42,520	7.0	564
			60	75	$\infty$	
Thapsic Acid	1	1	25	112,700	4.0	823
			60	137	34.7	
	1	2	25	131,100	3.6	776
			60	169	70.0	
	2	1	25	124,100	4.0	967
			60	128	138.9	
	2	2	25	128,700	3.7	934
			60	138	58.9	

<sup>1</sup> 1.0 rad/s; at 25 °C, 3% strain, 25 mm PP; at 60 °C, 50% strain, 25 mm PP

**Supplementary Table 3.30 Rheological Data for Mixtures of Model Compounds with AAD-1 at 25 °C and 60 °C<sup>1</sup>**

Model Compound	Run No.	Mass % Compound in Mixture	Temperature, °C	Viscosity (Pa · s)	Tan $\delta$	Visc 25/Visc 60
None	1	0	25	74,080	2.8	304
			60	243	23.8	
	2	0	25	47,920	3.1	297
			60	161	36.9	
Hexadecane	1	1	25	41,740	3.1	271
			60	154	107.3	
	1	2	25	23,310	3.4	235
			60	99	38.3	
	2	1	25	26,950	3.5	254
			60	106	33.6	
	2	2	25	16,100	3.6	197
			60	81	$\infty$	
1-hexadecanol	1	1	25	35,050	3.4	253
			60	138	31.8	
	1	2	25	21,740	3.9	234
			60	93	45.2	
	2	1	25	27,950	3.6	257
			60	109	48.2	
	2	2	25	19,150	3.9	223
			60	86	$\infty$	
Palmitic Acid	1	1	25	32,560	3.6	257
			60	127	38.1	
	1	2	25	27,280	3.7	267
			60	102	43.2	
	2	1	25	27,590	3.7	242
			60	114	117.7	
	2	2	25	23,230	3.9	235
			60	99	1,036	
Thapsic Acid	1	1	25	54,580	3.1	307
			60	178	32.9	
	1	2	25	52,120	3.0	322
			60	162	30.0	
	2	1	25	49,270	3.2	324
			60	152	36.6	
	2	2	25	36,020	3.3	252
			60	143	32.1	

<sup>1</sup> 1.0 rad/s; at 25 °C, 3% strain, 25 mm PP; at 60 °C, 50% strain, 25 mm PP



**Supplementary Table 3.31 Rheological Data for Mixtures of Model Compounds with AAF-1 at 25 °C and 60 °C<sup>1</sup>**

Model Compound	Run No.	Mass % Compound in Mixture	Temperature, °C	Viscosity (Pa · s)	Tan $\delta$	Visc 25/Visc 60
None	1	0	25	499,500	3.2	1,387
			60	360	68.8	
	2	0	25	354,700	3.7	1,198
			60	296	$\infty$	
Hexadecane	1	1	25	266,300	3.8	1,128
			60	236	135.5	
	1	2	25	125,100	4.5	941
			60	133	$\infty$	
	2	1	25	185,500	4.3	936
			60	198	48.9	
	2	2	25	99,070	5.0	805
			60	123	223.4	
	1	1	25	193,400	4.6	966
			60	200	586.7	
1-hexadecanol	1	2	25	106,500	5.5	858
			60	124	102.4	
	2	1	25	140,500	5.2	885
			60	159	362.7	
	2	2	25	104,800	5.2	792
			60	132	59.7	
	1	1	25	237,100	4.5	1,214
			60	195	55.0	
	1	2	25	133,500	4.8	980
			60	136	45.0	
Palmitic Acid	2	1	25	204,900	4.6	1,011
			60	202	75.5	
	2	2	25	129,700	5.2	891
			60	146	154.7	
	1	1	25	282,700	3.8	1,002
			60	282	73.7	
	1	2	25	322,500	2.5	872
			60	370	43.6	
Thapsic Acid	2	1	25	320,600	3.8	1,165
			60	275	69.7	
	2	2	25	332,900	3.5	1,059
			60	314	105.0	

<sup>1</sup> 1.0 rad/s; at 25 °C, 3% strain, 25 mm PP; at 60 °C, 50% strain, 25 mm PP

**Supplementary Table 3.32 Rheological Data for Mixtures of Model Compounds with AAG-1 at 25 °C and 60 °C<sup>1</sup>**

Model Compound	Run No.	Mass % Compound in Mixture	Temperature, °C	Viscosity (Pa · s)	Tan $\delta$	Visc 25/Visc 60
None	1	0	25	364,000	8.7	1,175
			60	310	86.2	
	2	0	25	312,900	9.6	1,246
			60	251	187.9	
Hexadecane	1	1	25	164,400	10.6	801
			60	205	78.0	
	1	2	25	65,700	10.6	543
			60	121	$\infty$	
	2	1	25	130,400	12.1	821
			60	159	$\infty$	
	2	2	25	58,390	15.5	615
			60	95	$\infty$	
	1	1	25	153,900	12.6	843
			60	182	54.2	
1-hexadecanol	1	2	25	76,610	16.7	654
			60	117	$\infty$	
	2	1	25	145,600	12.0	928
			60	157	$\infty$	
	2	2	25	88,410	15.8	771
			60	115	251.4	
	1	1	25	210,500	10.9	970
			60	217	106.4	
Palmitic Acid	1	2	25	169,200	11.2	643
			60	263	522	
	2	1	25	299,700	8.6	1,288
			60	233	94.3	
	2	2	25	188,400	10.7	867
			60	217	159.2	
	1	1	25	248,100	11.0	1,057
			60	235	542.2	
Thapsic Acid	1	2	25	230,000	11.3	
			60	219	66.3	
	2	1	25	284,300	9.9	1,165
			60	244	2,206	
	2	2	25	236,300	11.1	1,079
			60	219	$\infty$	

<sup>1</sup> 1.0 rad/s; at 25 °C, 3% strain, 25 mm PP; at 60 °C, 50% strain, 25 mm PP

**Supplementary Table 3.33 Rheological Data for Mixtures of Model Compounds with AAK-1 at 25 °C and 60 °C<sup>1</sup>**

Model Compound	Run No.	Mass % Compound in Mixture	Temperature, °C	Viscosity (Pa · s)	Tan $\delta$	Visc 25/Visc 60
None	1	0	25	148,000	2.6	264
			60	561	15.8	
	2	0	25	161,600	2.7	364
			60	443	14.8	
Hexadecane	1	1	25	88,430	2.8	241
			60	367	18.5	
	1	2	25	61,700	2.8	229
			60	270	18.9	
	2	1	25	82,370	2.8	249
			60	331	22.1	
	2	2	25	65,270	2.8	265
			60	246	24.6	
	1	1	25	86,230	3.0	250
			60	345	20.5	
1-hexadecanol	1	2	25	51,470	3.3	225
			60	229	26.4	
	2	1	25	96,940	2.8	311
			60	312	25.6	
	2	2	25	52,810	3.2	261
			60	203	29.9	
	1	1	25	95,170	3.0	261
			60	364	19.5	
	1	2	25	77,770	2.9	224
			60	346	22.4	
Palmitic Acid	2	1	25	100,200	2.9	296
			60	339	18.9	
	2	2	25	78,290	3.0	311
			60	252	33.5	
	1	1	25	138,100	2.7	324
			60	462	15.8	
	1	2	25	118,000	2.7	255
			60	462	16.1	
Thapsic Acid	2	1	25	124,300	2.8	346
			60	359	21.1	
	2	2	25	148,800	2.7	345
			60	432	17.1	

<sup>1</sup> 1.0 rad/s; at 25 °C, 3% strain, 25 mm PP; at 60 °C, 50% strain, 25 mm PP

**Supplementary Table 3.34 Rheological Data for Mixtures of Model Compounds with AAM-1 at 25 °C and 60 °C<sup>1</sup>**

Model Compound	Run No.	Mass % Compound in Mixture	Temperature, °C	Viscosity (Pa · s)	Tan $\delta$	Visc 25/Visc 60
None	1	0	25	264,700	2.4	744
			60	356	22.7	
	2	0	25	293,500	2.3	886
			60	331	40.6	
Hexadecane	1	1	25	140,800	2.7	629
			60	224	49.5	
	1	2	25	72,860	3.1	484
			60	150	35.1	
	2	1	25	125,600	2.8	552
			60	226	54.4	
	2	2	25	75,990	3.1	616
			60	123	57.1	
	1	1	25	142,400	2.8	698
			60	204	57.7	
1-hexadecanol	1	2	25	75,380	3.5	508
			60	148	55.0	
	2	1	25	134,100	2.9	698
			60	192	81.7	
	2	2	25	72,320	3.4	532
			60	136	78.2	
	1	1	25	132,900	2.7	591
			60	225	37.2	
	1	2	25	114,600	3.0	587
			60	195	40.0	
Palmitic Acid	2	1	25	183,700	2.6	715
			60	257	87.6	
	2	2	25	109,800	2.8	604
			60	182	36.7	
	1	1	25	310,100	2.1	735
			60	421	27.2	
	1	2	25	260,300	2.1	625
			60	417	24.6	
Thapsic Acid	2	1	25	247,500	2.2	668
			60	370	28.3	
	2	2	25	284,600	2.1	728
			60	391	29.4	

<sup>1</sup> 1.0 rad/s; at 25 °C, 3% strain, 25 mm PP; at 60 °C, 50% strain, 25 mm PP

**Supplementary Table 4.7 Potentiometric Titration of Bases in Expanded Set of Asphalts**

Asphalt	End Point #1		End Point #2		Total Base, meq/g
	mv	meq/g	mv	meq/g	
AAG-2	460	0.26	700	0.19	0.45
ABD	450	0.21	700	0.18	0.39
AAH	470	0.10	725	0.09	0.19
AAJ	460	0.11	720	0.11	0.22
AAK-2	440	0.12	700	0.09	0.21
AAV	470	0.09	720	0.11	0.20

**Supplementary Table 4.8 Potentiometric Titration of Acids in Core Asphalts**

Asphalt	Total Acids (meq/g)			Strong Acids (meq/g) run 1	Moderate and Weak Acids (meq/g) run 1
	run 1	run 2	Avg.		
AAA-1	0.228	0.246	0.237	0.041	0.187
AAB-1	0.262	0.246	0.254	-	0.262
AAC-1	0.246	0.217	0.232	0.027	0.219
AAD-1	0.348	0.402	0.375	0.043	0.305
AAF-1	0.307	0.297	0.302	0.040	0.267
AAG-1	0.567	0.441	0.504	0.038	0.529
AAK-1	0.279	0.333	0.306	0.024	0.255
AAM-1	0.236	0.265	0.250	0.030	0.206

**Supplementary Table 4.9 Potentiometric Titrations of Acids in Aged Core Asphalts**

Asphalt <sup>1</sup>	Total Titratable Acids (meq/g) <sup>2</sup>		
	Run 1	Run 2	Avg.
AAA-1	0.378	0.315	0.346
AAB-1	0.326	0.307	0.316
AAC-1	0.318	0.332	0.325
AAD-1	0.516	0.506	0.511
AAF-1	0.424	0.437	0.430
AAG-1	0.612	0.589	0.600
AAK-1	0.614	0.623	0.618
AAM-1	0.322	0.399	0.360

<sup>1</sup> Asphalts were TFO-PAV aged at 60 °C and 300 psi for 1,000 hours.

<sup>2</sup> Titrations were performed 15 minutes after dissolution of samples.

**Supplementary Table 4.10 Potentiometric Titrations of Acids in Iso-octane Maltenes of Core Asphalts**

Asphalt	Total Titratable Acids (meq/g)		
	Run 1	Run 2	Avg.
AAA-1	0.156	0.171	0.163
AAB-1	0.200	0.192	0.196
AAC-1	0.207	0.196	0.201
AAD-1	0.266	0.271	0.268
AAF-1	0.254	0.223	0.238
AAG-1	0.545	0.475	0.510
AAK-1	0.242	0.247	0.244
AAM-1	0.266	0.215	0.241

**Supplementary Table 4.11 Potentiometric Titrations of IEC Strong Acid Fractions of Core Asphalts**

Asphalt	Titration Time After Dissolution of Sample (hrs)	Run No.	Total Titratable Acids (meq/g)
AAA-1	0.25	1	0.861
	0.25	2	0.866
AAB-1	0.25	1	0.960
	0.25	2	0.943
AAD-1	0.25	1	1.108
	0.25	2	1.009
AAF-1	0.25	1	1.112
	0.25	2	1.047
AAG-1	0.25	1	1.642
	0.25	2	1.692
	4.0	1	1.493
	4.0	2	1.475
	72.0	1	1.516
	72.0	2	1.553
	168.0	1	1.530
	168.0	2	1.522
	0.25	1	0.952
	0.25	2	0.968
AAM-1	0.25	1	0.721
	0.25	2	0.766
	72.0	1	0.627
	72.0	2	0.732

**Supplementary Table 4.12 Potentiometric Titrations of IEC Amphoteric and Total Acid Fractions of Core Asphalts**

Asphalt	IEC Fraction	Titration Time After Dissolution of Sample (hrs)	Run No.	Total Titratable Acids (meq/g)
AAD-1	Amphoteric	0.25	1	1.004
		0.25	2	1.030
		4.0	1	0.969
		72.0	1	0.863
		72.0	2	0.798
		168.0	1	0.791
		168.0	2	0.777
AAG-1	Amphoteric	0.25	1	1.266
		0.25	2	1.138
	Total Acid	0.25	1	1.365
AAK-1	Amphoteric	0.25	1	0.651
		0.25	2	0.679
	Total Acid	0.25	1	1.041
AAM-1	Amphoteric	0.25	1	0.642
		0.25	2	0.640
	Total Acid	0.25	1	0.777



**Supplementary Table 4.13 Potentiometric Titrations of Core Asphalts Performed at Various Times After Dissolution of Sample**

Asphalt	Titration Time After Dissolution of Sample (hrs)	Run No.	Total Titratable Acids (meq/g)
AAC-1	72.0	1	0.148
	72.0	2	0.200
AAD-1	4.0	1	0.238
	4.0	2	0.288
	72.0	1	0.244
	72.0	2	0.274
	168.0	1	0.261
	168.0	2	0.274
AAG-1	4.0	1	0.451
	4.0	2	0.384
	72.0	1	0.369
	72.0	2	0.388
	168.0	1	0.365
AAK-1	72.0	1	0.223
	72.0	2	0.191

**Supplementary Table 5.12 Tan  $\delta$  Values at Three Temperatures of Mixtures of SEC Fractions of Asphalts AAD-1 and AAK-1**

Mixture Designation	Run No.	Components and Composition (mass %) of Mixture				Tan $\delta$ , 1.0 rad/s		
		AAD-1		AAK-1		25 °C	45 °C	60 °C
		SEC-I	SEC-II	SEC-I	SEC-II			
A <sup>1</sup>	1	23.4	76.6	-	-	2.4	5.4	15.8
	2					2.5	5.9	18.1
B	1	23.4	-	-	76.6	2.2	4.0	9.2
	2					2.2	4.2	10.3
C	1	26.0	74.0	-	-	2.0	3.9	8.7
	2					2.1	4.2	10.1
D	1	26.0	-	-	74.0	1.9	3.0	5.7
	2					1.9	3.2	6.5
E	1	-	76.6	23.4	-	2.8	6.6	26.0
	2					2.7	6.5	18.5
F	1	-	-	23.4	76.6	2.5	5.0	11.8
	2					2.4	5.1	12.9
G	1	-	74.0	26.0	-	2.3	4.3	11.0
	2					2.3	4.5	13.4
H <sup>2</sup>	1	-	-	26.0	74.0	2.1	3.8	7.6
	2					2.1	3.7	7.8

<sup>1</sup> Asphalt AAD-1 (natural abundance)

<sup>2</sup> Asphalt AAK-1 (natural abundance)

A value of  $\sigma = 0.013$  was calculated for the tan  $\delta$  at 25 °C for AAK-1.

**Supplementary Table 5.13** Tan  $\delta$  Values at Three Temperatures of Mixtures of SEC Fractions of Asphalts AAD-1 and AAM-1

Mixture Designation	Run No.	Components and Composition (mass %) of Mixture				Tan $\delta$ , 1.0 rad/s		
		AAD-1 SEC-I	AAD-1 SEC-II	AAM-1 SEC-I	AAM-1 SEC-II	25 °C	45 °C	60 °C
A <sup>1</sup>	1	23.4	76.6	-	-	2.3	5.0	13.8
	2					2.5	5.7	16.9
B	1	23.4	-	-	76.6	0.8	1.4	1.8
	2					0.8	1.0	1.8
C	1	30.6	69.4	-	-	1.6	2.2	3.9
	2					1.6	2.4	4.5
D	1	30.6	-	-	69.4	0.5	0.7	1.1
	2					0.5	0.8	1.2
E	1	-	76.6	23.4	-	22.2	-	-
	2					24.7	373	-
F	1	-	-	23.4	76.6	3.0	16.3	41.2
	2					3.1	15.3	54
G	1	-	69.4	30.6	-	7.9	65.8	714
	2					7.3	57.0	158
H <sup>2</sup>	1	-	-	30.6	69.4	1.9	6.0	19.8
	2					2.0	6.8	19.7

<sup>1</sup> Asphalt AAD-1 (natural abundance)

<sup>2</sup> Asphalt AAM-1 (natural abundance)

A value of  $\sigma = 0.015$  was calculated for the tan  $\delta$  value at 25 °C for asphalt AAM-1.

Supplementary Table 5.14 Tan  $\delta$  Values at Three Temperatures of Mixtures of SEC Fractions of Asphalts AAG-1 and AAK-1

Mixture Designation	Run No.	Components and Composition (mass %) of Mixture				Tan $\delta$ , 1.0 rad/s		
		AAG-1 SEC-I	AAG-1 SEC-II	AAK-1 SEC-I	AAK-1 SEC-II	25 °C	45 °C	60 °C
A <sup>1</sup>	1	11.8	88.2	-	-	8.0	47.2	-
	2					7.8	44.3	-
B	1	11.8	-	-	88.2	15.5	230.2	-
	2					18.7	161.0	-
C	1	26.0	74.0	-	-	1.7	5.9	22.4
	2					2.0	7.0	27.5
D	1	26.0	-	-	74.0	3.3	16.2	115.6
	2					3.4	18.8	98.7
E	1	-	88.2	11.8	-	5.0	14.2	38.5
	2					4.5	15.6	63.8
F	1	-	-	11.8	88.2	8.8	56.0	-
	2					8.8	35.5	-
G	1	-	74.0	26.0	-	1.5	3.1	5.1
	2					1.6	2.9	4.7
H <sup>2</sup>	1	-	-	26.0	74.0	2.1	3.5	7.2
	2					2.1	3.7	7.9

<sup>1</sup> Asphalt AAG-1 (natural abundance)

<sup>2</sup> Asphalt AAK-1 (natural abundance)

A value of  $\sigma = 0.013$  was calculated for the tan  $\delta$  value at 25 °C of asphalt AAK-1.

Supplementary Table 5.15 Tan  $\delta$  Values at Three Temperatures of Mixtures of SEC Fractions of Asphalts AAG-1 and AAM-1

Mixture Designation	Run No.	Components and Composition (mass %) of Mixture				Tan $\delta$ , 1.0 rad/s		
		AAG-1 SEC-I	AAG-1 SEC-II	AAM-1 SEC-I	AAM-1 SEC-II	25 °C	45 °C	60 °C
A <sup>1</sup>	1	11.8	88.2	-	-	7.6	60.4	-
	2					7.7	58.6	-
B	1	11.8	-	-	88.2	3.4	21.9	84.5
	2					3.6	23.6	77
C	1	30.6	69.4	-	-	1.4	4.1	12.4
	2					1.5	4.3	13.8
D	1	30.6	-	-	69.4	0.8	1.9	3.4
	2					0.9	2.0	4.2
E	1	-	88.2	11.8	-	14.4	215.8	-
	2					13.8	98	-
F	1	-	-	11.8	88.2	6.0	74.2	54.5
	2					6.5	48.5	83
G	1	-	69.4	30.6	-	3.6	13.8	70.2
	2					4.0	14.3	59.4
H <sup>2</sup>	1			30.6	69.4	1.9	6.6	19.4
	2					1.9	6.5	17.4

<sup>1</sup> Asphalt AAG-1 (natural abundance)

<sup>2</sup> Asphalt AAM-1 (natural abundance)

A value of  $\sigma = 0.015$  was calculated for the tan  $\delta$  value at 25 °C for asphalt AAM-1.

Supplementary Table 5.16 Viscosities at Three Temperatures of Mixtures of SEC Fractions of Asphalts AAD-1 and AAK-1

Mixture Designation	Run No.	Components and Composition (mass %) of Mixture				Viscosity, Pa · s, 1.0 rad/s		
		AAD-1 SEC-I	AAD-1 SEC-II	AAK-1 SEC-I	AAK-1 SEC-II	25 °C	45 °C	60 °C
A <sup>1</sup>	1	23.4	76.6	-	-	86,320	2,880	342
	2					74,330	2,453	285
B	1	23.4	-	-	76.6	245,500	8,312	907
	2					243,800	7,461	819
C	1	26.0	74.0	-	-	179,800	6,163	718
	2					125,300	5,167	596
D	1	26.0	-	-	74.0	530,700	17,220	1,922
	2					429,800	14,260	1,588
E	1	-	76.6	23.4	-	54,490	1,888	233
	2					56,850	1,891	233
F	1	-	-	23.4	76.6	159,100	4,761	554
	2					172,800	5,348	572
G	1	-	74.0	26.0	-	108,500	3,965	489
	2					96,420	3,541	432
H <sup>2</sup>	1	-	-	26.0	74.0	275,500	8,868	1,146
	2					270,800	9,916	1,179

<sup>1</sup> Asphalt AAD-1 (natural abundance)

<sup>2</sup> Asphalt AAK-1 (natural abundance)

A value of  $\sigma = 1.7 \times 10^4$  was calculated for the viscosity at 25 °C for asphalt AAK-1.

Supplementary Table 5.17 Viscosities at Three Temperatures of Mixtures of SEC Fractions of Asphalts AAD-1 and AAM-1

Mixture Designation	Run No.	Components and Composition (mass %) of Mixture				Viscosity, Pa · s, 1.0 rad/s		
		AAD-1 SEC-I	AAD-1 SEC-II	AAM-1 SEC-I	AAM-1 SEC-II	25 °C	45 °C	60 °C
A <sup>1</sup>	1	23.4	76.6	-	-	93,310	2,995	347
	2					81,350	2,605	302
B	1	23.4	-	-	76.6	5,397,000	201,000	25,030
	2					6,037,000	468,400	23,390
C	1	30.6	69.4	-	-	482,800	22,710	2,843
	2					456,500	19,760	2,522
D	1	30.6	-	-	69.4	16,550,000	2,172,000	384,700
	2					18,710,000	2,153,000	324,900
E	1	-	76.6	23.4	-	2,794	101	17
	2					2,438	96	18
F	1	-	-	23.4	76.6	175,400	2,014	213
	2					130,000	1,955	211
G	1	-	69.4	30.6	-	7,700	234	36
	2					8,051	238	38
H <sup>2</sup>	1	-	-	30.6	69.4	404,000	6,779	535
	2					368,600	5,359	547

<sup>1</sup> Asphalt AAD-1 (natural abundance)

<sup>2</sup> Asphalt AAM-1 (natural abundance)

A value of  $\sigma = 5.2 \times 10^4$  was calculated for the viscosity at 25 °C of asphalt AAM-1.

Supplementary Table 5.18 Viscosities at Three Temperatures of Mixtures of SEC Fractions of Asphalts AAG-1 and AAK-1

Mixture Designation	Run No.	Components and Composition (mass %) of Mixture				Viscosity, Pa·s, 1.0 rad/s		
		AAG-I SEC-I	AAG-I SEC-II	AAK-I SEC-I	AAK-I SEC-II	25 °C	45 °C	60 °C
A <sup>1</sup>	1	11.8	88.2	-	-	307,400	3,975	311
	2					412,500	4,502	333
B	1	11.8	-	-	88.2	7,955	205	29
	2					8,260	212	32
C	1	26.0	74.0	-	-	7,387,000	91,970	5,233
	2					4,591,000	62,840	3,747
D	1	26.0	-	-	74.0	205,500	3,731	373
	2					159,000	3,537	337
E	1	-	88.2	11.8	-	603,600	6,584	507
	2					445,300	5,911	459
F	1	-	-	11.8	88.2	10,510	280	42
	2					10,730	305	40
G	1	-	74.0	26.0	-	5,364,000	91,970	7,884
	2					5,157,000	108,800	9,129
H <sup>2</sup>	1	-	-	26.0	74.0	291,100	10,430	1,226
	2					283,200	9,755	1,122

<sup>1</sup> Asphalt AAG-1 (natural abundance)

<sup>2</sup> Asphalt AAK-1 (natural abundance)

A value of  $\sigma = 1.7 \times 10^4$  was calculated for the viscosity at 25 °C of asphalt AAK-1.



**Supplementary Table 5.19 Viscosities at Three Temperatures of Mixtures of SEC Fractions of Asphalts AAG-1 and AAM-1**

Mixture Designation	Run No.	Components and Composition (mass %) of Mixture				Viscosity, Pa · s, 1.0 rad/s		
		AAG-I SEC-I	AAG-I SEC-II	AAM-I SEC-I	AAM-I SEC-II	25 °C	45 °C	60 °C
A <sup>1</sup>	1	11.8	88.2	-	-	392,500	4,387	327
	2					367,000	4,667	338
B	1	11.8	-	-	88.2	254,200	2,622	255
	2					276,300	2,777	232
C	1	30.6	69.4	-	-	10,810,000	183,100	11,240
	2					7,715,000	144,500	8,668
D	1	30.6	-	-	69.4	9,536,000	397,700	32,670
	2					7,375,000	282,600	21,560
E	1	-	88.2	11.8	-	98,740	1,371	129
	2					89,950	1,373	127
F	1	-	-	11.8	88.2	66,930	669	86
	2					57,170	651	84
G	1	-	69.4	30.6	-	290,800	4,975	436
	2					356,300	4,687	410
H <sup>2</sup>	1	-	-	30.6	69.4	500,600	5,170	571
	2					418,700	5,176	536

<sup>1</sup> Asphalt AAG-1 (natural abundance)

<sup>2</sup> Asphalt AAM-1 (natural abundance)

A value of  $\sigma = 5.2 \times 10^4$  was calculated for the viscosity at 25 °C of asphalt AAM-1.

**Supplementary Table 5.20 Comparison of Viscosities (60 °C) of Sets of Mixtures of SEC Fractions of Asphalts AAD-1 and AAK-1**

Mixture Designation	Viscosity, Pa · s, 60 °C	Mixture Designation	Viscosity, Pa · s, 60 °C
<u>SOLVENT PHASE COMPARISON</u>			
A	314	B	863
C	657	D	1,755
E	233	F	563
G	461	H	1,162
<u>DISPERSED PHASE COMPARISON</u>			
A	314	E	233
B	863	F	563
C	657	G	461
D	1,755	H	1,162
<u>NATURAL ABUNDANCE COMPARISON</u>			
A	314	C	657
B	863	D	1,755
E	233	G	461
F	563	H	1,162

**Supplementary Table 5.21 Comparison of Viscosities (60 °C) of Sets of Mixtures of SEC Fractions of Asphalts AAD-1 and AAM-1**

Mixture Designation	Viscosity, Pa · s, 60 °C	Mixture Designation	Viscosity, Pa · s, 60 °C
<u>SOLVENT PHASE COMPARISON</u>			
A	325	B	24,210
C	2,682	D	354,800
E	18	F	212
G	37	H	541
<u>DISPERSED PHASE COMPARISON</u>			
A	325	E	18
B	24,210	F	212
C	2,682	G	37
D	354,800	H	541
<u>NATURAL ABUNDANCE COMPARISON</u>			
A	325	C	2,682
B	24,210	D	354,800
E	18	G	37
F	212	H	541

**Supplementary Table 5.22 Comparison of Viscosities (60 °C) of Sets of Mixtures of SEC Fractions of Asphalts AAG-1 and AAK-1**

Mixture Designation	Viscosity, Pa · s, 60 °C	Mixture Designation	Viscosity, Pa · s, 60 °C
<u>SOLVENT PHASE COMPARISON</u>			
A	322	B	31
C	4,490	D	355
E	483	F	41
G	8,506	H	1,174
<u>DISPERSED PHASE COMPARISON</u>			
A	322	E	483
B	31	F	41
C	4,490	G	8,506
D	355	H	1,174
<u>NATURAL ABUNDANCE COMPARISON</u>			
A	322	C	4,490
B	31	D	355
E	483	G	8,506
F	41	H	1,174

**Supplementary Table 5.23 Comparison of Viscosities (60 °C) of Sets of Mixtures of SEC Fractions of Asphalts AAG-1 and AAM-1**

Mixture Designation	Viscosity, Pa · s, 60 °C	Mixture Designation	Viscosity, Pa · s, 60 °C
<u>SOLVENT PHASE COMPARISON</u>			
A	332	B	244
C	9,954	D	27,115
E	128	F	85
G	423	H	553
<u>DISPERSED PHASE COMPARISON</u>			
A	332	E	128
B	244	F	85
C	9,954	G	423
D	27,115	H	553
<u>NATURAL ABUNDANCE COMPARISON</u>			
A	332	C	9,954
B	244	D	27,115
E	128	G	423
F	85	H	553

**Supplementary Table 5.24 Relative Viscosities at 25 °C of Mixtures of SEC Fractions**

Mixture <sup>1</sup> Designation	Asphalts Comprising Mixtures and $\eta_{rel}$			
	AAD-1/AAK-1, $\eta_{rel}$	AAD-1/AAM-1, $\eta_{rel}$	AAG-1/AAK-1, $\eta_{rel}$	AAG-1/AAM-1, $\eta_{rel}$
A	238	260	5.7	6.1
B	218	217	7.1	10
C	453	1,395	95.5	148
D	427	669	161	321
E	165	7.7	8.4	1.5
F	148	5.8	9.4	2.3
G	304	22.5	85	5.2
H	241	14.5	255	17.4

<sup>1</sup> See Supplementary Tables 5.12 - 5.15 for exact compositions of mixtures.

**Supplementary Table 5.25 Polarity Factors of Mixtures of SEC Fractions**

Mixture <sup>1</sup> Designation	Asphalts Comprising Mixtures and Polarity Factors			
	AAD-1/AAK-1	AAD-1/AAM-1	AAG-1/AAK-1	AAG-1/AAM-1
A	125	125	105	105
B	122	136	74	90
C	133	147	131	140
D	130	157	105	128
E	109	83	109	96
F	106	94	77	81
G	115	93	139	115
H	112	97	112	97

<sup>1</sup> See Supplementary Tables 5.12-5.15 for Exact Compositions of Mixtures.

**Supplementary Table 6.4    Viscoelastic Properties of AAM-1 Asphalt after Extended Cure Time at 45 °C**

Cure Time, hr.	Elastic Modulus, $G'$ , dyne/cm <sup>2</sup>	Viscous Modulus, $G''$ , dyne/cm <sup>2</sup>	Viscosity <sup>1,2</sup> (Pa · s)	Tan $\delta$ <sup>2</sup>	Torque, g-cm
2	*	$2.13 \times 10^3$	$2.13 \times 10^3$	-	4
6	*	$2.35 \times 10^3$	$2.35 \times 10^3$	-	5
24	*	$3.11 \times 10^3$	$3.12 \times 10^3$	-	6
48	*	$3.91 \times 10^3$	$3.91 \times 10^3$	-	8
73	*	$5.06 \times 10^3$	$5.07 \times 10^3$	-	10
97	*	$4.07 \times 10^3$	$4.08 \times 10^3$	-	8
901	*	$3.94 \times 10^3$	$3.95 \times 10^3$	-	8
2,009	$4.47 \times 10^2$	$4.61 \times 10^3$	$4.63 \times 10^3$	10.31	9

<sup>1</sup> 0.1 rad/s

<sup>2</sup> See footnote 2, Tables 6.1 and 6.2

**Supplementary Table 6.5    Viscoelastic Properties of AAM-1 Asphalt after Extended Cure Time at 60 °C**

Cure Time, hr.	Viscous Modulus, $G''$ , dyne/cm <sup>2</sup>	Viscosity <sup>1,2</sup> (Pa · s)	Torque, g-cm
2	$2.21 \times 10^2$	$2.21 \times 10^3$	2
6	$2.20 \times 10^2$	$2.20 \times 10^3$	2
30	$2.36 \times 10^2$	$2.36 \times 10^3$	2
48	$2.37 \times 10^2$	$2.37 \times 10^3$	2
72	$2.34 \times 10^2$	$2.34 \times 10^3$	2
96	$2.50 \times 10^2$	$2.50 \times 10^3$	3
815	$3.01 \times 10^2$	$3.07 \times 10^3$	3
2,560	$4.06 \times 10^2$	$4.06 \times 10^3$	4

<sup>1</sup> 0.1 rad/s

<sup>2</sup> See footnote 2, Tables 6.1 and 6.2

**Supplementary Table 6.6 Viscoelastic Properties of AAG-1 Asphalt after Extended Cure Time at 60°C, 25 mm PP**

Cure Time, hr.	Viscous Modulus, $G''$ , dyne/cm <sup>2</sup>	Viscosity <sup>1,2</sup> (Pa · s)	Torque, g-cm
2	$2.19 \times 10^2$	$2.19 \times 10^2$	2
6	$2.19 \times 10^2$	$2.19 \times 10^2$	2
24	$2.17 \times 10^2$	$2.18 \times 10^2$	2
48	$2.28 \times 10^2$	$2.28 \times 10^2$	2
73	$1.94 \times 10^2$	$1.94 \times 10^2$	2
96	$2.10 \times 10^2$	$2.10 \times 10^2$	2
867	$2.11 \times 10^2$	$2.11 \times 10^2$	2
2,224	$2.27 \times 10^2$	$2.27 \times 10^2$	2

<sup>1</sup> 0.1 rad/s

<sup>2</sup> See footnote 2, Tables 6.1 and 6.2

**Supplementary Table 6.7 Rheological Properties of Aged AAK-1 at 25°C, 25 mm PP, 110°C Loading Temperature**

Cure Time, hr.	Elastic Modulus, $G'$ , dyne/cm <sup>2</sup>	Viscous Modulus, $G''$ , dyne/cm <sup>2</sup>	Viscosity <sup>1,2</sup> (Pa · s)	$G^*$ , dyne/cm <sup>2</sup>	Tan $\delta$ <sup>2</sup>	Torque, g-cm
2	$1.024 \times 10^6$	$1.951 \times 10^6$	$2.203 \times 10^6$	$2.203 \times 10^6$	1.906	169.6
7	$1.102 \times 10^6$	$2.059 \times 10^6$	$2.336 \times 10^6$	$2.336 \times 10^6$	1.868	179.6
24	$1.189 \times 10^6$	$2.177 \times 10^6$	$2.480 \times 10^6$	$2.480 \times 10^7$	1.831	190.6
48	$1.210 \times 10^6$	$2.201 \times 10^6$	$2.512 \times 10^6$	$2.512 \times 10^7$	1.819	192.9
121	$1.197 \times 10^6$	$2.161 \times 10^6$	$2.470 \times 10^6$	$2.470 \times 10^7$	1.806	189.8
493	$1.384 \times 10^6$	$2.416 \times 10^6$	$2.784 \times 10^6$	$2.784 \times 10^7$	1.746	213.5
614	$1.459 \times 10^6$	$2.532 \times 10^6$	$2.922 \times 10^6$	$2.922 \times 10^7$	1.736	224.0
1,050	$1.432 \times 10^6$	$2.472 \times 10^6$	$2.857 \times 10^6$	$2.857 \times 10^7$	1.727	223.8
5,091	$1.701 \times 10^6$	$2.847 \times 10^6$	$3.316 \times 10^6$	$3.316 \times 10^7$	1.673	253.6

<sup>1</sup> 0.1 rad/s, 0.64% strain

<sup>2</sup> See footnote 2, Tables 6.1 and 6.2



**Supplementary Table 6.8 Rheological Properties of Aged AAK-1 at 25 °C, 25 mm PP, 150 °C Loading Temperature**

Cure Time, hr.	Elastic Modulus, $G'$ , dyne/cm <sup>2</sup>	Viscous Modulus, $G''$ , dyne/cm <sup>2</sup>	Viscosity <sup>1,2</sup> (Pa · s)	$G^*$ , dyne/cm <sup>2</sup>	Tan $\delta$ <sup>2</sup>	Torque, g-cm
2	$9.203 \times 10^5$	$1.782 \times 10^6$	$2.005 \times 10^7$	$2.005 \times 10^6$	1.936	154.5
8	$9.989 \times 10^5$	$1.884 \times 10^6$	$2.132 \times 10^7$	$2.132 \times 10^6$	1.886	164.1
30	$1.143 \times 10^6$	$2.095 \times 10^6$	$2.387 \times 10^7$	$2.387 \times 10^6$	1.833	183.4
51	$1.210 \times 10^6$	$2.205 \times 10^6$	$2.515 \times 10^7$	$2.515 \times 10^6$	1.822	193.2
169	$1.240 \times 10^6$	$2.211 \times 10^6$	$2.535 \times 10^7$	$2.535 \times 10^6$	1.783	194.7
607	$1.222 \times 10^6$	$2.162 \times 10^6$	$2.483 \times 10^7$	$2.483 \times 10^6$	1.769	194.8
4,648	$1.634 \times 10^6$	$2.729 \times 10^6$	$3.180 \times 10^7$	$3.180 \times 10^6$	1.670	243.3

<sup>1</sup> 0.1 rad/s, 0.64% strain.

<sup>2</sup> See footnote 2, Tables 6.1 and 6.2

**Supplementary Table 6.9 Viscoelastic Properties of Aged Asphalt AAM-1 After Extended Cure Time at 25 °C, 25 mm PP**

Cure time, hr.	Elastic Modulus, $G'$ , dyne/cm <sup>2</sup>	Viscous Modulus, $G''$ , dyne/cm <sup>2</sup>	Viscosity <sup>1,2</sup> (Pa · s)	Tan $\delta$ <sup>2</sup>	Torque, g-cm
2	$2.62 \times 10^6$	$3.03 \times 10^6$	$4.00 \times 10^6$	1.16	304
6	$3.25 \times 10^6$	$3.54 \times 10^6$	$4.81 \times 10^6$	1.09	363
25	$3.54 \times 10^6$	$3.73 \times 10^6$	$5.14 \times 10^6$	1.05	387
49	$3.17 \times 10^6$	$3.39 \times 10^6$	$4.65 \times 10^6$	1.07	351
72	$3.36 \times 10^6$	$3.52 \times 10^6$	$4.87 \times 10^6$	1.05	367
96	$3.75 \times 10^6$	$3.82 \times 10^6$	$5.35 \times 10^6$	1.02	403
768	$3.95 \times 10^6$	$3.88 \times 10^6$	$5.54 \times 10^6$	0.98	416
2,401	$4.35 \times 10^6$	$4.06 \times 10^6$	$5.95 \times 10^6$	0.93	445

<sup>1</sup> 0.1 rad/s, 0.64% strain.

<sup>2</sup> See footnote 2, Tables 6.1 and 6.2

**Supplementary Table 6.10 Viscoelastic Properties of TFO-POV Aged Asphalt AAM-1 After Extended Cure Time at 45°C**

Cure time, hr.	Elastic Modulus, $G'$ , dyne/cm <sup>2</sup>	Viscous Modulus, $G''$ , dyne/cm <sup>2</sup>	Viscosity <sup>1,2</sup> (Pa · s)	Tan $\delta$ <sup>2</sup>	Torque, g-cm
2	$4.62 \times 10^3$	$2.95 \times 10^4$	$2.98 \times 10^4$	6.37	2
6	$9.07 \times 10^3$	$4.11 \times 10^4$	$4.21 \times 10^4$	4.53	3
24	$7.52 \times 10^3$	$3.20 \times 10^4$	$3.28 \times 10^4$	4.25	3
48	$9.67 \times 10^3$	$4.28 \times 10^4$	$4.39 \times 10^4$	4.43	3
72	$8.77 \times 10^3$	$3.59 \times 10^4$	$3.69 \times 10^4$	4.09	3
97	$9.21 \times 10^3$	$3.84 \times 10^4$	$3.95 \times 10^4$	4.17	3
839	$1.50 \times 10^4$	$4.87 \times 10^4$	$5.10 \times 10^4$	3.25	4
1,841	$1.97 \times 10^4$	$5.51 \times 10^4$	$5.85 \times 10^4$	2.80	5

<sup>1</sup> 0.1 rad/s

<sup>2</sup> See footnote 2, Tables 6.1 and 6.2

**Supplementary Table 6.11 Viscoelastic Properties of TFO-POV Aged Asphalt AAM-1 after Extended Cure Time at 60°C**

Cure Time, hr.	Viscous Modulus, $G''$ , dyne/cm <sup>2</sup>	Viscosity <sup>1,2</sup> (Pa · s)	Torque, g-cm
2	$8.80 \times 10^2$	$8.81 \times 10^2$	9
6	$9.10 \times 10^2$	$9.11 \times 10^2$	9
25	$9.18 \times 10^2$	$9.20 \times 10^2$	9
48	$1.06 \times 10^3$	$1.06 \times 10^2$	11
74	$1.08 \times 10^3$	$1.09 \times 10^2$	11
98	$1.16 \times 10^3$	$1.16 \times 10^2$	12
792	$1.78 \times 10^3$	$1.79 \times 10^2$	18
1,812	$1.23 \times 10^3$	$1.24 \times 10^2$	12

<sup>1</sup> 0.1 rad/s

<sup>2</sup> See footnote 2, Tables 6.1 and 6.2

**Supplementary Table 6.12      Viscoelastic Properties of Asphalt AAM-1 n-heptane  
Maltenes After Extended Cure Time at 0 °C**

Cure time, hr.	Elastic Modulus, G', dyne/cm <sup>2</sup>	Viscous Modulus, G'', dyne/cm <sup>2</sup>	Viscosity <sup>1,2</sup> (Pa · s)	Tan δ <sup>2</sup>	Torque, g-cm
2	6.66 x 10 <sup>6</sup>	6.51 x 10 <sup>6</sup>	3.73 x 10 <sup>7</sup>	0.98	683
6	9.38 x 10 <sup>6</sup>	8.17 x 10 <sup>6</sup>	4.97 x 10 <sup>7</sup>	0.87	892
24	1.40 x 10 <sup>6</sup>	1.06 x 10 <sup>7</sup>	7.01 x 10 <sup>7</sup>	0.76	1,212
48	1.36 x 10 <sup>7</sup>	1.04 x 10 <sup>7</sup>	6.82 x 10 <sup>7</sup>	0.76	1,183
73	1.53 x 10 <sup>7</sup>	1.12 x 10 <sup>7</sup>	7.58 x 10 <sup>7</sup>	0.73	1,295
96	1.49 x 10 <sup>7</sup>	1.10 x 10 <sup>7</sup>	7.41 x 10 <sup>7</sup>	0.74	1,271
762	2.40 x 10 <sup>7</sup>	1.42 x 10 <sup>7</sup>	1.12 x 10 <sup>8</sup>	0.59	1,789
2,556	2.19 x 10 <sup>7</sup>	1.32 x 10 <sup>7</sup>	1.02 x 10 <sup>8</sup>	0.60	1,662

<sup>1</sup> 0.025 rad/s, 0.64% strain

<sup>2</sup> See footnote 2, Tables 6.1 and 6.2

**Supplementary Table 6.13      Viscoelastic Properties of Asphalt AAM-1 Neutral Fraction  
after Extended Cure Time at 0 °C**

Cure time, hr.	Elastic Modulus, G', dyne/cm <sup>2</sup>	Viscous Modulus, G'', dyne/cm <sup>2</sup>	Viscosity <sup>1,2</sup> (Pa · s)	Tan δ <sup>2</sup>	Torque, g-cm
2	8.34 x 10 <sup>5</sup>	1.06 x 10 <sup>6</sup>	1.35 x 10 <sup>6</sup>	1.27	104
7	9.96 x 10 <sup>5</sup>	1.22 x 10 <sup>6</sup>	1.58 x 10 <sup>6</sup>	1.23	121
26	1.05 x 10 <sup>6</sup>	1.42 x 10 <sup>6</sup>	1.76 x 10 <sup>6</sup>	1.35	136
48	1.15 x 10 <sup>6</sup>	1.55 x 10 <sup>6</sup>	1.93 x 10 <sup>6</sup>	1.35	148
73	1.06 x 10 <sup>6</sup>	1.41 x 10 <sup>6</sup>	1.76 x 10 <sup>6</sup>	1.33	135
97	9.41 x 10 <sup>5</sup>	1.35 x 10 <sup>6</sup>	1.65 x 10 <sup>6</sup>	1.43	127
765	1.66 x 10 <sup>6</sup>	2.23 x 10 <sup>6</sup>	2.78 x 10 <sup>6</sup>	1.34	213
2,579	1.14 x 10 <sup>6</sup>	1.58 x 10 <sup>6</sup>	1.95 x 10 <sup>6</sup>	1.39	150

<sup>1</sup> 0.1 rad/s

<sup>2</sup> See footnote 2, Tables 6.1 and 6.2

**Supplementary Table 6.14 Viscoelastic Properties of Aged Core Asphalts after 2 Hour and 45 Day Cure at 25 °C**

Asphalt	Cure time, hr.	Elastic Modulus, $G'$ , dyne/cm <sup>2</sup>	Viscous Modulus, $G''$ , dyne/cm <sup>2</sup>	Viscosity <sup>1,2</sup> (Pa · s)	Tan $\delta$ <sup>2</sup>
AAA-1	2	$3.684 \times 10^5$	$1.358 \times 10^6$	$1.650 \times 10^4$	3.6
	1,080	$3.875 \times 10^5$	$1.358 \times 10^6$	$2.482 \times 10^4$	3.5
AAB-1	2	$1.624 \times 10^6$	$4.293 \times 10^6$	$4.941 \times 10^4$	2.6
	1,080	$1.582 \times 10^6$	$3.918 \times 10^6$	$6.366 \times 10^4$	2.4
AAC-1	2	$1.851 \times 10^5$	$1.027 \times 10^6$	$1.338 \times 10^4$	5.5
	1,080	$2.133 \times 10^5$	$1.025 \times 10^6$	$1.900 \times 10^4$	4.8
AAD-1	2	$7.035 \times 10^5$	$1.961 \times 10^6$	$2.321 \times 10^4$	2.7
	1,080	$7.434 \times 10^5$	$1.957 \times 10^6$	$3.128 \times 10^4$	2.6
AAF-1	2	$3.265 \times 10^6$	$1.023 \times 10^7$	$1.793 \times 10^5$	3.1
	1,080	$3.559 \times 10^6$	$1.024 \times 10^7$	$2.561 \times 10^5$	2.8
AAG-1	2	$1.674 \times 10^6$	$1.045 \times 10^7$	$2.153 \times 10^5$	6.2
	1,080	$1.771 \times 10^6$	$1.045 \times 10^7$	$2.113 \times 10^5$	5.9
AAK-1	2	$1.591 \times 10^6$	$3.942 \times 10^6$	$8.440 \times 10^4$	2.4
	1,080	$1.681 \times 10^6$	$3.918 \times 10^6$	$1.036 \times 10^5$	2.3
AAM-1	2	$2.691 \times 10^6$	$5.812 \times 10^6$	$1.132 \times 10^5$	2.1
	1,080	$2.862 \times 10^6$	$5.792 \times 10^6$	$1.696 \times 10^5$	2.0

<sup>1</sup> 0.1 rad/s, 25 mm parallel plates

<sup>2</sup> See footnote 2, Tables 6.1 and 6.2

**Supplementary Table 8.37 Viscosities and Aging Indices of Core Asphalts after TFO**

Asphalt	Run No.	Viscosity (Pa·s), <sup>1</sup> 60°C, 0.1 rad/s, after TFO	Aging Index
AAA-1	1	208	1.8
	2	<u>185</u>	
	Avg.	196	
AAB-1	1	331	1.9
	2	<u>270</u>	
	Avg.	300	
AAC-1	1	225	1.9
	2	<u>191</u>	
	Avg.	208	
AAD-1	1	390	2.7
	2	<u>319</u>	
	Avg.	355	
AAF-1	1	616	2.3
	2	<u>443</u>	
	Avg.	530	
AAG-1	1	349	1.4
	2	<u>333</u>	
	Avg.	341	
AAK-1	1	1,040	2.5
	2	<u>1,050</u>	
	Avg.	1,045	
AAM-1	1	448	1.7
	2	<u>418</u>	
	Avg.	433	

<sup>1</sup> Viscosity measurements on the Rheometrics Mechanical Spectrometer are estimated to have an error bar of  $\pm 10\%$ .

**Supplementary Table 8.38 Changes in Rheological and Chemical Properties During Thin-Film Oven + 60°C PAV (300 psi) Oxidation of SIIRP Asphalts**

Asphalt	Oxidation Time, hrs	Dynamic Viscosity ( $\eta^*$ ) <sup>1</sup> 60°C, Pa·s	Carbonyl Absorbance <sup>2</sup> Units	Sulfoxide <sup>2</sup> M/L	Aging Index
AAC-2	0	53.0	0.025	0.144	5.30
	144	$2.81 \times 10^1$	0.09	0.217	
AAD-2	0	72.3	0.053	0.016	10.69
	144	$7.73 \times 10^2$	0.07	0.284	
AAG-2	0	121.2	0.14	0.237	4.83
	144	$5.85 \times 10^2$			
AAK-2	0	121.1	0.03	0.107	8.84
	144	$1.07 \times 10^3$	0.06	0.226	
AAM-2	0	130.5	0.015	0.016	8.89
	144	$1.16 \times 10^3$	0.11	0.101	
AAE	0	513.6	0.025	0.028	11.89
	96	$5.11 \times 10^3$	0.06	0.187	
	144	$6.11 \times 10^3$	0.07	0.223	
	400	$1.46 \times 10^4$	0.09	0.317	
AAH	0	149.0	<0.005	0.073	10.47
	144	$1.56 \times 10^2$	0.09	0.227	
	400	$2.62 \times 10^3$	0.13	0.249	
AAJ	0	269.0	0.02	0.036	10.93
	144	$2.94 \times 10^3$	0.10	0.163	
	400	$5.63 \times 10^3$	0.12	0.141	
AAL	0	106.0	0.024	0.031	8.49
	144	$9.00 \times 10^2$	0.06	0.243	
AAN	0	191.0	0.01	0.033	7.33
	96	$9.36 \times 10^2$	0.05	0.227	
	144	$1.40 \times 10^3$	0.05	0.261	
	400	$2.26 \times 10^3$	0.08	0.309	
AAO	0	154.0	0.016	0.052	5.73
	144	$8.82 \times 10^2$	0.06	0.201	

Continued on next page

Supplementary Table 8.38 continued

AAP	0	325.0	0.03	0.041	10.68
	144	$3.47 \times 10^3$	0.11	0.124	
AAQ	0	135.0	0.01	0.073	5.93
	144	$8.01 \times 10^2$	0.08	0.206	
AAR	0	284.0	0.025	0.040	7.85
	144	$2.23 \times 10^3$	0.06	0.24	
AAS-1	0	283.0	<0.005	0.022	7.07
	96	$1.72 \times 10^3$	0.04	0.211	
	144	$2.00 \times 10^3$	0.04	0.224	
	400	$3.36 \times 10^3$	0.07	0.275	
AAT	0	285.4	0.018	0.057	8.65
	144	$2.47 \times 10^3$	0.05	0.249	
AAU	0	286.2	0.026	0.039	12.44
	144	$3.56 \times 10^3$	0.06	0.265	
AAV	0	79.4	<0.005	0.033	4.61
	144	$3.66 \times 10^2$	0.07	0.230	
	400	$4.83 \times 10^2$	0.11	0.254	
AAW	0	286.0	<0.005	0.030	13.39
	96	$2.34 \times 10^3$	0.04	0.235	
	144	$3.83 \times 10^3$	0.05	0.265	
	400	$8.18 \times 10^3$	0.08	0.307	
AAX	0	254.0	0.011	0.075	8.82
	144	$2.24 \times 10^3$	0.08	0.213	
	400	$4.84 \times 10^3$	0.13	0.226	
AAZ	0	260.0	0.01	0.045	3.88
	144	$1.01 \times 10^3$	0.07	0.227	
	400	$1.81 \times 10^3$	0.11	0.274	
ABD	0	245.0	0.03	0.024	6.04
	48	$8.39 \times 10^2$	0.07	0.136	
	144	$1.48 \times 10^3$	0.10	0.256	

<sup>1</sup> Viscosity measurements on the Rheometrics Mechanical Spectrometer are estimated to have an error bar of  $\pm 10\%$ .

<sup>2</sup> Based on prior experience with asphalts, standard deviations are (mol/L): sulfoxides, 0.027; ketones, 0.006.

**Supplementary Table 8.39 Changes in Rheological and Chemical Properties During Thin-Film Oven + 70 °C PAV (300 psi) Oxidation of SHRP Asphalts**

Asphalt	Oxidation Time, hrs	Dynamic Viscosity ( $\eta^*$ ) <sup>1</sup> 60 °C, Pa · s	Carbonyl Absorbance <sup>2</sup> Units	Sulfoxide <sup>2</sup> M/L	Aging Index
AAC-2	0	53.0	0.025	0.144	7.68
	144	4.07 x 10 <sup>2</sup>	0.12	0.23	
AAD-2	0	72.3	0.053	0.016	22.54
	144	1.63 x 10 <sup>3</sup>	0.09	0.37	
AAG-2	0	121.2	0.19	0.24	6.54
	144	7.93 x 10 <sup>2</sup>			
AAK-2	0	121.1	0.03	0.107	15.44
	144	1.87 x 10 <sup>3</sup>	0.08	0.31	
AAM-2	0	130.5	0.015	0.016	17.09
	144	2.23 x 10 <sup>3</sup>	0.13	0.11	
AAE	0	513.6	0.025	0.028	24.14
	144	1.24 x 10 <sup>4</sup>	0.09	0.34	
AAH	0	149.0	<0.005	0.073	17.80
	144	2.65 x 10 <sup>3</sup>	0.13	0.28	
AAJ	0	269.0	0.02	0.036	15.28
	144	4.11 x 10 <sup>3</sup>	0.13	0.19	
AAN	0	191.0	0.01	0.033	12.98
	144	2.48 x 10 <sup>3</sup>	0.07	0.33	
AAS-1	0	283.0	<0.005	0.022	10.31
	144	2.92 x 10 <sup>3</sup>	0.07	0.29	
AAV	0	79.4	<0.005	0.033	6.85
	144	5.44 x 10 <sup>2</sup>	0.10	0.27	
AAW	0	286.0	<0.005	0.030	22.89
	144	6.55 x 10 <sup>3</sup>	0.07	0.34	
AAX	0	254.0	0.011	0.075	13.29
	144	3.38 x 10 <sup>3</sup>	0.12	0.24	
AAZ	0	260.0	0.01	0.045	-
	144	-	-	-	
ABD	0	245.0	0.03	0.024	8.29
	144	2.03 x 10 <sup>3</sup>	0.15	0.30	

<sup>1</sup> Viscosity measurements on the Rheometrics Mechanical Spectrometer are estimated to have an error bar of  $\pm 10\%$ .

<sup>2</sup> Based on prior experience with asphalts, standard deviations are (mol/L): sulfoxides, 0.027; ketones, 0.006.



**Supplementary Table 8.40 Changes in Rheological and Chemical Properties During Thin-Film Oven + 80°C PAV (300 psi) Oxidation of SHRP Asphalts**

Asphalt	Oxidation Time, hrs	Dynamic Viscosity ( $\eta^*$ ) <sup>1</sup> 60°C, Pa·s	Carbonyl Absorbance <sup>2</sup> Units	Sulfoxide <sup>2</sup> M/L	Aging Index
AAC-2	0 144	53.0 $7.47 \times 10^2$	0.025 0.14	0.144 0.18	14.09
AAD-2	0 144	72.3 $4.98 \times 10^3$	0.053 0.10	0.016 0.42	68.88
AAG-2	0 144	121.2 $1.04 \times 10^3$	0.24	0.18	8.58
AAK-2	0 144	121.1 $5.59 \times 10^3$	0.03 0.12	0.107 0.37	46.16
AAM-2	0 144	130.5 $4.00 \times 10^3$	0.015 0.16	0.016 0.08	30.65
AAE	0 144	513.6 $5.41 \times 10^4$	0.025 0.12	0.028 0.38	105.30
AAH	0 144	149.0 $5.98 \times 10^3$	<0.005 0.16	0.073 0.25	40.16
AAJ	0 144	269.0 $1.29 \times 10^4$	0.02 0.16	0.036 0.16	47.96
AAN	0 144	191.0 $6.23 \times 10^3$	0.01 0.11	0.033 0.37	32.62
AAS-1	0 144	283.0 $6.80 \times 10^3$	<0.005 0.11	0.022 0.34	24.02
AAV	0 144	79.4 $6.72 \times 10^2$	<0.005 0.14	0.033 0.23	8.46
AAW	0 144	286.0 $2.45 \times 10^4$	<0.005 0.11	0.030 0.32	85.63
AAX	0 144	254.0 $6.88 \times 10^3$	0.011 0.15	0.075 0.21	27.04
AAZ	0 144	260.0	0.01	0.045	
ABD	0 144	245.0 $3.83 \times 10^3$	0.03 0.17	0.024 0.24	15.64

<sup>1</sup> Viscosity measurements on the Rheometrics Mechanical Spectrometer are estimated to have an error bar of  $\pm 10\%$ .

<sup>2</sup> Based on prior experience with asphalts, standard deviations are (mol/L): sulfoxides, 0.027; ketones, 0.006.

**Supplementary Table 8.41 Viscosities and Yields of SEC Fraction-II Materials of Core Asphalts and TFAAT (130°C; 4 Hrs; 12 Hrs) Aged Asphalts**

Asphalt	Mass Fraction SEC Fraction II Core Asphalt	Viscosity (Pa·s), <sup>1</sup> SEC Fraction II, 1.0 Radians/sec. <u>Core Asphalt</u> 25 °C	Mass Fraction SEC Fraction II, TFAAT Aged (4 hrs) Asphalt	Viscosity (Pa·s), SEC Fraction II TFAAT Aged (4 hrs) <u>Asphalt, 1.0 Radians/sec</u> 25 °C	Mass Fraction SEC Fraction II TFAAT Aged (12 hrs) Asphalt	Viscosity (Pa·s), SEC Fraction II TFAAT Aged (12 hrs) <u>Asphalt, 1.0 Radians/sec</u> 25 °C	45 °C
AAA-1	78.2	506	74.0	520	72.0	452	232
AAB-1	78.3	1,367	74.7	1,434	72.7	1,482	438
AAC-1	85.8	8,602	82.6	11,170	81.8	15,230	2,173
AAD-1	76.6	337	72.4	360	70.1	369	161
AAF-1	85.6	53,350	81.3	-	78.7	35,530	3,631
AAG-1	87.1	62,380	85.0	98,570	83.1	98,510	12,070
AAK-1	74.1	1,124	70.9	1,313	68.1	10,090	407
AAM-1	69.5	26,350	65.4	29,840	63.7	20,760	2,963

<sup>1</sup> Viscosity measurements on the Rheometrics Mechanical Spectrometer are estimated to have an error bar of ± 10%.

**Supplementary Table 8.42 Molecular Weights of SEC Fraction I of Both Unaged Asphalts and of TFAAT (130 °C; 12 Hrs) Aged Asphalts, and S Concentrations of Parent Asphalts**

Asphalt	Molecular Weight, <sup>1</sup> SEC-Fraction I, Core Asphalt 60 °C, VPO, toluene	Molecular Weight, <sup>1</sup> SEC-Fraction I, TFAAT Aged (12 hr. 130 °C) 60 °C, VPO, toluene	Sulfur <sup>2</sup> Conc. of Asphalt mass %
AAA-1	11,000	11,500	5.5
AAB-1	9,200	9,800	4.7
AAC-1	7,300	8,400	1.9
AAD-1	7,000	13,900	6.9
AAF-1	8,690	10,100	3.4
AAG-1	7,900	7,800	1.3
AAK-1	10,000	13,000	6.4
AAM-1	4,600	5,700	1.2

<sup>1</sup> ASTM Method D 2503 is estimated to have an error bar of  $\pm 10\%$  in this molecular weight range.

<sup>2</sup> Based on experience with a large number of fossil fuel samples, the standard deviation for the analysis of sulfur is 0.36.

**Supplementary Table 8.43 Sulfoxide and Carbonyl Concentrations of SEC Fractions of TFO-PAV (60°C; 144 hours) Aged Asphalts**

Asphalt	Run No.	SEC Fraction	Sulfoxide Conc. (M/L)	Ketone Absorbance Units
AAA-1	1	I	0.27	0.09
		II	0.19	0.10
	2	I	0.25	0.07
		II	0.20	0.09
AAB-1	1	I	0.21	0.10
		II	0.25	0.08
	2	I	0.23	0.08
		II	0.27	0.09
AAC-1	1	I	0.27	0.14
		II	0.15	0.12
	2	I	-	-
		II	0.19	0.11
AAD-1	1	I	0.56	0.09
		II	0.27	0.11
AAF-1	1	I	0.25	0.10
		II	0.23	0.08
	2	I	0.27	0.10
		II	0.25	0.09
AAG-1	1	I	0.20	0.13
		II	0.17	0.16
AAK-1	1	I	0.20	0.08
		II	0.25	0.12
	2	I	0.22	0.08
		II	0.24	0.09
AAM-1	1	I	0.08	0.11
		II	0.08	0.14
	2	I	0.08	0.12
		II	0.12	0.15

Standard deviations were estimated by multiplying the average of the ranges of each of the replicate determinations by 0.886. Thus the standard deviation for sulfoxides of SEC Fraction-I materials is 0.021, and 0.0009 for carbonyl content of SEC Fraction-I materials. For the SEC Fraction-II materials, the standard deviation is 0.014 for sulfoxides and 0.012 for carbonyls. For three oxidized asphalts a value of 0.027 was calculated for the standard deviation of sulfoxides and 0.006 for carbonyls using the standard method of calculation.

Supplementary Table 8.44 Mass Fractions of Core Asphalt SEC Fraction-II, Aged<sup>1</sup> Asphalt SEC Fraction-II, and Molecular Weights<sup>2</sup> of Core Asphalt SEC Fraction-I and Aged<sup>1</sup> Asphalt SEC Fraction-I

Asphalt	Mass Fraction, SEC Fraction-II Unaged Asphalt	Mass Fraction <sup>3</sup> , SEC Fraction-II Aged Asphalt	Difference (Column 2 - Column 3)	MW, SEC Fraction-I Unaged Asphalt	MW, SEC Fraction-I Aged Asphalt	Aging Index <sup>4</sup>
AAA-1	78.2	75.9	2.3	11,000	8,970	6.11
AAB-1	78.3	75.3	3.0	9,200	8,660	6.75
AAC-1	85.8	83.1	2.7	7,300	7,460	6.24
AAD-1	76.6	72.6	4.0	7,000	13,710	11.83
AAF-1	85.6	81.7	3.9	8,690	7,370	9.79
AAG-1	87.1	85.7	1.4	7,900	5,380	3.84
AAK-1	74.1	71.5	2.6	10,000	10,600	8.34
AAM-1	69.5	65.3	4.2	4,600	5,640	9.33

<sup>1</sup> Aging was by TFO-PAV, 60 °C, 144 hours

<sup>2</sup> MW values were determined in toluene at 60 °C by VPO, and so these values are number-average MW's. There were no replicate determinations. At these levels, errors are estimated to be  $\pm 10\%$  by this method.

<sup>3</sup> These are averages of two determinations. The standard deviation of 0.53 is calculated by determining the average of the ranges and multiplying by 0.886.

<sup>4</sup> Aging indices were calculated by dividing dynamic viscosities of aged asphalts measured at 60 °C and 0.1 radians/sec by viscosities of unaged asphalts measured under the same conditions. Aged and unaged asphalts were subjected to the same annealing protocol. The statistical analyses of these measurements is presented in the report for subtask 1.1.5.

Supplementary Table 8.45 Viscosities and Yields of SEC Fraction-II of Core Asphalts and Aged<sup>1</sup> Asphalts

Asphalt	Unaged Core Asphalt		Run No. <sup>2</sup>	TFO-PAV Aged Asphalt	
	Mass Fraction SEC Fraction-II	Viscosity (Pa·s) SEC Fraction-II 1.0 Radians/Sec		Mass Fraction <sup>3</sup> SEC Fraction-II	Viscosity (Pa·s) SEC Fraction-II
		25 °C      45 °C			25 °C      45 °C
AAA-1	78.2	506      28.5	1 2	75.3 76.4	678.6 749.7
AAB-1	78.3	1,367      42.2	1 2	75.6 75.1	2,023 2,227
AAC-1	85.8	8,620      176.2	1 2	83.3 82.9	16,770 16,740
AAD-1	76.6	337      16.9	1 2	72.6 72.7	648.3 -
AAF-1	85.6	53,350      381.0	1 2	82.0 81.4	65,120 66,630
AAG-1	87.1	62,380      864.1	1 2	85.4 85.9	155,100 1,621
AAK-1	74.1	1,124      46.3	1 2	71.9 71.2	1,459 1,374
AAM-1	69.5	26,350      384	1 2	65.8 64.9	37,730 24,790

<sup>1</sup> Aging conditions were 60 °C, 144 hrs, TFO-PAV

<sup>2</sup> These runs represent different SEC separations of the same aged samples

<sup>3</sup> The standard deviation of 0.532 for these determinations was estimated by multiplying the average of the sum of the ranges by 0.886.

**Supplementary Table 8.46 Carbonyl Absorbance and Sulfoxide Concentrations of PSU Aged Asphalts**

Asphalt	Aging Temperature, °C	Sulfoxide <sup>1</sup> Concentration, mol/L	Ketones, <sup>1</sup> Absorbance Units
AAD-1	100	0.25	0.11
	113	0.32	0.15
AAG-1	100	0.15	0.19
	113	0.14	0.26
AAK-1	100	0.26	0.10
	113	0.30	0.17
AAM-1	100	0.08	0.15
	113	0.06	0.22

<sup>1</sup> Replicate runs have not yet been performed. Based on prior experience, standard deviations are: sulfoxides - 0.027 mol/L, carbonyl - 0.006 absorption units.

**Supplementary Table 8.47 Reduced Specific Viscosity Measurements of TFAAT Aged AAA-1 Maltenes and Asphaltenes**

Asphaltene Content <sup>1</sup>		Viscosity (Pa·s) <sup>2</sup>		Reduced Specific Viscosity	
mass %	% natural abundance	25 °C	60 °C	25 °C	60 °C
0	0	285	4	-	-
7.6	25	12,600	62	570	186
15.2	50	109,000	170	2,500	265
22.7	75	175,000	916	2,710	977
30.3	100	846,000	9,030	9,810	7,246
37.9	125	-	78,100	-	50,120

<sup>1</sup> The standard deviation for asphaltene precipitation with n-heptane is estimated to be 0.78.

<sup>2</sup> Viscosity measurements on the Rheometrics Mechanical Spectrometer are estimated to have an error bar of ± 10%.

**Supplementary Table 8.48 Reduced Specific Viscosity Measurements of TFAAT Aged AAB-1 Maltenes and Asphaltenes**

Asphaltene Content <sup>1</sup>		Viscosity (Pa·s) <sup>2</sup>		Reduced Specific Viscosity	
mass %	% natural abundance	25 °C	60 °C	25 °C	60 °C
0	0	731	5	-	-
1.5	5	1,190	6	42	11
7.6	25	3,110	17	43	29
15.1	50	13,900	56	119	64
22.6	75	153,000	1,430	922	1,190
30.2	100	11,800,000	332,000	53,400	207,000
37.8	125	12,500,000	925,000	45,200	462,000

<sup>1</sup> See footnote 1, Supplementary Table 8.47.

<sup>2</sup> See footnote 2, Supplementary Table 8.47.

**Supplementary Table 8.49 Reduced Specific Viscosity Measurements of TFAAT Aged AAC-1 Maltenes and Asphaltenes**

Asphaltene Content <sup>1</sup>		Viscosity (Pa·s) <sup>2</sup>		Reduced Specific Viscosity	
mass %	% natural abundance	25 °C	60 °C	25 °C	60 °C
0	0	539	16	-	-
5.2	25	13,900	28	30	15
10.5	50	40,500	84	62	41
15.8	75	514,000	544	598	214
21.0	100	445,000	952	388	285
26.2	125	-	40,200	-	9,778

<sup>1</sup> See footnote 1, Supplementary Table 8.47.

<sup>2</sup> See footnote 2, Supplementary Table 8.47.



**Supplementary Table 8.50 Reduced Specific Viscosity Measurements of TFAAT Aged AAD-1 Maltenes and Asphaltenes**

Asphaltene Content <sup>1</sup>		Viscosity (Pa · s) <sup>2</sup>		Reduced Specific Viscosity	
mass %	% natural abundance	25 °C	60 °C	25 °C	60 °C
0	0	170	2	-	-
9	25	660	6	32	30
18	50	11,700	52	377	167
27	75	153,000	107	3,328	2,368
36	100	-	13,900	-	23,160
45	125	-	215,000	-	286,600

<sup>1</sup> See footnote 1, Supplementary Table 8.47.

<sup>2</sup> See footnote 2, Supplementary Table 8.47.

**Supplementary Table 8.51 Reduced Specific Viscosity Measurements of TFAAT Aged AAF-1 Maltenes and Asphaltenes**

Asphaltene Content <sup>1</sup>		Viscosity (Pa · s) <sup>2</sup>		Reduced Specific Viscosity	
mass %	% natural abundance	25 °C	60 °C	25 °C	60 °C
0	0	8,271	10	-	-
1.4	5	7,819	16	-3.82	44
7.2	25	23,720	33	26	33
14.3	50	252,000	218	206	152
21.4	75	2,658,000	2,665	1,500	1,290
28.6	100	11,090,000	44,120	4,680	11,100
35.8	125	31,350,000	316,900	10,600	92,000

<sup>1</sup> See footnote 1, Supplementary Table 8.47.

<sup>2</sup> See footnote 2, Supplementary Table 8.47.

**Supplementary Table 8.52 Reduced Specific Viscosity Measurements of TFAAT Aged AAG-1 Maltenes and Asphaltenes**

Asphaltene Content <sup>1</sup>		Viscosity (Pa·s) <sup>2</sup>		Reduced Specific Viscosity	
mass %	% natural abundance	25 °C	60 °C	25 °C	60 °C
0	0	117,000	133	-	-
3.6	25	257,000	235	33	21
7.3	50	742,000	514	73	39
10.9	75	993,000	794	69	46
14.5	100	1,550,000	1,400	85	66
18.1	125	4,190,000	4,050	193	163

<sup>1</sup> See footnote 1, Supplementary Table 8.47.

<sup>2</sup> See footnote 2, Supplementary Table 8.47.

**Supplementary Table 8.53 Reduced Specific Viscosity Measurements of TFAAT Aged AAK-1 Maltenes and Asphaltenes**

Asphaltene Content <sup>1</sup>		Viscosity (Pa·s) <sup>2</sup>		Reduced Specific Viscosity	
mass %	% natural abundance	25 °C	60 °C	25 °C	60 °C
0	0	378	9	-	-
1.9	5	836	9	81	8
9.7	25	2,020	19	53	15
19.4	50	36,900	149	571	95
29.2	75	233,000	48,700	2,410	21,700
38.9	100	20,100,000	1,580,000	157,000	529,000
48.6	125	50,500,000	6,960,000	315,000	1,860,000

<sup>1</sup> See footnote 1, Supplementary Table 8.47.

<sup>2</sup> See footnote 2, Supplementary Table 8.47.

Supplementary Table 9.11 Elemental Analyses and Molecular Weights of Expanded Set Asphalts

Asphalt	Element <sup>1</sup>						H/C (atomic ratio)	M <sub>n</sub> (Daltons) <sup>2</sup> Toluene	
	(mass %)					(ppm)			
	C	H	N	S	O				
AAE	83.8	10.1	0.7	5.2	1.0	90.8	179	1.44	820
AAH	86.3	10.1	0.8	2.8	1.0	43.1	84	1.39	840
AAJ	86.5	10.7	0.6	1.9	0.7	74.0	148	1.47	1,030
AAL	83.4	10.1	0.6	5.5	1.0	97.8	244	1.44	760
AAN	84.5	10.2	0.7	4.3	0.8	65.4	157	1.44	890
AAO	83.8	10.1	0.4	5.0	0.5	45.7	163	1.44	930
AAP	85.9	10.9	0.6	1.7	0.8	68.1	128	1.51	1,090
AAQ	85.5	10.1	0.6	3.6	0.5	51.4	127	1.41	810
AAR	84.1	10.1	0.7	4.6	0.6	79.0	334	1.43	880
AAS-1	84.0	10.0	0.6	5.4	0.8	52.4	159	1.42	960
AAT	83.9	10.1	0.6	5.1	0.7	80.1	201	1.43	880
AAU	84.4	10.2	0.8	4.0	0.7	97.6	197	1.44	880
AAV	86.4	10.5	0.8	2.4	1.1	40.8	92.1	1.45	890
AAW	84.5	10.1	0.7	4.5	0.9	80.3	334	1.42	890
AAX	86.6	10.4	0.8	2.4	1.1	55.9	116	1.43	970
AAZ	83.7	10.1	0.6	5.4	0.5	88.4	439	1.44	860
AAZ	85.0	10.0	0.6	4.4	0.9	35.0	102	1.40	970
ABC	83.2	9.9	0.3	6.4	0.4	25.1	37	1.42	870
ABD	86.8	10.7	1.2	1.6	1.2	123	61.9	1.47	728
AAC-2	86.6	10.6	0.9	1.9	1.0	54.9	100	1.46	870

<sup>1</sup> Analyses for C, H, N, S, O are standard methods and their standard deviations are (mass %): carbon, 0.36; hydrogen, 0.20; nitrogen, 0.09; oxygen, 0.41; sulfur, 0.36. For nickel and vanadium, standard deviations are (ppm): 14.7 and 18.4, respectively.

<sup>2</sup> The MW data was obtained by a vapor phase osmometry method at 60°C in toluene. For most of these values, error bars are  $\pm 5\%$ . It is the nature of the method that for the error increases as MW's increase, so that for values over 1,000 Daltons, the error bar is  $\pm 10\%$ .

**Supplementary Table 9.12 Infrared Functional Group Analysis of Expanded Set of Asphalts**

Sample	Functional Group (Moles/L) <sup>1</sup>						
	Sulfoxide	Ketone	Carboxylic Acid	Carboxylic Acid Salt	2-Quinolone	Pyrrolic N-H	Phenolic O-H
AAE	0.028	<0.005	0.015	<0.005	0.008	0.132	0.029
AAH	0.073	<0.005	<0.005	<0.005	0.008	0.180	0.017
AAJ	0.036	<0.005	<0.005	<0.005	0.008	0.218	0.036
AAL	0.031	<0.005	0.013	<0.005	0.011	0.166	0.045
AAN	0.033	<0.005	<0.005	<0.005	0.014	0.168	0.030
AAO	0.052	<0.005	0.008	<0.005	0.008	0.171	0.003
AAP	0.041	0.022	<0.005	<0.005	0.010	0.183	0.047
AAQ	0.073	<0.005	<0.005	<0.005	0.011	0.173	0.015
AAR	0.040	<0.005	0.009	<0.005	0.018	0.190	0.013
AAS-1	0.022	<0.005	<0.005	<0.005	0.009	0.118	0.013
AAT	0.057	<0.005	0.006	<0.005	0.012	0.214	0.017
AAU	0.039	<0.005	0.007	<0.005	0.019	0.239	0.043
AAV	0.033	<0.005	<0.005	<0.005	0.007	0.196	0.036
AAW	0.030	<0.005	<0.005	<0.005	0.017	0.155	0.052
AAX	0.075	<0.005	0.009	<0.005	0.011	0.196	0.048
AAZ	0.048	<0.005	<0.005	<0.005	0.012	0.204	0.027
AAZ	0.045	<0.005	0.008	<0.005	0.008	0.166	0.022
ABD	0.024	<0.005	0.025	<0.005	0.015	0.376	0.077
AAC-2	0.144	<0.005	<0.005	<0.005	0.010	0.214	0.010
AAD-2	0.016	<0.005	0.020	<0.005	0.018	0.213	0.032
AAK-2	0.107	<0.005	0.023	<0.005	0.010	0.182	0.006
AAM-2	0.016	<0.005	0.008	<0.005	0.006	0.187	0.034

<sup>1</sup> Based on prior experience with asphalts, standard deviations are (mol/L): sulfoxides, 0.027; ketones, 0.006; carboxylic acids, 0.005; 2-quinolones, 0.002. The analyses for N-H and O-H are qualitative.

**Supplementary Table 9.13 Asphaltene Yields of Expanded Set Asphalts Determined by Different Operators**

Asphalt	Operator (Initials)	Heptane <sup>1</sup> Asphaltenes H <sub>A</sub> (mass %)	Iso-octane <sup>2</sup> Asphaltenes I <sub>A</sub> (mass %)	ACI, [I <sub>A</sub> / (H <sub>A</sub> + I <sub>A</sub> )] × 10
AAE	MC	22.5	2.0	0.77
	AG	<u>23.4</u>	<u>1.8</u>	
	Average	22.9	1.9	
AAH	MC	15.8	3.9	1.92
	MC	<u>16.0</u>	<u>3.7</u>	
	Average	15.9	3.8	
AAJ	MC	10.1	3.9	2.59
	AG	<u>11.1</u>	<u>3.5</u>	
	Average	10.6	3.7	
AAN	MC	15.3	3.1	1.51
	AG	<u>16.2</u>	<u>2.6</u>	
	Average	15.7	2.8	
AAS-1	MC	17.7	3.3	1.36
	AG	<u>19.1</u>	<u>2.5</u>	
	Average	18.4	2.9	
AAV	MC	9.2	3.8	2.54
	AG	<u>10.2</u>	<u>2.8</u>	
	Average	9.7	3.3	
AAW	MC	17.4	2.9	1.39
	AG	<u>18.5</u>	<u>2.9</u>	
	Average	17.9	2.9	
AAX	MC	11.9	3.2	2.05
	AG	<u>12.1</u>	<u>2.9</u>	
	Average	12.0	3.1	
AAZ	MC	8.9	3.8	3.03
	DG	<u>9.5</u>	<u>4.1</u>	
	Average	9.2	4.0	
ABD	MC	6.7	3.2	3.14
	AG	<u>7.3</u>	<u>3.1</u>	
	Average	7.0	3.2	

<sup>1</sup> For the ten asphalts for which there are duplicate determinations, a standard deviation of 0.700 for heptane asphaltene yield was calculated by multiplication of the average of the ranges by 0.886. The standard deviation for n-heptane asphaltene preparations from a wide variety of tar sands and heavy oil has been determined to be 1.15 (mass %).

<sup>2</sup> For the ten asphalts for which there are duplicate determinations, a standard deviation of 0.337 was calculated by multiplication of the average of the ranges by 0.886.

**Supplementary Table 9.14 Comparison of Asphaltene Yields and Asphaltene Compatibility Indices of Selected Core Asphalts and Lower Viscosity Grades of Core Asphalts**

Asphalt	Heptane Asphaltenes $H_A$ (mass %)	Iso-octane Asphaltenes $I_A$ (mass %)	ACI, $[I_A / (H_A + I_A)] \times 10$
AAC-1 (Avg.)	9.9	3.3	2.45
AAC-2	9.8	3.4	
	<u>11.0</u>	<u>2.2</u>	
	10.5 (Avg.)	2.8 (Avg.)	2.10
AAD-1 (Avg.)	20.2	3.4	1.44
AAD-2	20.1	3.1	1.34
AAG-1 (Avg.)	5.0	3.3	3.97
AAG-2	4.8	2.7	
	<u>5.2</u>	<u>2.8</u>	
	5.0 (Avg.)	2.8 (Avg.)	3.59
AAK-1 (Avg.)	20.1	2.8	1.22
AAK-2	18.7	2.5	
	<u>19.7</u>	-	
	19.2 (Avg.)		1.15
AAM-1 (Avg.)	3.7	5.4	5.93
AAM-2	3.8	4.8	
	5.3	-	
	<u>5.3</u>	<u>4.1</u>	
	4.8 (Avg.)	4.5 (Avg.)	4.84

**Supplementary Table 9.15 Heithaus Parameters of Members of the Expanded Set of Asphalts**

Asphalt	P <sup>1</sup>	p <sub>a</sub> <sup>1</sup>	p <sub>o</sub> <sup>1</sup>	ACI
AAE	3.4 3.2	0.7 0.7	1.1 1.1	0.77
AAJ	4.1	0.8	0.9	2.59
AAN	3.4 3.8	0.7 0.7	1.0 1.2	1.51
AAS-1	3.7 3.6	0.7 0.7	1.1 1.1	1.36
AAV	4.5	0.8	1.1	2.54
AAW	2.9 2.8	0.6 0.6	1.1 1.1	1.39

<sup>1</sup> Standard deviations determined for each of the eight core asphalts for P range from  $\pm 0.05$  to  $\pm 2.80$ ; for p<sub>a</sub>, standard deviations range from 0.01 to 0.03; for p<sub>o</sub>, standard deviations range from 0.02 to 0.15.

**Supplementary Table 9.16 Core Asphalt Viscosities by Brabender Rheotron and Rheometric Mechanical Spectrometer at 45°C**

Asphalt	Viscosity (Pa · s) <sup>1</sup>	
	Mechanical Spectrometer, 0.1 rad/s	Brabender
AAA-1	848	893
AAB-1	1,710	1,230
AAC-1	1,510	1,460
AAD-1	1,190	1,280
AAF-1	2,240	-
AAG-1	3,240	-
AAK-1	4,600	-
AAM-1	2,940	-

<sup>1</sup> Viscosity measurements on the Rheometrics Mechanical Spectrometer are estimated to have an error bar of  $\pm 10\%$ .

**Supplementary Table 9.17** Viscosities of Expanded Set of Asphalts at 60 °C after Argon Annealing, 50% Strain, 25 mm PP

Asphalt	Viscosity (Pa · s) <sup>1</sup> , 0.1 rad/s
AAE	514
AAH	149
AAJ	269
AAN	191
AAS-1	283
AAV	79
AAW	286
AAX	254
AAZ	260
ABD	245
AAC-2	53
AAD-2	72
AAG-2	121
AAK-2	121
AAM-2	130

<sup>1</sup> Viscosity measurements on the Rheometrics Mechanical Spectrometer are estimated to have an error bar of ± 10%.



**Supplementary Table 9.18 Viscosities of Heptane Maltenes of Core Asphalts at Three Temperatures**

Parent Asphalt	Viscosity (Pa·s) <sup>2</sup>		
	25 °C	45 °C	60 °C
AAA-1	804	40	8
AAB-1	3,020	58	17
AAC-1	10,520	169	25
AAD-1	329	17	4
AAF-1	25,000	368	33
AAG-1 <sup>1</sup>	90,300; 76,080; 81,000	1,250; 1,040; 1,130	104; 96; 103
AAK-1	1,620	72	12
AAM-1	10,180	1,079	139

<sup>1</sup> Averages and standard deviations calculated for the three determinations of AAG-1 are: 25 °C, 82,460 ± 5,896; 45 °C, 1,140 ± 86; 60 °C, 101 ± 3.6.

<sup>2</sup> Viscosity measurements on the Rheometrics Mechanical Spectrometer are estimated to have an error bar of ± 10%.

**Supplementary Table 9.19 Reduced Specific Viscosity Measurements of Mixtures of AAA-1 Maltenes and Asphaltenes**

Asphaltene Content <sup>1</sup>		Viscosity (Pa·s) <sup>2</sup>		Reduced Specific Viscosity	
mass %	% natural abundance	25 °C	60 °C	25 °C	60 °C
0.8	5	864	8	9	10
4.2	25	1,850	13	31	17
8.4	50	5,180	26	65	29
12.6	75	17,600	69	165	63
16.8	100	58,400	222	426	165
21.0	125	138,000	422	815	255
33.6	200	1,170,000	9,740	4,327	3,745

<sup>1</sup> The standard deviation for asphaltene precipitation with n-heptane is estimated to be 0.78.

<sup>2</sup> Viscosity measurements on the Rheometrics Mechanical Spectrometer are estimated to have an error bar of ± 10%.

**Supplementary Table 9.20    Reduced Specific Viscosity Measurements of Mixtures of AAB-1 Maltenes and Asphaltenes**

Asphaltene Content <sup>1</sup>		Viscosity (Pa · s) <sup>2</sup>		Reduced Specific Viscosity	
mass %	% natural abundance	25 °C	60 °C	25 °C	60 °C
0.9	5	2,610	10	-15.2	24
4.3	25	7,420	17	34	23
8.6	50	13,000	35	38	36
13.0	75	41,600	78	98	63
17.3	100	216,000	333	408	221
21.6	125	534,000	1,500	813	815
34.6	200	12,400,000	52,500	11,900	17,880

<sup>1</sup> See footnote 1, Supplementary Table 9.19.

<sup>2</sup> See footnote 2, Supplementary Table 9.19.

**Supplementary Table 9.21    Reduced Specific Viscosity Measurements of Mixtures of AAC-1 Maltenes and Asphaltenes**

Asphaltene Content <sup>1</sup>		Viscosity (Pa · s) <sup>2</sup>		Reduced Specific Viscosity	
mass %	% natural abundance	25 °C	60 °C	25 °C	60 °C
0.5	5	11,630	28	21	22
2.1	20	17,520	36	32	21
5.2	50	36,050	58	46	26
7.9	75	77,410	113	81	45
10.5	100	201,600	189	173	73
13.1	125	275,300	393	192	113

<sup>1</sup> See footnote 1, Supplementary Table 9.19.

<sup>2</sup> See footnote 2, Supplementary Table 9.19.

**Supplementary Table 9.22 Reduced Specific Viscosity Measurements of Mixtures of AAD-1 Maltenes and Asphaltenes**

Asphaltene Content <sup>1</sup>		Viscosity (Pa · s) <sup>2</sup>		Reduced Specific Viscosity	
mass %	% natural abundance	25 °C	60 °C	25 °C	60 °C
1.1	5	326	4.0	-0.7	10.2
4.3	20	866	6.6	38	19
10.8	50	3,510	21.2	90	45
16.1	75	20,800	76.4	386	125
21.5	100	31,700	162.0	444	203
26.9	125	93,900	535.0	1,060	544

<sup>1</sup> See footnote 1, Supplementary Table 9.19.

<sup>2</sup> See footnote 2, Supplementary Table 9.19.

**Supplementary Table 9.23 Reduced Specific Viscosity Measurements of Mixtures of AAF-1 Maltenes and Asphaltenes**

Asphaltene Content <sup>1</sup>		Viscosity (Pa · s) <sup>2</sup>		Reduced Specific Viscosity	
mass %	% natural abundance	25 °C	60 °C	25 °C	60 °C
0.7	5	36,800	38	68	18
2.6	20	45,600	47	32	15
6.5	50	113,000	87	54	25
9.8	75	202,000	158	72	38
13.0	100	415,000	380	120	80
16.3	125	1,020,000	963	245	171

<sup>1</sup> See footnote 1, Supplementary Table 9.19.

<sup>2</sup> See footnote 2, Supplementary Table 9.19.

**Supplementary Table 9.24 Reduced Specific Viscosity Measurements of Mixtures of AAG-1 Maltenes and Asphaltenes**

Asphaltene Content <sup>1</sup>		Run No.	Viscosity (Pa · s) <sup>2</sup>		Reduced Specific Viscosity	
mass %	% natural abundance		25 °C	60 °C	25 °C	60 °C
0.5	5	1	91,000	116	1.6	23
		2	112,800	139	96	88
1.25	25	1	157,000	158	60	42
		2	109,300	131	35	29
2.5	50	1	221,000	200	58	37
		2	342,900	316	140	91
3.75	75	1	304,000	252	63	38
		2	192,300	199	41	28
5.0	100	1	428,000	322	75	42
		2	287,300	238	56	29
6.25	125	1	523,000	391	77	44
		2	332,800	272	54	29

<sup>1</sup> See footnote 1, Supplementary Table 9.19.

<sup>2</sup> See footnote 2, Supplementary Table 9.19.

**Supplementary Table 9.25 Reduced Specific Viscosity Measurements of Mixtures of AAK-I Maltenes and Asphaltenes**

Asphaltene Content <sup>1</sup>		Viscosity (Pa·s) <sup>2</sup>		Reduced Specific Viscosity	
mass %	% natural abundance	25 °C	60 °C	25 °C	60 °C
1.0	5	2,310	14	42	15
5.0	25	4,450	23	35	17
10.1	50	17,800	61	99	39
15.2	75	75,400	206	300	104
20.2	100	138,000	596	416	235
25.2	125	447,000	3,140	1,088	1,010
40.4	200	18,600,000	358,000	28,700	72,800

<sup>1</sup> See footnote 1, Supplementary Table 9.19.

<sup>2</sup> See footnote 2, Supplementary Table 9.19.

**Supplementary Table 9.26 Reduced Specific Viscosity Measurements of Mixtures of AAM-I Maltenes and Asphaltenes**

Asphaltene Content <sup>1</sup>		Viscosity (Pa·s) <sup>2</sup>		Reduced Specific Viscosity	
mass %	% natural abundance	25 °C	60 °C	25 °C	60 °C
0.2	5	176,900	172	321	101
1.4	30	232,500	250	92	57
2.3	50	326,800	372	96	73
3.4	75	330,200	453	66	66
4.6	100	451,300	656	75	81
5.8	125	756,000	1,302	111	144

<sup>1</sup> See footnote 1, Supplementary Table 9.19.

<sup>2</sup> See footnote 2, Supplementary Table 9.19.

## **Appendix B**

### **List of Data Tables Available in Database**

## 1.1

A2A111A1.D01  
A2A111A1.D02  
A2A111A1.D03  
A2A111A1.D04  
A2A111A1.D05

A2A111B1.D01  
A2A111B1.D02  
A2A111B1.D03  
A2A111B1.D04  
A2A111B1.D05  
A2A111B1.D06  
A2A111B1.D07  
A2A111B1.D08  
A2A111B1.D09  
A2A111B1.D10  
A2A111B1.D11  
A2A111B1.D12  
A2A111B1.D13  
A2A111B1.D14  
A2A111B1.D15  
A2A111B1.D16  
A2A111B1.D17

A2A111B2.D01  
A2A111B2.D02  
A2A111B2.D03  
A2A111B2.D04  
A2A111B2.D05  
A2A111B2.D06  
A2A111B2.D07  
A2A111B2.D08  
A2A111B2.D09  
A2A111B2.D10  
A2A111B2.D11  
A2A111B2.D12

A2A111C1.D01  
A2A111C1.D02

A2A111D1.D01  
A2A111D1.D02  
A2A111D1.D03  
A2A111D1.D04

A2A112A1.D01  
A2A112A1.D02

A2A112B1.D01  
A2A112B1.D02  
A2A112B1.D03  
A2A112B1.D04  
A2A112B1.D05  
A2A112B1.D06  
A2A112B1.D07  
A2A112B1.D08

A2A112C1.D01  
A2A112C1.D02

A2A113A1.D01  
A2A113A1.D02  
A2A113A1.D03  
A2A113A1.D04

A2A113B1.D01  
A2A113B1.D02

A2A115B1.D01  
A2A115B1.D02

A2A117A1.D01  
A2A117A1.D02  
A2A117A1.D03

### 1.3

A2A131A1.D01  
A2A131A1.D02  
A2A131A1.D03  
A2A131A1.D04  
A2A131A1.D05  
A2A131A1.D06  
A2A131A1.D07  
A2A131A1.D08

A2A131C1.D01  
A2A131C1.D02

A2A131C2.D01  
A2A131C2.D02

A2A131D1.D01  
A2A131D1.D02  
A2A131D1.D03  
A2A131D1.D04  
A2A131D1.D05  
A2A131D1.D06  
A2A131D1.D07  
A2A131D1.D08

A2A132A1.D01  
A2A132A1.D02  
A2A132A1.D03

A2A132B1.D01  
A2A132B1.D02  
A2A132B1.D03

A2A132D1.D01  
A2A132D1.D02  
A2A132D1.D03

A2A134A1.D01

A2A135A1.D01  
A2A135A1.D02  
A2A135A1.D03  
A2A135A1.D04



**Appendix C**  
**Lot Numbers for Resins Used in Ion Exchange**  
**Chromatography Separations**

Tables C-1 through C-4 correspond to tables found in chapter 1 and appendix A. Individual runs can be matched up using individual asphalts and run numbers. Table C-1 corresponds to the separations whose results are reported in table 1.8. In table 1.8, the results of separation of AAD-1 into amphotericics, bases, and neutrals plus acids are listed for run MC1. In run MC1, cation resin lot number 30431 was used. Anion resin lot number 36250 was used in this and two other runs. In run SK1 of AAD-1, portions of two cation resin lot numbers were used to fill one of the columns. Similarly, table C-2 corresponds to table 1.15, table C-3 corresponds to supplementary table 1.18, and table C-4 corresponds to supplementary table 1.19.

**Table C-1 IEC Resin Lot Numbers from Separation of Amphoteric, Base, Acid, and Neutral Fractions Isolated from Four Core Asphalts Reported in Table 1.8**

Asphalt	Operator Initials and Run Number	Sample code number	Resin Lot Number		
			Total Base + Amphoterics (cation)	Amphoterics (anion)	Total Acids (anion)
AAD-1	MC1	608-109	30431	36250	-
	SK1	689-15	30431, 41882A	36250	-
	MC2	689-35	41191	36250	-
	SK2	689-85	42526A	41975A	41975A
	DG1	737-24	41882A	41975A	41975A
AAG-1	MC3	689-5	30431	36250	-
	SK3	689-18	41882A	36250	-
	DG2	689-98	42526A	41975A	41975A
	DG3	737-32	41882A	41975A	41975A
AAK-1	MC4	608-110	30431	36250	-
	SK4	689-17	41882A	36250	-
	SK5	689-94	42526A	41975A	41975A
	DG4	737-13	42526A	41975A	-
	DG5	737-26	42526A, 41882A	41975A	41975A
AAM-1	MC5	689-3	30431	36250	-
	SK6	689-29	41191, 41882A	36250	-
	SK7	689-95	42526A	41975A	41975A
	DG6	737-33	41882A	-	41975A

**Table C-2 IEC Resin Lot Numbers from Separation of Four Aged (TFO-POV-air; 60 °C, 144 hours) Asphalts Reported in Table I.15**

Asphalt	Run No.	Sample code number	Resin Lot Number	
			Total Base + Amphoteric (cation)	Amphoteric (anion)
AAD-1	1	689-41	41191	36250
	2	689-66	41191	41721A
AAG-1	1	689-43	41191	36250
AAK-1	1	689-33	41191	41721A
	2	689-70	41191	41721A
AAM-1	1	689-42	41191	36250
	2	689-50	41191	41721A

**Table C-3 IEC Resin Lot Numbers from Separation of Seven Asphalts Reported in Supplementary Table 1.18 (Appendix A)**

Asphalt	Operator Initials and Run Number	Sample code number	Resin Lot Number			
			Strong Acid (anion)	Strong Base (cation)	Weak Acid (anion)	Weak Base (cation)
AAA-1	MC6	487-52	13190	14244	13190	14244
	MC7	487-63	13190	30064	32443	30064
	MC8	608-36	35189	-	-	-
	SP1	608-41	36250	33813	-	-
	MC9	608-72	36250	33813	-	-
AAB-1	MC10	487-27	32443	14244	32443, NA <sup>1</sup>	30064
	MC11	487-31	13190	14244	13190	14244
	MC12	608-35	35189	33813	-	-
	MC13	608-42	36250	-	-	-
AAD-1	MC14	487-2	NA	NA	NA	NA
	MC15	487-7	NA	NA	NA	NA
	MC16	487-47	13190	14244	-	-
	MC17	608-18	35189	-	-	-
AAF-1	SP2	487-87	35189	33813	35189	33813
	MC18	487-102	35189	33813	35189	33813
	MC19	608-32	35189	33813	-	-
	MC20	608-91	36250	-	-	-
AAG-1	MC21	487-57	13190	30064	NA	30064
	SP3	487-68	32443	33813	32216	30064, 33813
	MC22	608-54	36250	33813	-	-
	MC23	608-92	36250	-	-	-
AAK-1	MC24	487-15	NA	NA	NA	NA
	MC25	487-23	NA	NA	NA, 32443	14244, 30064
	SP4	608-43	35189	33813	-	-
	MC26	608-67	36250	33813	-	-
	MC27	608-70	36250	-	-	-
	MC28	608-104	36250	-	-	-
	DG7	689-53	36250, 41721A	41191	41721A	41191
AAM-1	MC29	487-38	13190	14244	13190	14244
	MC30	487-42	13190	14244	13190	14244, 30064

<sup>1</sup> NA = not available

**Table C-4 IEC Resin Lot Numbers from Separation of AAC-1 Reported in Supplementary Table 1.19 (Appendix A)**

Run	Sample code number	Resin Lot Number	
		Total Acid (anion)	Total Base (cation)
1	608-25	35189	33813
2	608-30	35189	33813
3	608-59	36250	-

**Appendix D**  
**Separation of a Quinolone-Enriched Fraction**  
**from SHRP Asphalts**

# Separation of a Quinolone-Enriched Fraction From SHRP Asphalts

Stephen C. Preece<sup>1</sup>, J.F. Branthaver<sup>2</sup>, and Sang-Soo Kim<sup>2</sup>

<sup>1</sup>Arizona Department of Public Safety  
P.O. Box 6638  
Phoenix, AZ 85005-6638

<sup>2</sup>Western Research Institute  
Box 3395 University Station  
Laramie, WY 82071-3395

**Keywords:** Asphalt, Modified Silica, Quinolone

## ABSTRACT

A method originally designed to separate a carboxylic acid concentrate from asphalts has been modified so that quinolone concentrates also can be extracted from asphalts. The quinolone concentrates are high in molecular weight and contain large amounts of oxygen, nitrogen, and sulfur. Infrared spectra of the quinolone concentrates are similar to those obtained from petroleum distillates by a multistep separation scheme. Some of the sulfur atoms associated with the quinolones are readily oxidizable.

## INTRODUCTION

The rheological properties of asphalts are believed to be influenced by associative interactions of polar, polyfunctional molecules in a non-polar hydrocarbon matrix (1). The identities of some of the functional groups involved in associative interactions in asphalts are carboxylic acids, phenols, pyridines, and quinolones. Other heteroatom-containing functional groups are probably involved. Compounds containing one or more of these groups have been identified in petroleum.

Asphalts contain non-volatile constituents of petroleum, which are also the largest and most polar components. The isolation of individual compounds, and even compound types, from asphalts for special study is a formidable task. This is because of the existence of large numbers of multifunctional compounds and extended methylene homologues in these residua.

As mentioned above, quinolones are one of a number of polar, associating species in asphalts, and thus may be major viscosity-controlling components of asphalts. Therefore the isolation and study of these compounds would be of interest. Quinolones were identified in petroleum by Copelin (2), who concentrated them from a gas oil fraction using a separation scheme involving hydrochloric acid treatment, ion exchange separation, and alumina chromatography. The quinolone fraction was characterized by a prominent peak at  $1655\text{ cm}^{-1}$



in the infrared spectrum. Based on a comparison with infrared spectra of model compounds, Copelin deduced that the quinolones were 2-quinolones and not 4-quinolones. Snyder et al. (3) detected the same materials in gas oil fractions of other crude oils. Petersen et al. (4) observed the  $1655\text{ cm}^{-1}$  peak in the infrared spectrum of asphalts, and assigned the peak to 2-quinolones. These workers observed that asphalts contain molecules that are too large to be typical pyridones. They showed that the  $1655\text{ cm}^{-1}$  peak was unaffected by treatments with hydrochloric acid or sodium hydroxide solutions, but disappeared when asphalts were treated with hexamethyldisilazane, which reacts with the enol form of the quinolones. Lithium aluminum hydride treatment of asphalts also resulted in loss of the  $1655\text{ cm}^{-1}$  peak in the infrared spectrum of treated asphalts. In this reaction, carbonyl groups are reduced.

The work of Petersen et al. (4) identifies 2-quinolones as probable constituents of asphalts. The complex separation schemes of Copelin (2) and Snyder et al. (3) are not easily applied to asphalts, due to irreversible adsorption of asphalt components on alumina and difficulties in extracting asphalts with acids. However, separation of highly polar carboxylic acids from asphalts using base-treated silica gels have been reported by Ramljak et al. (5). In this report, a modification of the Ramljak et al. (5) separation scheme was developed as a rapid method for the concentration of 2-quinolones from asphalts.

## EXPERIMENTAL

Asphalts used in this study were obtained from the Materials Reference Library of the Strategic Highway Research Program (SHRP).

The modified silica gel was prepared according to the procedure of Ramljak et al. (5). A typical preparation consists of slurring 400 g silicic acid (BIO-SIL A, 100-200 mesh, Bio-Rad Labs) in 4.0 L dichloromethane and then adding in portions a solution of 40 g potassium hydroxide (J.T. Baker) in 800 mL 2-propanol (J.T. Baker). After stirring the mixture for 30 minutes, it was poured onto a Buchner funnel having a sintered glass disc (C porosity) and washed with another 500 mL 2-propanol. Then the filter cake was washed with dichloromethane to remove alcohol.

The isolation of carboxylic acid concentrates was performed according to the procedure of Ramljak et al. (5), except that chromatographic columns were employed in place of extractors. In order to successfully concentrate quinolones, carboxylic acids must be removed from asphalts first. A flow sheet for the separation of asphalts into carboxylic acid concentrate, quinoline concentrates, and quinolone-free material is illustrated in Figure 1.

After the adsorption of the carboxylic acid concentrate on the modified silica gel, chloroform was removed from the eluted fraction on a rotary evaporator. The flask containing the chloroform solution was immersed in a hot water bath, and a vacuum of about 2 Torr was applied to remove the last of the chloroform. Approximately 20 g of this eluted fraction, which comprises 95% or more of the parent asphalt, was dissolved in 80 mL dichloromethane (Omni Solv, HPLC Grade). This solvent was poured onto the top of a column 2.5 cm i.d. x 100 cm filled about three-fourths full with modified silica gel. A small layer of sand was placed in the bottom of the column before adding the modified silica gel. In filling the

column, dichloromethane was poured into the column and then the gel slurry was added while the column stopcock was opened. Gel was added to fill the column with a well-packed bed to the 75 cm level. Flow rates for the separation were set by opening the column stopcock fully. About 4.0 L dichloromethane were required to complete the separation. Eluates were divested of solvent as described above, and designated the quinolone-free fraction. The modified silica gel and adsorbate were transferred to a Buchner funnel (M porosity) and a mixture of 20% formic acid (Aldrich Chemical Co.) and 80% dichloromethane was poured onto it to desorb the quinolone concentrate. These eluates were dried on a rotary evaporator as described above and then redissolved in dichloromethane and again filtered to remove potassium silicate associated with the quinolone concentrate. It may be necessary to use benzene as solvent for the quinolone concentrate in order to remove residual formic acid on the rotary evaporator.

Infrared Spectra of films of the quinolone concentrates were obtained on a Perkin-Elmer 983 Spectrophotometer. Molecular weights were determined by vapor phase osmometry using ASTM method D 2503 using toluene (60°C; 140°F) as solvent.

Elemental analyses were performed by the Analytical Research Division of Western Research Institute using standard methods.

## RESULTS AND DISCUSSION

The Strategic Highway Research Program (SHRP) has designated eight asphalts for special study. Four of these asphalts, AAA-1, AAD-1, AAG-1, and AAK-1 were separated on modified silica gel to collect carboxylic acid concentrates and quinolone concentrates. The asphalts contain about 0.01 to 0.02 M/L of quinolones (Table 1), based on the infrared functional group analysis of Petersen (6). Recoveries of material range from 96-98% in each step, so that the two concentrates are small in amount compared with the whole asphalts. The replication of the separation for AAK-1, using two different operators was not good, but this does not affect the utility of the method in concentrating quinolones.

Elemental analyses and number-average molecular weights of the parent asphalts and the quinolone concentrates (Table 2) show that in each case, the quinolone concentrates are more aromatic and contain more nitrogen, oxygen, and sulfur than the parent asphalts. Large sulfur contents in quinolone concentrates in distillates were observed by Copelin (2), who claimed that substantial amounts of thioquinolines were present in the materials he studied. Number-average molecular weight ( $\bar{M}_n$ ) values of the asphalt quinolone concentrates determined by vapor phase osmometry (VPO) in toluene at 60°C (140°F) are much higher than those reported by Copelin (2), which were about 300 Daltons. These materials were derived from 340-450°C (644-842°F) distillates. Evidently quinolones occur in crude oils over a large molecular weight range. The  $\bar{M}_n$  value of the quinoline concentrate of AAK-1 also was determined by VPO in pyridine at 60°C (140°F). This value is about half that of the  $\bar{M}_n$  value determined in toluene, which demonstrates that quinolones have strong tendencies to associate. In contrast,  $\bar{M}_n$  values for whole asphalts are similar in pyridine and toluene.

Infrared spectra of quinolone concentrates of asphalts are shown in Figures 2-5. Copelin (2) identified the peak at about 1650  $\text{cm}^{-1}$  as the carbonyl peak of the quinolone amide

function. This peak is prominent in Figures 2-5. The quinolone concentrate of AAG-1 (Figure 4) is contaminated by some carboxylic acids, as shown by the presence of a peak at about  $1705\text{ cm}^{-1}$ . No peak corresponding to thioquinolones is observed in any of the asphalt quinolone concentrates. Instead, large sulfoxide peaks ( $\sim 1020\text{ cm}^{-1}$ ) are observed. The quinolones contain (or possibly are associated with) readily oxidizable sulfur functionalities.

In another study, the quinolone concentrate of AAD-1 was further separated into fractions using a column of modified silica gel (7). Retention times of most of the components of the concentrates were similar to those of model compounds having 2-pyridone or 2-quinolone structural units.

It is possible to collect both carboxylic acids and quinolones by eliminating the initial step and directly separating the original asphalt on activated silica with dichloromethane. Yield of the combination of quinolones and acids for AAA-1 is 4.8 wt %.

## CONCLUSIONS

Quinolones can be concentrated from four asphalts by a modification of a method originally developed to concentrate carboxylic acids from asphalts. The quinolone concentrates are characterized by a prominent peak in their infrared spectra at about  $1650\text{ cm}^{-1}$ . Nitrogen, oxygen, and sulfur concentrations in these materials also are high. The sulfur functionality associated with the quinolone concentrates is readily oxidizable. The number-average molecular weights of the quinolone concentrates are approximately twice those of the parent asphalts.

The method used to concentrate quinolones from asphalts is rapid and simple and it presumably can be extended to other petroleum-derived fractions. It is estimated that quinolones are concentrated about ten- to twenty-fold by this method based on concentrations of these compounds in parent asphalts. The concentrates can be further purified by other separation methods (7).

## DISCLAIMER

The contents of this report reflect the views of the authors, who are solely responsible for the facts and accuracy of the data presented. The contents do not necessarily reflect the official view or policies of the Strategic Highway Research Program (SHRP) or SHRP's sponsors. The results reported here are not necessarily in agreement with the results of other SHRP research activities. They are reported to stimulate review and discussion within the research community. This report does not constitute a standard, specification, or regulation. Mention of specific brands of materials does not imply endorsement by SHRP or Western Research Institute.

## ACKNOWLEDGMENTS

The work reported herein has been conducted as a part of Project A002A of the Strategic Highway Research Program (SHRP). SHRP is a unit of the National Research Council that was authorized by Section 128 of the Surface Transportation and Uniform Relocation Assistance Act of 1987. This project is titled "Binder Characterization and Evaluation" and is being conducted by the Western Research Institute, Laramie, Wyoming, in cooperation with the Pennsylvania Transportation Institute, Texas Transportation Institute, and SRI International. Dr. Raymond E. Robertson is the principal investigator. Dawn Geldien is the project administrator. The support and encouragement of Dr. Edward Harrigan, SHRP Asphalt Program Manager, and Dr. Jack Youtcheff, SHRP Technical Contract Manager, are gratefully acknowledged. Analytical work was performed by G.W. Gardner. The manuscript was prepared by J. Greaser.

## LITERATURE CITED

- (1) Petersen, J.C. 1984. *Transport. Res. Rec.*, 999, 13-30.
- (2) Copelin, E.C. 1964. *Anal. Chem.*, 36, 2274-2277.
- (3) Snyder, L.E., B.E. Buell, and H.E. Howard. 1968. *Anal. Chem.*, 40, 1303-1317.
- (4) Petersen, J.C., R.V. Barbour, S.M. Dorrence, F.A. Barbour, and R.V. Helm. 1971. *Anal. Chem.*, 43, 1491-1496.
- (5) Ramljak, Z., A. Solc, P. Arpino, J.M. Schmitter, and G. Guichon. 1977. *Anal. Chem.*, 49, 1222-1225.
- (6) Petersen, J.C. 1986. *Transport. Res. Rec.*, 1096, 1-11.
- (7) Preece, S.C. 1992. Master of Science Dissertation, University of Wyoming, Laramie, Wyoming.

**TABLE 1**  
**Yields of Quinolone Concentrates from Four Asphalts**

Asphalt	Yield of Quinolone Concentrate, wt % of Asphalt
AAA-1	2.6
AAD-1	6.7
AAG-1	2.7
AAK-1	5.0; 6.8

**TABLE 2**  
**Elemental Analyses and Number-Average Molecular Weights of Four Asphalts and Their Quinolone Concentrates**

Substrate	Element, wt %					$\bar{M}_n$ (Daltons)	
	C	H	N	O	S	H/C	toluene pyridine
Asphalt AAA-1	84.2	10.5	0.48	0.6	5.5	1.48	790
AAA-1 Quinolone Concentrate	-	-	0.90	2.8	8.4	-	1,400
Asphalt AAD-1	81.4	10.8	0.77	0.9	6.9	1.58	710
AAD-1 Quinolone Concentrate	78.5	9.3	1.50	2.9	8.6	1.41	1,500
Asphalt AAG-1	85.6	10.5	1.10	1.1	1.3	1.46	710
AAG-1 Quinolone Concentrate	-	-	1.57	3.6	1.9	-	1,360
Asphalt AAK-1	80.7	10.2	0.71	0.8	6.5	1.51	860
AAK-1 Quinolone Concentrate, run 1	79.6	8.5	1.20	2.7	7.2	1.27	1,800
AAK-1 Quinolone Concentrate, run 2 <sup>1</sup>	76.6/76.3	9.0/9.0	1.1/1.2	3.9/3.9	8.3/8.4	1.40	2,172
							1,113

<sup>1</sup> Replicate elemental analyses were performed for this sample

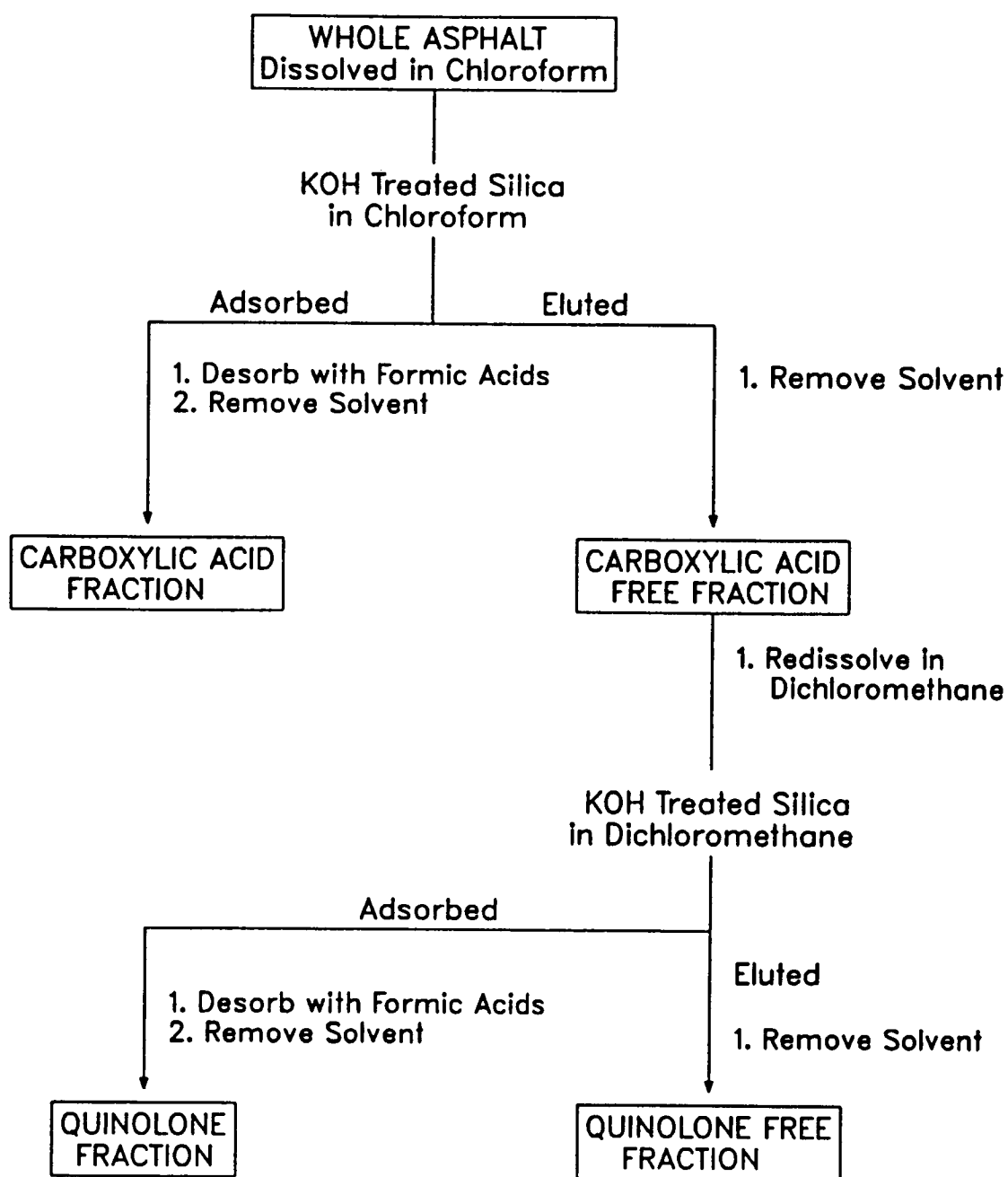


Figure 1. Flow Scheme for the Isolation of Quinolones

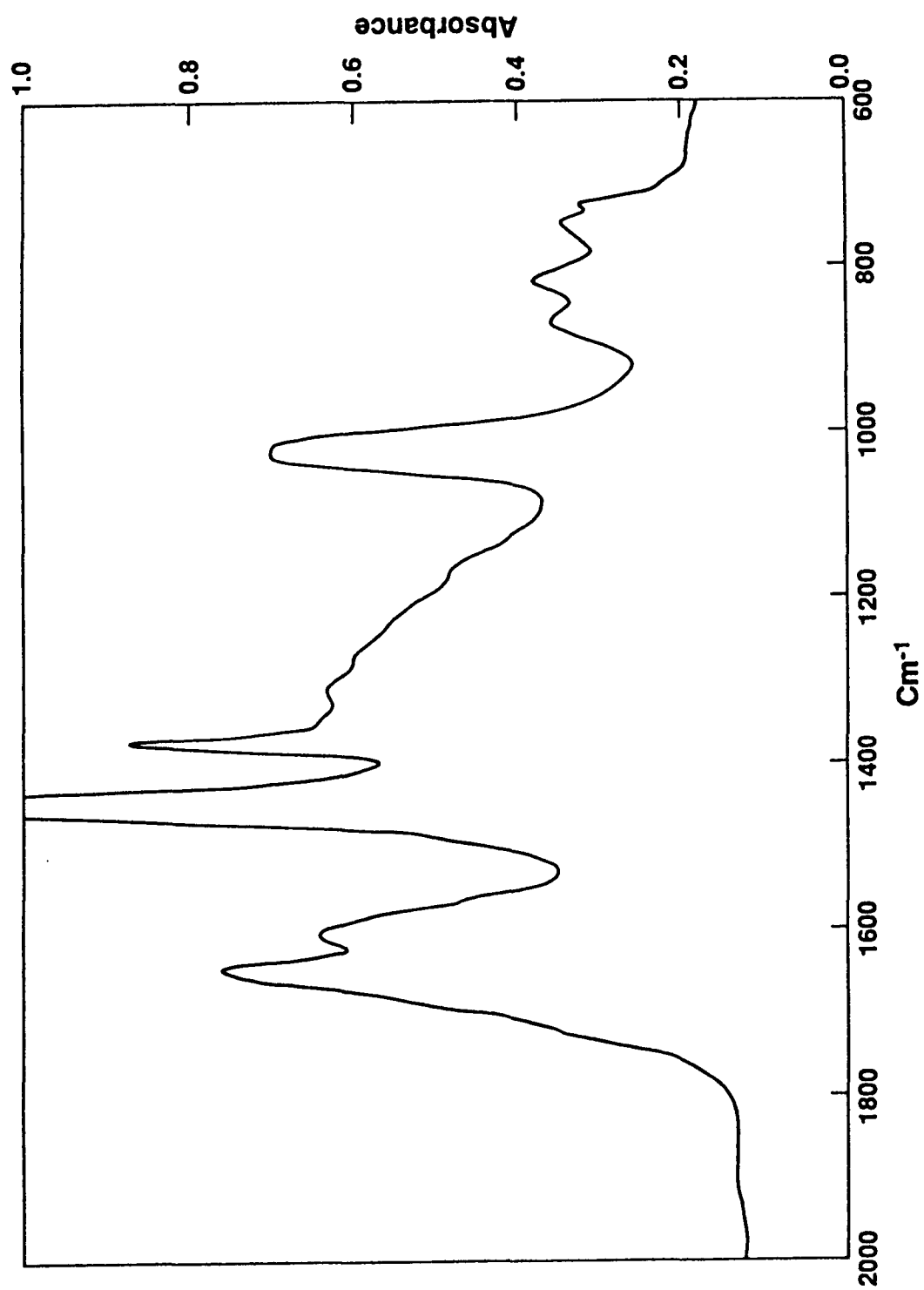


Figure 2. Quinolone Concentrate from AAA-1

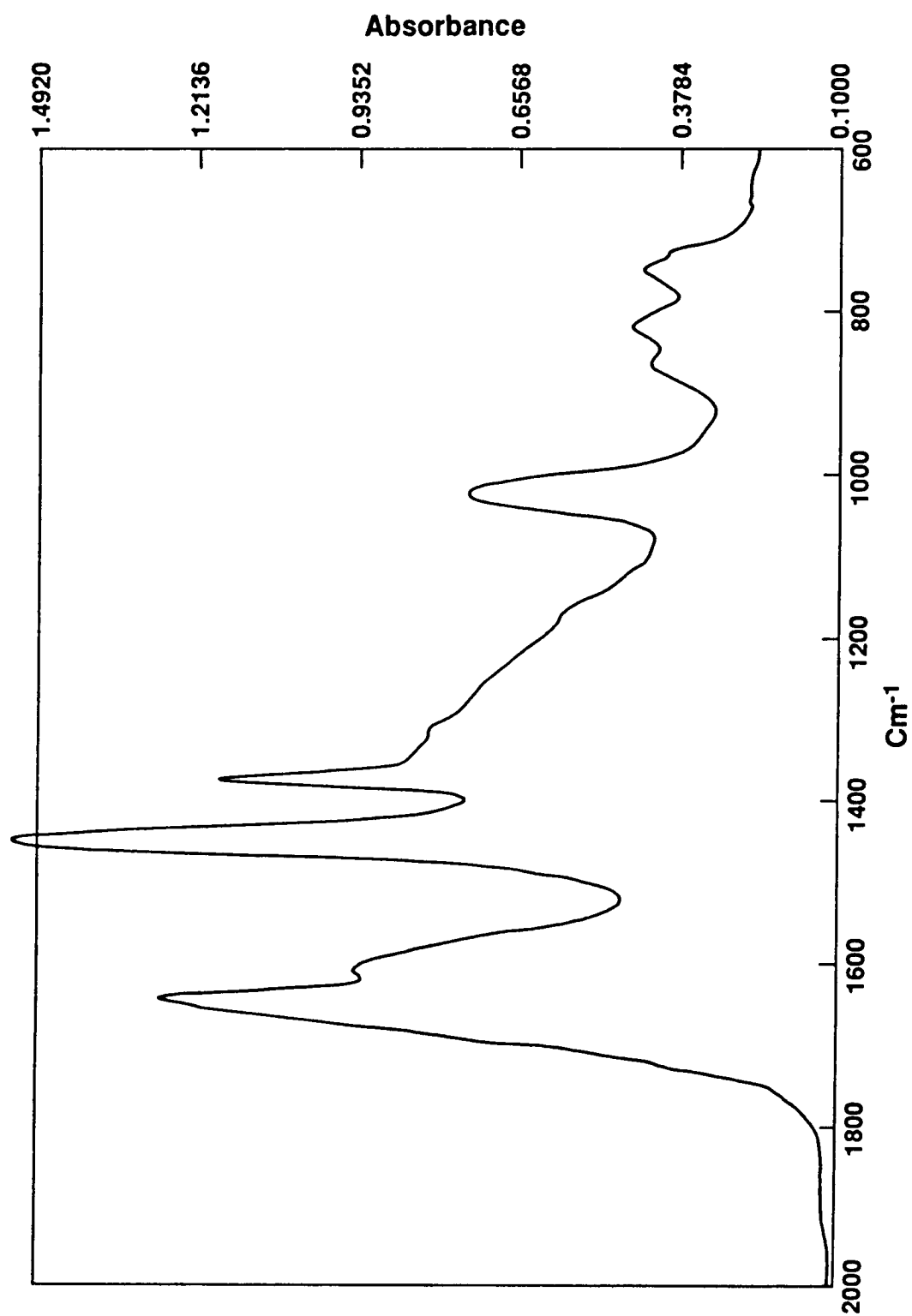


Figure 3. Quinolone Concentrate from AAD-1



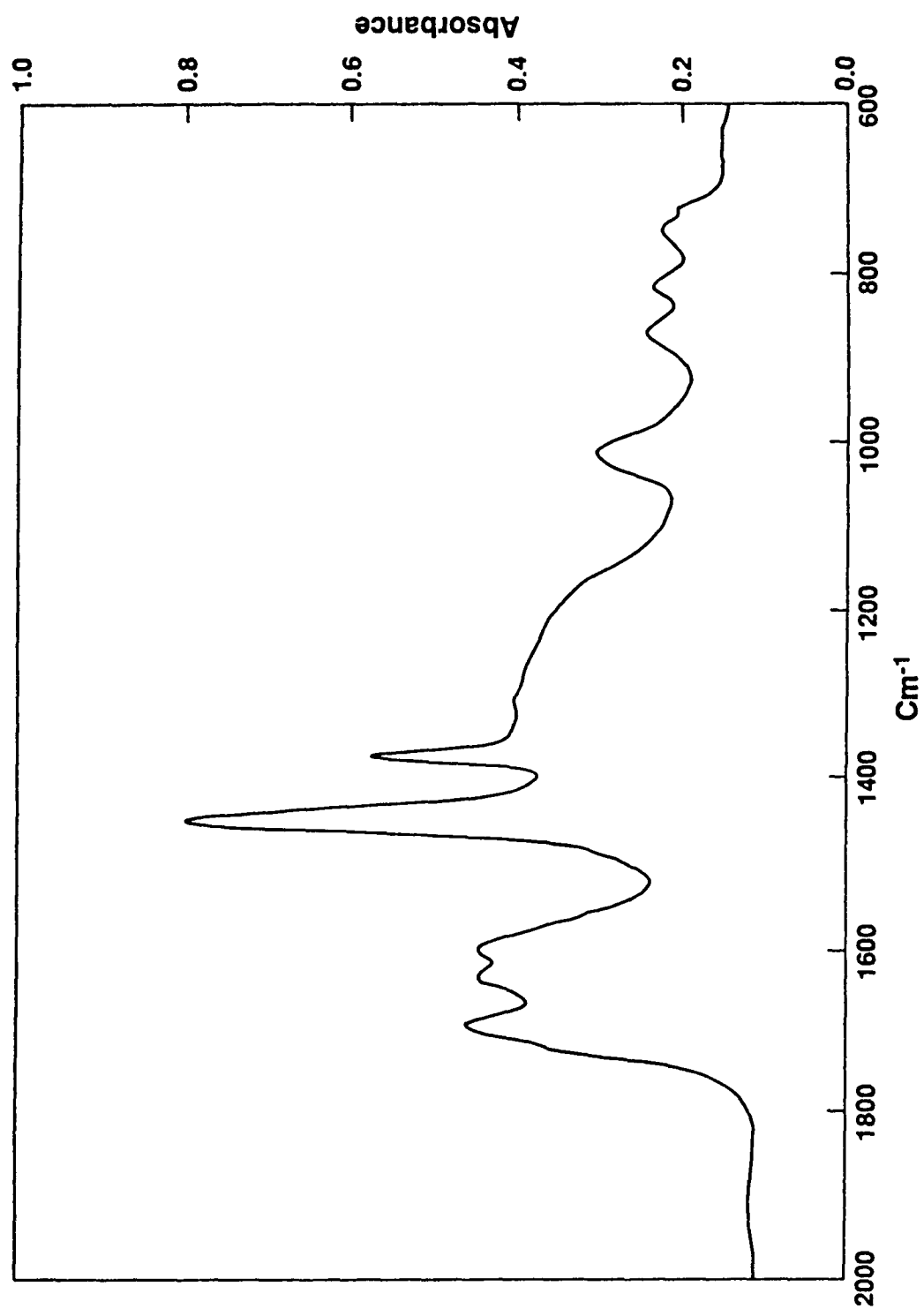


Figure 4. Quinolone Concentrate from AAG-1

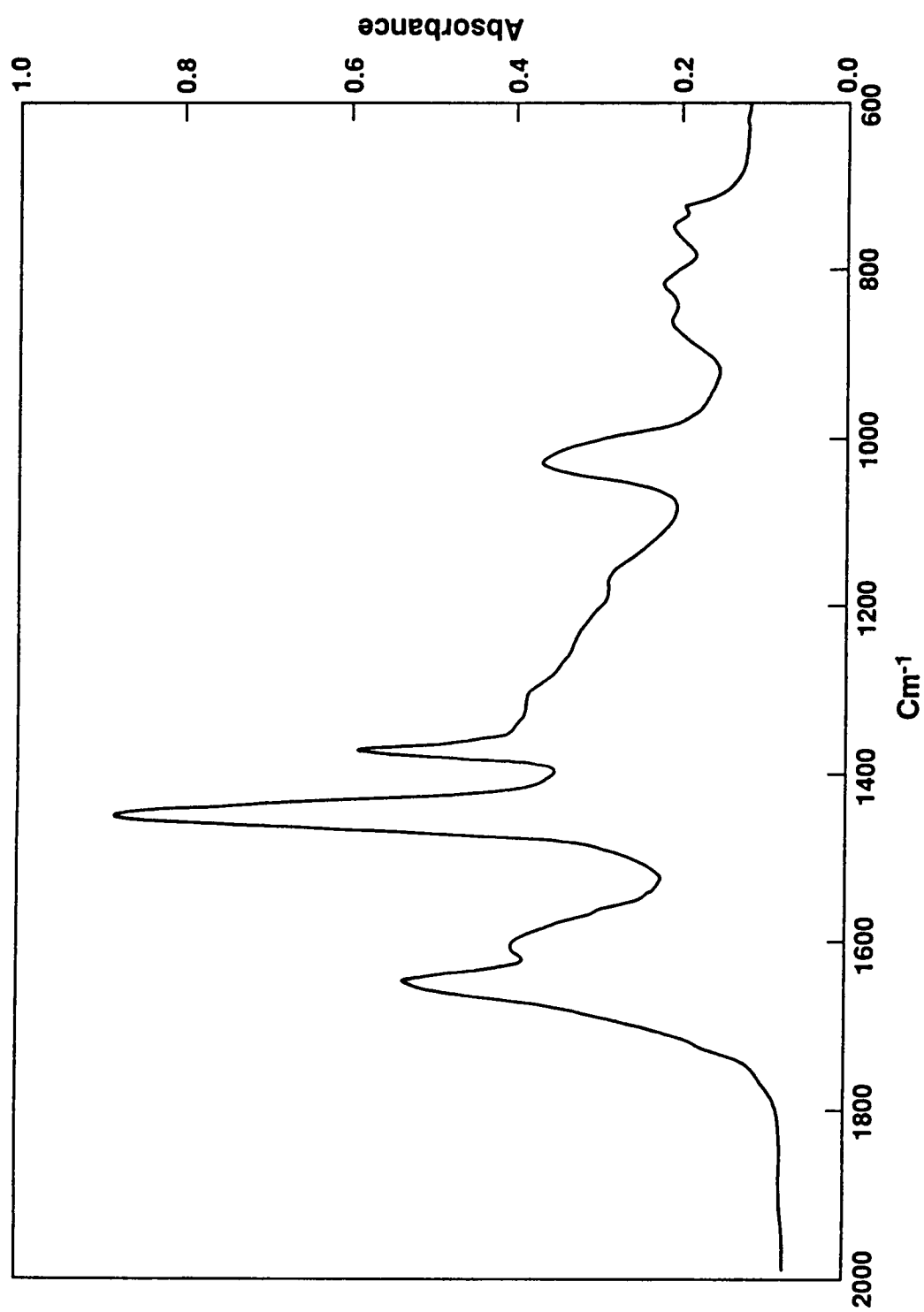


Figure 5. Quinolone Concentrate from AAK-1

## **Asphalt Advisory Committee**

Thomas D. Moreland, *chairman*  
*Moreland Altobelli Associates, Inc.*

Gale C. Page, *vice chairman*  
*Florida Department of Transportation*

Peter A. Bellin  
*Niedersachsisches Landesamt  
für Strassenbau*

Dale Decker  
*National Asphalt Paving Association*

Joseph L. Goodrich  
*Chevron Research Company*

Eric Harm  
*Illinois Department of Transportation*

Charles Hughes  
*Virginia Highway & Transportation Research Council*

Robert G. Jenkins  
*University of Cincinnati*

Anthony J. Kriech  
*Heritage Group Company*

Richard Langlois  
*Universite Laval*

Richard C. Meininger  
*National Aggregates Association*

Nicholas Nahas  
*EXXON Chemical Co.*

Charles F. Potts  
*APAC, Inc.*

Ron Reese  
*California Department of Transportation*

Donald E. Shaw  
*Georgia-Pacific Corporation*

Scott Shuler  
*The Asphalt Institute*

Harold E. Smith  
*City of Des Moines*

Thomas J. Snyder  
*Marathon Oil Company*

Richard H. Sullivan  
*Minnesota Department of Transportation*

A. Haleem Tahir  
*American Association of State Highway and  
Transportation Officials*

Jack Telford  
*Oklahoma Department of Transportation*

George West  
*Shell Oil Company*

## **Liaisons**

Avery D. Adcock  
*United States Air Force*

Ted Ferragut  
*Federal Highway Administration*

Donald G. Fohs  
*Federal Highway Administration*

Fredrick D. Hejl  
*Transportation Research Board*

Aston McLaughlin  
*Federal Aviation Administration*

Bill Weseman  
*Federal Highway Administration*

## **Expert Task Group**

Ernest Bastian, Jr.  
*Federal Highway Administration*

Wayne Brule  
*New York State Department of Transportation*

Joseph L. Goodrich  
*Chevron Research Company*

Woody Halstead  
*Consultant*

Gayle King  
*Bituminous Materials Co., Inc.*

Robert F. LaForce  
*Colorado Department of Transportation*

Mark Plummer  
*Marathon Oil Company*

Raymond Pavlovich  
*Exxon Chemical Company*

Ron Reese  
*California Department of Transportation*

Scott Shuler  
*Colorado Paving Association*

**Table 8.16 Oxidation Products Formed in Asphalt AAG-1 as a Function of Time During TFAAT Aging at 113°C**

Oxidation Time, hrs	Functional Group Concentration, <sup>1</sup> mol/L	
	Ketones	Sulfoxides
0		
3	0.01	0.05
6	0.06	0.12
9	0.08	0.14
16	0.10	0.14
24	0.12	0.16
40	0.15	0.17
56	0.21	0.17
72	0.28	0.18
	0.32	0.17

<sup>2</sup> Based on prior experience with asphalts, standard deviations are (mol/L): sulfoxides, 0.027; ketones, 0.006.

**Table 8.17 Comparison of POV (Oxygen) and PAV (Air) Aging of Selected SHRP Asphalts, 300 psi, 60°C, 144 Hours**

Asphalt	Log Viscosity Change in Aging <sup>1</sup>		Infrared Analysis of Surface and Bottom of Samples after Aging in Air	
	In Oxygen	In Air	Carbonyl <sup>2</sup> , abs.	Sulfoxides <sup>2</sup> , mol/L
AAA-1	0.88	0.76	-	-
AAA-1, Run 2	-	-0.80	-	-
AAB-1	1.00	0.87	-	-
AAD-1	1.02	0.95	-	-
AAG-1	0.71	0.47	0.12	0.18
AAG-1, Run 2	-	-0.48	0.11	0.17
AAK-1	1.16	1.06	0.05	0.19
AAK-1, Run 2	-	1.03	0.05	0.18
AAM-1	<u>1.05</u>	<u>0.72</u>	-	-
Average	0.97	0.81		

<sup>1</sup> POV and PAV aging conducted on asphalts subjected to prior TFO aging.

<sup>2</sup> Based on prior experience with asphalts, standard deviations are (mol/L): sulfoxides, 0.027; ketones, 0.006.

**Table 8.18 Comparison of Results from Thin-Film Oven (TFO) Oxidation and TFO Followed by 60°C Pressure Oxidation Vessel (POV)-Argon (300 psi) Oxidation of SHRP Asphalts**

Asphalt	POV Oxidation Time, hrs	Oxidation Type	Dynamic Viscosity ( $\eta^*$ ) <sup>1</sup> 60°C, Pa·s	Carbonyl <sup>2</sup> Absorbance Units	Sulfoxide <sup>2</sup> M/L
AAA-1	--	TFO	$1.85 \times 10^2$	0.02	0.04
	144	TFO-POV-Argon, 60°C	$1.96 \times 10^2$	0.02	0.04
AAB-1	--	TFO	$3.01 \times 10^2$	0.00	0.07
	144	TFO-POV-Argon, 60°C	$2.98 \times 10^2$	0.00	0.09
AAC-1	--	TFO	$1.91 \times 10^2$	0.02	0.04
	144	TFO-POV-Argon, 60°C	$1.97 \times 10^2$	0.02	0.04
AAD-1	--	TFO	$3.19 \times 10^2$	0.04	0.06
	144	TFO-POV-Argon, 60°C	$3.45 \times 10^2$	0.04	0.06
AAF-1	--	TFO	$4.43 \times 10^2$	0.00	0.06
	144	TFO-POV-Argon, 60°C	$4.73 \times 10^2$	0.00	0.10
AAG-1	--	TFO	$3.33 \times 10^2$	0.03	0.05
	144	TFO-POV-Argon, 60°C	$3.29 \times 10^2$	0.03	0.05
AAK-1	--	TFO	$1.05 \times 10^3$	0.02	0.03
	144	TFO-POV-Argon, 60°C	$1.15 \times 10^3$	0.03	0.03
AAM-1	--	TFO	$4.48 \times 10^2$	0.02	0.03
	144	TFO-POV-Argon, 60°C	$4.74 \times 10^2$	0.02	0.03

<sup>1</sup> Viscosity measurements on the Rheometrics Mechanical Spectrometer are estimated to have an error bar of  $\pm$  10%.

<sup>2</sup> Based on prior experience with asphalts, standard deviations are (mol/L): sulfoxides, 0.027; ketones, 0.006.

# APPENDIX IX

# APPENDIX VI

# APPENDIX III



## **Asphalt Advisory Committee**

Thomas D. Moreland, *chairman*  
*Moreland Altobelli Associates, Inc.*

Gale C. Page, *vice chairman*  
*Florida Department of Transportation*

Peter A. Bellin  
*Niedersachsisches Landesamt  
für Strassenbau*

Dale Decker  
*National Asphalt Paving Association*

Joseph L. Goodrich  
*Chevron Research Company*

Eric Harm  
*Illinois Department of Transportation*

Charles Hughes  
*Virginia Highway & Transportation Research Council*

Robert G. Jenkins  
*University of Cincinnati*

Anthony J. Kriech  
*Heritage Group Company*

Richard Langlois  
*Universite Laval*

Richard C. Meininger  
*National Aggregates Association*

Nicholas Nahas  
*EXXON Chemical Co.*

Charles F. Potts  
*APAC, Inc.*

Ron Reese  
*California Department of Transportation*

Donald E. Shaw  
*Georgia-Pacific Corporation*

Scott Shuler  
*The Asphalt Institute*

Harold E. Smith  
*City of Des Moines*

Thomas J. Snyder  
*Marathon Oil Company*

Richard H. Sullivan  
*Minnesota Department of Transportation*

A. Haleem Tahir  
*American Association of State Highway and  
Transportation Officials*

Jack Telford  
*Oklahoma Department of Transportation*

George West  
*Shell Oil Company*

## **Liaisons**

Avery D. Adcock  
*United States Air Force*

Ted Ferragut  
*Federal Highway Administration*

Donald G. Fohs  
*Federal Highway Administration*

Fredrick D. Hejl  
*Transportation Research Board*

Aston McLaughlin  
*Federal Aviation Administration*

Bill Weseman  
*Federal Highway Administration*

## **Expert Task Group**

Dave Allen  
*University of Kentucky*

Daniel W. Dearasaugh, Jr.  
*Transportation Research Board*

Ervin Dukatz  
*Vulcan Materials*

Charles Manzione  
*United States Air Force*

Bill Maupin, Jr.  
*Virginia Transportation Research Council*

Richard May  
*The Asphalt Institute*

Roy McQueen  
*Rajan-McQueen and Associates*

James A. Sherwood  
*Federal Highway Administration*

George Way  
*Arizona Department of Transportation*

8/16/93

## **Asphalt Advisory Committee**

Thomas D. Moreland, *chairman*  
*Moreland Altobelli Associates, Inc.*

Gale C. Page, *vice chairman*  
*Florida Department of Transportation*

Peter A. Bellin  
*Niedersachsisches Landesamt  
für Strassenbau*

Dale Decker  
*National Asphalt Paving Association*

Joseph L. Goodrich  
*Chevron Research Company*

Eric Harm  
*Illinois Department of Transportation*

Charles Hughes  
*Virginia Highway & Transportation Research Council*

Robert G. Jenkins  
*University of Cincinnati*

Anthony J. Kriech  
*Heritage Group Company*

Richard Langlois  
*Universite Laval*

Richard C. Meininger  
*National Aggregates Association*

Nicholas Nahas  
*EXXON Chemical Co.*

Charles F. Potts  
*APAC, Inc.*

Ron Reese  
*California Department of Transportation*

Donald E. Shaw  
*Georgia-Pacific Corporation*

Scott Shuler  
*The Asphalt Institute*

Harold E. Smith  
*City of Des Moines*

Thomas J. Snyder  
*Marathon Oil Company*

Richard H. Sullivan  
*Minnesota Department of Transportation*

A. Haleem Tahir  
*American Association of State Highway and  
Transportation Officials*

Jack Telford  
*Oklahoma Department of Transportation*

George West  
*Shell Oil Company*

## **Liaisons**

Avery D. Adcock  
*United States Air Force*

Ted Ferragut  
*Federal Highway Administration*

Donald G. Fohs  
*Federal Highway Administration*

Fredrick D. Hejl  
*Transportation Research Board*

Aston McLaughlin  
*Federal Aviation Administration*

Bill Weseman  
*Federal Highway Administration*

## **Expert Task Group**

Ernest Bastian, Jr.  
*Federal Highway Administration*

Wayne Brule  
*New York State Department of Transportation*

Joseph L. Goodrich  
*Chevron Research Company*

Woody Halstead  
*Consultant*

Gayle King  
*Bituminous Materials Co., Inc.*

Robert F. LaForce  
*Colorado Department of Transportation*

Mark Plummer  
*Marathon Oil Company*

Raymond Pavlovich  
*Exxon Chemical Company*

Ron Reese  
*California Department of Transportation*

Scott Shuler  
*Colorado Paving Association*

**Table 4.8 Failure Energy (MPa) Master Curve Parameters for All SHRP Asphalts in Unaged (Tank) Condition at Reference Temperature of  $-10^{\circ}\text{C}$  ( $14^{\circ}\text{F}$ )**

Asphalt	A	B1	95% Confidence Intervals for B1		B3	95% Confidence Intervals for B3	
AAA-1	1.10	43.90	42.90	44.90	6.63	6.55	6.70
AAB-1	0.78	30.80	29.00	32.60	9.52	9.27	9.76
AAC-1	0.89	21.30	19.90	22.60	9.62	9.35	9.89
AAD-1	1.20	36.00	33.40	38.50	8.03	7.78	8.29
AAE-1	0.71	44.40	39.70	49.10	8.46	7.84	9.11
AAF-1	0.56	19.40	18.60	20.10	12.20	12.10	12.40
AAG-1	0.38	16.50	12.40	20.60	12.30	10.80	13.90
AAH-1	1.17	22.80	17.80	27.80	7.77	6.93	8.66
AAJ-1	0.67	29.50	24.30	34.70	9.45	8.41	10.60
AAK-1	0.72	34.00	31.30	36.60	9.09	8.80	9.38
AAL-1	1.24	36.50	27.30	45.60	6.60	5.94	7.29
AAM-1	0.82	26.30	24.80	27.80	10.00	9.79	10.30
AAN-1	0.52	32.40	26.20	38.60	8.76	7.56	10.10
AAO-1	1.12	32.70	23.40	42.00	8.77	7.45	10.20
AAP-1	1.27	29.20	24.60	33.70	8.75	7.96	9.58
AAQ-1	0.45	22.10	17.90	26.40	9.40	8.17	10.70
AAR-1	0.67	41.60	30.60	52.60	10.90	9.42	12.40
AAS-1	0.93	41.80	35.90	47.70	10.60	9.73	11.50
AAT-1	0.47	51.70	45.50	58.00	13.30	12.20	14.40
AAU-1	0.55	51.20	49.20	53.20	13.30	12.90	13.60
AAV-1	0.59	18.90	14.10	23.80	8.23	7.16	9.38
AAW-1	0.36	52.40	49.20	55.60	12.80	12.30	13.30
AAX-1	0.36	30.90	27.40	34.40	12.50	11.60	13.60
AAY-1	0.65	36.10	29.10	43.10	8.60	7.76	9.49
AAZ-1	0.46	33.90	28.10	39.70	12.70	11.30	14.20
ABA-1	1.51	27.00	20.50	33.60	8.27	7.36	9.23
ABC-1	1.04	34.00	25.00	43.00	8.21	7.23	9.24
ABD-1	0.43	2.71	2.10	3.32	7.20	6.11	8.38

**Table 4.9 Specification-Type Testing Experimental Layout of Replicate 1  
for One Asphalt (at Least Four Replicates Were Tested)**

Temperature Levels	Tank (Unaged)	Age Levels	
		TFOT	PAV
1	X	X	X
2	X	X	X
3	X	X	X

## **Asphalt Advisory Committee**

Thomas D. Moreland, *chairman*  
*Moreland Altobelli Associates, Inc.*

Gale C. Page, *vice chairman*  
*Florida Department of Transportation*

Peter A. Bellin  
*Niedersachsisches Landesamt  
für Strassenbau*

Dale Decker  
*National Asphalt Paving Association*

Joseph L. Goodrich  
*Chevron Research Company*

Eric Harm  
*Illinois Department of Transportation*

Charles Hughes  
*Virginia Highway & Transportation Research Council*

Robert G. Jenkins  
*University of Cincinnati*

Anthony J. Kriech  
*Heritage Group Company*

Richard Langlois  
*Universite Laval*

Richard C. Meininger  
*National Aggregates Association*

Nicholas Nahas  
*EXXON Chemical Co.*

Charles F. Potts  
*APAC, Inc.*

Ron Reese  
*California Department of Transportation*

Donald E. Shaw  
*Georgia-Pacific Corporation*

Scott Shuler  
*The Asphalt Institute*

Harold E. Smith  
*City of Des Moines*

Thomas J. Snyder  
*Marathon Oil Company*

Richard H. Sullivan  
*Minnesota Department of Transportation*

A. Haleem Tahir  
*American Association of State Highway and  
Transportation Officials*

Jack Telford  
*Oklahoma Department of Transportation*

George West  
*Shell Oil Company*

## **Liaisons**

Avery D. Adcock  
*United States Air Force*

Ted Ferragut  
*Federal Highway Administration*

Donald G. Fohs  
*Federal Highway Administration*

Fredrick D. Hejl  
*Transportation Research Board*

Aston McLaughlin  
*Federal Aviation Administration*

Bill Weseman  
*Federal Highway Administration*

## **Expert Task Group**

Dallas Little, *chairman*  
*Texas Transportation Institute*

Campbell Crawford  
*National Asphalt Paving Association*

Daniel W. Dearasaugh  
*Transportation Research Board*

Francis Fee  
*Westbank Oil, Incorporated*

Eric Harm  
*Illinois Department of Transportation*

Charles Hughes  
*Virginia Highway & Transportation Research Council*

Kevin Stuart  
*Federal Highway Administration*

Roger L. Yarbrough  
*Apcon Corporation*

## **Asphalt Advisory Committee**

Thomas D. Moreland, *chairman*  
*Moreland Altobelli Associates, Inc.*

Gale C. Page, *vice chairman*  
*Florida Department of Transportation*

Peter A. Bellin  
*Niedersachsisches Landesamt  
für Strassenbau*

Dale Decker  
*National Asphalt Paving Association*

Joseph L. Goodrich  
*Chevron Research Company*

Eric Harm  
*Illinois Department of Transportation*

Charles Hughes  
*Virginia Highway & Transportation Research Council*

Robert G. Jenkins  
*University of Cincinnati*

Anthony J. Kriech  
*Heritage Group Company*

Richard Langlois  
*Universite Laval*

Richard C. Meininger  
*National Aggregates Association*

Nicholas Nahas  
*EXXON Chemical Co.*

Charles F. Potts  
*APAC, Inc.*

Ron Reese  
*California Department of Transportation*

Donald E. Shaw  
*Georgia-Pacific Corporation*

Scott Shuler  
*The Asphalt Institute*

Harold E. Smith  
*City of Des Moines*

Thomas J. Snyder  
*Marathon Oil Company*

Richard H. Sullivan  
*Minnesota Department of Transportation*

A. Haleem Tahir  
*American Association of State Highway and  
Transportation Officials*

Jack Telford  
*Oklahoma Department of Transportation*

George West  
*Shell Oil Company*

## **Liaisons**

Avery D. Adcock  
*United States Air Force*

Ted Ferragut  
*Federal Highway Administration*

Donald G. Fohs  
*Federal Highway Administration*

Fredrick D. Hejl  
*Transportation Research Board*

Aston McLaughlin  
*Federal Aviation Administration*

Bill Weseman  
*Federal Highway Administration*

## **Expert Task Group**

Dallas Little, *chairman*  
*Texas Transportation Institute*

Campbell Crawford  
*National Asphalt Paving Association*

Daniel W. Dearasaugh  
*Transportation Research Board*

Francis Fee  
*Westbank Oil, Incorporated*

Eric Harm  
*Illinois Department of Transportation*

Charles Hughes  
*Virginia Highway & Transportation Research Council*

Kevin Stuart  
*Federal Highway Administration*

Roger L. Yarbrough  
*Apcon Corporation*

## **Asphalt Advisory Committee**

Thomas D. Moreland, *chairman*  
*Moreland Altobelli Associates, Inc.*

Gale C. Page, *vice chairman*  
*Florida Department of Transportation*

Peter A. Bellin  
*Niedersachsisches Landesamt  
für Strassenbau*

Dale Decker  
*National Asphalt Paving Association*

Joseph L. Goodrich  
*Chevron Research Company*

Eric Harm  
*Illinois Department of Transportation*

Charles Hughes  
*Virginia Highway & Transportation Research Council*

Robert G. Jenkins  
*University of Cincinnati*

Anthony J. Kriech  
*Heritage Group Company*

Richard Langlois  
*Universite Laval*

Richard C. Meininger  
*National Aggregates Association*

Nicholas Nahas  
*EXXON Chemical Co.*

Charles F. Potts  
*APAC, Inc.*

Ron Reese  
*California Department of Transportation*

Donald E. Shaw  
*Georgia-Pacific Corporation*

Scott Shuler  
*The Asphalt Institute*

Harold E. Smith  
*City of Des Moines*

Thomas J. Snyder  
*Marathon Oil Company*

Richard H. Sullivan  
*Minnesota Department of Transportation*

A. Haleem Tahir  
*American Association of State Highway and  
Transportation Officials*

Jack Telford  
*Oklahoma Department of Transportation*

George West  
*Shell Oil Company*

## **Liaisons**

Avery D. Adcock  
*United States Air Force*

Ted Ferragut  
*Federal Highway Administration*

Donald G. Fohs  
*Federal Highway Administration*

Fredrick D. Hejl  
*Transportation Research Board*

Aston McLaughlin  
*Federal Aviation Administration*

Bill Weseman  
*Federal Highway Administration*

## **Expert Task Group**

Dallas Little, *chairman*  
*Texas Transportation Institute*

Campbell Crawford  
*National Asphalt Paving Association*

Daniel W. Dearasaugh  
*Transportation Research Board*

Francis Fee  
*Westbank Oil, Incorporated*

Eric Harm  
*Illinois Department of Transportation*

Charles Hughes  
*Virginia Highway & Transportation Research Council*

Kevin Stuart  
*Federal Highway Administration*

Roger L. Yarbrough  
*Apcon Corporation*

## **Asphalt Advisory Committee**

Thomas D. Moreland, *chairman*  
*Moreland Altobelli Associates, Inc.*

Gale C. Page, *vice chairman*  
*Florida Department of Transportation*

Peter A. Bellin  
*Niedersachsisches Landesamt  
für Strassenbau*

Dale Decker  
*National Asphalt Paving Association*

Joseph L. Goodrich  
*Chevron Research Company*

Eric Harm  
*Illinois Department of Transportation*

Charles Hughes  
*Virginia Highway & Transportation Research Council*

Robert G. Jenkins  
*University of Cincinnati*

Anthony J. Kriech  
*Heritage Group Company*

Richard Langlois  
*Universite Laval*

Richard C. Meininger  
*National Aggregates Association*

Nicholas Nahas  
*EXXON Chemical Co.*

Charles F. Potts  
*APAC, Inc.*

Ron Reese  
*California Department of Transportation*

Donald E. Shaw  
*Georgia-Pacific Corporation*

Scott Shuler  
*The Asphalt Institute*

Harold E. Smith  
*City of Des Moines*

Thomas J. Snyder  
*Marathon Oil Company*

Richard H. Sullivan  
*Minnesota Department of Transportation*

A. Haleem Tahir  
*American Association of State Highway and  
Transportation Officials*

Jack Telford  
*Oklahoma Department of Transportation*

George West  
*Shell Oil Company*

## **Liaisons**

Avery D. Adcock  
*United States Air Force*

Ted Ferragut  
*Federal Highway Administration*

Donald G. Fohs  
*Federal Highway Administration*

Fredrick D. Hejl  
*Transportation Research Board*

Aston McLaughlin  
*Federal Aviation Administration*

Bill Weseman  
*Federal Highway Administration*



## **Asphalt Advisory Committee**

Thomas D. Moreland, *chairman*  
*Moreland Altobelli Associates, Inc.*

Gale C. Page, *vice chairman*  
*Florida Department of Transportation*

Peter A. Bellin  
*Niedersachsisches Landesamt  
für Strassenbau*

Dale Decker  
*National Asphalt Paving Association*

Joseph L. Goodrich  
*Chevron Research Company*

Eric Harm  
*Illinois Department of Transportation*

Charles Hughes  
*Virginia Highway & Transportation Research Council*

Robert G. Jenkins  
*University of Cincinnati*

Anthony J. Kriech  
*Heritage Group Company*

Richard Langlois  
*Universite Laval*

Richard C. Meininger  
*National Aggregates Association*

Nicholas Nahas  
*EXXON Chemical Co.*

Charles F. Potts  
*APAC, Inc.*

Ron Reese  
*California Department of Transportation*

Donald E. Shaw  
*Georgia-Pacific Corporation*

Scott Shuler  
*The Asphalt Institute*

Harold E. Smith  
*City of Des Moines*

Thomas J. Snyder  
*Marathon Oil Company*

Richard H. Sullivan  
*Minnesota Department of Transportation*

A. Haleem Tahir  
*American Association of State Highway and  
Transportation Officials*

Jack Telford  
*Oklahoma Department of Transportation*

George West  
*Shell Oil Company*

## **Liaisons**

Avery D. Adcock  
*United States Air Force*

Ted Ferragut  
*Federal Highway Administration*

Donald G. Fohs  
*Federal Highway Administration*

Fredrick D. Hejl  
*Transportation Research Board*

Aston McLaughlin  
*Federal Aviation Administration*

Bill Weseman  
*Federal Highway Administration*

## **Asphalt Advisory Committee**

Thomas D. Moreland, *chairman*  
*Moreland Altobelli Associates, Inc.*

Gale C. Page, *vice chairman*  
*Florida Department of Transportation*

Peter A. Bellin  
*Niedersächsisches Landesamt  
für Strassenbau*

Dale Decker  
*National Asphalt Paving Association*

Joseph L. Goodrich  
*Chevron Research Company*

Eric Harm  
*Illinois Department of Transportation*

Charles Hughes  
*Virginia Highway & Transportation Research Council*

Robert G. Jenkins  
*University of Cincinnati*

Anthony J. Kriech  
*Heritage Group Company*

Richard Langlois  
*Universite Laval*

Richard C. Meininger  
*National Aggregates Association*

Nicholas Nahas  
*EXXON Chemical Co.*

Charles F. Potts  
*APAC, Inc.*

Ron Reese  
*California Department of Transportation*

Donald E. Shaw  
*Georgia-Pacific Corporation*

Scott Shuler  
*The Asphalt Institute*

Harold E. Smith  
*City of Des Moines*

Thomas J. Snyder  
*Marathon Oil Company*

Richard H. Sullivan  
*Minnesota Department of Transportation*

A. Haleem Tahir  
*American Association of State Highway and  
Transportation Officials*

Jack Telford  
*Oklahoma Department of Transportation*

George West  
*Shell Oil Company*

## **Liaisons**

Avery D. Adcock  
*United States Air Force*

Ted Ferragut  
*Federal Highway Administration*

Donald G. Fohs  
*Federal Highway Administration*

Fredrick D. Hejl  
*Transportation Research Board*

Aston McLaughlin  
*Federal Aviation Administration*

Bill Weseman  
*Federal Highway Administration*

## **Expert Task Group**

Dallas Little, *chairman*  
*Texas Transportation Institute*

Campbell Crawford  
*National Asphalt Paving Association*

Daniel W. Dearasaugh  
*Transportation Research Board*

Francis Fee  
*Westbank Oil, Incorporated*

Eric Harm  
*Illinois Department of Transportation*

Charles Hughes  
*Virginia Highway & Transportation Research Council*

Kevin Stuart  
*Federal Highway Administration*

Roger L. Yarbrough  
*Apcon Corporation*

## **Asphalt Advisory Committee**

Thomas D. Moreland, *chairman*  
*Moreland Altobelli Associates, Inc.*

Gale C. Page, *vice chairman*  
*Florida Department of Transportation*

Peter A. Bellin  
*Niedersachsisches Landesamt  
für Strassenbau*

Dale Decker  
*National Asphalt Paving Association*

Joseph L. Goodrich  
*Chevron Research Company*

Eric Harm  
*Illinois Department of Transportation*

Charles Hughes  
*Virginia Highway & Transportation Research Council*

Robert G. Jenkins  
*University of Cincinnati*

Anthony J. Kriech  
*Heritage Group Company*

Richard Langlois  
*Universite Laval*

Richard C. Meininger  
*National Aggregates Association*

Nicholas Nahas  
*EXXON Chemical Co.*

Charles F. Potts  
*APAC, Inc.*

Ron Reese  
*California Department of Transportation*

Donald E. Shaw  
*Georgia-Pacific Corporation*

Scott Shuler  
*The Asphalt Institute*

Harold E. Smith  
*City of Des Moines*

Thomas J. Snyder  
*Marathon Oil Company*

Richard H. Sullivan  
*Minnesota Department of Transportation*

A. Haleem Tahir  
*American Association of State Highway and  
Transportation Officials*

Jack Telford  
*Oklahoma Department of Transportation*

George West  
*Shell Oil Company*

## **Liaisons**

Avery D. Adcock  
*United States Air Force*

Ted Ferragut  
*Federal Highway Administration*

Donald G. Fohs  
*Federal Highway Administration*

Fredrick D. Hejl  
*Transportation Research Board*

Aston McLaughlin  
*Federal Aviation Administration*

Bill Weseman  
*Federal Highway Administration*

8/16/93

## **Expert Task Group**

Dallas Little, *chairman*  
*Texas Transportation Institute*

Campbell Crawford  
*National Asphalt Paving Association*

Daniel W. Dearasaugh  
*Transportation Research Board*

Francis Fee  
*Westbank Oil, Incorporated*

Eric Harm  
*Illinois Department of Transportation*

Charles Hughes  
*Virginia Highway & Transportation Research Council*

Kevin Stuart  
*Federal Highway Administration*

Roger L. Yarbrough  
*Apcon Corporation*

8/23/93